

# **Taxonomy of fossil eagles and vultures (Aves, Accipitridae) from Australia**

By

**Ellen K. Mather**

BSc (Hons)

*Thesis  
Submitted to Flinders University  
for the degree of*

**Doctor of Philosophy**

College of Science and Engineering  
3<sup>rd</sup> December 2021

# CONTENTS

<b>LIST OF FIGURES</b> .....	<b>V</b>
<b>LIST OF TABLES</b> .....	<b>VII</b>
<b>THESIS SUMMARY</b> .....	<b>VIII</b>
<b>DECLARATION</b> .....	<b>X</b>
<b>PAPERS AND MANUSCRIPTS PUBLISHED DURING CANDIDATURE</b> .....	<b>X</b>
<b>ACKNOWLEDGEMENTS</b> .....	<b>XI</b>
<b>PREFACE</b> .....	<b>XIII</b>
<b>STATEMENT OF AUTHORSHIP</b> .....	<b>XIV</b>
<b>CHAPTER 1: INTRODUCTION</b> .....	<b>1</b>
1.1 The Accipitridae .....	1
1.2 Phylogenetic relationships .....	2
1.2.1 Relatives of the Accipitridae .....	2
1.2.2 Resolution of relationships within the Accipitridae .....	3
1.3 Fossil Record .....	14
1.3.1 Cathartidae and Teratornithidae .....	15
1.3.2 Sagittariidae .....	16
1.3.3 Pandionidae .....	16
1.3.4 Accipitrid-like Fossil Lineages .....	17
1.3.5 Accipitridae of Europe .....	18
1.3.6 Accipitridae of Asia .....	19
1.3.7 Accipitridae of Africa .....	21
1.3.8 Accipitridae of the Americas .....	22
1.3.9 Accipitridae of Australasia .....	25
1.4 Diversity and distribution of modern Australasian accipitrids .....	27
1.5 Summary and material of interest .....	28
1.6 Thesis aims and objectives .....	30
1.7 Thesis structure .....	30
<b>CHAPTER 2: AN EXCEPTIONAL PARTIAL SKELETON OF A NEW BASAL RAPTOR (AVES: ACCIPITRIDAE) FROM THE LATE OLIGOCENE NAMBA FORMATION, SOUTH AUSTRALIA</b> .....	<b>31</b>
2.1 INTRODUCTION .....	33
2.1.1 The Accipitridae and Kin .....	33
2.1.2 Pre-Pleistocene Fossil Record of the Accipitridae .....	33
2.1.3 The Namba Formation .....	35
2.2 MATERIALS AND METHODS .....	39
2.2.1 Abbreviations .....	39
2.2.2 Nomenclature .....	39

2.2.3	Measurements .....	40
2.2.4	Photography.....	40
2.2.5	Comparative Material .....	40
2.2.6	Phylogenetic methods.....	41
2.2.7	Ecomorphological analyses.....	44
2.3	RESULTS.....	45
2.3.1	Systematic palaeontology .....	45
2.3.2	Size comparisons of the three fossils .....	87
2.3.3	Phylogenetic analyses.....	91
2.4	DISCUSSION .....	94
2.4.1	Relationships with fossil and extant Australian Accipitridae.....	94
2.4.2	Palaeobiology .....	97
2.5	Additional Information.....	100
	Thesis Appendices.....	100
	Supplementary Information .....	100
2.6	References .....	101
<b>CHAPTER 3: AN OLD-WORLD VULTURE FROM THE AUSTRALIAN PLEISTOCENE: “TAPHAETUS” LACERTOSUS DE VIS 1905 (AEGYPIINAE, ACCIPITRIDAE).....</b>		
3.1	INTRODUCTION .....	113
3.1.1	Pleistocene Australian Accipitridae .....	113
3.1.2	The history of “ <i>Taphaetus</i> ” <i>lacertosus</i> .....	113
3.2	MATERIALS AND METHODS.....	114
3.2.1	Abbreviations .....	114
3.2.2	Nomenclature.....	114
3.2.3	Comparative Material .....	115
3.2.4	Measurements .....	116
3.2.5	Photography and Scanning.....	116
3.2.6	Phylogenetic Methods.....	116
3.2.7	Fossil Sites.....	118
3.3	RESULTS.....	119
3.3.1	Systematic Palaeontology .....	119
3.3.2	Phylogenetic Analysis .....	137
3.4	DISCUSSION .....	138
3.4.1	Distribution of Scavenging Birds of Prey .....	138
3.4.2	Implications for the ecology of Nov. gen. <i>lacertosus</i> .....	140
3.5	Additional Information.....	142
	Thesis Appendices.....	142
	Supplementary Information .....	142
3.6	References .....	143

<b>CHAPTER 4: NEW LARGE PLEISTOCENE OLD WORLD VULTURES (ACCIPITRIDAE) FROM AUSTRALIA: MORPHOLOGY, SYSTEMATICS AND PALAEOECOLOGICAL IMPLICATIONS.</b> .....	<b>150</b>
4.1 INTRODUCTION .....	151
4.1.1 Australian Accipitridae .....	151
4.1.2 Pleistocene Australian fossil record of Accipitridae .....	152
4.1.3 Fossil record of accipitrid vultures .....	153
4.2 MATERIALS AND METHODS .....	156
4.2.1 Abbreviations: .....	156
4.2.2 Nomenclature .....	157
4.2.3 Comparative Material .....	157
4.2.4 Measurements .....	158
4.2.5 Phylogenetic methods .....	158
4.2.6 Mass estimates .....	160
4.2.7 Australian Pleistocene sites .....	160
4.2.8 Aims and Assumptions .....	169
4.3 RESULTS .....	170
4.3.1 Systematic palaeontology .....	170
4.3.2 Body mass estimation .....	226
4.3.3 Phylogenetic Analyses .....	228
4.4 DISCUSSION .....	234
4.4.1 Phylogenetic relationships .....	234
4.4.2 Diversity of Pleistocene Australian Accipitridae .....	235
4.4.3 Palaeoecology .....	236
4.4.4 Role in the Australian Pleistocene .....	240
4.5 Additional Information .....	242
Thesis Appendices .....	242
Supplementary Information .....	242
4.6 References .....	243
<b>CHAPTER 5. DISCUSSION</b> .....	<b>257</b>
5.1 Thesis summary and aims .....	257
5.2 Project Findings .....	258
5.2.1 An exceptionally complete new basal raptor (Aves: Accipitridae) from the late Oligocene Namba Formation, South Australia .....	258
5.2.2 <i>Taphaetus lacertosus</i> , a widespread aegyptine vulture from the Pleistocene of Australia .....	259
5.2.3 New large Pleistocene Old World vultures (Accipitridae) from Australia: morphology, systematics and palaeoecological implications. ....	260
5.3 Suggestions for future research .....	263
5.3.1 Oligocene Accipitridae of Australia .....	263
5.3.2 Pleistocene Accipitridae of Australia .....	264

5.3.3 Bridging the Oligocene and Pleistocene: Miocene Accipitridae .....	265
5.3.4 Phylogeny and systematics of Australia's fossil Accipitridae .....	266
5.4 Conclusions .....	266
<b>APPENDICES.....</b>	<b>267</b>
Appendix 1: Morphological character list .....	267
Appendix 2: Additional Measurements.....	292
Measurements from <i>Archaeohierax sylvestris</i> holotype .....	292
Appendix 3: Chapter 2 comparative descriptions with extant species .....	296
<i>Archaeohierax sylvestris</i> .....	296
Gen. et sp. Indet. ....	319
Appendix 4: Chapter 2 PCA analyses data, scree plots and biplots.....	324
Appendix 5: Chapter 2 additional phylogenetic trees .....	330
<b>BIBLIOGRAPHY .....</b>	<b>334</b>

## List of figures

<b>Figure 1.1</b> Simplified phylogeny of Accipitridae	6
<b>Figure 2.1</b> Map of South Australia with location of Callabonna Sub-Basin and study sites	39
<b>Figure 2.2</b> Accipitriform skeleton illustration showing bones preserved in fossil specimen	48
<b>Figure 2.3</b> <i>Archaeohierax sylvestris</i> rostrum, quadrate and vertebrae	50
<b>Figure 2.4</b> <i>Archaeohierax sylvestris</i> sternum, coracoid and scapula	53
<b>Figure 2.5</b> <i>Archaeohierax sylvestris</i> humerus	57
<b>Figure 2.6</b> <i>Archaeohierax sylvestris</i> ulna and radius	59
<b>Figure 2.7</b> <i>Archaeohierax sylvestris</i> os carpale radiale, os carpale ulnare, carpometacarpus and manual phalanges	63
<b>Figure 2.8</b> <i>Archaeohierax sylvestris</i> femur and tibiotarsus	68
<b>Figure 2.9</b> <i>Archaeohierax sylvestris</i> tarsometatarsus	72
<b>Figure 2.10</b> <i>Archaeohierax sylvestris</i> pedal and ungual phalanges	76
<b>Figure 2.11</b> Accipitrid genus et sp. indet. distal humerus	82
<b>Figure 2.12</b> Accipitrid genus et sp. indet. distal femur	86
<b>Figure 2.13</b> PCA plots of long bone measurements in <i>Archaeohierax sylvestris</i> and extant species	90
<b>Figure 2.14</b> Bayesian analysis phylogenetic tree of combined molecular and morphological data (ordered), molecular and morphological branches unlinked	93
<b>Figure 3.1</b> Comparisons of the scanned distal humeri of Nov. gen. <i>lacertosus</i> to <i>Aquila audax</i> and <i>Haliaeetus leucogaster</i>	124
<b>Figure 3.2</b> Comparisons of Nov. gen. <i>lacertosus</i> lectotype and Wellington Caves distal humeri	130
<b>Figure 3.3</b> Comparisons of Nov. gen. <i>lacertosus</i> and <i>Aquila audax</i> tarsometatarsi	131
<b>Figure 3.4</b> Comparisons of humerus and tarsometatarsus of Nov. gen. <i>lacertosus</i> and aegyptiine species	135
<b>Figure 3.5</b> Parsimony analysis phylogenetic tree of morphological (ordered) data	138
<b>Figure 4.1</b> Map of Australia with marked fossil site locations	161
<b>Figure 4.2</b> Map of Green Waterhole Cave	164
<b>Figure 4.3</b> Comparison between humeri of accipitrid GWC/VFC, Nov. gen. <i>lacertosus</i> and <i>Aquila audax</i>	175

<b>Figure 4.4</b> Accipitrid GWC/VFC quadrate, coracoid, scapula and carpometacarpus	182
<b>Figure 4.5</b> Accipitrid GWC/VFC ulna and radius	197
<b>Figure 4.6</b> Accipitrid GWC/VFC thoracic vertebra	199
<b>Figure 4.7</b> Accipitrid GWC/VFC pelvis and femur	200
<b>Figure 4.8</b> Accipitrid GWC/VFC tibiotarsus, tarsometatarsus and os metatarsale I	209
<b>Figure 4.9</b> Comparison between sterna of Mairs Cave accipitrid and <i>Gypohierax angolensis</i>	218
<b>Figure 4.10</b> Humeri of Mairs Cave accipitrid, <i>Gyps fulvus</i> , <i>Gypohierax angolensis</i> , <i>Gypaetus barbatus</i> and “ <i>Taphaetus</i> ” <i>lacertosus</i> , and unguis phalanges of Mairs Cave accipitrid	219
<b>Figure 4.11</b> Parsimony analysis phylogeny for accipitrid GWC/VFC, morphological (ordered) data only	230
<b>Figure 4.12</b> Parsimony analysis phylogeny for accipitrid GWC/VFC, molecular and morphological (ordered) data	232
<b>Figure 4.13</b> Bayesian analysis phylogeny for accipitrid GWC/VFC, molecular and morphological (ordered) data	233
<b>Figure 5.1</b> List of extinct and extant Australian megafauna	263
<b>Figure A4.1</b> Biplots of PC1 and PC2 of absolute data PCA (A)	325
<b>Figure A4.2</b> Scree plot of absolute data PCA (A)	325
<b>Figure A4.3</b> Biplots of PC1 and PC2 of log transformed data PCA (B)	327
<b>Figure A4.4</b> Scree plot of log-transformed data PCA (B)	327
<b>Figure A4.5</b> Biplots of PC1 and PC2 of size standardised PCA (C)	329
<b>Figure A4.6</b> Scree plot of size standardised PCA (C)	329
<b>Figure A5.1</b> Strict consensus tree of Analysis 1, Chapter 2 with bootstrap values	330
<b>Figure A5.2</b> Strict consensus tree of Analysis 2, Chapter 2 with bootstrap values	331
<b>Figure A5.3</b> Strict consensus tree of Analysis 3, Chapter 2 with bootstrap values	332
<b>Figure A5.4</b> Majority consensus tree of Analysis 4b, Chapter 2	333

## List of tables

<b>Table 3.1</b> Measurements of distal humeri from Nov. gen. and <i>Aquila audax</i>	128
<b>Table 3.2</b> Proximal and shaft measurements of tarsometatarsi from Nov. gen. and <i>Aquila audax</i>	128
<b>Table 3.3</b> Distal measurements of tarsometatarsi specimens of Nov. gen. and <i>Aquila audax</i>	129
<b>Table 4.1</b> U-series dating age estimates for Green Waterhole Cave	167
<b>Table 4.2</b> Key measurements (mm) of long bone fossils of accipitrid GWC/VFC	173
<b>Table 4.3</b> Comparative measurements of the humerus and femora in accipitrid GWC/VFC and selected extant species	227
<b>Table 4.4</b> Mass estimates for accipitrid GWC/VFC	228
<b>Table A2.1</b> Measurements for pedal and ungual phalanges of <i>Archaeohierax sylvestris</i>	294
<b>Table A2.2</b> Measurements of humeri and femora of fossil and extant specimens (Chapter 2)	295
<b>Table A4.1</b> Absolute data from <i>Archaeohierax sylvestris</i> and selected extant species for PCA (A).	324
<b>Table A4.2</b> Statistics for absolute data PCA (A)	325
<b>Table A4.3</b> Log transformed data from <i>Archaeohierax sylvestris</i> and selected extant species for PCA (B)	326
<b>Table A4.4</b> Statistics for log transformed data PCA (B)	327
<b>Table A4.5</b> Size standardised data from <i>Archaeohierax sylvestris</i> and selected extant species for PCA (C)	328
<b>Table A4.6</b> Statistics for size standardised data PCA (C)	329

## Thesis summary

The Accipitridae (eagles, hawks, and Old-World vultures) have a global distribution across all continents except Antarctica. Australia is home to seventeen accipitrid species, including the iconic wedge-tailed eagle *Aquila audax*. A review of their fossil record shows the group appeared in the late Eocene of Europe and North America, but our understanding of the evolution and fossil history of these birds in Australia is lacking. In this thesis, I address this gap by describing and interpreting fossils from the Oligocene and Pleistocene periods.

First, Chapter 2 presents a description of a late Oligocene accipitrid (~24 Ma) from the Namba Formation at Lake Pinpa, South Australia (SA). This new species is represented by an exceptionally complete partial skeleton. Detailed analyses and comparisons revealed that it is not closely related to any living subfamily, but instead represents a new subfamily sister to possibly all accipitrids other than elanine kites.

The lectotype (a distal humerus) and the originally referred quadrate of the Pleistocene fossil species "*Taphaetus*" *lacertosus* de Vis, 1905 from Kalamurina, SA, is redescribed in Chapter 3. The original assessment of the humerus as a distinct species of accipitrid is valid, but the quadrate is from a species of Ardeidae. A new genus is required for this distinct species, as *Taphaetus* de Vis 1905 is a junior homonym of *Taphaetus* de Vis 1891, a synonym of *Aquila*. Undescribed fossil distal humeri from the Wellington Caves, New South Wales, were referable to "*T.*" *lacertosus* based on their similar morphology. A tarsometatarsus from Wellington Caves is also referred to the taxon due to its association with the humeri and its appropriate size and concordant aegyptine morphology. A second tarsometatarsus, from Leaena's Breath Cave (Nullarbor Plains, WA), is also referred to the species. Phylogenetic analysis of the taxon supported its position within the Old World vultures (Aegyptinae).

The Pleistocene fossil remains of large accipitrids from across southern Australia were assessed to determine the number of species they represented in Chapter 4. These included the sites Leaena's breath Cave, Mairs Cave (Flinders Ranges, SA), Victoria Fossil Cave (Naracoorte, SA), Green Waterhole Cave (Tantanoola district, SA), Wellington Caves (Wellington, New South Wales), and Cooper Creek (SA). Two species are present, which are described within as the Mairs Cave accipitrid and accipitrid GWC/VFC. Phylogenetic analyses resolved accipitrid GWC/VFC as an aegyptine vulture despite aspects of its morphology being much more like active predators such as eagles. Mass estimates predict the smaller sex was up to twice the size of the largest female *Aquila audax* and rivalled Haast's eagle *Hieraaetus moorei* in size. The Mairs Cave accipitrid was not included in phylogenetic analyses due to the few bones available for it, but the morphology of the sternum and partial distal humerus strongly support a relationship with gypaetine vultures. It was at least twice as large as *Aquila audax*. The discovery that Pleistocene Australia was

home to both aegyptine and gypaetine vultures reveals that the modern accipitrid raptor guild is markedly reduced in diversity and function.

## Declaration

I certify that this thesis:

- 1) Does not incorporate without acknowledgement any material previously submitted for a degree or diploma in any university; and
- 2) To the best of my knowledge and belief, does not contain any material previously published or written by another person except where due reference is made in the text.

A handwritten signature in black ink that reads "E. Mather". The letters are cursive and fluid, with a large initial 'E'.

## Papers and manuscripts published during candidature

Mather, E. K., Tennyson, A. J. D., Scofield, R. P., De Pietri, V. L., Hand, S. J., Archer, M. and Worthy, T. H. (2018) [2019] Flightless rails (Aves: Rallidae) from the early Miocene St Bathans Fauna, Otago, New Zealand. *Journal of Systematic Palaeontology*, 17(5), 423–449.

Chapter 2 - Mather, E. K., Lee, M. S. Y., Camens, A. B. and Worthy, T. H. (2021) An exceptional partial skeleton of a new basal raptor (Aves: Accipitridae) from the late Oligocene Namba Formation, South Australia. *Historical Biology*, DOI: 10.1080/08912963.21.1966777

## **Acknowledgements**

To my supervisors, Trevor Worthy and Mike Lee, I would like to extend my deepest gratitude. Trevor, you have been an invaluable source of guidance and information since before my PhD candidature even began. It's because of you that I know a tibiotarsus from a tarsometatarsus, and I sometimes wonder how you ever put up with me! Mike, without you I wouldn't understand how to run and interpret a phylogeny half as well as I do.

I'd like to thank the Flinders Palaeontology PhD students, present and former, with whom I shared a workspace and who were a vital source of support, advice, and distraction: Kailah Thorn, Jacob Blokland, Jacob van Zoelen, Phoebe McInerney, Amy Tschirn, Diana Fusco, Warren Handley, Grant Gully, Lisa Nink, Elen Shute, Isaac Kerr, Cassia Paragnani, and Arthur Crichton. You are all amazing people, and I wish you all the best in the future. To Tim Niederer and Nicia Burgess, it's been great to get to know you and I wish you the best for your Honours projects.

To the extended Flinders Palaeontology Lab, it's been a delight to work with you and get to know you all. To Carey Burke, Aaron Camens, Gavin Prideaux, John Long, Rod Wells, and Vera Weisbecker; I've learned so much from you, and I hope to continue with that knowledge well into the future.

To my dear parents, Barb and Ian – you have always encouraged me from the very beginning, ever since I first said I wanted to be a palaeontologist as a child. I have truly been blessed to have you as my mum and dad. And to my brother and sister, Tom and Abby, thank you for showing interest in my project and asking about it whenever we caught up; it meant a lot to me.

Many thanks to the wonderful Elizabeth Scharsachs and her family, who provided valuable accommodation and company while I was in the UK.

This project has been many years in the making and would not have been possible if it weren't for the work of people before me. I would like to acknowledge the efforts of the following people: Charles Walter de Vis, who described many of the original Pleistocene accipitrid material, some of which were included in my own thesis; Pat Vickers-Rich and Jerry van Tets, for their extensive work on the Australian fossil avifauna, including accipitrids; Priscilla Gaff, who had previously worked on much of the same Pleistocene material in her own thesis; the following collection managers and staff: Mary-Anne Binnie, Maya Penck, Phillipa Horton (South Australia Museum), Tim Ziegler, Karen Roberts (Museums Victoria), Jacqueline Nguyen, Matthew McCurry (Australian Museum), Leo Joseph, Alex Drew (Australian National Wildlife Collection), Scott Hucknull (Queensland Museum), Mikael Siversson (Western Australian Museum), Chris Milensky (Smithsonian

Museum of Natural History), Mark Robbins (University of Kansas Institute of Biodiversity), Judith White and Joanne Cooper (London Museum of Natural History), without whom I would not have had access to vital comparative specimens and fossils; and a second shoutout to Isaac Kerr, who kindly took the scans of the "*Taphaetus*" lectotype while at Queensland Museum for his own PhD work, Elen Shute for identifying the Leaena's Breath Cave accipitrid material during her own thesis, and Judith White from the Natural History Museum at Tring for providing photographs of specimens when requested.

My PhD candidature and research was supported by the Flinders University Research Scholarship, as well as the Australian Government Research Training Program Scholarship.

## **Preface**

Throughout time, throughout cultures, humanity has been fascinated by eagles and their kin. Their talons and feathers have been used as jewellery and status symbols, their image appears in cave art and heraldry, they are the subject of poems and art, and are central to an entire form of hunting known as falconry. Naturally they are also the focus of scientific curiosity, and many studies have been performed to investigate their anatomy, ecology, taxonomy, evolution, and fossil record – which brings us to this thesis.

My attention was first drawn to Australian fossil Accipitridae (eagles, hawks and Old World vultures) by my supervisor Trevor Worthy, not long after I had completed my Honours thesis. He proposed a PhD project where I would describe and investigate the phylogeny of undescribed Oligocene and Pleistocene fossil accipitrids, as well as the ecomorphology of the latter. Having worked on fossil species of rails (Rallidae) from the Miocene deposits of New Zealand, switching over to a family of predatory birds was quite a change. But the project was very interesting to me, and I agreed to take it on.

This PhD project, as it is written out in this thesis, is not how it was originally envisioned. The ecomorphology chapter was later ruled out due to concerns for time constraints, and I chose to replace it with a chapter describing the fossil accipitrids of St Bathans, New Zealand, the site where the rails from my Honours project had come from. That chapter was abruptly derailed by the unexpected discovery that one of the ‘eagle’ fossil bones was in fact from a giant, flightless parrot. With not enough actual accipitrid material left for a chapter’s worth of content, I had to change focus again.

The third iteration of this chapter was a reassessment of a previously described fossil accipitrid. Simple enough; until we realised that some fossil material loaned to us from the Australian Museum could also be assigned to this species and could also be phylogenetically assessed. These aspects were added in, and thankfully there were no more changes beyond that point.

While stressful, switching chapter topics several times did have one benefit. It resulted in me researching parts of the literature I hadn’t previously looked at and resulted in discoveries that might not have otherwise been made. When it comes down to it, that’s really the whole point of undertaking a PhD.

This thesis and the results within were the product of four years of work. It is my hope that it will provide information and a basis for future research on fossil accipitrids for many more years to come.

## Statement of Authorship

This thesis was completed without the use of any professional editing services.

**Chapter 1: Introduction.** I conducted and wrote the literature review and prepared all figures.

**Chapter 2: An exceptional partial skeleton of a new basal raptor (Aves: Accipitridae) from the Late Oligocene Namba Formation, South Australia.** The chapter was co-authored with MSY Lee, AB Camens, and TH Worthy. I devised the methods with the suggestions of TH Worthy and MSY Lee, conducted the analyses, compared and described the fossil material, created the figures presented herein, and wrote the manuscript. THW helped with osteological terminology and interpretation. AB Camens and TH Worthy collected the Lake Pinpa fossil material. MSY Lee collated the molecular data. All authors edited the final draft of the manuscript I wrote.

**Chapter 3: An old-world vulture from the Australian Pleistocene: “*Taphaetus*” *lacertosus* de Vis 1905 (Aegyptiinae, Accipitridae).** The chapter was co-authored with MSY Lee and TH Worthy. I devised the methods with the suggestions of TH Worthy and MSY Lee, conducted the analyses, compared and described the fossil material, created the figures presented herein, and wrote the manuscript. THW helped with osteological terminology and interpretation. MSY Lee suggested the inclusion of a phylogenetic analysis and collated the molecular data. All authors edited the final draft of the manuscript I wrote.

**Chapter 4: New large Pleistocene Old World vultures (Accipitridae) from Australia: morphology, systematics and palaeoecological implications.** The chapter was co-authored with MSY Lee, DA Fusco and TH Worthy. I devised the methods with the suggestions of TH Worthy and MSY Lee, conducted the analyses, compared and described the fossil material, created the figures presented herein unless otherwise noted, and wrote the manuscript. THW helped with osteological terminology and interpretation. DA Fusco provided fossil material and stratigraphic dates from Cathedral Cave. MSY Lee collated the molecular data. J Hellstrom of Melbourne University analysed calcite raft samples and provided U-series dates for Green Waterhole Cave. All authors edited the final draft of the manuscript I wrote.

**Chapter 5: Discussion.** I prepared all figures, wrote up the summary of the thesis findings and discussed their implications.

Trevor H. Worthy and Michael S. Y. Lee read the drafts for each chapter and provided feedback and suggestions.

# Chapter 1: Introduction

The aim of this thesis is to describe the fossil eagles and hawks (Aves: Accipitridae) of the Namba Formation and Pleistocene deposits of Australia and determine their phylogenetic relationships with the living species where possible. This introductory chapter will provide a brief overview of the Accipitridae, and the topics presented in the three data chapters to familiarise the reader with them. The first section will summarise the literature on the phylogenetics of the Accipitridae, covering how our understanding of it has changed throughout history. This applies to both the position of Accipitridae in the overall phylogeny of Aves, particularly in relation to other families with similar ecologies, and the phylogenetic arrangement within the family Accipitridae itself. The second section reviews the known fossil record for the family, with the aim of reviewing all species described in the literature. This covers the late Eocene to the late Holocene, a time period that spans from roughly 34 million years ago to the present day, and all continents except for Antarctica. For simplicity, the fossil records of New Zealand and Australia are combined into an Australasian record.

## 1.1 The Accipitridae

The Accipitridae, commonly named as eagles, hawks and harriers, are one of several bird families that are colloquially referred to as 'raptors' and 'birds of prey', along with the Falconidae (falcons), Strigiformes (owls), Pandionidae (ospreys) and occasionally the Cathartidae (New World vultures/condors). Of these families, only the Pandionidae and Cathartidae are closely related in a clade with Accipitridae (Cathartidae more distantly), and the Sagittariidae (secretary birds) is also a close relative (see Claramunt and Cracraft 2015; Prum et al. 2015; Jarvis et al. 2014). Accipitrids have a cosmopolitan distribution; only Antarctica lacks endemic or established breeding species. Based on current knowledge, there are at least 69 genera and 240 extant species (Dickinson and Remsen 2013). I follow Dickinson and Remsen (2013) in taxonomic nomenclature wherein the authorities for all extant taxa are given.

Accipitrid species are primarily carnivorous, although a select few exhibit omnivorous tendencies. Prey can range in size from large insects and small vertebrates, such as lizards and rodents, to large mammals such as sub-adults of small to medium-sized species of Cervidae (see Kerley and Slaght 2013), albeit rarely. Body mass varies significantly between species, with the smallest accipitrids just under 100 g (Pearl Kite *Gampsonyx swainsonii* and Little Sparrowhawk *Accipiter minullus*) and the largest up to 14 kg (Cinereus Vulture *Aegypius monachus*).

Like most modern birds, the Accipitridae first appear in the fossil record after the K–PG extinction, in the late Eocene to early Oligocene and their fossil history is reviewed below. Fossil and molecular evidence indicates the accipitrids diversified into the modern lineages during the Miocene (reviewed below).

## **1.2 Phylogenetic relationships**

Historically, Accipitridae and Falconidae were grouped together alongside the Strigiformes and Cathartidae in an order often named the ‘Falconiformes’ (see Nitzsch 1840; Brandt 1853). As these birds were further studied, doubts began to emerge regarding this traditional taxonomic grouping. Strigiformes were the first group to be separated from the rest of the falconiform birds, with Fitzinger (1856), Milne-Edwards (1867–71) and Fürbringer (1888) placing them in their own order, although a handful of later authors grouped owls with diurnal raptors (see Engelmann 1928; Grassé 1950). Contemporary ornithologists now largely agree with the former assessment, as genetic studies have confirmed that the Strigiformes are not close relatives of the Accipitridae and are in fact related to the Coraciimorphae clade (Jetz et al. 2012; Prum et al. 2015), which includes a diverse group of bird families ranging from mousebirds to toucans.

Morphological data have shown that there are notable differences between the Accipitridae and Falconidae, which to some authors was enough to justify splitting them into separate orders as far back as the mid-twentieth century (Brown and Amadon 1968; Jollie 1976, 1977a, 1977b, 1977c). It was not until molecular phylogenies demonstrated that the Accipitridae and Falconidae were markedly genetically distinct from each other that it became widely accepted that the two were separate groups at the ordinal level. According to the latest studies, falconids are in fact more closely related to the parrots (Psittaciformes) than they are to the accipitrids (Jetz et al. 2012; Prum et al. 2015). As a result of this, the name ‘Accipitriformes’ came into use to describe the Accipitridae and their close relatives (see Gill et al. 2010), although Falconiformes has been used as recently as the last two decades (see Marchant and Higgins 1993; Sievwright and Macleod 2012) and Accipitriformes was used as early as the 1970’s with falcons included within it (Condon 1975).

### **1.2.1 Relatives of the Accipitridae**

The Cathartidae, which are commonly known as New World vultures including condors, also had doubts raised about their relationships with other birds of prey. Cathartids, along with falconids and accipitrids were originally grouped in Falconiformes (see Sharpe 1891; Wetmore 1934; Brown and Amadon 1968) but some authors were separating them

into a separate order, Cathartiformes, long ago (Chapman 1926; Griscom 1932; Hudson 1948). Friedmann (1950) retained the suborder 'Cathartae' within Falconiformes, but also noted many features that distinguished them from the 'Falcones' suborder of falconiforms (true birds of prey). Friedmann also attributed the resemblances of Cathartae to other orders of birds such as the Ciconiiformes as due to a lack of specialisation seen in most Falconiformes. Later, Ligon (1967) proposed that the Cathartidae, which were then known as Vulturidae, were a suborder of the Ciconiiformes (storks) based on certain morphological and physiological similarities. A relationship with the Ciconiiformes has been supported by some studies using molecular data (Sibley and Ahlquist 1990; Avise et al. 1994; Seibold and Helbig 1995; Wink et al. 1998; Song et al. 2014), but most recent phylogenies have retained the Cathartidae within the Accipitriformes, placing them as the most basal lineage within the group (Hackett et al. 2008; Jarvis et al. 2014; Prum et al. 2015). As such, the Cathartidae can be classified as either a primitive lineage of the Accipitriformes or form a very closely related sister group as the Cathartiformes. I follow Dickinson and Remsen (2013) in their family level taxonomy of the order Accipitriformes and include Cathartidae as an accipitriform.

The widely accepted close relatives of the Accipitridae are the monotypic families Sagittariidae (Secretary Bird *Sagittarius serpentarius*), and the Pandionidae (Osprey *Pandion haliaetus*). Pandionidae is directly sister to the Accipitridae clade, and the Sagittariidae fall sister to the clade comprising Pandionidae and Accipitridae. Both families are highly specialised in their niches, with *Sagittarius* having elongate legs that enable a more cursorial lifestyle and a shift to being a terrestrial predator (although it has retained its flight ability), while *Pandion* near-exclusively hunts fish and is adapted to plunging into the water from a height.

### **1.2.2 Resolution of relationships within the Accipitridae**

With the introduction of genetic data including eventually DNA sequences, the study of phylogeny was forever changed. Several phylogenetic studies of the Accipitridae and their closest relatives were conducted in the 1990s and early 2000s, usually using single gene loci (Sibley and Ahlquist 1990; Wink and Seibold 1996; Wink et al. 1998; Wink and Sauer-Gürth 2004). However, a comprehensive molecular phylogenetic study of the Accipitridae as a family was not conducted until Lerner and Mindell (2005) compared several molecular loci from exemplars of 14 recognised subfamilies, both from previous morphological works (Gadow 1893; Sushkin 1905; Peters 1931; Brown and Amadon 1968; Jollie 1976) and identified within their study, with a total of 27 genera and 68 species sampled. This study found that several subfamilies – the Harpiinae, Circaetinae and the Old World vultures (Aegyptiinae and Gypaetinae) – were not monophyletic, which had been suggested in some

earlier works. Furthermore, polyphyly, or at least a lack of monophyly, was found not only in the subfamilies Milvinae and Perninae but also quite extensively in multiple genera. Griffiths et al. (2007) found similar results in their study, which used the RAG-1 exon of almost all the same species sampled by Lerner and Mindell.

Prior to the advent of molecular study, both Jollie (1976, 1977a, 1977b, 1977c) and Holdaway (1994) conducted comprehensive morphological phylogenetic analyses of the Accipitridae. Jollie undertook both a literature review and the examination of specimens in many collections across the United States of America, assessing differences in feather distribution and development, osteological morphology, myology, visceral anatomy, and external features of Accipitridae to determine their phylogeny (Jollie 1976, 1977a, 1977b, 1977c). Holdaway used 188 qualitative discrete osteological characters identified across 66 species of Accipitridae plus *Pandion* and *Sagittarius*. His favoured phylogenetic tree placed the recently extinct *Harpagornis moorei* (now known as *Hieraaetus moorei*) as sister to the genus *Aquila*. Due to this and other factors such as large body size and geographical proximity, it was generally believed at the time that *Harpagornis* was derived from *Aquila audax*. However, when DNA sequenced from Holocene specimens of *Harpagornis* was compared to the DNA sequences of extant eagles, it was found that this species was extremely close to *Hieraaetus morphnoides* and *H. pennatus*, with a genetic distance of only 1.25% (Bunce et al. 2005). This extremely narrow genetic distance implies a very recent divergence between these species, with their most recent common ancestor dating back 1.8–0.7Ma. This was considered quite surprising as *H. morphnoides* and *H. pennatus* are quite small, their common names being the Little Eagle and Pygmy Eagle respectively, while *Harpagornis* was one of the largest eagles known to have existed.

In some cases, morphological features were considered so distinct and consistently distributed that they could be used to reliably identify clades. An example of this was the fused condition in the basal phalanges of pedal digit II found in some genera of Accipitridae. Olson (1982) found this condition to be present in the milvine accipitrids (*Milvus* and *Haliastur*), haliaeetine accipitrids (*Haliaeetus* and *Icthyophaga*), *Ictinia*, and *Busarellus*. He concluded that *Busarellus* could likely be included in the milvine clade based on the fusion and aspects of plumage and behaviour, while *Ictinia* could only be included by phalangeal fusion. However, later studies using molecular or morphological data suggested that the fused phalanges condition is actually convergent, and that *Ictinia* and *Busarellus* do not form a clade with the milvine and haliaeetine accipitrids (Holdaway 1994; Lerner et al. 2008; Nagy and Tökölyi 2014).

Nagy and Tökölyi (2014) took phylogenetic analyses of the Accipitridae a step further by using molecular data to estimate likely divergence dates of the accipitrid subfamilies, of

which they recognised 11. Their analysis found that most of the more basal subfamilies (Elaninae, Perninae, Gypaetinae, Harpiinae, Circaetinae) originated between 30–13 Ma, while more derived subfamilies (Aquilinae, Buteoninae and Haliaeetinae) tended to date between 17–10 Ma. Interestingly, the Aegypiinae dated between 13–7 Ma despite being more closely related to the older clades. In all other regards, their phylogeny largely agreed with that of Lerner and Mindell (2005).

The most recent published phylogenetic work was done by Mindell et al. (2018), which largely agreed with previous findings. An unpublished thesis by Migotto (2013) had similar findings. The authors also tested for divergence dates amongst the lineages, with results suggesting that the most basal living genera, *Gampsonyx* and *Elanus*, diverged from the rest of the Accipitridae roughly 34 Ma, and the split between the Perninae+Gypaetinae clade and the rest of the accipitrid subfamilies roughly 23 Ma, in agreement with Nagy and Tökölyi (2014).

Endemic accipitrid monotypic, or low diversity genera, within the same region, are not necessarily closely related. A molecular study using the RAG-1 exon of the endemic hawks of the Australo-Papuan region found that while the genera *Henicopernis*, *Lophoictinia* and *Hamirostra* grouped closely to each other and fell sister to the pernine kites in a phylogeny, *Harpyopsis* (New Guinea) proved to be sister to the two species of harpy eagles that inhabit South America (Barrowclough et al. 2014). This reveals the importance of understanding the factors of dispersal as well as in-situ speciation when accounting for diversity within a region.

Below, I will review the diversity, range, and relationships of genera in each widely accepted subfamily of the Accipitridae in the following sequence: Elaninae, Perninae, Gypaetinae + Aegypiinae, Circaetinae, Harpiinae, Aquilinae, Haliaeetinae, and Accipitrinae + Buteoninae. A simplified phylogenetic tree of these subfamilies is presented in Figure 1.1.

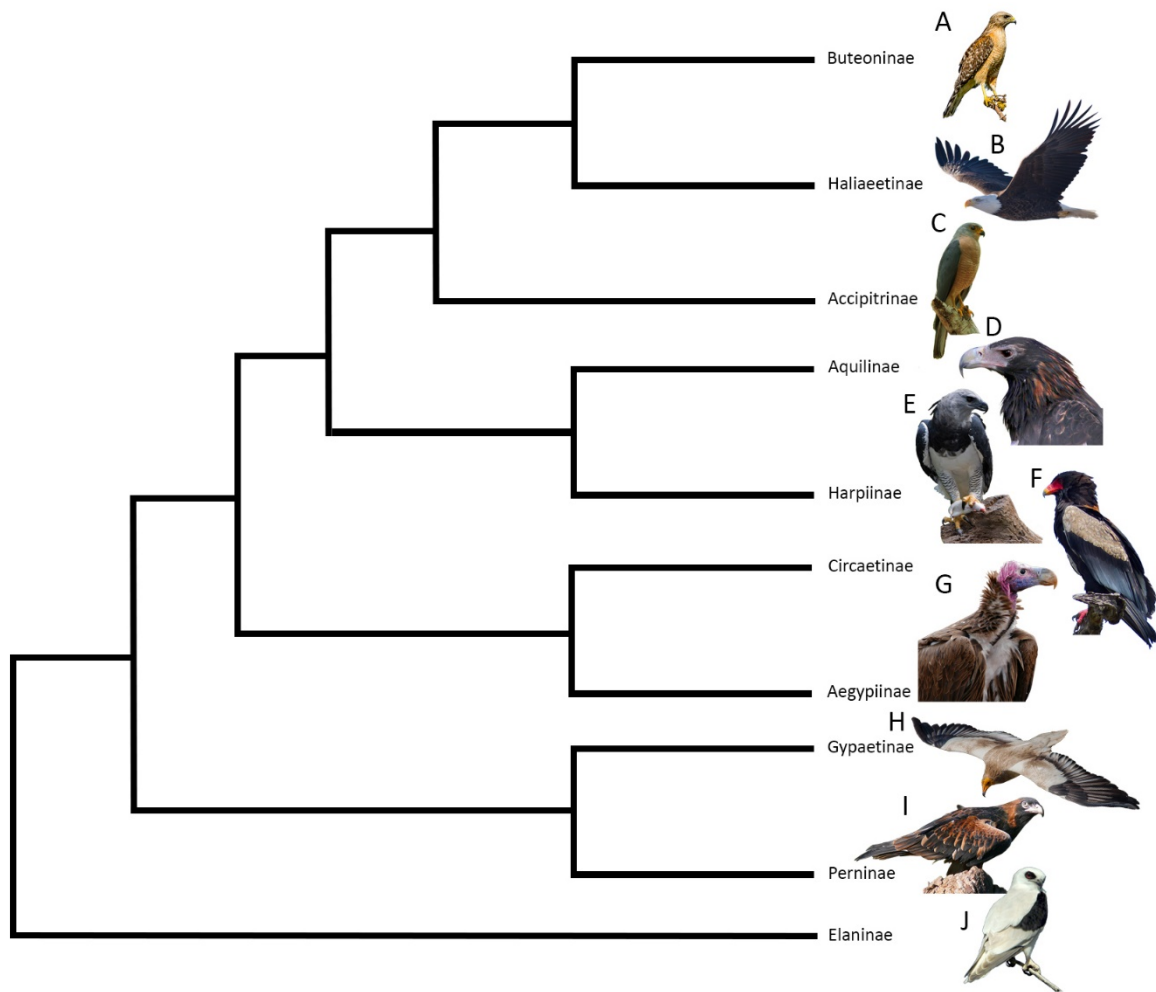


**Figure 1.1:** A simplified phylogeny of the Accipitridae (see Lerner and Mindell 2005; Nagy and Tökölyi 2014) representing all major subfamilies recognised in this thesis. Images: Buteoninae, (A) *Buteo lineatus* (Andy Morffew 2016); Haliaeetinae, (B) *Haliaeetus leucocephalus* (Steve Berardi 2010); Accipitrinae, (C) *Accipiter hiogaster* (Oleg Chernyshov 2012); Aquilinae, (D) *Aquila audax* (Susan 2012); Harpiinae, (E) *Harpia harpyja* (Tom Friedel 2008); Circaetinae, (F) *Terathopius ecaudatus* (Bernard Dupont 2013); Aegypiinae, (G) *Torgos tracheliotos* (Bernard Dupont 2016); Gypaetinae, (H) *Neophron percnopterus* (Artemy Viokhansky 2014); Perninae, (I) *Hamirostra melanosternon* (Benjamint444 2008); Elaninae, (J) *Elanus scriptus* (Frank Pierce 2007). All images sourced from Wikimedia commons.

### **Elanine kites (Elaninae)**

The elanine kites consistently form the most basal lineage of all true accipitrids in phylogenies, and comprise the genera *Elanus* (4 species), and the monotypic *Gampsonyx*, and *Chelictinia*. *Elanus* is distributed globally, being present on all continents, while *Gampsonyx* is restricted to South America and *Chelictinia* to Africa (Dickinson and Remsen 2013). The ancestral region of origin is thought to be the Neotropics (Nagy and Tökölyi 2014).

The genetic distance between *Elanus* and the rest of the Accipitridae is so considerable that some researchers involved in the early genetic phylogenies of Accipitridae

raised the possibility of placing them in their own family, the Elanidae (Wink 2000; Wink and Sauer-Gürth 2004). It should be noted that these studies did not incorporate other elanine species in their analyses. However, further studies with more comprehensive genetic data showed this to be unnecessary (Lerner and Mindell 2005). *Gampsonyx* has been both classified as an accipitrid (Vigors 1825) and as a falconid (Peters 1931) in the past, the latter of which was due to its morphology and plumage being similar to species in that family (see Brown and Amadon 1968) but has been shown to clearly be a true accipitrid by molecular data (Griffiths et al. 2007; Nagy and Tökölyi 2014).

### ***Pernine kites (Perninae)***

The Perninae, despite the common name of pernine kites, include not only the honey buzzards (*Pernis*, 4 species, and *Henicopernis*, 2), but also the bazas/cuckoo hawks (*Aviceda*, 5) and several groups of kites (*Elanoides*, *Leptodon*, 2, *Chondrohierax*, *Hamirostra*, *Lophoictinia*). Distribution for this subfamily is global, but with the exception of certain species in the genera *Pernis* and *Aviceda*, most are found in warm regions in Central to South America, Africa, South Asia, the Indonesian archipelago and Australia (Dickinson and Remsen 2013), with a possible Neotropical origin (Nagy and Tökölyi 2014).

Most species in this subgroup are small birds that inhabit forest or woodland environments and prey upon large invertebrates and small vertebrates (Brown and Amadon 1968). The kite-like genera *Hamirostra* and *Lophoictinia*, which were traditionally included in the milvine kite clade (see below), were revealed via molecular data to in fact be part of the pernine clade (Lerner and Mindell 2005; Griffiths et al. 2007).

*Henicopernis* was generally assumed to be closely related to *Pernis* due to their overall similar morphology. However, phylogenetic work using mitochondrial DNA by Gamauf and Haring (2004, 2005) placed them separately, with *Henicopernis* coming out between the gypaetines and *Buteo*. This was eventually debunked by Barrowclough et al. (2014), who showed via a molecular phylogeny of the RAG-1 exon that *Henicopernis* formed a clade with *Lophoictinia* and *Hamirostra* which was sister to *Aviceda*. While this demonstrated that *Henicopernis* was indeed a true pernine, it also showed that its relationship to *Pernis* was not as close as previously assumed.

The genus *Aviceda* was also recently suggested to be non-monophyletic, with *A. subcristata* forming the above-mentioned clade and *A. cuculoides* being sister to *Pernis* (Mindell et al. 2018). The two species in question have very different biogeographic ranges, with *subcristata* ranging throughout New Guinea and parts of tropical northern Australia, while *cuculoides* inhabits most forested areas of southern Africa. However, Mindell et al. commented that this non-monophyly may have been a result of the methodology rather than

actual molecular differences and cautioned against taxonomic revision before this novel finding is investigated further.

### **Accipitrid Old World vultures (*Gypaetinae* and *Aegyptiinae*)**

Despite morphological and ecological similarities with the New World vultures (Cathartidae), Old World vultures fall strictly within Accipitridae. They are not monophyletic, being divided into two subfamilies, the Aegyptiinae and Gypaetinae, the latter of which forms a clade with the perine kites and the former with the serpent eagles (Lerner and Mindell 2005; Griffiths et al. 2007; Nagy and Tökölyi 2014; Mindell et al. 2018).

The living Gypaetinae are typically recognised to comprise of the monotypic genera *Neophron*, *Gypaetus* (monotypic in present but more diverse in past; see 1.4.5 below), and *Gypohierax*. While Lerner and Mindell (2005) placed *Polyboroides* in its own subfamily, the Polyboroidinae, the phylogenetic trees of Griffiths et al. (2007), Nagy and Tökölyi (2014), and Mindell et al. (2018) included the genus in Gypaetinae. In contrast to the monotypic genera, *Polyboroides* consists of two species. Most of the subfamily is restricted to Africa with the only exception being *Gypaetus barbatus*, which is also present in South Asia and Europe (Dickinson and Remsen 2013). Unsurprisingly, there is strong support for their origin being Afrotropical (Nagy and Tökölyi 2014).

The Gypaetinae subfamily is particularly notable in that it comprises 'atypical' vultures, ones that do not scavenge meat from carcasses; *Neophron percnopterus* will hunt small live prey if the opportunity arises and is also known to feed on large bird eggs by cracking the shell with a pebble, the diet of *Gypohierax angolensis* includes oddities such as crabs, molluscs and the husk of the oil palm nut (which it apparently has a preference for), and *Gypaetus barbatus* specialises in feeding on bone marrow rather than meat (Brown and Amadon 1968). Species of *Polyboroides*, in contrast, are active foragers rather than scavengers, feeding on small vertebrates and large invertebrates (Brown and Amadon 1968), and possess an unusually high degree of flexibility at the intertarsal joint, something seen in only one other accipitrid genus, the buteonine *Geranospiza*.

The Aegyptiinae subfamily is considerably more diverse, comprising of the monotypic *Necrosyrtes*, *Sarcogyps*, *Trigonoceps*, *Aegyptius* and *Torgos*, and *Gyps* (8 species). It is also the most derived genus in the subfamily and has been estimated to have undergone a rapid diversification event within the last 3.57–1.1 Ma based on molecular data (Groth and Barrowclough 1999; Arshad et al. 2009). Much like those in Gypaetinae, most species are African, although there are multiple species that also occur in Asia and a few in Europe (Dickinson and Remsen 2013), and it is highly likely the subfamily originated from the Afrotropics (Nagy and Tökölyi 2014).

The relationships between the aegyptine genera have been debated over the last century. Delacour (1947) considered *Sarcogyps* to be a synonym of *Torgos* and united them as such. White (1951) noted that the differences between *Torgos* and *Trigonoceps* to *Aegyptus* were trivial enough that he believed they should be merged with *Aegyptus*. Amadon (1977) agreed with this in his review of vulture taxonomy, adding that L. H. Brown also agreed with this assessment, but ultimately disagreed with White's (1950) proposal to merge *Neophron* and *Necrosyrtes* based on certain morphological features differentiating the two – the later separation of these two genera into the Gypaetinae and Aegyptinae respectively would render this moot. As of writing, *Torgos* and *Trigonoceps* are still routinely referred to as separate genera to *Aegyptus*, although the three form a monophyletic group in most phylogenetic trees (Nagy and Tökölyi 2014; Mindell et al. 2018).

### **Serpent/Snake eagles (Circaetinae)**

As their common name suggests, the Circaetinae are comprised largely of reptile-hunting specialists, with a few exceptions. The most speciose genera in this subgroup are *Spilornis* (5) and *Circaetus* (6), while all other genera are monotypic (*Dryotriorchis*, *Eutriorchis*, *Terathopius*, *Pithecophaga*). The latter two are not reptile hunting specialists; *Terathopius ecaudatus* is known to predominantly feed on carrion, while *Pithecophaga jefferyi* prefers monkeys and lemurs (Brown and Amadon 1968). Species of *Spilornis* are spread throughout South Asia, the Indonesian archipelago and Africa, while most in *Circaetus* only occur in Africa, apart from *C. gallicus* which also occurs in Europe, South Asia and throughout the Indonesian archipelago (Dickinson and Remsen 2013). Members of *Dryotriorchis* are restricted to central Africa, those in *Pithecophaga* to the Philippines, in *Eutriorchis* to Madagascar, and in *Terathopius* throughout Africa (Dickinson and Remsen 2013). This subfamily is thought to have originated from the Indomalayan region (Nagy and Tökölyi 2014).

The monophyly of the subfamily was called into question by Lerner and Mindell (2005) when it was found that *Eutriorchis astur* would preferentially group with the gypaetine vultures rather than other traditional serpent eagles in their analyses. It was noted that Jollie (1977b) had previously written that *Eutriorchis*, along with *Dryotriorchis*, appeared to lack distinct sister relationships in the serpent eagles based on morphological data, suggesting that the placement of *Eutriorchis* is indeed unresolved. Unfortunately, Griffiths et al. (2007) was unable to sample *Eutriorchis*, and a dissertation by Kocum (2008) determined that *Eutriorchis* can be placed in the Perninae. The latter could be related to Lerner and Mindell's (2005) findings to some degree, as some regard the Gypaetinae and Perninae to be so closely related that they could be merged into a single subfamily (see Dickinson and Remsen 2013). Nagy and Tökölyi (2014) and Mindell et al. (2018) were finally able to

incorporate *E. astur* into a phylogenetic analysis with the other Accipitridae and found that it grouped closely with members of the Perninae such as *Chondrohierax* and *Leptodon*, corroborating the findings of Kocum (2008), and lending strong support to the hypothesis that *Eutriorchis* is not a true serpent eagle and is instead an example of convergent evolution arising from similar diets.

### **Harpy eagles (Harpiinae)**

The Harpiinae are a small clade that until recently was thought to be comprised solely of large eagles that primarily prey upon small to medium size mammals. Traditionally the clade was comprised of *Harpia harpyja*, *Morphnus guianensis*, *Harpyopsis novaeguineae*, and *Pithecophaga jefferyi*, until Lerner and Mindell (2005) showed that *Pithecophaga* was genetically more similar to the Circaetinae and had to be excluded to create monophyly in the Harpiinae without forcing additional parsimony steps. Similarly, the molecular phylogeny revealed that two taxa proposed to be harpiine eagles by Brown (1970), *Harpyhaliaetus solitarius* and *H. coronatus*, fell firmly within the Buteoninae instead (Lerner and Mindell 2005). Both findings were later corroborated by the phylogenetic results of Nagy and Tökölyi (2014). The subfamily is thought to have a Neotropical to Afrotropical ancestral distribution and origin (Nagy and Tökölyi 2014).

Interestingly, the bat hawk *Macheiramphus alcinus* came out as closely related to the harpiine eagles in the phylogenies of both Griffiths et al. (2007) and Nagy and Tökölyi (2014), although Griffiths et al. incorrectly referred to it as *M. anderssoni*; *M. alcinus anderssoni* is one of three subspecies recognised in the species (Dickinson and Remsen 2013). Lerner and Mindell (2005) did not sample *M. alcinus*, and so could not comment on its affinities. However, it had previously been assumed to be related to the elanine kites by Peters (1931), while Brown and Amadon (1968) noted it bore the most similarities to *Aviceda* in the pernine kites.

*Macheiramphus alcinus* represents a significant departure from other harpiines in size and ecology. It is a medium-sized pursuit hunter that preys primarily on bats, swallows, and swifts, and occurs in Africa, South Asia and New Guinea, wherein each population has been assigned a subspecies status. The only other harpiine eagle that occurs within that range is *Harpyopsis*, which is restricted to New Guinea, while *Harpia* and *Morphnus* are endemic to Central and South America. Given its position in the Harpiinae in both phylogenies where it was included (Griffiths et al. 2007; Nagy and Tökölyi 2014), it is possible *Macheiramphus* is the most basal member of the group.

### **Booted eagles (Aquilinae)**

The Aquilinae are a subfamily comprised of the genera *Aquila* (11 species), *Hieraaetus* (5), *Spizaetus* (4), *Nisaetus* (8), *Clanga* (3), and the monotypic *Ictinaetus*, *Stephanoaetus*, *Lophaetus*, *Lophotriorchis* and *Polemaetus* (see Amadon 1982; Dickinson and Remsen 2013). Distribution of this subfamily is widespread, with all continents except Antarctica inhabited (Dickinson and Remsen 2013), and their ancestral distribution is similarly broad, thought to encompass the Neotropics, Afrotropics, and Indomalayan region (Nagy and Tökölyi 2014). Their common name of 'booted eagles' refers to the fact that all species in this subfamily have feathered tarsi rather than the scaled tarsi seen in most other accipitrids. This subfamily has a history of poorly resolved relationships, particularly between the genera *Aquila* and *Hieraaetus*. This is largely due to what appears to be a very close relationship between the extant genera, to the point where many species have been reassigned multiple times over the past years.

The true extent of this degree of non-monophyly at the generic level can be observed in many studies of these genera; *Aquila* and *Hieraaetus* were found to be extensively paraphyletic in most phylogenetic reconstructions, forming clades where members from each genus grouped more closely to members of the other genus than to congeneric species (Helbig et al. 2005; Lerner et al. 2017). This has led to debate over whether one genus should be merged with the other, or certain species reassigned to better separate the genera. Clark (2012) argued for the latter, and claimed to show that after having *H. kienerii* reassigned to *Lophotriorchis* (Helbig et al. 2005; Lerner and Mindell 2005), the three spotted eagles into a new genus called *Clanga* (Wells and Inskipp 2012; Gregory and Dickinson 2012), the species *H. fasciatus* and *spilogaster* to *Aquila* (Helbig et al. 2005; Lerner and Mindell 2005), and by applying a set of morphological characters that Clark devised, it is possible to retain both *Hieraaetus* and *Aquila* while resolving both families into monophyletic clades. This was somewhat supported by Lerner et al. (2017), as their study found that while a few species of *Hieraaetus* should be reassigned to *Aquila*, the remaining species could be distinguished from those in *Aquila* by osteology, plumage and vocalisations, although it was noted further study would be needed to validate this.

While not as problematic, other lineages in the Aquilinae have also historically exhibited unresolved relationships with each other. However, most of these are now resolved. At the very least, it is known that Aquilinae is monophyletic, even if the genera within it are not (Jiang et al. 2015).

The genus *Spizaetus* was found to be divided into two clades, one comprising of the Asian species and the other of the American and African species (Lerner and Mindell 2005; Haring et al. 2007), which had been noted to differ slightly as far back as Brown and

Amadon (1968). This led to the Asian clade being assigned to a separate genus called *Nisaetus* (Gamauf et al. 2005; Haring et al. 2007). In the same study, *Oraetus isidori* was reassigned to *Spizaetus*, *Spizaetus africanus* (formerly *Cassinaetus*) to *Aquila*, and *Hieraaetus kienerii* to *Lophotriorchis* (Haring et al. 2007). The genera *Spizastur* and *Oraetus* were also later fully merged with *Spizaetus*, and *Cassinaetus/Spizaetus africanus* confirmed to form a clade with *Aquila* by Lerner et al. (2017).

### **Sea/Fish eagles (*Haliaeetinae*)**

The Haliaeetinae subfamily is widely accepted to be comprised of two genera, *Haliaeetus* (8 species) and *Ichthyophaga* (2), which are generally large fish specialists. More recent analyses have also supported the inclusion of species in the genera *Milvus* (2) and *Haliastur* (2) in this subfamily (Griffiths et al. 2007; Nagy and Tökölyi 2014), when in earlier works these genera were often regarded as comprising a separate subfamily called Milvinae (Lerner and Mindell 2005). *Ichthyophaga* occurs throughout South Asia and the Indonesian archipelago, *Haliaeetus* is present in North and Central America, Europe, Asia, Africa, the Indonesian archipelago, and Australia, *Milvus* on all continents except Antarctica and South and Central America, and *Haliastur* across South Asia, the Indonesian archipelago and Australia (Dickinson and Remsen 2013). Their ancestral range has been suggested to be Australasian (Nagy and Tökölyi 2014). Of particular note for this subfamily, is the fusion in the first and second phalanges of the second digit (Olson 1982; Holdaway 1994).

The most widespread species of *Milvus*, *M. migrans*, occurs across Europe, Africa, Asia and Australasia, and has around seven subspecies that vary in their genetic closeness to each other (Scheider et al. 2004). Its range overlaps with *M. milvus*, and the two are known to interbreed in mixed populations (Schreiber et al. 2000). A third species, *M. aegyptius*, has been proposed at times, but is now largely accepted to be a subspecies of *M. migrans* (e.g., Dickinson and Remsen 2013).

While the Haliaeetinae have been shown to be monophyletic, Lerner and Mindell's (2005) phylogenetic tree revealed that the genus *Haliaeetus* was not, as when *Ichthyophaga* was included it placed directly between two groups of *Haliaeetus*. The same was found by Nagy and Tökölyi (2014), which showed two groups of *Haliaeetus* with *Ichthyophaga* clustered within one group. These results, along with more recent literature, have led to the suggestion that *Ichthyophaga* should be merged into *Haliaeetus* (Lerner and Mindell 2005; Mindell et al. 2018).

### **Buzzards and true hawks (*Buteoninae* and *Accipitrinae*)**

The Buteoninae and Accipitrinae lineages are reasonably closely related in most phylogenies (see Griffiths et al. 2007; Nagy and Tökölyi 2014; Mindell et al. 2018), although

their exact affinities can be difficult to resolve. The Buteoninae is quite diverse with *Buteo* (26 sp.), and 15 other genera (*Parabuteo* (2 sp.), *Leucopternis* (3), *Geranoaetus* (3), *Buteogallus* (9), *Harpyhaliaetus*, *Busarellus*, *Rostrhamus*, *Cryptoleucopteryx*, *Geranospiza*, *Helicolestes*, *Rupornis*, *Butastur* (4), *Morphnarchus*, *Pseudastur* (3) and *Ictinia* (2)). It is typically closely related to the Haliaeetinae as its sister lineage (Lerner and Mindell 2005; Griffiths et al. 2007; Nagy and Tökölyi 2014). They are spread across the Americas, Europe, Africa and South Asia (Dickinson and Remsen 2013) and are believed to have an Afrotropical and Neotropical ancestral range and origin (Nagy and Tökölyi 2014). The Accipitrinae are similarly diverse, dominated by the genus *Accipiter* (46 sp.) while also including *Kaupifalco*, *Melierax* (3), *Micronisus*, *Circus* (14), *Erythrotriorchis* (2), *Megatriorchis* and *Urotriorchis*. *Circus* and *Accipiter* are both globally distributed, while *Kaupifalco*, *Melierax*, *Urotriorchis*, and *Micronisus* are restricted to Africa, *Megatriorchis* to New Guinea, and *Erythrotriorchis* to New Guinea and Australia (Dickinson and Remsen 2013). The subfamily is thought to be Afrotropical in origin (Nagy and Tökölyi 2014).

The genera *Buteo* and *Accipiter* are commonly found to be polyphyletic; Lerner et al. (2008) found that groups of *Buteo* formed clades that either grouped with or were separated by other Buteonine genera such as *Leucopternis* and *Parabuteo*, while Riesing et al. (2003) found similar results and that at least two species of *Buteo* did not group with other members of the genus. In the case of *Accipiter*, Oatley et al. (2015) found that the species *A. superciliosus* and *A. trivirgatus* did not fall within the main clade. A phylogenetic analysis using the DNA barcodes via the COI gene of 25 species of African and European *Accipiter* found strong support for three of the eight recognised superspecies and was able to identify 19 species distinctly from the rest (Breman et al. 2013). Further phylogenetic study has supported suggestions that certain species of *Accipiter*, namely *A. trivirgatus*, *A. griseiceps* and the lineage comprising *A. collaris* and *A. superciliosus*, fall outside of the *Accipiter* clade and are candidates for generic revision (Breman et al. 2013; Mindell et al. 2018). To this day, the boundaries between species, subspecies and populations are still being resolved genetically and morphologically (see Millsap et al. 2011; Etherington and Mobley 2016).

These two genera are both highly derived and highly speciose lineages (*Accipiter* in particular), which are noted for the number of species complexes they contain. In the case of *Buteo*, this has been attributed to the effects of range contractions and expansions related to Pleistocene climate oscillations and geographic barriers, which have created fluctuations in genetic connectivity and dispersal throughout time (Cade 1955; Riesing et al. 2003). For *Accipiter*, it has been proposed that some of the diversity is related to the long-distance migrations that certain *Accipiter* species make, which has resulted in new sedentary species arising from off-course migrants in a phenomenon described as 'migration dosing

speciation'. Some *Buteo* species have also possibly arisen through these circumstances (Bildstein 2004). Other Buteonine genera, such as *Leucopternis* and *Buteogallus*, also exhibit notable polyphyly (Amaral et al. 2006), which is likely a result of similar biogeographical factors as those affecting *Buteo* in the Neotropics.

*Buteo* as a whole appears to have a Neotropical origin (Amaral et al. 2009) and is apparently monophyletic (de Oliveira et al. 2013), while the Nearctic species seem to have arisen as a result of a colonisation event in South America 7.7–3.3 Ma (Amaral et al. 2009). The Palearctic species of *Buteo* (Europe) can be divided into West and East taxa subgroups, the latter of which is well differentiated genetically while the former is more differentiated morphologically (Kruckenhauser et al. 2004). *Accipiter*, comparatively, seems to have originated from the Afrotropics (Nagy and Tökölyi 2014).

The genus *Harpagus*, in which species are noted for the distinct notch on each side of the upper mandible resembling a tooth, comprises one species *H. bidentatus* inhabiting South America, and *H. diodon*, in Africa (Dickinson and Remsen 2013). It was originally assigned to the Milvinae, although noted to be positioned close to the Accipitrinae (Peters 1931). Miller (1937) also noted the similarities of *Harpagus* to *Accipiter* in his comparative study of the skeleton of *Harpagus*. Initially, molecular data seemed to confirm the placement of the genus in Milvinae (Lerner and Mindell 2005), but later works brought that into question. Griffiths et al. (2007) found that *Harpagus*, along with *Melierax* and *Kaupifalco*, each formed an isolated lineage sister to Accipitrinae, not forming a distinct clade with any other genera. Nagy and Tökölyi (2014) revised the relationship yet again, placing them as sister to the Buteoninae and Haliaeetinae subfamilies and giving them subfamily status as the Harpaginae. Mindell et al. (2018) placed *Harpagus* among a group of genera they classed as 'transitory Accipitrinae', stating that resolving exact subfamilial status would be dependent on having a mostly complete sampling of *Accipiter*. Until further molecular work is done, the exact affinities of *Harpagus* remain unresolved.

### 1.3 Fossil Record

The global fossil record of birds is one that has been extensively documented and reviewed most notably by Lambrecht (1933), Brodkorb (1964), and Olson (1985). Mayr (2009) provided a comprehensive summary of the avian fossil record for the Paleogene (Paleocene to Oligocene) and saw the rise of the modern bird families, with the Accipitridae and their relatives being no exception. The fossil record of these related non-accipitrid lineages is summarised below, along with all known fossil accipitrids.

### 1.3.1 Cathartidae and Teratornithidae

The Cathartidae (New World Vultures) have a relatively rich fossil record (see Cracraft and Vickers-Rich 1972), as do their sister lineage, the extinct Teratornithidae (Teratorns). While the extant Cathartidae have a strictly New World distribution (South America, North America), the species *Diatropornis ellioti* (Milne-Edwards, 1892) and *Parasarcoramphus milneedwardsi* Mourer-Chauviré, 2002 from the middle Eocene to late Oligocene Quercy fissure fillings in France have been attributed to this family (Mourer-Chauviré 2002). However, Mayr (2009) noted that the limited, disassociated material used to describe these species was only compared to members of Cathartidae, and there is a possibility that these fossils instead represent members of the stem group that forms the Cathartidae-Teratornithidae clade.

The late Eocene species *Phasmagyps patritus* Wetmore, 1927 from Colorado, North America, is thought to represent the oldest true cathartid, although some doubts have been raised about this (see Olson 1985). *Brasilogyps faustoi* Alvarenga, 1985, from late Oligocene to early Miocene deposits in Brazil, has much more certain affinities. The first known member of the condor lineage that makes up modern cathartids, *Hadrogyps aigialeus* Emslie, 1988a, occurred in middle Miocene deposits in California. The other known taxa, *Perugyps diazi* Stucchi and Emslie, 2005, and *Kuntur cardenasi* Stucchi et al., 2015, are found in late Miocene deposits in Peru, which suggests that the modern condors originated in North America and then dispersed south (Emslie 1988b; Stucchi and Emslie 2005; Stucchi et al. 2015). Two fossil condors have been recorded from Pliocene deposits of Argentina (Tambussi and Noriega 1996): *Vultur gryphus* Linnaeus, 1758 and *Dryornis pampeanus* Tonni and Noriega, 1998. From this point in time on, the South American Cathartidae rapidly diversified and produced a rich Pleistocene fauna, including *Pampagyps imperator* Agnolin et al., 2017 and *Gymnogyps howardae* Tambussi and Noriega, 1999 from late Pleistocene deposits in Argentina, *Geronogyps reliquus* Campbell, 1979 from Pleistocene tar pits in Peru, and *Pleistovultur nevesi* Alvarenga et al., 2008 from late Pleistocene Brazil. The North American cathartid fauna underwent a similar degree of diversification from the Pliocene onwards, with *Aizenogyps toomeyae* Emslie, 1998 known from the Pliocene of Florida, and at least several Pleistocene species known from sites such as Rancho La Brea (see Jefferson 1991).

The Teratornithidae, in comparison, seem to have originated in South America (Campbell and Tonni 1980; Emslie 1988b), with the oldest fossil taxon *Taubatornis* known from late Oligocene/early Miocene deposits in Brazil (Olson and Alvarenga 2002). Late Miocene deposits have revealed species such as *Argentavis magnificens* Campbell and Tonni, 1980 which is believed to have been one of the largest volant birds to have ever

existed (Campbell and Tonni 1983). The Teratornithidae did not reach North America until the Pliocene, but thereafter diversified and multiple species are known from the Pleistocene Rancho la Brea tar pits, California (see Brodkorb 1964; Mayr 2017), before becoming extinct by the end of the Pleistocene.

### 1.3.2 Sagittariidae

The sagittariid fossil record is remarkably poor, with only two genera currently described. Two species have been assigned to the late Oligocene to early Miocene genus *Pelargopappus* Stejneger, 1885 from France; *P. magnus* Milne-Edwards, 1867–71 and *P. schlosseri* Gaillard, 1908 (see Mourer-Chauviré and Cheneval 1983). A single early Miocene species has been assigned to a genus known as *Amanuensis* Mourer-Chauviré, 2003 from Namibia, Africa. At this stage, the relationships between the fossil genera and the extant *Sagittarius* have not been established (Mayr 2017), and the evolutionary history of this family remains unclear. However, based on molecular data it is likely that the family is older than the limited fossil record suggests, as all divergence dates estimated by molecular phylogenies suggest a split between Sagittariidae and Accipitridae + Pandionidae at least 40 Ma during the Eocene, probably earlier (see Nagy and Tökölyi 2014; Mindell et al. 2018). Until further fossils are discovered and described, this cannot be assessed.

### 1.3.3 Pandionidae

While multiple fossil specimens from the Eocene to Oligocene have been assigned to Pandionidae (Harrison and Walker 1976; Olson and Rasmussen 2001; Mayr 2006a), few have resulted in the description of distinct species. This is presumably due to the material being isolated bones such as pedal phalanges and fragmentary tarsometatarsi, which have limited diagnostic power.

Until recently, the oldest described fossil species of Pandionidae was the mid-Miocene *Pandion homalopteron* Warter, 1976 which occurred in California, with another American species *Pandion lovensis* Becker, 1985 that occurred in late Miocene deposits in Florida. A new publication on the fossils of diurnal birds of prey in the Carpathian or Pannonian Basin in central Europe (see Kessler 2018) described a late Oligocene osprey from Hungary, *Pandion pannonicus* Kessler, 2018.

Given the highly specialised nature of the single extant species *Pandion haliaetus*, there is a possibility that most character traits in early species of *Pandion* were plesiomorphic for all Accipitriformes. Therefore, other fossil specimens from early Oligocene or late Eocene deposits could in fact be unrecognised members of Pandionidae that did not survive past this period.

### 1.3.4 Accipitrid-like Fossil Lineages

While the exact time of origin for the Accipitridae is still unknown, the fact that there are undescribed fossil specimens identified/attributed to Pandionidae dating from the late Eocene (Harrison and Walker 1976) and the early Oligocene (Mayr 2006a) reveals that Accipitridae must have been present by this time, as the Pandionidae are sister to Accipitridae. Birds resembling accipitriforms occur in the European fossil record as early as the middle Eocene, but their exact affinities can be difficult to place due to the fragmentary nature of many fossils of this age (Mayr 2017). This is further confounded by the presence of extinct bird lineages that bear a notable resemblance to accipitrids and which lived at the same time.

One such lineage is represented by a bird fossil found from the middle Eocene Messel Lake Deposits in Germany named *Messelastur gratulator* Peters, 1994. It was described as a member of Accipitridae based on morphological characters of the skull. However, the discovery of a complete skeleton resulted in this species being placed within its own family, Messelasturidae (Mayr 2005), and it was eventually determined to be a member of the stem lineage of Psittaciformes upon the discovery of a specimen with well-preserved feet (Mayr 2011).

Another raptor-like lineage is Horusornithidae, found in Upper Eocene deposits in the La Bouffie locality of Quercy, France (Mourer-Chauviré 2006). Currently restricted to a single species, *Horusornis vianeyliaudae* Mourer-Chauviré, 1991, this family exhibits several traits in common with the Accipitridae such as a derived morphology of the hypotarsus and the pedal claws (Mayr and Clarke 2003) as well as a modified os metacarpale major of the carpometacarpus (Mourer-Chauviré 1991). Unlike the accipitrids, *H. vianeyliaudae* exhibits morphology in the tibiotarsus and tarsometatarsus which would have allowed considerably more flexion in the hind limb, which has been speculated to be related to its feeding habit (Mourer-Chauviré 1991).

Also from the middle Eocene Messel Lake is another raptorial bird, named *Masillaraptor parvunguis* Mayr, 2006. *Masillaraptor* was identified by Mayr as a 'falconiform', as it possesses the shortened middle phalanges of the fourth toe and first phalanx of the second toe seen in the Accipitridae and Falconidae but refrained from associating it with any families due to the largely unresolved relationships between them at the time (Mayr 2006b).

In his overview of avian evolution, Mayr (2017) noted that reliably identified fossils of the more derived subfamilies of Accipitridae (Aquilinae, Accipitrinae and Buteoninae) first appear in the early Miocene and hypothesised that the environmental conditions of the time that favoured open grassland and allowed the rise of the mammalian megafauna likely also resulted in the diversification of accipitrids. Certainly, these conditions would have resulted in

the diversification of the vulture clades; numerous fossils of this group have been found across Europe, Asia and America ranging between the early Miocene to late Pleistocene (see below). The fossil vulture taxa no doubt scavenged off the carcasses of the many large mammals that grazed across the land.

### 1.3.5 Accipitridae of Europe

Some of the oldest known true accipitrids have been found in European fossil deposits, although the remains are often isolated or fragmentary. *Milvodes kempi* Harrison and Walker, 1979, dated to the late Eocene of Britain and known from a distal tarsometatarsus, was accepted as a true accipitrid by Mayr (2009), although he was more cautious of assigning it to the family in later works (Mayr 2017). Of a similar age are *Aquilavus corroyi* (Gaillard, 1939) and *Aquilavus hypogaeus* (Milne-Edwards, 1892), found in the early Oligocene fissure fillings in Quercy, France (Mourer-Chauvire 2006), although it has been debated if there is enough evidence to support erecting two species or even placing them in the same genus given the lack of material (Mayr 2009, 2017).

One of the oldest confirmed accipitrids from Europe is the early Oligocene (30–31 Ma) *Aviraptor longicrus* Mayr and Hurum, 2020, which is known from Poland. Despite its age, it strongly resembles species of the extant genus *Accipiter*, and likely had a similar ecology as an avivore (specialist predator of birds).

From the late Oligocene/early Miocene of France, *Palaeohierax gervaisii* (Milne-Edwards, 1863), was considered the oldest representative of gypaetine vultures in Europe by some (Brodkorb 1964), but others have questioned if it can be referred to any extant accipitrid taxon (Mayr 2009). The similar-aged *Palaeocircus cuvieri* Milne-Edwards, 1871, is considered by most to be an accipitrid, but others have argued for its inclusion into Pandionidae (Brunet 1970).

Early Miocene deposits in France reveal the species *Promilio incertus* (Gaillard, 1939; see Brodkorb 1964), *Aquilavus priscus* (Milne-Edwards, 1863; see Lambrecht, 1933), and *Aquilavus depredator* (Milne-Edwards, 1871; see Lambrecht, 1933). Similarly, the middle Miocene species *Aquila pennatoides* Gaillard, 1939, *Aquila delphinensis* Gaillard, 1939 and *Hieraaetus edwardsi* (Sharpe, 1899) occurred in France as well, and likely replaced or were descended from the early Miocene species mentioned above. Another fossil bird of this age, *Aquilavus bilinicus* (Laube, 1909) which was originally proposed to be a species of *Cygnus*, was once assigned to the Accipitridae (Brodkorb 1964) but is now regarded as a species of stork (see Mlíkovský and Švec 1989).

The late Miocene has *Circaetus rhodopensis* Boev, 2012 and *Buteo spassovi* Boev and Korachev, 1998 from Bulgaria, as well as *Milvus deperditus* Milne-Edwards, 1871, and

*Haliaeetus piscator* Milne-Edwards, 1871, which inhabited France. In Ukraine, a further two species were described as *Buteo praebuteo* Sobolev, 2011 and *Buteo sarmathicus* Sobolev, 2011.

The Pliocene deposits of Europe reveal greater geographical spread of fossil species. Two species are known from Italy, *Garganoaetus freudenthali* Ballmann, 1973 and *Garganoaetus murivorus* Ballmann, 1973. *Aegyptius turgarinovi* Manegold and Zelenkov, 2015 is from Moldovak, and *Gyps bochenskii* Boev, 2014 and *Aquila kurochkini* Boev, 2013 are from Bulgaria. *Aegyptius turgarinovi* also holds the distinction of being the oldest representative of the Aegypiinae in Europe (Manegold and Zelenkov 2014).

The Pleistocene has a similar distribution of species, although across different sites and countries. *Aquila nipaloides* Louchart et al., 2005 has been found in deposits located in Corsica and Sardinia (Italy) and is believed to be an extinct relative of the extant Steppe Eagle *Aquila nipalensis*. *Gyps melitensis* Lydekker, 1890 is a vulture deriving from deposits on the islands of Malta and Crete, and some sites on mainland Europe. Another vulture, *Aegyptius prepyrenaicus* Hernández, 2001, was described from late Pleistocene cave deposits in northeast Spain, but due to a lack of any other material from outside the type locality and distinguishing morphological features, others consider it nomen dubium and likely a synonym of *Gyps melitensis* (e.g., Sánchez Marco 2007). A third vulture, *Gypaetus osseticus* Burchak-Abramovich, 1971, is known from localities in Russia, and was incorrectly listed under the name *Gypaetus asiaticus* by Kessler (2018).

From Bulgaria, a Serpent Eagle *Circaetus haemusensis* Boev, 2015 provides evidence of the Circaetinae having a continuous presence in Europe from the Miocene to the present. The remaining described Pleistocene species from this point of time are *Buthierax pouliani* Kretzoi, 1977 from Greece, which was later synonymised with another middle Pleistocene fossil subspecies *Buteo rufinus jansoni* Mourer-Chauviré, 1975 by Louchart et al. (2005), *Milvus brachypterus* Jánossy, 1977 from Hungary, and *Aquila fossilis* Giebel, 1847 from Sardinia, Italy. *Haliaeetus angustipes* (Jánossy, 1983) was thought to be an extinct early Pleistocene species from the Czech Republic but was later determined to be synonymous with the extant *H. albicilla* (see Mlíkovský 1997).

### **1.3.6 Accipitridae of Asia**

The Neogene fossil record of birds in Asia is currently poorly understood, mostly as a result of lack of investigation rather than any real lack of deposits (Zelenkov 2016). As a result, relatively few fossil accipitrids are known from this region of the world. Some of those known, however, are spectacularly preserved.

The Oligocene reveals three putative accipitrids: *Buteo circooides* Kurochkin, 1968, *Venerator (Tutor) dementjevi* (Kurochkin, 1968), and *Gobihierax edax* Kurochkin, 1968, from middle Oligocene deposits in Mongolia. This was later reduced to two, as *Gobihierax* was determined to be a galliform by Zelenkov and Kurochkin (2015). Early Oligocene specimens of large femora resembling Aegypiinae from Mongolia and an undescribed species speculated to be of the genus *Aquilavus* from late Oligocene *Indricotherium* Beds in Kazakhstan (Kurochkin 1976) were also noted.

China, during the Miocene and Pleistocene, was dominated by a very different environment than today, with many megafaunal mammals roaming open grassland and woodland, resulting in a great diversity of accipitrid vultures. The first of these to be described was *Mioaegyptus gui* Hou, 1984, which was found in the eastern province of Jiangsu, although its actual affinities with Accipitridae are considered questionable, and it may in fact be more primitive than any member of Accipitridae (Hou 1984; Rich et al. 1986; Manegold et al. 2014; Zelenkov 2016). Also from an eastern province, and of a similar age, is *Qiluornis taishanensis* Hou et al., 2000 from Shandong, which appears to be a member of the stem lineage of Aegypiinae (Manegold et al. 2014; Zelenkov 2016). Late Miocene age deposits in Gansu Province of northwest China yielded a remarkably complete specimen of another species of vulture, which was named *Gansugyps linxiaensis* Zhang et al., 2010. Another almost complete skeleton of a gypaetine vulture, *Mioneophron longirostris* Li et al., 2016, was also found in Gansu Province in deposits of the same age and represents the oldest known species of Gypaetinae in the Old World.

Pliocene deposits in Asia have so far revealed few avian fossils, with fossil sites dating to this age rare outside of Mongolia (Zelenkov 2016). Nevertheless, there are representatives of several lineages known from this time period; an undescribed accipitrid which bears resemblance to a gypaetine vulture has been identified in the early Pliocene Chono-Harayah locality of west Mongolia, based on a proximal phalanx of digit III (Zelenkov 2013), as well as *Haliaeetus fortis* Kurochkin, 1985, which has been found in both late Miocene and early Pliocene localities in the same region (Zelenkov 2013). Some species have yet to be named, including another species of *Haliaeetus* which has been found in the Tologoi locality in Transbaikalia (Kurochkin 1985) and a species of *Buteo* from the Ulugkhem locality of Tuva (Panteleyev et al. 2006), both of which are late Pliocene in age (Zelenkov 2016).

For the Pleistocene, there are at least four known Asian fossil accipitrids, three of them aegypiine vultures. Two taxa, *Aegyptus jinniushanensis* Zhang et al., 2012 and an unnamed species of *Torgos*, were recovered from middle Pleistocene deposits in Liaoning Province in China's northeast (Zhang et al., 2012a). While their morphology suggests that

they fed on similar parts of a carcass, it is likely that competition was reduced by the two species having different ecological preferences (Zhang et al. 2012a). A buteonine hawk, *Buteo sanya* Hou, 1998, has been found from deposits in Luobidang Cave. From South-east Asia, a fossil aegyptiine vulture belonging to the genus *Trigonoceps* has been found from Liang Bua Cave on Flores (Meijer et al. 2013), and a second has been noted from deposits on Java, although it is unknown if it represents an extinct novel species or an extant one (Wetmore 1940).

### 1.3.7 Accipitridae of Africa

Currently, the fossil avifauna of Africa is poorly described and there are few named and described accipitrid fossil species known from this region. A distal tarsometatarsus has been identified as a large accipitrid from the late Eocene Jebel Qatrani Formation in Egypt but has yet to be described beyond bearing a resemblance to the extant genus *Haliaeetus* (Rasmussen et al. 1987; Mayr 2009).

A possible accipitrid fossil consisting of a fragmented tarsometatarsus and pedal phalanx has been found in the late Miocene Middle Awash deposits in Ethiopia but cannot be reliably identified (Louchart et al. 2008). A further three accipitrid species have been identified from Miocene sites across Kenya and appear to be species in the extant genera of *Aegyptius*, *Accipiter* and *Melierax* (Walker and Dyke 2006). These fossil species appear to be very similar to certain extant species in the same genera, and it has been proposed that they could be informative regarding palaeoenvironmental conditions across Miocene Kenya.

The Pliocene has revealed few fossil species, with currently one vulture known as *Aegyptius varswaterensis* Manegold, Pavia and Haarhoff, 2014. From Holocene deposits in Madagascar, *Stephanoaetus mahery* Goodman, 1994a and up to two undescribed possible species of *Aquila* from Madagascar (Goodman 1994b; Goodman and Rakotozafy 1995) are known. In the case of the latter, it is currently uncertain if these species represent extinct endemics or locally extinct extant migrants from mainland Africa.

Ifri n'Ammar, Morocco has Pleistocene fossil material that reveals the extant vulture species *Aegyptius monachus* and *Gyps fulvus* once inhabited this region (Manegold and Hutterer 2021). Modern residential populations of *A. monachus* are restricted to Europe and Asia, while *G. fulvus* no longer seems to occur commonly in Morocco but is known from a few regions of North Africa. A third species was also identified by Manegold and Hutterer (2021), which was deemed to likely represent *Gyps melitensis*, although it could also be *Aegyptius prepyrenaicus*.

### 1.3.8 Accipitridae of the Americas

Like Europe, the avian fossil record of North America is very diverse in its accipitrid fauna. Most notable is the presence of Old World vultures in Gypaetinae, revealing that this clade was once far more widespread than it is today. South America, in contrast, shows much less diversity, with only a handful of accipitrids known from Cenozoic deposits, and some of these are disputed as Accipitridae.

One of the oldest confirmed accipitrids both globally and in the ‘New World’, is *Palaeoplancus dammanni* Mayr and Perner, 2020, known from the late Eocene deposits in Wyoming. This species is known from a nearly complete tarsometatarsus, the morphology of which indicates it engaged in a currently unidentified specific type of foraging behaviour or was specialised to a certain prey type.

Deriving from early Oligocene deposits, three species of “*Buteo*” have been described: *B. grangeri* Wetmore and Case, 1934, *B. fluviaticus* Miller and Sibley, 1942, and *B. antecursor* Wetmore, 1933. While the assignment to genus was based on morphological similarity, it has been remarked that this may simply be a result of plesiomorphy within the family (Mayr 2009), which would render any genus level assignment tentative at best. Furthermore, these species have been described based off isolated elements, and it has been admitted that *B. grangeri* and *B. fluviaticus* may be a single species instead (Miller and Sibley 1942). Another species has also been described from early to mid-Oligocene deposits in Wyoming, *Palaeoplancus sternbergi* Wetmore, 1933, which exhibits morphological similarities to modern accipitrids but appears to fall outside the crown group Accipitridae based on certain plesiomorphic features. This species was also identified from early Miocene deposits of South Dakota (Ducey, 1992).

The late Oligocene accipitrid fauna in North America is represented by the species *Buteo ales* (Wetmore, 1926) see Miller and Sibley (1942). Fossils, possibly of *B. ales*, have also been found in deposits dated to the early Miocene (Wetmore 1926). Only two Oligocene fossils are described from South America, both endemic to the region: *Cruschedula revola* Ameghino, 1899 and *Climacarthrus incompletus* Ameghino, 1899. Their status as true members of Accipitridae are regarded as dubious at best (Mayr 2009), although some argue that they are valid accipitrid genera (Agnolin 2006).

The Miocene of the Americas has a very rich accipitrid avifauna, possibly the richest globally for this time. While most of this diversity is concentrated in North America, isolated toe and skull elements of unidentified accipitrids in Panama and Patagonia hint at an unrecognised diversity in South America (Picasso et al. 2009; Steadman and MacFadden 2016). No named accipitrid species are known from South America; the two middle Miocene species from Argentina, *Thegornis musculosus* Ameghino, 1895 and *Thegornis debilis*

Ameghino, 1895 previously assigned to the Accipitridae (see Brodkorb 1964; Agnolin 2006), have now been reassigned to Falconidae (Noriega et al. 2011), confirming their original attribution.

Old World vultures in Gypaetinae first occur in the American fossil record during the Miocene, with numerous species described so far. *Neophrontops vetustus* Wetmore, 1943, *Palaeoborus howardae* Wetmore, 1936, and *Anchigyps voorhiesi* Zhang, Feduccia and James, 2012 all derive from sites in Nebraska (Zhang et al. 2012b). *Anchigyps* is particularly notable as it suggests the divergence of gypaetine vultures occurred during or just before the Miocene (Zhang et al. 2012b). An additional four species of gypaetine vultures have been described based on single bones or partial skeletons from other locations in America: *Arikarornis macdonaldi* Howard, 1966 and *Palaeoborus rosatus* A. H. Miller and Compton, 1939 from South Dakota, *Neophrontops americanus* L. H. Miller, 1916 from Wyoming (which appears to have persisted into the Pleistocene), and *Neophrontops ricardoensis* Rich, 1980 from California, along with an undescribed *Neophrontops* from Arizona (Bickart 1990).

Numerous non-vulturine accipitrid genera also existed during the Miocene. Nebraska, again, seems to have been a hotspot for diversity and has yielded *Palaeastur atavus* Wetmore, 1943, *Apatosagittarius terrenus* Feduccia and Voorhies, 1989, and *Promilio efferus* (Wetmore, 1923; see Wetmore 1958). *Apatosagittarius terrenus* is one of the more unusual species uncovered, as it converged with the extant secretary-bird *Sagittarius serpentarius* in morphology, suggesting it had a similar ecology. Florida also has yielded several species, albeit with less diversity: *Promilio floridanus* (Brodkorb, 1956), *P. epileus* Wetmore, 1958, and *P. brodkorbi* Wetmore, 1958. *Miohierax stocki* Howard, 1944 occurred in California, and is represented by a distal tarsometatarsus and several phalanges which indicate a buteonine relationship.

Several extant genera also appear in Miocene deposits in Nebraska, although all the contained species are extinct. So far these include *Buteo conterminus* (Wetmore, 1923) see Brodkorb (1964), *Buteo typhoius* Wetmore, 1923, *Buteo contortus* (Wetmore, 1923) see Brodkorb (1964), *Spizaetus schultzi* Martin, 1975, and *Buteogallus enectus* (Wetmore, 1923). The latter was described as *Urubitinga enecta* Wetmore, 1923, before the generic attribution was changed to *Hypomorphnus* by the 25<sup>th</sup> supplement of the American Ornithologists Union checklist of North American birds (1950), which is now considered to be a synonym of *Buteogallus*.

The Pliocene does not have as diverse a record as the Miocene, but still boasts an impressive range of species. *Amplibuteo concordatus* Emslie and Czaplewski, 1999, and *Aquila bivia* Emslie and Czaplewski, 1999, are recorded from deposits in Florida and

Arizona, *Neophrontops slaughteri* Feduccia, 1974 from Idaho, and *Palaeoborus umbrosus* (Cope, 1874: see Howard 1932), which was originally described as a cathartid, from Rancho La Brea, California. *Neophrontops dakotensis* Compton, 1935 was described from South Dakota, and *Proictinia gilmorei* Shufeldt, 1913 from Kansas, although it is also present in South Dakota in the early Miocene (Ducey 1992). Nebraska boasts two described species, *Buteo dananus* (Marsh, 1871) see Brodkorb (1964), and *Spizaetus tanneri* Martin, 1971.

The Pleistocene is very well represented in North America, with famous fossil deposits such as the tar deposits of Rancho La Brea in California providing valuable specimens from a range of fauna, including accipitrids. From Cuba and the Bahamas are *Buteogallus borraisi* (Arredondo, 1970) see Suárez and Olson (2007), *Titanohierax gloveralleni* Wetmore, 1937 and *Gigantohierax suarezi* Arredondo and Arredondo, 2002. *Amplibuteo woodwardi* L. H. Miller, 1911 is from Florida and California, and has also been found in Cuban cave deposits (Suárez 2004). The sheer size of these fossil species is their most impressive quality, with *B. borraisi* being roughly 30% larger overall than its extant relative *B. urubitinga*, but smaller and less robust compared to *T. gloveralleni*, *G. suarezi* and *A. woodwardi*, which inhabited the same biogeographic region (Suárez and Olson 2007).

Fossil accipitrid bones from the Bahamas were described as *Calohierax quadratus* (Wetmore 1937) but were later determined to be the extant *Buteo lineatus* (see Olson 2000). *Spizaetus pliogryps* Shufeldt, 1892, is the second oldest representative of its genus, following *S. tanneri* as mentioned above, and is so far restricted to Oregon, along with *Buteogallus sodalis* Shufeldt, 1891. Another slightly younger species of the former genus, *Spizaetus willetti* Howard, 1935, has been found in cave deposits from Nevada and New Mexico (Howard 1962).

Two species, *Amplibuteo hibbardi* Campbell, 1979 and *Buteogallus terrestris* Campbell, 1979 were described from Talara Tar Seeps in Peru (see Suárez and Olson 2009), making them the only extinct Pleistocene accipitrid taxa currently known from South America. Two bird species, *Lagopterus minutus* Moreno and Mercerat, 1891 and *Foetopterus ambiguous* Moreno and Mercerat, 1891 from Argentina, were once assigned to the Accipitridae but have since been synonymised with the extant species *Chloephaga picta* for the former (Tonni 1970) and *Polyborus plancus* for the latter (Tonni 1980), which are a goose and a falcon respectively.

*Buteogallus daggetti* (L. H. Miller, 1915) see L. H. Miller (1928) and Olson (2007), *Spizaetus grinelli* (L. H. Miller, 1911) see Wetmore (1956), and *Buteogallus fragilis* (L. H. Miller, 1911) see Brodkorb (1964), have been found in deposits from Rancho La Brea California and northern Mexico. The Old World vultures survived until roughly this point of

time; *Neophrontops vallecitoensis* Howard, 1963 and *Neogyps errans* L. H. Miller, 1916 have been discovered at the site, all of which lived in the region of California.

Known Holocene extinctions include *Circus dossensus* Olson and James, 1991, a currently undescribed species of *Haliaeetus* (Olson and James 1991) from the Hawaiian Islands that has been shown to differ from the extant *H. albicilla* in only three nucleotide base pairs out of 704 (see Fleischer et al. 2000), and *Bermuteo avivorus* Olson, 2008, a buteonine hawk from Bermuda Island.

### 1.3.9 Accipitridae of Australasia

Australasia has a poor pre-Miocene fossil record of accipitrids, and of birds in general (Vickers-Rich 1991). Fossil sites dating from between the late Cretaceous and late Miocene are far less common compared to their Pliocene and Quaternary counterparts, but those present reveal a very different landscape. Oligo-Miocene deposits in Riversleigh, Queensland reveal multiple transitions between open forest and rainforest environments over millions of years, based on faunal changes (Travouillon et al. 2009). In the similarly aged Namba and Etadunna formations in the Lake Frome/Munda – Kati Thanda-Lake Eyre region, South Australia (SA), deposits indicate a forest environment surrounding large, permanent lakes (Alley 1998). This leads to the conclusion that Australia was dominated by closed forests in a warm, wet environment at the time (Dawson and Dawson 2006).

The oldest fossil accipitrids in Australia and New Zealand date back to this late Oligocene to early Miocene environment, although they are few. All described species are known from fragmentary remains, with *Pengana robertbolesi* Boles, 1993 from the Oligo-Miocene Riversleigh Sticky Beak Site ('D-Site Equivalent', = Faunal Zone A deposits) in Queensland described from a distal tibiotarsus (Boles 1993), and *Aquila bullockensis* Gaff and Boles, 2010 from the Mid-Miocene Camfield Beds near Bullock Creek in the Northern Territory, from a distal humerus. The presence of at least two accipitrid species has been confirmed by fossil material from the early-middle Miocene St Bathans Fauna from the Manuherikia Group strata of the Bannockburn Formation Otago, New Zealand, but has yet to be officially named or described in detail (Worthy et al. 2007; Worthy et al. 2014; Worthy et al. 2017). Material that was claimed to be accipitrid but is undescribed, derives from Oligocene deposits at Lake Palankarina, SA (Vickers-Rich 1991; Boles 2006), and late Miocene deposits at Alcoota, Northern Territory (Vickers-Rich 1991). Worthy and Yates (2017) elaborated on the Alcoota accipitrid material, reporting multiple pedal and ungual phalanges and a tarsometatarsus representing a taxon the size of a male *Aquila audax*, and a pedal phalanx from another the size of the extant *Hamirostra melanosternon*.

From the end of the Miocene to the middle to late Pleistocene, Australia underwent a

series of climatic changes that changed the climate to a much more arid state that led to a grassland and open forest dominated landscape, similar to what is seen today (Martin 2006; McGowran and Hill 2015). It is these changes that led to the emergence of mammalian megafauna in Australia; the diprotodontoids, for example, went from the sheep-sized *Neohelos* of Oligo-Miocene Riversleigh to the rhinoceros-sized *Diprotodon* by the end of the Pleistocene, likely due to adaptations to open grassland grazing (Archer and Hand 2006). The vast majority of accipitrid fossils in Australia occur in this palaeoenvironmental context of gradual continuous aridification punctuated by a fluctuating climate.

The first fossil accipitrids to be described from Australia were recorded from deposits in Queensland by Charles de Vis from the 1890s to the early 1900s and are believed to be from Pliocene to Pleistocene in age (see Boles 2006). De Vis described a fossil distal humerus that he believed belonged to an undescribed relative of the Wedge-tailed Eagle (at the time named *Uroaetus audax*), naming it *Uroaetus brachialis* based on its greater size (de Vis 1890). This was revised to the newly erected genus *Taphaetus* upon the discovery of a femur, which showed some differences in morphology from *Uroaetus* and was assumed to be the same species described in the previous paper (de Vis 1891). An additional species, *Necrastur alacer* de Vis, 1892, was later described in a review of Queensland's extinct birds, with de Vis comparing it to the extant genus *Nisaetus* (de Vis 1892). The number of described species was pushed up to four after the turn of the century, with *Asturaetus furcillatus* and *Baza gracilis* described in a review of extinct Australian avifauna, another species being attributed to *Taphaetus* (*Taphaetus lacertosus* de Vis, 1905) and *T. brachialis* being returned to *Uroaetus* once more (de Vis 1905). The final fossil accipitrid to be described, although with great hesitation based on the specimen being a single phalanx, was *Palaeolestes gorei* de Vis, 1911.

Much later, as is common with fossil material collected many decades ago, the classifications of these accipitrids were heavily revised. After Falconidae and Accipitridae were separated, it was determined that *Asturaetus furcillatus* was a falcon, rather than a hawk or eagle, and was eventually revealed to be a specimen of the extant species *Falco berigora* by Rich et al. (1982). Out of the remaining accipitrids, *Baza gracilis* was determined to be a species of extant *Accipiter*, *Palaeolestes* was found to not even be a bird, *Uroaetus brachialis* was agreed to be an accipitrid and the remaining genera, *Necrastur* and *Taphaetus*, required further study (Van Tets and Rich 1990; Boles 2006). The results of any such further study on *Necrastur*, *Uroaetus* and *Taphaetus* have yet to be published, which presents an unfortunate limitation on our understanding of the evolution and fossil history of Australian accipitrids during this time period. Undescribed accipitrid material has also been mentioned to have been found in Chinchilla and Lake Kanunka, SA (Vickers-Rich 1991),

though the Chinchilla specimen was not listed by Louys and Price (2015) for unknown reasons.

Perhaps the most well-known of all Australasian fossil accipitrids is *Hieraaetus moorei* (Haast, 1872), a giant eagle that existed on the South Island of New Zealand until the arrival of humans around 700 years ago. It is presumed to have been driven to extinction due to humans hunting and subsequently exterminating the various species of moa that existed at the time, upon which it preyed. Remarkably complete specimens have been collected from Holocene fossil deposits, and the species is very well described (see Haast 1874; Owen 1879; Holdaway 1991; Worthy and Holdaway 2002). Another large accipitrid, the Eyles' Harrier *Circus teauteensis* Forbes, 1892, which includes the junior synonym *Circus eylesi* Scarlett, 1953, also went extinct around the same time, and is found in fossil deposits of a similar age. For a time, there was also believed to be an extinct sea eagle *Haliaeetus australis* (Harrison and Walker, 1973), see Olson (1984), which was thought to be native to the Chatham Islands (Dawson 1961). This was later revealed to be a specimen of the extant *Haliaeetus leucocephalus* that was accidentally mixed up with subfossil specimens (Worthy and Holdaway 2002).

#### **1.4 Diversity and distribution of modern Australasian accipitrids**

The Australian continent and surrounding islands are home to at least 17 species of resident breeding accipitrids, with a further four species that are occasional vagrants from regions of Asia and South-east Asia. In total, the resident species are distributed across 13 genera, two of which are wholly endemic to Australia, and represent six subfamilies out of the extant ten known globally: Elaninae, Perninae, Aquilinae, Haliaeetinae, Accipitrinae and Buteoninae.

New Zealand, in comparison, has only one living resident breeding species alive today; the accipitrine *Circus approximans*. Vagrant species from Australia include the Black Kite *Milvus migrans* and, very rarely, the White-Bellied Sea Eagle *Haliaeetus leucogaster* (see Gill et al. 2010). *Circus approximans* is itself a recent arrival to New Zealand, as it is absent from the fossil record prior to human inhabitation (Holdaway et al. 2001; Worthy and Holdaway 2002; Gill et al. 2010).

The Australasian region is historically completely lacking in resident species of Circaetinae, Harpiinae, Aegyptiinae and Gypaetinae. However, species of the former two subfamilies are present in the adjacent/nearby Melanesia and Wallacea biogeographic regions (Dickinson and Remsen 2013), and as noted above, the fossil record demonstrates that vultures from Aegyptiinae were also present at least in Wallacea (Meijer et al. 2013).

This raises the question of why these subfamilies would be absent in Australia, given their proximity and the presence of suitable habitat for these species.

## 1.5 Summary and material of interest

As noted above, the Australasian fossil record of Accipitridae is quite paltry; this is to the detriment of our understanding of past environments, as accipitrids tend to be apex predators and as such are an integral component of many terrestrial ecosystems. Different subfamilies tend to have different dietary preferences, so knowing which and how many lineages have been present throughout different times in Australian prehistory could provide valuable information on past ecosystems. However, there are at least several undescribed accipitrid or accipitrid-like fossil species from various epochs that could help clarify on the history of Australian Accipitridae.

A remarkable fossil accipitrid specimen preserving 63 bones of the skeleton (or potential accipitrid) and an isolated distal humerus, potentially from separate taxa, have been found in the late Oligocene Pinpa Local Fauna of the Namba Formation deposits at Lake Pinpa, SA, which have yet to be described. An isolated distal femur of an unknown accipitrid, possibly from the same species as one of the above from Lake Pinpa, is also known from the Ericmas LF, Namba Formation (T. H. Worthy pers comm), and there are additional reported bones from sites such as Palankarina (see Rich et al. 1991; Vickers-Rich 1991). This material is equivalent in age or slightly older than *Pengana robertbolesi*, whose phylogenetic affinities are currently unresolved (Boles 1993), and potential relationships between them have yet to be assessed.

The significance of accipitrid fossil material from the Namba Formation cannot be overstated. As mentioned above, Oligo-Miocene Australia was much wetter and more heavily forested than the Australia of later era (Martin 2006; McGowran and Hill 2015), and this had a profound influence on what fauna was present. The types of Accipitridae that can thrive in such environments are very different from those that favour open woodland and grasslands (for example, *Aviceda subcristata* compared to *Aquila audax*). The age also predicts that few of the crown lineages present today could have been present, limiting the number of lineages to which the fossil could be referred (Nagy and Tökölyi 2014; Mindell et al. 2018). This could mean that the fossil species of this time are members of one of these lineages, or they could be an unknown extinct lineage.

The Pleistocene accipitrid fauna, while more recent, is also poorly understood. While several fossil species are recognised, there has been little work done to determine their phylogenetic relationships to extant accipitrids, or even confirm that their status as distinct

taxa are valid. There has been commentary on the potential relationship of *Taphaetus* to Old World vultures (Rich and van Tets 1982; Baird 1991), but next to nothing has been published to confirm or disprove this intriguing theory.

An undescribed Pleistocene accipitrid is represented by fossils from several cave deposits across Western Australia (WA), South Australia and New South Wales (NSW), being first noted as an unknown species when a pair of several wing bones was collected from Green Waterhole Cave, SA (Baird 1985). While in that paper, it was noted to have been placed under study by several of the authors mentioned above who worked on the de Vis material, no published descriptions or any related papers have been forthcoming to date, though it was addressed in an unpublished thesis by Gaff (2002). It has since been mentioned in passing a handful of times in articles discussing faunal diversity of Australian deposits (see Baird 1991; Vickers-Rich 1991; Reed and Bourne 2000), and material believed to be from the same or a similar species has been uncovered in Leaena's Breath Cave, Nullarbor Plains, WA, Victoria Fossil Cave, Naracoorte, SA, Cooper Creek, SA, and Cathedral Cave, Wellington, NSW (unpubl. Data T. H. Worthy; D. Fusco 2021; Gaff 2002). The most remarkable feature of this fossil material is the large size; while wing bones uncovered so far are roughly equivalent in length to the extant large eagles in Australia, *Aquila audax* and *Haliaeetus leucogaster*, two femora have been found that are significantly larger than their counterparts. As leg bones are often considered indicative of mass, this could suggest a very large eagle was present on mainland Australia, potentially rivalling *Hieraaetus moorei* from neighbouring New Zealand in size.

A second large species is known from Mairs Cave, Flinders Ranges, SA, which was previously reported in Gaff (2002). Currently only known from this single site, the fossil material of the Mairs Cave taxon indicates a species much larger than *Aquila audax*. However, much less material is available, making assessment of its ecology and taxonomy more difficult.

The relevance of these species, in contrast to the Pinpa specimen, is regarding the biodiversity and ecological roles of the recent accipitrid fauna of Australia. Given their age it can be expected that they will be referable to extant subfamilies of Accipitridae, but possibly one that is no longer present in Australia. The ecological implications for large eagles and vultures being present in the Pleistocene are of particular interest, as they would represent a missing element of the modern fauna and demonstrate that the diversity and evolution of Australian accipitrids was much greater and more complex than previously believed.

## 1.6 Thesis aims and objectives

The overarching aim of this thesis is to provide a greater understanding of the evolution of Australian Accipitridae using the selected fossil material mentioned above. To address this aim, the following objectives were devised:

- 1) Taxonomically describe the fossil accipitrids using a wide selection of extant species and close relatives for comparison.
- 2) Using a comprehensive morphological and molecular data matrix, resolve the phylogenetic position of selected fossil Australian accipitrids in relation to the living species.
- 3) Based on their morphology, determine the likely ecology of the fossil species.
- 4) Based on the findings of the above objectives, discuss their implications for the history of accipitrid diversity, ecologies and evolution in Australia.

## 1.7 Thesis structure

Thesis chapters 2, 3 and 4 are written in a format of publications, with Chapter 2 already published. Chapters 3 and 4 will soon be submitted for publication. For this reason, they have standard journal article format of Abstract to Discussion, with multiple authors attributed (based on the planned author list for publication) and individual reference lists. Both Chapter 1 and Chapter 5 have their references located within the Bibliography.

In Chapter 2, the partial skeleton of an accipitrid from the late Oligocene Namba Formation is examined in a phylogenetic context with extant species of Accipitridae. This chapter has been published in *Historical Biology*. References in this chapter are formatted as per the styles of the journal.

In Chapter 3, the lectotype for "*Taphaetus*" *lacertosus* de Vis, 1905 is redescribed and compared to extant accipitrids, and new fossil material is assigned to the taxon. A parsimony phylogenetic analysis was performed to determine its position in Accipitridae, and the implications of the results for the ecology of "*Taphaetus*" discussed.

In Chapter 4, Pleistocene material from widespread sites across Australia is assessed and attributed to two large, accipitrid species. These are taxonomically described, and a phylogenetic analysis of their relationships undertaken. The likely ecology of the species is discussed, as well as the implications this has for the ecosystems of Pleistocene Australia.

## **Chapter 2: An exceptional partial skeleton of a new basal raptor (Aves: Accipitridae) from the Late Oligocene Namba Formation, South Australia**

Ellen K. Mather<sup>1,2</sup>, Michael S. Y. Lee<sup>1,3</sup>, Aaron B. Camens<sup>1</sup>, Trevor H. Worthy<sup>1</sup>

<sup>1</sup>College of Science and Engineering, Flinders University, GPO 2100, Adelaide, SA 5001, Australia

<sup>2</sup>Corresponding author, [math0083@flinders.edu.au](mailto:math0083@flinders.edu.au)

<sup>3</sup> Earth Sciences Section, South Australian Museum, North Terrace, Adelaide 5000, Australia

This chapter was published online in *Historical Biology* on the 28<sup>th</sup> of September 2021. The version presented in this thesis is the same in content and writing as the version sent for submission, with changes only made for formatting to fit the thesis and corrections of minor errors. The published version can be viewed at the link below:

<https://doi.org/10.1080/08912963.2021.1966777>

## Abstract

The Australian pre-Pleistocene fossil record of Accipitridae (eagles, hawks, old-world vultures) comprises one latest Oligocene or early Miocene and one middle Miocene species, each represented by partial bones. Globally, most fossil accipitrids are based on single bones. The recent discovery of an older and considerably more complete accipitrid from late Oligocene sediments in Australia is therefore significant. It is derived from the Pinpa Local Fauna from the Namba Formation at Lake Pinpa, South Australia (~26–24 Ma). The fossil, described as *Archaehierax sylvestris* n. gen. et sp., represents a raptor that was larger than the black-breasted buzzard *Hamirostra melanosternon* but smaller and more gracile than the wedge-tailed eagle *Aquila audax*. Comprehensive morphological and molecular phylogenetic analyses resolved *Archaehierax* as a basal accipitrid, not closely related to any living subfamily and perhaps the sister taxon to all other accipitrids exclusive of elanines. Relatively short wings similar to species of *Spizaetus* and *Spilornis* suggest it was adapted for flight within enclosed forests. Additional accipitrid fossils from the Namba Formation, a distal femur and a distal humerus, are incomparable with the holotype of *A. sylvestris*; they may represent distinct species or smaller individuals of the new taxon.

**Keywords:** Lake Pinpa, Accipitriformes, Cenozoic fossil birds, accipitrid evolution, Australia

## 2.1 INTRODUCTION

### 2.1.1 The Accipitridae and Kin

The Accipitriformes comprises four extant families and up to 259 species: the New-World vultures (Cathartidae, seven species), secretary birds (Sagittariidae, one species), ospreys (Pandionidae, one species) and the eagles, hawks and Old-World vultures (Accipitridae, ~250 species) (Dickinson and Remsen 2013). The accipitrids are the most widely distributed family in the order, being widespread on every continent except for Antarctica, and play key roles as apex predators and scavengers in many environments.

From the 19<sup>th</sup> to early 21<sup>st</sup> century, the Accipitridae were usually placed in Falconiformes with the Falconidae (falcons), Cathartidae, Sagittariidae and Pandionidae (Sharpe 1874; Ridgway 1874; Gadow 1891; Sushkin 1905; Peters 1934; Jollie 1976; Stresemann and Amadon 1979; Lerner and Mindell 2005; Hackett et al. 2008). Molecular data justified recognising Falconidae and Pandionidae as separate families from Accipitridae, though *Pandion* is very closely related to the Accipitridae (Sibley and Ahlquist 1990; Wink and Sauer-Gürth 2004; Lerner and Mindell 2005; Griffiths et al. 2007; Hackett et al. 2008). Accipitriformes was resurrected to include Accipitridae, Pandionidae, Sagittariidae and Cathartidae by Christidis and Boles (2008) and this usage has been followed thereafter (Dickinson and Remsen 2013; Gill et al. 2020). Accipitridae is recognised to include multiple subfamilies, though similarities in plumage and morphology (see Peters 1934; Amadon 1964; Jollie 1976) have obscured relationships and composition which are only recently being revealed by analyses of molecular data (refer to Ferguson-Lees and Christie 2001; Lerner and Mindell 2005; Dickinson and Remsen 2013; Mindell et al. 2018). Here we use the subfamilies Elaninae, Perninae, Gypaetinae, Aegyptiinae, Circaetinae, Harpiinae, Aquilinae, Accipitrinae, Haliaeetinae, and Buteoninae, following Nagy and Tökölyi (2014). We differ from Mindell et al. (2018) in recognising the Haliaeetinae as distinct from the Buteoninae, and Aquilinae from Harpiinae, based on differences in morphology and ecology, and the lack of justification provided by Mindell et al. (2018) for merging them.

Australia has 17 resident breeding accipitrid species in 12 genera, two of which are monotypic and endemic, in five subfamilies (Debus 1998; Christidis and Boles 2008; Dickinson and Remsen 2013).

### 2.1.2 Pre-Pleistocene Fossil Record of the Accipitridae

The fossil record of Accipitridae begins in the middle Eocene in Europe, although the fragmentary nature of the fossils prohibits definitive identification (Olson 1985; Mlíkovský 2002; Mayr 2017). A further complication is the presence of lineages that resemble Accipitridae, such as the Horusornithidae, thought to be an extinct lineage of Accipitriformes (Mourer-Chauviré 1991), and the Messelasturidae, predators in a lineage now thought to be

related to stem-group parrots (Mayr 2006a; Mayr 2011). The Eocene raptor *Masillaraptor parvunguis* Mayr, 2006, represented by several articulated skeletons, was considered to be either an accipitriform or a falconiform when first described (Mayr 2006b), but was later considered to be a falconid (Mayr 2009, 2017).

The Oligocene to Miocene record of accipitrids varies by continent. Africa is extremely poorly represented at the time of writing, with one indeterminate Oligocene fossil from Egypt bearing some similarity to *Haliaeetus* (Rasmussen et al. 1987); otherwise, African fossils attributable to extant genera are known from the Miocene onwards (Walker and Dyke 2006).

North America has numerous described species of late Oligocene to early Miocene age: four species have been described in the modern genus *Buteo*, (but see Mayr and Perner [2020] for caveats), and nine species in six fossil genera (Brodkorb 1964; Mayr 2009, 2017; Mayr and Perner 2020). Most species are described from a single bone, except for *Palaeoplancus sternbergi* Wetmore, 1933, which is represented by a partial skeleton with axial, pectoral and pelvic limb elements (Wetmore 1933). In contrast, South America has no definitive fossil accipitrids from this time period, possibly due to the dominance of the Cathartidae, Teratornithidae and Phorusrhacidae in the avian predatory and scavenging guilds (Mayr 2017).

Two accipitrids, each based on single bones, are known from Oligocene deposits of Asia: *Buteo circoides* Kurochkin, 1968 and *Venerator (Tutor) dementjevi* (Kurochkin, 1968). Other indeterminate fossil accipitrids of early Oligocene age are known from Mongolia and of late Oligocene age from Kazakhstan (Kurochkin 1976). Four species of vulturine accipitrids are recorded from middle to late Miocene deposits of China: *Mioaegyptus gui* Hou, 1984, *Mioneophron longirostris* Li et al., 2016, *Qiluornis taishanensis* Hou et al., 2000, and *Gansugyps linxiaensis* Zhang et al., 2010, each represented by a partial or near complete skeleton.

Seven fossil accipitrids are known from the early Oligocene to the early Miocene deposits of Europe, six of which are described from single bones: *Palaeohierax gervaisii* (Milne-Edwards, 1863), *Promilio incertus* (Gaillard, 1939), *Aquilavus priscus* Milne-Edwards, 1863, *Aquilavus depredator* Milne-Edwards, 1871, *Aquilavus corroyi* (Gaillard, 1939), and *Aquilavus hypogaeus* (Milne-Edwards, 1892). In contrast, *Aviraptor longicrus* Mayr and Hurum, 2020, is represented by a complete skeleton and is one of the oldest confirmed accipitrids known from Europe.

The pre-Pleistocene fossil record of the Australian Accipitridae is quite poor (Baird 1991; Vickers-Rich 1991). At the time of writing, Australia has two described pre-Pleistocene

accipitrids, the late Oligocene to early Miocene *Pengana robertbolesi* Boles, 1993 from the Riversleigh deposits in Queensland, and the middle Miocene *Aquila bullockensis* Gaff and Boles, 2010 from the Bullock Creek Site in the Northern Territory (Worthy and Nguyen 2020).

The global fossil record, and molecular divergence dating, suggests that by the early Miocene, about 20 Ma, all extant subfamilies of the Accipitridae had evolved (Walker and Dyke 2006; Zhang et al. 2012; Nagy and Tökölyi 2014; Mindell et al. 2018).

### **2.1.3 The Namba Formation**

The vast Kati Thanda-Lake Eyre catchment is approximately 1.2 million km<sup>2</sup>, extending over much of mid-central to north-eastern inland Australia. Sedimentary deposition in the central/southern Australian section of the basin occurred in three major phases; the first phase resulted in the Late Paleocene—Middle Eocene Eyre Formation, which is comprised of sandstone and carbonaceous conglomerates and clasts; the second phase resulted in the Late Oligocene—early Miocene Etadunna, Namba, Doonbarra and Cadelga Formations, which are comprised of clays, silts, fine sand, and carbonates; and the third phase saw the Pliocene—Quaternary Wipajiri, Tirari, Kutjitarra, Katipiri, Eurinilla, Millyera Coomb Spring and Coonarbine Formations deposited, which are comprised of a variety of sediments including cobbles, sands and clays from fluvial or lacustrine deposition (Drexel and Preiss 1995; Alley 1998).

Our focus is the Namba Formation, located in the Callabonna Sub-basin of the Lake Eyre Basin, in South Australia to the east of the Flinders Ranges (Alley 1998; see Figure 2.1). This is sometimes referred to as the Tarkarooloo Basin (see Woodburne et al. 1994) or the Frome Sub-basin (see Megirian et al. 2010). The age of this formation is correlated with that of the Etadunna Formation, in the Tirari Sub-basin of the Lake Eyre Basin (Alley 1998). The Namba Formation contains three primary Local Faunas (LFs): the Pinpa LF, the Ericmas LF, and the Tarkarooloo LF (Callen and Tedford 1976; Rich and Archer 1979; Rich et al. 1991; Thorn et al. 2021). The Pinpa LF derives from beds of olive and orange mottled clay and white dolomitic mudstone stained with manganese at the top of the lower member of the Namba Formation, which crops out at Lake Pinpa and Billeroo Creek (Tedford et al. 1977; Rich et al. 1991; Thorn et al. 2021). The Ericmas LF derives from fluvial sands deposited in channels cut into the lacustrine units of the Namba Formation, so is younger than the Pinpa LF, and derives from Ericmas Quarry and South Prospect Quarries at Lake Namba a few kilometres south of Lake Pinpa (Tedford et al. 1977; Rich et al. 1991). There is much overlap of species composition between Pinpa and Ericmas LFs suggesting broad similarity in age. While Rich et al. (1991) recognised the Ericmas LF to occur at Lake Pinpa, recent work by THW and ABC recognises only one local fauna from Lake Pinpa and restricts

the Ericmas LF to that derived from Ericmas and South Prospect quarries at nearby Lake Namba (Thorn et al. 2021). The Tarkarooloo LF derives from fluvial sands in Tom O's Quarry by Lake Tarkarooloo about 10 kilometres west of Lake Pinpa but the temporal relationship to the Ericmas LF is unknown, though co-occurrence of some species suggests a broadly similar age (Rich et al. 1991).

The accepted age of the Namba and Etadunna Formations has varied (see Pledge 2016). The Etadunna Formation, and therefore by proxy the Namba Formation, was initially considered to be of Oligocene age when it was first identified (Stirton et al. 1961). Subsequent analysis of the Pinpa and Ericmas LFs of the Namba Formation considered their likely age to be middle Miocene (16–12 Ma) (e.g., Tedford et al. 1977; Woodburne et al. 1985) based on the identification of grass pollen in the basal Namba Formation in Wooltana-1 bore that thereby indicated the presence of extensive grasslands (Callen and Tedford 1976). However, later studies of the same pollen slides determined that grass pollen was exceedingly rare and that of Restionaceae or sedges, which occur wherever wetlands are present, was common along with a host of rainforest taxa (Martin 1990). Therefore, Martin (1990) interpreted the palaeoenvironment as a rainforest surrounding swamps and via correlation with floras elsewhere, inferred a late Oligocene – early Miocene age for the basal Namba Formation.

Woodburne et al. (1994) detailed the biostratigraphy and revised the age of the Etadunna Formation, using four lines of evidence: 1, the presence of Oligocene age (24–28 Ma) foraminiferal fauna in the Etadunna Formation (Lindsay 1987); 2, a reported Rb-Sr age of 25 Ma on an authigenic illite (Norrish and Pickering 1983); 3, the presence of land mammal fossils consistent with those of known Oligocene age; and 4, the magnetostratigraphic record, to conclude that a late Oligocene age for the Etadunna Formation was most likely. As Woodburne et al. (1994) determined that the Pinpa LF correlated with the most basal Zone A “Wynyardiid” Fauna of the Etadunna Formation, a late Oligocene age was also inferred for it. Woodburne et al. (1994) did not cite Martin (1990) and were apparently unaware of it, as the pollen data provided compelling evidence to support their inferred late Oligocene age. This work was accepted by Megirian et al. (2010) who established a comprehensive land mammal biostratigraphy and advocated a late Oligocene age (28–24 Ma) for the Namba Formation. Some of the ages accepted by Megirian et al. (2010) have been robustly confirmed by direct dating of sites from Faunal Zones B and C at Riversleigh, northwest Queensland, to the early and middle Miocene respectively (Woodhead et al. 2016), supporting the prior correlation of Faunal Zone B sites with the Kutjamarpu LF (Wipajiri Fm) from Lake Ngapakaldi, Lake Eyre Basin on biochronological grounds; the Kutjamarpu LF is slightly younger than the uppermost

Etadunna local fauna – the Ngama LF – on biochronological grounds (Megirian et al. 2010). Therefore, we use the age range of 26–24 Ma advocated by Woodhead et al. (2016) for the Pinpa + Ericmas Local Faunas.

Aquatic or semiaquatic vertebrates are common in both the Pinpa and Ericmas LFs in the Namba Formation, including fish, turtles, crocodylians, and dolphins (Tedford et al. 1977; Fordyce 1983; Rich et al. 1991), revealing the presence of a permanent lake in the basin during this time period. The dolomitic layers at the site suggest periods of time when sections of the lake would seasonally dry out (Callen 1977). The afore-mentioned pollen record from the Namba Formation reveals that the depositional environment was dominated by a mix of rainforest and temperate forest surrounding sedge-lined lakes in the late Oligocene to early Miocene when the Pinpa LF was present (Martin 1990). The range in habitats resulted in a diverse vertebrate fauna inhabiting this area in the late Oligocene, resulting in a fossil fauna that is a key snapshot into our understanding of the evolution of Australian animals.

The Pinpa LF, found at Lake Pinpa and Wells Bog Site at Billeroo Creek (Rich et al. 1991; Thorn et al. 2021) (Figure 2.1), is extremely diverse, comprising fish and both aquatic and terrestrial reptiles, mammals, and birds (Rich et al. 1991). Reptiles are represented by an indeterminate species of chelid turtle, (*Emydura* sp.), an unnamed species of meiolaniid turtle (see Rich et al. 1991), the crocodylian *Australosuchus clarkae* Willis and Molnar, 1991 (see Willis 1997), and an egeriine skink *Proegernia mikebulli* Thorn et al., 2021.

The mammals of the Pinpa LF are well-documented, see Rich et al. (1991), or subsequently described; Monotremata: Ornithorhynchidae, *Obdurodon insignis* Woodburne and Tedford, 1975. Marsupialia, Vombatiformes: Phascolarctidae, *Madakoala devisi* Woodburne et al., 1987; Ilariidae, *Ilaria illumidens* Tedford and Woodburne, 1987; Mukupiridae, *Mukupirna nambensis* Beck et al., 2020 (=Vombatoidea genus A of Tedford et al. 1977); Diprotodontidae, *Raemeotherium yatkolai* Rich et al., 1978; Wynyardiidae, *Muramura pinpensis* Pledge, 2003. Marsupialia, Phalangeriformes: Pseudocheiridae, *Pildra antiquus* Woodburne, Tedford and Archer, 1987; *Pildra secundus* Woodburne, Tedford and Archer, 1987 (listed as from Ericmas LF, Lake Pinpa); Pilkipildridae, *Pilkipildra handae* Archer, Tedford and Rich, 1987; Miralinidae, *Miralina* sp. cf *M. minor*; Ektopodontidae, *Chunia* sp. cf *C. illuminata*; undetermined Petauridae; undetermined Macropodiformes, Macropodidae/Potoroidae; Placentalia, Cetacea: an unnamed species of extinct rhabdosteid dolphin (Fordyce 1983).

Birds are also abundant in the Pinpa LF, with many semi-aquatic taxa, see Rich et al. (1991), as modified by Boles and Ivison (1999), Worthy (2009, 2011), Boles et al. (2013) and

De Pietri et al. (2016). Presbyornithidae, *Wilaru tedfordi* Boles et al., 2013; Megapodiidae, *Ngawupodius minya* Boles and Ivison, 1999 (listed as from the Ericmas LF by Boles and Ivison [1999] but derives from the South end of Lake Pinpa where only deposits preserving the Pinpa LF occur (Thorn et al. 2021), and as a pigeon in Rich et al. [1991: 1025]). Anatidae: *Pinpanetta tedfordi* Worthy, 2009; *Pinpanetta vickersrichae* Worthy, 2009; *Pinpanetta fromensis* Worthy, 2009, *Australotadorna alecwillsoni* Worthy, 2009. Phalacrocoracidae: *Nambashag billeroensis* Worthy, 2011; *Nambashag microglaucus* Worthy, 2011. Pelecanidae: *Pelecanus tirarensis* Miller, 1966. Other taxa include undescribed species of rails (Rallidae), undetermined flamingos (Phoenicopteriformes), grebes (Podicipedidae), and passerines (authors' unpublished data).

From the dolomitic beds of the Namba Formation exposed at Site 12 on Lake Pinpa (Figure 2.1), and hence forming part of the Pinpa LF, a partial skeleton of an accipitrid was recovered in 2016 by a Flinders University expedition, led by THW and ABC. Sixty-three recognisable bones are represented, spanning the tip of the rostrum to the pedal digits (Figure 2.2). The pelvic limb elements are well preserved, except for the femur for which only the caput is preserved. This skeleton represents not only the oldest fossil representative of Accipitridae in Australia, but also the most complete (cf. Boles 1993; Gaff and Boles 2010). This relatively complete state is also rare on a global scale, and only observed in a handful of cases, such as the Miocene vultures of China which are near complete (Hou et al. 2000; Zhang et al. 2010; Li et al. 2016), *Palaeoplancus sternbergi* (see Wetmore 1933; Mayr and Perner 2020) and *Aviraptor longicrus* (see Mayr and Hurum 2020). Besides the new skeleton, there are another two accipitrid fossils recognised from the Namba Formation; a distal right humerus, from the dolomitic layers at Site 11, Lake Pinpa (also of the Pinpa LF) and a distal femur from Ericmas Quarry, Lake Namba, of the Ericmas LF. It is the aim of this contribution to formally describe these fossils and determine their phylogenetic relationships in the Accipitridae.

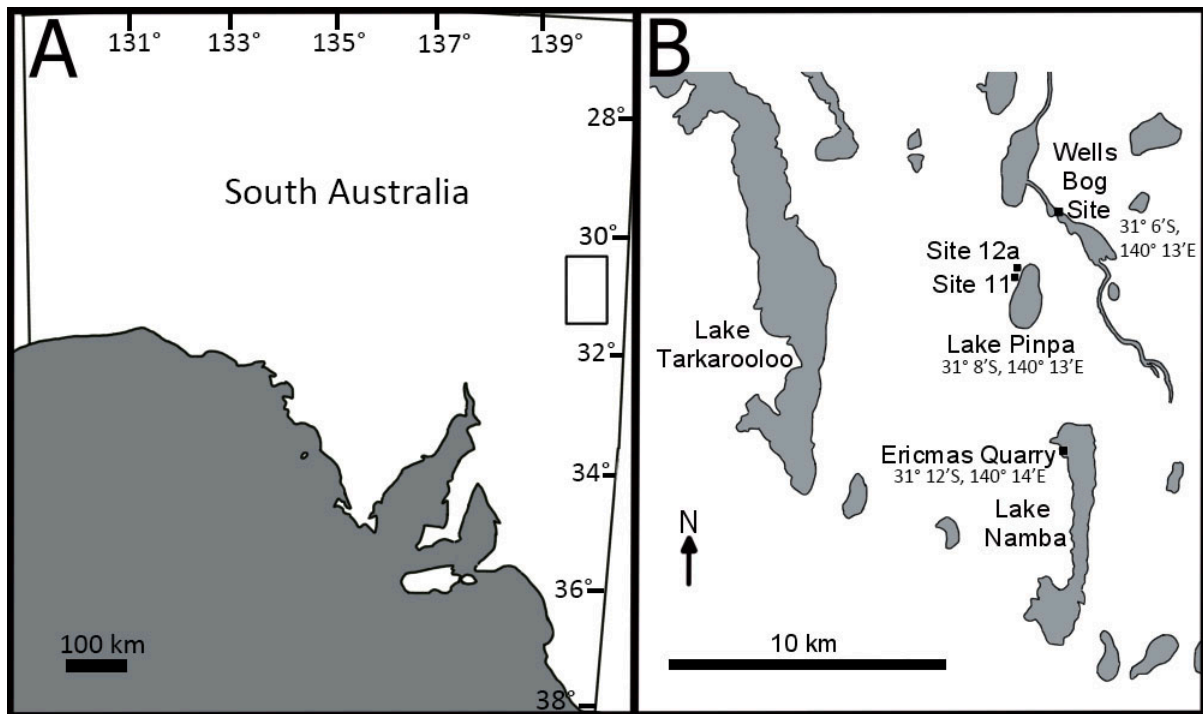


**Figure 2.1:** (A) Map of South Australia with general location of Callabonna Sub-Basin fossil sites marked with a rectangle, (B) detailed map of the study sites in the Callabonna Sub-Basin. Lake Pinpa Sites 11 and 12, Ericmas Quarry, and Wells Bog Site located by black squares.

## 2.2 MATERIALS AND METHODS

### 2.2.1 Abbreviations

Institutions: South Australia Museum, Adelaide, SA, Australia (SAMA); Museums Victoria, Melbourne, VIC, Australia (NMV); Australian National Wildlife Collection, Canberra, ACT, Australia (ANWC); University of Kansas Institute of Biodiversity, Lawrence, KS, USA (KU); Smithsonian Museum of Natural History, Washington DC, USA (USNM); Natural History Museum, London, UK (NHMUK).

Anatomical: Pedal phalanges are identified by the digit first (Roman numeral) and phalanx second (number), e.g., II.2 is digit II, phalanx 2; cmc, carpometacarpus; cor, coracoid; DW, distal width; L, left; PW, proximal width; R, right; SW, shaft width; tmt, tarsometatarsus.

Manus digits are identified akin to the pedal phalanges, e.g., MI.1 is manus digit I, phalanx 1.

### 2.2.2 Nomenclature

The anatomical nomenclature advocated by Baumel and Witmer (1993) is followed for all bones except for the os carpal radiale, which follows Mayr (2014), and the quadrate, which follows Elzanowski and Zelenkov (2015). Taxonomic nomenclature follows Dickinson and Remsen (2013) and Gill et al. (2020) for composition of Accipitriformes, and Nagy and Tökölyi (2014) for subfamilial composition (excluding Milvinae).

### 2.2.3 Measurements

Bones were measured with an accuracy of 0.1 mm using digital callipers.

### 2.2.4 Photography

Photographs were taken using a focus stacking method using a Canon 5DS-r digital camera 50.0 MP with either a Canon EF 100 mm or a 65 mm f2.8 IS USM professional macro lens with multiple images then compiled into a single photo using the program Zerene Stacker. Some fossil specimens were whitened with ammonium chloride powder before imaging (see Feldmann 1989) to retain shape as the primary feature captured rather than variable staining and reflective surfaces.

### 2.2.5 Comparative Material

Skeletons of a broad range of accipitrids and outgroup taxa were loaned from museums and other institutions from Australia and internationally to compare to the fossil as follows.

#### Extant species (in taxonomic groupings)

##### Falconiformes.

**Falconidae.** *Falco berigora* SAMA B55605; *Falco longipennis* SAMA B49055; *Falco peregrinus* SAMA B32515.

##### Ciconiiformes.

**Threskiornithidae.** *Threskiornis spinicollis* SAMA B48351.

**Ciconiidae.** *Ciconia ciconia* SAMA B49223, SAMA B11601.

##### Accipitriformes.

**Cathartidae.** *Coragyps atratus* SAMA B36873.

**Sagittariidae.** *Sagittarius serpentarius* USNM 223836.

**Pandionidae.** *Pandion haliaetus* SAMA B37096, NMV B30256.

**Accipitridae.** Elaninae: *Elanus axillaris* NMV B34037; *Elanus scriptus* NMV B8617, NMV B30263, ANWC 22680; *Gampsonyx swainsonii* USNM 623110; *Chelictinia riocourii* NHMUK S.1904.4.28.3. Perninae: *Elanoides forficatus* USNM 622340; *Chondrohierax uncinatus* USNM 289784; *Aviceda subcristata* ANWC 22665, NMV B19826; *Pernis apivorus* SAMA B59278; *Lophoictinia isura* NMV B18533, ANWC 44373; *Hamirostra melanosternon* ANWC (FALS-41), SAMA B36200. Gypaetinae: *Polyboroides typus* USNM 430434; *Neophron percnopterus* SAMA B11449; *Gypohierax angolensis* USNM 291316; *Gypaetus barbatus* NHMUK S.1972.1.59, NHMUK S.1896.2.16.120, NHMUK S.1952.3.61. Circaetinae:

*Spilornis cheela* USNM 562001; *Terathopius ecaudatus* NMV 18575; *Pithecophaga jefferyi* NHMUK S.1910.2.11.1a, NHMUK S.1961.23.1. Aegyptiinae: *Necrosyrtes monachus* USNM 620646; *Gyps coprotheres* ANWC 22724; *Gyps fulvus* NMV 18574, NMV B30269; *Aegyptius monachus* NMV R553; *Sarcogyps calvus* NHMUK S.2013.22.1, NHMUK S.2007.30.1; *Trionocephus occipitalis* NHMUK S.1954.30.54; *Torgos tracheliotos* NHMUK S.1930.3.24.248, NHMUK S.1952.1.172. Harpiinae: *Harpia harpyja* NHMUK S.1862.3.19, NHMUK S.1909.8.18.1. Aquilinae: *Stephanoaetus coronatus* NHMUK S.1954.30.42, NHMUK S.1862.3.14.19; *Aquila audax* SAMA B46613, NMV B19228; *Aquila chrysaetos* NMV B32659, ANWC 22682 (FALS-123); *Aquila fasciata* (formerly *Hieraaetus fasciatus*) NMV B30575; *Hieraaetus morphnoides* SAMA B47128, NMV B8643, NMV B20224; *Hieraaetus* (= *Harpagornis*) *moorei*, casts of the original type material, NMV P33032 (tibiotarsus), NMV P33031 (pedal phalanx), NMV P33030 (tarsometatarsus), NMV P33029 (femur), NMV P33028 (humerus), NMV P33027 (femur), NMV P33026 (ulna); *Spizaetus tyrannus* KU 35007; *Spizaetus ornatus* KU 72077. Haliaeetinae: *Haliaeetus leucogaster* NMV B8847, SAMA B49459; *Haliaeetus leucocephalus* ANWC 22723 (16500), NMV B15601; *Haliaeetus albicilla* NMV B34417; *Haliastur indus* ANWC 22719, NMV B13753; *Haliastur sphenurus* NMV B11661, SAMA B33998; *Milvus migrans* SAMA B47130, NMV B20404. Accipitrinae: *Melierax metabates* NHMUK S.1954.30.29; *Kaupifalco monogrammicus* NHMUK S.1869.10.19.28; *Circus assimilis* SAMA B56454, ANWC 22727; *C. approximans* ANWC 22728, ANWC 22729; *C. cyaneus* ANWC 22735; *C. aeruginosus* NMV B12891; *Accipiter fasciatus* NMV B13444, SAMA B36355; *A. cooperii* ANWC 22764, ANWC 22765; *A. striatus* ANWC 22747, NMV B12666; *A. novaehollandiae* NMV B18401; *A. cirrocephalus* NMV B16071, NMV B10346; *A. nisus* NMV B12413, ANWC 22742; *A. gentilis* ANWC 22736, NMV B12927. Buteoninae: *Erythrotriorchis radiatus* NHMUK S.1872.10.22.9; *Geranospiza caerulescens* NHMUK S.1903.12.20.318; *Ictinia mississippiensis* ANWC 22681 (21655), NMV B13343; *Buteo buteo* SAMA B46558, NMV B24505; *B. nitidus* NMV B13222; *Buteo rufofuscus* NMV B24503; *Buteo lagopus* ANWC 22776 (21694), NMV B24884.

## 2.2.6 Phylogenetic methods

### **Morphological analysis**

A total of 300 morphological characters were coded for both extant and fossil specimens, from the following elements: cranium, sternum, coracoid, humerus, ulna, carpometacarpus, ossa carpi, ossa digitorum manus, pelvis, femur, tibiotarsus, tarsometatarsus, and pedal phalanges (see Appendix 1; SI 1). A total of 154 characters were derived from Migotto (2013, unpublished thesis), two from Elzanowski and Stidham (2010), two from Elzanowski and Zelenkov (2015), six from Gaff and Boles (2010), one from Worthy et al. (2016), three from Mayr (2018) and three from Mayr (2014). The remaining 129

characters were novel traits derived from observations and comparisons between the extant and fossil specimens.

### **Molecular data**

Molecular data from Burleigh et al. (2015) was added to the morphological data to improve estimated relationships between living species (Lerner and Mindell 2005; Nagy and Tökölyi 2014; Burleigh et al. 2015). This allows the fossil taxa to be placed phylogenetically according to the signal in the morphological data, but in the context of a DNA-informed tree for living taxa which better accommodates homoplasy in skeletal morphology (see Holdaway 1994; Griffiths et al. 2007). The following genes, well-sampled in accipitrids, were used: cytochrome b, cytochrome oxidase 1, NADH dehydrogenase 2, 12s RNA, RAG 1, and fibrinogen B beta introns 6 and 7, for an aligned matrix totalling seven gene regions and six loci.

Genomic data for the above gene regions from Burleigh et al. (2015) were used for the following species: *Ciconia ciconia*, *Coragyps atratus*, *Sagittarius serpentarius*, *Pandion haliaetus*, *Gampsonyx swainsonii*, *Elanoides forficatus*, *Chondrohierax uncinatus*, *Aviceda subcristata*, *Pernis apivorus*, *Lophoictinia isura*, *Hamirostra melanosternon*, *Polyboroides typus*, *Neophron percnopterus*, *Gypohierax angolensis*, *Gypaetus barbatus*, *Spilornis cheela*, *Terathopius ecaudatus*, *Pithecophaga jefferyi*, *Necrosyrtes monachus*, *Gyps fulvus*, *Gyps coprotheres*, *Aegyptius monachus*, *Sarcogyps calvus*, *Trigonoceps occipitalis*, *Torgos tracheliotos*, *Harpia harpyja*, *Aquila chrysaetos*, *Hieraaetus morphnoides*, *Hieraaetus fasciatus/Aquila fasciata*, *Hieraaetus moorei*, *Spizaetus tyrannus*, *Spizaetus ornatus*, *Haliaeetus leucogaster*, *Haliaeetus leucocephalus*, *Haliaeetus albicilla*, *Milvus migrans*, *Melierax metabates*, *Kaupifalco monogrammicus*, *Circus aeruginosus*, *Circus cyaneus*, *Accipiter cooperii*, *Accipiter striatus*, *Accipiter novaehollandiae*, *Accipiter gentilis*, *Ictinia mississippiensis*, *Geranospiza caerulescens*, *Buteo buteo*, *Buteo lagopus*, *Buteo rufofuscus*, and *Platalea leucorodia*. To reduce missing data, genetic data from *Platalea leucorodia* was paired with *Threskiornis spinicollis*, and *Elanus caeruleus* paired with *Elanus scriptus*, as these species pairs consist of closely related taxa (see Campbell and Lapointe 2009 regarding this method).

### **Phylogenetic analysis**

Phylogenetic comparisons were aimed primarily at determining the relationships of the fossil specimen SAMA P.54998. A total of 47 species of Accipitridae, and one species each of Pandionidae, Sagittariidae, Cathartidae, Threskiornithidae, and Ciconiidae were sampled. The non-accipitrid species were selected for the following reasons: Pandionidae, Sagittariidae and Cathartidae are successive sister-taxa to the Accipitridae within the

Accipitriformes; the species of Ciconiidae and Threskiornithidae (Ciconiiformes), are examples of bird families outside of Accipitriformes that share similar size and flight morphology, as well as a history of grouping with the Cathartidae in older phylogenies (see Sibley and Ahlquist 1990; Wink 1995).

Both parsimony and Bayesian analyses were used to explore the data. The parsimony analyses of the morphological, molecular, and combined morphological-molecular datasets used PAUP 4.0b10, and heuristic searches. Each search was comprised of 1000 random addition replicates, and enabled TBR branch swapping, with NCHUCK set to 1000. Characters that were inapplicable to a specimen were coded using '-', while missing data were coded as '?'. The taxa *Threskiornis spinicollis*, *Ciconia ciconia*, *Coragyps atratus*, *Sagittarius serpentarius* and *Pandion haliaetus* were all defined as outgroup taxa in all analyses, with *Threskiornis spinicollis* and *Ciconia ciconia* being the most basal outgroups. Once the heuristic searches had generated a set of most parsimonious trees (MPT), a strict consensus tree was created from them. The support for clades on these trees were then assessed using bootstrapping, with 1000 replicates, and majority-rule consensus trees set to conlevel 50 (support shown if >50%). See SI.2 for the input file.

For the Bayesian analyses, MrBayes 3.2.7 was used via the CIPRES platform (Miller et al. 2010). The morphological partition used the standard (Lewis) model for discrete data, with correction for non-sampling of invariant characters. The among-character rate variability was modelled using the gamma parameter, with distribution approximated using four categories. The molecular partitioning scheme and substitution models were identified using PartitionFinder (Lanfear et al. 2016), using BIC. The data was thus treated as three partitions: morphological data (morph); molecular partition 1 (pfinder Molec1), which contains Cyt-B codons 1 and 2, CO1 codons 1 and 2, ND2 codons 1 and 2, 12s, Rag-1 codons 1, 2 and 3, and FGBint67; and molecular partition 2 (pfinder Molec2), which contains Cyt-B codon 3, CO1 codon 3, and ND2 codon 3. The Molec1 and Molec2 partitions each had a GTR model using a Dirichlet prior for the state frequencies. The among-character rates were set to InvGamma, with the gamma distribution approximated as above. All substitution parameters were unlinked across these molecular partitions. See SI.3 for the input file.

Each analysis entailed four runs, each run comprising four MCMC chains (incrementally heated to 0.1), the number of generations set to 50,000,000, the sample and print frequency set to 5000. Burnin was set to 20% (and confirmed sufficient using PSRF and SDSF values in MrBayes) and the majority-rule consensus tree was obtained from all post-burnin samples. During the MrBayes runs, *Ciconia ciconia* was set as the sole outgroup taxon, due to limitations of MrBayes, but trees were later rerooted so that both *Ciconia ciconia* and *Threskiornis spinicollis* were the most distal outgroup clade. The Bayesian

analyses were performed twice: with morphological and molecular branch lengths linked or unlinked.

### **2.2.7 Ecomorphological analyses**

Measurements of selected elements for a sample of extant accipitrids were used to correlate morphology with ecology of living forms and so to retrodict the ecology and feeding strategy of the fossil taxon. Measurements used reflected their availability in the fossil: height of the quadrate; length and proximal width of the carpometacarpus; length, shaft width and distal width of the ulna; length, shaft width, distal width, height of the condylus lateralis, depth of the condylus lateralis, height of the condylus medialis and depth of the condylus medialis of the tibiotarsus; length, shaft width, distal width, and width and height of trochleae metatarsorum 2, 3 and 4 of the tarsometatarsus; length of the first phalanx of pedal digit 1; and the length of the first and second phalanges of pedal digit 2. The fossil species was compared to *Elanus scriptus*, *Hamirostra melanosternon*, *Pernis apivorus*, *Lophoictinia isura*, *Neophron percnopterus*, *Aegypius monachus*, *Gyps coprotheres*, *Spilornis cheela*, *Haliaeetus leucogaster*, *Aquila audax*, *Hieraaetus morphnoides*, *Spizaetus tyrannus*, and *Circus assimilis* in principal components analyses (PCA). These species were chosen as they were considered to be either, exemplars of the different hunting strategies of Accipitridae, or were potential analogues for the fossil. The PCA was performed on measurements of the wings and legs: raw, log-transformed, and standardised for size by division by the height of the quadrate in each individual (as this was possible for the fossil). The extant taxa were classed based on their preferred habitat (open, woodland, or forest) as determined from the literature (Brown and Amadon 1968; Ferguson-Lees and Christie 2001).

Widths of the distal femur, distal humerus, proximal humerus and distal tibiotarsus were measured for both extant and fossil specimens so that the relationships between these values could be used to predict the width of the distal humerus and distal femur for SAMA P.54998, and thereby to assess whether size precluded the isolated distal humerus from Site 11 Lake Pinpa and the distal femur from Ericmas Quarry from being the same taxon as SAMA P.54998.

## 2.3 RESULTS

### 2.3.1 Systematic palaeontology

**Class Aves Linnaeus, 1758**

**Order Accipitriformes Vieillot, 1816**

**Family Accipitridae Vigors, 1824**

**Subfamily Archaehieraxinae subfam. Nov.**

**Type genus:** *Archaehierax* gen. nov.

**Remarks:** The fossil is identified as an accipitrid due to the following combination of characters: Skull - Rostrum deep and narrow, with hooked tip and a large, broad nasal aperture; Tibiotarsus - Pons supratendineus ossified, aligned steeply transversely, medially placed, with unbranched canalis tendinosus, and distal condyles much wider than craniocaudally deep; Tarsometatarsus - Robust, with monosulcate hypotarsus, the lateral and medial hypotarsal crests widely separated and trochleae metatarsorum splayed both medially and laterally, and dorsally arched in distal view; Foot - Four digits with raptorial unguals, those of digits 1 and 2 relatively large; Digit IV - Phalanges 2 and 3 are very short compared to phalanx 4.

The fossil can be excluded from Falconiformes (Falconidae) and the other families of Accipitriformes (Cathartidae, Sagittariidae, Pandionidae) by the morphology of the tarsometatarsal hypotarsus cristae and sulcus. The cristae are fused or partially fused together to enclose the sulcus in Cathartidae, Sagittariidae, and Pandionidae, while in Falconidae the medial crista is connected to the shaft by a ridge that extends two-thirds of its length, features that are absent in the fossil.

**Diagnosis:** Accipitrids in which the following autapomorphic features are found: the pila medialis of the sternum dorsally separates two deep pneumatic fossae, the humerus has the caput humeri only slightly elevated proximally past the tuberculum ventralis, the tip of the processus procoracoideus of the coracoid sharply curves inwards ventrally towards the medial face of the bone, the tibiotarsus has the lateral/distal retinaculum scar in a deep fossa, the tarsometatarsus is relatively elongate with narrow trochleae metatarsorum that are separated by wide incisurae, and the incisura for the m. flexor hallucis brevis tendon is large, distinct, and extends distal to the fossa metatarsi I. In addition to this, the following features occur: the rostral tip of the rostrum is hooked below the tomial margin at a relatively shallow 30–40° angle, the quadrate has a deep, distinct foramen pneumaticum caudomediale, and the sternum has the apex carinae displaced caudally from the base of the spina externa.

**Genus *Archaehierax* Mather, Lee, Camens and Worthy gen. nov.**

**Type species:** *Archaehierax sylvestris* sp. nov.

<http://zoobank.org/urn:lsid:zoobank.org:act:8C4B01F2-12CE-46F4-A444-C63B18C90BAE>

**Etymology:** *Archaehierax* is derived from the Greek words 'archaios', meaning ancient, and 'hierax', meaning hawk. Gender masculine.

**Diagnosis:** An accipitrid distinguished by the combination of the following features;

**Rostrum. (1)** The nares are large and fully open, **(2)** processus maxillopalatini not fused;

**Quadrate. (3)** the condylus pterygoideus projects less medially than the condylus medialis,

**(4)** a deep, distinct fossa caudomedialis with a small amount of pneumatism; **Sternum. (5)**

The apex carinae is displaced caudally from the base of the spina externa, **(6)** the medial

crista on the carina does not extend to the spina externa; **(7)** The pila medialis on the dorsal

face separates two deep fossae (autapomorphy); **Humerus. (8)** The caput humeri is only

slightly elevated proximally past the tuberculum ventralis (autapomorphy); **Os carpale**

**ulnare. (9)** Deepened depression on ulnaris face; **Tarsometatarsus. (10)** The trochleae

metatarsorum are splayed and separated by wide incisurae, especially laterally, with the

individual trochleae themselves quite narrow in width (autapomorphy); **(11)** The incisura for

the m. flexor hallucis brevis tendon is large, distinct, and extends distal to the fossa metatarsi

I (autapomorphy); **Phalanx IV.4. (12)** The distal articular end that articulates with phalanx

IV.5, is considerably wider than the shaft.

**Type Locality/Stratigraphy/Age:** 31° 07.499' S; 140° 12.755' E. Site 12a, Lake Pinpa, Frome Downs Station, Callabonna Sub-Basin, S.A. Dolomite bed of Namba Formation, Pinpa LF, late Oligocene, 26–24 Ma.

***Archaehierax sylvestris* Mather, Lee, Camens and Worthy gen. et sp. nov. (Figures 3–10)**

<http://zoobank.org/urn:lsid:zoobank.org:act:092140CA-E937-43B3-B3F1-7127C97094F4>

**Holotype:** SAMA P.54998, 63 elements and associated fragments of a single skeleton (see Figure 2.2) as follows:

Fragments of mandible; rostral majority of rostrum; R pterygoid; L quadratojugal; L quadrate; ceratohyal; atlas vertebra; axis vertebra; partial cervical vertebra #3; caudal

vertebrae x3 (position in tail indeterminate); cranial part sternum; LR scapulae; cranial and sternal parts LR coracoids; sternal parts LR coracoids; proximal LR humeri; L and distal R ulna; L and distal R radius; L carpometacarpus; LR os carpi ulnare; L os carpi radiale; R manual phalanges, proximal fragment MI.1, proximal fragment MII.1 and MII.2; L manual phalanges MI.1, MII.2 with distal end eroded, and MIII.1; LR proximal femur fragments; R tibiotarsus reconstructed in two parts; L tibiotarsus; fragmented LR fibulae; LR tarsometatarsi; LR ossa metatarsalia; pedal phalanges: RI.1, RII.1, RII.2, RIII.1, RIII.2, RIII.3 (partial), RIII.4, LI.1, LI.2 (fragmented), LII.1, LII.2, LIII.1, LIII.2, LIII.3 (partial), LIII.4, LIV.1, LIV.2, LIV.3, LIV.4, LIV.5. The skeleton was found eroding out on the surface with surviving elements recovered in a semi-articulated state from within dolomitic clays (equivalent to layer 5 of Thorn et al. 2021), with most large elements fractured into many roughly articulated pieces, presumably by expansion and contraction associated with the wetting and drying of the clays. The fragments for each element were, where possible, separated, cleaned and reassembled by THW.

**Measurements (mm):** See Appendix 2 Table 1.

**Etymology:** the species name 'sylvestris' is derived from the Greek word 'sylvas', meaning forest, and the Latin suffix '-estris', meaning 'belonging to'.

**Type locality/Stratigraphy and age:** As per genus.

**Diagnosis:** as for genus.

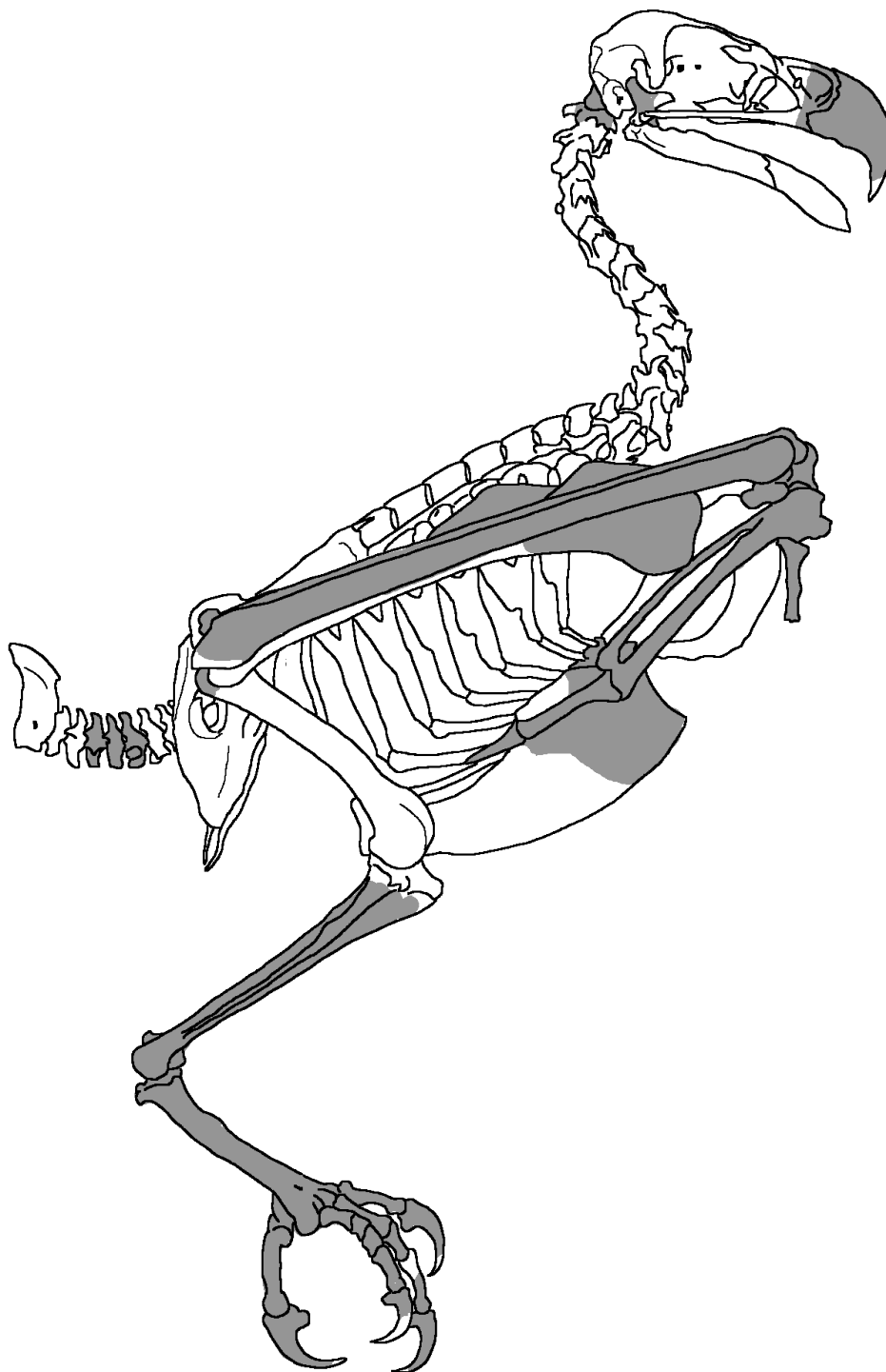


**Figure 2.2:** Exemplar accipitriform skeleton, *Pandion haliaetus cristatus*, derived from an illustration in Eyton (1867), showing the bones preserved in the fossil accipitrid specimen SAMA P.54998 shaded in grey. The illustrated taxon and fossil material are not identical in terms of the morphology of individual elements.

## Descriptions

### ***Rostrum maxillare* (Figure 2.3A, B).**

The rostral section of the rostrum maxillare is preserved in reasonably good condition. The morphology of its rostral tip, tomial margin, rostral margin of the nares, and the palatines is visible. The rostrum has a preserved length of 32.6 mm from the rostral tip to the posterior base of the nares, and a preserved depth of 17.3 mm from the tomial margin to the dorsal side of the rostrum taken at the rostral end of the nares. **(Trait 1)** The rostral tip of the rostrum is hooked, descending below the tomial margin at a 30–40° angle. **(2)** The lateral tomial margin (Figure 2.3A: CT), positioned distal to the nares, is ventrally convex. **(3)** The nasal aperture (Figure 2.3A: N) is large (height 8.7 mm) and fully open as in most accipitrids, spanning just over half the rostrum depth. **(4)** The ossified section rostral to the incisura ventromedialis is of small to moderate size (10.1 mm preserved length) relative to the total length of the rostrum. **(5)** In ventral aspect, an incisura ventromedialis (Figure 2.3B: IV) (sensu Livezey and Zusi 2007) is present (sediment filled) extending from where damage destroys it rostrally to the preserved caudal end of the palate; it is narrow and widens caudally, rather than being closed forming a fenestra. The pars maxillaris palatini (Figure 2.3B: PM) are unfused and diverge slightly caudally, the left being least fragmented although it has broken from the adjacent lateral margin creating a false incision. A small fragment of bone preserved between the pars maxillaris palatini is interpreted as a displaced fragment of the processus maxillopalatinus. **(6)** Damage precludes ascertaining the presence/form of the fenestra ventrolaterale.

Other accipitrid subfamilies differ as follows:

**(Trait 1)** Compared to the fossil, the rostral tip of the rostrum is much more sharply hooked ventrally in most subfamilies. Only members of Elaninae, Perninae (except *Chondrohierax uncinatus*, which is sharper), Buteoninae, and Gypaetinae have similar or shallower angled tips.

The rostrum maxillare is overall most similar to that of species of Buteoninae (see Appendix 3 for further comparisons with extant species).

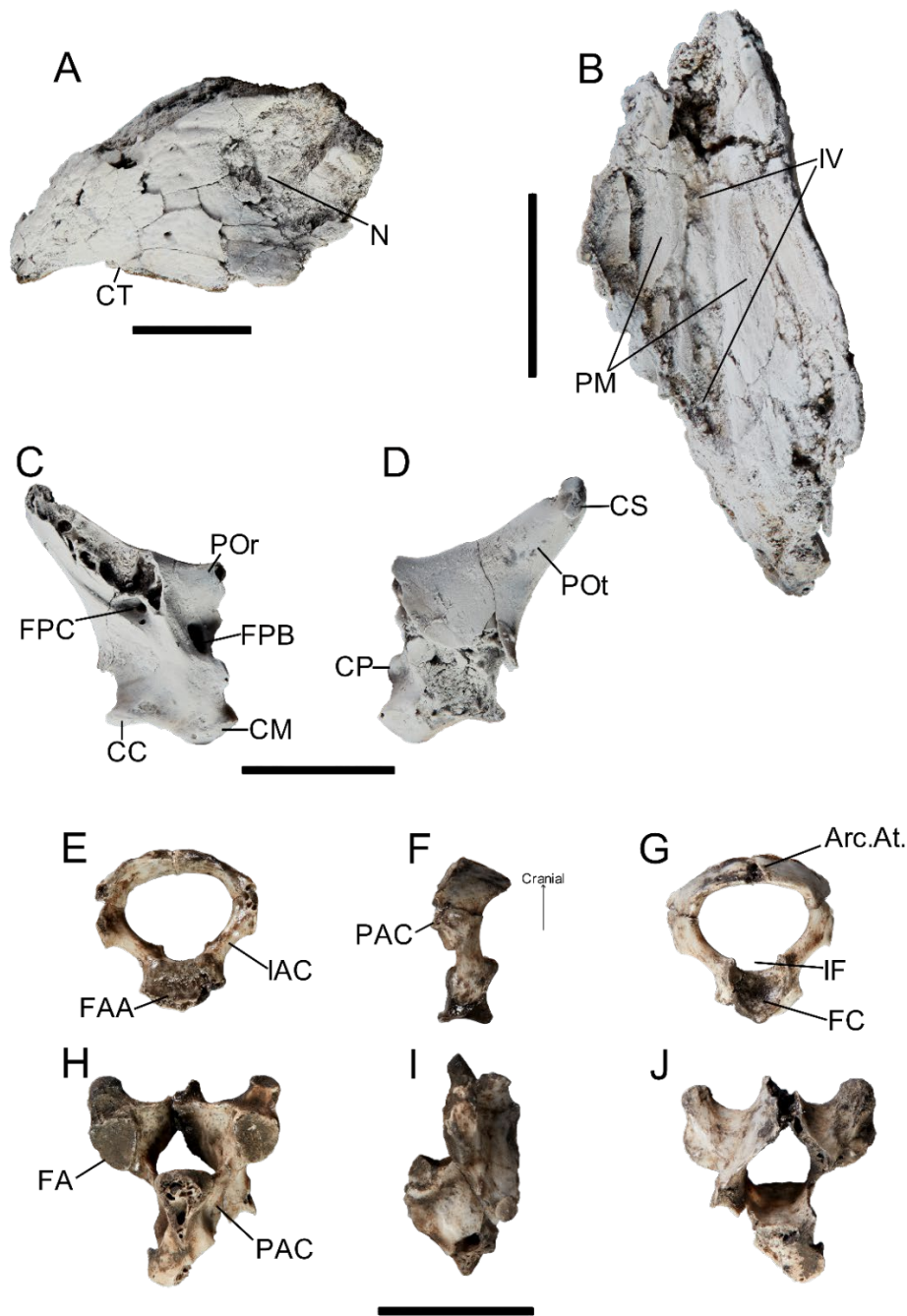


**Figure 2.3:** *Archaehierax sylvestris* gen. et. Sp. nov. SAMA P.54998 rostrum in lateral (A) and ventral (B) view; quadrate in medial (C) and lateral (D) view; atlas vertebra in caudal (E), lateral (F) and cranial (G) view; and axis vertebra in caudal (H), lateral (I) and cranial (J) view. Specimens in A-D are coated in ammonium chloride. Abbreviations: Arc. At., arcus atlantis; CC, condylus caudalis; CM, condylus medialis; CP, condylus pterygoideus; CS, capitulum squamosum; CT, crista tomialis; FA, facies articularis; FAA, facies articularis axialis; FC, fossa condyloidea; FPB, fossa pneumaticum basiorbitale; FPC, fossa/depressio pneumaticum caudomediale; IAC, incisura caudalis arcus; IF, incisura fossae; IV, incisura ventromedialis; N, nasale; PAC, processus articularis caudalis; PM, pars maxillaris palatini; POr, processus orbitalis; POt, processus oticus. Scale bars are 10 mm.

### **Quadrate (Figure 2.3C, D).**

The left quadrate has considerable breakage affecting the lateral side ventrally, the medial side of the processus oticus, and loss of the processus orbitalis. Preservation of morphological detail is best medially. On the processus oticus, only about half of the capitulum squamosum is preserved and the dorsal half of the crista medialis is lost. Of the processus orbitalis, only the well-preserved base remains. Both the condylus pterygoideus and medialis are intact, but the entire condylus lateralis and caudal half of the condylus caudalis are lost.

**(Trait 1)** The processus oticus (Figure 2.3D: POt) is short and broad leading up to the capitulum squamosum. **(2)** The capitulum squamosum (Figure 2.3D: CS), as preserved is relatively small, and has a tuberculum subcapitulare forming a distinct hook projecting ventrally on its cranial margin. **(3)** The processus orbitalis (Figure 2.3C: POr) is dorsomedially oriented. **(4)** The processus is set entirely in the ventral half of the quadrate, creating a gentle, shallow sloping arc between the base of the processus and the capitulum. **(5)** A large and deep foramen pneumaticum basiorbitale (Figure 2.3C: FPB) is present between the processus orbitalis and the condylus pterygoideus. **(6)** Breakage prohibits assessing the status of the foramen rostromediale. **(7)** The ventral section of the crista medialis is preserved and is quite broad and flat with no projecting ridge. **(8)** A thin, distinct sulcus runs along the ventral margin of the crista to connect to the foramen pneumaticum caudomediale. **(9)** A distinct, deep fossa pneumatica caudomediale (Figure 2.3C: FPC) is present just medial of the ventral-most point of the crista medialis. **(10)** The condylus pterygoideus (Figure 2.3D: CP) is distinct, high-set and well separated from the condylus medialis. **(11)** The condylus medialis (Figure 2.3C: CM) is well preserved, showing a large (4.0 mm wide by 2.8 mm deep), semi-ovular facet, with a pointed medial margin that extends further medially than the condylus pterygoideus. **(12)** The portion of the condylus caudalis (Figure 2.3C: CC) preserved indicates a facet of a similar size to the condylus medialis, with a semicircular shape.

Other accipitrid subfamilies differ as follows (variable characters excluded):

**(Trait 8)** The sulcus running along the ventral crista is broad and indistinct in all other taxa except in species of *Milvus* and *Haliaeetus* (Haliaeetinae) where it is narrow and indistinct. **(9)** The fossa caudomediale is practically absent in the subfamilies Circaetinae and Aegyptiinae, as well as the species in *Hamirostra*, *Lophoictinia* (Perninae), *Neophron* (Gypaetinae), and *Haliaeetus* (Haliaeetinae); shallow in Aquilinae and species of *Elanoides*, *Chondrohierax* (Perninae), *Polyboroides* and *Gypohierax* (Gypaetinae); and deep in Elaninae, Accipitrinae and Buteoninae, as well as species in *Pernis* (Perninae). The depressio was indistinctly shaped (i.e. a gradually deepened area rather than a defined pit)

in all species, and apneumatic in all species except in *Pernis* and *Haliaeetus*.

The quadrate is overall most similar to that of species of Aegypiinae (see Appendix 3 for further comparisons with extant species).

### **Vertebrae (Figure 2.3E–J).**

The atlas vertebra of SAMA P.54998 is 10.7 mm wide by 10.7 mm high (from the proximal margin of arcus atlantis to the distal margin of fossa condyloidea). **(Trait 1)** The arcus atlantis (Figure 2.3G: Arc. At.) forms a low, flat arch, which dorsally has a maximum proximodistal width of 3.2 mm at the centre, overhanging the fossa condyloidea cranially. **(2)** The incisura fossae (Figure 2.3G: IF) is shallow and broad, forming a semicircular shape in cranial aspect. **(3)** The fossa condyloidea (Figure 2.3G: FC) is 4.3 mm wide by 4.2 mm long. **(4)** The dorsolateral eminences of the fossa condyloidea are small. **(5)** The ventral margin of the fossa forms a rounded point in cranial aspect and is prominent cranially in lateral aspect. **(6)** The zygopophyses caudales are badly worn and difficult to assess, but what is preserved indicates they were distinct and caudally projected from the rest of the arcus atlantis. **(7)** The incisurae caudales arcus (Figure 2.3E: IAC) are very shallow. **(8)** The facies articularis axisialis (Figure 2.3E: FAA) is 5.7 mm wide by approximately 3.8 mm long. **(9)** The rest of the distal corpus atlantis is worn away and cannot be assessed, but what is present suggests that few additional structures were present, and that there was some asymmetry in the shape of the lateral fossa condyloidea.

The axis vertebra is quite fragmented, with most of the neural spine, facies articularis atlantica, dens, facies articularis caudalis, processus ventralis and the area of incisurae caudales arcus broken away. Its width is 12.7 mm across processus articulares caudales and mid-line length of the corpus vertebra is 8 mm. The facies articularis on zygopophyses caudales are 3.1 mm wide by 3.8–4.1 mm long. **(10)** A short but caudally-prominent projection is present dorsal to each facet (Figure 2.3H: FA), measuring 2–2.5 mm in width. **(11)** There is no evidence of a bridge enclosing the incisurae caudales arcus (Figure 2.3F, H: PAC).

The three known caudal vertebrae are too broken to identify their position in the caudal series.

The vertebrae are overall most similar to that of species of Elaninae (see Appendix 3 for comparisons with extant species).

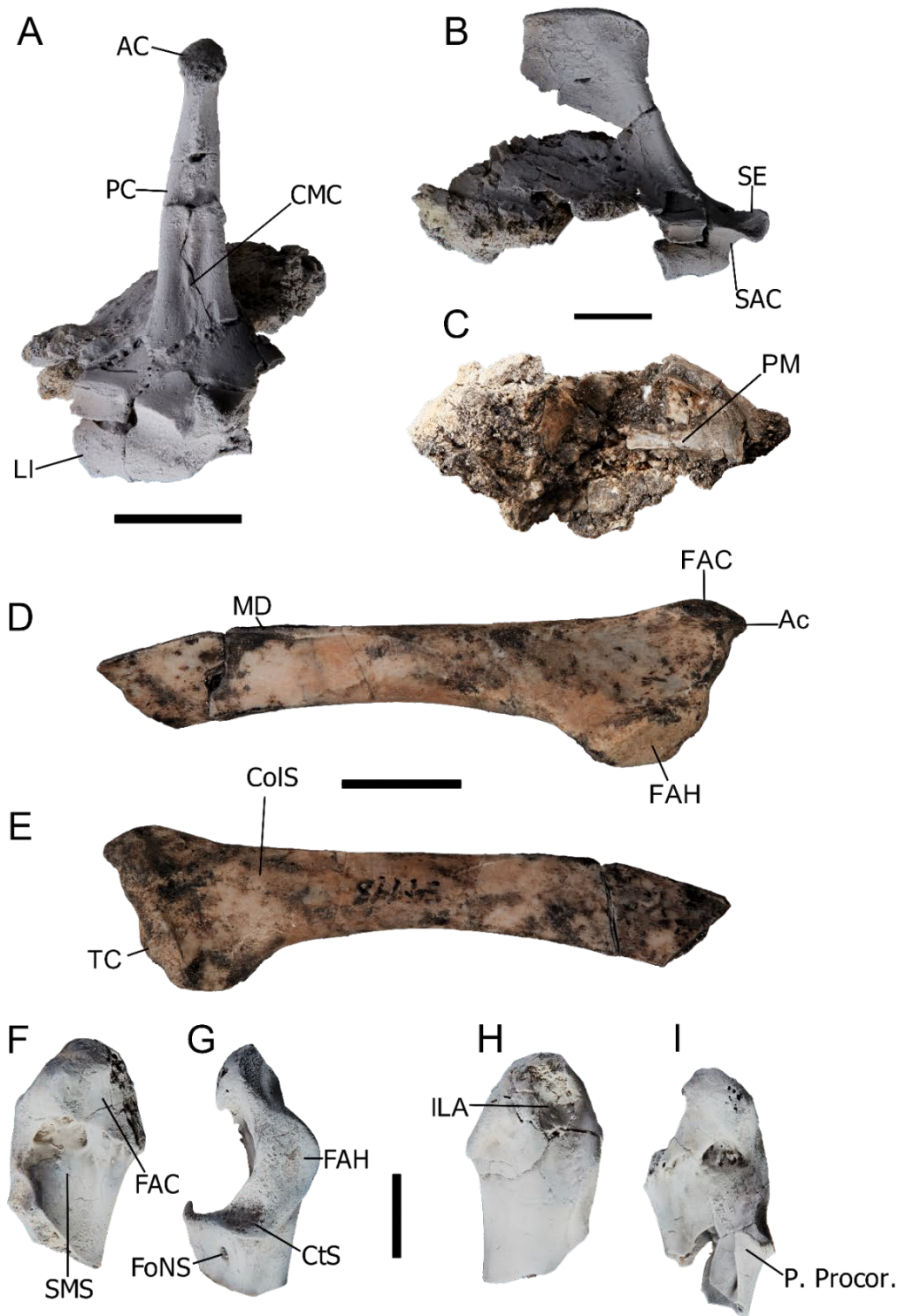


**Figure 2.4:** *Archaeohierax sylvestris* gen. et. sp. nov. SAMA P.54998 partial sternum in cranial (A), left lateral (B) and dorsal (C) view; right scapula in lateral (D) and medial (E) view; omal fragments of the left coracoid in medial (F) and lateral (H) view and of the right coracoid in dorsal (G) and medial (I) view. Specimens in A, B, and F-I are coated in ammonium chloride. Abbreviations: AC, apex carina; Ac, acromion; CMC, crista medialis carinae; CtS, cotyla scapularis; CoIS, collum scapulae; FAC, facies articularis clavicularis; FAH, facies articularis humeralis; FoNS, foramen nervi supracoracoidei; ILA, impressio ligamenti acrocoracohumeralis; LI, labrum internum; MD, margo dorsalis; PC, pila carinae; PM, pila medialis; P. Procor., processus procoracoideus; SAC, sulcus articularis coracoideus; SE, spina externa; SMS, sulcus m. supracoracoidei; TC, tuberculum coracoideum. Scale bars are 10 mm.

### **Sternum (Figure 2.4A–C).**

The cranial section of the sternum of SAMA P.54998 is preserved, retaining the structure of the spina externa, pila carinae, crista medialis carinae, apex carinae, the left sulcus articularis coracoideus, and the left labrum internum. It is characterised by:

**(Trait 1)** A spina interna is absent; a small notch exists in its place. **(2)** The spina externa (Figure 2.4B: SE) is 6.4 mm wide at its base, 4.7 mm wide at its blunt tip and 4.2 mm long. In cranial view, the spina externa is triangular as a medial crista forming a lobe projecting 3.6 mm ventrally. The base of the spina externa is broader than the apex carinae (4.0 mm). **(3)** The crista medialis carinae (Figure 2.4A: CMC) is short, extending dorsally from the apex carinae to mid-height of the pila carinae with a low profile in lateral view. More dorsad, the pila carinae is smooth to the base of the spina externa. **(4)** The pila carinae (Figure 2.4A: PC) is robust for its size, measuring 5.2 mm at mid-depth. It is 23.3 mm long from the ventral margin of the carina sterni to where the pila carinae meets the spina externa. **(5)** The apex carinae (Figure 2.4A: AC) at 4.0 mm wide, is noticeably expanded from the width of the pila carinae immediately dorsal to it (3.0). **(6)** The apex carinae is rounded, with no hooked projection extending cranially. **(7)** The maximum carina depth below the sternal basin is roughly equivalent to basin depth below the costal margin, typical of most accipitrids except for certain vulture species (Aegypiinae). **(8)** The apex carinae is set well caudally [assuming the junction of the carina with the pars cardiaca is aligned horizontally] from the base of the spina externa. **(9)** There are no small, dispersed pneumatic foramina present dorsally in the body of the sternum. **(10)** The small part of the carina sterni preserved narrows caudally from the pila carinae. **(11)** The left sulcus articularis coracoideus (Figure 2.4B: SAC) is 4.3 mm dorsoventrally deep, and extends to the midline of the sternum, directly dorsal to the spina externa, where it does not overlap the right sulcus. **(12)** The left labrum internum (Figure 2.4A: LI) is maximally 4.2 mm deep and 2.8 mm wide in dorsal view as preserved. **(13)** A pila medialis (Figure 2.4C: PM), 2.1 mm wide, on the dorsal face of the sternum separates two deep, pneumatic fossae in the pars cardiaca.

Extant accipitrid subfamilies differ as follows:

**(3)** The crista medialis extends to the base of the spina externa in members of all subfamilies except Aegypiinae. **(8)** The apex carinae lies directly ventral to the base of the spina externa, or projects more cranially, in species in all subfamilies except for Gypaetinae and Aegypiinae. **(11)** The sulci articularis coracoidei overlap in all species except for *Gampsonyx swainsonii* (Elaninae) and *Sarcogyps calvus* (Aegypiinae). **(13)** No species in any subfamily has a distinct pila medialis separating pneumatic fossae in the pars cardiaca, which is thus an autapomorphy suggesting subfamilial distinction for the new species.

The sternum is overall most similar to that of species of Aegyptiinae (see Appendix 3 for comparisons with extant species).

**Coracoid (Figure 2.4F–I).**

The well-preserved left and right omal ends and fragments of both sternal ends of the coracoids of SAMA P.54998 were recovered. They reveal the following:

**(Trait 1)** A foramen nervi supracoracoidei (Figure 2.4G: FoNS) is present and located adjacent to the shaft rather than near the medial margin of the processus procoracoideus; **(2)** The foramen lacks an opening into the corpus; and **(3)** it is small, about 1 mm in width, and positioned just sternal of the cotyla scapularis. **(4)** A large (6 mm wide) pneumatic foramen is present in the sulcus m. supracoracoidei (Figure 2.4F: SMS). The width of the sulcus is approximately 14.5 mm from the ventrosternal corner of the facies articularis clavicularis to the facies articularis humeralis, and 12.8 mm from the medial margin to the laterodorsal margin immediately cranial to the cotyla scapularis. **(5)** The facies articularis clavicularis (Figure 2.4F: FAC) is large, broad, and clearly delineated sternally by a crista that dorsally overhangs the aforementioned foramen, and ventrally is a low non-overhanging crista. The sternal margin of this facet is straight with no notch, nor dorsal or ventral projections directed sternally. **(6)** The cotyla scapularis (Figure 2.4G: CtS), preserved on the right omal fragment, is deep and large (6.7 mm wide by 5.7 mm long) in relation to the processus procoracoideus and triangular shaped. **(7)** The facies articularis humeralis (Figure 2.4G: FAH) is 7.7 mm wide and 12.8 mm long. **(8)** The impressio lig. acrocoracohumeralis (Figure 2.4H: ILA), best seen on the left specimen, forms a distinct sulcus ~7 mm wide by 18.1 mm long on the processus acrocoracoideus, although this may be exaggerated by damage to the fossil. **(9)** The processus procoracoideus (Figure 2.4I: P. Procor.) forms a short projection medially, barely as long again as the cotyla scapularis width, with its tip sharply angling ventrally towards the medial face to partly enclose the triosseal canal. **(10)** The best preserved sternal-end fragment shows that the angulus medialis is acute, forming a 30-45° angle. **(11)** The medial side of the facies articularis sternalis is 6.5 mm wide at its broadest point, and shallow, with little deepening towards the dorsal margin.

Extant accipitrid subfamilies differ as follows:

**(Trait 5)** The sternal margin of the facies articularis clavicularis does not form a crest overhanging the sulcus supracoracoideus in Elaninae, Perninae (except *Chondrohierax uncinatus*), Gypaetinae (except *Polyboroides typus*), Aegyptiinae, Haliaeetinae, Accipitrinae, and Buteoninae. **(8)** The impressio lig. acrocoracohumeralis is shallow in Elaninae, Perninae, Gypaetinae, Accipitrinae, and Buteoninae. **(9)** In all subfamilies, the processus

procoracoideus does not, or barely, angles ventrally towards the medial face.

The coracoid is overall most similar to that of species of Aegyptiinae, Accipitrinae and Buteoninae (see Appendix 3 for further comparisons with extant species).

### **Scapula (Figure 2.4D, E).**

Both the left and right scapulae of *Archaeohierax sylvestris* gen. et. sp. nov. are almost complete, lacking only the distal third or less of the corpus scapulae. In total, the preserved craniocaudal length of the scapulae is 56.8 mm (left) and 53.3 mm (right).

The proximal dorsoventral width of the scapula is 14.4 mm from the acromion to the ventral side of the facies articularis humeralis. **(1)** The tuberculum coracoideum (Figure 2.4E: TC) is low and barely cranially prominent dorsal of the facies articularis humeralis. **(2)** The acromion (Figure 2.4D: Ac) has a distinct cranio-laterally oriented crista lig. acrocoracoacromiali dorsally, and a robust rounded medial prominence. **(3)** There are no pneumatic foramina or fossae present in the acromion cranially, **(4)** nor on the lateral or medial facies between the acromion and the facies articularis humeralis. **(5)** The facies articularis humeralis (Figure 2.4D: FAH) is quite large and broad, measuring 6.3 mm dorsoventrally by 10.8 mm craniocaudally on the left specimen; 6.3 mm by 10.4 mm on the right. **(6)** The acromion barely projecting proximally/cranially of the tuberculum coracoideum. **(7)** Minimum dorsoventral depth of the collum scapulae (Figure 2.4E: CoIS) is 6.3 mm. **(8)** While the extremitas caudalis is broken off, the corpus scapulae is elongate and moderately narrow, **(9)** but it greatly increases in depth caudal to the margo dorsalis ridge (Figure 2.4D: MD), attaining a maximum dorsoventral depth of 8.1 mm. **(10)** The lateral face dorsal to and immediately posterior to the facies articularis humeralis is flat. **(11)** The ligamental attachment on the margo dorsalis has a very small prominence and is not elevated dorsally above the rest of the margo dorsalis.

Extant accipitrid subfamilies differ as follows (key characters only):

**(Trait 6)** The acromion strongly projects cranially in all species except in pernines (*Chondrohierax uncinatus*, *Pernis apivorus*, *Aviceda subcristata*), and *Ictinia mississippiensis* (Buteoninae).

The scapula is overall most similar to that of species of Elaninae (see Appendix 3 for further comparisons with extant species).

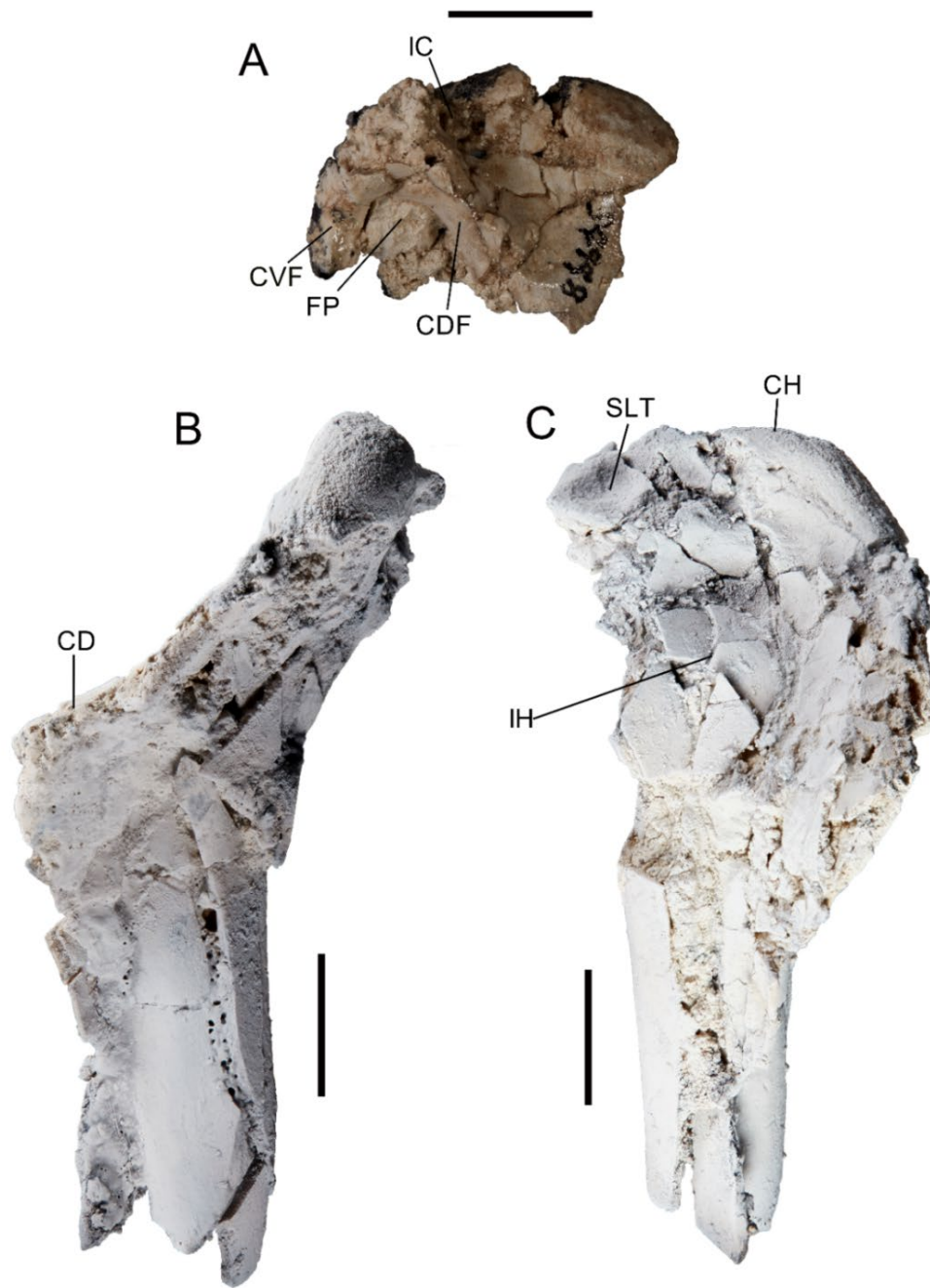


**Figure 2.5:** Proximal humerus fragments of *Archaehierax sylvestris* gen. et. sp. nov. SAMA P.54998: right, in caudal view (A); left, in dorsal (B) and cranial (C) views. Specimens in B and C are coated in ammonium chloride. Abbreviations: CD, crista deltopectoralis; CDF, crus dorsale fossae; CH, caput humeri; CVF, crus ventrale fossae; FP, fossa pneumotricipitalis; IC, incisura capitis; IH, intumescencia humeri; SLT, sulcus ligamenti transversus. Scale bars are 10 mm.

***Humerus (Figure 2.5).***

The humeri are poorly preserved in SAMA P.54998. Only the caput humeri, crus

dorsale fossae, fossa pneumotricipitalis, and the incisura capitis of the proximal end of the right humerus is preserved. The left humerus is more complete, preserving about 60 mm of proximodistal length of the proximal end including the caput humeri, crus dorsale fossae, fossa pneumotricipitalis, incisura capitis, sulcus lig. transversus, facies bicipitalis, crista deltopectoralis, and some of the proximal shaft. However, there is also significant breakage and fracturing of the bone surface in this specimen, which has resulted in the loss of the tuberculum dorsale, the ventral margin of the crista bicipitalis, tuberculum ventrale, and sulcus n. coracobrachialis. These specimens reveal the following:

(1) The incisura capitis (Figure 2.5A: IC), as best observed in the left humerus, is shallow and lacks secondary deepening. (2) There is no visible ligamental scar in the distal incisura capitis. (3) The caput humeri (Figure 2.5A: CH) is quite flattened, projecting proximal to the incisura capitis only a few millimetres. (4) The fossa pneumotricipitalis (Figure 2.5A: FP) was large and deep, although breakage precludes assessing its former width. The better-preserved left specimen shows it was minimally 7.7 mm wide. (5) The crus dorsale fossae (Figure 2.5A: CDF) is broad, measuring 4.0 mm wide, and is caudally convex. (6) The sulcus lig. transversus (Figure 2.5C: SLT), best seen in the left humerus, is shallow but well defined, and seems continuous between the ventral and dorsal sections. Ventrally, the sulcus is deep and round, measuring 6.3 mm wide by 4.5 mm long cranial to the incisura capitis. The crista deltopectoralis (Figure 2.5B: CrD), while quite fractured, is preserved in its entirety in the left specimen. Preserved length is 42.7 mm from the assumed position of the tuberculum dorsale to its distal end. (7) The profile of the proximal section of the dorsal margin of the crista between its origin near the tuberculum dorsale and the angulus cristae of the crista deltopectoralis is flat in a ventro-cranial view. (8) The angulus cristae of the crista deltopectoralis is very prominent and distinctly triangular in dorsal view. (9) Distally, the crista deltopectoralis, while fractured, projected mainly cranially (shaft margin visible proximal to the distal point of crista).

Extant accipitrid subfamilies differ as follows:

(Trait 1) In all subfamilies except Aegypiinae and *Spilornis cheela* in Circaetinae, species have a deep incisura capitis; (3) The caput humeri is more elevated proximal to the incisura capitis and tuberculum ventrale, ranging from a moderate (Elaninae) to a large proximal projection (all other subfamilies) so a low flattened caput is identified as an autapomorphy of the species.

The proximal humerus is overall most similar to that of species of Elaninae, Aegypiinae, Aquilinae, Haliaeetinae and Buteoninae (see Appendix 3 for comparisons with extant species).



**Figure 2.6:** *Archaehierax sylvestris* gen. et. sp. nov. SAMA P.54998 left radius in ventral (A) and dorsal (B) view, and left ulna in ventral (C), cranial (D) and caudal (E) view. Abbreviations: CD, condylus dorsalis; CrI, crista intercotylaris; CtV, cotyla ventralis; CV, condylus ventralis; DL, depressio ligamentosa; DR, depressio radialis; FAR, facies articularis radiocarpalis; FAU, facies articularis ulnaris; IB, impressio brachialis; IR, incisura radialis; IST, impressio scapulotricipitis; IT, incisura tendinosa; ITC, incisura tuberculum carpalis; PCD, processus cotylaris dorsalis; SI, sulcus intercondylaris; ST, sulcus tendineus; T, tuberculum; TAV, tuberculum aponeurosis ventralis; TBR, tuberculum bicipitale radiale; TCr, tuberculum carpalis; TLCV, tuberculum ligamentum collateralis ventralis. Scale bar 10 mm.

### ***Ulna (Figure 2.6C–E).***

SAMA P.54998 preserves a near-complete left ulna, reassembled from fragments, that is only missing the olecranon, parts of the ventral margin of the cotyla ventralis contiguous with the olecranon, and the caudodorsal margin of the cotyla dorsalis. The distal right ulna is also preserved with the condyles mostly intact, with only the ventrocaudal margin of the condylus dorsalis and condylus ventralis worn away. They reveal the following features:

**(1)** The ulna is largely straight in dorsal and ventral view, with only very slight caudal curvature towards the proximal and distal ends. The processus cotylaris dorsalis projects distally of the cotyla ventralis (Figure 2.6E: PCD), is 5.8 mm wide, and **(2)** is quadrangular in shape with a flattened dorsal tip between parallel equal-length proximodorsal and distoventral sides. **(3)** The cotylae are shallow, separating by a moderately proximally protruding crista intercotylaris (Figure 2.6D: Cri). Breakage precludes assessing if a pneumatic fossa or foramen was present caudal of the cotylaris dorsalis. **(4)** The impressio scapulo-tricipitis (Figure 2.6E: IST) is shallow. **(5)** The incisura radialis (Figure 2.6D: IR), defined by the margin of the cotyla ventralis proximoventrally, the tuberculum cranialis distally, and a ridge descending ventrodistally from the base of the processus cotylaris dorsalis dorsally, is shallow. **(6)** Distal to the incisura radialis two tubercula are present, one on the cranial face is large and round (3.8 mm wide) and distinctly projects from the shaft (Figure 2.6D, E: T), the other smaller (1.9 mm wide) and flatter positioned adjacent to it on the ventral face. **(7)** The impressio brachialis (Figure 2.6C: IB) is shallow, with the base flat and not depressed relative to the shaft and is 12 mm long proximodistally. The midshaft of the left specimen is 7.7 mm craniocaudally wide in dorsal aspect. **(8)** The papillae remigales caudales form low, barely prominent scars, which is typical of most accipitrids. The distal end of the ulna measures 12.9 mm wide (left) and 12.2 mm wide (right) between the cranial point of the tuberculum carpale (Figure 2.6C: TCr) and the caudal margin of the condylus dorsalis (Figure 2.6C: CD) in ventral aspect. **(9)** The tuberculum carpale is short and blunt, or rounded, in dorsal and ventral view, **(10)** with a flattened facet directed ventrodistally. **(11)** The incisura tuberculum carpale (Figure 2.6C: ITC) forms a distinct notch separating the tuberculum carpale and condylus ventralis (Figure 2.6C: CV) when viewed in dorsal aspect. The condylus dorsalis (left specimen) is 13.5 mm long proximodistally along its caudal margin in ventral aspect, and 9.3 mm deep from the caudal margin to the incisura tendinosa, in caudodorsal view. **(12)** The caudal margin of the condylus dorsalis forms a continuous curve in the proximal half, best visible in either craniodorsal or caudodorsal view, interrupted only by a small notch for the incisura tendinosa (Figure 2.6E: IT). **(13)** The incisura tendinosa lies between the condylus dorsalis and the condylus ventralis (dorsal aspect), though it does

not quite separate the two proximodistally. **(14)** The depressio radialis (Figure 2.6C: DR) is shallow and not pneumatized. **(15)** The sulcus intercondylaris (Figure 2.6C: SI) forms a relatively deep v-shape in ventral aspect. **(16)** The condylus ventralis distinctly projects distocranially, and measures 5.7 mm wide (in ventral aspect) by 11.2 mm deep (in cranial aspect).

Extant accipitrid subfamilies differ as follows:

**(Trait 1)** The proximal shaft is notably curved cranially in elanines, most pernines (excepting *Aviceda subcristata*, *Lophoictinia isura* and *Hamirostra melanosternon*), and buteonines (except species of *Circus*).

The ulna is overall most similar to that of species of Circaetinae (see Appendix 3 for comparisons with extant species).

### **Radius (Figure 2.6A, B).**

In SAMA P.54998 the left radius is complete, preserving most features of the proximal (cotyla humeralis slightly worn ventrocaudally) and distal ends.

The cotyla humeralis is large, measuring 5.5 mm deep dorsoventrally, and 4.1 mm wide. It shows the following:

A tuberculum bicipitale radiale (Figure 2.6A: TBR) is located 5.4 mm distal of the facies articularis ulnaris on the dorsal face. The tuberculum has **(1)** a large, deep, non-pneumatic fossa (2.6 mm wide by 3.8 mm proximodistal length) on it, and **(2)** has a distinct profile in cranial view as a low, quadrangular ridge. **(3)** The sulcus tendineus (Figure 2.6B: ST) is very shallow, barely differentiated from the corpus. **(5)** The tuberculum aponeurosis ventralis (Figure 2.6A: TAV) projects ventrally at approximately 60-70°, and its tip is rounded. **(6)** The facies articularis radiocarpalis (Figure 2.6A: FAR) is quite flat in dorsal view, but slightly curves out distally from the tuberculum aponeurosis ventralis to the opposite margin. **(7)** The depressio ligamentosa (Figure 2.6A: DL) on the ventral face of the distal end is deep but lacks pneumatism. **(8)** The facies articularis ulnaris (Figure 2.6A, B: FAU) forms a prominent bulb that projects out ventrally, and which has a deep notch on the proximal margin that gives it a double-peaked appearance.

Extant accipitrid subfamilies differ as follows:

**(Trait 1)** The fossa associated with the tuberculum bicipitalis is shallow in all species except some pernines e.g., *Elanoides forficatus* (absent) and *Pernis apivorus* (deep). **(5)** The tuberculum aponeurosis ventralis projects at a more abrupt angle in all taxa except *N. percnopterus* (Gypaetinae), species of *Gyps* (Aegypiinae), and *H. morphnoides* and *A.*

*chrysaetos* (Aquilinae). **(7)** The depressio ligamentosa is shallower in Perninae (except *E. forficatus*), Gypaetinae, Circaetinae, Aquilinae, Haliaeetinae, and Buteoninae.

The radius is overall most similar to that of species of Haliaeetinae and Gypaetinae (see Appendix 3 for comparisons with extant species).

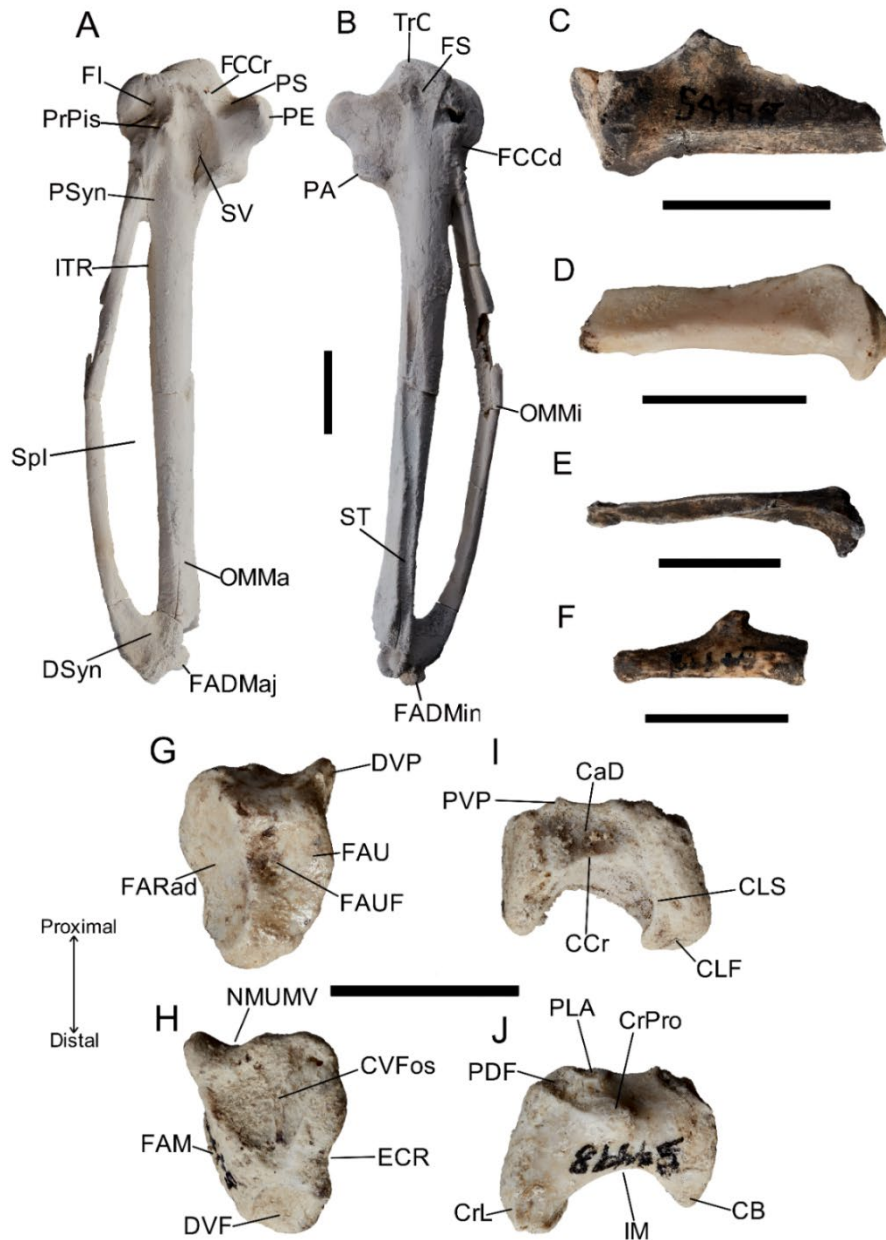


**Figure 2.7:** *Archaeohierax sylvestris* Gen. et. sp. nov. SAMA P.54998 left carpometacarpus in ventral (A) and dorsal (B) view, manual phalanx digiti majoris II.1 broken distally (C), manual phalanx digiti majoris II.2 (D), manual phalanx digiti alularis I.1 (E), manual phalanx digiti minoris III.1 (F), os carpale radiale in caudal (G) and cranial (H) view, and os carpale ulnare in caudal (I) and cranial (J) view. Carpometacarpus coated with ammonium chloride. Abbreviations: CaD, caudal fossa; CB, crus breve; CCr, caudal crista; CrL, crus longus; CLF, crus longus fossa; CLS, crus longus sulcus; CrPro, cranial projection; CVFos, cranial ventral fossa; DSyn, distal synostosis; DVF, dorsal ventral fossa; DVP, distoventral projection; ECR, extensor carpi radialis; FADMaj, facies articularis digitalis major; FADMin, facies articularis digitalis minor; FAM, facies articularis metacarpalis; FARad, facies articularis radialis; FAU, facies articularis ulnaris; FAUF, facies articularis ulnaris fossa; FCCr, fovea carpalis cranialis; FCCd, fovea carpalis caudalis; FI, fossa infratrochlearis; FS, fossa supratrochlearis; IM, incisura metacarpalis; ITR, intermetacarpal tuberosity; NMUMV, notch for musculus ulnometacarpalis ventralis; OMMa, os metacarpale majus; OMMi, os metacarpale minus; PA, processus alularis; PDF, proximodorsal fossa; PE, processus extensorius; PLA, proximal ligament attachment; PrPis, processus pisiformis; PS, proximal sulcus; PSyn, proximal synostosis; PVP, proximoventral projection; Spl, spatium intermetacarpale; ST, sulcus tendineus; SV, sulcus on ventral facies; TrC, trochlea carpalis. Scale bars 10 mm.

### ***Os carpale radiale (Figure 2.7G, H).***

The left os carpale radiale is complete in SAMA P.54998.

Measurements: proximodistal length 8.6 mm, dorsoventral width 12.3 mm, and depth 5.4 mm.

It has the following features, terminology from Mayr (2014): **(1)** The distoventral projection (Figure 2.7G: DVP) is small and pointed, oriented at an angle between 45-60°. **(2)** The notch for the musculus ulnometacarpalis ventralis (Figure 2.7H: NMUMV) is distinct, but shallow. **(3)** The facies articularis metacarpalis (Figure 2.7H: FAM) slightly projects distally from the cranial face in cranial view. **(4)** The sulcus for the musculus extensor carpi radialis (Figure 2.7H: ECR) is shallow, forming a gentle curve at about a 160° angle between the ventral and dorsal ends. **(5)** A broad, deep fossa covers most of the ventral half of the cranial face (Figure 2.7H: CVFos), which is open towards the proximo-ventral corner. **(6)** A second smaller and deep fossa is present on the dorsal half of the cranial face (Figure 2.7H: DVF) and is apneumatic and oriented more craniodorsally. **(7)** The facies articularis radialis (Figure 2.7G: FARad) is broad (depth ~5.7 mm, dorsoventral width 11.0 mm) and strongly marked on the caudal face. **(8)** The caudal face has a small but deep fossa (Figure 2.7G: FAUF), set in the facies articularis ulnaris (Figure 2.7G: FAU) close towards the ventral end. **(9)** The caudal margin of the facies articularis metacarpalis forms a convex continuous curve from the ventral margin to the dorsal margin.

The os carpale radiale is overall most similar to that of species of Elaninae and Buteoninae (see Appendix 3 for comparisons with extant species).

### ***Os carpale ulnare (Figure 2.7I, J).***

Both the right and left os carpale ulnare are complete in SAMA P.54998.

Measurements (mm) right/left: dorsoventral width 12.2/11.8, craniocaudal depth (excluding cranial projection) 4.4/4.6, and proximodistal length 9.9/9.2. They show:

**(1)** A distinct projection, roughly in the centre of the cranial face (Figure 2.7J: CrPro), extends well cranially above the margin of the proximal ligament attachment, and lacks a prominent ridge that makes it contiguous with the proximodorsal corner. **(2)** The rest of the cranial face is roughly equal in cranial height towards the crus breve (Figure 2.7: CB) and the crus longus (Figure 2.7J: CrL). **(3)** The proximodorsal corner of the crus longus is distinctly notched by a deepened apneumatic fossa (Figure 2.7J: PDF). **(4)** The proximal margin of the cranial face has a distinct ligament attachment point (Figure 2.7J: PLA), projecting slightly proximally above the face and positioned ventrally adjacent to the proximal end of the crus longus. **(5)** The crus breve is slightly shorter (8.7 mm long) in the right

specimen, than total length (9.4 mm) from the proximal point of the crus longus to the distal margin, **(6)** and has a flattened, ventral face. **(7)** On the caudal face, a very low projection is present on the proximal margin immediately adjacent to the ventral crus breve (Figure 2.7I: PVP). **(8)** A distinct, deep impression is present in the caudal surface (Figure 2.7I: CaD). **(9)** This depression is separated from the rest of the distal face by a distinct but low crista that extends dorsoventrally across the face from the caudal projection (Figure 2.7I: CCr), connecting to both the crus breve and crus longus. **(10)** The incisura metacarpalis is deep and broadly v-shaped (Figure 2.7J: IM), with the peak offset towards the crus breve. **(11)** A very shallow sulcus is seen running along the proximodistal extent of the caudal face of the crus longus (Figure 2.7I: CLS), **(12)** which terminates in a shallow fossa on the distal point of the crus (Figure 2.7I: CLF).

Extant accipitrid subfamilies differ as follows:

**(Trait 2)** The ventral cranial face is higher set cranially than the dorsal cranial face in all subfamilies except Accipitrinae. **(3)** There is no notch on the proximal end of the crus longus in all subfamilies except in the genera *Aquila* (Aquilinae), *Haliaeetus* (Haliaeetinae) and *Buteo* (Buteoninae), which have a shallow notch. **(8)** There is no deepened depression on the caudal face in all subfamilies except Aquilinae, *Aegypius monachus* (Aegyptiinae), Accipitrinae, and the genus *Buteo* (Buteoninae). **(9)** There is no raised crista on the caudal face in all subfamilies except in the genus *Buteo* (Buteoninae).

The os carpale ulnare is overall most similar to that of species of Elaninae, Perninae, Gypaetinae and Aquilinae (see Appendix 3 for further comparisons with extant species).

### ***Carpometacarpus* (Figure 2.7A, B).**

For SAMA P.54998, the left carpometacarpus is almost complete, missing only the cranial section of the facies articularis digitalis majus.

**(1)** The fossa infratrochlearis (Figure 2.7A: FI) is deep and lacks pneumatization. **(2)** A rounded ridge extending from the processus pisiformis to the trochlear rim separates the fossa infratrochlearis from **(3)** an extremely deep sulcus (Figure 2.7A: SV) between the processus pisiformis and the processus extensorius. This sulcus is elongate and extends from the trochlea carpalis (Figure 2.7B: TrC) to adjacent to the processus alularis (Figure 2.7B: PA). **(4)** The fossa supratrochlearis (Figure 2.7B: FS), which is caudoventrally positioned on the ventral face of the proximal end, is shallow and lacks pneumatization. **(5)** There is a shallow sulcus on the ventral face, on the proximal margin at the base of the processus extensorius just distal to the trochlea carpalis (Figure 2.7A: PS). **(6)** The fovea carpalis cranialis (Figure 2.7A: FCCr) is shallow and apneumatic. **(7)** The fovea carpalis

caudalis (Figure 2.7B: FCCd) is very shallow and apneumatic. **(8)** The ventral rim of the trochlea carpale projects strongly caudally and distally is short, terminating slightly distal to the level of the processus pisiformis. **(9)** The proximal margin of the processus extensorius (Figure 2.7A: PE) and the trochlea carpale forms an approximately 120° angle, with the proximal margin slightly upturned proximally. From base to tip, the processus extensorius measures 7.7 mm in craniocaudal width, and is 39% of the 19.6 mm proximal width of the carpometacarpus. **(10)** The proximodorsal margin of the processus extensorius forms a sharp crista that dorsally overhangs the dorsal face of the processus. **(11)** The processus alularis protrudes slightly cranially in a triangular bulge, with a single curved articular facet distally. **(12)** The processus alularis is separated from the caudal surface of the shaft by a small notch on the dorsal face. **(13)** The processus pisiformis (Figure 2.7A: PrPis) strongly projects ventrally in caudal and cranial view and is positioned central on the ventral face between the processus extensorius and the caudal margin of the trochlea carpalis. It is separated from the spatium intermetacarpale (Figure 2.7A: Spl) by a dorsoventral length of 10.5 mm. **(14)** This region of separation between the processus pisiformis and spatium intermetacarpale is occupied by a shallow sulcus that is bound by the os metacarpale minus in its distal half. **(15)** The synostosal region distal to the processus alularis is wider craniocaudally than it is long dorsoventrally. **(16)** The intermetacarpal tuberosity (Figure 2.7A: ITR), which is the scar for the insertion of the m. extensor metacarpi ulnaris has almost no caudal projection and is positioned well distal of the proximal synostosis (Figure 2.7A: Psyn). **(17)** The sulcus tendineus (Figure 2.7B: ST) is primarily located on the dorsal face of the shaft. **(18)** The sulcus tendineus is broad. **(19)** The proximal region of the os metacarpale minus has a distinct groove on the caudal face, which lacks any pneumatisation. **(20)** The os metacarpale minus (Figure 2.7B: OMMi) is slightly arched caudally when viewed in ventral and dorsal aspect. **(21)** The facies articularis digitalis minor (Figure 2.7B: FADMin) projects further distally than the preserved facies articularis digitalis major (Figure 2.7A: FADMaj). **(22)** The length between the distal point of the facies articularis digitalis minor and the spatium intermetacarpale is approximately equal to the width of the spatium. **(23)** The distal synostosis (Figure 2.7A: DSyn) is very short. **(24)** The os metacarpale majus (Figure 2.7A: OMMa) has a markedly flattened cranial face and is dorsoventrally deeper than it is craniocaudally wide. **(25)** The sulcus interosseus positioned in the distal synostosis is slightly deepened.

Measurements – see Appendix 2 Table 1; overall, the carpometacarpus has a proximal craniocaudal width that is equivalent to 25% of the total length, which is moderately gracile.

Extant accipitrid subfamilies differ as follows:

**(Trait 1)** The fossa infratrochlearis is shallow, except in Perninae (deep in *Pernis apivorus* and *Chondrohierax uncinatus*, the latter also pneumatic) and Gypaetinae (deep).

**(19)** The proximal section of the os metacarpale minus has a shallower groove, except in *P. typus* (Gypaetinae, deep) and *Haliaeetus leucocephalus* (Haliaeetinae, deep), or in Elaninae (flat, ungrooved).

The carpometacarpus is overall most similar to that of species of Buteoninae (see Appendix 3 for further comparisons with extant species).

### **Manus (Figure 2.7C–F).**

The manus bones are moderately well-preserved in SAMA P.54998, with a mostly intact left phalanx digiti alulae (L MI.1), complete left phalanx digiti minoris (L MIII.1) and left phalanx digiti majoris 2 (L MII.2), and a mostly intact R MI.1, partial R MII.1 and fragment of the R MII.2.

**(1)** The proximal L MI.1 has a dorsoventral width of 6.6 mm and a craniocaudal depth of 6.5 mm, and from proximal view is triangular. **(2)** The cranial margin is tapered into a thin crista that continues along the length of the preserved bone. **(3)** A small tuberculum is present on the caudal margin of the ventral face, close to the proximal end. **(4)** The dorsal margin and face of the proximal end is much more protruding than the ventral margin and face and has two ligament attachment points on its dorsal surface. **(5)** The width of the bone narrows distally. **(6)** The L MIII.1 is 14.2 mm long and has a prominent caudal projection slightly less than halfway distally along its length, the tip of which is oriented caudoproximally. **(7)** Both the dorsal and ventral face lack any sort of depression or sulcus. Only the proximal end of the MII.1 is preserved, which is 8.3 mm wide by 6.9 mm deep. **(8)** The caudal margin projects caudally into a thin crista, and a deep depression is visible just distal of the projecting point. The left MII.2 is 24.1 mm long and proximally has a dorsoventral height of 5.8 mm and a craniocaudal depth of 4.8 mm. **(9)** The caudal margin forms a thin crista. **(10)** The proximal quarter of the cranial margin is also flattened, but then expands notably with the presence a shallow sulcus extending to the distal end. **(11)** On the dorsal surface, a low ridge is present at the proximal end, with a small but deep fossa set into the caudal side of it. **(12)** A similar fossa is also set into the caudal side of this ridge in proximal view, just distal of the articular facet. **(13)** The ventral face has a deep depression lacking pneumatic foramina just distal of the proximal end.

The manus bones are overall most similar to those of species of Perninae (see Appendix 3 for further comparisons with extant species).

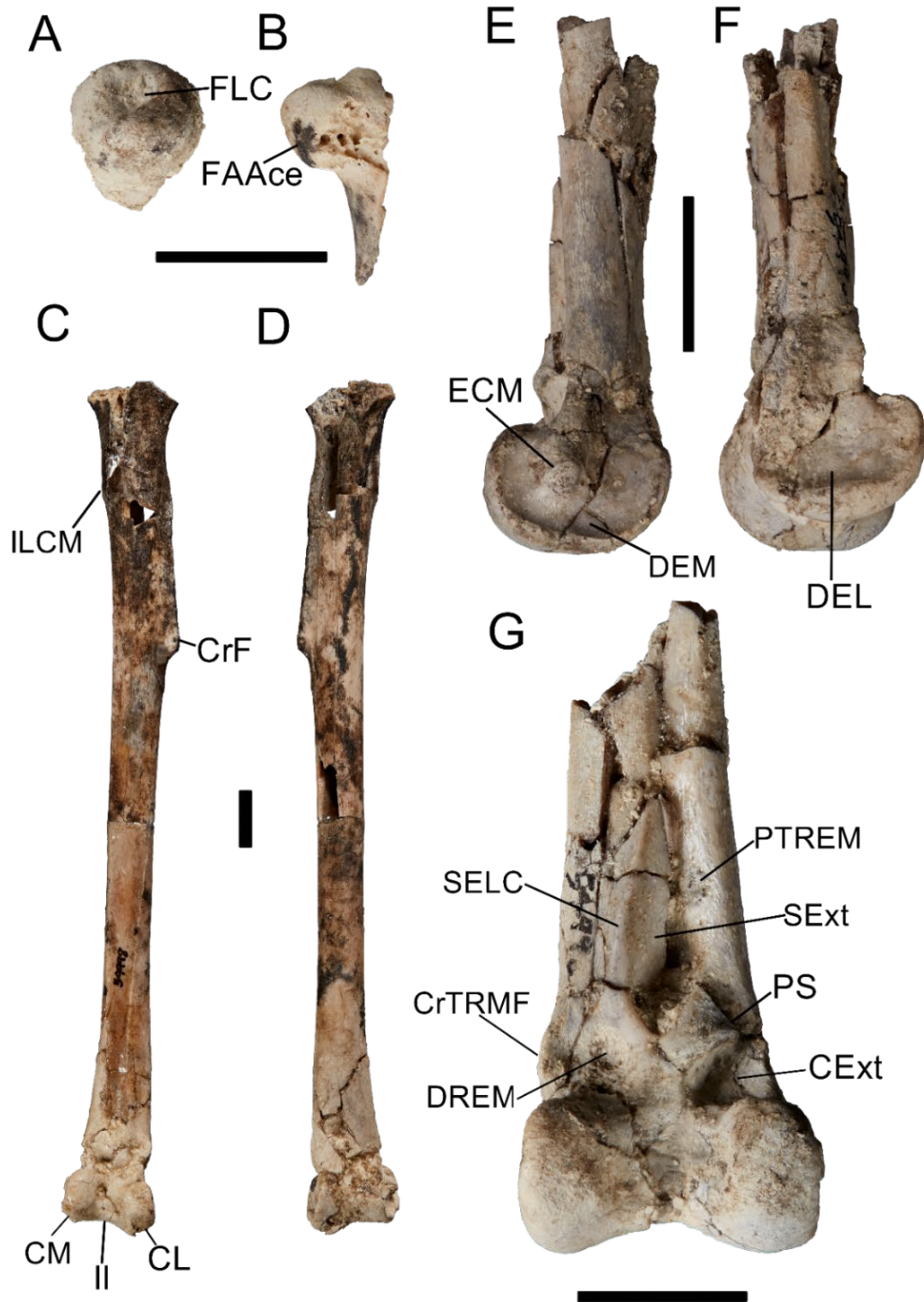


**Figure 2.8:** *Archaeohierax sylvestris* gen. et. sp. nov. SAMA P.54998 proximal left and right femoral fragments in medial (A) and cranial (B) view, left tibiotarsus in cranial (C) and caudal (D) aspect, and distal right tibiotarsus (E-G) in medial (E) lateral (F) and cranial (G) view. Abbreviations: CExt, canalis extensorius; CrF, crista fibularis; CL, condylus lateralis; CM, condylus medialis; CrTRMF, cranial tuberculum retinaculi musculus fibularis; DEL, depressio epicondylaris lateralis; DEM, depressio epicondylaris medialis; DREM, distal insertion retinaculum extensorium tibiotarsi; ECM, epicondylus medialis; FAAce, facies articularis acetabularis; FLC, fovea ligamenti capitis; II, incisura intercondylaris; ILCM, impressio ligamenti collateralis medialis; PTREM, proximal insertion scar retinaculum extensorium tibiotarsi; PS, pons supratendineus; SExt, sulcus extensorius; SELC, lateral crista beside sulcus extensorius. Scale bars 10 mm.

### ***Femur (Figure 2.8A, B).***

In SAMA P.54998, only the caput of both femora has been preserved, preserving the articularis acetabularis face and the fovea ligamenti capitis. The width of the caput is 7.6 mm. The fovea ligament capitis (Figure 2.8A: FLC) is shallow and set in the proximal margin of the caput. The articularis acetabularis face (Figure 2.8B: FAAce) is not well defined from the medial face.

### ***Tibiotarsus (Figure 2.8C–G).***

Both the right and left tibiotarsi are preserved in SAMA P.54998. The left tibiotarsus is almost complete with only the proximal articular surfaces missing. It preserves the base of the cnemial crests and the entire crista fibularis, but damage to the distal end obscures the details of the pons supratendineus, the tuberculum retinaculum m. fibularis, and the distal insertion scar for the retinaculum extensorium tibiotarsi. The right tibiotarsus is missing the entire proximal end, and the distal end could not be reconnected to the shaft but is very well-preserved revealing most features of interest.

As observed on the left element, **(1)** the impressio lig. collateralis medialis (Figure 2.8C: ILCM) is a slightly elevated tuberculum on the medial face, measuring 4.5 mm wide and 8.9 mm long. **(2)** The crista fibularis (Figure 2.8C: CrF) is approximately 33.3 mm long, or roughly 24% of the preserved length (135.7 mm). **(3)** The crista fibularis is prominent, maximally projecting 2.4 mm, or approximately 26% of shaft width (9.3 mm) at the same point. **(4)** The width of the crista fibularis is greatest distally. **(5)** The cranial face directly adjacent to the crista fibularis is slightly convex. **(6)** The scar for the ligament that connected to the distal end of the fibula is approximately 34.5 mm long and extends distally along the lateral margin of the shaft, from 38 mm distal to the crista fibularis. **(7)** A distinct linea is visible on the medial margin of the shaft that extends approximately 77.4 mm proximodistally from the distal base of the impressio lig. collateralis medialis. **(8)** The cross-section of the shaft at mid length is roughly circular. **(9)** The sulcus extensorius (Figure 2.8G: SExt) is medially positioned on the distal third of the shaft and is approximately 5 mm wide at broadest, compared to a shaft width of 10.5 mm at the same section. **(10)** The lateral margin of the sulcus is bordered by a raised crista (Figure 2.8G: SELC). **(11)** The canalis extensorius (Figure 2.8G: CExt) is deep, and both openings are quite large. **(12)** The pons supratendineus (Figure 2.8G: PS) is obliquely angled at roughly 45° to the long axis, and **(13)** is distinctly arched cranially. **(14)** The distomedial margin of the pons supratendineus lies close (1.3 mm) to the medial shaft margin. **(15)** The cranial tuberculum retinaculi m. fibularis (Figure 2.8G: CrTRMF) is craniolaterally prominent. **(16)** The caudal tuberculum

retinaculi m. fibularis is low and barely projecting, but preservation is poor in this region of the bone. **(17)** The proximal scar (tuberositas retinaculum extensoris medialis, Figure 2.8G: PTREM) is separated proximally from the pons supratendineus by a distance equal to the proximodistal width of the pons. **(18)** The distal/lateral attachment of the extensor retinaculum (Figure 2.8: DREM) is marked by a deep, round fossa. **(19)** Distal width (17.5 mm) is greater than the maximum distal depth (13.4 mm) by roughly 24% (right element). **(20)** The increase in width from the shaft to the distal end is gradual and symmetrical either side. **(21)** The condyles have roughly equal craniocaudal depth in distal view, **(22)** with a deep incisura intercondylaris roughly 25% of depth of the distal end, **(23)** and the impression in the trochlea cartilaginis tibialis in caudal view forms an inverted v-shape. **(24)** The epicondylus medialis (Figure 2.8E: ECM) is large and projects well medial to the condylus medialis, being visible in cranial view, and is of moderate robustness. **(25)** The epicondyle is surrounded by a deep depressio medialis (Figure 2.8E: DEM), which is bordered by a thin but prominent crista on the margins of the condyle. **(26)** The depressio lateralis (Figure 2.8F: DEL) is shallow, and bordered by a flattened, broad crista on the distal margin of the lateral condyle. The trochlea cartilaginis tibialis is difficult to assess due to breakage, **(27)** but appears largely flat.

Extant accipitrid subfamilies differ as follows:

The medial side of the pons supratendineus is more widely separated from the medial shaft margin (**Trait 14**) in elanines, pernines except *E. forficatus*, gypaetines, aegyptiines, circaetines, aquilines, and haliaetines. **(10)** There is no crista on the lateral margin of the sulcus extensorius in elanines, gypaetines, aegyptiines, circaetines, aquilines, haliaetines, accipitrines or buteonines. **(18)** No species in any subfamily has the lateral/distal retinaculum scar in a deep fossa; it ranges from a shallow fossa (pernines, aegyptiines, circaetines, aquilines, haliaetines), to flat (elanines, some pernines, gypaetines), or slightly elevated rugose surface (accipitrines, buteonines), identifying the deep pit for the distolateral insertion of the retinaculum extensoris medialis as an autapomorphy of the fossil.

The tibiotarsus is overall most similar to that of species of Buteoninae (see Appendix 3 for further comparisons with extant species).

### ***Fibula.***

The proximal ends of the left and right fibulae are preserved in *Archaeohierax sylvestris* gen. et. sp. nov. Craniocaudal depth is about 10.2 mm, while width is 3.7 (right) and 4.0 mm (left).

**(1)** A shallow fossa is present in the cranial half of the proximal lateral face. **(2)** The caudal face has a very shallow depression just distal to the caudal projection. **(3)** The medial face has a broad but shallow sulcus that extends from near the proximal margin down the shaft.

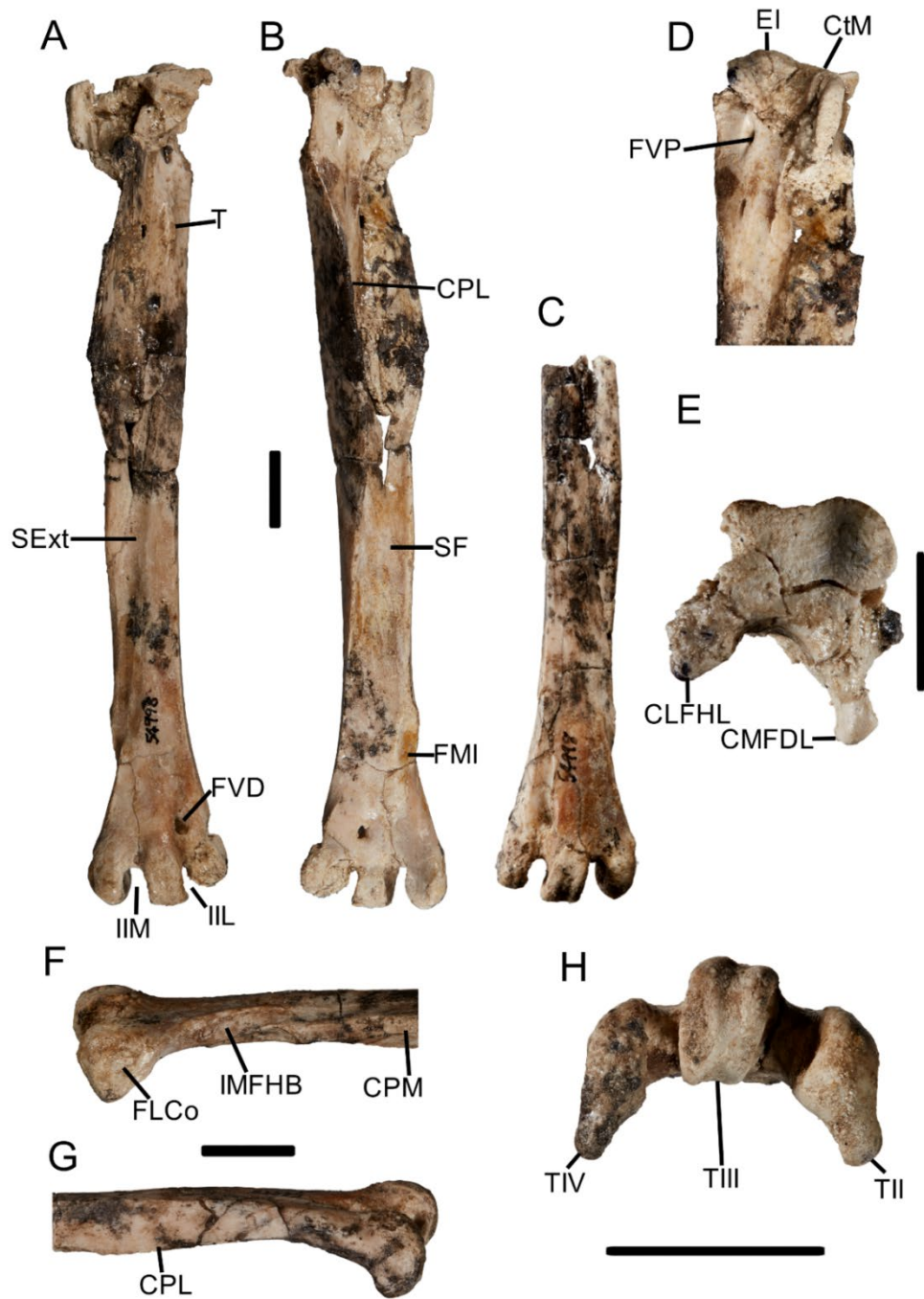


**Figure 2.9:** Tarsometatarsi of *Archaehierax sylvestris* gen. et. sp. nov. SAMA P.54998, left in dorsal (A), plantar (B), proximal end plantar (D) and proximal end (E) view, and distal right in dorsal (C), medial (F), lateral (G), and distal (H) view. Abbreviations: CLFHL, crista lateralis flexoris hallucis longus; CtM, cotyla medialis; CMFDL, crista medialis flexoris digitorum longus; CPL, crista plantares lateralis; CPM, crista plantares medialis; EI, eminentia intercotylaris; FLCo, fovea ligamentosa collateralis; FMI, fossa metatarsi I; FVD, foramen vasculare distale; FVP, foramen vasculare proximale; IIL, incisura inter lateralis; IIM, incisura intertrochlearis medialis; IMFHB, incisura musculus flexor hallucis brevis; SExt, sulcus extensorius; SF, sulcus flexorius; T, tuberculum; TII, trochlea metatarsi II; TIII, trochlea metatarsi III; TIV, trochlea metatarsi IV. Scale bars 10 mm.

### ***Tarsometatarsus (Figure 2.9).***

The right and left tarsometatarsi are both imperfectly preserved in SAMA P.54998. The left tarsometatarsus preserves the original length of the bone, though the medial half and the proximal end, from mid-length on the medial side to and including the area proximal to the foramen vasculare proximale laterale, has been dorsolaterally twisted approximately 90° relative to the rest of the bone. The lateral half is thus undistorted from just proximal to the foramen vasculare proximale laterale distally. The cotyla lateralis is missing with about half of the eminentia intercotylaris. The foramen vasculare proximale mediale is obscured by the distortion on both the dorsal and plantar side.

The right specimen has the distal half preserved well with all features, but the proximal half is so badly fragmented that nearly all identifying features are lost. Only the crista medialis hypotarsi is recognisable. The specimens reveal the following features:

**(1)** The length of the tarsometatarsus is about 66-75% of the length of the tibiotarsus (uncertainty allows for the missing proximal end of the tibiotarsus). **(2)** The length to distal width (maximal across trochleae) ratio is approximately 1:6 and shows the tarsometatarsus is moderately elongate among accipitrids. **(3)** The cotyla medialis (Figure 2.9D: CtM) is deep and with a notably convex dorsal margin. **(4)** The eminentia intercotylaris (Figure 2.9D: EI) projects a few millimetres proximally to the rim of the cotyla medialis. **(5)** The crista lateralis flexoris hallucis longus (sensu Mayr 2016) (lateral hypotarsal crista) and the crista medialis flexoris digitorum longus (medial hypotarsal crista) (Figure 2.9E: CMFDL) are not fused together plantarly, and so form a wide monosulcate hypotarsus. **(6)** The medial hypotarsal crista is distinctly proximodistally longer (8.9 mm from proximal margin to distal hook, 11.4 mm from proximal margin to distal termination point) than the lateral hypotarsal crista (6.0 mm). **(7)** The plantar depth of the lateral hypotarsal crista is 13.6 mm (76%) of the depth of the medial hypotarsal crista 17.8 mm. **(8)** In medial view, the medial hypotarsal crista has little or no hook distally. **(9)** The sulcus flexorius (Figure 2.9B: SF) is moderately deep, with the cristae plantares lateralis and medialis quite distinct and projecting plantarly. **(10)** The tuberositas m. cranialis (Figure 2.9A: T) is positioned towards the lateral side of the shaft, moderately projects dorsally to the adjacent laterodorsal margin, **(11)** is short and oval shaped, **(12)** and is positioned well distal (5.2 mm) of the lateral foramina vascularia proximalia. **(13)** The impressio retinaculi extensorii, preserved on the dislocated cotyla medialis, are a pair of distinctly projecting cristae, with the retinaculum itself unossified, which is the typical state among the accipitrids. **(14)** The fossa infracotylaris dorsalis is shallow in the undamaged section distal to the eminentia intercotylaris and towards the retinaculi. **(15)** There is a distinct sulcus extensorius (Figure 2.9A: SExt) at mid-length, which opens to the medial face around two-thirds of the distance distally along the shaft. **(16)** The

medial half of the proximal 40% of the shaft is highly compressed as it is in many accipitrids, forming a crista 1.3 mm thick. **(17)** The crista plantaris lateralis (Figure 2.9G: CPL) is well-developed, extending from the hypotarsus to level with the fossa metatarsi I. **(18)** In lateral aspect the crista plantaris lateralis is markedly projecting plantarly, deepest just proximal to mid-length. **(19)** The foramen vasculare distale (Figure 2.9A: FVD) has a diameter of about 1.6 mm and is positioned close to the incisura intertrochlearis lateralis. **(20)** The fossa metatarsi I (Figure 2.9B: FMI) is set largely on the plantar face, though partially faces medially, and measures 6.7 mm long by 3.5 mm wide. **(21)** The incisura m. flexor hallucis brevis (Figure 2.9F: IMFHB) is very distinct, passing dorsally above and distal to the fossa metatarsi I, to open plantarly between the facet in metatarsi I and trochlea metatarsi II. This state of the incisura was rarely seen in our comparative sample, with a similar but shallower incisura in species of *Haliaeetus* and *Harpia harpyja* (slightly deeper) that ends just proximal to the fossa metatarsi I. **(22)** The fossa supratrochlearis plantaris is very shallow. **(23)** The incisura intertrochlearis medialis (Figure 2.9A: IIM) and incisura intertrochlearis lateralis (Figure 2.9A: IIL) are extremely wide compared to in other Accipitridae. **(24)** From distal view, the trochleae are arched dorsally. All trochleae are higher than they are wide (excluding extension from flanges). **(25)** The plantar extent of trochleae metatarsorum II (Figure 2.9H: TII) and IV are almost identical (9.1 mm and 9.5 mm respectively, measured from right specimen). **(26)** Trochlea metatarsi III (Figure 2.9H: TIII) is located comparatively much higher dorsally, and while it has a depth of 7.7 mm, the plantar-most point of it is separated from that of trochlea metatarsi IV by about 6.6 mm. **(27)** Trochlea metatarsi II has a robust profile in distal view, with a short, robust plantar projection on its outer margin and a deep fovea ligamentosa collateralis. **(28)** Trochlea metatarsi III has a robust profile in distal view and has a shallow medial groove dorsodistally. **(29)** Trochlea metatarsi III is laterally directed relative to the shaft axis. **(30)** Trochlea metatarsi IV is the narrowest of the trochleae in distal view, with a short, thin plantar projection on the lateral margin. **(31)** The flange on trochlea metatarsi II is moderately projecting plantarly, **(32)** while the flange on trochlea metatarsi IV is quite prominent and plantar oriented. **(33)** The distal extent of the trochleae metatarsorum II and III is roughly equal and surpass distally the distal margin of IV.

Extant accipitrids differ across all subfamilies as follows:

**(9)** The sulcus flexorius is shallower, with the cristae plantares lateralis and medialis relatively low in elanines, gypaetines, circaetines, haliaeetines, and buteonines. **(21)** The incisura m. flexor hallucis brevis is shallower and shorter ending at or proximal to the fossa metatarsi I in all observed species. **(23)** In all subfamilies, the incisura intertrochleae are relatively narrower and the autapomorphically wide incisura in the fossil is one of its most characteristic features.

The tarsometatarsus is overall most similar to that of species of Elaninae (although more elongate), Aquilinae and Circaetinae (see Appendix 3 for further comparisons with extant species).



**Figure 2.10:** Image showing left pedal phalanges and os metatarsale 1 of *Archaeohierax sylvestris* gen. et. sp. nov. SAMA P.54998, digit 1 (A), digit 2 (B), digit 3 (C) and digit 4 (D) with RI.2 added given the left counterpart was broken. Scale bar 10 mm.

### ***Digit 1 (Figure 2.10A).***

The os metatarsale I in SAMA P.54998 is fairly robust, with the proximal end attenuated to a thin point. In dorsal and plantar view, the region immediately proximal to the medial side of the articular surface for I.1 is inflated, creating a  $>90^\circ$  angle just distal of the mid-length point along the 'shaft'. The attachment facet for the tarsometatarsus is quite long, extending to be adjacent with the previously mentioned inflation, but is not prominent in lateral view. The sulcus for a tendon on the distal dorsal face is bordered by a reduced crest that is positioned slightly medial of centre in the metatarsal. The phalanx I.1 is long and moderately robust, with the enlarged proximal end much wider than the corpus. Plantarly, the tubercula flexoria are enlarged, enclosing a broad sulcus that extends as a shallow attachment point to roughly midway on the corpus distally. The lateral side of the face dorsalis of the proximal end is slightly inflated into a ligamental attachment point, forming a modest, rounded mound. The foveae lig. collaterales on the distal end are very deep, and there is only a very shallow indentation set between the two foveae on the dorsal face. The ungual phalanx I.2 (as seen in right side) is slightly larger than the ungual phalanx II.3, with mild curvature along the ungual phalanx. The phalanx I.1 and ungual I.2 exhibit notable hypertrophy in contrast to digits III and IV, a trait that is present in almost all Accipitridae (Fowler et al. 2009).

### ***Digit II (Figure 2.10B).***

Like most accipitrids, there is no fusion of the phalanges II.1 and II.3. The species in Haliaeetinae and *Ictinia* are notable for such fusion (see Jollie 1976). The phalanx II.1 is quite short compared to phalanx II.2, being just under half its length and considerably shortened lengthwise (not compressed lateromedially), which is a common trait in Accipitridae. All phalanges are notably hypertrophied compared to those in digits III and IV.

### ***Digit III (Figure 2.10C).***

Four phalanges are present. The medial face of the ungual phalanx (III.4) lacks the central ridge present in most accipitrids and falconids, though it is possibly that this feature has been poorly preserved.

### ***Digit IV (Figure 2.10D).***

The midshaft width of phalanx IV.4 is 3.2 mm, compared to the 3.8 mm of phalanx I, and the distal end of phalanx IV.4 is distinctly widened, measuring 4.6 mm. This dramatic

shift in width along the digit does not appear in the sampled elanine genera (*Elanus*, *Gampsonyx*), species of *Hieraaetus* (though the section before the articular end is swollen) or *Spizaetus* species, but appears to a lesser degree in the pernines, gypaetines, circaetines, aegypiines, species of *Aquila*, and species of *Haliaeetus*.

### **Summary**

*Archaeohierax sylvestris* shares a mosaic of characters across a broad range of taxa and thus the above comparisons do not reveal clear affinity with any one taxon. Different elements in the fossil skeleton differ markedly as to which subfamilies they most closely resemble: the rostrum maxillare – buteonines; the quadrate – aegypiines; the vertebrae – elanines; the sternum – aegypiines; the coracoid – aegypiines, accipitrines, and buteonines; the scapula – elanines; the humerus – elanines, aegypiines, aquilines, haliaeetines and buteonines; the ulna – circaetines; the carpometacarpus – buteonines; the os carpi ulnare – elanines, pernines, gypaetines and aquilines; the os carpi radiale – elanines and buteonines; the tibiotarsus – buteonines; and the tarsometatarsus – elanines (fossil is more elongate), aquilines and circaetines. There are several autapomorphies which further differentiates it from all extant subfamilies. Notably these include the sternal basin having a medial bar separating deep pneumatic fossae, humerus with very low proximal projection of the caput, and tarsometatarsus with broad incisurae intertrochleae and the incisura for the m. flexor hallucis brevis tendon extending distal to the fossa metatarsi I. Together, these support differentiation of this taxon with separate subfamilial status, consistent with the phylogenetic results discussed below.

### **Comparison with fossil accipitrids**

Australia has only two described pre-Pleistocene accipitrids. *Pengana robertbolesi*, from Sticky Beak Site in the Riversleigh World Heritage Area, of ?Late Oligocene—Early Miocene age, which is now considered one of the Faunal Zone A sites (Travouillon et al. 2006) and that on biochronological grounds are slightly younger than the Pinpa LF (Woodhead et al. 2016). It is represented by a distal tibiotarsus (Boles 1993), and while of similar size, is easily distinguished from *Archaeohierax sylvestris* by the following characters: the distal margin of the pons supratendineus is angled less steeply, ~30° relative to the long axis; the condyles have flattened sides in cranial aspect and are not medially and laterally expanded relative to the distal end of the shaft. *Aquila bullockensis* from the mid-Miocene Camfield Beds (12 Ma) of Bullock Creek (Gaff and Boles 2010; Megirian et al. 2010) was described from a distal humerus - which was not preserved in *Archaeohierax sylvestris*.

However, *A. bullockensis* is very much (>10 Ma) younger than *Archaeohierax sylvestris*, much larger, and the morphology of the distal humerus was interpreted to be typical of species of *Aquila*. *Archaeohierax sylvestris* has many features on other bone elements that exclude close affinity with both *Aquila* and the Aquilinae, so conspecificity with *A. bullockensis* can be ruled out.

In relation to Oligocene-age fossil accipitrids from elsewhere in the world, the geographic isolation of Australia makes it unlikely that any described species are closely related to *Archaeohierax sylvestris*. As reviewed in the Introduction, most late Oligocene and early Miocene accipitrid species are found in North America and Europe. Nearly all of them are described from a single skeletal element, making assessment of relationships with *Archaeohierax sylvestris* difficult. The late Oligocene – early Miocene accipitrids from North America, including the relatively complete *Palaeoplancus sternbergi*, are all easily distinguished from *Archaeohierax sylvestris* by size, and by morphology of the distal tarsometatarsus; specifically, trochlea metatarsi II is relatively broader and/or the intertrochlear incisions are much narrower.

Four Oligocene fossil accipitrids are described from Europe, all but one of which is based on a single bone:

“*Aquila*” (“*Aquilavus*”) *hypogaea* Milne-Edwards, 1892 from the Quercy fissure fillings is incomparable as it is based on a femur.

“*Aquila*” (“*Aquilavus*”) *corroyi* Gaillard, 1939, also from Quercy fissure fillings, was described from a tarsometatarsus that resembles *Milvus* according to Mayr (2009). It lacks the wide incisura intertrochleae of *Archaeohierax sylvestris*, and the flange on the trochlea metatarsi II is oriented more medially (Gaillard 1939, Figure 1).

*Palaeohierax gervaisii* (Milne-Edwards, 1863), late Oligocene France, is described from a tarsometatarsus and is larger than “*A.*” *corroyi*. Compared to *Archaeohierax sylvestris*, the incisura intertrochleae are narrow and the flange on trochlea metatarsi II is oriented more medially (Milne-Edwards, 1863, Plate 183, Figures 1–10).

*Aviraptor longicrus* Mayr and Hurum 2020, of early Oligocene age from Poland, is described from a complete skeleton. It is a very small accipitrid with highly elongate legs like those seen in species of Accipitrinae, which clearly distinguishes it from *Archaeohierax sylvestris*.

There are two Middle Oligocene species from Mongolia; *Buteo circoides* Kurochkin, 1968 (distal ulna), and *Venerator* (“*Tutor*”) *dementjevi* (Kurochkin, 1968) (distal humerus). Only *B. circoides* can be directly compared to *Archaeohierax sylvestris*, with images indicating

the tuberculum carpale is less prominent of the ventral condyle, and the ventral condyle has greater distal extent than the dorsal condyle (Kurochkin 1968, Figure 1).

Three fossil accipitrids are known from early Miocene deposits of Europe:

*Promilio incertus* (Gaillard, 1939) was described from a right tarsometatarsus from Chavroches, France, which lacks the wide incisura of *Archaeohierax sylvestris*, the flange on the trochlea metatarsi II is oriented more medially, and the hypotarsal crests are of roughly equal craniocaudal depth (Gaillard 1939, Figure 19).

*Aquilavus priscus* (Milne-Edwards, 1863), described from a tarsometatarsus, tibiotarsus and carpometacarpus, is from Auvergne, France. It is larger than *P. gervaisii*. Compared to *Archaeohierax sylvestris*, the incisura intertrochleae are narrow and the flange on trochlea metatarsi II is oriented more medially (Milne-Edwards 1863, Plate 184, Figures 1–4). On the carpometacarpus, the os metacarpale minus is flat, the processus alularis is less distinct from the distal processus extensorius, and the facies articularis digitalis major has less distal extent than the facies articularis digitalis minor (Milne-Edwards 1863, Plate 184, Figures 14–16). The tibiotarsus seems to lack a distinct scar or rugosity for the distal retinaculum extensorium (Milne-Edwards 1863, Plate 184, Figures 11–13).

*Aquilavus depredator* (Milne-Edwards, 1871), described from a tarsometatarsus, is from Saint-Gérard le Puy, France. Compared to *Archaeohierax sylvestris*, the incisura intertrochleae are narrow and the flange on trochlea metatarsi II is oriented more medially (Milne-Edwards 1871, Plate 183 Figures 11–14; Plate 184, Figures 5–10).

The middle Miocene accipitrids from Asia are all aegyptiine vultures (Hou et al. 2000; Zhang et al. 2010; Zhang et al. 2012; Li et al. 2016) and so are not closely related (see phylogenetic analysis below).

**Family Accipitridae Vigors, 1824**

**Subfamily indet.**

**Genus and sp. indet.**

**Material:** Distal right humeral fragment, preserving a relatively unworn distal end and 16.2 mm of shaft, and some associated fragments of the shaft, SAMA P.58917.

**Measurements (mm):** Distal width 15.4, least shaft width 8.3, total depth 8.5, condylus dorsalis depth 8.3, condylus dorsalis width 5.2, condylus ventralis depth 5.1, condylus ventralis width 7.3, epicondylus ventralis depth 7.0.

**Locality, stratigraphy and age:** 31° 07.568' S; 140° 12.737' E. Site 11, Lake Pinpa, Frome Downs Station, South Australia, Namba Formation, Pinpa LF, late Oligocene. Collected by A. Camens, T. Worthy and W. Handley, 24–26 September 2015.

**Remarks:**

The fossil can be excluded from other raptor families on the following features:

Falconidae (falconid state in brackets): the condylus dorsalis is thickened and rounded distally (consistently narrow and rectangular); the processus flexorius ends proximal to the condylus ventralis (equidistant).

Pandionidae (state for *Pandion haliaetus* in brackets): a shallow fossa m. brachialis (deep); a flat epicondylus dorsalis (prominently projecting); a flat epicondylus ventralis (prominent); the fossa olecrani is shallow (deep); the sulcus scapulotricipitalis is shallow (deep).

Cathartidae (cathartid state in brackets): a shallow fossa m. brachialis (deep); a lack of pneumatization in the fossa m. brachialis (present); a flat epicondylus ventralis (prominent).

Sagittariidae (sagittariid state in brackets): the two fossae marking the attachment points for the lig. collaterale dorsale are positioned roughly adjacent to each other (cranial-most fossa slightly proximal to and abutting caudal fossa in sagittariids).

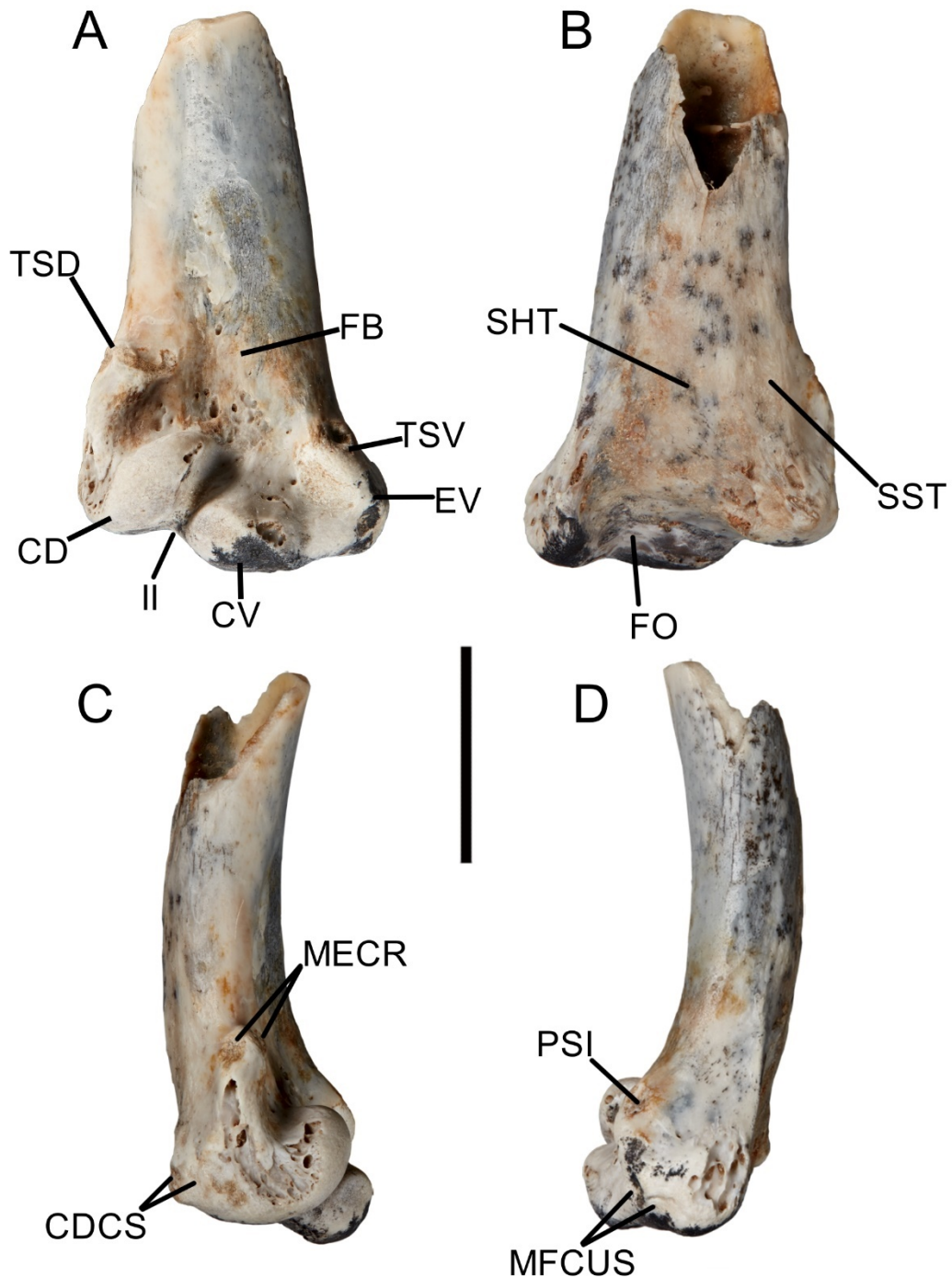


**Figure 2.11:** Accipitrid distal right humerus SAMA P.58917 in cranial (A), caudal (B), dorsal (C) and ventral (D) view. Abbreviations: CD, condylus dorsalis; CDCS, condylus dorsalis caudal scars; CV, condylus ventralis; EV, epicondylus ventralis; FB, fossa brachialis; FO, fossa olecrani; II, incisura intercondylaris; MECR, m. extensor carpi radialis insertion scars; MFCUS, musculus flexor carpi ulnaris scars; PF, processus flexorius; PSI, pronator superficialis insertion; SHT, sulcus humerotricipitalis; SST, sulcus scapulotricipitalis; TSD, tuberculum supracondylare dorsale; TSV, tuberculum supracondylare ventrale. Scale bar 10 mm.

The fossil is broadly similar to accipitrids and displays the following features: **(1)** The tuberculum supracondylare dorsale (Figure 2.11A: TSD) is located well-proximal to the condylus dorsalis (Figure 2.11A: CD) and is small, barely projecting dorsally of the shaft, but projects slightly cranially as a proximodistally elongate rugosity; **(2)** the dorsal face/shaft margin between the tuberculum supracondylare dorsale and the epicondylus dorsalis is mildly inflated; Two shallow scars for the m. extensor carpi radialis are present on the tuberculum supracondylare dorsale (Figure 2.11C: MECR), **(3)** the larger palmar attachment scar on the cranial face adjacent to the dorsal margin is oval **(4)** and the smaller dorsal scar is located on the dorsal face of the processus. **(5)** In caudal view, the processus flexorius (Figure 2.11: PF) terminates proximal to the condylus ventralis (Figure 2.11A: CV) but is prominent ventrally. **(6)** The sulcus scapulothoracalis (Figure 2.11B: SST) forms a shallow but broad notch roughly 2 mm wide on the caudal face. **(7)** The fossa olecrani (Figure 2.11B: FO) is moderately deep, defining well the dorsal margin to the processus flexorius but does not create a discontinuity with the sulcus humerotricipitalis. **(8)** The sulcus humerotricipitalis (Figure 2.11B: SHT) is very shallow, and at 5.3 mm wide extends over half of shaft width of 9.7 mm at the same point. **(9)** The fossa m. brachialis (Figure 2.11A: FB) is shallow but distinct, with a proximodistal length of 13.8 mm extending well proximal to the tuberculum supracondylare dorsale, and a maximum dorsoventral width of 7.3 mm level with the proximal margin of the tuberculum supracondylare dorsale. In contrast, the shaft width measures 10.1 mm at the same point. Within the fossa, the impressio m. brachialis is slightly deeper. **(10)** The fossa is well separated (3 mm) from the dorsal margin of the shaft. **(11)** The epicondylus ventralis (Figure 2.11A: EV) is indistinct from the ventral margin and does not project ventrally past the processus flexorius. **(12)** A single distinct, shallow insertion scar is present on the ventrodistal section of the epicondylus ventralis, with a very faint and shallow second insertion ventrally adjacent to it. These insertions serve as the attachment point for the m. flexor carpi ulnaris. **(13)** The tuberculum supracondylare ventrale (Figure 2.11A: TSV) projects cranially but not ventrally from the shaft. **(14)** A shallow insertion scar for the pronator superficialis is present just proximal to the tuberculum on the dorsal face. **(15)** The condylus dorsalis (Figure 2.11A: CD) is 5.9 mm proximodistally long, 4.7 mm dorsoventrally wide and 8.6 mm craniocaudally deep. **(16)** Two small, very shallow insertion scars are present on the caudal section of the dorsal face of the condylus dorsalis by the distal margin (Figure 2.11C: CDCS), directly craniocaudally adjacent to each other. **(17)** The condylus ventralis is 4.5 mm proximodistally long, 7.3 mm dorsoventrally wide and 5 mm craniocaudally deep. **(18)** The condylus dorsalis is separated by a distinct notch from and set well proximal to the distal margin of the condylus ventralis in cranial view. **(19)** The incisura intercondylaris (Figure 2.11: II) is narrow, roughly 1.1 mm wide, but distinct. **(20)** The processus flexorius is surpassed distally by the condylus ventralis in caudal view, and

strongly projects ventrally in caudal view. **(21)** The ventral margin of the condylus ventralis is not separated by a notch from the processus flexorius in cranial view.

Extant accipitrids differ as follows:

**(Trait 1)** The tuberculum supracondylare dorsale projects much further dorsally in all subfamilies and species except *Pernis apivorus* (Perninae), *Polyboroides typus* (Gypaetinae, non-projecting), Aquilinae, Accipitrinae and species of *Buteo* (Buteoninae). **(16)** The insertion scars towards the caudal margin of the condylus dorsalis are both deep in all subfamilies except Elaninae and Accipitrinae, with the latter having the cranial-most insertion being shallow and the caudal-most deep.

(See Appendix 3 for further comparisons with extant species).

### **Summary**

The fossil has the most similarities to species from the subfamily Elaninae (see Appendix 3), but differs markedly in regards to the inflation of the dorsal face between the tuberculum supracondylare dorsale and the epicondylus dorsalis, the size and shape of the palmar and dorsal attachment scars for the m. extensor carpi radialis, the distinct depression in the section of dorsal face caudal to the tuberculum supracondylaris and the epicondylus dorsalis, the sulcus humerotricipitalis width, the fossa m. brachialis length, the configuration of the insertion scars on the distal epicondylus ventralis, the position of the distal margin of the condylus dorsalis relative to that of the condylus ventralis in cranial view, the ventral projection of the processus flexorius, and the connectivity of the condylus ventralis and entepicondyle in cranial view.

As the *Archaeohierax sylvestris* specimen SAMA P.54998 lacks a preserved distal humerus, it cannot be compared to SAMA P.58917. However, it is not believed to belong to the same species due to the significantly smaller size of SAMA P.58917 from the humerus size predicted for SAMA P.54998 (see comparative measurements below).

**Family Accipitridae Vigors, 1824**

**Subfamily indet.**

**Gen. et Sp. indet.**

**Material:** NMV P.222435, distal left femur preserving intact distal end and 15.5 mm of shaft.

**Measurements (mm):** Preserved length 26, DW 13.3, least SW 7.3, preserved condylus medialis depth 9.7, condylus medialis width 5.6, condylus lateralis depth 11.0, condylus lateralis width 6.1.

**Locality, stratigraphy and age:** 31° 11.237'S 140° 13.944'E Ericmas Quarry, Lake Namba, Frome Downs Station, South Australia, Namba Formation, Ericmas LF, late Oligocene. Collected by T. Flannery, 7/4/83.

**Remarks:**

The specimen can be excluded from the Pandionidae and Cathartidae by the presence of a single muscular attachment on the planum popliteum, and from Falconidae and Sagittariidae by the linea intermuscularis caudalis remaining level and visible on the medial margin of the caudal face.

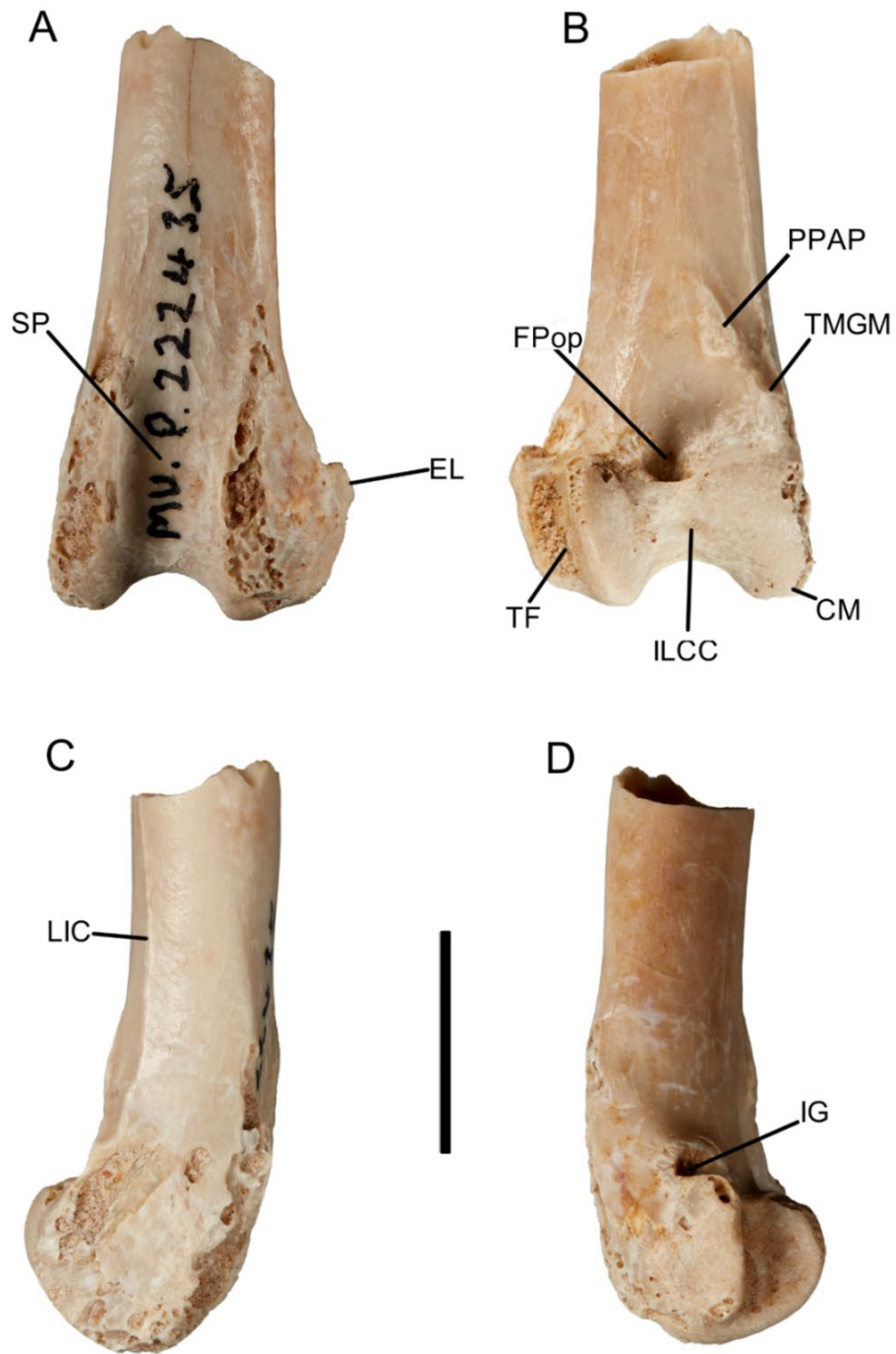


**Figure 2.12:** Distal left femur NMV P.222435 depicted in cranial (A), caudal (B), medial (C) and lateral (D) view. Abbreviations: CM, condylus medialis; EL, epicondylus lateralis; FPop, fossa poplitea; IG, impressio m. gastrocnemialis lateralis; ILCC, impressio lig. cruciati cranialis; LIC, linea intermuscularis caudalis; PPAP, planum popliteum attachment point; SP, sulcus patellaris; TF, trochlea fibularis; TMGM, tuberculum muscularis gastrocnemialis medialis. Scale bar 10 mm.

The femur is consistent with accipitrids and has the following morphology.

**(Trait 1)** The linea intermuscularis caudalis (Figure 2.12C: LIC) is highly distinct, running along the medial border of the caudal shaft face in a raised line, **(2)** but is not continuous with the tuberculum m. gastrocnemialis medialis, so there is no crista supracondylaris medialis. **(3)** The secondary origin point for the ligamentum collateralis lateralis is very faint and shallow, barely distinct from the surface of the bone. **(4)** The fovea tendineus m. tibialis cranialis is shallow. **(5)** The fossa poplitea (figure 2.12B: FPop) is shallow, deepening slightly towards the distal end immediately proximal to the condyles. **(6)** The attachment scar on the planum popliteum (Figure 2.12B: PPAP) is positioned medially. **(7)** The impressio m. gastrocnemialis lateralis (Figure 2.12D: IG) is large and shallow. **(8)** The epicondylus lateralis (Figure 2.12A: EL) is short and very robust but has little projection from the condylus lateralis.

(See Appendix 3 for comparisons with extant species).

### **Summary**

The distal femur NMV P.222435 is from an accipitrid which exhibits the most similarity to those of species in Buteoninae, Aegypiinae, and most of Elaninae (see Appendix 3). It mainly differs from species in these subfamilies in lacking a prominent crista supracondylaris medialis, the position and shape of the attachment point on the planum popliteum, and the weak projection of the epicondylaris lateralis.

As the distal femur is not a highly diagnostic section of the accipitrid skeleton, and the distal femur is not preserved in *Archaeohierax sylvestris* specimen SAMA P.54998, NMV P.222435 is regarded as gen. et. sp. indet. The size difference between NMV P.222435 and the predicted size of the distal femur of SAMA P.54998 is greater than would be predicted from typical sexual dimorphism, which makes it unlikely the two are representatives of the same species (see comparative measurements below).

### **2.3.2 Size comparisons of the three fossils**

The width measurements of the proximal humerus, distal humerus, distal tibiotarsus and distal femur of extant taxa were compared (see Appendix 2 Table 2) and showed that the distal width of the humerus was between 80–90% of the proximal width of the humerus, while the distal width of the tibiotarsus was between 75–110% the distal width of the femur in extant accipitrids. If the bones of *Archaeohierax sylvestris* had similar ratios, then it can be predicted that the width of the missing distal humerus should fall in the range 23.4–26.4 mm,

while that of the missing distal femur should be between 15.8–22.0 mm broad. Based on this, both the isolated distal femur NMV P222435 and the isolated distal humerus SAMA P.58917 are too small to belong to an individual the size of the *A. sylvestris* holotype. However, sexual dimorphism is known to be considerable and common in accipitrids (Brown and Amadon 1968; Marchant and Higgins 1993) and raises the possibility that these isolated fossils may belong to a smaller sex of the one species if they fall within a certain size range. Field et al. (2013) devised multiple algorithms for predicting body mass from skeletal measurements, while Campbell and Marcus (1992) predicted body mass based on the femur and tibiotarsus circumference. Using these, the mass of the bird for the *Archaeohierax sylvestris* holotype is estimated as 3.7 kg based on the length of the coracoid facies articularis humeralis, 4.6 kg by the least shaft diameter/width of the tarsometatarsus, and 3.2 kg based on tibiotarsus least shaft circumference. The mass of the bird represented by the distal femur is calculated at 2 kg based on femur shaft width/diameter, or 1.6 kg based on shaft circumference. The mass of the bird represented by the distal humerus is calculated at 1.5 kg based on shaft width/diameter, or 1.6 kg based on circumference. Assuming these predictions are accurate, the femur represents a bird 46–67% smaller than the skeleton specimen, and the humerus one 60–67% smaller. This would be pushing accipitrid sexual dimorphism to its extreme limits, making it unlikely that the fossils represent a single species. However, these mass predictions use different elements, limiting their comparability. Nevertheless, while considering it likely that at least two accipitrids are represented, we consider it unwise to describe the smaller as a second species when size would be the only distinguishing factor and their congeneric status cannot be assessed.

### **PCA analysis of limb measurements**

Length data for a range of post cranial measurements were visualised in PCA plots to determine if there was any correlation between them and preferred habitat. All PCAs used a variance-covariance matrix, iterative imputation for missing data (in the case of I.2 length of *Gyps coprotheres*), and 1000 bootstrap replicates. See Appendix 4 for datasets, scree plots, biplots, PCA values.

The first PCA used absolute length measurements of the carpometacarpus, ulna, tibiotarsus, tarsometatarsus, pedal digit 1 and pedal digit 2 (Figure 2.13A). In the resulting scatterplot PC1 (92.1% variance) was most strongly driven by the ulna, with some influence from the carpometacarpus (wings), the tarsometatarsus and tibiotarsus and PC2 (7% variance) by the tarsometatarsus and tibiotarsus (legs). *Archaeohierax sylvestris* was positioned as a long-legged, short-winged taxon, well separated from other species. Both *Spizaetus tyrannus* and *Spilornis cheela* grouped closely together, creating a cluster for forest-habitat accipitrids. *Circus assimilis*, which inhabits grassland and open woodland, was

positioned intermediate between *Archaeohierax sylvestris* and the forest taxa.

A second PCA was run after log-transforming the measurements. In the resulting scatterplot (Figure 2.13B) PC1 (91.4% variance), was driven by almost all measurements, with those of the tibiotarsus and tarsometatarsus having slightly more influence than those of the wings and digits, and PC2 (3.3% variance) revealed that species were separated most strongly based on the tarsometatarsus length, with lesser influence from the digit lengths and tibiotarsus length. *Archaeohierax sylvestris* grouped with the long-legged and short winged taxa, but the distribution of the extant taxa changed. *Spizaetus tyrannus* and *Spilornis cheela* were more widely separated, with the open-habitat taxon *Circus assimilis* positioned more closely to *Spizaetus tyrannus*.

As size dominated the first two PCAs, a third PCA was performed with measurements standardised for size, by division of postcranial data by the height of the quadrate, an element which correlates strongly with skull size and therefore body size (Elzanowski et al. 2001). In the resulting scatterplot (Figure 2.13C), PC1 (67.2%) was most strongly driven by ulna length and to a lesser degree by carpometacarpus length, while PC2 (28.9%) was most strongly driven by tibiotarsus length and tarsometatarsus length. *Archaeohierax sylvestris* occupied a more negative position on PC2 relative to *Circus assimilis* as the peak of the long-legged, short-winged taxa, and *Spizaetus* and *Spilornis* clustered together closely once more. *Archaeohierax sylvestris* fell intermediate between *Circus assimilis* and the forest accipitrid cluster.

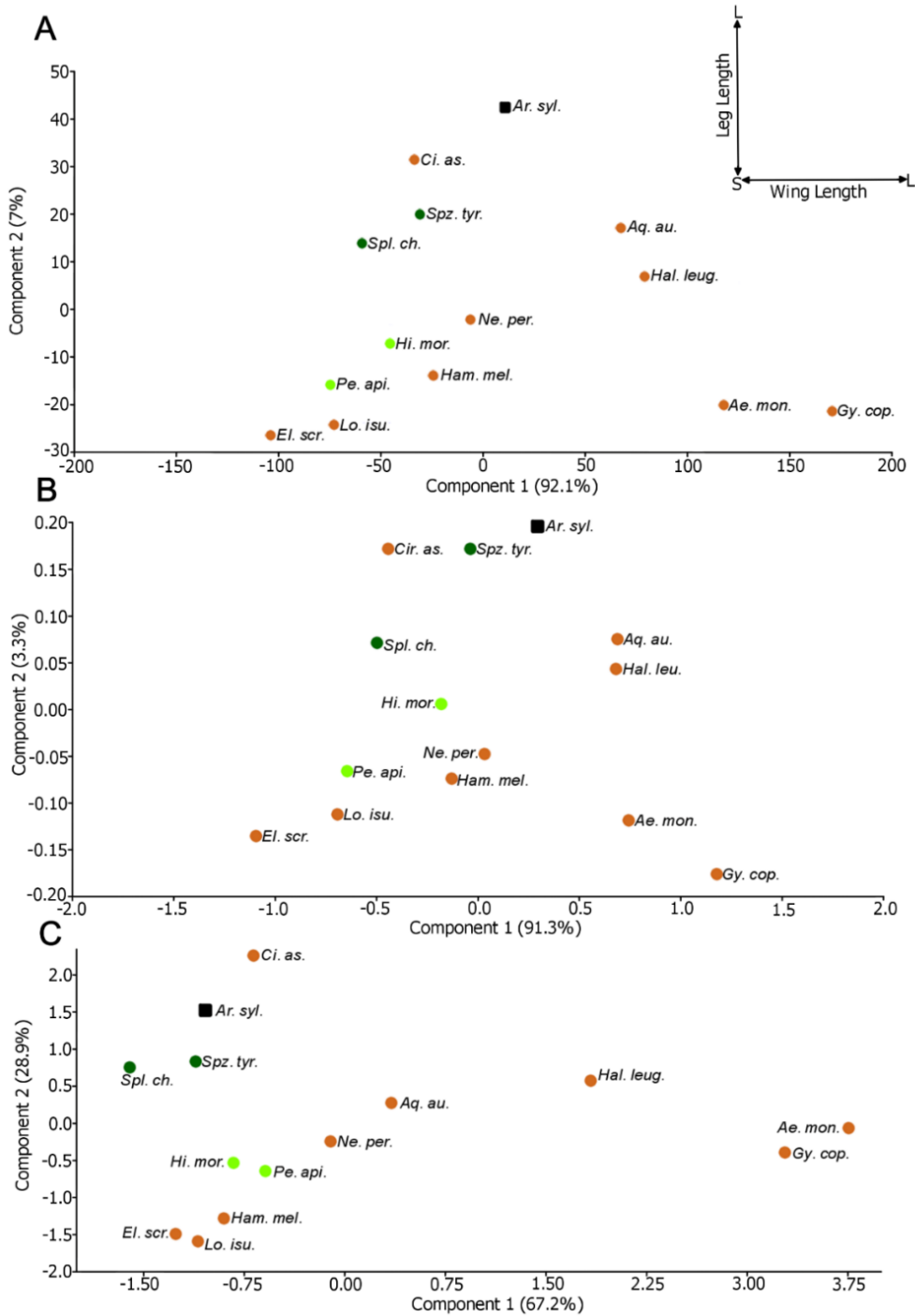


**Figure 2.13:** PCA plots using length measurements of the carpometacarpus, ulna, humerus, tibiotarsus, tarsometatarsus, pedal digit 1 and pedal digit 2 treated in three ways. (A) Absolute data, (B) log-transformed data, (C) size standardised data with variables proportional to quadrate height. Directional arrows at top right indicate directionality of limb length (S, short and L, long) along the PC axes. Note: axes in A and B have been scaled for better visualization, so 2D distances do not represent true 2D distances in PCA space. Abbreviations: *Ae. mon.*, *Aegypius monachus*; *Ar. syl.*, *Archaeohierax sylvestrus*; *Aq. au.*, *Aquila audax*; *Ci. as.*, *Circus Assimilis*; *El. scr.*, *Elanus scriptus*; *Gy. cop.*, *Gyps coprotheres*; *Ham. mel.*, *Hamirostra melanosternon*; *Hal. leug.*, *Haliaeetus leucogaster*; *Hi. mor.*, *Hieraaetus morphnoides*; *Lo. isu.*, *Lophoictinia isura*; *Ne. per.*, *Neophron percnopterus*; *Pe. api.*, *Pernis Apivorus*; *Spl. ch.*, *Spilornis cheela*; *Spz. tyr.*, *Spizaetus tyrannus*. Dark green, forested habitat; light green, woodland/open forest; orange, open habitat (grassland, savannah etc.). Fossil (*Archaeohierax*) indicated by black square.

### 2.3.3 Phylogenetic analyses

We performed phylogenetic analyses of morphological data only, and combined morphological and molecular data, using parsimony and Bayesian methods. We discuss all analyses below but have most confidence in the analyses combining morphology and molecules, in particular the unlinked Bayesian analyses, for reasons discussed at the end.

#### **Analysis 1: Parsimony, morphology only, unordered characters**

The first analysis used only morphological data, with no ordering, constraints or weighting applied to the characters. The resulting 30 most parsimonious trees (hereafter MPTs) had a tree length of 1686 steps (Appendix 5 Figure A5.1). *Coragyps atratus*, *Ciconia ciconia*, *Threskiornis spinicollis*, and *Sagittarius serpentarius* were rooted as the outgroup (Bootstrap= 97%), while *Pandion* resolved as sister to Accipitridae with a support value of 97%. This is broadly concordant with independent molecular phylogenetic studies.

Within Accipitridae, the tree is less congruent with DNA trees. The Accipitridae as a family had strong support (87%) with the non-Australian Perninae resolved as the most basal clade, which was strongly supported (87%) but had species left in a polytomy.

The fossil *Archaeohierax sylvestris* n. gen. et sp. resolved as a branch between the Circaetinae-Harpiinae-Aquilinae clade and all other subfamilies higher up the tree. However, support for this position was very weak (<50%).

#### **Analysis 2: Parsimony, morphology only, ordered characters**

Analysis 2 differed from Analysis 1 by ordering certain multistate characters which formed morphoclines (see Appendix 1). This generated four MPTs with a tree length of 1720. The resulting strict consensus tree (Appendix 5 Figure A5.2) is largely the same as for analysis 1, but with the following differences. The Accipitridae resolved with strong support slightly higher than the previous analysis (Bootstrap=88%).

The fossil *Archaeohierax sylvestris* was resolved as being between the Elaninae and the Australian endemic Perninae on the phylogenetic tree, though support for this position was very weak (<50%).

#### **Analysis 3: Parsimony, morphology and DNA, ordered characters**

As the analyses based on morphology failed to resolve the taxa in a way that reflects strongly supported clades based on comprehensive molecular data, and the primary aim of the analysis was to assess how the fossil related to the well-corroborated clades of modern taxa, molecular data from six genes was added for 47 taxa (see Methods) forming a combined morphology and molecular data matrix used in Analysis 3. Parsimony analysis of this matrix produced three MPTs with a tree length of 1831, for which the strict consensus

tree is shown in Figure 2.16.

Given the molecular data largely constrains the tree to the relationships dictated by molecular data alone, relationships were mostly the same as those in recent molecular studies (Nagy and Tökölyi 2014; Mindell et al. 2018).

The position of the fossil *Archaeohierax sylvestris* varied between the strict consensus tree and the bootstrap majority consensus tree of the same analysis. In the strict consensus tree (Appendix 5 Figure A5.3) the fossil resolved as nested within the Circaetinae, sister to *Pithecophaga jefferyi*. However, the bootstrap consensus tree resolved the fossil as its own branch between the Perninae-Gypaetinae and the Circaetinae-Aegyptiinae clades with moderate (68%) support.

#### **Analysis 4: Bayesian inference, morphology + DNA, ordered**

The Bayesian analysis with molecular and morphological branch lengths unlinked produced a broadly similar tree for living taxa to the bootstrap consensus of the corresponding parsimony analysis, but with overall much stronger supports for higher-level clades (Figure 2.14). All subfamilies resolved as monophyletic, and the divergence nodes for all subfamilies and major clades were greater than 70% except for one.

The fossil *Archaeohierax sylvestris* resolved as a lineage positioned between the Elaninae and the Perninae-Gypaetinae clades (i.e., non-elanine accipitrids). Support for *Archaeohierax* plus a clade of all non-Elanine accipitrids was weak (44%), but there was moderate support (73%) for monophyly of all other non-elanine accipitrids excluding *Archaeohierax*.

When the branch lengths for the molecular and morphological data were linked (Appendix 5 Figure A5.4), the position of the fossil changed. *Archaeohierax sylvestris* moved up the phylogeny and resolved as an independent branch above the Circaetinae-Aegyptiinae clade but below the Harpiinae and relatives. Support for this node was stronger than that of the position resolved by the unlinked analysis, but still weak (56%).

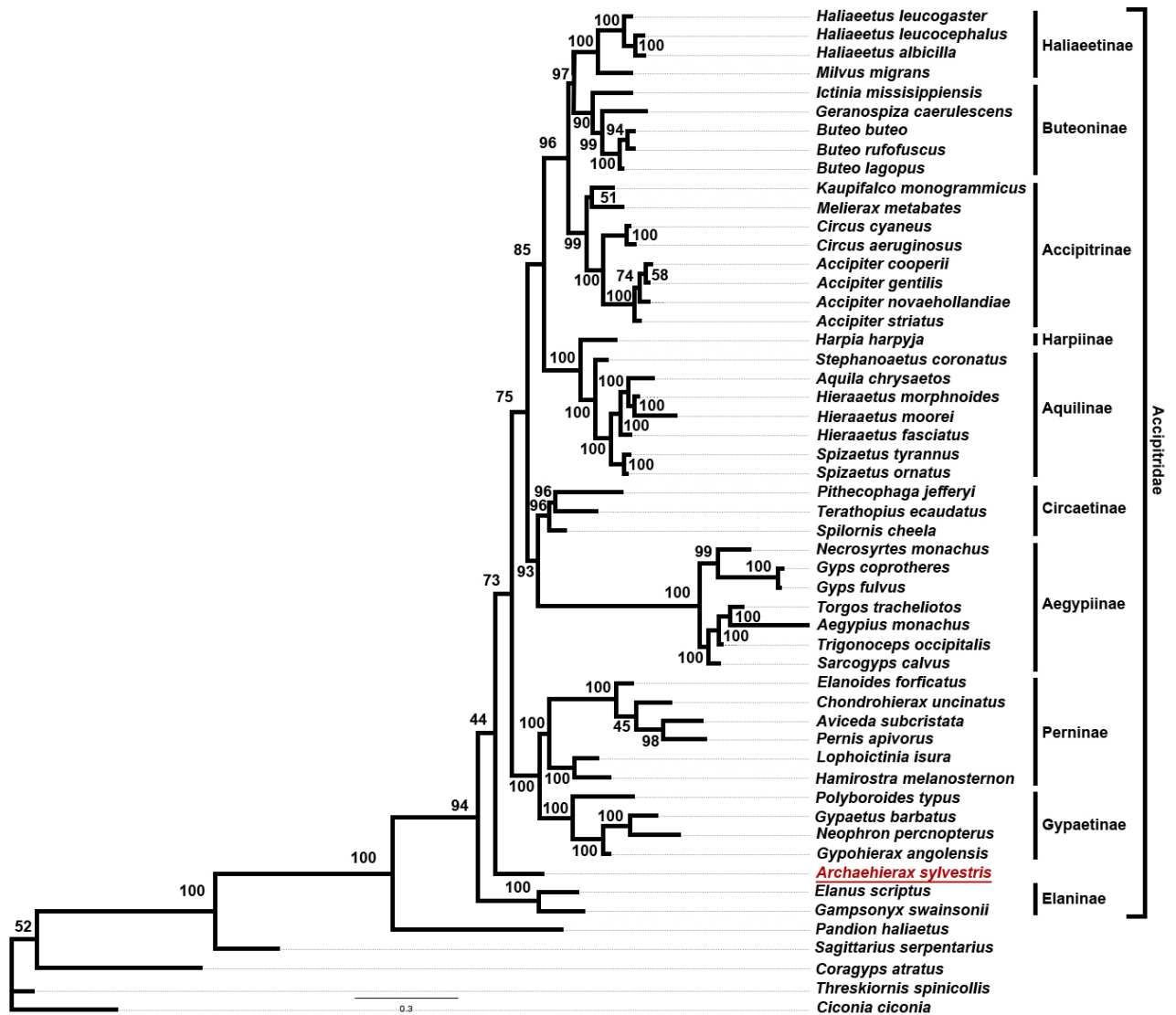


**Figure 2.14:** Analysis 4a: combined molecular and morphological data (ordered) analysed with Bayesian methods; molecular and morphological partition branch lengths unlinked. Node values show posterior probability. Majority-rule consensus tree.

### Summary

All phylogenetic analyses resolved *Archaehierax sylvestris* with the Accipitridae, consistent with the conclusions drawn from the morphological descriptions, though its precise position within that family varied. Some analyses found it deeply nested within Accipitridae, closely related to, but outside buteonines, haliaeetines and accipitrines. These analyses include the morphology-only parsimony analyses, morphology+molecular parsimony and morphology+molecular Bayesian analysis with linked branch lengths. However, as discussed below, these deeply nested affinities for *Archaehierax* are problematic, and appear less plausible than the topology retrieved in the Bayesian analysis with branch lengths unlinked - where it was one of the most basal accipitrid lineages, with

only Elaninae diverging before it (Figure 2.17).

A more precise and robust position for *Archaeohierax sylvestris* is perhaps prohibited by missing data. Even with the 63 preserved elements, there is still a significant amount of missing data. The mandible and cranium, most of the sternum, the distal ends of the humeri, the pelvis, and most of the femora were not preserved. Thus, only 45% (135/300) of phylogenetic characters could be assessed in SAMA P.54998.

## 2.4 DISCUSSION

*Pengana robertbolesi* was previously the only accipitrid raptor known from the late Oligocene in Australia (Boles 1993; Worthy and Nguyen 2020), being slightly younger than *Archaeohierax sylvestris* at 24–20 Ma (Travouillon et al. 2006; Woodhead et al. 2016) and represented only by a distal tibiotarsus making relationships within Accipitridae difficult to establish. The specimens from the late Oligocene Namba Formation are the oldest accipitrids in Australia and extend the fossil record of the Australian Accipitridae to 26–24 Ma, when Australia was much warmer and heavily forested.

### 2.4.1 Relationships with fossil and extant Australian Accipitridae

*Archaeohierax sylvestris* is unambiguously an accipitrid based on many skeletal features, but notably the morphology of the tarsometatarsal hypotarsus, the lack of a spina interna on the sternum, and the shortened second and third phalanges of the fourth digit. Unsurprisingly, *Archaeohierax sylvestris* has multiple unique features of its skeletal morphology that distinguish it from other accipitrids, such as the low caput humeri (humerus), the two fossae in the pars caudale separated by a pila medialis (sternum), and the wide incisurae intertrochleares (tarsometatarsus). However, as summarised above, the different elements of *Archaeohierax sylvestris* do not reveal a consistent closer relationship to the species in any one subfamily. Some elements, such as the rostrum, carpometacarpus and tibiotarsus, show much similarity to species in more derived subfamilies like the Buteoninae, while others, such as the quadrate, vertebrae, and sternum resemble those of more basal subfamilies like Elaninae and Aegypiinae. Other elements, like the humerus, ossa carpalia and the tarsometatarsus, share features with multiple subfamilies. The scapula, ulna, radius, carpometacarpus, carpal phalanges, fibula and pedal phalanges do not align well with the species of any one subfamily. The morphology of the os carpi radiale also excludes the fossil from an accipitrid clade comprising Harpiinae, Aquilinae, Haliaeetinae, Buteoninae and Accipitrinae (see Mayr 2014). This mix of affinities among characters contributes to understanding why the fossil does not group robustly in any subfamily in the phylogenetic analyses. This typifies many Paleogene fossil bird species

across multiple families (see Mayr 2009), along with the phylogenetic results, supports the idea that *Archaeohierax* does not belong to an extant subfamily. Missing data probably exacerbates the problem as about 55% of characters could not be coded.

In our parsimony analysis using combined morphological and molecular data (Figure 2.16), *Archaeohierax sylvestris* resolved either deeply nested within Circaetinae as sister to *Pithecophaga jefferyi* (strict consensus tree) or as a stem lineage situated between the clade Gypaetinae-Perninae and Aegyptiinae-Circaetinae (bootstrap consensus tree). The Bayesian analysis of combined morphological and molecular data with morphology and molecular branch lengths linked had *A. sylvestris* resolved as above the Aegyptiinae-Circaetinae clade but lower than the Harpiinae and Aquilinae. In contrast, the Bayesian analysis of combined morphological and molecular data, with unlinked molecular and morphological branch lengths, resolved *Archaeohierax sylvestris* near the base of the Accipitridae, immediately above the Elaninae. The topology of the unlinked molecular and morphology branch lengths tree (Figure 2.17, analysis 4a) is preferred for several reasons; firstly, given the age of the fossil, the more basal position on the accipitrid phylogenetic tree is more plausible. Dated molecular phylogenies imply that most of the extant accipitrid subfamilies had not diverged by the late Oligocene, with only the Elaninae, which diverged at 33.7 Ma (Mindell et al. 2018), likely present, as the Perninae + Gypaetinae clade diverged at 23.8 Ma from remaining accipitrids (Mindell et al. 2018). Other lineages emerged during or after the middle Miocene (Nagy and Tökölyi 2014; Oatley et al. 2015; Prum et al. 2015; Mindell et al. 2018). Secondly, while many analyses of combined morphological and molecular datasets link branch lengths between these data types (e.g. Ronquist et al. 2012), this might be justifiable only under certain circumstances. Duchéne et al. (2020) compared the effects of linking branch lengths of gene loci trees and demonstrated that partitioning and linking loci to create proportionate branch lengths gave the strongest support, while analyses that had unlinked loci, or loci that were linked to produce identical branch lengths, received weaker support. Goloboff et al. (2019) explored the question of whether assuming a common mechanism of evolution to both all genetrees and morphological data was warranted and concluded that morphological data was generally not compatible with the common clock assumption used when linking branch lengths, producing low levels of branch length correlation. Similarly, Barba-Montoya et al. (2020) found a poor linear relationship between branch lengths for morphological and molecular data, consistent with the idea that the morphological traits were evolving at much more variable rates compared to the molecular ones. Based on this, the results estimated by linking morphological and molecular branch lengths (see Appendix 5) should be regarded with caution.

The molecular-based divergence dates for Aquilinae (Nagy and Tökölyi 2014; Mindell

et al. 2018) suggest that *Aquila bullockensis*, at 14–12 Ma (Woodhead et al. 2016), predates the inferred age of the *Aquila* genus by at least 5 Ma. Morphologically the holotype distal humerus has several distinct differences from *Aquila audax*, including a reduced distal projection of the processus flexorius, a tuberculum supracondylare ventrale with less cranial projection and no proximal narrowing, little to no convexity between the tuberculum supracondylare dorsale and epicondylus dorsalis, and the dorsal insertion for the m. extensor radii is positioned offset from the tuberculum supracondylare dorsale. This does not necessarily mean that *A. bullockensis* is not an aquiline, but rather that it is unlikely to be a member of the crown *Aquila* or any other extant aquiline genus, and that the initial comparative descriptions were too limited to support referral of the species to *Aquila*. Since the description of the holotype more fossil material that likely belongs to *A. bullockensis* has been discovered and is awaiting description, which may change interpretations of the relationship of *A. bullockensis* to the extant Aquilinae.

In relation to size, it is clear that *Archaeohierax sylvestris* was a large accipitrid, smaller than the wedge-tailed eagle *Aquila audax* and the white-bellied sea eagle *Haliaeetus leucogaster* but larger than the black-breasted buzzard *Hamirostra melanosternon* among the extant Australian fauna. It is tempting to assume from this that it must belong to a lineage of large accipitrids. However, while size is sometimes useful in diagnosing clade membership, there are notable exceptions. Haast's eagle *Hieraaetus moorei*, one of the largest eagles ever known at an estimated 15 kg (Worthy and Holdaway 2002), is most closely related to the little eagle *Hieraaetus morphnoides* (Bunce et al. 2005; Knapp et al. 2019), which weighs under 1 kg, the two diverging from a common ancestor approximately 1 million years ago (Knapp et al. 2019). Another example is seen among extant species; the Philippine eagle *Pithecophaga jefferyi* is morphologically convergent on the Harpiinae in terms of large body size, prey preference, and preferred habitat, but groups molecularly with the Circaetinae, most of which are medium-sized reptile specialists.

Regardless of its closest extant relative, *Archaeohierax sylvestris* demonstrates the presence of Accipitridae in Australia since the late Oligocene and that there were at least two divergent clades (*A. sylvestris* and *Pengana robertbolesi*) in Australia around the Oligo-Miocene boundary. All well-sampled Australian faunas from the late Oligocene onwards are now known to have contained accipitrids (Baird et al. 1991; Boles 1993; Gaff and Boles 2010; Rich and van Tets 1982; Louys and Price 2015; Worthy and Yates 2018). However, the geographic origin of these austral accipitrids is difficult to infer, given the presence of accipitrids across multiple continents at this time and a lack of phylogenetic analyses of them with fossils elsewhere.

Conspecificity of the isolated distal humerus and femur specimens from other sites in

the Namba Formation with *Archaeohierax sylvestris* could not be excluded based on morphology given the holotype lacks these elements, although their much smaller size makes this unlikely, exceeding differences attributable to sexual dimorphism. However, in the absence of overlapping skeletal elements, establishing whether they are congeneric or not is impossible, so we refrain from describing them as a species.

#### 2.4.2 Palaeobiology

*Archaeohierax sylvestris* is inferred to have inhabited forested areas, based on the pollen records from the Namba Formation (Martin 1990) and the associated fauna in the Pinpa LF, which contains many arboreal taxa such as koalas (phascolarctids), and members of four families of possums and kin (phalangeriforms) (see above; Rich et al. 1991). Our principal component analyses show the fossil taxon grouped most closely to species with relatively shorter wings and longer legs. This body form is observed in forest dwelling eagles and hawks, such as species of *Spizaetus*, *Spilornis*, *Harpia harpyja* and *Pithecophaga jefferyi*, which are adapted to flying through more constricted spaces among the trees and vegetation (Brown and Amadon 1968; Holdaway 1991 unpublished thesis). However, it is also present in the spotted harrier *Circus assimilis*, which *Archaeohierax sylvestris* was also closely associated with in PCA plots, which favours open grassland and lightly wooded areas for its habitat (Brown and Amadon 1968; Marchant and Higgins 1993; Debus 1998). In the case of *Circus assimilis*, however, wingspan to leg length proportion is less the result of the wings being shortened, but more the product of the legs being hyper-elongate compared to other accipitrids, especially in the tarsometatarsus, to facilitate a specialised hunting strategy. *Circus assimilis* is known to forage by slowly flying less than five metres above vegetation (Aumann 2001) and has been documented pursuing small prey such as lizards on foot (Buij 2014). It is likely that the high ratio between the wing and leg length in *C. assimilis* is therefore being driven by a need to reach into grass cover to quickly grab small vertebrates before they can escape. As *Archaeohierax sylvestris* does not exhibit the extreme elongate tarsometatarsus morphology observed in *C. assimilis*, and more closely resembles that of the crested serpent-eagle *Spilornis cheela* and the black hawk-eagle *Spizaetus tyrannus*, it can be inferred that the ecology of *Archaeohierax sylvestris* was more akin to the latter species.

With its shorter wings allowing manoeuvrability, *Archaeohierax* would not have been a particularly fast flier, but would have been capable of more agile twists and turns in flight than an accipitrid of its size with a typical wingspan. If we use extant forest eagle species such as those in *Spizaetus* as a morphological analogue, it can be assumed that *Archaeohierax sylvestris* was likely an ambush hunter, waiting on a perch within forest cover until prey came into range, and then attacking with a quick burst of speed (Whitacre and

Jenny 2013).

The potential diet of *Archaeohierax* can be inferred based on that of living analogues, such as species in *Spizaetus*. A female ornate hawk-eagle *Spizaetus ornatus* was recorded feeding on the remains of an estimated 3.2 kg Central American agouti (*Dasyprocta punctata*) and later, on a great curassow (*Crax rubra*), which can weigh between 3.1–4.8 kg (though it was not directly observed killing these animals). Whitacre and Jenny (2013) recorded a male with an adult great tinamou (*Tinamus major*) around 1 kg in weight, which is also the average weight for male *Spizaetus ornatus*. *Archaeohierax sylvestris* is notably larger than the species of *Spizaetus* observed in this project (*Spizaetus ornatus*, *Spizaetus tyrannus*), and assuming similar prey hunting abilities, would have been quite capable of preying on many of the mammals and birds known from the Pinpa Local Fauna.

Based on its larger physical size, phylogenetic position, and the proportions of the tibiotarsus to the tarsometatarsus, it is unlikely that *Archaeohierax sylvestris* was restricted to preying on large invertebrates and small vertebrates as seen in the elanines and some of the pernines. The extant Australian elanines, the letter-winged kite *Elanus scriptus* and the black-shouldered kite *Elanus axillaris*, primarily feed upon small mammals (typically mouse-sized), lizards, and large insects such as beetles, grasshoppers and locusts (Brown and Amadon 1968; Marchant and Higgins 1993). The pernine kite *Hamirostra melanosternon* feeds upon small mammals (rabbit-sized at largest), reptiles, and birds, and has been observed to break open eggs of large ground-dwelling birds using either stones or its beak (Brown and Amadon 1968; Marchant and Higgins 1993). The square-tailed kite *Lophoictinia isura* preys on a wide array of small birds, reptiles, large insects, and even bird eggs from nests (Brown and Amadon 1968; Marchant and Higgins 1993).

However, *Archaeohierax sylvestris* also lacks the robustness of legs seen in the species of aquilines and harpiines that feed on larger birds and small to medium mammals. The morphology and tibiotarsus-tarsometatarsus ratio of the fossil are also slenderer compared to the fish eagles/haliaeetines, which require the sturdiness to strike through water and the grip to maintain a hold on struggling prey so despite living near a lake this bird likely did not fish like these species. *Aquila audax* feeds on mammals ranging in size from rabbits to small wallabies, and is also a frequent scavenger of roadkill, while *Haliaeetus leucogaster* near exclusively preys on large fish and sea-snakes (Brown and Amadon 1968; Marchant and Higgins 1993). *Hieraaetus morphnoides*, a smaller bird that is closely related to *Aquila*, preys upon small rabbits and other mammals of a similar size, as well as small ground birds (Brown and Amadon 1968; Marchant and Higgins 1993). *Archaeohierax* is larger than *H. morphnoides*, but its more gracile morphology may have restricted it to prey of a similar size to that preferred by this species.

The reduced size of the flange on trochlea metatarsi II in *Archaeohierax sylvestris*, as well as its strongly plantar orientation, differs greatly from most Accipitridae. As this marks the point where the musculature for digit II connects to the tarsometatarsus, this could indicate a reduced ability to manoeuvre this digit in the plantar-medial direction, which is the orientation present in most accipitrids. However, the wider spacing of the trochleae could indicate a greater foot span when the toes are extended for prey capture, which might compensate for the loss of potential manoeuvrability.

The Pinpa Local Fauna contains a diverse array of animals (see above), some of which would have been potential prey for *Archaeohierax sylvestris*. If a diet of small to medium birds and mammals ranging in habitat from arboreal, terrestrial and littoral is inferred, prey species may have included *Wilaru tedfordi* (a presbyornithid), *Ngawupodius minya* (a dwarf megapode), smaller individuals and juveniles of *Madakoala devisi* (an early koala), a huge diversity of possums and many of the waterbirds that appear in abundance in the Local Fauna.

## **Acknowledgements**

We would like to thank Phillipa Horton, Maya Penck and Mary-Anne Binnie (SAMA), Judith White and Joanne Cooper (NHMUK), Chris Milensky (Smithsonian), Mark Robbins (KU), Tim Ziegler and Karen Roberts (NMV), and Leo Joseph and Alex Drew (ANWC) for allowing access to collections and loans of specimens, without which this project could not have been done. We would also like to thank Warren Handley for his input regarding mass allometry, Elizabeth Scharsachs and her family for providing accommodation in Tring, and the PhD students of Flinders Palaeontology for their support and willingness to talk over thoughts and concerns.

We thank the Mark Mitchell Foundation for a grant to T.H. Worthy, A. B. Camens that funded some of the fieldwork component. For assistance in the field, we thank Amy Tschirn and Warren Handley. We acknowledge the support of Andrew Black (Blackie), manager, for access to Frome Downs Station that allowed this work.

## **Authors Contributions**

EKM and THW designed the study. EKM collected all data, compiled the morphological matrix and did all analyses. MSYL collated the molecular data used in the combined analyses or morphological and molecular data. THW and MSYL contributed to data interpretation. EKM wrote the manuscript, and all authors edited the manuscript. THW and ABC collected the fossil material of *Archaeohierax sylvestris* while on field work.

## 2.5 Additional Information

### Thesis Appendices

#### Please See:

**Appendix 1: List of morphological characters.** Full descriptions of all 300 morphological characters used in the analyses, including character states and whether the character was ordered, with references.

**Appendix 2: Additional tables of measurements.** Measurements for the holotype of *Archaehierax sylvestris* and comparative measurements for all fossils and selected extant species used in size inferences in section 2.3.2.

**Appendix 3: Comparative descriptions.** Descriptive comparisons of *Archaehierax sylvestris* and Gen et. Sp. indet to extant subfamilies and species of Accipitridae for each bone represented in the fossils.

**Appendix 4: PCA analyses data, scree plots and biplots.** Data used in Chapter 2 PCA plots, PC eigenvalues, PC1 and PC2 biplots, and PC scree plots.

**Appendix 5. Additional phylogenetic trees.** Strict consensus trees from Chapter 2 analyses 1–3, and majority-consensus tree of Chapter 2 analysis 4b.

### Supplementary Information

All files available at <https://figshare.com/s/7b9b1a551576ab5ce767>

**SI.1: Morphological character data matrix.** Mesquite file containing character states for all fossil and extant species used in this thesis.

**SI.2: *Archaehierax* parsimony analysis file.** Command file for the parsimony analyses involving *Archaehierax sylvestris*.

**SI.3: *Archaehierax* Bayesian infile.** Nexus command file for the Bayesian analyses involving *Archaehierax sylvestris*.

## 2.6 References

- Alley NF. 1998. Cainozoic stratigraphy, palaeoenvironments and geological evolution of the Lake Eyre Basin. *Palaeogeogr Palaeoclimatol Palaeoecol*, 144(3-4): 239–263.
- Amadon D. 1964. Taxonomic notes on birds of prey. *Am Mus Novit*, 2166: 1–24.
- Archer M, Tedford RH, Rich TH. 1987. The Pilkipildridae, a new family and four species of ?petauroid possums (Marsupialia: Phalangerida) from the Australian Miocene. In: Possums and opossums: studies in evolution. M Archer editor. Surrey Beatty & Sons Pty Ltd and The Royal Zoological Society of New South Wales, Sydney, Australia; p. 607–627.
- Aumann T. 2001. Habitat use, temporal activity patterns and foraging behaviour of raptors in the south-west of the Northern Territory, Australia. *Wildl Res*, 28: 365–378.
- Baird RF. 1991. Avian fossils from the Quaternary of Australia. In: *Vertebrate palaeontology of Australasia*, P Vickers-Rich, JM Monaghan, RF Baird, TH Rich (Eds). Pioneer Design Studio Ltd, Lilydale, & Monash University Publications Committee, Melbourne; p. 809–870.
- Baird RF, Rich PV, van Tets GF. 1991. Localities yielding avian assemblage of Quaternary age in Australia. In: *Vertebrate palaeontology of Australasia*, P Vickers-Rich, JM Monaghan, RF Baird, TH Rich (Eds). Pioneer Design Studio Ltd, Lilydale, & Monash University Publications Committee, Melbourne; p. 850–870.
- Barba-Montoya J, Tao Q, Kumar S. 2021. Molecular and morphological clocks for estimating evolutionary divergence times. *BMC Ecology and Evolution*, 21(1): 1–15.
- Baumel JJ, Witmer LM. (1993) Osteologia. In: *Handbook of avian anatomy: nomina anatomica avium, 2<sup>nd</sup> edition*, J.J. Baumel, A.S. King, J.E. Breazile, H.E. Evans and J.C. Vanden Berge (Eds). Publications of the Nuttall Ornithological Club 23. Nuttall Ornithological Club Cambridge, MA; p. 45–132
- Beck RMD, Louys J, Brewer P, Archer M, Black KH, Tedford RH. 2020. A new family of diprotodontian marsupials from the latest Oligocene of Australia and the evolution of wombats, koalas, and their relatives (Vombatiformes). *Sci Rep*, 10, 9741, <https://doi.org/10.1038/s41598-020-66425-8>.
- Boles WE. 1993. *Pengana robertbolesi*, a peculiar bird of prey from the Tertiary of Riversleigh, northwestern Queensland, Australia. *Alcheringa*, 17: 19–25.
- Boles WE, Finch MA, Hofheins RH, Vickers-Rich P, Walters M, Rich TH. 2013. A fossil stone-curlew (Aves: Burhinidae) from the Late Oligocene/Early Miocene of South Australia. In: *International Meeting of the Society-for-Avian-Paleontology-and-*

- Evolution* 2012, Naturhistorisches Museum Wien, Vienna, Austria; p 43–62.
- Boles WE, Ivison TJ. 1999. A new genus of dwarf megapode (Galliformes: Megapodiidae) from the Late Oligocene of central Australia. *Smithson. Cont. Paleobiol.*, 89: 199–206.
- Brodkorb P. 1964. Catalogue of fossil birds: Part 2 (Anseriformes through Galliformes). *Bull Flo Mus Nat Hist*, 8(3): 195–335.
- Brown L, Amadon D (Eds). 1968. *Eagles, hawks and falcons of the world*. Michelin House, London, England.
- Buij R. 2014. Spotted Harrier hunting lizards on foot. *Aust Field Ornithol*, 31(2): 107–112.
- Bunce M, Szulkin M, Lerner HRL, Barnes I, Shapiro B, Cooper A, Holdaway RN. 2005. Ancient DNA provides new insights into the evolutionary history of New Zealand's extinct giant eagle. *PLoS Biology*, 3(1): e9, DOI: 10.1371/journal.pbio.0030009.
- Burleigh JG, Kimball RT, Braun EL. 2015. Building the avian tree of life using a large-scale, sparse supermatrix. *Mol Phylogenet Evol*, 84: 53–63.
- Callen RA. 1977. Late Cainozoic environments of part of Northeastern South Australia. *J Geol Soc Aust*, 24(3–4): 151–169.
- Callen RA, Tedford RH. 1976. New late Cainozoic rock units and depositional environments, Lake Frome area, South Australia. *Trans R Soc S Aust*, 100(3): 125–167.
- Campbell KE, Marcus L. 1992. The relationship of hindlimb bone dimensions to body weight in birds. In: *Papers in avian paleontology honoring Pierce Brodkorb*. KE Campbell (Ed). Natural History Museum of Los Angeles County Science Series, 36, Los Angeles, California; p. 395–412.
- Campbell V, Lapointe FJ. 2009. The use and validity of composite taxa in phylogenetic analysis. *Syst Biol*, 58(6): 560–572.
- Christidis L, Boles W. 2008. *Systematics and taxonomy of Australian birds*. CSIRO Publishing, Melbourne, Australia.
- De Pietri V, Scofield RP, Zelenkov N, Boles WE, Worthy TH. 2016. The unexpected survival of an ancient lineage of anseriform birds into the Neogene of Australia: the youngest record of Presbyornithidae. *Roy Soc Open Sci*, 3: 150635, <http://dx.doi.org/10.1098/rsos.150635>.
- Debus SJS. 1998. *The birds of prey of Australia: a field guide*. Oxford University Press, Melbourne, Australia.

- Dickinson EC, Remsen JV Jr (Eds). 2013. *The Howard & Moore Complete Checklist of Birds of the World*. 4<sup>th</sup> edition, vol 1. Aves Press: Eastbourne, UK.
- Drexel JF, Preiss WV (Eds). 1995. *The Geology of South Australia: the Phanerozoic*. Vol 2. Geol. Surv. S. Aust. Bull. 54.
- Duchéne DA, Jun Tong K, Foster CSP, Duchéne S, Lanfear R, Ho SYW. 2020. Linking branch lengths across sets of loci provides the highest statistical support for phylogenetic inference. *Mol Biol Evol*, 37(4): 1202–1210.
- Elzanowski A, Paul GS, Stidham TA. 2001. An avian quadrate from the Late Cretaceous Lance Formation of Wyoming. *J Vert Paleo*, 20(4): 712–719.
- Elzanowski A, Stidham TA. 2010. Morphology of the quadrate in the Eocene anseriform *Presbyornis* and extant galloanserine birds. *J Morphol*, 271: 305–323.
- Elzanowski A, Zelenkov NV. 2015. A primitive heron (Aves: Ardeidae) from the Miocene of Central Asia. *J Ornithol*, 156: 837–846.
- Eyton TC. 1867. *Osteologia Avium; or, A Sketch of the Osteology of Birds*. Vol 2. R Hobson, Wellington, Salop/Shropshire, England.
- Feldmann R. 1989. Whitening fossils for photographic purposes. *The Paleontological Society Special Publications*, 4: 342–346.
- Ferguson-Lees J, Christie DA (Eds). 2001. *Raptors of the World*. Christopher Helm Publishers, London: p. 992.
- Field DJ, Lynner C, Brown C, Darroch SAF. 2013. Skeletal correlates for body mass estimation in modern and fossil flying birds. *PLoS One*, 8(11): e82000. doi: 10.1371/journal.pone.0082000
- Fordyce RE. 1983. Rhabdosteid dolphins (Mammalia: Cetacea) from the Middle Miocene, Lake Frome area, South Australia. *Alcheringa*, 7(1): 27–40. DOI: 10.1080/03115518308619631.
- Fowler DW, Freedman EA, Scannella JB. 2009. Predatory functional morphology in raptors: interdigital variation in talon size is related to prey restraint and immobilisation technique. *PloS One*, 4: e7999.
- Gadow H. 1891-1893. Anatomischer Theil. Dr HG Bronn's Klassen und Ordnungen des Thier-Reichs. Leipzig: wissenschaftlich dargestellt in Wort und Bild. CF Winter'sche Verlagshandlung. Vögel. Anatomischer Theil. Bronn's Klassen und Ordnungen des Thier-Reichs. Leipzig: CF Winter Verlagshandlung. Vol. 6. pt 4, p.1008.
- Gaff P, Boles WE. 2010. A new eagle (Aves: Accipitridae) from the Mid Miocene Bullock

- Creek Fauna of northern Australia. *Rec Aust Mus*, 62: 71–76.
- Gaillard C. 1939. Contribution à l'étude des oiseaux fossils. *Arch Mus Hist Nat Lyon*, 15: 1–100.
- Gill F, Donsker P, Rasmussen P (Eds). 2020. IOC World Bird List (v10.2). doi: 10.14344/IOC.ML.10.2.
- Goloboff PA, Pittman M, Pol D, Xu X. 2019. Morphological data sets fit a common mechanism much more poorly than DNA sequences and call into question the Mk model. *Syst Biol*, 68(3): 494–504.
- Griffiths CS, Barrowclough GF, Groth JG, Mertz LA. 2007. Phylogeny, diversity, and classification of the Accipitridae based on DNA sequences of the RAG-1 exon. *J Avian Biol*, 38: 587–602.
- Hackett SJ, Kimball RT, Reddy S, Bowie RC, Braun EL, Braun MJ, Chojnowski JL, Cox WA, Han K-L, Harshman J, Huddleston CJ, Marks BD, Miglia KJ, Moore WS, Sheldon FH, Steadman DW, Witt CC, Yuri T. 2008. A phylogenomic study of birds reveals their evolutionary history. *Science*, 320: 1763–1768.
- Holdaway RN. 1991. Systematics and palaeobiology of Haast's eagle (*Harpagornis moorei* Haast, 1872) (Aves: Accipitridae). Unpublished PhD thesis. Department of Zoology, University of Canterbury, Christchurch (New Zealand). 472 p.
- Holdaway RN. 1994. An exploratory phylogenetic analysis of the genera of the Accipitridae, with notes on the biogeography of the family. In: *Raptor conservation today*. Meyburn B-U, Chancellor RD (Eds). London, UK: World Working Group on Birds of Prey and Owls; p. 601–649.
- Hou L. 1984. The Aragonian vertebrate fauna of Xiacaswan, Jiangsu 2. Aegypinae (Falconiformes [sic], Aves). *Vert PalAs*, 22(1): 14–22.
- Hou L, Zhou Z, Zhang F, Li J. 2000. A new vulture from the Miocene of Shandong, eastern China. *Vert PalAs*, 38(2): 108–112.
- Jollie M. 1976. A contribution to the morphology and phylogeny of the Falconiformes. *Evolutionary Theory*, 1, 285–298.
- Knapp M, Thomas JE, Haile J, Prost S, Ho SYW, Dussex N, Cameron-Christie S, Kardailsky O, Barnett R, Bunce M, Gilbert MTP, Scofield RP. 2019. Mitogenomic evidence of close relationships between New Zealand's extinct giant raptors and small-sized Australian sister-taxa. *Mol Phylogenet Evol*, 134: 122–128.
- Kurochkin EN. 1968. Fossil remains of birds from Mongolia. *Ornitologiya*: 9, 323–330.

- Kurochkin EN. 1976. A survey of the Paleogene birds of Asia. *Smithson. Cont. Paleobiol.*, 27: 75–86.
- Lanfear R, Frandsen PB, Wright AM, Senfeld T, Calcott B. 2016. PartitionFinder 2: new methods for selecting partitioned models of evolution formolecular and morphological phylogenetic analyses. *Mol Biol Evol.* DOI: dx.doi.org/10.1093/molbev/msw260
- Lerner HRL, Mindell DP. 2005. Phylogeny of eagles, Old World vultures, and other Accipitridae based on nuclear and mitochondrial DNA. *Mol Phylogenet Evol*, 37: 327–346.
- Li Z, Clarke JA, Zhou Z, Deng T. 2016. A new Old World vulture from the late Miocene of China sheds light on Neogene shifts in the past diversity and distribution of the Gypaetinae. *Auk*, 133: 615–625.
- Lindsay JM. 1987. Age and habitat of a monospecific foraminiferal fauna from near-type Etadunna Formation, Lake Palankarina, Lake Eyre Basin. *South Australian Department of Mines Report*, 87: 93.
- Linnaeus, C. 1758. *Systema Naturae per Regna Tria Naturae*, 10th Edition, revised, Vol 1: Regnum Animale. Salvii, L. Holmiae, Stockholm, Sweden, iv + 824 pp.
- Livezey BC, Zusi RL. 2007. Higher-order phylogeny of modern birds (Theropoda, Aves: Neornithines) based on comparative anatomy. II. Analysis and discussion. *Zool J Linn Soc-Lond*, 149: 1–95.
- Louys J, Price GJ. 2015. The Chinchilla Local Fauna: an exceptionally rich and well-preserved Pliocene vertebrate assemblage from fluvial deposits of south-eastern Queensland, Australia. *Acta Palaeontologica Polonica*, 60(3): 551–572.
- Marchant S, Higgins PJ. 1993. *Handbook of Australian, New Zealand and Antarctic Birds. Vol. 2: Raptors to Lapwings*. Melbourne, Victoria: Oxford University Press.
- Martin HA. 1990. The palynology of the Namba Formation in the Wooltana-1 bore, Callabonna Basin (Lake Frome), South Australia, and its relevance to Miocene grasslands in central Australia. *Alcheringa*, 14 (3): 247–255.
- Mayr G. 2006a. The post-cranial osteology and phylogenetic position of the Middle Eocene *Messelastur gratulator* Peters, 1994 – a morphological link between owls (Strigiformes) and falconiform birds? *J Vert Palaeontol*, 25(3): 635–645.
- Mayr G. 2006b. A new raptorial bird from the Middle Eocene of Messel, Germany. *Hist Biol*, 18(2): 99–106.
- Mayr G. 2009. A well-preserved skull of the “falconiform” bird *Masillaraptor* from the middle

- Eocene of Messel (Germany). *Palaeodiversity*, 2: 315–320.
- Mayr G. 2011. Well-preserved new skeleton of the Middle Eocene *Messelastur* substantiates sister group relationship between Messelasturidae and Halcyornithidae (Aves, ?Pan-Psittaciformes). *J Syst Palaeontol*, 9: 159–171.
- Mayr G. 2014. Comparative morphology of the radial carpal bone of neornithine birds and the phylogenetic significance of character variation. *Zoomorphology*, 133: 425–434.
- Mayr G. 2016. Variations in the hypotarsus morphology of birds, and their evolutionary significance. *Acta Zool*, 97(2): 196–210.
- Mayr G. 2017. *Avian Evolution*. Chichester, West Sussex, John Wiley and Sons.
- Mayr G. 2018. Size and number of the hypoglossal nerve foramina in the avian skull and their potential neuroanatomical significance. *J Morphol*, 279(2): 274–285.
- Mayr G, Hurum JH. 2020. A tiny, long-legged raptor from the early Oligocene of Poland may be the earliest bird-eating diurnal bird of prey. *Sci Nat*, 107(48), <https://doi.org/10.1007/s00114-020-01703-z>.
- Mayr G, Perner T. 2020. A new species of diurnal birds of prey from the late Eocene of Wyoming (USA) – one of the earliest New World records of the Accipitridae (hawks, eagles and allies). *Neues Jahrb Geol Paläontol-Abh*, 297(2): 205–215.
- Megirian D, Prideaux GJ, Murray PF, Smit N. 2010. An Australian land mammal biochronological scheme. *Paleobiology*, 36(4): 658–671.
- Migotto, R. 2013. Phylogeny of Accipitridae (Aves: Accipitriformes) based on osteological characters. PhD Dissertation, Universidade de São Paulo, Instituto de Biociências, Departamento de Zoologia.
- Miller AH. 1966. The fossil pelicans of Australia. *Mem Qld Mus*, 14(5): 181–190.
- Miller MA, Pfeiffer W, Schwartz T. 2010. Creating the CIPRES Science Gateway for inference of large phylogenetic trees. In: *Proceedings of the Gateway Computing Environments Workshop (GCE)*, New Orleans, LA; p. 1–8.
- Milne-Edwards A. 1863. Mémoire sur la distribution géologique des oiseaux fossils et description de quelques espèces nouvelles. *Ann Sci Nat Zool*, 4(20): 133–176.
- Milne-Edwards A. 1871. Des caracteres ostéologiques des oiseaux de proie diurnes. In: *Recherches anatomiques et paléontologiques pour servir a l'histoire des oiseaux fossils de la France*. Victor Masson et Fils, Paris, France; p. 406–473.
- Milne-Edwards A. 1892. Sur les oiseaux fossiles des dépôts Eocenes de Phosphate de

Chaux du sud de la France. *Comptes Rendus du Second Congrès Ornithologique International, Budapest*: 60–80.

- Mindell DP, Fuchs J, Johnson JA. 2018. Phylogeny, taxonomy and geographic diversity of diurnal raptors: Falconiformes, Accipitriformes and Cathartiformes. In: *Birds of Prey: biology and conservation in the XXI century*, J. H. Sarasola, J. Grande, J. Negro (Eds). Springer, Cham, Switzerland; p. 3–32.
- Mlíkovský J. 2002. *Cenozoic birds of the world part 1: Europe*. Ninox Press, Praha, Czech Republic.
- Mourer-Chauviré C. 1991. The Horusornithidae nov. fam., Accipitriformes (Aves) with a hyperflexible intertarsal joint from the Eocene of Quercy. *Geobios*, 13: 183–192.
- Nagy J, Tökölyi J. 2014. Phylogeny, historical biogeography and the evolution of migration in accipitrid birds of prey (Aves: Accipitriformes). *Ornis Hungarica*, 22: 15–35.
- Norrish K, Pickering JG. 1983. Clay Minerals. In: *Soils: an Australian viewpoint*. CSIRO Division of Soils. CSIRO Academic, Melbourne; p. 281–308.
- Oatley G, Simmons RE, Fuchs J. 2015. A molecular phylogeny of the harriers (*Circus*, Accipitridae) indicate the role of long distance dispersal and migration in diversification. *Mol Phylogenet Evol*, 85: 150–160.
- Olson SL. 1985. The fossil record of birds. In: *Avian Biology*, vol. 8, DS Farmer, JR King, KC Parkes. Academic Press, New York; p. 79–252.
- Peters JL. 1934. *Check-list of the birds of the world: Vol. 1*. Harvard University Press, Cambridge.
- Pledge NS. 2003. A new species of *Muramura* Pledge (Wynyardiidae: Marsupialia) from the Middle Tertiary of the Callabonna Basin, Northeastern South Australia. *Bull Am Mus Nat Hist*, 279: 541–555.
- Pledge NS. 2016. New specimens of ektopodontids (Marsupialia: Ektopodontidae) from South Australia. *Mem Mus Vic*, 74: 173–187.
- Prum RO, Berv JS, Dornburg A, Field DJ, Townsend JP, Lemmon EM, Lemmon AR. 2015. A comprehensive phylogeny of birds (Aves) using targeted next-generation DNA sequencing. *Nature*, 526(7574): 569–573.
- Rasmussen DT, Olsen SL, Simons EL. 1987. Fossil birds from the Oligocene Jebel Qatrani Formation, Fayum Province, Egypt. *Smithson. Cont. Paleobiol.*: 62, 1–19.
- Rich P, van Tets J. 1982. Fossil birds of Australia and New Guinea: their biogeographic, phylogenetic and biostratigraphic input. In: *The Fossil Vertebrate Record of*

- Australasia*. P. V. Rich, and E. M. Thompson (Eds). Monash University Offset Printing Unit, Clayton, Victoria; p. 235–384.
- Rich TH, Archer M, Hand SJ, Godthelp H, Muirhead J, Pledge NS, Flannery TF, Woodburne MO, Case JA, Tedford RH, Turnbull WD, Lundelius EL Jr, Rich LSV, Whitelaw MJ, Kemp A, Vickers-Rich P. 1991. Australian Mesozoic and Tertiary terrestrial mammal localities. In: *Vertebrate palaeontology of Australasia*, P Vickers-Rich, JM Monaghan, RF Baird, TH Rich (Eds). Pioneer Design Studio Ltd, Lilydale, & Monash University Publications Committee, Melbourne; p. 1005–1057.
- Rich TH, Archer M, Tedford RH. 1978. *Raemotherium yatkolai*, gen. et. sp. nov., a primitive diprotodontid from the medial Miocene of South Australia, *Mem Mus Vic*, 39: 85–91.
- Rich THV, Archer M. 1979. *Namilamadeta snideri*, a new diprotodontan (Marsupialia, Vombatoidea) from the medial Miocene of South Australia. *Alcheringa*, 3(3): 197–208.
- Ridgway R. 1874. Catalogue of the ornithological collection of the Boston Society of Natural History Part II: Falconidae. *Proc Boston Soc Nat*, 16: 43–72.
- Ronquist F, Klopfstein S, Vilhelmsen L, Schulmeister S, Murray DL, Rasnitsyn AP. 2012. A total-evidence approach to dating with fossils, applied to the early radiation of the Hymenoptera. *Syst Biol*, 61(6): 973–999.
- Sharpe RB. 1874. *Catalogue of the Accipitres, or diurnal birds of prey, in the collection of the British Museum (Volume 1)*. Order of the Trustees, UK, London.
- Sibley CG, Ahlquist JE. 1990. *Phylogeny and classification of birds: a study in molecular evolution*. Yale University Press, New Haven, Connecticut.
- Stirton RA, Tedford RH, Miller AH. 1961. Cenozoic stratigraphy and vertebrate palaeontology of the Tirari Desert, South Australia. *Rec South Aust Mus*, 14: 19–61.
- Stresemann E, Amadon D. 1979. Order Falconiformes. In: *Check-list of the birds of the world, Volume 1, 2<sup>nd</sup> edition; revision of the work of James L. Peters*. E. Mayr, G. Cottrell (Eds). Museum of Comparative Zoology, Cambridge, Massachusetts; p. 271–425.
- Sushkin PP. 1905. Zur Morphologie des Vogelskelets: vergleichende Osteologie der normalen Tagraubvögel (Accipitres) und die Fragen der Classification: mit IV Taf. *Nouv MémSoc Imp Naturalistes Moscou*, 16: 164–247.
- Tedford RH, Archer M, Bartholomai A, Plane M, Pledge NS, Rich, T., Rich, P. & Well, R. T. (1977) The discovery of Miocene vertebrates, Lake Frome area, South Australia.

*BMR J Aust Geol Geop*, 2: 53–57.

- Tedford RH, Woodburne MO. 1987. The Illariidae, a new family of vombatiform marsupials from Miocene strata of South Australia and an evaluation of the homology of molar cusps in the Diprotodontia. In: *Possums and opossums: studies in evolution*, M Archer (ed). Surrey Beatty and Sons, Chipping Norton, New South Wales. Vol. 2; p. 401–418.
- Thorn KM, Hutchinson MN, Lee MSY, Brown NJ, Camens AB, Worthy TH. 2021. A new species of *Proegernia* from the Namba Formation in South Australia and the early evolution and environment of Australian egeriine skinks. *Roy Soc Open Sci*, 8: 201686.
- Travouillon KJ, Archer M, Hand SJ, Godthelp H. 2006. Multivariate analyses of Cenozoic mammalian faunas from Riversleigh, north-western Queensland. *Alcheringa: an Australasian Journal of Palaeontology*, 30(S1): 323-349.
- Vickers-Rich P. 1991. The Mesozoic and Tertiary history of birds on the Australian plate. In: *Vertebrate palaeontology of Australasia*, P Vickers-Rich, JM Monaghan, RF Baird & TH Rich (Eds). Pioneer Design Studio Ltd, Lilydale, & Monash University Publications Committee, Melbourne; p. 721–809.
- Vieillot, LJP. 1816. *Analyse d'une nouvelle ornithologie elementaire*. D'eterville, Paris, France; 70 pp.
- Vigors, NA. 1824. Sketches in ornithology; or, observations on the leading affinities of some of the more extensive groups of birds. On the groups of the Falconidae. *Zoological Journal* 1: 308–346.
- Walker CA, Dyke GJ. 2006. New records of fossil birds of prey from the Miocene of Kenya. *Hist Biol*, 18(2): 95–98.
- Wetmore A. 1933. An Oligocene eagle from Wyoming. *Smithsonian Miscellaneous Collections*, 87(19): 1–9.
- Whitacre D, Jenny JP. 2013. *Neotropical birds of prey: biology and ecology of a forest raptor community*. Cornell University Press, Sage House, Ithaca.
- Willis PMA. 1997. Review of fossil crocodiles from Australasia. *Aust Zool*, 30(3): 287–298.
- Willis PMA, Molnar RE. 1991. A new middle Tertiary crocodile from Lake Palankarina, South Australia. *Rec South Aust Mus*, 25(1): 39–55
- Wink M. 1995. Phylogeny of Old and New World vultures (Aves: Accipitridae and Cathartidae) inferred from nucleotide sequences of the mitochondrial cytochrome b

- gene. *Z Naturforsch C*, 50(11-12): 868–882.
- Wink M, Sauer-Gürth H. 2004. Phylogenetic relationships in diurnal raptors based on nucleotide sequences of mitochondrial and nuclear marker genes. In: *Raptors Worldwide*, R. D. Chancellor, B. -U. Meyburg (Eds). World Working Group on Birds of Prey and Owls, MME/Birdlife Hungary, Budapest; p. 483–498.
- Woodburne MO, MacFadden BJ, Case JA, Springer MS, Pledge NS, Power JD, Woodburne JM, Springer KB. 1994. Land mammal biostratigraphy and magnetostratigraphy of the Etadunna Formation (Late Oligocene) of South Australia. *J Vert Paleontol*, 13(4): 483–515.
- Woodburne MO, Tedford RH. 1975. The first Tertiary monotreme from Australia. *Am Mus Novit*, 2588: 1–11.
- Woodburne MO, Tedford RH, Archer M, Pledge NS. 1987. *Madakoala*, a new genus and two species of Miocene koalas (Marsupialia: Phascolarctidae) from South Australia and a new species of *Perikoala*. In: *Possums and opossums: studies in evolution*, M. Archer (ed). Surrey Beatty and Sons, Chipping Norton, New South Wales. Vol. 1; p. 293–317.
- Woodburne MO, Tedford RH, Archer M, Turnbull WD, Plane MD, Lundelius EL. 1985. Biochronology of the continental mammal record of Australia and New Guinea. *Special Publication South Australian Department of Mines and Energy*, 5: 347–363.
- Woodburne MO, Tedford RH, Archer M. 1987. New Miocene pseudocheirids (Pseudocheiridae: Marsupalia) from South Australia. In: *Possums and opossums: studies in evolution*, M. Archer (ed). Surrey Beatty and Sons, Chipping Norton, New South Wales. Vol. 2; p. 639–679.
- Woodhead J, Hand SJ, Archer M, Graham I, Sniderman K, Arena DA, Black KH, Godthelp H, Creaser P, Price E. 2016. Developing a radiometrically-dated chronologic sequence for Neogene biotic change in Australia, from the Riversleigh World Heritage Area of Queensland. *Gondwana Res*, 29(1): 153–167.
- Worthy TH. 2009. Descriptions and phylogenetic relationships of two new genera and four new species of Oligo-Miocene waterfowl (Aves: Anatidae) from Australia. *Zool J Linn Soc-Lond*, 156: 411–454.
- Worthy TH. 2011. Descriptions and phylogenetic relationships of a new genus and two species of Oligo-Miocene cormorants (Aves: Phalacrocoracidae) from Australia. *Zool J Linn Soc-Lond*, 163(1): 277–314.

- Worthy TH, Holdaway RN. 2002. *The lost world of the moa: prehistoric life of New Zealand*. Indiana University Press, Bloomington, Indiana.
- Worthy TH, Mitri M, Handley WD, Lee MS, Anderson A, Sand C. 2016. Osteology supports a stem-galliform affinity for the giant extinct flightless bird *Sylviornis neocaledoniae* (Sylviornithidae, Galloanseres). *PLOS ONE*, 11(3), DOI: 10.1371/journal.pone.0150871.
- Worthy TH, Nguyen JMT. 2020. An annotated checklist of the fossil birds of Australia. *Trans R Soc S Aust*, 144(1): 66–108.
- Worthy TH, Yates A. 2018. A review of the smaller birds from the late Miocene Alcoota local faunas of Australia with a description of a new anatids species. *Contribuciones del MACN*, 7: 221–252.
- Zhang Z, Feduccia A, James HF. 2012. A Late Miocene accipitrid (Aves: Accipitriformes) from Nebraska and its implications for the divergence of Old World vultures. *PLOS ONE*, 7(11): e48842.
- Zhang Z, Zheng X, Zheng G, Hou L. 2010. A new Old World vulture (Falconiformes: Accipitridae) from the Miocene of Gansu Province, northwest China. *J Ornithol*, 151: 401–408.

## Chapter 3: An old-world vulture from the Australian Pleistocene: “*Taphaetus*” *lacertosus* de Vis 1905 (Aegypiinae, Accipitridae).

Ellen K. Mather<sup>1, 2</sup>, Michael S. Y. Lee<sup>1, 3</sup>, Trevor H. Worthy<sup>1</sup>

<sup>1</sup>College of Science and Engineering, Flinders University, GPO 2100, Adelaide, SA 5001, Australia

<sup>2</sup>Corresponding author, [math0083@flinders.edu.au](mailto:math0083@flinders.edu.au)

<sup>3</sup> Earth Sciences Section, South Australian Museum, North Terrace, Adelaide 5000, Australia

### Abstract

The Australian Pleistocene fossil record of Accipitridae is poorly understood. Only two extinct species have been described from fossils for this time period, which have had little further investigation beyond confirming their accipitrid status. One of these species is “*Taphaetus*” *lacertosus* de Vis, 1905, described from a distal humerus and a quadrate from north-eastern South Australia. While this species was verified as an accipitrid in subsequent studies, its exact taxonomic affinities remain conjectural. In this study, new material, comparisons of bones to living species, and phylogenetic analyses reveals that “*T.*” *lacertosus* is an Old-World vulture, in the subfamily Aegypiinae, and new fossils from Wellington Caves (NSW) and the Nullarbor Plains (WA) reveal it had a wide geographical range across Pleistocene Australia. A referred tarsometatarsus exhibiting a lack of hyper-developed trochleae indicates that “*T.*” *lacertosus* was most likely a scavenger like other aegypiines based on the lack of hyper-developed trochleae. This significantly expands the palaeogeographical range of the Old-World vultures and reveals for the first time the existence of large, obligate scavenging birds of prey, an avian guild absent in the modern fauna, in the megafaunal-rich biotas of the Australian Pleistocene.

**Keywords:** Fossil birds, extinction, scavengers, Old World vultures, biogeography, Australia

### 3.1 INTRODUCTION

#### 3.1.1 Pleistocene Australian Accipitridae

In Australia, the Pleistocene (2.56 Ma–11.7 Ka) was marked by dry, arid climatic conditions, with the environment dominated by grasslands, open woodland (Sniderman et al. 2007) and desert (Hesse et al. 2004), similar to the present day. The Australian megafauna, which included at least 20 genera of large mammals, four of large birds, and three of large reptiles (Wroe et al. 2013; Johnson et al. 2021), inhabited these environments until most of them went extinct between 50–40 Ka (Roberts et al. 2001; van der Kaars et al. 2017). The raptor guild of the Pleistocene can be assumed to have comprised most of the living Australian species, with fossil material of *Aquila audax* at least 500–200 Ka old (Baird 1991; EKM, THW unpublished data). However, two extinct species have been described from this epoch; *Aquila brachialis* (de Vis, 1889) and “*Taphaetus*” *lacertosus* de Vis, 1905, that represent potential additional diversity (Gaff 2002 unpublished thesis; Boles 2006; Boles 2017; Worthy and Nguyen 2020).

#### 3.1.2 The history of “*Taphaetus*” *lacertosus*

“*Taphaetus*” *lacertosus* de Vis, 1905 was described from a distal humerus and a quadrate collected from Kalamurina on the Warburton River in north-eastern South Australia (de Vis 1905). De Vis compared the fossil material with living Australian bird species of similar size and noted that the fossil humerus was not much larger than that of *Haliaeetus leucogaster*. However, it was also highly distinct from both that species and *Aquila audax*.

The generic assignment of “*T.*” *lacertosus* is problematic. The genus *Taphaetus* was first established by de Vis (1891) with *Uroaetus brachialis* de Vis, 1889, the type species by monotypy, forming the new combination *Taphaetus brachialis* (de Vis, 1889) to which taxon he also assigned a fossil femur. The holotype of “*Taphaetus*” *brachialis*, a distal humerus, along with a femur were reassigned back to *Uroaetus* by de Vis (1905); *Uroaetus* Kaup, 1844 is a junior synonym of *Aquila* Brisson, 1760, so *brachialis* is now listed in *Aquila* (see Worthy and Nguyen 2020). In their review of the Australian fossil avifauna, Worthy and Nguyen (2020) noted that the reassignment of its type species *Uroaetus brachialis* back from *Taphaetus* de Vis, 1891, to *Uroaetus*, meant that *Taphaetus* de Vis, 1891 then became a synonym of *Uroaetus* Kaup, 1844 and so is now a synonym of *Aquila*. However, de Vis (1905), after reverting *brachialis* back to *Uroaetus*, then used the genus name *Taphaetus* for the description of “*Taphaetus*” *lacertosus* de Vis, 1905. As a result, *Taphaetus* de Vis, 1905, with the type species by monotypy *Taphaetus lacertosus* de Vis, 1905, is a junior homonym for *Taphaetus* de Vis, 1891, and so is unavailable as a genus name.

*Aquila brachialis* was found to be correctly identified as an eagle in van Tets and Rich’s (1990) review of avian taxa named by de Vis, while “*Taphaetus*” *lacertosus* was

stated to require more scrutiny. The relationships of “*Taphaetus*” *lacertosus* were first commented on by van Tets (1974), who designated the humerus as the lectotype, and suggested it was a member of the living genus *Ichthyophaga*, a genus of fish eagle now a synonym of *Haliaeetus*. Later, van Tets (1984) without rationale suggested it was related to the living accipitrid subfamily Gypaetinae, which all accipitrid vultures were assigned to at the time. Other works have also suggested the presence of Old-World vultures in the Pleistocene Australian avifauna (Rich and van Tets 1982; Tedford and Wells 1990; Gaff 2002 unpublished thesis) but little has been done to verify these claims.

Given ‘*lacertosus*’ is an available species name in nomenclatural terms, determining whether it is a species distinct from living and other fossil taxa, and thus its taxonomic (including generic) affinity, is a necessary precursor to investigating the diversity of Australian Pleistocene accipitrids and assignment of such fossils to taxa. Therefore, the aim of this chapter is to redescribe the lectotype of ‘*lacertosus*’, establish whether it is a distinct taxon, and if so correct its nomenclature by assigning it to either an existing or a new genus as required. In doing so, other large fossil accipitrid fossils from Pleistocene sites in Australia will be surveyed for possible assignment to the taxon and then the relationships reassessed for the taxon. The quadrate described by de Vis (1905) was unavailable for study due to collection closure at Queensland Museum. Comparisons were instead made to extant specimens on hand using the description and illustrations of the fossil of de Vis (1905).

## 3.2 MATERIALS AND METHODS

### 3.2.1 Abbreviations

**Institution.** South Australia Museum, Adelaide, SA, Australia (SAMA); Museums Victoria, Melbourne, VIC, Australia (NMV); Australian National Wildlife Collection, Canberra, ACT, Australia (ANWC); Australian Museum, Sydney, NSW, Australia (AM); University of Kansas Institute of Biodiversity, Lawrence, KS, USA (KU); Natural History Museum, London, UK (NHMUK); Smithsonian Museum of Natural History, Washington DC, USA (USNM); Queensland Museum, Brisbane, QLD, Australia (QM); Western Australian Museum, Perth, WA, Australia (WAM).

**Bones.** Humerus (hum); tarsometatarsus (tmt).

### 3.2.2 Nomenclature

The anatomical nomenclature advocated by Baumel and Witmer (1993) is followed for all bones. Avian nomenclature follows Nagy and Tökölyi (2014) for subfamilial composition (excluding Milvinae) and Dickinson and Remsen (2013) for species, wherein the

authors for living taxa can be found. Subfamily nomenclature differs from that in Mindell et al. (2018) by recognising Haliaeetinae as distinct from Buteoninae, and Harpiinae from Aquilinae.

### 3.2.3 Comparative Material

Specimens were obtained on loan from museums and other institutions from across Australia and overseas.

Ciconiiformes.

**Threskiornithidae.** *Threskiornis spinicollis* SAMA B48351. **Ciconiidae.** *Ciconia ciconia* SAMA B49223, SAMA B11601.

Accipitriformes.

**Cathartidae.** *Coragyps atratus* SAMA B36873.

**Sagittariidae.** *Sagittarius serpentarius* USNM 223836.

**Pandionidae.** *Pandion haliaetus* SAMA B37096, NMV B30256.

#### Accipitridae specimens (in phylogenetic order):

Elaninae: *Elanus axillaris* NMV B34037; *Elanus scriptus* NMV B8617, NMV B30263, ANWC 22680. Perninae: *Elanoides forficatus* USNM 622340; *Chondrohierax uncinatus* USNM 289784; *Pernis apivorus* SAMA B59278; *Lophoictinia isura* NMV B18533, ANWC 44373; *Hamirostra melanosternon* ANWC (FALS-41), SAMA B36200. Gypaetinae: *Polyboroides typus* USNM 430434; *Neophron percnopterus* SAMA B11449; *Gypohierax angolensis* USNM 291316; *Gypaetus barbatus* NHMUK S.1972.1.59, NHMUK S.1896.2.16.120, NHMUK S.1952.3.61. Circaetinae: *Spilornis cheela* USNM 562001; *Terathopius ecaudatus* NMV 18575; *Pithecophaga jefferyi* NHMUK S.1910.2.11.1a, NHMUK S.1961.23.1. Aegyptiinae: *Necrosyrtes monachus* USNM 620646; *Gyps coprotheres* ANWC 22724; *Gyps fulvus* NMV 18574, NMV B30269; *Aegyptius monachus* NMV R553; *Sarcogyps calvus* NHMUK S.2013.22.1, NHMUK S.2007.30.1; *Trigonoceps occipitalis* NHMUK S.1954.30.54; *Torgos tracheliotos* NHMUK S.1930.3.24.248, NHMUK S.1952.1.172. Aquilinae: *Aquila audax* SAMA B46613, NMV B19228; *Aquila chrysaetos* NMV B32659, ANWC 22682 (FALS-123); *Aquila fasciata* (labelled as *Hieraaetus fasciatus*) NMV B30575; *Hieraaetus morphnoides* SAMA B47128, NMV B8643, NMV B20224; *Hieraaetus* (= *Harpagornis*) *moorei* casts of original type material, NMV P33032 (tibiotarsus), NMV P33031 (pedal phalanx), NMV P33030 (tarsometatarsus), NMV P33029 (femur), NMV P33028 (humerus), NMV P33027 (femur), NMV P33026 (ulna); *Spizaetus tyrannus* KU 35007; *Spizaetus ornatus* KU 72077. Harpiinae: *Morphnus guianensis* NHMUK 1851.12.2.10; *Harpia harpyja* NHMUK 1862.3.19.14, 1909.8.18.1. Haliaeetinae: *Haliaeetus leucogaster* NMV B8847, SAMA

B49459; *Haliaeetus leucocephalus* ANWC 22723 (16500), NMV B15601; *Haliaeetus albicilla* NMV B34417; *Haliastur indus* ANWC 22719, NMV B13753; *Haliastur sphenurus* NMV B11661, SAMA B33998; *Milvus migrans* SAMA B47130, NMV B20404. Accipitrinae: *Circus assimilis* SAMA B56454, ANWC 22727; *Circus cyaneus* ANWC 22735; *Circus aeruginosus* NMV B12891; *Accipiter fasciatus* NMV B13444, SAMA B36355; *Accipiter cooperii* ANWC 22764, ANWC 22765; *Accipiter striatus* ANWC 22747, NMV B12666; *Accipiter novaehollandae* NMV B18401; *Accipiter cirrocephalus* NMV B16071, NMV B10346; *Accipiter nisus* NMV B12413, ANWC 22742; *Accipiter gentilis* ANWC 22736, NMV B12927. Buteoninae: *Ictinia mississippiensis* ANWC 22681 (21655), NMV B13343; *Geranospiza caerulescens* NHMUK S.1903.12.20.318; *Buteo buteo* SAMA B46558, NMV B24505; *Buteo lagopus* NMV B24884, ANWC 22776 (21694); *Buteo nitidus* NMV B13222; *Buteo rufofuscus* NMV B24503.

### 3.2.4 Measurements

Bones were measured to an accuracy of 0.1 mm using digital callipers.

### 3.2.5 Photography and Scanning

All photographs created at Flinders were taken using a focus stacking method using a Canon 5DS-r digital camera 50.0 MP and either a Canon EF 100 mm or 65 mm f2.8 IS USM professional macro lens. Multiple images were then compiled into a single photo using the program Zerene Stacker.

The type specimen for “*Taphaetus*” *lacertosus*, QM F5507 distal humerus, was photographed and surface scanned using an Einscan Pro+ handheld 3D scanner, Industrial Pack tripod and turntable at Queensland Museum by Isaac Kerr, accurate to roughly 200 microns. The resulting point cloud scan files were then processed into triangle meshes in Einscan Software V3.0. This was then compiled into a 3D image using the digital program Blender, which was used to assess the morphological features of the fossil in a way that photography alone could not capture.

### 3.2.6 Phylogenetic Methods

#### ***Morphological data***

Three hundred morphological characters ranging from the cranium to the pedal digits were coded for living species and where applicable in the fossil material. A total of 154 characters was derived from Migotto (2013, unpublished thesis), two from Elzanowski and Stidham (2010), two from Elzanowski and Zelenkov (2015), six from Gaff and Boles (2010), one from Worthy et al. (2016), three from Mayr (2018) and three from Mayr (2014). The remaining characters were novel traits derived from observations and comparisons between the living and fossil specimens.

### **Molecular data**

Molecular data from Burleigh et al. (2015) was added to the morphological data to improve estimated relationships among living species (Lerner and Mindell 2005; Nagy and Tökölyi 2014; Burleigh et al. 2015). The following genes, well-sampled in accipitrids, were used: cytochrome b, cytochrome oxidase 1, NADH dehydrogenase 2, 12s RNA, RAG 1, and fibrinogen B beta introns 6 7.

The following species were sampled for available genes from the above loci: *Ciconia ciconia*, *Coragyps atratus*, *Sagittarius serpentarius*, *Pandion haliaetus*, *Elanus caeruleus*, *Gampsonyx swainsonii*, *Elanoides forficatus*, *Chondrohierax uncinatus*, *Aviceda subcristata*, *Pernis apivorus*, *Lophoictinia isura*, *Hamirostra melanosternon*, *Polyboroides typus*, *Neophron percnopterus*, *Gypohierax angolensis*, *Gypaetus barbatus*, *Spilornis cheela*, *Terathopius ecaudatus*, *Pithecophaga jefferyi*, *Necrosyrtes monachus*, *Gyps fulvus*, *Gyps coprotheres*, *Aegyptius monachus*, *Sarcogyps calvus*, *Trionoceph occipitalis*, *Torgos tracheliotos*, *Harpia harpyja*, *Stephanoaetus coronatus*, *Aquila chrysaetos*, *Hieraaetus morphnoides*, *Hieraaetus fasciatus*, *Aquila fasciata*, *Hieraaetus moorei*, *Spizaetus tyrannus*, *Spizaetus ornatus*, *Haliaeetus leucogaster*, *Haliaeetus leucocephalus*, *Haliaeetus albicilla*, *Milvus migrans*, *Melierax metabates*, *Kaupifalco monogrammicus*, *Circus aeruginosus*, *Circus cyaneus*, *Accipiter cooperii*, *Accipiter striatus*, *Accipiter novaehollandiae*, *Accipiter gentilis*, *Ictinia mississippiensis*, *Geranospiza caerulescens*, *Buteo buteo*, *Buteo lagopus*, *Buteo rufofuscus*, and *Platalea leucorodia*. To reduce missing data, genomic data from *Platalea leucorodia* was used instead of *Threskiornis spinicollis*, and *Elanus caeruleus* for *Elanus scriptus*, as these species pairs consist of closely related taxa (see Campbell and Lapointe 2009 regarding this method).

### **Phylogenetic analysis**

Forty-seven species of Accipitridae and one each from Pandionidae, Sagittariidae, Cathartidae, Threskiornithidae and Ciconiidae were sampled. The list of 300 characters (67 ordered) is in Appendix 1, the data matrix is in SI.1, and the input file is in SI.5. Phylogeny was assessed using the parsimony program PAUP 4.0a169, using a combined molecular-morphological dataset and heuristic searches. Each search comprised of 1000 random addition replicates, and enabled TBR branch swapping, with NCHUCK set to 1000. Characters that were inapplicable to a specimen were coded using '-', while missing data were coded as '?' for recoding purposes, though PAUP treats these identically. The taxa *Threskiornis spinicollis*, *Ciconia ciconia*, *Coragyps atratus*, and *Sagittarius serpentarius* were set as outgroups to the Accipitridae. The support for clades on these trees was then assessed using bootstrapping, which was set to a conlevel of 50 (support shown on bootstrap consensus tree if >50%) and 1000 replicates.

### **3.2.7 Fossil Sites**

#### ***Kalamurina, Warburton River***

The Kalamurina locality is located near the Kalamurina Homestead, on the Warburton River approximately 55 km north-east of Lake Eyre in north-eastern South Australia. Fossils from this site were collected during an expedition in 1901-1902 led by J. W. Gregory, most likely from the riverbed beside fluvial deposit outcroppings on the riverbank just north of the homestead itself and contribute to the Kalamurina Fauna (see Tedford et al. 1986; Tedford and Wells 1990). Tedford and Wells (1990) noted that the course of the Warburton River between Kalamurina and Toolapinna Waterhole cuts through the Katipiri Formation, from which the Kalamurina Fauna originates. The Katipiri Formation itself is now considered to be Middle to Late Pleistocene in age (Nanson et al. 2008; Megirian et al. 2010). Only a distal humerus and a quadrate have been identified as accipitrid material from this site (de Vis 1905).

#### ***Wellington Caves***

The Wellington Caves are located in central-western New South Wales, seven km south of the town Wellington, and the fossiliferous deposits within are believed to have formed between the Pliocene to late Pleistocene (Dawson et al. 1999; Megirian et al. 2010). The caves are set in Devonian-age limestone at a boundary between facies of limestone-mudstone containing calcarenite (Frank 1971, 1975) and a thinly bedded limestone facies (Osborne 2007). Cathedral Cave is the largest of these caves and has yielded many fossils of great significance, most of them from the Cathedral Chamber and Well Chamber (Dawson 1985; Dawson and Augee 1997; Prideaux et al. 2007a). An estimated 7–10 m of fossil-bearing sediment covers the floors of the Cathedral and Well Chambers (Osborne 1991). Fossils have also been found at other caves in this complex, most notably Bone Cave, Phosphate Mine and Mitchell's Cave (Osborne 1991; Osborne 1997). Mitchell Cave and Phosphate Mine are the source of huge collections of Pleistocene material (Dawson 1985).

While numerous authors have attempted dating the stratigraphy of the Wellington Caves assemblages (see Dawson and Augee 1997), many of these dates are now regarded as problematic and are currently under Revision (D. Fusco pers. comms.). The age of the fossils from the Wellington Caves deposits are therefore largely inferred based on biochronological comparisons with other sites (Megirian et al. 2010).

The accipitrid material from Wellington Caves has poor provenance data, with most fossils lacking stratigraphic details and site from which they were collected. Specimens used in this project are two distal humeri and a tarsometatarsus, which are a part of the "Old Collection". The Old Collection refers to a large number of fossils that were excavated from

the Wellington Caves throughout the mid-19<sup>th</sup> century to early 20<sup>th</sup> century, most of which were not properly sorted or registered until 1926 (Dawson 1985). The specimens used in this study were first transferred to the Australian Museum in 1976 and most likely were among the fossils acquired by the NSW Department of Mines between 1884 and 1917 (Dawson 1985). Due to their lack of precise collection data, they can only be determined as Pleistocene in age.

### ***Leaena's Breath Cave***

Leaena's Breath Cave (alternate spelling; Leana's Breath Cave) is a 73 m long limestone cave located in the Nullarbor Plains of Western Australia, located directly south of Old Homestead Cave, and is part of a collective of caves known as the Thylacoleo Caves. The cave itself has been dated as minimally 4 million years old using U-PB geochronology techniques on speleothems (Woodhead et al. 2006). Leaena's Breath Cave was first discovered in 2002, and along with other caves in the Thylacoleo Caves complex has yielded Pleistocene age fossils of remarkable quality, including complete skeletons (Prideaux et al. 2007b). The age of these fossils is thought to range between 400–200 Ka for specimens in the upper sediment of the excavation pit based on optical dating, to as old as 780–400 Ka for those in the lower sediment based on U-Th and palaeomagnetic dating (Prideaux et al. 2007b).

Very little accipitrid material has been collected from Leaena's Breath Cave, but what is present has good provenance data. Only a proximal tarsometatarsus, identified as an indeterminate accipitrid by Shute (2018), was attributable to "*Taphaetus*".

## **3.3 RESULTS**

### **3.3.1 Systematic Palaeontology**

#### **Accipitriformes Vieillot, 1816**

#### **Accipitridae Vigors, 1824**

The lectotype humerus is identified as an accipitrid based on the presence of the following characters: The distal margin of the fossa brachialis extends distal to the tuberculum supracondylare dorsale; a distinct sulcus scapulo-tricipitalis; the proximal margin of the condylus dorsalis is roughly level with the ventral-tip of the epicondylus ventralis; a distinct circular dorsal insertion for the m. extensor metacarpi radialis on the dorsal projection of the tuberculum supracondylare dorsale; a distinct pit for the insertion of the

proximal m. pronator superficialis ventrally-adjacent or proximal to the tuberculum supracondylare ventrale; and the epicondylus ventralis is markedly ventrally prominent.

This fossil is easily distinguished from the following similar-sized birds likely to be encountered in Pleistocene Australian fossil sites.

The fossil is distinguished from Ciconiidae (*Ephippiorhynchus asiaticus*) by the following characters (ciconiid state in brackets): The tuberculum supracondylare dorsale is strongly projecting (little to no projection); the dorsal sulcus of the m. humerotricipitalis is narrow, just under a third of the shaft width (broad, roughly half the shaft width); the ventral sulcus of the m. humerotricipitalis is broad, twice the width of the dorsal sulcus (narrow, half the width); the epicondylus ventralis and the tuberculum supracondylare ventrale are distinctly separated from each other (continuous/overlapping); the dorsal insertion of the m. extensor metacarpi radialis is a circle/oval shape restricted to the dorsal facies (circle with ventrally projecting line leading onto cranial facies).

The fossil is distinguished from Pelecanidae (*Pelecanus conspicillatus*) by the following characters (pelecanid state in brackets): The tuberculum supracondylare dorsale is strongly projecting (little to no projection); the origin of m. extensor digitorum communi is a small, circular pit on the dorsal facies between the tuberculum supracondylare dorsale and the epicondylus dorsalis (large, oval-shaped attachment scar); the tuberculum supracondylare ventrale is weakly projecting cranially (cranially flattened); there is no pneumatism of the distal end (pneumatic region present on cranial facies adjacent to tuberculum supracondylare ventrale); the epicondylus ventralis strongly projects ventrally (weak projection); the distal margin of the fossa brachialis is positioned distal to the tuberculum supracondylare dorsale (positioned proximal to the processus).

The fossil is distinguished from Phoenicopteriformes (*Phoenicopterus ruber*) by the following characters (phoenicopterid state in brackets): the epicondylus ventralis projects prominently ventrally (little to no projection), the dorsal sulcus for the m. humerotricipitalis is under a third of the shaft width (half of shaft width), the ventral sulcus for the m. humerotricipitalis is twice the width of the dorsal sulcus (half the width of the dorsal sulcus), the tuberculum supracondylare ventrale is weakly projecting cranially (cranially flattened), the condylus dorsalis and condylus ventralis are separated by a distinct, deep incisura (narrow, shallow incisura).

The fossil is distinguished from Ardeidae by the following characters (ardeid state in brackets): A deep fossa m. brachialis (shallow); a broad fossa m. brachialis, approximately two thirds of shaft width or more (narrow, one third of shaft width); a narrow sulcus for the dorsal belly of the m. humerotricipitalis (broad).

Several features of the bone, notably its large size, are only matched by *Aquila audax* and *Haliaeetus leucogaster* in the Australian fauna. However, the combination of a narrow dorsal part of sulcus humerotricipitalis, a markedly prominent epicondylus ventralis, a dorsally inflated facies between the tuberculum supracondylare dorsale and epicondylaris dorsalis, and a distally short processus flexorius, distinguish it from all other accipitrids. As this humerus is unambiguously identifiable as that of an accipitrid and is distinguished from all known genera and species, '*Taphaetus*' *lacertosus* is confirmed as a distinct taxon. However, as *Taphaetus* de Vis, 1905 is a junior homonym of *Taphaetus* de Vis, 1891, which is a junior synonym of *Uroaetus* Kaup, 1844 and so of *Aquila* Brisson, 1760, it requires a new name.

As the quadrate was unavailable for study, we instead used the descriptions and illustrations in de Vis (1905) to assess if the original identification was valid. The fossil quadrate differs distinctly from those of accipitrids and instead agreed with those of Ardeidae, particularly species in the genera *Ardea* and *Egretta*, by the following characters (accipitrid state in brackets): A large foramen pneumaticum caudomediale positioned ventral to the capitulum oticum articular surface (no foramen pneumaticum, though a depressio caudomediale is present in some species); The capitulum oticum is positioned further dorsally relative to the capitulum squamosum (capitulum squamosum further dorsal); The width of the capitula and the width of the shaft are very similar, with little narrowing between the dorsal and ventral ends (shaft distinctly narrower than dorsal end); In caudal view, the condylus mandibularis medialis is positioned to be level with the condylus mandibularis lateralis, with both being equally visible (condylus mandibularis medialis set back rostrally, less visible than condylus lateralis); The condylus mandibularis caudalis is prominently projecting caudally (projecting medially); The condylus mandibularis lateralis barely extends laterally from the shaft (extends prominently caudally); The condylus mandibularis medialis extends prominently medially from the shaft (little to no extension); A prominent secondary facet is present on the condylus mandibularis medialis (no secondary facet); In ventral view, the condyles project rostrally past the rostral margin of the articular surface (roughly in line with margin). The reported dorsal height of 22 mm is distinctly larger than that observed in the bittern *Botarus poiciloptilus* (~15–16 mm), and the morphology is a better match for a heron. It is much larger than compared specimens of white-faced heron *Egretta novaehollandiae* and grey heron *Ardea cinerea* but could potentially be a match in size to the great-billed heron (*Ardea sumatrana*). As it is not of an accipitrid, it is not considered further.

**Nov. gen.**

**Type species:** *Taphaetus lacertosus* de Vis, 1905: Annals of the Queensland Museum 6: 4, pl. 1, fig. 1.

**Revised Diagnosis:**

A large accipitrid similar in size to *Aquila audax*, with humeri differing from all other Accipitridae by the following combination of characters: **(1)** A prominent dorsal convexity of the facies between the tuberculum supracondylare dorsale and the epicondylus dorsalis; **(2)** A strongly dorsally projecting tuberculum supracondylare dorsale; **(3)** A distinct and deepened attachment for the origin of m. extensor digitorum communi; **(4)** A large, shallow, circular attachment scar for the origin of the proximal head of m. pronator superficialis (=pronator brevis); **(5)** The epicondylus ventralis strongly projected ventrally as a craniocaudally elongate peak; **(6)** Processus flexorius distally short, ending proximal to the distal margin of the condylus ventralis; **(7)** and a narrow sulcus/groove for the dorsal belly of the m. humerotricipitalis.

**Nov. gen. *lacertosus* (de Vis, 1905)**

**Lectotype:** QM F5507, distal R humerus (designated by van Tets, 1974, p. 58).

**Type Locality:** Kalamurina, Warburton River, Lake Eyre Basin, SA. Collected by John W Gregory in April 1902 (de Vis 1905).

**Stratigraphy and Geological age:** Katipiri Formation; mid- to late Pleistocene; assumed to derive from fluvial sediments that outcrop in the banks of the river at this point. Associated fauna comprise the Kalamurina Fauna and is typical of late Pleistocene (Tedford and Wells 1990; Tedford et al. 1992).

**Measurements of Lectotype:** QM F.5507 distal R humerus: preserved distal width 35.5, condylus dorsalis lateromedial width 9.1, condylus dorsalis depth 22.3, condylus dorsalis proximodistal length 12.3, condylus ventralis width 14.1 mm.

**Amended Diagnosis:** As for genus.

**Description**

In addition to the diagnostic characters described above, the following characters serve to distinguish the species:

**(8)** The palmar attachment for the m. extensor metacarpi radialis (Figure 3.1A, C; PEMR) on the cranial facies immediately ventral of the tuberculum supracondylare dorsale (Figure 3.1A; TSD), is shallow, roughly oval shaped, and orientated dorsoventrally; **(9)** The

dorsal attachment sulci for the m. extensor metacarpi radialis (Figure 3.1A, B; DEMR) consists of a large, deep sulcus on the dorsal facies of the tuberculum supracondylare dorsale and is directed dorsoproximally; **(10)** The epicondylus dorsalis is dorsally flat and does not project dorsally of the condylus dorsalis; **(11)** The fossa m. brachialis (Figure 3.1A; FB) is deep, with the distal margin positioned well proximal to the tuberculum supracondylare ventrale; **(12)** The dorsal margin of the fossa m. brachialis extends close to (~2 mm) the dorsal margin of the shaft; **(13)** The tuberculum supracondylare ventrale (Figure 3.1A; TSV) is not inflated ventrally and is moderately projected cranially; **(14)** The interior margin of the tuberculum supracondylare ventrale is aligned roughly parallel to the adjacent medial surface; **(15)** The attachment scars for the origin of the distal head of m. pronator superficialis and of m. pronator profundus are deep, with that for the m. pronator superficialis attachment point being deeper than that of the m. pronator profundus; **(16)** The incisura intercondylaris (Figure 3.1A; II) is relatively broad, roughly 3 mm in width, and distinctly separates the two condyles cranially; **(17)** The distal margin of the condylus dorsalis (Figure 3.1A; CD) is set well proximal of the distal margin of the condylus ventralis, with the distal margin forming a broad, shallow notch between the two condyles; **(18)** The distoventral margin of the condylus ventralis (Figure 3.1A; CV) is continuous with the entepicondyle; **(19)** and the sulcus scapulothoracicus (Figure 3.1D; SST) is shallow and relatively broad.

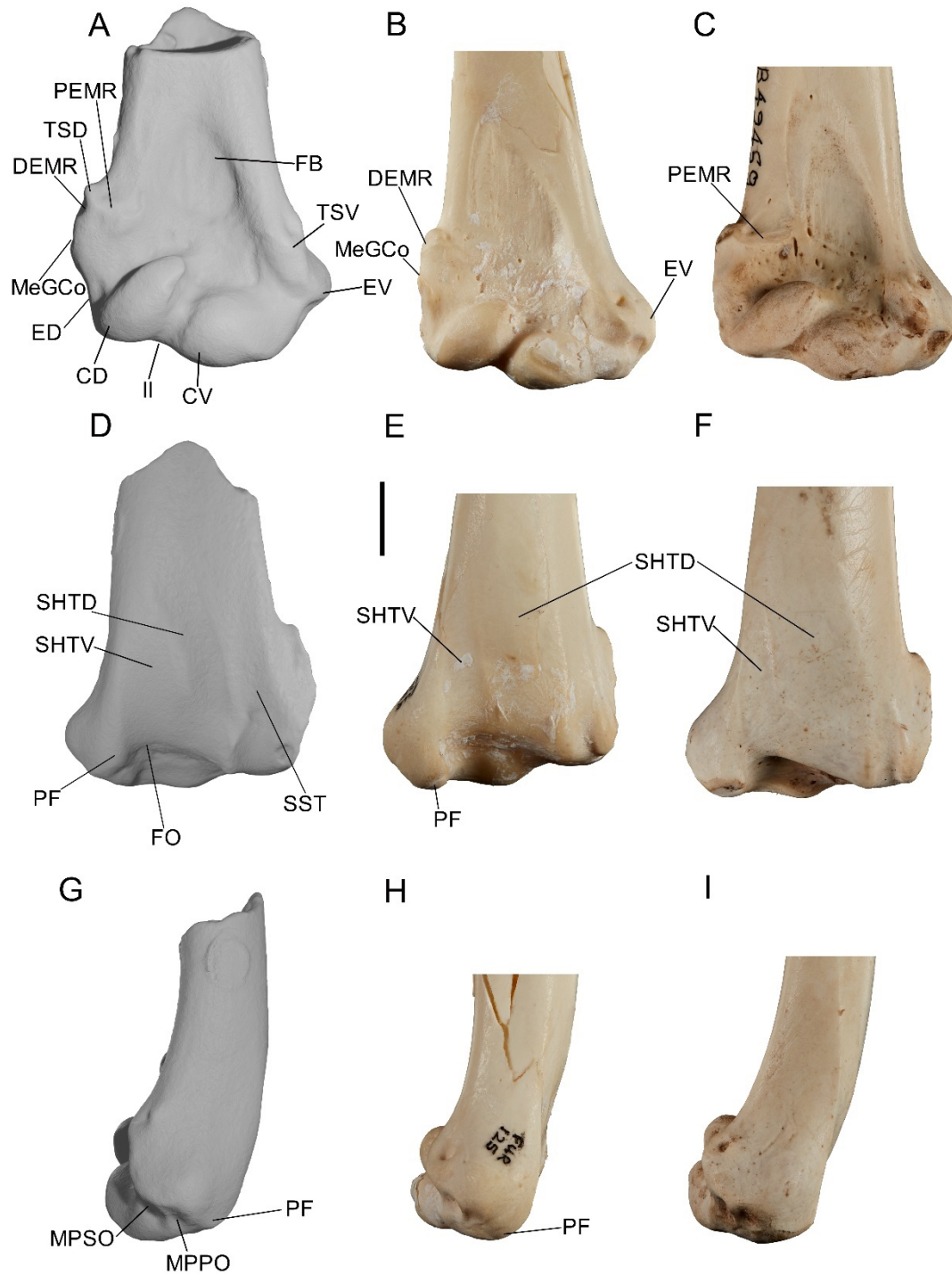


**Figure 3.1:** Comparisons of the scanned distal humeri of Nov. gen. *lacertus* QM F5507 (A, D, G), *Aquila audax* (B, E, H) and *Haliaeetus leucogaster* (C, F, I) in cranial (A, B, C), caudal (D, E, F) and ventral (G, H, I) view. Abbreviations: CD, condylus dorsalis; CV, condylus ventralis; DEMR, dorsal attachment m. extensor metacarpi radialis; ED, epicondylus dorsalis; EV, epicondylus ventralis; FB, fossa brachialis; FO, fossa olecrani; II, incisura intercondylaris; MeGCo, m. extensor gitorum communi origin; MPSO, origin of distal head of m. pronator superficialis; MPPO, m. pronator profundus origin; PF, processus flexorius; PEMR, palmar attachment m. extensor metacarpi radialis; SHTD, dorsal sulcus humerotricipitalis; SHTV, ventral sulcus humerotricipitalis; SST, sulcus scapulo-tricipitalis; TSD, tuberculum supracondylare dorsale; TSV, tuberculum supracondylare ventrale. Scale bar 10 mm.

## Comparisons of lectotype.

### *Humerus*

The lectotype humerus of Nov. gen. *lacertosus* differs markedly from humeri of all species of accipitrid present in Australia. It is larger than all except those of *Aquila audax* and *H. leucogaster* and differs from these by the above diagnostic characters and especially **(1)** the convex projecting dorsal facies distal to the tuberculum supracondylare dorsale; **(12)** the more projecting entepicondyle ventrale and **(7)**, the narrow groove for the dorsal belly of m. humerotricipitalis. The following comparisons therefore seek to establish to which subfamily it should be attributed.

Referral of Nov. gen. *lacertosus* to the Elaninae, Perninae, Accipitrinae and Buteoninae can be excluded based on size, as all species in these subfamilies are significantly smaller than the fossil.

The Circaetinae, Aquilinae (e.g. *Aquila audax*), Harpiinae and Haliaeetinae (e.g. *Haliaeetus leucogaster*) can be excluded by the following differences species in these groups exhibit: **(1)** The dorsal facies between the tuberculum supracondylare dorsale and epicondylus dorsalis has low dorsal convexity; **(2)** The tuberculum supracondylare dorsale is weakly to moderately projecting and flattened; **(4)** The attachment scar for the proximal head of pronator superficialis is small; **(5)** The epicondylus ventralis is weakly projecting ventrally; **(6)** The distal extent of the processus flexorius is equal to the condylus ventralis; **(7)** The dorsal sulcus of the m. humerotricipitalis is broad, occupying roughly half of the shaft width, while the ventral sulcus is quite narrow; **(13)** The tuberculum supracondylare ventrale is proximocranially prominent; and **(14)** The interior margin of the tuberculum supracondylare ventrale is aligned across the shaft at a low angle.

The humerus of Nov. gen. *lacertosus* most closely resembles those of species in the subfamilies Aegyptiinae and Gypaetinae, with both subfamilies sharing similar states for 6, 7, 9, 10, and 12, gypaetines in addition share states for characters 2, 11, and 18, and aegyptiines share states for 1, 14, 16 and 19.

The subfamilies differ from Nov. gen. *lacertosus* in the following characters:

#### Gypaetinae.

**(1)** The dorsal facies between the tuberculum supracondylare dorsale and epicondylus dorsalis is less inflated as a convex surface compared to the fossil, barely projecting dorsal of these two points. **(3)** The insertion point for the m. extensor digitorum communi does not form a distinct pit. **(4)** The attachment scar for the proximal head pronator superficialis is small and deep. **(5)** The epicondylus ventralis forms a moderate, rounded peak. **(8)** The palmar attachment scar of the m. extensor metacarpi radialis is a small,

narrow, and shallow circle in all species except *Polyboroides typus*, where it is a circular shape, rather than a broad robust elevated scar as in the fossil. **(13)** The tuberculum supracondylare ventrale is more flattened, not elevated cranially. **(14)** The interior margin of the tuberculum supracondylare ventrale is oriented at a lower angle across the shaft. **(15)** The insertions of the distal m. pronator superficialis and profundus are roughly the same depth in *G. angolensis*, while the m. pronator profundus insertion is shallower in *P. typus* and *N. percnopterus*. **(16)** The incisura intercondylaris is broad in *N. percnopterus* (as in the fossil) and narrow in *P. typus*. **(17)** The distal margin of the condylus dorsalis forms a deep narrow notch between the condyles. **(19)** The sulci m. humerotricipitalis are shallow in all taxa, with the dorsal sulcus roughly one third of shaft width in *N. percnopterus* and half the width in *P. typus* and *G. angolensis*. The sulcus for the ventral belly is a third to a quarter of the shaft width in all species.

#### Aegyptiinae.

**(2)** The tuberculum supracondylare dorsale does not project cranially in aegyptiines. **(3)** The insertion point for the m. extensor digitorum communi does not form a distinct pit. **(4)** The attachment scar for the proximal pronator superficialis is small and deep. **(5)** The ventral tip of the epicondylus ventralis is rounded, not angular. **(11)** The fossa m. brachialis is shallower than Nov. gen. *Iacertosus* in all species except those in *Gyps* and *Aegyptius*. **(13)** The tuberculum supracondylare ventrale is flattened cranially. **(15)** Only the origins for the distal m. pronator superficialis and profundus are distinct in *Necrosyrtes monachus*, while in all other taxa the origin for the m. extensor metacarpi ulnaris is also distinct along with the others. The cranial-most attachment point is deeper than the caudal-most attachment, with the caudal insertion being almost flat in *A. monachus*, *G. fulvus* and *G. coprotheres*, and the third insertion present in the aforementioned taxa being shallow with very slight deepening. **(17)** The distal margin of the condylus dorsalis forms a shallow, broad notch in the species of *Gyps* and *N. monachus*, and narrow and deep in *A. monachus*. **(18)** The distal margin of the condylus ventralis is not continuous with the entepicondyle in all species except *N. monachus* (continuous).

#### ***Newly Referred Material***

**Localities and age:** Leaena's Breath Cave, Nullarbor, WA, Australia, 31.4°S 128.1°E; excavation Pit B1, Unit 3, depth 115-120 cm; Pleistocene; collected by G. Prideaux et al. 2013, identified by Shute (2018): WAM 15.9.73 L proximal tarsometatarsus.

'Old Collection', Wellington Caves, NSW, Australia, 32°31' S, 148°51' E; Pleistocene; likely acquired by NSW Mining Department 1884–1917: AM F.58093 L tarsometatarsus; AM F.58092 RL distal humeri.

The new material has been assigned to Nov. gen. *lacertosus* for the following reasons: The two distal humeri fragments AM F.58092 are a similar size (see Table 3.1) and have identical morphology to the lectotype QM F5507, and so are unambiguously referred to this same species. Specifically, these two fragments show the same unique sharp ventrally projecting entepicondyle and the same distally abbreviated processus flexorius (see Figure 3.2).

The L tarsometatarsus AM F.58093 is associated with the distal humeri AM F.58092 in that it also derives from the 'Old Collections' from Wellington Caves. Its size (see Table 3.2, 3.3) is appropriate for the bird the humeri derive from and it differs markedly from all known taxa and has a morphology concordant with that of vultures, as does the humerus (see below). Moreover, it is from a distinctly smaller bird than another large accipitrid from Pleistocene deposits in Australia that will be described elsewhere. Therefore, it is considered more parsimonious to refer this tarsometatarsus to the same taxon as the humeri, rather than erect a second similar sized taxon. The proximal L tarsometatarsus WAM 15.9.73 from Leaena's Breath Cave is identical in morphology to the Wellington Cave tarsometatarsus, and so is also referred to Nov. gen. *lacertosus*.

Specimen	Distal width	CD width	CD length	CV width
QM F.5507	35.5	9.1	12.3	14.4
AM F.58092 R	31.8	9.2	13.3	13.7
AM F.58092 L	29.8	8.2	12.5	14.9
<i>A. audax</i>	30.3, (10) 28–32.3, 1.4	8.8, (10), 7.9– 10.2, 0.8	10.7, (10), 10.2–11.7, 0.5	12.4, (10), 11.6–13.6, 0.7

**Table 3.1:** Measurements (mm) of distal humeri of Nov. Gen. (QM F. 5507, AM F. 58092) compared to *Aquila audax*. For *Aquila audax*, the data are the mean, number, range and standard deviation. *A. audax* specimen numbers: FUR 125, FUR 085, SAMA B46613, SAMA B49025, SAMA B47814, SAMA B39628, SAMA B46633, SAMA B55112, SAMA B31109, SAMA B46992. Abbreviations: CD, condylus dorsalis; CV, condylus ventralis.

Specimen	Length	PW	PD (w/o hypotarsus)	PD (w hypotarsus)	CL length	Width (midshaft)
AM F.58093	91.4	22	11.9	15.5	10.4	12.8
WAM 15.9.73	NA	21.8	11.4	16.2 (preserved)	12.8 (preserved)	13.4 (preserved)
<i>A. audax</i>	104.1, (10), 101.5–108.2, 2.3	20.1, (10), 18.7–21.6, 1.1	8.6, (10), 7.7–9.1, 0.5	16.1, (10), 14.8–17.2, 0.9	6.4, (10), 5.1–7.5, 0.7	10.8, (10), 9.3–11.8, 1.0

**Table 3.2:** Proximal and shaft measurements (mm) of tarsometatarsi of Nov. Gen. (AM F.58093, WAM 15.9.73) compared to *Aquila audax*. For *Aquila audax*, the data are the mean, number, range and standard deviation. *A. audax* specimen numbers: FUR 125, FUR 085, SAMA B46613, SAMA B49025, SAMA B47814, SAMA B39628, SAMA B46633, SAMA B55112, SAMA B31109, SAMA B46992. Abbreviations: PW, proximal width; PD, proximal depth; CL, crista lateralis hypotarsi.

Specimen	DW (w/o flange)	DW (flange)	TII Width (no flange)	TII Width (flange)	TII height	TIII width	TIII height	TIV width	TIV height
AM F.58093	23	24.8	5.8	8.1	8.9	8.6	12.1	5.8	12.5
<i>A. audax</i>	20.2, (10), 18–22.1, 1.4	23.6, (10), 21.5–25.4, 1.5	5.5, (10), 4.7–6.3, 0.5	9.8, (10), 9.0–10.8, 0.6	8.1, (10), 7.5–8.8, 0.5	6.8, (10), 6.2–7.3, 0.4	10.1, (10), 9.3–10.9, 0.6	4.4, (10), 3.7–4.8, 0.4	12.5, (10), 11.2–13.3, 0.7

**Table 3.3:** Distal measurements (mm) of tarsometatarsi specimens of Nov. Gen. (AM F.58093) compared to *Aquila audax*. For *Aquila audax*, the data are the mean, number, range and standard deviation. *A. audax* specimen numbers: FUR 125, FUR 085, SAMA B46613, SAMA B49025, SAMA B47814, SAMA B39628, SAMA B46633, SAMA B55112, SAMA B31109, SAMA B46992. ‘Flange’ refers to the projection of bone out from the main trochlea. Abbreviations: DW, distal width; TII, trochlea metatarsi II; TIII, trochlea metatarsi III; TIV, trochlea metatarsi IV.

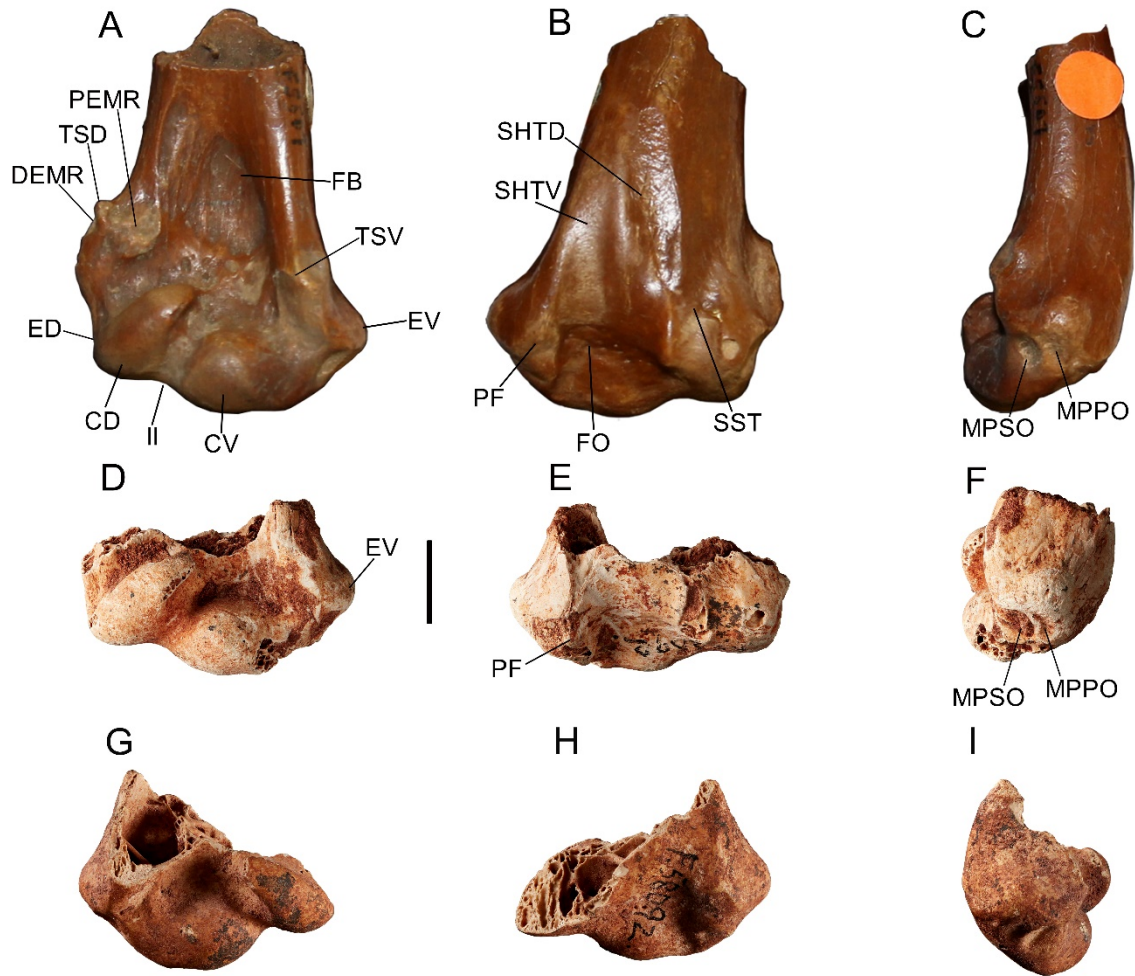


**Figure 3.2:** Photographs of Nov. gen. *lacertus* lectotype QM F.5507 (A-C), right distal AM F.58092 (D-F) and left distal AM F.58092 (G-I) in cranial (A, D, G), caudal (B, E, H) and ventral (C, F, I) views. Abbreviations: CD, condylus dorsalis; CV, condylus ventralis; DEMR, dorsal attachment m. extensor metacarpi radialis; ED, epicondylus dorsalis; EV, epicondylus ventralis; FB, fossa m. brachialis; FO, fossa olecrani; II, incisura intercondylaris; MPPO, origin of m. pronator profundus; MPSO, origin of distal head m. pronator superficialis; PF, processus flexorius; PEMR, palmar attachment m. extensor metacarpi radialis; SHTV, ventral belly of sulcus humerotricipitalis; SHTD, dorsal belly of sulcus humerotricipitalis; SST, sulcus scapulotricipitalis; TSD, tuberculum supracondylare dorsale; TSV, tuberculum supracondylare ventrale. Scale bar 10 mm.

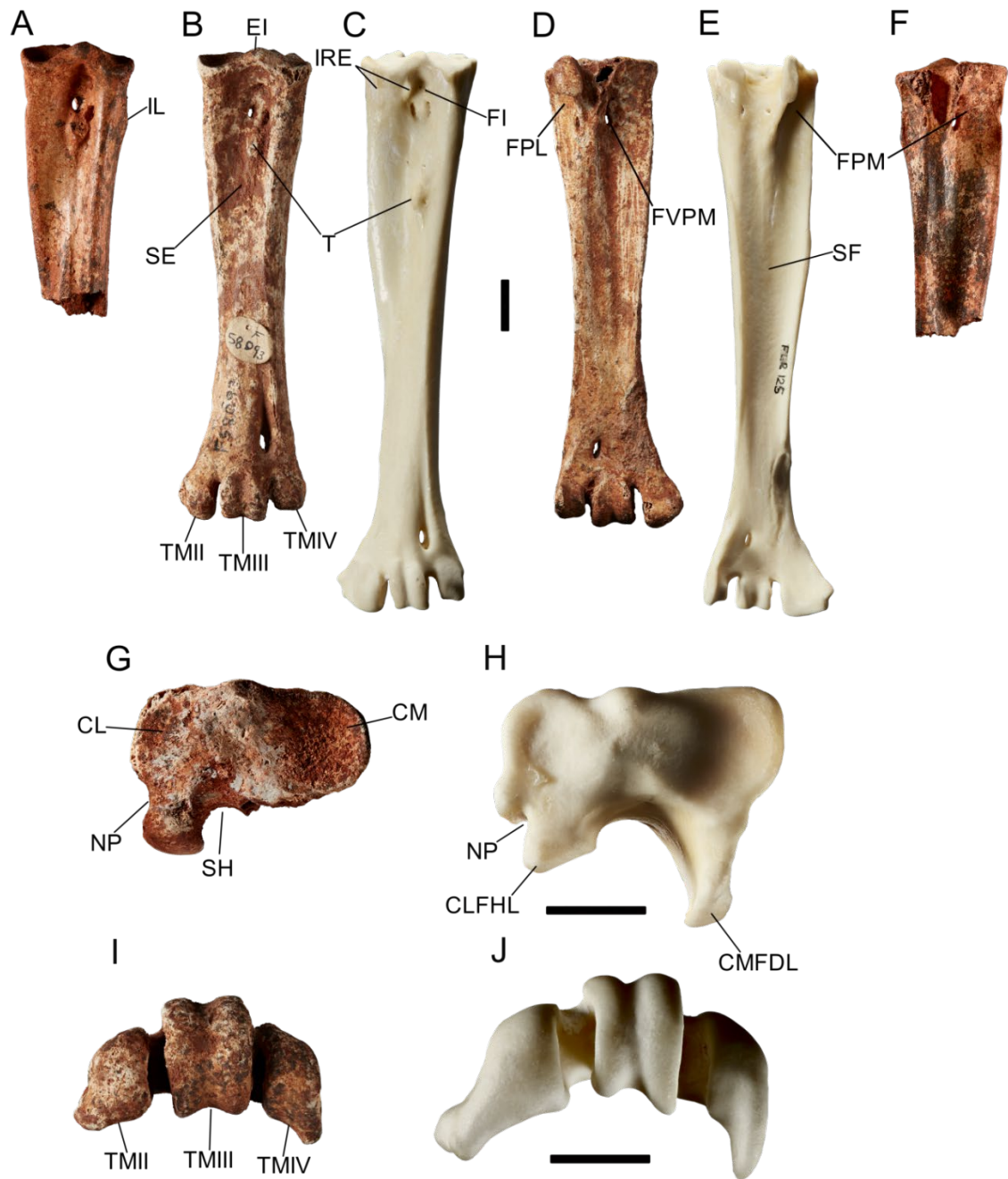


**Figure 3.3:** Tarsometatarsi of Nov. gen. *lacertosus* (A, B, D, F, G, I) compared to that of *Aquila audax* FUR 125 (C, E, H, J). Left tarsometatarsus AM F.58093 (B, D, I): proximal tarsometatarsus WAM 15.9.73 (A, F, G), in dorsal (A-C), plantar (D-F), proximal (G, H) and distal (I, J) views. Abbreviations: CL, cotyla lateralis; CLFHL, crista lateralis flexoris hallucis longus; CM, cotyla medialis; CMFDL, crista medialis flexoris digitorum longus; EI, eminentia intercotylaris; FI, fossa infracotylaris; FPL, fossa parahypotarsalis lateralis; FPM, fossa parahypotarsalis medialis; FVPM, foramen vascularia proximalia medialis; IL, impressio ligamentum collateralis lateralis; IRE, impressio retinaculi extensorii; NP, nervus peroneus notch; SE, sulcus extensorius; SF, sulcus flexorius; SH, sulcus hypotarsus; T, tuberositas m. tibialis cranialis; TMII, trochlearis metatarsi II; TMIII, trochlearis metatarsi III; TMIV, trochlearis metatarsi IV. Scale bars 10 mm.

### **Tarsometatarsus (Figure 3.3A, B, D, F, G, I).**

The specimen AM F.58093 from Wellington Caves is near-perfectly preserved, missing only the crista medialis hypotarsi. The specimen from Leaena's Breath Cave WAM 15.9.73 preserves the proximal half of the tarsometatarsus except for the plantar parts of the hypotarsal crests.

These specimens reveal the following features: **(1)** The eminentia intercotylaris (Figure 3.3B; EI) projects proximally prominently; **(2)** The sulcus hypotarsi (Figure 3.3G; SH) is narrow in width; **(3)** The base of the sulcus hypotarsi (dorsal surface) is located plantar to the sulcus flexorius; **(4)** The fossa parahypotarsalis lateralis (Figure 3.3D; FPL) is shallow, about 5-6 mm wide between the crista plantaris lateralis and the base of the crista lateralis hypotarsi, extends about 25 mm distally to where the crista plantaris lateralis and the crista extending from the crista lateralis hypotarsi converge on the lateral margin; **(5)** The notch for the nervus peroneus (Figure 3.3G, H; NP) in proximal aspect is shallow; **(6)** A sulcus for the musculus fibularis longus cannot be distinguished [in *Aquila audax* it is shallow and wholly on the lateral facies]; **(7)** The cotylae are roughly level, not with the medial one relatively distally located; **(8)** The fossa infracotylaris dorsalis (Figure 3.3C; FI) is deepened proximally; **(9)** The impressio ligamentum collateralis lateralis (Figure 3.3A; IL) is laterally prominent (this margin is worn in AM F.58093); **(10)** The plantar facies of the crista lateralis hypotarsi is broadly ellipsoid (5.2 x 8.7 mm); **(11)** The distal end of the crista medialis hypotarsi is adjacent to the foramen vasculare proximale medialis; **(12)** The medial foramen vasculare is positioned medial to the crista medianoplantaris; **(13)** The medial shaft margin is relatively thick dorsal to the fossa parahypotarsalis medialis; **(14)** The proximal end of the fossa parahypotarsalis medialis (Figure 3.3E, F; FPM) is deep and makes up over 1/3<sup>rd</sup> of shaft width; **(15)** The impressiones retinaculi extensorii (Figure 3.3C; IRE) are not discernible in either specimen; **(16)** The tuberositas m. tibialis cranialis (Figure 3.3B, C; T) directly abuts the foramina vascularia proximalia in WAM 15.9.73, but in AM F.58093 the medial foramen is slightly separated proximally from the tuberositas (separated far from the foramina in *A. audax*); **(17)** The tuberositas is roughly ellipsoidal in shape; **(18)** The tuberositas is set roughly central in the shaft; **(19)** The sulcus extensorius (Figure 3.3B; SE) is moderately deepened and indistinct; **(20)** The sulcus flexorius (Figure 3.3E; SF) is slightly deepened and joins the medial facies by midlength; **(21)** The sulcus for the tendon of m. abductor digiti IV is broad and shallow, and opens laterally over a wide (10 mm) length of the shaft just proximal to TIV; **(22)** The trochlea metatarsi II (Figure 3.3I; TMII) is slightly longer than trochlea metatarsi III (Figure 3.3I; TMIII) by ~1 mm; **(23)** The relative distal extent of trochlea metatarsi II is slightly longer than trochlea metatarsi IV (Figure 3.3I; TMIV) by at least 2 mm; **(24)** The fovea lig. collateralium is shallow; **(25)** The plantar flange on trochlea metatarsi II is

very short; **(26)** The plantar flange on trochlea metatarsi IV is short; **(27)** The trochlea metatarsi II is relatively narrow (compared with *A. audax*); **(28)** and the trochlea metatarsi IV is relatively broad (compared with *A. audax*).

The tarsometatarsi referred to Nov gen. *lacertosus* can be excluded from the Elaninae, Perninae, Accipitrinae and Buteoninae based on their much larger size, the lack of shaft width constriction immediately proximal to the fossa metatarsi I, and fossa metatarsi I being positioned entirely on the plantar facies.

Species in the Circaetinae, Aquilinae, Harpiinae and Haliaeetinae are excluded by these characteristics of the fossil: **(2)** the narrow width of the sulcus hypotarsi; **(3)** the shallow depth of the sulcus hypotarsi; **(5)** the shallow notch for the nervus peroneus; **(15)** the absence of impressiones retinaculi extensorii; **(21)** the sulcus for the m. abductor digiti IV being broad; **(24)** the shortened length of the trochlearis metatarsi II flange; **(26)** the shortened length of the trochlea metatarsi IV flange; **(21)** the relatively narrow width of the trochlea metatarsi II; **(28)** and the relatively broad width of the trochlea metatarsi IV.

The fossil shows the most resemblance to species in the Gypaetinae and Aegyptiinae, with the similarities and differences expanded upon below:

#### Gypaetinae.

The gypaetines share with the fossil the following six character states: **(1)** The eminentia intercotylaris projects proximally as in the fossil in all species except *Polyboroides typus*, where it is hyper-protruding proximally; **(2)** A narrow sulcus hypotarsus; **(3)** The base of the sulcus hypotarsus is set plantar to the sulcus flexorius, though in *Gypohierax angolensis* it is to a lesser degree than in the fossil; **(8)** A deep fossa infracotylaris dorsalis; **(21)** The sulcus for the m. abductor digit IV being broad; **(22)** and the trochlearis metatarsi II is slightly longer than trochlea metatarsi IV in *Gypohierax angolensis* and *P. typus* and is longer by at least half its length in *Neophron percnopterus* and *Gypaetus barbatus*.

The gypaetines differ from the fossil as follows: **(5)** The notch for the nervus peronius forms a shallow yet distinct notch in all species except *Gypaetus barbatus*, where it is deep; **(6)** The fossa parahypotarsalis lateralis spans a quarter of the shaft length or less in all species except *Neophron percnopterus*, where it spans a third of shaft length; **(9)** The impressio ligamentum collateralis lateralis is indistinct in all species except *P. typus*; **(10)** The plantar facies of the hypotarsus crista lateralis is wider than it is long in all species except *P. typus*, where it is longer than wide; **(13)** The medial shaft margin is thin dorsal to the fossa parahypotarsalis medialis in all species except *N. percnopterus*, where it is thick like the fossil; **(14)** The proximal end of the fossa parahypotarsalis medialis takes up at least a third of the shaft width in all species, and is deep in all species except *G. barbatus*, which

is shallow; **(15)** The impressio retinaculi extensorii are present as small ridges in *P. typus* and *G. angolensis*, and practically absent in *G. barbatus* and *N. percnopterus*; **(16)** The tuberositas m. tibialis cranialis is separated distally from the proximal foramina by a distance equivalent to its length; **(17)** The tuberositas is oval in *G. barbatus* and *N. percnopterus*, and an elongate narrow ridge in *P. typus* and *G. angolensis*; **(20)** The sulcus flexorius is shallow in all species except *P. typus*, where it is deep; **(22)** The trochlea metatarsi III has greater distal extent than trochlea metatarsi II in all species except *Gypohierax angolensis*, where trochlea metatarsi II is longer than trochlea metatarsi III; **(27)** The trochlea metatarsi II is relatively broad; **(28)** and the trochlea metatarsi IV is relatively narrow.

#### Aegyptiinae.

The fossil is very similar to aegyptiines species (see Figure 3.4), and agrees with them in the following 13 characters: **(2)** A narrow sulcus hypotarsus; **(3)** The sulcus hypotarsus is set plantar to the sulcus flexorius, though in species of *Gyps* and *Aegyptius monachus* it is to a lesser degree than the fossil; **(5)** The notch for the nervus peroneus is very shallow in proximal view in all species except those in *Gyps* and *Sarcogyps calvus* (shallow but distinct notch); **(6)** The fossa parahypotarsalis lateralis extends over a third of the shaft length in all species except *Aegyptius monachus*, where it is barely present; **(8)** The fossa infracotyloidea dorsalis is deepened proximally in all species except those in *Gyps* and *Necrosyrtes monachus*, where it is shallow; **(13)** The medial shaft margin is thin dorsal to the fossa parahypotarsalis medialis. **(15)** The impressio retinaculi extensorii are extremely flattened or absent; **(16)** The tuberositas m. tibialis cranialis directly abuts the foramina in all species except *Trionocephus occipitalis* and *S. calvus* (separated by one tuberositas length); **(21)** The sulcus for the m. abductor digit IV being broad; **(22)** The distal extent of trochlea metatarsi II is slightly longer than or roughly equal to that of trochlea metatarsi III in all species except those in *Gyps*, *Aegyptius monachus* and *Necrosyrtes monachus*, where trochlea metatarsi III has slightly greater extent than trochlea metatarsi II; **(24)** The plantar flange of the trochlea metatarsi II is short; **(25)** The plantar flange of the trochlea metatarsi IV is short; **(27)** and the trochlea metatarsi II is relatively narrow.

Differences from the living Aegyptiinae are expanded on in the next section below.

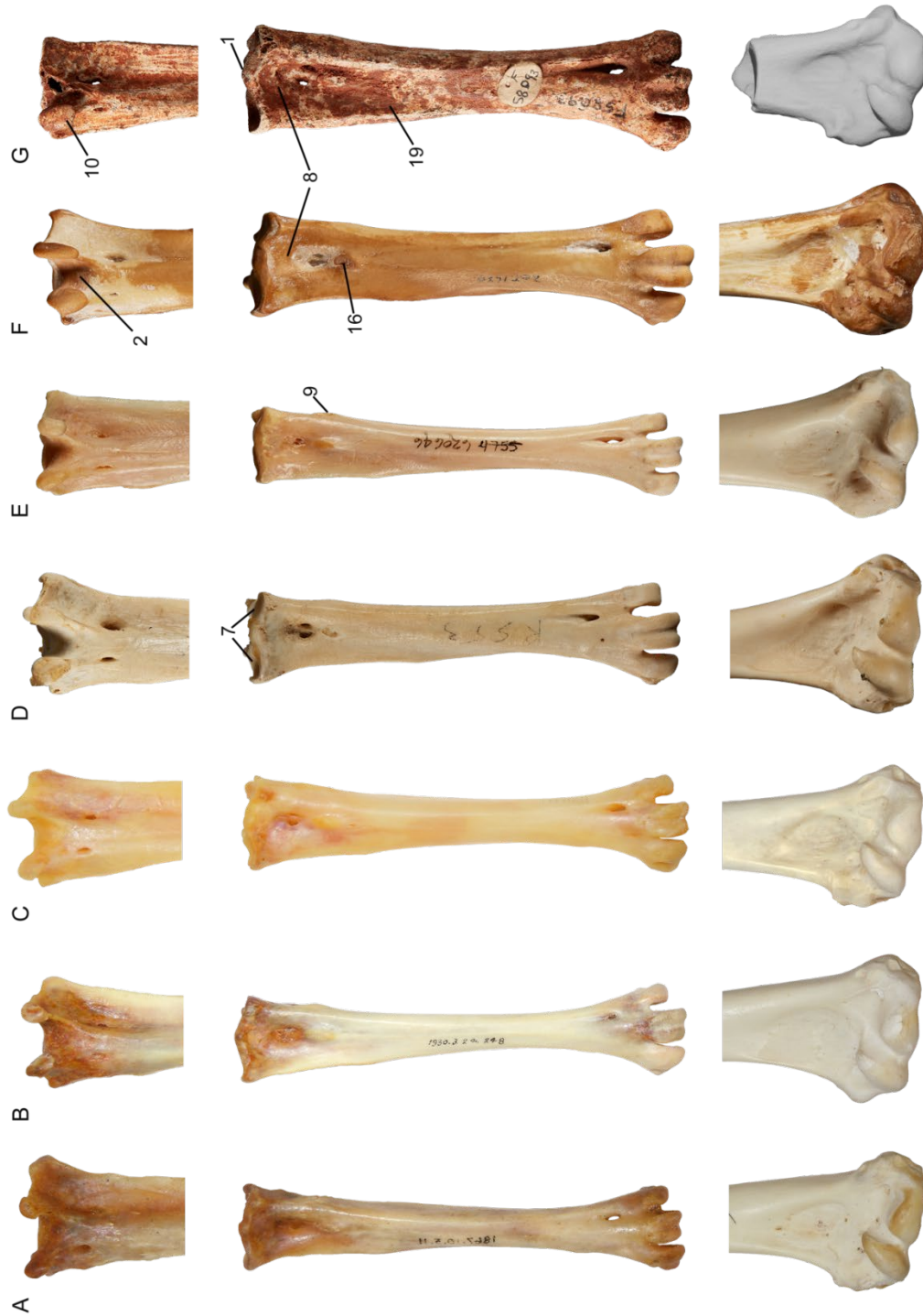


**Figure 3.4:** Comparisons of the elements of Nov. gen. *lacertus* to those of six species of Aegypiinae: tarsometatarsus in plantar view to show structure of the hypotarsus (top), tarsometatarsus in dorsal view (middle) and distal humerus in cranial view (bottom). *Trigonoceps occipitalis* (A), *Torgos tracheliotos* (B), *Sarcogyps calvus* (C), *Aegypius monachus* (D), *Necrosyrtes monachus* (E), *Gyps coprotheres* (F) and Nov. gen. *lacertus* (G). Numbers reflect the characters given in the tarsometatarsus description. Images are scaled to similar size.

### **Comparison with extant Aegyptiinae**

Nov. gen. *lacertosus* can be distinguished from all aegyptiines as follows (aegyptiine state in brackets).

The humerus has a more prominently projecting tuberculum supracondylare dorsale (tuberculum supracondylare dorsale non-projecting), moderate cranial projection of the tuberculum supracondylare ventrale (flattened or reduced cranial projection), a shallow, large attachment scar for the proximal head pronator superficialis (small scar), and the epicondylus ventralis is highly distinct from the tuberculum supracondylaris ventralis. The tarsometatarsus has a prominent eminentia intercotylaris (flattened or barely projecting), medial and lateral cotylae of roughly equal depth (medial shallower), a deepened notch for the nervus peroneus (shallow or no notch), a broad and deep fossa parahypotarsalis lateralis (shallow), a deep sulcus extensorius (shallow), a deep sulcus flexorius (shallow), a shallow fovea lig. collateralis (deep in all species except *Gyps coprotheres*), and the length of trochlea metatarsi II being slightly greater relative to trochlea metatarsi IV (significantly longer than trochlea metatarsi IV). The fossil can further be distinguished from individual genera by the following characters:

- From species of *Torgos*, *Trigonoceps*, *Sarcogyps*, and *Necrosyrtes* by a deeper fossa m. brachialis (shallow).
- From species of *Torgos*, *Sarcogyps*, *Aegyptius* and *Gyps* by lacking a prominent, visible m. extensor metacarpi ulnaris origin (distinct).
- *Torgos*, *Trigonoceps*, *Sarcogyps*, *Aegyptius* and *Gyps* by the condylus ventralis being continuous with the entepicondyle (not continuous).
- *Torgos*, *Trigonoceps*, *Sarcogyps*, *Aegyptius* and *Necrosyrtes* by the trochlea metatarsi IV being relatively broad (narrow).
- *Trigonoceps*, *Sarcogyps*, *Aegyptius* and *Gyps* by the impressio ligamentum collateralis lateralis being prominent laterally (flattened).
- From *Torgos*, *Trigonoceps*, and *Sarcogyps* by the lateral crista hypotarsus being longer than wide (wider than long) and the tarsometatarsus being overall short and robust in length (comparatively long and elongate, narrows between proximal and distal ends).
- From *Necrosyrtes*, *Gyps* and *Aegyptius* by a deep fossa infracotylaris (shallow fossa)
- From *Torgos* and *Necrosyrtes* by the convexity between the supracondylaris dorsalis and epicondylus dorsalis being relatively flattened (forms prominent peak)

- From *Torgos* and *Aegypius* by the flange of trochlea metatarsi II being extremely short (short but notably projecting medioplantarily from trochlea)
- From *Torgos* and *Trigonoceps* by the crista medianoplantaris ending adjacent to the foramina vascularia proximalia (ends proximal to the foramina), and the foramen vasculare distale being set close to the incisura intertrochlearis lateralis (positioned well proximal to the incisura).
- From *Trigonoceps* and *Sarcogyps* by the position of the tuberositas m. tibialis cranialis being adjacent to the foramina proximalia (set one tuberositas length distal) and the impressio ligamentum collateralis lateralis distinctly projecting dorsally (flat).
- From *Necrosyrtes* and *Gyps* by the length of trochlearis metatarsi III being roughly equal with II (III longer than II)
- From *Aegypius* by the broad and shallow notch between the condylus dorsalis and ventralis (deep and narrow)

### 3.3.2 Phylogenetic Analysis

The parsimony analysis of the combined molecular and morphological data resulted in three most parsimonious trees (MPTs), with a tree length of 1792, for which the strict consensus tree is shown in Figure 3.5.

The clade Accipitridae had very strong support (Bootstrap 94%). Branching order for living forms is as for Mindell et al. (2018), as expected given the overlapping molecular data. Most subfamilies were well resolved with strong support greater than 60%, with the exception of Buteoninae (Paraphyletic, *Ictinia mississippiensis* grouped closer to Haliaeetinae with 51% support), Circaetinae (57%) and Accipitrinae (57%).

The fossil species Nov. gen. *lacertosus* was strongly supported as a member of the large accipitrid clade that includes Circaetinae and Aegyptiinae (83%). Within this, it was moderately supported as a member of the aegyptiine + circaetine clade (62%), strongly supported as an aegyptiine (81%), and weakly supported as the sister group to the two species of *Gyps* (30%).

Thirty-eight unambiguous (optimization-independent) synapomorphies defined the Aegyptiinae clade but only eight were compelling: Character 37 state 1 (CI 0.5) (nares of rostrum partially covered by a caudal bone shield), 71 state 1 (CI 1.0) (sternum abutment of crista medialis to spina externa base), 101 state 1 (CI 0.5) (coracoid omal margin of processus procoracoideus oriented in distal slope relative to sternal margin), 102 state 0 (CI 1.0) (coracoid cotyla scapularis less than a quarter of the shaft width), 236 state 0 (CI 0.5) (tibiotarsus height to width ratio of medial condyle roughly equal), 237 state 0 (CI 0.5)

(tibiotarsus height to width ratio of lateral condyle roughly equal), 261 state 0 (CI 0.5)  
 (tarsometatarsus attachment ridges for impressioes retinaculi extensorii absent) and 274  
 state 1 (CI 0.5) (tarsometatarsus width of abductor muscle IV sulcus narrow).

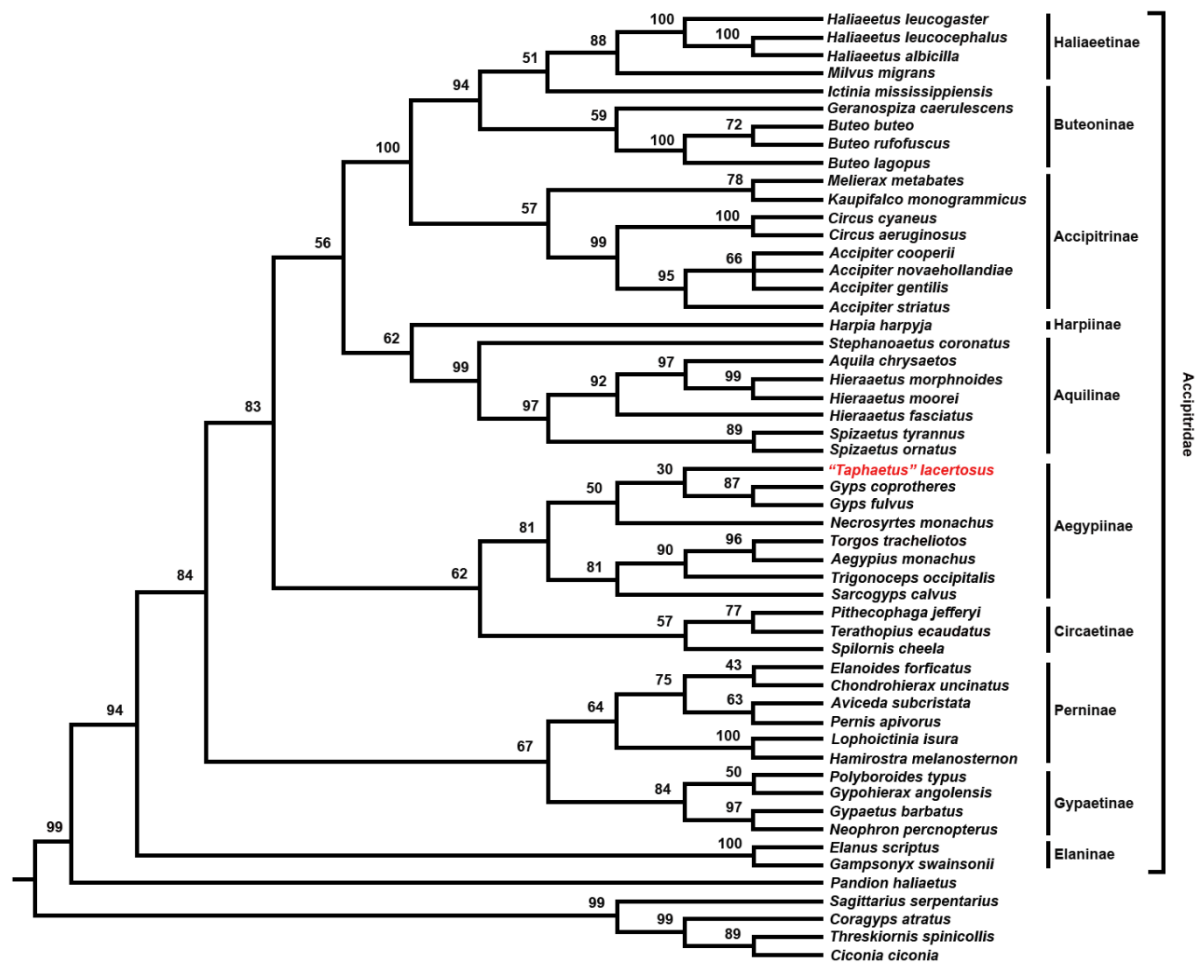


**Figure 3.5:** Parsimony analysis of morphological (ordered) data. Strict consensus of three most parsimonious trees. Tree length = 1792, MPT = 3, CI = 0.2176, HI = 0.7824, RI 0.5755. Bootstrap values are given at each node.

### 3.4 DISCUSSION

#### 3.4.1 Distribution of Scavenging Birds of Prey

The identity of Nov. gen. *lacertosus* as a member of Aegyptiinae fills a prominent and puzzling ecological void in Pleistocene Australia. Living aegyptiines are restricted to Africa, Europe and parts of Asia, but the fossil record reveals that their range once extended to the Americas (see Brodkorb 1964), leaving Antarctica and Australia as the only continents

where they were apparently absent (Ferguson-Lees and Christie 2001; Bildstein 2017). While their absence from Antarctica is easily explicable based on environment, Pleistocene Australia had extensive areas of grasslands, open woodlands and desert, and a diverse assemblage of up to 27 genera of megafaunal animals that would seem well suited to supporting vulture populations. Australia currently has only one large accipitrid living in inland terrestrial environments, the wedge-tailed eagle *Aquila audax*, which currently is both an active predator and scavenger. The lack of any other large, predatory, scavenging birds to fill a typical vulture niche in Australia in the absence of vultures makes this even stranger. Australia only has one documented species of stork (Ciconiidae), the black-necked stork *Ephippiorhynchus asiaticus*, which does not scavenge carcasses like storks do in the genus *Leptoptilus*. There is no evidence that any other large, volant scavenging bird lineages such as the Teratornithidae of South America were ever present in Australia. Despite some claims to the contrary, all the current evidence indicates the large, flightless Dromornithidae of Australia were herbivorous (Murray and Vickers-Rich 2004; Handley and Worthy 2021), unlike the flightless, predatory Phorusrhacidae from South America.

The Pleistocene avifauna of all continents outside Antarctica and Australia has included multiple species of both vultures and large eagles. In Europe the vulture guild had at least one additional species, *Gyps melitensis* Lydekker, 1890, that presumably existed alongside the four species of vultures and ten eagles still present today (Dickinson and Renssen 2013). The African vulture guild similarly also had at least one additional species, *Aegyptius varswaterensis* Manegold et al., 2014 alongside the 11 living vultures and 17 eagles (Dickinson and Renssen 2013). Mainland Asia had at least two extinct species of vultures, *Aegyptius jinniushanensis* Zhang et al., 2012, and an unnamed species of *Torgos* (Zhang et al. 2012) alongside seven species of living vultures and 21 eagles (Dickinson and Renssen 2013), while throughout the South-East Asian islands at least one fossil vulture, an unnamed species of *Trigonoceps* (Meijer et al. 2013) existed along with 22 species of eagles (Dickinson and Renssen 2013). From North America, sites such as the Rancho La Brea tar pits demonstrate the existence of at least two species of accipitrid vultures, four cathartid vultures, two teratorns and six large eagles during the same time period (see Stock 1930; Howard 1930; Jefferson 1991). Compared to these diverse faunas, the Australian accipitrid guild of only two large eagles, only one of which occurs inland, and no vultures is extremely unusual.

Nov. gen. *lacertosus* is the first recorded vulture species in the Australian continental region (Australia and New Guinea, or Sahul), and its phylogenetic and morphological distinctiveness indicates the existence of an endemic lineage of Australian or Australasian vultures. Most notably it fills the ecological void of an obligate avian scavenger that is

lacking in modern Australia. This absence has possibly resulted in the ecological release of now generalist accipitrid species like *Aquila audax*, allowing them to fulfil multiple roles as hunter and scavenger (Olsen 2005). *A. audax* is not unique in this regard; many species of *Aquila* and other genera of large eagles also scavenge frequently as part of their diet. In these species scavenging is typically more frequent in winter seasons when live prey is scarce (Blázquez et al. 2009), or among younger individuals with lower hunting success compared to older adults (Margalida et al. 2017). In places such as Africa where large eagles and large vultures coexist, it has been noted that some vultures utilise eagles in foraging, following them to carcasses and then forcing them away (Kane et al. 2014). The relationship between Nov. gen. *lacertosus* and *Aquila audax* may have been similar in nature, and only the extinction of the former has allowed the latter to utilise carcasses like it does in the present day.

### 3.4.2 Implications for the ecology of Nov. gen. *lacertosus*

The morphology of both the humerus and the tarsometatarsus of Nov. gen. *lacertosus* are consistent with that of aegyptine vultures. The reduced size of the flange on trochlea metatarsi II, the shallow fovea lig. collateralis, and the small, shallow sulcus hypotarsi show the musculature on the limb was much weaker than on active hunters like *Aquila audax*. While Nov. gen. *lacertosus* has comparatively deeper muscular sulci and fossae than most of its aegyptine relatives, it seems most likely that Nov. gen. *lacertosus* was still primarily a scavenger, flying great distances to track down dead or dying large mammals.

Compared to other aegyptines, Nov. gen. *lacertosus* was likely a medium-sized species. It was notably larger than the smallest aegyptine vulture, *Necrosyrtes monachus*, but smaller than the species like *Gyps fulvus* and *Aegypius monachus*. Given this size, it can be predicted that Nov. gen. *lacertosus* would have had a ‘gulper’ or ‘ripper’ type diet based (see Hertel 1994), feeding either on the soft viscera or the outer skin and flesh of carcasses.

Nov. gen. *lacertosus* resolves phylogenetically as the sister group to the genus *Gyps*, though bootstrap support is low. It especially resembles *Gyps* in some features of the tarsometatarsus. Many species of *Gyps* are social, gathering in large numbers to feed at a single carcass, and are heavily reliant on the presence of conspecifics for successful foraging (Jackson et al. 2008; Dermody et al. 2011). It is possible that Nov. gen. *lacertosus* may have behaved similarly, and likewise maintained a competitive edge at carcasses by grouping together to overwhelm other avian or smaller mammalian scavengers that were present at this time.

The geographical range of Nov. gen. *lacertosus* has been expanded by the discovery of the new material. Previously known only from Kalamurina on the Warburton River in

north-east South Australia (de Vis 1905), newly referred material shows the species to have been present around the Wellington Caves in New South Wales and on the Nullarbor Plains of Western Australia. Both these new sites are over a thousand kilometers away from Kalamurina, though in terms of the flight range of a large accipitrid this is not a great distance. There is no reason that Nov. gen. *lacertosus* would not have been widespread across Australia, occupying grassland and open woodlands environments wherever they occurred, barring competitive exclusion via other species occupying the same niche.

As the first vulture of any lineage recorded in Australia, Nov. gen. *lacertosus* demonstrates that the Australian avifauna once included obligate avian scavengers like all continents (excluding Antarctica) do to the present day. As such, it would have provided a valuable service to Australian ecosystems by reducing the transmission of certain diseases (see Ogada et al. 2012) and facilitating energy flow through food webs (Wilson and Wolkovich 2011). Its presence indicates that the diversity of Pleistocene Australian accipitrids was significantly greater than it is today, not only in diversity but in realized niche space, and its extinction would have likely had a distinct impact on the ecological systems.

## **Acknowledgements**

We would like to thank Jacqueline Nguyen for the transportation of the Wellington Cave fossil material to our institute, Isaac Kerr for photographing and scanning the lectotype specimen at QM, Elizabeth Scharsachs and her family for providing accommodation in Tring, Judith White for providing the photographic material for *Torgos tracheliotos*, *Trigonoceps occipitalis*, *Sarcogyps calvus* and *Gypaetus barbatus*, and the following collection managers and curators; Phillipa Horton, Maya Penck and Mary-Anne Binnie (SAMA), Matthew McCurry (AM), Judith White and Joanne Cooper (NHMUK), Chris Milensky (Smithsonian), Mark Robbins (KU), Tim Ziegler and Karen Roberts (NMV), Scott Hucknull (QM), Mikael Siverson (WAM), and Leo Joseph and Alex Drew (ANWC).

## **Author Contributions**

EKM and THW designed the study. All authors contributed to the manuscript, with EKM writing the initial draft and THW and MSYL particularly providing feedback, revisions and suggestions. EKM compared and described the fossil material, with THW providing corrections and feedback. MSYL suggested the inclusion of a phylogenetic analysis and collated the molecular data, while EKM collected the morphological data and performed the analyses, with MSYL and THW providing feedback.

## 3.5 Additional Information

### Thesis Appendices

Please see:

**Appendix 1: List of morphological characters.** Full descriptions of all 300 morphological characters used in the analyses, including character states and whether the character was ordered, with references.

### Supplementary Information

All files available at <https://figshare.com/s/7b9b1a551576ab5ce767>

**SI.1: Morphological character data matrix.** Mesquite file containing character states for all fossil and extant species used in this thesis.

**SI.4: STL file of “*Taphaetus*” *lacertosus* lectotype.** A 3D image of the lectotype distal humerus QM F5507 of Nov. gen. compiled in the computer program Blender. Data will also be published by Queensland Museum in either Morphosource or their own repository when chapter is formally published.

**SI.5: Nov. gen. parsimony analysis file.** Command file for the parsimony analyses involving Nov. gen. *lacertosus*.

### 3.6 References

- Baird R. F. (1991) The Quaternary Avifauna of Australia. In: Vickers-Rich, P., J. M. Monahan, R. F. Baird, and T. H. Rich (Eds). *Vertebrate Palaeontology of Australasia*, Pioneer Design Studio, Melbourne. pp 809–870.
- Baumel, J. J., & Witmer, L. M. (1993) Osteologia. 45–132. In: J.J. Baumel, A.S. King, J.E. Breazile, H.E. Evans and J.C. Vanden Berge (Eds). *Handbook of avian anatomy: nomina anatomica avium, 2<sup>nd</sup> edition*. Publications of the Nuttall Ornithological Club 23. Nuttall Ornithological Club Cambridge, MA.
- Bildstein, K. L. (2017). *Raptors: the curious nature of diurnal birds of prey*. Cornell University Press, New York.
- Blázquez, M., Sánchez-Zapata, J., Botella, F., Carrete, M. & Eguía, S. (2009) Spatio-temporal segregation of facultative avian scavengers at ungulate carcasses. *Acta Oecologica*, 35(5), 645–650.
- Boles, W. E. (2006) The Avian Fossil Record of Australia: An Overview. In: *Evolution and Biogeography of Australasian Vertebrates*, J. R. Merrick, M. Archer, G. M. Hickey and M. S. Y. Lee (Eds). Auscipub, Oatlands, NSW; p. 387–411.
- Boles, W. E. (2017) A Brief History of Avian Paleontology in Australia. In: *Contributions to the History of Australasian Ornithology Volume III*, W. E. Davis Jr., W.E. Boles, H. F. Recher (Eds). Cambridge, Massachusetts; p. 265–362.
- Brisson, M-J. (1760) *Ornithologia sive synopsis methodica sistens avium divisionem in ordines, sectiones, genera, species, ipsarumque varietates. Cum accurata cujusque speciei descriptione, citationibus auctorum de iis tractantium, nominibus eis ab ipsis & nationibus impositis, nominibusque vulgaribus*. Apud Cl. Joannem-Baptistam Bauche, Parisiis.
- Brodkorb, P. (1964). Catalogue of fossil birds: Part 2 (Anseriformes through Galliformes). *Bulletin of the Florida State Museum, Biological Sciences*, 8(3), 195–335.
- Burleigh, J. G., Kimball, R. T. & Braun, E. L. (2015) Building the avian tree of life using a large-scale, sparse supermatrix. *Molecular and Phylogenetic Evolution*, 84, 53–63.
- Campbell, V. & Lapointe, F. J. (2009) The use and validity of composite taxa in phylogenetic analysis. *Systematic Biology*, 58(6), 560–572.
- Dawson, L. (1985) Marsupial fossils from Wellington Caves, New South Wales; the historic and scientific significance of the collections in the Australian Museum. *Records of the Australian Museum*, 37(2), 55–69.

- Dawson, L. & Augee, M. L. (1997) The late Quaternary sediments and fossil vertebrate fauna from Cathedral Cave, Wellington Caves, New South Wales. *Proceedings of the Linnean Society of New South Wales*, 117, 51–78.
- Dawson, L., Muirhead, J. & Wroe, S. (1999) The Big Sink Local Fauna: a lower Pliocene mammalian fauna from the Wellington Caves complex, Wellington, New South Wales. *Records of the Western Australian Museum*, supplement 57, 265–290.
- de Vis, C. W. (1889) Addition to the list of fossil birds. *Proceedings of the Royal Society of Queensland*, 6, 55–58.
- de Vis, C. W. (1891) Note on an extinct eagle. *Proceedings of the Linnean Society of New South Wales*, 6, 123–125.
- de Vis, C. W. (1905) A contribution to the knowledge of the extinct avifauna of Australia. *Annals of the Queensland Museum*, 6, 3–25.
- Dermody, B. J., Tanner, C. J. & Jackson, A. L. (2011) The evolutionary pathway to obligate scavenging in *Gyps* vultures. *PloS one*, 6(9), e24635.
- Dickinson, E. C. & Remsen J. V. Jr (Eds). 2013. *The Howard & Moore Complete Checklist of Birds of the World*. 4<sup>th</sup> edition, vol 1. Aves Press: Eastbourne, UK.
- Elzanowski, A. & Stidham, T. A. (2010) Morphology of the quadrate in the Eocene anseriform *Presbyornis* and extant galloanserine birds. *Journal of Morphology*, 271, 305–323.
- Elzanowski, A. & Zelenkov, N. V. (2015) A primitive heron (Aves: Ardeidae) from the Miocene of Central Asia. *Journal of Ornithology*, 156, 837–846.
- Ferguson-Lees, J. & Christie, D. A. (2001) *Raptors of the world*. Houghton MiZin Company, Boston.
- Frank, R. (1971) The clastic sediments of the Wellington Caves, New South Wales. *Helictite*, 9, 3–34.
- Frank, R. (1975) Late Quaternary climatic change: evidence from cave sediments in central eastern New South Wales. *Australian Geographical Studies*, 13.
- Gaff, P. (2002) The fossil history of the family Accipitridae in Australia. Unpublished Master of Science thesis, Monash University, Victoria, Australia.
- Gaff, P. & Boles, W. E. (2010) A new eagle (Aves: Accipitridae) from the Mid Miocene Bullock Creek Fauna of northern Australia. *Records of the Australian Museum*, 62, 71–76.

- Handley, W. D. & Worthy, T. H. (2021) Endocranial anatomy of the giant extinct Australian mihirung birds (Aves, Dromornithidae). *Diversity*, 13(3), 124, <https://doi.org/10.3390/d13030124>.
- Hertel, F. (1994) Diversity in body size and feeding morphology in past and present vultures. *Ecology*, 75(4), 1074–1084.
- Hesse, P. P., Magee, J. W. & van der Kaars, S. (2004) Late Quaternary environments of the Australian arid zone: a review. *Quaternary International*, 118–119, 87–102.
- Howard, H. (1930) A census of the Pleistocene birds of Rancho la Brea from the collections of the Los Angeles Museum. *The Condor*, 32(2), 81–88.
- Jackson, A. L., Ruxton, G. D. & Houston, D. C. (2008) The effect of social facilitation on foraging success in vultures: a modelling study. *Biology Letters*, 4, 311–313.
- Jefferson, G. T. (1991) A catalogue of late Quaternary vertebrates from California: Part one, nonmarine lower vertebrate and avian taxa. *Natural History Museum of Los Angeles County, Technical Reports*, 5, 1–60.
- Johnson, C. N., Dortch, J. & Worthy, T. H. (2021) Interactions with megafauna. The Oxford Handbook of the Archaeology of Indigenous Australia and New Guinea. DOI: 10.1093/oxfordhb/9780190095611.013.10.
- Kane, A., Jackson, A. L., Ogada, D. L., Monadjem, A. & McNally, L. (2014) Vultures acquire information on carcass location from scavenging eagles. *Proceedings of the Royal Society B: Biological Sciences*, 281, 20141072.
- Kaup, J. J. (1844) *Classification der säugethiere und vögel*. Druck und Verlag von C. W. Leske, Darmstadt.
- Lerner, H. R. L. & Mindell, D. P. (2005) Phylogeny of eagles, Old World vultures, and other Accipitridae based on nuclear and mitochondrial DNA. *Molecular and Phylogenetic Evolution*, 37, 327–346.
- Lydekker, R. (1890) On the remains of some large extinct birds from the cavern-deposits of Malta. *Proceedings of the Zoological Society of London*, 28, 403–411.
- Manegold, A., Pavia, M. & Haarhoff, P. (2014) A new species of *Aegyptius* vulture (Aegyptiinae, Accipitridae) from the early Pliocene of South Africa. *Journal of Vertebrate Paleontology*, 34(6), 1394–1407.
- Margalida, A., Colomer, M., Sánchez, R., Sánchez, F. J., Oria, J. & González, L. M. (2017) Behavioural evidence of hunting and foraging techniques by a top predator suggests the importance of scavenging for preadults. *Ecology and Evolution*, 7, 4192–4199.

- Mayr, G. (2014) Comparative morphology of the radial carpal bone of neornithine birds and the phylogenetic significance of character variation. *Zoomorphology*, 133, 425–434.
- Mayr, G. (2018) Size and number of the hypoglossal nerve foramina in the avian skull and their potential neuroanatomical significance. *Journal of Morphology*, 279(2), 274–285.
- Megirian, D., Prideaux, G. J., Murray, P. F. & Smit, N. (2010) An Australian land mammal age biochronological scheme. *Paleobiology*, 36(4), 658–671.
- Meijer, H. J. M., Sutikna, T., Saptomo, E. W., Awe, R. D., Jatmiko, Wasisto, S., James, H. F., Morwood, M. J. & Tocheri, M. W. (2013) Late Pleistocene-Holocene non-passerine avifauna of Liang Bua (Flores, Indonesia). *Journal of Vertebrate Palaeontology*, 33(4), 877–894.
- Migotto, R. (2013) Phylogeny of Accipitridae (Aves: Accipitriformes) based on osteological characters. PhD Dissertation, Universidade de São Paulo, Instituto de Biociências, Departamento de Zoologia.
- Mindell, D. P., Fuchs, J. & Johnson, J. A. (2018) Phylogeny, taxonomy and geographic diversity of diurnal raptors: Falconiformes, Accipitriformes and Cathartiformes. In: *Birds of Prey*, J. H. Sarasola, J. Grande, J. Negro (Eds). Springer, Cham; p. 3–32.
- Murray, P. F. & Vickers-Rich, P. (2004) *Magnificent mihirungs: the colossal flightless birds of the Australian dreamtime*. Indiana University Press.
- Nagy, J. & Tökölyi, J. (2014) Phylogeny, historical biogeography and the evolution of migration in accipitrid birds of prey (Aves: Accipitriformes). *Ornis Hungarica*, 22, 15–35.
- Nanson, G. C., D. M. Price, B. G. Jones, J. C. Maroulis, M. Coleman, H. Bowman, T. J. Cohen, T. J. Pietsch, and J. R. Larsen. (2008) Alluvial evidence for major climate and flow regime changes during the middle and late Quaternary in eastern central Australia. *Geomorphology*, 101, 109–129.
- Ogada, D. L., Torchin, M. E., Kinnaird, M. F. & Ezenwa, V. O. (2012) Effects of vulture declines on facultative scavengers and potential implications for mammalian disease transmission. *Conservation Biology*, 26(3), 453–460.
- Olsen, P. (2005) Wedge-tailed eagle. *Molecular Phylogenetics and Evolution*, 37, 327–346.
- Osborne, R. A. L. (1991) Red earth and bones: the history of cave sediment studies in New South Wales, Australia. *Earth Sciences History*, 10(1), 13–28.

- Osborne, R. A. L. (1997) Rehabilitation of the Wellington Caves phosphate mine: implications for Cainozoic stratigraphy. *Proceedings of the Linnean Society of New South Wales*, 117, 175–180.
- Osborne, R. A. L. (2007) Cathedral Cave, Wellington Caves, New South Wales, Australia. A multiphase, non-fluvial cave. *Earth Surface Processes and Landforms*, 32, 2075–2103.
- Prideaux, G. J., Long, J. A., Ayliffe, L. K., Hellstrom, J. C., Pillans, B., Boles, W. E., Hutchinson, M. N., Roberts, R. G., Cupper, M. L., Arnold, L. J., Devine, P. D. & Warburton, N. M. (2007b) An arid adapted middle Pleistocene vertebrate fauna from south-central Australia. *Nature*, 445, 422–425.
- Prideaux, G. J., Roberts, R. G., Megirian, D., Westaway, K. E., Hellstrom, J. C. & Olley, J. M. (2007a) Mammalian responses to Pleistocene climate change in southeastern Australia. *Geology*, 35(1), 33–36.
- Rich, P. & J. van Tets. 1982. Fossil birds of Australia and New Guinea: their biogeographic, phylogenetic and biostratigraphic input. In: *The Fossil Vertebrate Record of Australasia*, P. V. Rich and E. M. Thompson (Eds).. Monash University Offset Printing Unit, Clayton, Victoria; p. 235–384.
- Roberts, R. G., Flannery, T. F., Ayliffe, L. K., Yoshida, H., Olley, J. M., Prideaux, G. J., Laslett, G. M., Baynes, A., Smith, M. A., Jones, R. & Smith, B. L. (2001) New ages for the last Australian megafauna: Continent-wide extinction about 46,000 years ago. *Science*, 292, 1888–1892.
- Shute, E. (2018) Early and Middle Pleistocene non-passerine birds from the Thylacoleo Caves, Nullarbor Plain. Unpublished PhD thesis, Flinders University, South Australia, Australia.
- Sniderman, J. M. K., Pillans, B., O'Sullivan, P. B. & Kershaw A. P. (2007) Climate and vegetation in southeastern Australia respond to Southern Hemisphere insolation forcing in the late Pliocene–early Pleistocene. *Geology*, 35, 41–44.
- Stock, C. (1930) Rancho La Brea: a record of Pleistocene life in California. *Los Angeles County Museum of Natural History Science Series 1, Palaeontology 1*, 1–84.
- Tedford, R. H. & Wells, R.T. (1990) Pleistocene deposits and fossil vertebrates from the “dead heart of Australia”. *Memoirs of the Queensland Museum*, 28(1), 263–284.

- Tedford, R. H., Wells, R. T. & Barghoorn, S. F. (1992) Tirari Formation and contained faunas, Pliocene of the Lake Eyre Basin, South Australia. *Beagle: Records of the Museums and Art Galleries of the Northern Territory*, 9(1), 173–194.
- Tedford, R. H., Williams, D., and Wells, R. T. (1986). Late Cenozoic sediments and fossil vertebrates. In: *The Lake Eyre Basin – Cainozoic Sediments, Fossil Vertebrates and Plants, Landforms, Silcretes and Climatic Implications*. Australasian Sedimentologists Group Field Guide Series No. 4. R. T. Wells and R. A. Callen (Eds). Geological Society of Australasia: Sydney; p. 42–72.
- van der Kaars, S., Miller, G. H., Turney, C. S. M., Cook, E. J., Nürnberg, D., Schönfeld, J., Kershaw, A. P. & Lehman, S. J. (2017) Humans rather than climate the primary cause of Pleistocene megafaunal extinction in Australia. *Nature Communications*, 8(1), 1–7.
- van Tets, G. F. (1974) Was ‘*Taphaetus*’ *lacertosus* De Vis a fishing eagle, *Ichthyophaga* Lesson? *Emu*, 74, 58.
- van Tets, G. F. (1984) A checklist of extinct fossil Australasian birds. pp 469-475. In: M. Archer & G. Clayton (Eds.), *Vertebrate Zoogeography & Evolution in Australasia*. Hesperian Press.
- van Tets, G. F. & Rich, P. V. (1990) An evaluation of de Vis’ fossil birds. *Memoirs of the Queensland Museum*, 28(1), 165–168.
- Vieillot, L. J. P. (1816) *Analyse d’une nouvelle ornithologie elementaire*. D’eterville, Paris, France; 70 pp.
- Vigors, N. A. (1824) Sketches in ornithology; or, observations on the leading affinities of some of the more extensive groups of birds. On the groups of the Falconidae. *Zoological Journal* 1: 308–346.
- Wilson, E. E. & Wolkovich, E. M. (2011) Scavenging: how carnivores and carrion structure communities. *Trends in Ecology and Evolution*, 26(3), 129–35.
- Woodhead, J., Hellstrom, J., Maas, R., Drysdale, R., Zanchetta, G., Devine, P. & Taylor E. (2006) U-Pb geochronology of speleothems by MC-ICPMS. *Quaternary Geochronology*, 1, 208–221.
- Worthy, T. H. & Nguyen, J. M. T. (2020) An annotated checklist of the fossil birds of Australia. *Transactions of the Royal Society of Australia*, 144(1), 66–108.
- Worthy, T. H., Mitri, M., Handley, W. D., Lee, M. S., Anderson, A. & Sand, C. (2016) Osteology supports a stem-galliform affinity for the giant extinct flightless bird

*Sylviornis neocaledoniae* (Sylviornithidae, Galloanseres). *PLOS ONE*, 11(3), DOI: 10.1371/journal.pone.0150871.

Wroe, S., Field, J. H., Archer, M., Grayson, D. K., Price, G. J., Louys, J., Faith, J. T., Webb, G. E., Davidson, I. & Mooney, S. D. (2013) Climate change frames debate over the extinction of megafauna in Sahul (Pleistocene Australia-New Guinea). *Proceedings of the National Academy of Sciences*, 110(22), 8777–8781.

Zhang, Z., Huang, Y., James, H. F. & Hou, L. (2012) Two Old World vultures from the middle Pleistocene of northeastern China and their implications for interspecific competition and biogeography of Aegypiinae. *Journal of Vertebrate Paleontology*, 32(1), 117–124.

## Chapter 4: New large Pleistocene Old World vultures (Accipitridae) from Australia: morphology, systematics and palaeoecological implications.

Ellen K. Mather<sup>1, 2</sup>, Michael S. Y. Lee<sup>1, 3</sup>, Diana A. Fusco<sup>1</sup>, Trevor H. Worthy<sup>1</sup>

<sup>1</sup>College of Science and Engineering, Flinders University, GPO 2100, Adelaide, SA 5001, Australia

<sup>2</sup>Corresponding author, [math0083@flinders.edu.au](mailto:math0083@flinders.edu.au)

<sup>3</sup> Earth Sciences Section, South Australian Museum, North Terrace, Adelaide 5000, Australia

### Abstract

The Pleistocene fossil record of Australian Accipitridae (eagles, hawks and Old World vultures) is very poorly understood with only one distinct extinct species named until now. This presents a severe limitation on our understanding of how the Australian accipitrid fauna has changed during the Pleistocene and into the present, particularly in relation to the megafaunal extinctions roughly 50–40 Ka. However, recent work on the species “*Taphaetus lacertosus*” has revealed it belonged to the vulture subfamily Aegypiinae, and several other taxa from this time period have yet to be described. Fossil material from multiple Pleistocene cave deposits is here identified as representing two new taxa. One species from Green Waterhole/Fossil Cave in the Tantanoola District, Victoria Fossil Cave at Naracoorte and Cooper Creek, all in South Australia, Leaena’s Breath Cave on the Nullarbor Plain, Western Australia, and Wellington Caves in New South Wales, is described as ‘accipitrid GWC/VFC’ gen. et sp. nov. A second, from Mairs Cave in Buckalowie Gorge of the Flinders Ranges, South Australia is described as ‘Mairs Cave accipitrid’ gen et sp. nov. The Green Waterhole Cave taxon was sufficiently complete for a phylogenetic analysis, which found strong support for a close relationship between it and the living aegypiine vultures, while the Mairs Cave taxon had features characteristic of gypaetine vultures. Thus, the guild of Old World vultures in Pleistocene Australia included three species, of which one uniquely was an actively predatory aegypiine vulture, and another is the first gypaetine vulture recorded from Australia.

**Keywords:** Pleistocene extinction, Aegypiinae, Gypaetinae, biogeography, avian predators, avian scavengers, new taxa, taxonomy

## 4.1 INTRODUCTION

### 4.1.1 Australian Accipitridae

Mainland Australia has seventeen resident breeding species of accipitrid raptors (Accipitridae), comprising twelve genera and five subfamilies (Marchant and Higgins 1993; Debus 1998). Most genera that are present in Australia are also present elsewhere, with the exception of the endemic *Lophoictinia* and *Hamirostra*. The Australian taxa are varied in their preferred habitats and diets, ranging from species in the genus *Elanus* (open grassland and woodland predators of small vertebrates and large invertebrates), to those in *Haliaeetus* (coastal, fish), and *Aquila* (open habitat, small to medium mammals) (Brown and Amadon 1968). Today, there are only two large (>2 kg) extant Australian eagles; the white-bellied sea eagle *Haliaeetus leucogaster*, which predominantly inhabits the coastal regions, and the widely distributed wedge-tailed eagle *Aquila audax*.

The modern Australian avifauna notably lacks several subfamilies of large accipitrids, with no species from Circaetinae (snake eagles), Harpiinae (harpy eagles and kin), Gypaetinae (aberrant Old World vultures) or Aegyptiinae (typical Old World vultures) present. Harpiine eagles are currently represented by four living species, all but one of which inhabits rainforest environments exclusively. Two species, *Harpia harpyja* and *Morphnus guianensis*, are endemic to South and Central America, *Macheiramphus alcinus* is found in Africa, South-East Asia and New Guinea, and *Harpyopsis novaeguineae* is restricted to New Guinea. Similarly, many species of the circaetine genus *Spilornis* and *Pithecophaga jefferyi* also prefer enclosed rainforest habitat and are present in South-east Asia, with open habitat genera restricted to Africa (Dickinson and Remsen 2013). The lack of harpiine and circaetine species in Australia is unusual given their occurrence in New Guinea, but perhaps can be attributed to a limited amount of suitable habitat and climate change, as the extent of Australian rainforest habitat oscillated through the Quaternary (Donders et al. 2006; Sniderman et al. 2007; Sniderman and Haberle 2012; Sniderman et al. 2012).

In the case of the Gypaetinae and Aegyptiinae, their absence is less explicable. Species in both subfamilies of Old World vultures favour open environments such as grassland, mountains/hills and open woodland (Brown and Amadon 1968; Ferguson-Lees and Christie 2001), most of which were predominant in Pleistocene to Holocene Australia. At least 27 genera of megafaunal species existed in Australia and New Guinea at the time (Wroe et al. 2013; Johnson et al. 2021), which would have provided food for vultures and large birds of prey. Furthermore, the fossil record of South-east Asia has documented extinct species within extant vulture genera being present as far south as Flores, Indonesia (Meijer et al. 2013). The lack of vultures in modern-day Australia is therefore extremely unusual and

not easily explained. This raises the question of whether there is an unrecognised presence of vultures from the Pleistocene.

The Old World/accipitrid vultures are comprised of species that predominantly specialise in scavenging rather than hunting. They are divided into two subfamilies: the Gypaetinae are 'aberrant' vultures with more varied diets and hunting ability (such as the omnivorous Palm-nut Vulture *Gypohierax angolensis*, or the hunting and hollow-foraging Harrier-hawks in *Polyboroides*), while the Aegypiinae are 'typical' vultures that subsist almost entirely off carcasses (Brown and Amadon 1968). However, these subfamilies are not monophyletic. The Aegypiinae are most closely related to the Circaetinae, while the Gypaetinae form a clade with the Perninae (Lerner and Mindell 2005; Griffiths et al. 2007; Nagy and Tökölyi 2014; Mindell et al. 2018). Despite their name the Old World vultures are not closely related to the New World vultures, which belong to a separate accipitriform family of scavenging specialists known as the Cathartidae (see Livezey and Zusi 2007; Hackett et al. 2008; Jarvis et al. 2014; Prum et al. 2015).

#### **4.1.2 Pleistocene Australian fossil record of Accipitridae**

The Pleistocene fossil record of Australian accipitrids is sparse, with most identified fossil specimens being highly fragmentary. Until recently, five extinct accipitrid species were recognised from Australian late Pliocene to Pleistocene deposits. These species were described by the naturalist and palaeontologist Charles Walter de Vis, who named *Aquila brachialis* (de Vis, 1889), "*Taphaetus*" *lacertosus* de Vis, 1905, *Necrastur alacer* de Vis, 1892, *Asturaetus furcillatus* de Vis, 1905, and *Palaeolestes gorei* de Vis, 1911. *Palaeolestes* was hesitantly assigned to the 'Accipitres', as the Accipitridae were known at the time, due to being based on a single phalanx that de Vis thought bore some similarity to those seen in living hawks and eagles (de Vis 1911).

The status of these species named by de Vis was later brought into question. Vickers-Rich et al. (1982) determined that *Asturaetus furcillatus* was a synonym of the living Brown falcon *Falco berigora*. *Aquila brachialis* has been suggested to be either a synonym of the extant *A. audax* (e.g., Condon 1975) or an indeterminate accipitrid (van Tets 1984). A reassessment by van Tets and Vickers-Rich (1990) of the 'accipitrid' species named by de Vis found that only *Aquila brachialis*, "*Taphaetus*" *lacertosus* and *Necrastur alacer* were likely correctly identified as accipitrids; *Asturaetus furcillatus* was a brown falcon as already noted and *Palaeolestes gorei* was likely to be a mammal. *Necrastur alacer* has nothing published specifically on it in the literature outside its initial description, but an unpublished thesis by Gaff (2002) considered it to be distinct from living Australian accipitrids in terms of its small size and morphology.

The affinities of “*Taphaetus*” *lacertosus* have long been a subject of debate, with speculation that it belonged to the Gypaetinae (the only vulture subfamily recognised at the time, see Brodkorb 1964; Olson 1985; Holdaway 1994) of the Accipitridae (Rich and van Tets 1982; van Tets 1984), though some authors were skeptical of this claim (see Baird 1991). Morphological comparisons and phylogenetic analysis on “*Taphaetus*” *lacertosus* determined that the species is an aegyptiine vulture (Mather et al. Chapter 3 herein). It is the first species of Old World vulture to be recorded in Australia and demonstrates that the geographical range of at least one vulture subfamily included that continent.

#### **4.1.3 Fossil record of accipitrid vultures**

##### ***Europe***

The oldest potential vulture known from Europe is *Palaeohierax gervaisii* (Milne-Edwards, 1863; 1871), which was described from a Miocene-age tarsometatarsus and existed during the late Oligocene and early Miocene of France (Mlíkovský 2002; Mayr 2009). It was first assigned to the Gypaetinae by Brodkorb (1964), with it apparently resembling the living *Gypohierax angolensis* in its morphology (Rich 1980; Olson 1985). However, its assignment to vulturine accipitrids is considered tenuous by some (Mayr 2009; Zhang et al. 2012a; Li et al. 2016).

Four fossil European vulture species are known from Pliocene and Pleistocene deposits, three of which are aegyptiines. *Aegyptius tugarinovi* Manegold and Zelenkov, 2015, is from the early Pliocene of Moldova, and was described from a left tarsometatarsus. This bone was initially described by Tugarinov (1940), who attributed it to another fossil species of vulture known at the time, *Gyps melitensis* Lydekker, 1890. *Gyps bochenskii* Boev, 2010 is a late Pliocene species known from a Middle Villafranchian site near Varshets, Bulgaria, and was described from sternal, coracoid, and digital phalanx elements, and is currently the oldest known species of *Gyps*. *Gyps melitensis* is known from several sites in Europe dated to the middle Pleistocene and was described from cervical vertebrae and leg bones from Zebbug Cave, Malta. A fossil proximal ulna from the Pleistocene site of Gabasa, Spain was considered to represent a new species by Hernandez (2001), which he named *Aegyptius prepyrenaicus*, but this was later considered to be a nomen dubium (Sánchez-Marco 2007). The only known gypaetine from Pleistocene deposits in Europe, *Gypaetus osseticus* Burchak-Abramovich, 1971, was described from material found in Tsona Cave, Georgia.

##### ***Asia***

The fossil record of accipitrid vultures in Asia begins in the early Miocene. The first Chinese fossil to be identified as an accipitrid vulture was *Mioaegyptius gui* Hou, 1984, which was part of the Aragonian fauna excavated from the Xiacaswan Formation, Jiangsu

Province, dated to the middle Miocene (Hou 1984). The species was described from a largely complete left tarsometatarsus. While it is definitively an accipitrid, the assignment to Aegypiinae is considered to be uncertain and requires more material to be verified (Rich et al. 1986; Manegold et al. 2014).

Another Chinese species, *Qiluornis taishanensis* Hou et al., 2000, was found in the early Miocene Shanwang Formation of Shandong Province (Hou et al. 2000). It consisted of a partial vertebral column, a complete pelvis, and bones of a complete right leg, and is regarded to have been reliably identified as an early stem Aegypiinae (Hou et al. 2000; Manegold et al. 2014).

*Gansugyps linxiaensis* Zhang et al., 2010 was found in the late Miocene Upper Liushu Formation in Gansu Province and is the third fossil taxon from China to be attributed to the accipitrid vultures (Zhang et al. 2010). It was described based on two skeletons, one nearly complete and another partially complete, missing the right wing, vertebral column and right femur, and was considered a crown aegypiine by Zhang et al. (2010) but was regarded to be a stem aegypiine by Manegold et al. (2014).

In addition to these three taxa assigned to the Aegypiinae, there is one species attributed to Gypaetinae. *Mioneophron longirostris* Li et al., 2016 comes from the Upper Liushu Formation, where with *Gansugyps linxiaensis* it formed part of a vulture guild that existed in Gansu Province during the late Miocene (Li et al. 2016). It was described based on a nearly complete skeleton and is the oldest known species of Gypaetinae from the Old World (Li et al. 2016).

At least two extinct species are reported from Pleistocene deposits of China: *Aegyptius jinniushanensis* Zhang et al., 2012b and a currently unnamed species thought to belong to the genus *Torgos* (Zhang et al. 2012b). Another unnamed species is known from Flores, Indonesia, and is believed to belong to the genus *Trigonoceps* (Meijer et al. 2013). A potential second Southeast Asian species was noted by Wetmore (1940) based on a distal ulna and radius from late Pleistocene deposits at Wataluang, Java, but the current location of these fossils is uncertain, and their vulturine affinities are currently unconfirmed (see Meijer 2014).

## **Africa**

The fossil record of African birds is quite poorly described, and the accipitrids are no exception. Currently the only known fossil vulture unique to Africa is *Aegyptius varswaterensis* Manegold et al., 2014 from the early Pliocene Upper Varwater Formation in South Africa. It was described from a partial skeleton comprising cervical and thoracic vertebrae, most of the wing bones, a proximal femur, fragmented fibula, and several pedal

phalanges. Fossils described from Ifri n'Ammar, Morocco, have extended the geographic range of the living species *Aegyptius monachus* and *Gyps fulvus* into the northern region of Africa, along with a third species that might possibly be referred to the extinct European taxon *Gyps melitensis* or even *Aegyptius prepyrenaicus* (see Manegold and Hutterer 2021).

### **Americas**

While all living accipitrid vultures are restricted to the Old World, the fossil record demonstrates that this was not always the case. North America has a very rich fossil record of accipitrid vultures extending from the early Miocene into the late Pleistocene (see Brodkorb 1964). Outside of China, most Miocene accipitrid vultures are from sites in North America. The oldest of these is *Arikarornis macdonaldi* Howard, 1966 from early Miocene deposits of South Dakota, which was described from the distal end of a tibiotarsus. The slightly younger *Anchigyps voorhiesi* Zhang et al., 2012a, from the late Miocene Ash Hollow Formation in Nebraska, USA, was described from a paired set of ulnae, tibiotarsi, tarsometatarsi, and the tip and left part of the ramus. It is believed to belong to a basal lineage that represents the divergence of Gypaetinae from other accipitrids (Zhang et al. 2012a), making it quite significant for estimates of divergence dates.

The American fossil aegyptiine genus *Neophrontops* is the most speciose of the extinct accipitrid vulturine genera, with six species currently described. The genus is also notable in that it spans multiple epochs. The oldest is the species *Neophrontops vetustus* Wetmore, 1943, from the middle Miocene Stonehouse Draw Quarry, Nebraska, described from a distal humerus (Wetmore 1943), and *N. ricardoensis* Rich, 1980, which is known from a partial articulated skeleton from middle Miocene deposits in California. *Neophrontops dakotensis* Compton, 1935 is known from the middle Pliocene Drewsey Formation of Oregon and the lower Pliocene Ogallala Formation of South Dakota and was described from a distal right humerus. *Neophrontops slaughteri* Feduccia, 1974, was described from a distal tibiotarsus from the upper Pliocene Glenns Ferry Formation of Idaho and a mandible and various wing and leg elements from the late Pliocene Inglis Quarry in Florida have been referred to the species (Emslie 1998). Two Pleistocene species are *N. americanus* Miller 1916, described from a tarsometatarsus from the upper Pleistocene Rancho La Brea tar pits, California and *N. vallecitoensis* Howard, 1963, described from a distal left tarsometatarsus from the upper Palm Spring Formation, California. A currently unidentified species of *Neophrontops* from the late Miocene to early Pliocene Big Sandy Formation of Arizona is known from an associated left radius, carpometacarpus and coracoid, as well as other specimens of coracoidei, humeri, ulnae, and tarsometatarsi (Bickart 1990).

Another genus of fossil accipitrid vulture known through multiple epochs is *Palaeoborus*. *Palaeoborus rosatus* Miller and Compton, 1939 and *P. howardae* Wetmore, 1936, with the former being from the middle to late Miocene Flint Hill North site in southern Dakota, and the latter from the middle Miocene Sheep Creek in Nebraska. The genus is known to have survived into the Pliocene, with the species *Palaeoborus umbrosus* (Cope, 1874) known from the lower Pliocene Santa Fe Formation in New Mexico.

One of the last American Old World vultures to exist was *Neogyps errans* Miller, 1916. The species was described based on a tarsometatarsus and is known from upper Pleistocene deposits of the tar pits of Rancho La Brea, Mckittrick, and Carpinteria, California (Miller 1916; Miller 1927a; Miller 1927b), as well as Smith Creek Cave, Nevada (Howard 1952), and San Josecito Cavern, Mexico (Miller 1943).

## **Australia**

*“Taphaetus” lacertosus* (de Vis, 1905) is the first confirmed species of Australian Old-World vulture. Named from material originating from the Pleistocene deposits at Kalamurina, South Australia (SA), it is also reported from other Pleistocene sites such as Wellington Caves, New South Wales (NSW), and Leaena’s Breath Cave, Western Australia (WA) (Mather et al. Chapter 3 herein). With the knowledge that Old World vultures were indeed present in the Sahul (Australia + New Guinea) region, the systematics of other undescribed Australian Pleistocene forms is of particular interest. Fossil material from large accipitrids has been documented from multiple sites (Baird 1985; Rich and van Tets 1982; Baird 1991) and were reported in an unpublished Monash University thesis by Gaff (2002), with some material being from birds even larger than *Aquila audax*, but these species have yet to be formally described. The aim of this project is therefore to describe these fossils and determine whether they also represent Old World vultures from both descriptive and phylogenetic comparisons where possible.

## **4.2 MATERIALS AND METHODS**

### **4.2.1 Abbreviations:**

**Institutes:** Australian Museum, Sydney, New South Wales, Australia (AMF); Australian National Wildlife Collection, Canberra, Australian Capital Territory, Australia (ANWC); Flinders University, Adelaide, South Australia, Australia (FU/FUR); Museums Victoria, Melbourne, Victoria, Australia (NMV); South Australia Museum, Adelaide, South Australia, Australia (SAMA); Western Australian Museum, Perth, Western Australia, Australia (WAM); Smithsonian Museum of Natural History, Washington D. C., United States of America (USNM); University of Kansas Institute of Biodiversity (KU), Lawrence, Kansas, United

States of America; Natural History Museum, London, UK (NHMUK); Canterbury Museum, Christchurch, New Zealand (CM).

**Skeletal:** DI.1 = digit 1, phalanx 1; DII.1 = digit II, phalanx 1; DII.2 = digit II, phalanx 2; DIII.1; DIII.2; DIII.3.

#### 4.2.2 Nomenclature

The anatomical nomenclature advocated by Baumel and Witmer (1993) is followed for all bones. Taxonomic nomenclature follows Dickinson and Remsen (2013) and Gill et al. (2020) for composition of Accipitriformes, and Nagy and Tökölyi (2014) for subfamilial composition (excluding Milvinae).

#### 4.2.3 Comparative Material

Skeletons of extant taxa were obtained on loan from museums and other institutions from across Australia and overseas as follows:

**CICONIIFORMES. Threskiornithidae.** *Threskiornis spinicollis* SAMA B48351. **Ciconiidae.** *Ciconia ciconia* SAMA B49223, SAMA B11601.

**ACCIPITRIFORMES. Cathartidae.** *Coragyps atratus* SAMA B36873. **Sagittariidae.** *Sagittarius serpentarius* USNM 223836. **Pandionidae.** *Pandion haliaetus* SAMA B37096, NMV B30256.

**Accipitridae.** Elaninae: *Elanus axillaris* NMV B34037; *Elanus scriptus* NMV B8617, NMV B30263, ANWC 22680; *Gampsonyx swainsonii* USNM 623110; *Chelictinia ricourii* NHMUK S.1904.4.28.3. Perninae: *Elanoides forficatus* USNM 622340; *Chondrohierax uncinatus* USNM 289784; *Aviceda subcristata* ANWC 22665, NMV B19826; *Pernis apivorus* SAMA B59278; *Lophoictinia isura* NMV B18533, ANWC 44373; *Hamirostra melanosternon* ANWC (FALS-41, SAMA B36200. Gypaetinae: *Polyboroides typus* USNM 430434; *Neophron percnopterus* SAMA B11449; *Gypohierax angolensis* USNM 291316; *Gypaetus barbatus* NHMUK S.1972.1.59, NHMUK S.1896.2.16.120, NHMUK S.1952.3.61. Circaetinae: *Spilornis cheela* USNM 562001; *Terathopius ecaudatus* NMV 18575; *Pithecophaga jefferyi* NHMUK S.1910.2.11.1a, NHMUK S.1961.23.1. Aegyptiinae: *Necrosyrtes monachus* USNM 620646; *Gyps coprotheres* ANWC 22724; *Gyps fulvus* NMV 18574, NMV B30269; *Aegyptius monachus* NMV R553; *Sarcogyps calvus* NHMUK S.2013.22.1, NHMUK S.2007.30.1; *Trigonoceps occipitalis* NHMUK S.1954.30.54; *Torgos tracheliotos* NHMUK S.1930.3.24.248, NHMUK S.1952.1.172. Harpiinae: *Harpia harpyja* NHMUK S.1862.3.19, NHMUK S.1909.8.18.1. Aquilinae: *Stephanoaetus coronatus* NHMUK S.1954.30.42; *Stephanoaetus coronatus* NHMUK S.1862.3.14.19; *Aquila audax* SAMA B46613; *Aquila audax* NMV B19228; *Aquila chrysaetos* NMV B32659; *Aquila chrysaetos* ANWC 22682 (FALS-123); *Aquila fasciata* (labelled as *Hieraaetus fasciatus*) NMV B30575; *Hieraaetus morphnoides* SAMA B47128; *Hieraaetus morphnoides* NMV B8643; *Hieraaetus*

*morphnoides* NMV B20224; *Spizaetus tyrannus* KU 35007; *Spizaetus ornatus* KU 72077. Haliaeetinae: *Haliaeetus leucogaster* NMV B8847, SAMA B49459; *Haliaeetus leucocephalus* ANWC 22723 (16500), NMV B15601; *Haliaeetus albicilla* NMV B34417; *Haliastur indus* ANWC 22719, NMV B13753; *Haliastur sphenurus* NMV B11661, SAMA B33998; *Milvus migrans* SAMA B47130, NMV B20404. Accipitrinae: *Melierax metabates* NHMUK S.1954.30.29; *Kaupifalco monogrammicus* NHMUK S.1869.10.19.28; *Circus assimilis* SAMA B56454, ANWC 22727; *Circus approximans* ANWC 22728, ANWC 22729; *Circus cyaneus* ANWC 22735; *Circus aeruginosus* NMV B12891; *Accipiter fasciatus* NMV B13444, SAMA B36355; *Accipiter cooperii* ANWC 22764, ANWC 22765; *Accipiter striatus* ANWC 22747, NMV B12666; *Accipiter novaehollandiae* NMV B18401; *Accipiter cirrocephalus* NMV B16071, NMV B10346; *Accipiter nisus* NMV B12413, ANWC 22742; *Accipiter gentilis* ANWC 22736, NMV B12927. Buteoninae: *Erythrotriorchis radiatus* NHMUK S.1872.10.22.9; *Ictinia mississippiensis* ANWC 22681 (21655), NMV B13343; *Geranospiza caerulescens* NHMUK S.1903.12.20.318; *Buteo buteo* SAMA B46558, NMV B24505; *Buteo lagopus* NMV B24884, ANWC 22776 (21694); *Buteo nitidus* NMV B13222; *Buteo rufofuscus* NMV B24503.

In addition, casts of bones of the type series of the extinct *Hieraaetus moorei* (Haast, 1872) were examined as follows: NMV P33032 (tibiotarsus CM AV 5104pt); NMV P33031 (ungual phalanx CM AV 5104pt); NMV P33030 (tarsometatarsus CM AV 5104pt); NMV P33029 (femur, CM AV 5104pt); NMV P33028 (humerus, CM AV 5104pt); NMV P33027 (femur CM AV 5102pt); NMV P33026 (ulna CM AV 5104pt); and additional observations were made from figures in Holdaway (1991).

#### 4.2.4 Measurements

Measurements were made with digital callipers, and rounded to the nearest 0.1 mm.

#### 4.2.5 Phylogenetic methods

**Morphological analysis:** A total of 300 morphological characters (see Appendix 1; SI.1) were sampled across the skeleton of both extant and fossil specimens, from the following elements: cranium, sternum, coracoid, humerus, ulna, carpometacarpus, ossa digitorum manus, pelvis, femur, tibiotarsus, tarsometatarsus, and pedal phalanges. A total of 154 characters were derived from Migotto (2013), two from Elzanowski and Stidham (2010), one from Elzanowski and Zelenkov (2015), eight from Gaff and Boles (2010), one from Worthy et al. (2016), and three from Mayr (2014). The remaining 129 characters were derived from observations and comparisons between the extant and fossil specimens.

**Molecular data:** Data from Burleigh et al. (2015) was used to provide molecular data for species used in this study, with the following genes being selected due to their good

sampling across accipitriforms: cytochrome b, cytochrome oxidase 1, NADH dehydrogenase 2, 12s RNA, RAG 1, and fibrinogen B beta introns 6 7.

Genomic data from these genes was used for the following species: *Ciconia ciconia*, *Coragyps atratus*, *Sagittarius serpentarius*, *Pandion haliaetus*, *Gampsonyx swainsonii*, *Elanoides forficatus*, *Chondrohierax uncinatus*, *Aviceda subcristata*, *Pernis apivorus*, *Lophoictinia isura*, *Hamirostra melanosternon*, *Polyboroides typus*, *Gypohierax angolensis*, *Neophron percnopterus*, *Gypaetus barbatus*, *Spilornis cheela*, *Terathopius ecaudatus*, *Necrosyrtes monachus*, *Torgos tracheliotos*, *Trigonoceps occipitalis*, *Gyps coprotheres*, *Gyps fulvus*, *Aegyptius monachus*, *Sarcogyps calvus*, *Aquila chrysaetos*, *Hieraaetus morphnoides*, *Hieraaetus fasciatus*/*Aquila fasciata*, *Hieraaetus moorei*, *Spizaetus tyrannus*, *Spizaetus ornatus*, *Haliaeetus leucogaster*, *Haliaeetus leucocephalus*, *Haliaeetus albicilla*, *Milvus migrans*, *Circus aeruginosus*, *Circus cyaneus*, *Accipiter cooperii*, *Accipiter striatus*, *Accipiter novaehollandiae*, *Accipiter gentilis*, *Buteo buteo*, *Buteo lagopus*, *Buteo rufofuscus*, and *Platalea leucorodia*. Genomic data from *Platalea leucorodia* was used as a stand in for *Threskiornis spinicollis*, and *Elanus caeruleus* for *Elanus scriptus*, as the species pairs are closely related taxa (see Campbell and Lapointe 2009).

**Phylogenetic analysis:** Phylogenetic comparisons were aimed primarily at determining the relationships of fossil specimens. A total of 47 species of Accipitridae, one species each of Pandionidae, Sagittariidae, Cathartidae, Threskiornithidae, and Ciconiidae was sampled. The non-accipitrid species were selected for the following reasons: Pandionidae, Sagittariidae and Cathartidae are all members of the order Accipitriformes along with the Accipitridae; the Ciconiidae and Threskiornithidae, both from the order Ciconiiformes, are examples of bird families that fall outside of Accipitriformes but are similar in size and flight morphology, as well as having a history of grouping with the Cathartidae morphologically.

A combination of parsimony and Bayesian analyses were used to analyse the data. The parsimony analyses of the morphological, molecular, and combined morphological-molecular matrices were analysed using PAUP 4.0b10, using heuristic searches (see SI.6). Each search comprised of 1000 random addition replicates, and enabled TBR branch swapping, with NCHUCK set to 1000. Characters that could not be assessed on a specimen were coded using '-' to indicate missing data. The taxa *Ciconia ciconia*, *Threskiornis spinicollis*, *Coragyps atratus* and *Sagittarius serpentarius* were set as the most distal outgroup clade. Once the heuristic searches had generated a set of most parsimonious trees (MPT), a strict consensus tree was created from them. The clades formed by these trees were then assessed using bootstrapping (200 replicates), and the majority-rule consensus was set to a conlevel of 50 (only clades >50% shown).

For the Bayesian analyses (see SI.7), MrBayes 3.2.7 was used via the platform CIPRES. The analyses were set into three partitions: morph, which focused on morphological data; pfinder molec1, which included Cyt-B codons 1 and 2, CO1 codons 1 and 2, ND2 codons 1 and 2, 12s, Rag-1 codons 1, 2 and 3, and FGBint67; and pfinder molec2, which included Cyt-B codon 3, CO1 codon 3, and ND2 codon 3. Each partition was subject to four runs, from which a consensus tree was then derived. The Morph partition had standard type data with variable coding of up to 10 states, which were fixed to be equal. The rates were set to gamma, with distribution approximated using four categories. The Molec1 partition had the GTR model, with a Nst of 6, with substitution rates and frequencies having (separate) Dirichlet priors. The rates were set to Invgamma, with the gamma distribution approximated using four categories. The Molec2 partition also had a (separate) GTR model. The rates were set to Gamma, with the distribution approximated based on four categories. The number of MCMC chains was set to 4 (incrementally heated at 0.1), the number of generations set to 50 000 000, the sample frequency set to 5000. *Ciconia ciconia* was initially set as the sole outgroup taxon, due to limitations with MrBayes, but trees were later re-rooted on the *Ciconia+Threskionis* clade.

#### **4.2.6 Mass estimates**

The femora, humeri, tibiotarsi and coracoids were used for mass estimates. To achieve this, a range of measurements were taken from the bones, using a digital calliper for lengths and widths, or with a length of string for shaft circumference. These measurements were then used to predict the body mass with established formulae (Campbell and Tonni 1983; Campbell and Marcus 1992; Field et al. (2013).

#### **4.2.7 Australian Pleistocene sites**

Australia has many Pleistocene fossil sites that are widely distributed across the country. Four have produced fossil accipitrid material that cannot be assigned to any extant Australian species, and in some cases even appear to have traits typical of accipitrid vultures. These sites are Leaena's Breath Cave, in the Nullarbor of WA; Mairs Cave, in the Flinders Ranges, SA; Victoria Fossil Cave, at Naracoorte, SA; Green Waterhole Cave (also known as Fossil Cave), at Tantanoola near Mt Gambier, SA; Cooper Creek, in the Lake Eyre Basin, SA; and Wellington Caves, NSW (see Figure 4.1).



**Figure 4.1: Map of Australia with location of fossil sites used in this study marked and labelled. Mairs Cave**

Mairs Cave is located in Buckalowie Gorge of the central Flinders Ranges, and is approximately 400 m long, with the entrance chamber being 120 m long by 10 m wide (Kraehenbuehl et al. 1997; Treble et al. 2017). The cave is predominantly in Cambrian limestone (Kraehenbuehl et al. 1997; Lawrence 2009) and is only accessible via a 17 m entrance shaft. The floor of the cave is rockfall with little stratified sediment and is occasionally flooded due to being on the same level as the current Buckalowie Creek (Lawrence 2009), which limits determining the age and succession of fossil taxa from this site (Liddle et al. 2018).

The presence of a very large accipitrid from this site has been acknowledged in multiple works (Rich and van Tets 1982; Baird 1991; Baird et al. 1991). Accipitrid material included in this study from this site includes a nearly complete sternum, a distal humerus, and two ungual phalanges. This material was recovered roughly 55 m [60 yards] from the

cave entrance under loose rocks on the surface, as per the collection data of ungual phalanx SAMA P.17139. Most have/had some calcite deposits on them indicating that they lay on the surface. The sternum and ungual phalanges had previously been considered by Gaff (2002).

### **Victoria Fossil Cave**

Victoria Fossil Cave is the most significant cave for fossils in the Naracoorte Caves National Park and is key to the inclusion of the park in the *Australian Fossil Mammal Sites (Riversleigh/Naracoorte)* World Heritage Area, having extensive deposits that have provided fossils of many species of Pleistocene megafauna, as well as smaller vertebrates such as birds (van Tets and Smith 1974; Reed and Bourne 2000; Fraser and Wells 2006; Reed and Bourne 2009). The cave itself has multiple fossil sites within it, the most significant being Fossil Chamber, Grant Hall, and the Ossuaries (Reed 2003, 2006; Fraser and Wells 2006). Fossil Chamber was discovered in 1969 (Wells 1975) and played a crucial role in the successful World Heritage nomination in 1994. Like all caves at Naracoorte, Victoria Fossil Cave was formed in Tertiary limestone beds in the phreatic zone during the late Miocene or early Pliocene and has since been uplifted above the local water table (Sprigg 1952; Wells et al. 1984). Accumulation of fossil material did not begin until the middle Pleistocene, when erosion of the surrounding Naracoorte East Dune exposed openings into the caves (Wells et al. 1984), and it has been estimated that sites in the cave range between 500 Ka and the present (Grün et al. 2001; Prideaux et al. 2007a; Macken et al. 2011; Macken and Reed 2013; Macken et al. 2013).

The diversity of extinct mammal fauna (birds and the herpetofauna have yet to be described in any detail) recorded from Victoria Fossil Cave has made it an extremely valuable site for assessing changes in environment, climate, and fauna through the Pleistocene. However, very little has been documented on the accipitrid fossils from this site, with most existing records not mentioning accipitrids among their lists of birds (van Tets and Smith 1974; Reed and Bourne 2000, 2009), although Gaff (2002) discussed some specimens.

The material assessed in this study originates from the Main Fossil Chamber of Victoria Fossil Cave, which has produced fossil material between 500–213 Ka based on U/Th dating of flowstone caps (Ayliffe et al. 1998). Material excavated from this site had their stratigraphic data captured by recording the 3D location of the excavation unit in decimal feet with X, Y, and Z coordinates relative to a fixed datum near the base of the talus cone (see Reed 2003). For example, SAMA P.28008 has coordinates of 60.5'–62.5' [along the datum line], R1'–2' [R = right of datum line], and -0.5' to -1.0' D/D [depth relative to datum].

Accipitrid material from Fossil Chamber of Victoria Fossil Cave includes a complete quadrate, humerus, ulna, carpometacarpus, a partial pelvis, two complete femora and a partial tarsometatarsus preserving the distal second and third trochleae. Gaff (2002) only mentioned the ulna.

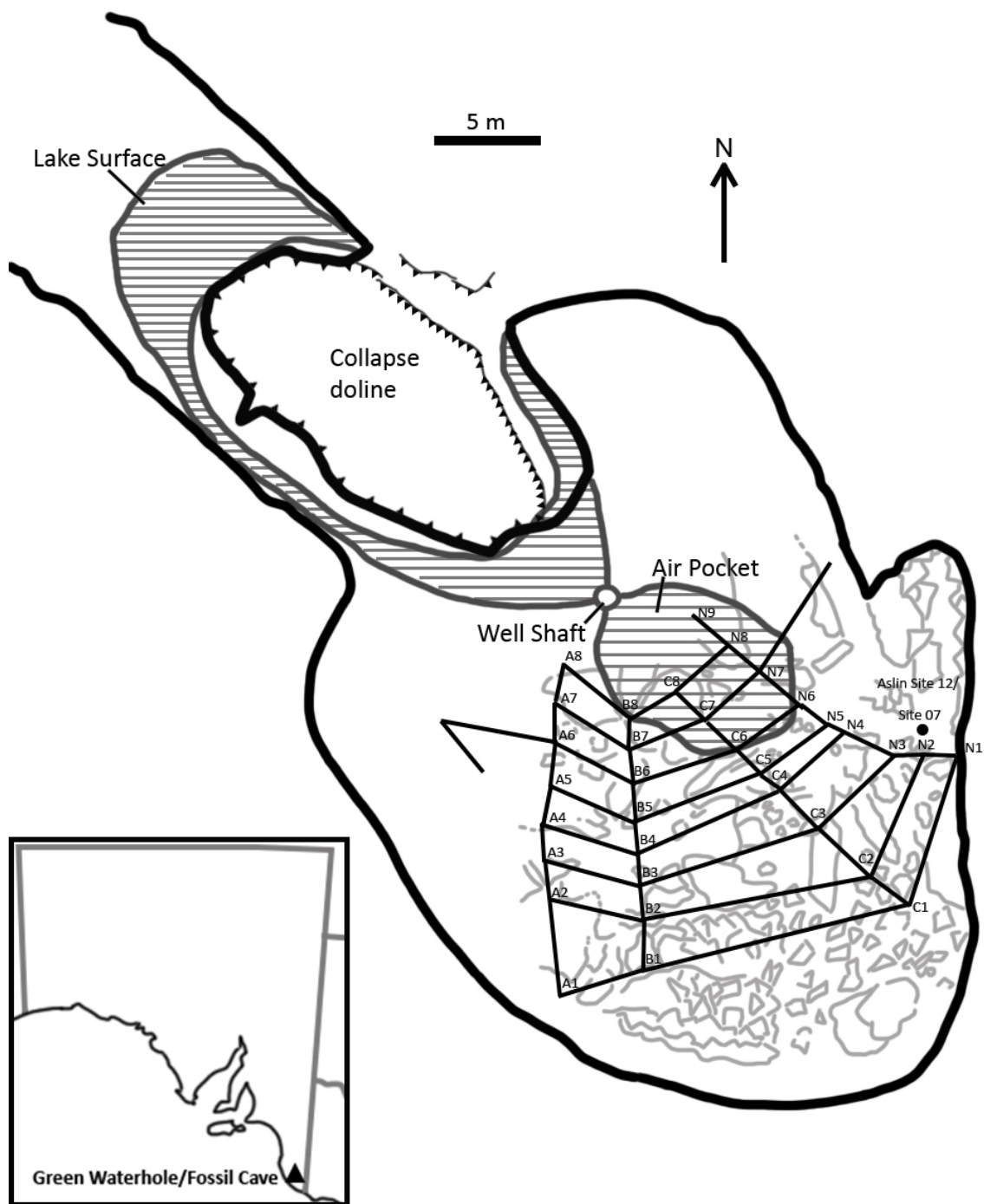


**Figure 4.2:** Map of Green Waterhole Cave modified from original (Horne 1988), with location of the cave in South Australia inset on bottom-left. Connecting points of the grid within the cave mark out the positions of the underwater anchor points for dive lines defining areas within which fossil bones were collected. Inward arrows around collapse doline indicate a vertical drop. Black dot noted as Aslin Site 12/Site 07 marks the position of where the fossil material described in this study was found. Thick black lines mark the walls of the cave. Light grey outlines mark the presence of rocks and boulders. The well shaft affords entry from the surface to the underground lake.

### **Green Waterhole Cave**

Green Waterhole Cave, also known by the name Fossil Cave and the Cave register numbers 5L81 and S123 of the Cave Exploration Group of South Australia (Inc.), Adelaide, is located in the Tantanoola district approximately 24 km northwest from Mt Gambier in SA. Like the Naracoorte Caves, those in the Gambier region are formed within the Oligo-Miocene limestone shelf that is spread across south-east South Australia (Boutakoff 1963). Unlike the Naracoorte Caves, which are mostly dry, caves in the Gambier region are largely below the water table, with Green Waterhole Cave being no exception. Green Waterhole Cave is assumed to have first been formed during the late Miocene (Pledge 1980). The fossils occurred on the floor of the chamber at depths of 1 to 9 metres.

The age of the fossils from Green Waterhole Cave has long been debated. Baird (1985) noted that recorded data on sea level transgressions indicated the cave entrance would have opened 125 Ka at most, and that the fauna indicated that it could be no younger than 15 Ka. This lower estimate was based off the findings of Horton (1984) indicating the Australian megafaunal extinction took place 26–15 Ka, which has since been revised to 50–40 Ka (Roberts et al. 2001; Gillespie et al. 2006; Saltré et al. 2016; Johnson et al. 2021). Fossils in the area about Site 7 were deposited in sediment with minimal terrigenous material and largely comprised of cave rafts, speleothems that form by crystallization on the surface of a water body, usually a pool. Their presence shows that a pool of water existed in the lower reaches of this chamber when the cave was largely drained of water during lower water tables. Many other fossils accumulated on the subaerial surface of the now drowned slopes in this entrance chamber. It is likely that this pool was a primary attractant to the very numerous birds that accumulated in it (Baird 1985). THW sent John Hellstrom, University of Melbourne, several samples of cave rafts collected in 2006 for U-series dating and five ages were obtained (Table 4.1) that reveal they formed in a narrow time interval 61.1–59.1 ka. Therefore, we consider that the birds and associated mammalian megafauna, including the accipitrid described herein, accumulated during the marine lowstand in MIS 4-3, probably mostly between 70–30 Ka when lower water tables will have enabled a discrete pool to exist in the lower parts of the main entrance chamber; the earlier MIS 5a, 5b had sea levels similar to the present and so the chamber will have then been below the water level then, as at present.

The fossil fauna from Green Waterhole Cave was first formally described by Pledge (1980), after multiple diving trips in the cave during the 1960s–1970s had yielded fossil bones and skeletons of extinct sthenurine and macropodine kangaroos. While the paper mostly focused on the kangaroo species present, Pledge noted the presence of many small bird bones. A formal survey of the cave was undertaken by the South Australian Underwater

Speleological Society Inc. over the course of 1987 to 1988. It was determined that the cave was approximately 70 metres long overall, 30 metres wide at the lowest chamber, and observed depths of over 15 metres at certain points (Horne 1988; Newton 1988). There are minimally 23 bird species listed from Green Waterhole Cave, which includes accipitrids (Baird 1985; Baird et al. 1991; Reed and Bourne 2000). Currently, more than 958 lots (most passerines remain unidentified) are registered in SA Museum.

#### *Accipitrids from Green Waterhole Cave*

The presence of bones of a large accipitrid has been noted from this site for nearly four decades (Rich and van Tets 1982; Baird 1985; Baird 1991; Baird et al. 1991; Reed and Bourne 2000; Gaff 2002). The first accipitrid fossils were recovered from Green Waterhole Cave in 1979 and 1987 by dives initiated by Rod Wells of Flinders university, and included paired sets of carpometacarpi, ulnae and radii, a scapula, os metatarsale I, and a thoracic vertebra (Baird 1985; Newton 1988). Most were collected from 'Site 7' or close to it, see Figure 4.2. An almost complete right coracoid, missing only the omal end, was later uncovered on an expedition led by TH Worthy and A Camens with Horne, Skinner, Albano, Nielsen and Lewis as divers in 2006, 2 m upslope of Aslin Site 12 tag, which is equivalent to Site 7. The radii, ulnae and carpometacarpi were observed by Gaff (2002) and interpreted as belonging to a large species of Perninae.

Sample ID	Lab number	Sample Mass/g	238 ng/g ± 2SE	238/V	230/238 A ± 95%	234/238 A ± 95%	Age/Ka ± 95%	232/238 A ± SE	230/232 i ± 2SD	230/232 A	Age cr (Ka) ± 2SE	[4/8] i Corr ± 2SE	Age CR/Age	Age Ka 1950 ± 95%
Site 2L81.1	UMA015 63 Mar-2007	0.0350	313±24	5.45	0.5334 ±0.0038	1.1907 ±0.0026	63.43 ±0.597	0.033 ± 0.0003	150 ±150	16.1	59.1± 4.6	1.225± 0.0041	93%	59.0± 4.6
Site 2L81.2	UMA015 64 Mar-2007	0.1124	286±21	4.36	0.5375 ±0.0064	1.1867 ±0.0056	64.38 ±1.021	0.035 ± 0.0013	150 ±150	15.2	59.7± 5.1	1.221± 0.0071	92%	59.7± 5.0
Site 2L81.3	UMA016 80 Jul-2007	0.0454	311±23	7.48	0.5469 ±0.0055	1.1900 ±0.0027	65.64 ±0.871	0.035 ± 0.0003	150 ±150	15.8	61.1± 5.0	1.226± 0.0044	93%	61.0± 4.9
Site 2L81.4	UMA016 81 Jul-2007	0.0651	341±26	8.41	0.5446 ±0.0023	1.1895 ±0.0022	65.30 ±0.380	0.036 ± 0.002	150 ±150	15.2	60.6± 5.0	1.225± 0.0041	92%	60.5± 5.0
Site 2L81.5	UMA016 82 Jul-2007	0.0386	314±24	6.02	0.5389 ±0.0017	1.1941 ±0.0029	64.04 ±0.307	0.033 ± 0.0002	150 ±150	16.1	59.7± 4.7	1.230± 0.0045	93%	59.6± 4.7

**Table 4.1:** U-series dating age estimates on five calcite raft samples from near Site 7, in Green Waterhole Cave. Analyses performed by John Hellstrom, University of Melbourne.

### ***Leaena's Breath Cave***

Leaena's (= Leana's) Breath Cave is a 73 m long limestone karst cave located in the Nullarbor Plains of WA and is part of a collective of caves known as the Thylacoleo Caves (Prideaux et al. 2007b). The cave is minimally 4 million years old based on U-PB geochronology techniques on speleothems (Woodhead et al. 2006). Leaena's Breath Cave along with other caves in the Thylacoleo Caves assemblage has yielded fossils of remarkable quality, including complete skeletons (Prideaux et al. 2007b). The age of these fossils based on optical dating, U-Th dating and palaeomagnetic dating is thought to range between 400–200 Ka for specimens in the upper levels of the excavation, to 780–400 Ka for specimens in the deepest part of the excavation (Prideaux et al. 2007b).

Accipitrid materials included in this study from this site are a sternal part of coracoid and the synsacrum of a pelvis. The coracoid was identified as an indeterminate accipitrid by E. Shute (2018).

### ***Wellington Caves***

The Wellington Caves are located in central-western NSW, 7 km south of the town Wellington, and the fossiliferous deposits within the complex are believed to have formed between the Pliocene and late Pleistocene (Dawson and Augee 1997; Dawson et al. 1999; Megirian et al. 2010). Cathedral Cave is the largest of these caves and has yielded many fossils of great significance, most of them from the Cathedral Chamber and Well Chamber (Dawson 1985; Dawson and Augee 1997; Prideaux et al. 2007a). This material is mostly mid- to late Pleistocene in age. An estimated 7–10 m of fossil-bearing sediment covers the floors of the Cathedral and Well Chambers (Osborne 1991). Fossils have also been found at other caves in this complex, most notably Bone Cave, Phosphate Mine and Mitchell's Cave which all have produced Pleistocene material that is likely somewhat older than in Cathedral Cave, perhaps mid-early Pleistocene in age (Dawson 1985; Osborne 1991; Osborne 1997). There are also Pliocene deposits from the site known as Big Sink in this complex (Dawson et al. 1999; Fusco 2021). The fossils from Cathedral Cave have provided valuable in determining faunal responses to climatic change (Fusco 2021).

The 'Old collections' of Wellington Caves include fossil material that was excavated during the 19<sup>th</sup> and 20<sup>th</sup> century and accumulated by the NSW Department of Mines, who oversaw the caves at the time. These specimens do not have their provenance and stratigraphic data well documented, and so the age of many of these fossils cannot be established beyond being from the Pleistocene.

While numerous authors have attempted dating the stratigraphy of the Wellington Caves assemblages (see Dawson and Augee 1997), many of these dates are now regarded as problematic and are currently under revision (Fusco 2021). The age of the fossils from the

Wellington Caves deposits are therefore largely inferred based on biochronological comparisons with other sites (e.g., Megirian et al. 2010).

Accipitrid materials from the Wellington Caves included in this study are a distal ulna, a partial carpometacarpus and a distal tibiotarsus. Two unguis phalanges are also known from this site, AM F.129563 and AM F.129564, but cannot be referred to any one species due to the presence of multiple large accipitrids known from this site including *Aquila audax* (distal ulna ID 4879), "*Taphaetus*" *lacertosus* (distal humeri AM F.58092, tarsometatarsus AM F.58093), and nov. gen. et sp. (right carpometacarpus AM F.152515). The tibiotarsus, unguis phalanges and the ulna are from the Old Collections, making their precise site of origin unknown. The carpometacarpus is from Cathedral Cave and is believed to be late Pleistocene in age (see Fusco 2021). The tibiotarsus had been previously noted by Gaff (2002).

### **Cooper Creek**

Cooper Creek is a river system within the Lake Eyre Basin spanning 1520 km in length and with a catchment area of up to 306 000 km<sup>2</sup> (Coleman 2002), originating in south-west Queensland. Numerous fossil sites are present along its banks, many of Pleistocene age. One such site, Waralamanko Waterhole, is located within South Australia, the fossils from which are estimated to be middle to late Pleistocene based on biocorrelation with other sites (Tedford and Wells 1990; Couzens and Prideaux 2018).

A distal tibiotarsus was collected from the Waralamanko Waterhole site at Cooper Creek and catalogued into the SA Museum collections and was studied by Gaff (2002) whom included images of it. This specimen could not be located at the time of writing, so these images were the only means of assessing the fossil.

#### **4.2.8 Aims and Assumptions**

We argue that the material from Victoria Fossil Cave and Green Waterhole Cave represent one unknown accipitrid species, as the same wing elements (ulna, carpometacarpus) occur in both sites, allowing direct comparison. Moreover, only a single individual is represented at Green Waterhole. At least two individuals are present in Victoria Fossil Cave (based on femora). Minimally, only one species is represented by these specimens and so we follow the parsimonious approach of referring the pelvic girdle elements found in Victoria Fossil cave to the same taxon as that represented by the wing bones. We also assume that the material from Mairs Cave represents a separate taxon on the basis that the humerus from this site differs substantially from that in Victoria Fossil Cave.

Here we describe these taxa and establish their relationships among accipitrids. Comparisons specifically include the fossil taxa "*Taphaetus*" *lacertosus* (a sympatric and contemporary similar-sized species) and the New Zealand *Hieraaetus moorei*, the gigantic extinct

eagle formerly known as *Harpagornis moorei*, from New Zealand, because of its similarly relatively robust pelvic elements.

## 4.3 RESULTS

### 4.3.1 Systematic palaeontology

**Class Aves Linnaeus, 1758**

**Order Accipitriformes Vieillot, 1816**

**Family Accipitridae Vigors, 1824**

**Accipitrid GWC/VFC Gen. et Sp. nov. (Figs. 1–5)**

**Holotype:** SAMA P.41517 (=FU 1141) left humerus missing only tuberculum ventrale (Fig. 1).

**Diagnosis:** A large accipitrid with short stout wing bones and very large and robust leg bones that exhibits the following unique combination of characters: Quadrate with (1) the processus orbitalis having a deepened sulcus on its medial facies; (2) The base of the processus orbitalis lacking either a foramen basiorbitale or a foramen rostromediale; (3) A prominent medially projecting condylus pterygoideus with greater extent than the condylus medialis. Scapula with (4) a large, pneumatic fossa present in the base of the acromion visible in cranial view; (5) The corpus strongly curving ventrally towards the caudal end. Coracoid with (6) the processus procoracoideus angling distally relative to the cotyla scapularis. Humerus with (7) a deep m. scapulohumeralis cranialis and (8) a markedly sigmoid curvature to the shaft. Pelvis with (9) a large, deep anterior fossa renalis. Femur with (10) the ligamental attachment scar proximal to the fossa poplitea circular in shape and positioned centrally in the shaft; and an os metatarsale I with (11) a largely straight profile of the lateral margin.

**Etymology:** to be determined with naming of species.

**Type locality/stratigraphy:** excavation co-ordinates (decimal feet) 64.5–67, R9–10, D/D -0.5 to -1.0, Main Fossil Chamber, Victoria Fossil Cave, Naracoorte, South Australia.

**Age of Holotype:** Early-Middle Pleistocene.

**Measurements (mm):** Total length 178.3, proximal width [tuberculum dorsale – crista bicipitalis] 37.1, width fossa pneumotricipitalis 11.7, length crista deltopectoralis from tuberculum dorsale 59.2, least shaft width 18.7, maximum distal width 33.3, condylus dorsalis width 9.3, condylus

dorsalis depth 19.4, condylus ventralis width 14.8, condylus ventralis depth 10.7, tuberculum supracondylaris ventralis to processus flexorius depth 15.0.

### **Paratypes:**

#### ***Victoria Fossil Cave, South Australia***

SAMA P.59030, complete right quadrate (62.75'–64.75', R13.5–15.5, D/D -2.0 to -2.5); SAMA P.59029, complete left ulna (-7' to -3', R5.5–7.5, D/D -1.72 to -1.97); SAMA P.41515, right carpometacarpus missing distal end and most of os metacarpale minus (57'–60.5', R12–13, D/D -1.75 to -2.75); SAMA P.41516, partial pelvis preserving synsacrum and most of right lateral side (57.5'–62.5', R13–14.5, D/D -0.5 to -1.0); SAMA P.41514, complete right femur (57.5'–60', R14–15, D/D -1.0 to -1.5); SAMA P.41513, complete right femur (56.5'–58.5', R1–2, D/D -0.5 to -1.0); SAMA P.28008, distal right tarsometatarsus preserving trochleae metatarsorum II and III (60.5'–62.5', R1–2, D/D -0.5 to -1.0). Seven specimens, MNI = 2. All can be attributed to the upper part of Unit 7 as defined by Reed (2003) Fig 6.3O.

Stratigraphy, age and locality as per Holotype.

#### ***Green Waterhole Cave, South Australia***

SAMA P.24329 fragmented thoracic vertebra; SAMA P.53845 near complete right scapula, with only the distal end worn away; SAMA P.42487 almost complete right coracoid with only the facies articularis clavicularis, processus acrocoracoideus and processus lateralis worn away; SAMA P.24324 complete right ulna; SAMA P.24323 complete left ulna; SAMA P.24326 complete right radius; SAMA P.24325 complete left radius; SAMA P.24328 complete right carpometacarpus; SAMA P.24327 complete left carpometacarpus; SAMA P.53845 complete os metatarsale I.

We argue that the fossil material represents a single individual on the following evidence: (1) A lack of duplicated elements; (2) that left and right sides are identical in all aspects; (3) the close proximity in which all fossil material was found; and (4) the size of all elements being within an appropriate range for a single skeleton.

**Locality:** All from Site 7, Green Waterhole/Fossil Cave, 37° 43.91'S; 140° 31.86'E. Tantanoola district, South Australia, Australia, except SAMA P.53845 from the area encompassed by the grid C5-C6/N5-N6 (Figure 4.2).

**Stratigraphy and Age:** See Table 4.1.

***Leaena's Breath Cave, Western Australia***

WAM 15.9.72 right coracoid missing omal end.

**Locality:** Leaena's Breath Cave, Nullarbor, WA, Australia, 31.4°S 128.1°E.

**Stratigraphy/Age:** Pit B, Quadrat 5, 100–105 cm depth, Early Pleistocene; collected by G. Prideaux et al. 2013, identified by E. Shute (2018).

**Referred Material**

***Wellington Caves, New South Wales***

AM F.129566 distal left ulna; AM F.152515 right carpometacarpus; AM F.106562 distal right tibiotarsus.

Locality: Old collections, Wellington Caves (tibiotarsus, ulna); Cathedral Cave, Wellington Caves (carpometacarpus collected by D. Fusco February 2017).

Stratigraphy/Age: Cathedral Cave, Flinders University excavation, quadrant II, layer 13, column 2 495–500 mm (see Fusco 2021) (carpometacarpus).

***Cooper Creek, South Australia***

SAMA P25218 [one of two bones catalogued under this number], distal right tibiotarsus, see Gaff (2002, Plate 5.1, O, Plate 5.2, C).

Locality: Waralamanko Waterhole, Cooper Creek, South Australia (Tedford and Wells 1990).

Stratigraphy/Age: late Pleistocene.

**Measurements (mm):** See Table 4.2.

Cat No	Element	Total L	PW	SW	DW
<b>Green Waterhole Cave</b>					
SAMA P.24323	Ulna (L)	208.0	22.2	9.5	20.0
SAMA P.24324	Ulna (R)	208.8	22.7	9.6	19.9
SAMA P.24325	Radius (L)	196.6	10.9	6.5	15.3
SAMA P.24326	Radius (R)	195.2	9.1	6.5	15.3
SAMA P.24327	Cmc (L)	108.4	26.1	-	17.0
SAMA P.24328	Cmc (R)	108.7	26.1	-	16.5
<b>Victoria Fossil Cave</b>					
SAMA P.41517	Hum (L)	178.3	37.1	18.7	33.3
SAMA P.59029	Ulna (L)	195.4	21.4	9.7	15.8
SAMA P.41514	Femur	145.5	38.3	20.5	35.2
SAMA P.41513	Femur	131.1	32.5	18.9	32.3
<b>Wellington Caves</b>					
AM F.106562	Tib (distal R)	NA	NA	16.6	28.1
AM F.129566	Ulna (distal L)	NA	NA	10.5	20.5

**Table 4.2:** Key measurements (mm) of limb bone fossils from Green Waterhole Cave, Victoria Fossil Cave, and Wellington Caves. Abbreviations: Cmc, carpometacarpus; DW, distal width; Hum, humerus; L, length; PW, proximal width; SW, shaft width; Tib, tibiotarsus.

### Additional measurements.

**Green Waterhole Individual: Coracoid SAMA P.42487, right:** preserved omal-sternal length 73.0, preserved proximal height (cotyla scapularis to preserved processus acrocoracoideus) 33.8, facies articularis humeralis length 20.9, midshaft width 16.1, preserved sternal width 36.1; **Radius, left SAMA P.24325** proximal depth (dorsal aspect) 10.1; **Radius, right SAMA P.24326:** proximal depth 11.4; **Carpometacarpus, left SAMA P.24327:** distal width excluding facies articularis digitalis minor 11.5; **Carpometacarpus, right SAMA P.24328:** distal width excluding facies articularis digitalis minor 12.1; **Thoracic vertebra SAMA P.24329:** preserved height 33.9, preserved width 23.0, preserved length of centrum 21.7, cranial width of centrum 10.3, preserved cranial height of centrum 9.5, preserved caudal width of centrum 11.3, preserved caudal height centrum 12.6; **Os metatarsale I SAMA P.53845:** length 26.1, distal width 12.5.

**Victoria Fossil Cave: Quadrate SAMA P.59030:** height 21.3, mediolateral width across condyles 15.5; **Pelvis SAMA P.41516:** length synsacrum 104.7; **Femur (P.41514):** preserved proximal depth 31.4, least shaft circumference 69, distal width 39.8 (with lateral projection), width condylus medialis 18.7, height condylus medialis 22.5, depth condylus medialis 29.3, width condylus lateralis 17.8, height condylus lateralis 22.4, depth condylus lateralis 34.8; **Femur (P.41513):** preserved proximal depth 23.8, least shaft circumference 59, distal width 35.8 (with lateral projection), width condylus medialis 17.1, height condylus medialis 19.2, depth condylus medialis 25.5, width condylus lateralis 13.1, height condylus lateralis 19.0, depth condylus lateralis 31.3; **Tarsometatarsus SAMA P.28008:** width trochlea metatarsi II 8.8, depth trochlea metatarsi II 12.4, width trochlea metatarsi III 9.9, depth trochlea metatarsi III 14.8.

**Wellington Cave: Tibiotarsus AM F.106562:** preserved length 97.8, least shaft circumference 53.0, least shaft width 14.6, distal width 27.8, craniocaudal depth of condyles 16.3 (preserved).

**Leaena's Breath Cave: Coracoid WAM 15.9.72:** preserved length 52.9, midshaft width 15.4, preserved sternal width 32.9.

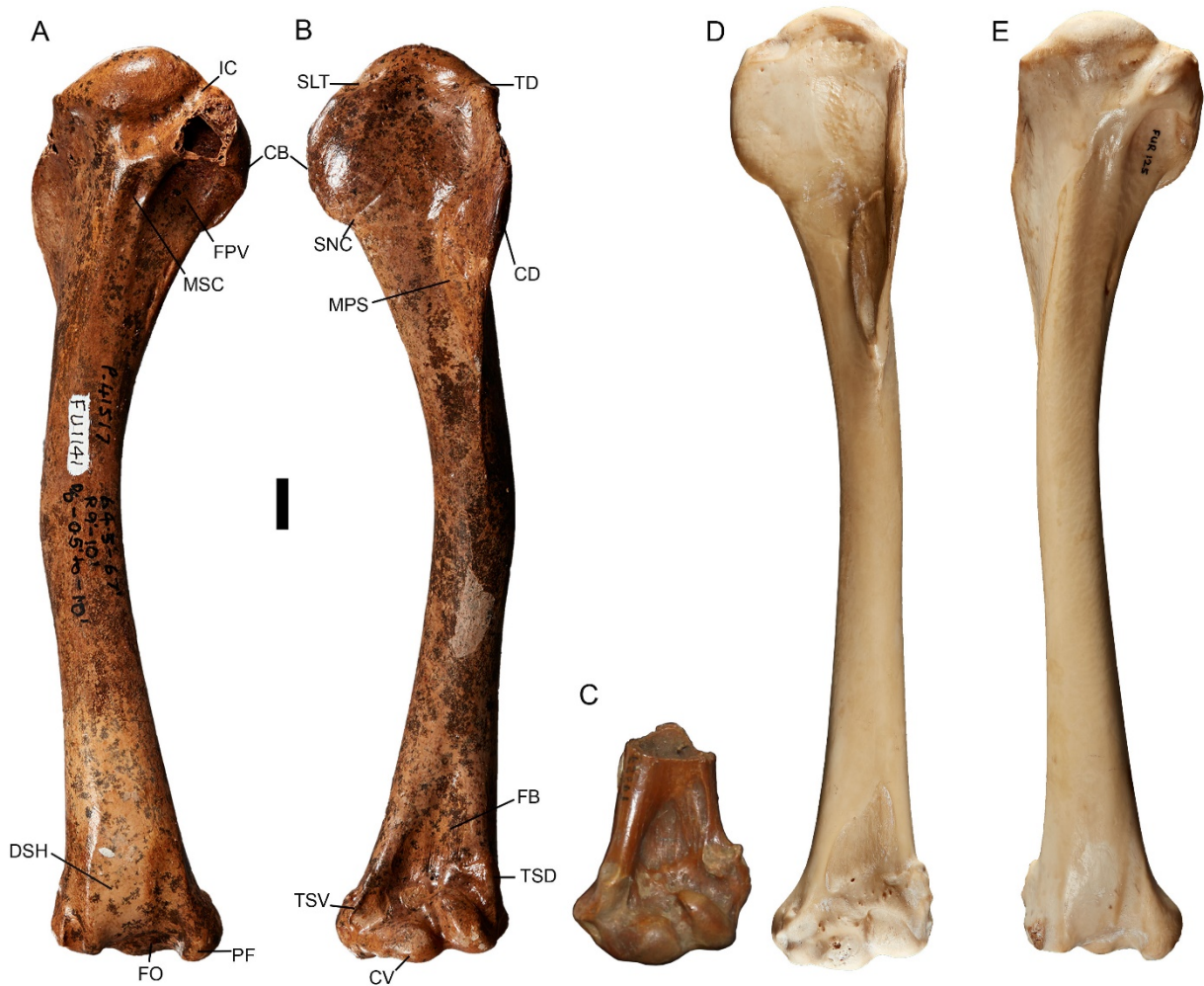


**Figure 4.3:** Holotype humerus SAMA P.41517 in caudal (A) and cranial (B) view, “*Taphaetus*” *lacertosus* lectotype distal humerus QM F5507 in cranial view (C), and *Aquila audax* FUR 125 humerus in cranial (D) and caudal (E) view. Abbreviations: CB, crista bicipitalis; CD, crista deltopectoralis; CV, condylus ventralis; DSH, dorsal sulcus humerotricipitalis; FB, fossa brachialis; FO, fossa olecrani; FPV, fossa pneumaticum ventralis; IC, incisura capitis; MPS, m. pectoralis scar; MSC, insertion of m. scapulohumeralis cranialis; PF, processus flexorius; SLT, sulcus lig. transversus; SNC, sulcus nervi coracobrachialis; TD, tuberculum dorsalis; TSD, tuberculum supracondylare dorsale; TSV, tuberculum supracondylare ventrale. Scale bar 10 mm.

## Description and comparisons of accipitrid GWC/VFC.

### *Humerus (Figure 4.3A, B).*

A near-perfect right humerus is lacking only the tuberculum ventrale. It is roughly comparable in length to that of a female *Aquila audax* and based on the dimorphism indicated by the fossil femora (see below), this suggests the fossil belongs to an individual of the smaller sex (most likely a male). Description is as follows:

The humerus is quite robust for its length (see Table 4.3).

(1) The tuberculum dorsale (Figure 4.3B: TD) is proximodistally aligned/level with the sulcus lig. transversus (Figure 4.3B: SLT) in cranial view. (2) The sulcus lig. transversus is deep. (3) The intumescencia humeri is inflated into a slight mound. (4) The margin of the fossa pneumotricipitalis ventralis (Figure 4.3A: FPV) forms a broad semi-circle. (5) The insertion of the m. scapulohumeralis cranialis (Figure 4.3A: MSC) is deep. (6) The attachment scar for the m. scapulohumeralis caudalis is not prominent and forms a broad scar on the ventral rim of the crista bicipitalis. (7) The incisura capitis (Figure 4.3A: IC) is shallow relative to the caput (tuberculum ventrale is broken so depth relative to it not assessable). (8) The insertion scar at the base dorsally of the incisura capitis is round and very faint. (9) The angulus deltopectoralis of the crista deltopectoralis (Figure 4.3B: CD) is roughly level with the distal margin of the crista bicipitalis (Figure 4.3A, B: CB). (10) The dorsal margin of the section of the crista deltopectoralis proximal to the angulus is flat. (11) The angulus deltopectoralis forms a rounded angle (~100°) in ventral view. (12) The distal termination of the crista is positioned within the shaft adjacent to the margin, allowing the shaft margin to be visible alongside it, (13) and is flat as it merges with the shaft in ventral view. (14) In cranial view, the crista prominently projects dorsally from the shaft, distinctly further than the tuberculum dorsale. (15) A sulcus is present on the proximal caudal face of the crista deltopectoralis. (16) In cranial view, the insertion scar for the m. pectoralis (Figure 4.3B: MPS) is robust and extends proximally to level with the distal base of the crista bicipitalis. (17) The crista bicipitalis forms a distinct distoventrally convex flange distally. (18) A faint sulcus nervus coracobrachialis (Figure 4.3B: SNC) is present extending proximodorsally from the distal margin of the crista bicipitalis. (19) The shaft is markedly sigmoid in its curvature. (20) The scar for m. latissimus dorsi forms a distinct line caudally on the shaft. (21) The processus flexorius (Figure 4.3A: PF) does not protrude caudally in ventral view. (22) In cranial view, the processus flexorius and condylus ventralis (Figure 4.3B: CV) are roughly equal in distal extent. (23) Distally, the processus flexorius is rounded. (24) The insertion scar for the pronator superficialis is large and deep and close to the ventrocranial margin of the tuberculum supracondylare ventralis. (25) The tuberculum supracondylare dorsale (Figure 4.3B: TSD) lacks dorsal projection but is slightly prominent cranially. (26) The fossa olecrani (Figure 4.3A: FO) is broad. (27) The fossa m. brachialis (Figure 4.3B: FB) is deep, (28) and non-pneumatic. (29) The dorsal margin of this fossa is broadly separated from the ventral shaft margin by a distance over a third of fossa width. (30) The palmar scar for the m. extensor carpi radialis is a shallow oval/line, while the dorsal scar is a large, shallow circle. (31) There are two shallow insertion scars for the m. flexor carpi ulnaris. (32) The tuberculum supracondylare ventrale (Figure 4.3B: TSV) is aligned proximodorsally across the shaft. (33) The proximoventral margin of the tuberculum supracondylare ventrale is sharply prominent cranially. (34) The dorsal sulcus for the m. humerotricipitalis is broad, spanning roughly half the dorsoventral shaft width beside it and is twice as wide as its ventral counterpart.

Extant accipitrids differ as follows (intraspecifically variable characters excluded):

The fossil species differs from all species of Elaninae and Accipitrinae by its much larger size. All accipitrines also have relatively elongate and narrow wing and leg bones.

#### Perninae.

**Nine characters differ for all pernines:** (4) The margin of the fossa pneumotricipitalis ventralis is shaped as a narrow half-oval. (5) The insertion for the m. scapulohumeralis cranialis is shallow. (6) The attachment scar for the m. scapulohumeralis caudalis is indistinct. (9) The angulus deltopectoralis of the crista deltopectoralis is distal to the crista bicipitalis. (14) The crista has roughly equal dorsal projection with the tuberculum dorsale in cranial view. (19) The shaft has little to no curvature. (20) The scar for m. latissimus dorsi is faint. (25) There is a weakly projecting tuberculum supracondylare dorsale. (29) The dorsal margin of fossa brachialis is more narrowly separated from the ventral shaft margin (distance less than a quarter of the fossa width).

**12 characters differ variably among pernines:** (3) The intumescencia humeri is inflated similar to the fossil in all species except *Lophoictinia isura* and *Hamirostra melanosternon*, where it is flat. (10) The dorsal margin of the crista deltopectoralis proximal to the angulus is flat in all species except *Chondrohierax uncinatus*, where it is concave. (11) The angulus deltopectoralis is distinctly angular in all species except *H. melanosternon* and *L. isura*, where it is rounded. (16) The insertion scar for the m. pectoralis ends distal to the base of the crista bicipitalis in all species except *H. melanosternon* and *C. uncinatus*, where it extends level to the distal margin of the crista bicipitalis. (17) The ventrodiscal margin of crista bicipitalis is unflared in all species except *H. melanosternon* and *L. isura*. (23) The distal end of the processus flexorius is flattened in all species except *L. isura*, where it is rounded. (24) The insertion scar for the pronator superficialis is shallow and close to the ventrocranial margin in all species except *H. melanosternon*, where it is deep. (26) The fossa olecrani is shallow in all species except *H. melanosternon* and *L. isura*, where it is deep. (31) The insertion scars are shallow in all species except *H. melanosternon* and *P. apivorus*, where they are deep. (32) The facet of the tuberculum supracondylare is angled across the shaft in all species except *Elanoides forficatus*, where it is nearly parallel to the shaft. (34) The dorsal sulcus m. humerotricipitalis is narrow, about a third of the shaft width in *H. melanosternon*, *L. isura*, and *E. forficatus*, and broad in *C. uncinatus* and *P. apivorus*, about half the shaft width.

#### Gypaetinae.

**Ten characters differ for all gypaetines:** (2) The sulcus lig. transversus is shallow. (3) The intumescencia humeri is flattened. (7) The incisura capitis is deep. (9) The angulus deltopectoralis of the crista deltopectoralis is distal to the crista bicipitalis. (14) The crista has equal dorsal extent with the tuberculum dorsale. (19) The shaft is weakly sigmoid. (22) In cranial view, the condylus ventralis extends further distally than the processus flexorius. (24) The insertion scar for the pronator superficialis is shallow. (31) The insertion scars for the m. flexor carpi ulnaris are

deep. **(33)** The tuberculum supracondylare ventrale is flattened cranially, lacking a prominent proximoventral rim.

**Four characters differ variably for all gypaetines:** **(1)** The tuberculum dorsale is distal to the sulcus lig. transversus in all species except *Polyboroides typus*, which is positioned level with it. **(5)** The insertion for the m. scapulohumeralis cranialis is shallow in all species except *P. typus*, where it is deep. **(16)** The insertion scar for the m. pectoralis terminates distal to the crista bicipitalis in all species except *P. typus*, where it extends to level with the crista. **(34)** The dorsal sulcus of m. humerotricipitalis is narrow in *N. percnopterus* and *G. barbatus* and broad in *P. typus*, and *G. angolensis*.

#### Aegyptiinae.

**12 characters differ for all aegyptiines:** **(2)** The sulcus lig. transversus is shallow. **(3)** The intumescentia humeri is flattened. **(5)** The insertion for the m. scapulohumeralis cranialis is shallow. **(16)** The m. pectoralis scar terminates well distal of the crista bicipitalis. **(19)** The shaft is weakly sigmoid in its curvature. **(22)** In cranial view, the condylus ventralis extends further distally than the processus flexorius. **(24)** The insertion scar for the pronator superficialis is small. **(29)** The dorsal margin of the fossa brachialis is more narrowly separated from the shaft by a distance ranging from less than a third to less than a quarter of the fossa width in all species. **(31)** There are three insertion scars for the m. flexor carpi ulnare, with the cranial-most scar being deep and the others shallow. **(32)** The angle of the interior margin of the tuberculum supracondylare ventrale is aligned almost parallel to the shaft margin. **(33)** The proximoventral margin of the tuberculum supracondylare ventrale is flattened cranially. **(34)** The dorsal sulcus of m. humerotricipitalis is narrow, roughly a third of the shaft width or less.

**Two characters differ variably for all aegyptiines:** **(12)** The distal termination of the crista is directly on the shaft margin in all species except those in *Gyps* and *Aegyptius*, which are positioned within the shaft. **(14)** The crista extends slightly further dorsally than the tuberculum dorsale in *Gyps* and *Necrosyrtes*, and distinctly further in *Aegyptius*.

#### Circaetinae.

**Ten characters differ for all circaetines:** **(2)** The sulcus lig. transversus is shallow. **(3)** The intumescentia humeri is flattened. **(4)** The margin of the fossa pneumotricipitalis ventralis forms a broad semi-circle. **(5)** The insertion for the m. scapulohumeralis cranialis is shallow. **(6)** The attachment scar for the m. scapulohumeralis caudalis is prominent. **(7)** The incisura capitis is deep. **(14)** The crista has equal dorsal extent with the tuberculum dorsale. **(19)** The shaft is slightly sigmoid. **(30)** The dorsal palmar scar is a small, shallow circle. **(31)** There are two insertion scars for the m. flexor carpi ulnaris, with the cranial insertion deep and the caudal insertion shallow.

**Seven characters differ variably for all circaetines:** (1) The tuberculum dorsale is roughly aligned with the sulcus lig. transversus in *Terathopius ecaudatus* and is distal to it in *Spilornis cheela*. (8) The insertion scar dorsally at the base of the incisura capitis is prominent in *T. ecaudatus* and faint in *S. cheela*. (12) The distal termination of the crista positioned within the shaft in *S. cheela* and on the shaft margin in *T. ecaudatus*. (13) The distal termination of the crista is flat against the shaft in *S. cheela* and angled in *T. ecaudatus*. (17) The crista bicipitalis has a distinct distoventrally convex flange at its distal base in *S. cheela* and lacks a flange in *T. ecaudatus*. (25) The tuberculum supracondylare dorsale has weak (*S. cheela*) to strong (*T. ecaudatus*) dorsal projection. (29) The dorsal margin of the fossa brachialis is more narrowly separated from the ventral shaft margin (~a third of fossa width in *S. cheela* and less than a quarter in *T. ecaudatus*).

#### Aquilinae.

**Seven characters differ for all aquilines:** (1) The tuberculum dorsale is distal to the sulcus lig. transversus. (2) The sulcus lig. transversus is shallow. (3) The intumescencia humeri is flattened. (4) The margin of the fossa pneumotricipitalis ventralis forms a narrow half-oval. (5) The insertion for the m. scapulohumeralis cranialis is shallow. (13) The distal termination of the crista is angled as it merges with the shaft in ventral view. (14) The crista is marginally more dorsally projecting than the tuberculum dorsale.

**Eight characters differ variably for all aquilines:** (6) The attachment scar for the m. scapulohumeralis caudalis is prominent in *Aquila* and *Hieraaetus* and flattened in *Spizaetus*. (7) The incisura capitis is shallow in *Aquila* and *Hieraaetus*, and deep in *Spizaetus*. (10) The dorsal margin of the section of the crista deltopectoralis proximal to the angulus is flat in *Aquila* and *Hieraaetus*, and concave in *Spizaetus*. (11) The angulus deltopectoralis forms a broad angle in *Aquila* and *Hieraaetus*, and sharply angled in *Spizaetus*. (17) The crista bicipitalis has a distinct distoventrally convex flange at its distal base in *Aquila* and *Hieraaetus* and is flattened in *Spizaetus*. (19) The shaft is markedly sigmoid in *Spizaetus* and is slightly sigmoid in *Aquila* and *Hieraaetus*. (25) The tuberculum supracondylare dorsale has moderate dorsal projection in all species except *Spizaetus*, which is flattened; (29) The dorsal margin of fossa brachialis is more narrowly separated from the shaft (~a third of the fossa width in *Spizaetus*, and less than a quarter of the width in *Hieraaetus* and *Aquila*).

#### Haliaeetinae.

**Nine characters differ for all haliaeetines:** (5) The insertion for the m. scapulohumeralis cranialis is shallow. (12) The distal termination of the crista is positioned within the shaft. (14) The crista is marginally more dorsally projecting than the tuberculum dorsale. (16) The insertion scar for the m. pectoralis terminates proximally distal to the crista bicipitalis. (19) The shaft is almost entirely straight. (22) In cranial view, the processus flexorius extends further distal than the

condylus ventralis. **(24)** The insertion scar for the pronator superficialis is small. **(25)** The tuberculum supracondylare dorsale has a small degree of dorsal projection. **(31)** There are two deep insertion scars for the m. flexor carpi ulnaris.

**Nine characters differ variably for all haliaeetines:** **(3)** The intumescencia humeri is flattened in all species except *Haliaeetus albicilla* and *Haliaeetus leucocephalus*. **(4)** The fossa pneumotricipitalis ventralis is broad in *Haliaeetus* and narrow in *Milvus migrans* and *Haliastur*. **(6)** The attachment scar for the m. scapulohumeralis caudalis is prominent in *Haliaeetus* and flat in *M. migrans* and *Haliastur*. **(7)** The incisura capitis is shallow in *Haliaeetus* and deep in *Haliastur* and *M. milvus*. **(9)** The angulus deltopectoralis of the crista deltopectoralis is roughly level with the distal margin of the crista bicipitalis in *Haliaeetus* and is distal to it in *Haliastur* and *M. migrans*. **(13)** The distal termination of the crista forms an angle in ventral view in all species except *M. migrans*, where it is rounded. **(20)** The scar for m. latissimus dorsi forms a distinct line in *Haliaeetus* and is faint in *M. migrans* and *Haliastur*. **(23)** The distal end of the processus flexorius is flattened in *Haliaeetus* and *Haliastur* and rounded in *M. migrans*. **(34)** The dorsal sulcus m. humerotricipitalis is approximately a third of the shaft width in *H. sphenurus*, *H. indus* and *M. migrans* and half the shaft width in species of *Haliaeetus*.

#### Buteoninae.

**12 characters differ for all buteonines:** **(2)** The sulcus lig. transversus is shallow. **(3)** The intumescencia humeri is flattened. **(4)** The margin of fossa pneumotricipitalis ventralis forms a half-oval. **(7)** The incisura capitis is deep. **(9)** The angulus deltopectoralis of the crista deltopectoralis is distal to the crista bicipitalis. **(11)** The angulus deltopectoralis is acutely angular. **(12)** The distal termination of the crista is positioned on the shaft margin. **(20)** The scar for the m. latissimus dorsi is faint. **(22)** The processus flexorius extends further distal than the condylus ventralis. **(25)** The tuberculum supracondylare dorsale has weak dorsal projection. **(27)** The fossa m. brachialis is shallow. **(31)** There are two insertion scars for the m. flexor carpi ulnaris, which are deep.

**Six characters differ variably for all buteonines:** **(6)** The attachment scar for the m. scapulohumeralis caudalis is prominent in *Buteo* and flat in *Ictinia mississippiensis*. **(13)** The distal termination of the crista forms a distinct angle with the shaft in ventral view in all species except *Buteo rufofuscus*, where it is flattened. **(14)** The crista has equal dorsal extent with the tuberculum dorsale in *Ictinia* and extends slightly further dorsally in *Buteo*. **(19)** The shaft is slightly sigmoid in all species except *Buteo nitidus*, where it is strongly so. **(24)** The insertion scar for the pronator superficialis is shallow in *I. mississippiensis* and deep in *Buteo*. **(29)** The dorsal margin of the fossa brachialis is more narrowly separated from the shaft margin (a quarter of the fossa width in all species except *B. nitidus*, which is by a third).

### Summary.

In terms of the least number of differences, the fossil is most similar to species of Aquilinae, with only seven invariant characters (**1, 2, 3, 4, 5, 13, 14**) separating them. However, in terms of unique characters, the fossil shares characters **25** (lack of dorsally prominent tuberculum supracondylare dorsale) with Aegypiinae, Gypaetinae, and the aquiline *Spizaetus*, and **29** (broad separation of fossa brachialis from the ventral shaft margin) with Aegypiinae, Gypaetinae and Haliaeetinae, to the exclusion of all other taxa. Only gypaetines and aegypiines have this combination of character states for **25** and **29** shared with the fossil. Only aegypiines share a similar character state for **14** (dorsal extent of crista greater than tuberculum dorsale), suggesting that the fossil has more in common with the Aegypiinae, despite its other differences.

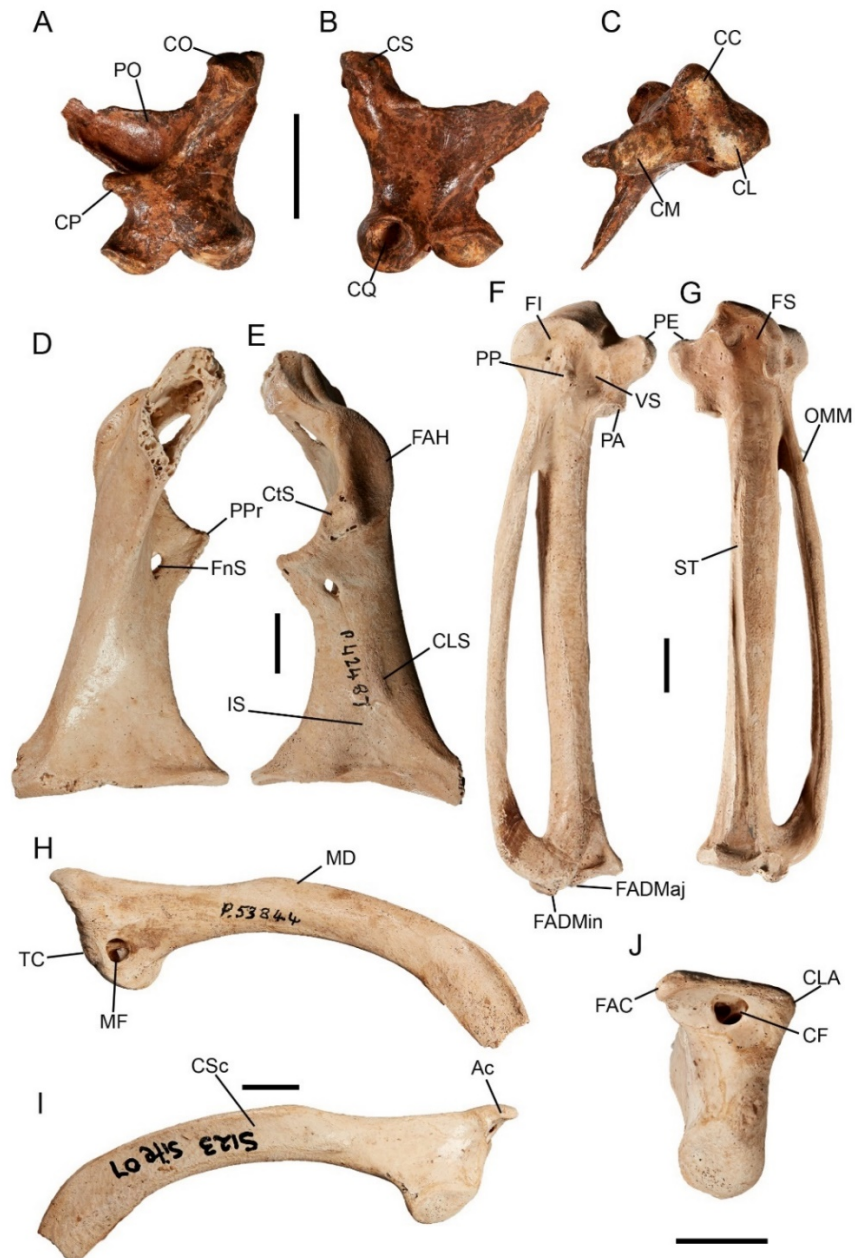


**Figure 4.4:** Accipitrid GWC/VFC quadrate SAMA P.59030 in medial (A), lateral (B) and ventral (C) view, coracoid SAMA P.42487 in ventral (D) and dorsal (E) view, carpometacarpus SAMA P.24327 in ventral (F) and dorsal (G) view, and scapula SAMA P.53845 in right lateral (H), left lateral (I) and cranial (J) view. Abbreviations: Ac, acromion; CC, condylus caudalis; CF, cranial fossa; CL, condylus lateralis; CLA, crista lig. acroracoroacromiali; CLS, coracobrachialis ligament attachment scar; CM, condylus medialis; CO, capitulum oticum; CP, condylus pterygoideus; CQ, cotyla quadratojugalis; CS, capitulum squamosum; CSc, capitulum scapulae; CtS, cotyla scapularis; FAC, facies articularis clavicularis; FADMaj, facies articularis digitalis major; FADMin, facies articularis digitalis minor; FAH, facies articularis humeralis; FI, fossa infratrochlearis; FnS, foramen n. supracoracoidei; FS, fossa supratrochlearis; IS, impressio m. supracoracoidei; MD, margo dorsalis; MF, medial fossa; OMM, os metacarpale minus; PA, processus alularis; PE, processus extensorius; PO, processus orbitalis; PP, processus pisiformis; PPr, processus procoracoideus; ST, sulcus tendineus; TC, tuberculum coracoideum; VS, ventral sulcus. Scale bars 10 mm.

### **Quadrate (Figure 4.4A–C).**

The right quadrate (SAMA P.59030) from Victoria Fossil Cave is almost completely intact, revealing all details of the processus oticus, cotylae and most of the processus orbitalis.

(1) The capitulum oticum (Figure 4.4A: CO) is twice as large as the capitulum squamosum (Figure 4.4B: CS). (2) There is no caudal foramen under the capitulum. (3) There is no foramen pneumaticum caudomediale. (4) There is no foramen pneumaticum basiorbitale. (5) There is no foramen rostromediale. (6) The condylus lateralis (Figure 4.4C: CL) is roughly twice the size of the condylus medialis (Figure 4.4C: CM). (7) The processus orbitalis has a deepened sulcus on its medial face. (8) The cotyla quadratojugalis (Figure 4.4B: CQ) takes up two thirds of the lateral face and is deep and fully enclosed. (9) The condylus pterygoideus (Figure 4.4A: CP) is very prominent medially (extends rostrally and medially past the condylus medialis) that is well separated dorsally from the condylus medialis.

Extant accipitrids differ as follows (intraspecifically variable characters excluded):

### Perninae.

**Three characters differ for all pernines:** (2) Caudal foramen present. (4) Foramen pneumaticum basiorbitale present. (7) The sulcus is absent on medial face of processus orbitalis.

**Four characters differ variably among pernines:** (1) The capitula are roughly equal in size in all species except *Pernis apivorus* (oticum twice as large as squamosum) and could not be assessed in *Elaenoides forficatus* and *Chondrohierax uncinatus*. (3) The foramen pneumaticum caudomediale is absent in all species except *P. apivorus*. (6) The condylus lateralis is equal in size to the condylus medialis in all species except *C. uncinatus*, where it is twice as large. (9) The condylus pterygoideus has no medial extent and is directly dorsally adjacent to the condylus medialis in all species except *Hamirostra melanosternon* and *Lophoictinia isura*, in which it is prominent and has equal medial extent to the condyle and is dorsally separated from it.

### Gypaetinae.

**Two characters differ for all gypaetines:** (4) Foramen pneumaticum basiorbitale present. (7) No sulcus on the processus orbitalis.

**Four characters differ variably among gypaetines:** (2) There is no caudal foramen under the capitulum in all species except *Neophron percnopterus*, where it is present. (6) The condylus lateralis is roughly twice the size of the condylus medialis in all species except *Gypaetus barbatus*, where they are roughly equal in size. (8) The cotyla quadratojugalis is roughly two thirds the size of the lateral face in all species except *N. percnopterus*, where it is half the size. (9) The condylus pterygoideus forms a very prominent medial protrusion (equal extent to condylus medialis) that is well separated in *N. percnopterus*, extends further than the condylus medialis and is directly dorsal to it in *P. typus*, and is non-projecting and indistinguishable in *G. angolensis*.

### Aegyptiinae.

**No characters differed for all aegyptiines.**

**Five characters differ variably among aegyptiines:** (1) The capitulum oticum is twice as large as the capitulum squamosum in all species except *Torgos tracheliotos*, where the capitula are roughly equal. (2) A caudal foramen is present under the capitulum in all species except *Sarcogyps calvus*, where it is absent. (4) Foramen pneumaticum basiorbitale absent in all species except *Necrosyrtes monachus*, *Trigonoceps occipitalis* and *S. calvus*. (7) Shallow sulcus present in species of *Gyps* and *Aegyptius monachus*, absent in *N. monachus*. (9) The condylus pterygoideus projects medially less than the condylus medialis in all species but extends dorsal to the condyle in species of *Gyps*, *A. monachus* and *N. monachus*.

### Circaetinae.

**Two characters differ for all circaetines:** (4) Foramen pneumaticum basiorbitale present. (7) No sulcus.

**One character differs variably among circaetines:** (9) The condylus pterygoideus forms a moderate protrusion with the same extent as the condylus medialis, which is directly dorsal to the condyle in *S. cheela* and well separated proximally in *T. ecaudatus*.

### Aquilinae.

**Four characters differ for all aquilines:** (4) Foramen pneumaticum basiorbitale present. (7) No sulcus. (8) The cotyla quadratojugalis is roughly half the size of the condylus lateralis face. (9) Condylus pterygoideus forms a moderate protrusion with less extent than the condylus medialis, which is positioned directly dorsal to it.

**Four characters differ variably among aquilines:** (1) Capitula are of equal size in species of *Aquila* and *Spizaetus*, capitulum oticum twice as large as squamosum in species of *Hieraaetus*. (2) Caudal foramen present in species of *Aquila*, absent in species of *Hieraaetus* and *Spizaetus*. (3) Foramen pneumaticum caudomediale absent in species of *Aquila*, *Hieraaetus moorei*, and *Hieraaetus morphnoides*, present in species of *Spizaetus* and *Hieraaetus fasciatus*. (6) The condylus lateralis et medialis are equal in size in species of *Aquila*, *H. morphnoides* and *H. moorei*, while in *H. fasciatus* and species of *Spizaetus* the lateral condylus lateralis is twice the size of the condylus medialis.

### Haliaeetinae.

**Three characters differ for all haliaeetines:** (1) Capitula are of equal size. (7) No sulcus on the processus orbitalis. (9) Condylus pterygoideus forms a prominent protrusion (equal extent to condylus medialis) that is directly dorsal to the condylus medialis.

**Five characters differ variable among haliaeetines:** (3) Foramen pneumaticum caudomediale absent in *Haliaeetus leucogaster*, *Haliaeetus albicilla*, *Haliastur sphenurus* and *Milvus migrans*, present in *Haliaeetus leucocephalus* and *Haliastur indus*. (4) Foramen pneumaticum basiorbitale present in all species except *H. leucocephalus* (possible intraspecific variation). (5) Foramen rostromediale present in all species except *H. albicilla*, *H. sphenurus* and *M. migrans*. (6) The condylus lateralis is roughly twice the size of the condylus medialis in all species except *M. migrans*, where they are equally sized. (8) The cotyla quadratojugalis is roughly half the size of the lateral face in species of *Haliaeetus*, and two-thirds the size in species of *Haliastur* and *M. migrans*.

#### Buteoninae.

**Four characters differ for all buteonines:** (4) Foramen pneumaticum basiorbitale present. (6) The condylus lateralis et medialis are roughly equal in size. (7) No sulcus on the processus orbitalis. (8) The cotyla quadratojugalis is roughly half the size of the lateral face.

**One character differs variably among buteonines:** (9) Condylus pterygoideus is directly proximal to the condylus medialis and has equal extent, forming a weak protrusion in *Ictinia mississippiensis* and a moderate protrusion in *Buteo*.

#### Summary.

In terms of least number of exclusionary differences, the fossil is most similar to the Aegypiinae, as there are no characters that consistently differ between it and all aegypiine species. However, it is also supported as an aegypiine by similarities in character 4 (lack of foramen pneumaticum basiorbitale) and character 7 (presence of a sulcus on the processus orbitalis), which only appear in this subfamily.

#### **Coracoid (Figure 4.4D, E).**

Two coracoids are available: one from the Green Waterhole Cave individual and one from Leaena's Breath Cave. These differ in no significant way from each other. The Green Waterhole coracoid is well preserved, lacking only the tip of the processus lateralis, the facies articularis clavicularis, and the ventral section of the processus acrocoracoideus.

(1) The foramen n. supracoracoidei (Figure 4.4D: FS) is set against the corpus of the shaft rather than adjacent to the margin of the processus procoracoideus and is positioned 7 mm distal to the cotyla scapularis. (2) The foramen has a medial pneumatic opening within it. (3) The sulcus m. supracoracoidei has a large pneumatic foramen dorsally within it that opens into the processus acrocoracoideus. (4) The facies articularis humeralis (Figure 4.4E: FAH) is roughly twice as long as it is wide. (5) The cotyla scapularis (Figure 4.4E: CtS) is small, being less than a quarter of the

width of the shaft, (6) and is shallow (7) and ellipsoidal (6 by 5 mm) in shape. (8) The omal margin of the processus procoracoideus (Figure 4.4D: PP) slopes sternomedially from the cotyla scapularis, (9) and has a short (8 mm) medial projection (10) with little to no curvature ventrally of the medial tip. (11) The coracobrachialis ligament attachment scar (Figure 4.4E: CLS) is positioned centrally in the shaft, (12) and is roughly triangular. (13) The impressio m. supracoracoidei (Figure 4.4E: IS) is extremely shallow. (14) The angulus medialis projects in a robust point that forms a 45° angle. (15) The facies articularis sternalis dorsalis forms a dorsally prominent flange over the medial third of its extent, which is broad and rounded. (16) The shaft is broad and robust for its length.

Extant Accipitridae differ as follows (intraspecifically variable characters excluded):

#### Perninae.

**No characters differ for all pernines.**

**Two characters differ variably among pernines:** (8) The processus procoracoideus weakly slopes sternally from the cotyla scapularis in all species except *Hamirostra melanosternon* and *Lophoictinia isura* (horizontal line). (15) The facies articularis sternalis dorsalis forms a dorsally prominent flange over the medial third of its extent, which is broad in all taxa except *Hamirostra* and *Chondrohierax* (narrow and projecting in a peak).

#### Gypaetinae.

**Three characters differ for all gypaetines:** (5) The cotyla scapularis is greater than a quarter of the width of the shaft. (6) The cotyla scapularis is deep. (8) The omal margin of the processus procoracoideus is oriented at a right angle to the shaft.

**Four characters differ variably among gypaetines:** (11) The coracobrachialis ligament attachment scar is positioned laterally on the shaft in all species except *Gypohierax angolensis*, where it is centrally positioned. (14) The angulus medialis forms a 45° angle in *N. percnopterus* and *P. typus*, and a 70–80° angle in *G. angolensis*. (15) The flange on the facies articularis sternalis dorsalis spans the medial third of the faces, and is broad and rounded in *Neophron* and *Polyboroides*, and a projecting peak in *Gypohierax*. (16) The shaft is broad and robust in *Gypohierax*, and slightly narrow and elongate in *Neophron* and *Polyboroides*.

#### Aegyptiinae.

**Two characters differ for all aegyptiines:** (8) The omal margin of the processus procoracoideus slightly slopes distomedially from the cotyla scapularis. (11) The coracobrachialis ligament attachment scar is positioned laterally on the shaft.

**Three characters differ variably among aegyptiines:** (3) The sulcus m. supracoracoidei has a foramen in all species except *Gyps coprotheres*, where it is absent. (14) The angulus

medialis projects in a 45° angle in species of *Gyps* and *Aegypius monachus*, and 70–80° in *Necrosyrtes monachus*. **(15)** The flange on the facies articularis sternalis dorsalis spans the medial third of the faces, and is broad and rounded in *Gyps*, and peaked in *Aegypius* and *Necrosyrtes*.

#### Circaetinae.

**Six characters differ for all circaetines:** **(5)** The cotyla scapularis is greater than a quarter of the width of the shaft. **(8)** The processus procoracoideus is oriented right angles to the shaft. **(9)** The processus has moderate medial projection. **(14)** The angulus medialis projects in a robust, broad point that forms a 70–80° angle. **(15)** The flange on the facies articularis sternalis dorsalis spans just under half the medial section of the facies. **(16)** The shaft is slightly narrow and elongate relative to length.

**No characters differ variably among circaetines.**

#### Aquilinae.

**Eight characters differ for all aquilines:** **(1)** The foramen n. supracoracoidei is directly adjacent to the medial margin of the processus procoracoideus. **(2)** There is no medial pneumatic opening within the foramen. **(5)** The cotyla scapularis is greater than a quarter of the width of the shaft. **(6)** The cotyla scapularis is deep. **(8)** The processus procoracoideus is oriented horizontal relative to the cotyla scapularis **(9)** and has moderate medial projection. **(15)** The flange on the facies articularis sternalis dorsalis spans the medial half of the facies. **(16)** The shaft is slightly narrow and elongate relative to length.

**One character differs variably among aquilines:** **(11)** The coracobrachialis ligament attachment scar is positioned centrally on the shaft in all species except *Hieraaetus morphnoides* and *Hieraaetus moorei*.

#### Haliaeetinae.

**Five characters differ for all haliaeetines:** **(5)** The cotyla scapularis is greater than a quarter of the width of the shaft. **(8)** The processus procoracoideus is oriented horizontal relative to the cotyla scapularis. **(14)** The angulus medialis projects in a narrow point which forms >45° angle. **(15)** The flange on the facies articularis sternalis dorsalis is narrow, rounded, very prominently projecting and spans the medial third of the facies. **(16)** The shaft is slightly narrow and elongate relative to length.

**Three characters differ variably among haliaeetines:** **(1)** The foramen n. supracoracoidei is set against the corpus of the shaft in *Haliaeetus* and *Milvus*, and against the shaft margin in *Haliastur*. **(2)** There is no medial pneumatic opening within the foramen in all species except *Haliaeetus leucogaster*, where it is present. **(11)** The coracobrachialis ligament

attachment scar is positioned laterally on the shaft in all species except *H. leucogaster*, where it is central.

#### Buteoninae.

**Eight characters differ for all buteonines:** **(1)** The foramen n. supracoracoidei is set directly adjacent to the medial margin of the processus procoracoideus. **(2)** There is no medial pneumatic opening within the foramen. **(8)** The processus procoracoideus forms a right angle with the shaft. **(12)** The coracobrachialis ligament attachment scar is an elongate vertical ridge. **(15)** The flange on the facies articularis sternalis dorsalis is narrow, rounded, very prominently projecting, and spans the medial half the facies width. **(16)** The shaft is narrow and elongate relative to length.

**No characters differ variably among buteonines.**

#### Summary.

In terms of the least number of differences, the fossil most closely resembles species in the Perninae. However, the fossil is much larger than any known species of pernine accipitrid. The largest extant species is *Hamirostra melanosternon*, with females weighing an average of 1.3 kg (Debus 1998), while the fossil is much larger than this. In terms of size, the fossil is more similar to species of Gypaetinae, Aegypiinae, Circaetinae, Aquilinae and Haliaeetinae. Out of these subfamilies, the fossil is most similar to Aegypiinae, which is only differentiated by two characters that are invariant among all members from the fossil, and which is the only subfamily wherein species share the same states for characters **5** (cotyla scapularis >1/4 shaft width), **8** (distal sloping of processus procoracoideus) and **16** (shaft broad and robust) as the fossil.

#### **Scapula (Figure 4.4H–J).**

The right scapula is near perfectly preserved, lacking only the caudal-most extremity.

**(1)** The acromion (Figure 4.4I: Ac) strongly projects cranially relative to the rest of the cranial end. **(2)** The facies articularis clavicularis is laterally prominent, overhanging the lateral facies. **(3)** The crista lig. acrocoracoacromiali has slight projection medially. **(4)** A large, pneumatic fossa is present in the base of the acromion and visible in cranial view (Figure 4.4J: CF). **(5)** The tuberculum coracoideum (Figure 4.4H: TC) is flat, with very little cranial projection from the rest of the cranial end. **(6)** A large pneumatic fossa is present in the medial face adjacent to the tuberculum coracoideum (Figure 4.4H: MF), **(7)** while there is no foramen on the lateral face. **(8)** The corpus scapulae (Figure 4.4I: CSc) is elongate and narrow, **(9)** and weakly expands in width distally. **(10)** The margo dorsalis (Figure 4.4H: MD) projects slightly dorsally relative to the collum. **(11)** The corpus strongly curves ventrally towards the distal end.

Extant Accipitridae differ as follows (intraspecifically variable characters excluded):

#### Perninae.

**Two characters differ for all pernines: (3)** The crista lig. acrocoracoacromiali is flattened medially. **(11)** The corpus is weakly curved ventrally.

**Two characters differ variably among pernines: (1)** The acromion strongly projects cranially in all species except *Chondrohierax uncinatus*, where it is flattened. **(4)** All species lack a fossa cranially in the acromion except *Pernis apivorus*.

#### Gypaetinae.

**One character differs for all gypaetines: (3)** The crista lig. acrocoracoacromiali is flattened medially.

**Four characters differ variably among gypaetines: (2)** The facies articularis clavicularis is laterally prominent in *Neophron* and *Gypohierax*, and weakly projecting laterally in *Polyboroides*. **(4)** A pneumatic fossa is present cranially in the acromion in *Gypohierax angolensis* and *Neophron percnopterus*, absent in *Polyboroides typus* and *Gypaetus barbatus*. **(6)** *G. angolensis* has no medial pneumatic foramen, *P. typus* has one present on the medial face, and **(7)** *G. barbatus* and *N. percnopterus* have one present on the ventral face.

#### Aegyptiinae.

**Two characters differ for all aegyptiines: (6)** All species lack a fossa on the medial facies. **(9)** There is no widening of the corpus scapulae towards the caudal end.

**Three characters differ variably among aegyptiines: (2)** The facies articularis clavicularis is laterally prominent in *Gyps* and *Necrosyrtes*, and extremely prominent in *Aegyptius*. **(3)** The crista lig. acrocoracoacromiali has slight projection medially in *Necrosyrtes* and is very small or flattened in *Gyps* and *Aegyptius*. **(7)** *Aegyptius monachus* and *Sarcogyps calvus* have a pneumatic foramen on the lateral face, which is absent in other species.

#### Circaetinae.

**Three characters differ for all circaetines: (3)** The crista lig. acrocoracoacromiali is flattened medially. **(9)** The corpus distinctly widens past the margo dorsalis towards the caudal end. **(11)** The corpus is weakly curved ventrally.

**Two characters differ variably among circaetines: (4)** Pneumatic fossa present cranially on the acromion in *Spilornis cheela*, absent in *Terathopius ecaudatus*. **(6)** *S. cheela* lacks a pneumatic foramen, while *T. ecaudatus* has one.

### Aquilinae.

**Three characters differ for all aquilines: (2)** The facies articularis clavicularis is weakly prominent laterally. **(3)** The crista lig. acrocoracoacromiali is flattened medially. **(9)** The corpus scapulae distinctly widens past the cranial point of the margo dorsalis towards the caudal end.

**Two characters differ variably among aquilines: (6)** A pneumatic fossa is present in the medial face of the cranial end in *Aquila*, *Hieraaetus morphnoides* and *Hieraaetus fasciatus*, but is lacking in all other species. **(11)** The corpus is weakly curved ventrally in all species except *Spizaetus tyrannus*, where it is strongly curved.

### Haliaeetinae.

**Four characters differ for all haliaeetines: (2)** The facies articularis clavicularis is weakly prominent laterally. **(3)** The crista lig. acrocoracoacromiali is weakly protruding to flattened medially. **(9)** The corpus scapulae distinctly widens past the cranial point of the margo dorsalis towards the caudal end. **(11)** The corpus is weakly curved ventrally.

**Two characters differ variably among haliaeetines: (4)** Pneumatic fossa present in base of acromion in all species except *Haliaeetus leucogaster* and species of *Haliastur*. **(6)** A fossa is present in the medial face of the cranial end in *H. leucogaster* and *Haliastur indus*, which is absent in all other species.

### Buteoninae.

**Four characters differ for all buteonines: (3)** The crista lig. acrocoracoacromiali is flattened medially. **(6)** There are no fossae on the medial face. **(9)** The corpus scapulae distinctly widens past the cranial point of the margo dorsalis towards the caudal end. **(11)** The corpus is weakly curved ventrally towards the distal end.

**One character differs variably among buteonines: (4)** A large, pneumatic fossa is present cranially in the acromion in *Buteo*, and absent in *Ictinia mississippiensis*.

### Summary.

The fossil bears the greatest resemblance to Gypaetinae, differing only in character **3** (flattening of the crista lig. acrocoracoacromiali). In terms of similarities, both the fossil and gypaetines share states for characters **9** (slight distal widening of the corpus) and **11** (strong curvature of the corpus ventrally). However, **11** is also shared with the Aegyptiinae, and only in this later subfamily do the character states for **2** (facies articularis clavicularis is laterally prominent) and **3** (weakly prominent crista lig. acrocoracoacromiali) found in the fossil both co-occur. The fossil could therefore belong to either vulturine subfamily.

### ***Ulna (Figure 4.5A, C, E, F–H).***

Four ulnae are attributed to accipitrid GWC/VFC.; three are complete - two from Green Waterhole Cave and one from Victoria Fossil Cave which are identical, and a distal part of one from Wellington Caves, which in so far as it is comparable does not differ either. Measurements are as seen above (Table 4.2).

The ulnae are quite robust for their length e.g., 11.2 vs 8.4 mm mid SW for ulna of very similar length P.24323 (208 mm) vs *Aquila audax* FUR 085 (205 mm). **(1)** The olecranon (Figure 4.5G: O) is set quite low, barely projecting proximal of the cotyla ventralis. **(2)** The cotyla ventralis is quite large, area about twice the size of the cotyla dorsalis, **(3)** circular, and **(4)** deeply concave. **(5)** The cotyla dorsalis is square-like in shape, with a short, distally projecting well rounded processus cotylaris dorsalis. **(6)** The cotylae are separated by a prominent crista intercotylaris. **(7)** A shallow, distinct fossa is present caudodorsal of the cotyla ventralis (Figure 4.5C: CF), **(8)** which is non-pneumatic. **(9)** The impressio m. scapulothoracalis (Figure 4.5E: ScT) located caudal to the cotyla dorsalis is large and distinct, and **(10)** shaped like an upside-down triangle. **(11)** The incisura radialis (Figure 4.5G: IR) is shallow and non-pneumatic. **(12)** There are two ligamental scars present on the cranial face just distal of the incisura radialis, neither of which prominently protrudes cranially. **(13)** The larger of the two is the dorsal scar (Figure 4.5C: DS), which forms a short, concave, robust line orientated proximodistally, with the distal half curving ventrally. **(14)** The ventral scar (Figure 4.5C: VS) is a small circle about a quarter of the size of the dorsal tuberculum, is not concave, and is positioned ventrodistally adjacent to the dorsal scar. Viewed in combination, the scars form a shape that greatly resembles a slanted exclamation mark. **(15)** The tuberculum ligamentosa collateralis ventralis (Figure 4.5G: TLCV) has an extremely low profile in cranial view, not even extending as far ventrally as the margin of the cotyla ventralis and the ligamental attachment scar on it extends caudally on the ventral face (Figure 4.5A: PLS) and extending proximally towards the olecranon. **(16)** The impressio brachialis (Figure 4.5F: IB) is quite long (~46.3 mm on P.24324), and moderately deep for its size. **(17)** When viewed in dorsal and ventral aspect, very little curvature is present in the shaft. **(18)** The papillae remigales caudales are small and have a low profile in dorsal and ventral aspect. **(19)** The tuberculum carpale (Figure 4.5F: TC) prominently projects cranioventrally in dorsal and ventral view. **(20)** The proximal dorsal margin of the tuberculum carpale is undifferentiated from the rest of the shaft, lacking any flattening of its surface or the presence of a fossa. **(21)** The incisura tuberculum carpale (Figure 4.5F: ITC) is quite deep and distinct, well separating the tuberculum carpale from the condylus ventralis ulnaris (Figure 4.5A: CV). **(22)** The sulcus intercondylaris (Figure 4.5A: SI) is shallow, forming a u-shape in ventral view. **(23)** The depressio radialis (Figure 4.5F: DR) is shallow. **(24)** The incisura tendineus (Figure 4.5C: IT) is shallow, with the distal point of the caudal margin forming a projecting point that slightly overhangs the incisura in SAMA P.24323 that is absent in SAMA P.59029 but connects to a slightly deepened fossa on the condylus dorsalis ulnaris (Figure 4.5A:

CD). **(25)** The dorsal margin of the dorsal condyle (Figure 4.5F: DC) is oriented at an angle across the shaft. **(26)** The length of the dorsal condyle is roughly equal to its width.

Extant Accipitridae differ as follows (variable characters excluded):

#### Perninae.

**Two characters differ for all pernines: (7)** There is no fossa caudal of the cotyla ventralis. **(15)** The tuberculum ligamentosa collateralis ventralis extends roughly equal to the margin of the cotyla ventralis.

**One character differs variably among pernines: (6)** The crista intercotylaris is flat in all species except *Pernis apivorus* and *Hamirostra melanosternon*.

#### Gypaetinae.

**One character differs for all gypaetines: (6)** The crista intercotylaris is flattened.

**Once character differs variably among gypaetines: (22)** The sulcus intercondylaris is shallow in all species except *Polyboroides typus*, where it is deep.

#### Aegyptiinae.

**Two characters differ for all aegyptiines: (1)** The olecranon projects strongly proximal to the cotyla ventralis. **(6)** The crista intercotylaris is flattened.

**Eight characters differ variably among aegyptiines: (4)** The cotyla ventralis is deep in species of *Gyps* and *Aegyptius monachus*, and shallow in *Necrosyrtes monachus*. **(7)** A fossa is present in all species except *N. monachus* and *Sarcogyps calvus*. **(8)** Where present the fossa is pneumatic. **(11)** The incisura radialis is non-pneumatic in all species except *A. monachus* and *S. calvus*. **(15)** The tuberculum ligamentosa collateralis ventralis has an extremely prominent ventral projection in species of *Gyps*, *A. monachus* and *Torgos tracheliotos*, and a moderate projection in all other species. **(20)** The proximal margin of the tuberculum is differentiated from the rest of the shaft by a flattening of its surface in species of *Gyps* and *A. monachus*, and by the presence of a shallow fossa in all other species. **(22)** The sulcus intercondylaris is slightly deepened in species of *Gyps* and *A. monachus*, and shallow in all species. **(23)** The depressio radialis is shallow in species of *Gyps* and *N. monachus* and is deep with some pneumatisation in *A. monachus*.

#### Circaetinae.

**Three characters differ for all circaetines: (6)** The crista intercotylaris is flattened. **(15)** The tuberculum ligamentosa collateralis ventralis has a moderate projection in cranial view. **(22)** The sulcus intercondylaris is deep.

**Two characters differ variably among circaetines: (12)** There are two ligamental scars on the cranial face, which are flattened in *Spilornis cheela* and *Terathopius ecaudatus*. **(26)** The

condylus dorsalis is longer than wide in *Spilornis cheela*, and roughly equal in *Terathopius ecaudatus*.

#### Aquilinae.

**Four characters differ for all aquilines:** (7) There is no fossa caudal to the cotyla medialis. (15) The tuberculum ligamentosa collateralis ventralis is prominent in cranial view, extending level with the dorsal margin of the cotyla dorsalis. (25) The dorsal margin of the dorsal condyle is oriented parallel to the shaft. (26) The dorsal condyle is longer proximodistally than wide.

**Two characters differ variably among aquilines:** (1) The olecranon is more strongly projecting proximally than the fossil in all species except *Hieraaetus fasciatus*. (9) The impressio m. scapulotricipitis is large and distinct in *Aquila* and small and distinct in *Hieraaetus* and *Spizaetus*.

#### Haliaeetinae.

**Six characters differ for all haliaeetines:** (6) The crista intercotylaris is flattened. (7) A deep fossa is present caudal to the cotyla ventralis. (15) The tuberculum ligamentosa collateralis ventralis has a prominent projection, equal to the dorsal margin of the cotyla dorsalis. (20) The proximal dorsal margin of the tuberculum is differentiated from the rest of the shaft by a flattening of its surface. (25) The dorsal margin of the dorsal condyle is oriented parallel to the shaft. (26) The dorsal condyle is longer than wide.

**One character differs variably among haliaeetines:** (1) The olecranon is low projecting in all species except *Milvus migrans*, where it projects prominently proximally.

#### Buteoninae.

**Eight characters differ for all buteonines:** (1) The olecranon is well projecting proximally. (15) The tuberculum ligamentosa collateralis ventralis has equal extent with the margin of the cotyla ventralis. (16) The impressio brachialis is shallow. (17) The shaft is distinctly curved. (19) The tuberculum carpale is weakly protruding. (21) The incisura tuberculum carpale is shallow. (22) The sulcus intercondylaris is deep. (23) The depressio radialis is slightly deepened.

**One character differs variably among buteonines:** (12) There are two ligamental scars, both on the cranial face in *Ictinia mississippiensis*, and one on the cranial, one on the ventral in *Buteo*.

#### Summary.

The fossil ulna is most similar to species in Gypaetinae, with only one invariant character differentiating all members. However, across the Gypaetinae and Aegyptiinae, the differentiating characters (1, projection of the olecranon; and 6, flattening of the crista intercotylaris) are arguably not significant, and the fossil could be considered to belong to either subfamily.

### ***Carpometacarpus* (Figure 4.4F, G).**

Complete left and right carpometacarpi exist for the Green Waterhole Cave individual, and a near- complete right specimen missing only the distal end and the os metacarpale minus is known from Victoria Fossil Cave. A partial third specimen is known from Cathedral Cave, Wellington Caves.

(1) The fossa infratrochlearis (Figure 4.4F: FI) lacks pneumatization and is shallow. (2) The fossa supratrochlearis (Figure 4.4G: FS) lacks pneumatization and is shallow. (3) A shallow sulcus is present in the ventral face between the processus pisiformis and processus extensorius (Figure 4.4F: VS). This sulcus extends from the cranial margin of the trochlea carpalis to the processus alularis. (4) The proximal margin of the processus extensorius has a shallow, non-pneumatic sulcus that extends to the base of the trochlea carpalis. (5) The fovea carpalis caudalis is slightly deepened and non-pneumatic. (6) The processus pisiformis (Figure 4.4F: PP) moderately projects ventrally. (7) The dorsal facies between the processus alularis (Figure 4.4G: PA) and the shaft has a shallow notch. (8) The processus extensorius (Figure 4.4F, G: PE) projects mostly cranially with only slight proximal projection. (9) The sulcus tendineus (Figure 4.4G: ST) is primarily located on the dorsal face, gradually curving onto the cranial face at the half-shaft length. (10) The sulcus tendineus is narrow. (11) The facies articularis digitalis minor (Figure 4.4F: FADMin) projects further distally than the facies articularis digitalis major (Figure 4.4F: FADMaj). (12) The os metacarpale minus (Figure 4.4G: OMM) is slightly arched caudally. (13) The proximal end of the os metacarpale minus is non-pneumatic.

Extant Accipitridae differ as follows (intraspecifically variable characters excluded):

#### Perninae.

**One character differs for all pernines:** (5) The fovea carpalis caudalis is shallow.

**Four characters differ variably among pernines:** (1) The fossa infratrochlearis lacks pneumatization and is shallow in all species except *Chondrohierax uncinatus*, which is pneumatic. (4) The fovea carpalis cranialis is shallow and non-pneumatic in all species except *C. uncinatus*, where it is pneumatic. (7) Dorsally the processus alularis is not separated by a notch from the shaft except in *C. uncinatus*, where it is. (13) The proximal end of the os metacarpale minus is non-pneumatic in all species except *C. uncinatus*.

#### Gypaetinae.

**One character differs for all gypaetines:** (7) The processus alularis is continuous with the shaft.

**One character differs variably among pernines:** (3) The sulcus is present in all species except *Gypaetus barbatus*.

### Aegyptiinae.

**One character differs for all aegyptiines: (12)** The os metacarpale minus is flattened.

**Seven characters differ variably among aegyptiines: (1)** All species have a pneumatized fossa infratrochlearis except *Necrosyrtes monachus*, where it is absent. **(2)** The fossa supratrochlearis is pneumatized in *N. monachus* and not pneumatized in all other species. **(3)** A sulcus is present in all species except *N. monachus*, *Trigonoceps occipitalis* and *Sarcogyps calvus*. **(5)** The fovea carpalis cranialis is deep and pneumatic in all species except *T. occipitalis*, which is non-pneumatic. **(6)** The processus pisiformes strongly projects in *Aegyptius* and *Gyps*, and moderately projects in *Necrosyrtes*. **(7)** The processus alularis is separated from the main face of the proximal end by a small notch in dorsal view in all species except *Torgos tracheliotos*, which is continuous with the shaft. **(13)** The proximal end of the os metacarpale minus is pneumatic in all species except *T. occipitalis* and *Sarcogyps calvus*.

### Circaetinae.

**One character differs for all circaetines: (4)** The proximal margin of the processus extensorius has a deep, non-pneumatic sulcus that extends to the base of the trochlea carpalis.

**One character differs variably among circaetines: (13)** The os metacarpale minus is slightly arched caudally in *Spilornis cheela* and flattened in *Terathopius ecaudatus*.

### Aquilinae.

**One character differs for all aquilines: (8)** The processus extensorius has strong proximal projection.

**One character differs variably among aquilines: (13)** The os metacarpale minus is flattened in species of *Aquila* and *Hieraaetus* and arched in species of *Spizaetus*.

### Haliaeetinae.

**One character differs for all haliaeetines: (8)** The processus extensorius has strong proximal projection.

**Two characters differ variably among haliaeetines: (3)** A sulcus is present in all species except *Haliaeetus leucogaster* and *Haliaeetus albicilla*. **(13)** The os metacarpale minus is flattened in species of *Haliaeetus* and slightly arched in all other species.

### Buteoninae.

**Six characters differ for all buteonines: (1)** The fossa infratrochlearis is deep. **(4)** The proximal margin of the processus extensorius has a deep, non-pneumatic sulcus that extends to the base of the trochlea carpalis. **(5)** The fovea carpalis caudalis is shallow. **(8)** The processus extensorius has strong proximal projection. **(9)** The distal third of the sulcus tendineus is located on

the dorsal face, which curves proximally onto the cranial face. **(13)** The os metacarpale minus is flattened.

**No characters differ variably among buteonines.**

Summary.

The fossil most closely resembles species of Gypaetinae, Aegyptiinae, Circaetinae and Aquilinae on the basis of size and the fewest invariant differences. When it comes to characters shared with most genera within these subfamilies, however, the Gypaetinae and Circaetinae are more similar to the fossil than the Aegyptiinae due to the lack of pneumatization, and Aquilinae due to the reduced proximal projection of the processus extensorius.

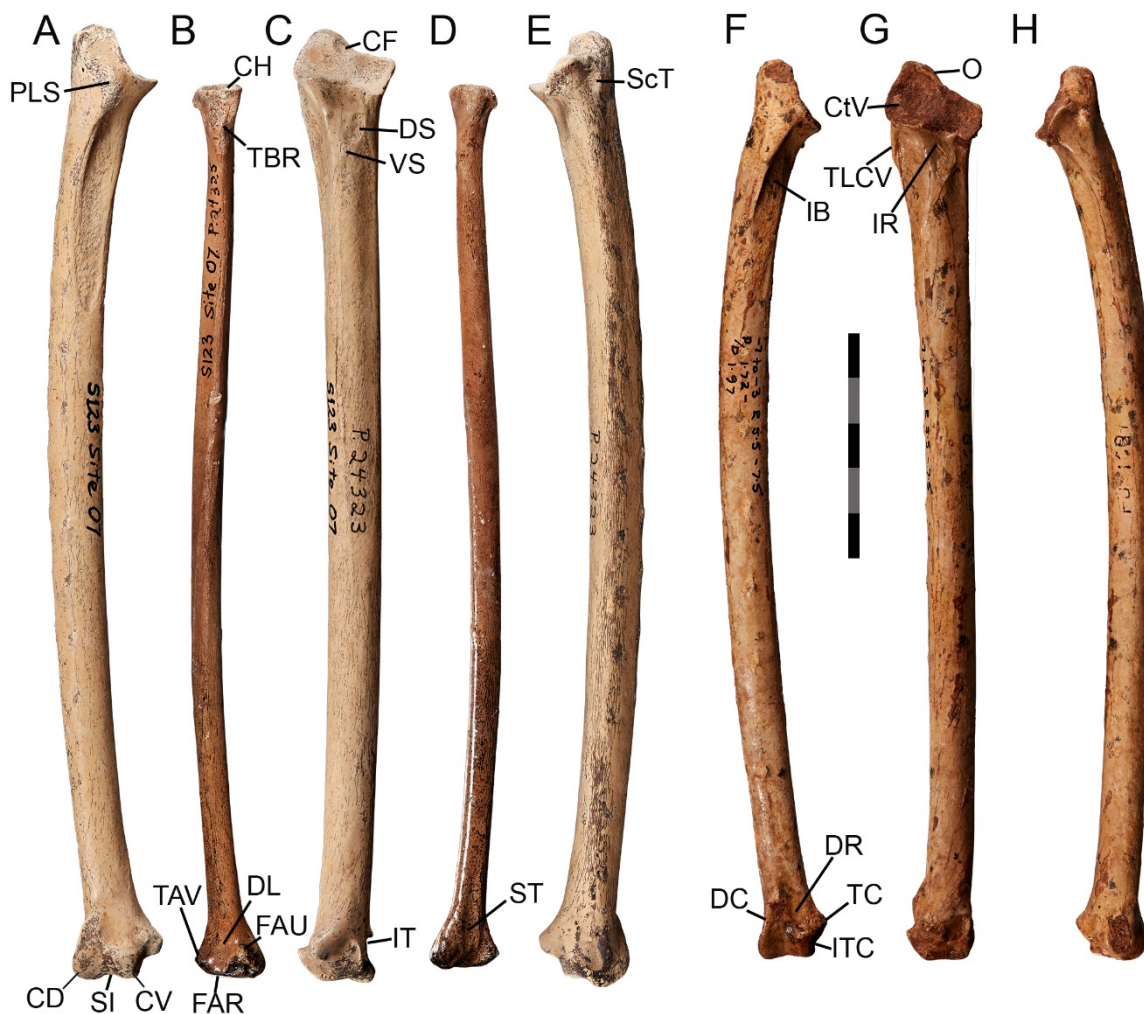


**Figure 4.5:** Accipitrid GWC/VFC ulna SAMA P.24323 in ventral (A), cranial (C) and dorsal (E) view, ulna SAMA P.59029 in ventral (F), cranial (G) and dorsal (H) view, radius SAMA P.24325 in ventral (B) and dorsal (D) view. Abbreviations: CD, condyles dorsalis; CF, caudal fossa; CH, cotyla humeralis; CtV, cotyla ventralis; CV, condylus ventralis; DC, condylus dorsalis; DL, depressio ligamenti; DR, depressio radialis; DT, dorsal tuberculum; FAR, facies articularis radialis; FAU, facies articularis ulnaris; IB, impressio brachialis; IR, incisura radialis; IT, incisura tendineus; ITC, incisura tuberculum carpale; O, olecranon; PLS, proximal ligamental scar; ScT, impressio m. scapulotricipitis; SI, sulcus intercondylaris; ST, sulcus tendineus; TAV, tuberculum aponeurosis ventralis; TBR, tuberculum bicipitalis radialis; TC, tuberculum carpale; TLCV, tuberculum ligamentosa collateralis ventralis; VT, ventral tuberculum. Scale bar 50 mm.

### **Radius (Figure 4.5B, D).**

Both the left and right radii are complete and in near perfect condition, allowing for comparison of all features across taxa.

(1) The cotyla humeralis (Figure 4.5B: CH) has a large, semi-circular facet, (2) which is shallow with little convexity. (3) The tuberculum bicipitalis radialis (Figure 4.5B: TBR) is quite prominent in dorsal view, (4) with a shallow fossa dorsally. (5) The tuberculum aponeurosis ventralis (Figure 4.5B: TAV) is prominent ventrally. (6) The ridges bounding the sulcus tendineus (Figure 4.5D: ST) dorsally are flat, (7) and the sulcus itself is shallow. (8) The facies articularis

radiocarpalis (Figure 4.5B: FAR) is flat in dorsal view, **(9)** and orientated at a slight dorsoventral angle. **(10)** The depressio ligamentosa (Figure 4.5B: DL) is very shallow, and practically indistinguishable on the ventral face of the distal end. **(11)** The depressio ligamentosa is non-pneumatic. **(12)** The facies articularis ulnaris (Figure 4.5B: FAU) forms a roughly circular and prominent protrusion on the ventral face of the distal end.

Extant Accipitridae differ as follows (variable characters excluded):

#### Perninae.

**No characters differ for all pernines.**

**One character differs variably among pernines: (3)** The tuberculum bicipitalis radialis is flattened in all species except *Lophoictinia isura* and *Hamirostra melanosternon*, where it is prominent dorsally.

#### Gypaetinae.

**One character differs for all gypaetines: (10)** The depressio ligamentosa is slightly deepened.

**One character differs variably among gypaetines: (3)** The tuberculum bicipitalis radialis is quite prominent in dorsal view in *Neophron percnopterus* and flattened in all other species.

#### Aegyptiinae.

**Three characters differ for all aegyptiines: (7)** The sulcus tendineus is slightly deepened. **(10)** The depressio ligamentosa is deep. **(11)** The depressio ligamentosa is pneumatic.

**No characters differ variably among aegyptiines.**

#### Circaetinae, Aquilinae.

No significant differences.

#### Haliaeetinae.

**No characters differ for all haliaeetines.**

**One character differs variably among haliaeetines: (10)** The depressio ligamentosa is very shallow in all species except those in *Haliaeetus*, where it is deepened.

#### Buteoninae.

**No characters differ for all buteonines.**

**One character differs variably among buteonines: (5)** The tuberculum aponeurosis ventralis is prominently projecting out ventrally in *Buteo*, and barely projecting in *Ictinia*.

Summary.

The fossil radius could not be meaningfully distinguished from species in *Circaetinae* and *Aquilinae* and is within the size range of known species of these subfamilies, as well as those in *Aegypiinae* and *Gypaetinae* for which differences are minor.

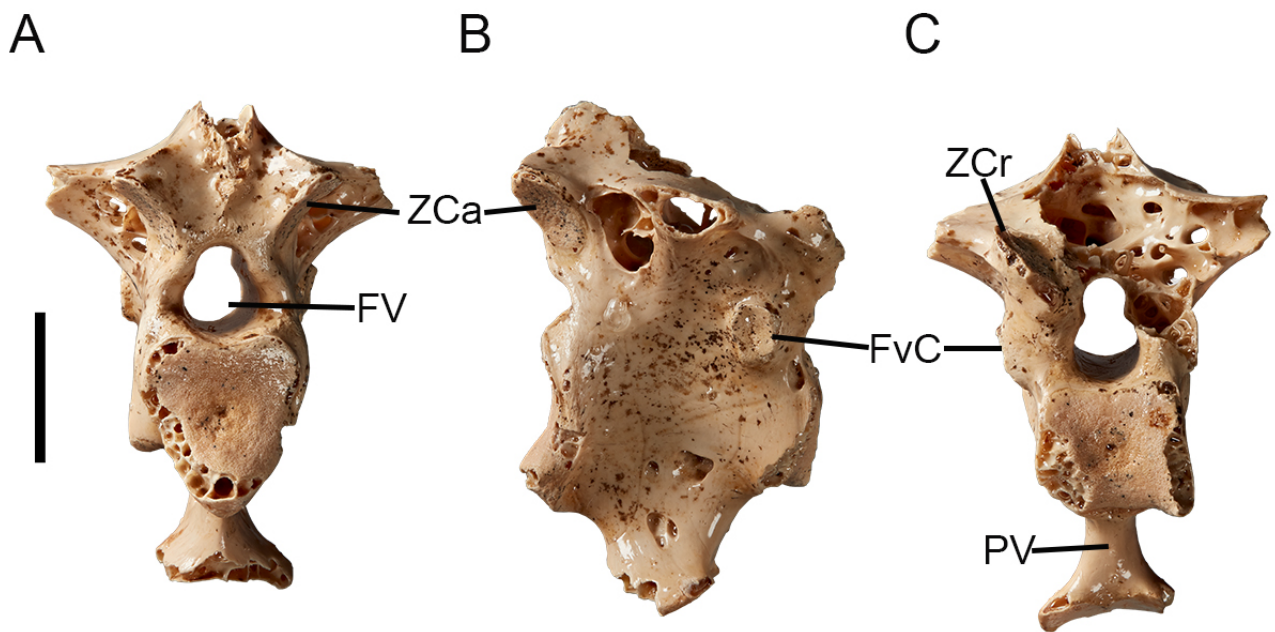


**Figure 4.6:** Accipitrid GWC/VFC thoracic vertebra SAMA P.24329 in caudal (A), lateral (B), and cranial (C) view. Abbreviations: FvC, fovea costalis; FV, foramen vertebrae; PV, processus ventralis; ZCa, zygapophysis caudalis; ZCr, zygapophysis cranialis. Scale bar 10 mm.

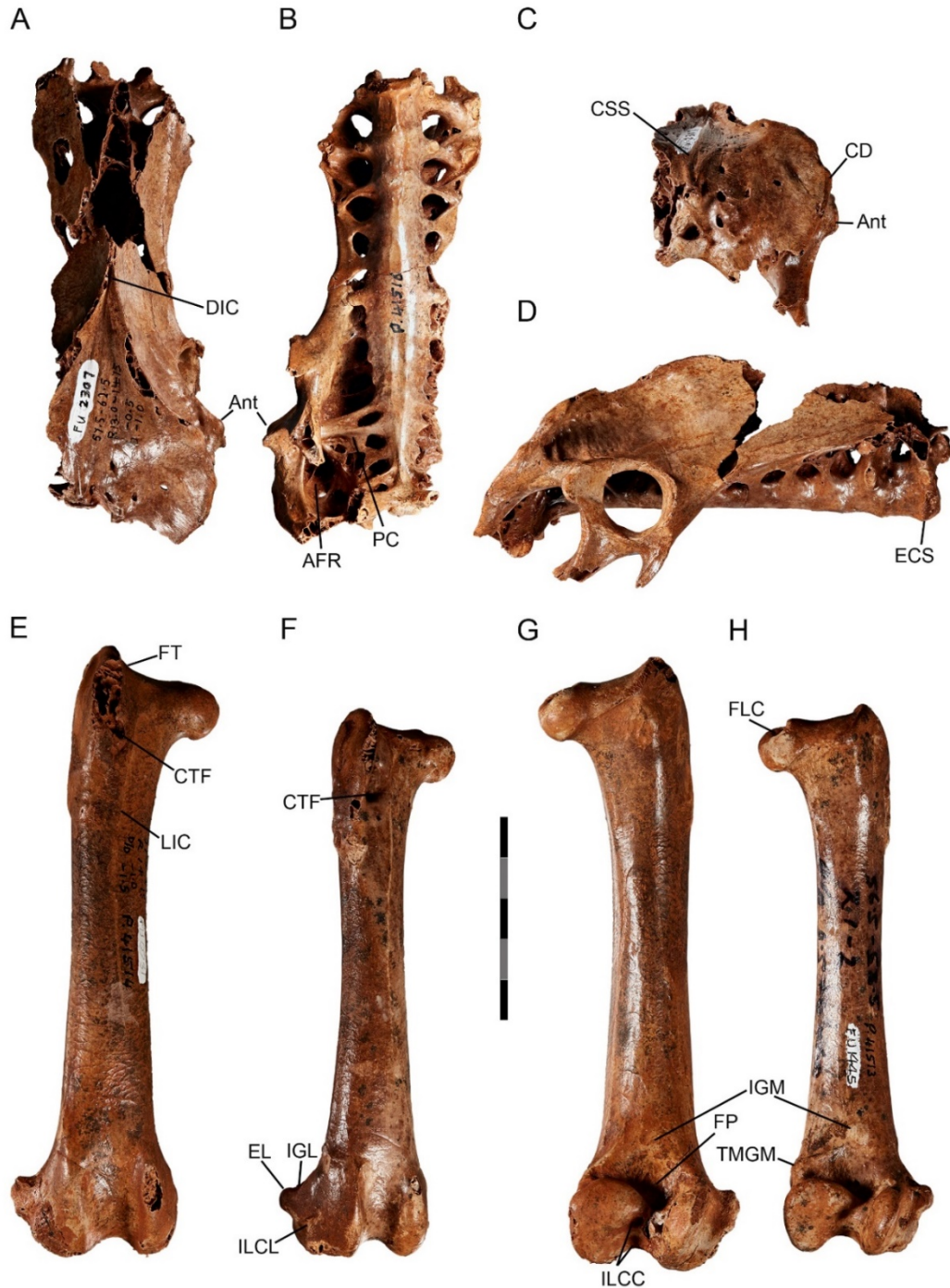


**Figure 4.7:** Images of Accipitrid GWC /VFC pelvis and femora. Pelvis SAMA P.41516 in dorsal (A), ventral (B), caudal (C), and right lateral (D) view. Femur SAMA P.41514 in cranial (E) and caudal (G) view, and femur SAMA P.41513 in cranial (F) and caudal (G) view. Abbreviations: Ant, antitrochanter; AFR, anterior fossa renalis; CD, crista dorsolateralis; CSS, crista spinosa synsacri; CTF, crista trochanteris foramen; DIC, dorsal iliac crests; ECS, extremitas cranialis synsacra; EL, epicondylus lateralis; FLC, fovea lig. capitis; FT, fossa trochanteris; FP, fossa poplitea; IGL, impressio gastrocnemialis lateralis; IGM, impressio gastrocnemialis intermedia; ILCC, impressio lig. cruciati caudalis et cranialis; ILCL, impressio lig. collateralis lateralis; LA, ligamental attachment scar; LIC, linea intermuscularis cranialis; PC, processus costales; TMGM, tuberculum muscularis gastrocnemialis medialis. Scale bar 50 mm.

### ***Thoracic vertebra (Figure 4.6A–C).***

The thoracic vertebra SAMA P.24329 from Green Waterhole Cave preserves the process ventralis, both the cranial and caudal articular facets of the heterocoelous corpus, both zygapophyses caudales, one zygapophysis cranialis, and the foramen vertebrae. The shape of the facies articularis caudalis indicates it is the fourth thoracic vertebra (see summary for greater detail), and this assumption was used when making comparisons. The description is as follows:

**(1)** A large pneumatic foramen exists just proximal to the zygapophyses caudales (Figure 4.6A, B: ZCa). **(2)** The foveae costales (Figure 4.6B, C: FvC) are adjacent to the margin of the facies articularis caudalis of the corpus. **(3)** The foveae costales prominently protrude from the corpus vertebrae in cranial view. **(4)** A small, pneumatic foramina is present in the ventral half of the corpus. **(5)** The shaft of the processus ventralis (Figure 4.6C: PV) is robust, with its cranial mid-shaft width roughly a third (3.4 mm) of the width of the facies articularis cranialis of the corpus (10.3 mm). **(6)** The processus ventralis ends in a broad, bifid projection that would have been roughly equivalent in width to that of the facies articularis cranialis of the corpus, with the bifid tips strongly projecting laterally.

Extant Accipitridae differ as follows:

#### Perninae.

**Two characters differ for all pernines:** **(5)** The shaft of the processus ventralis is thin, and a third or less of the width of the facies articularis cranialis. **(6)** The tip of the processus ventralis is not bifid in the 4<sup>th</sup> thoracic vertebra, and in all cases is narrower than the width of the facies articularis cranialis and weakly projecting laterally.

**Three characters differ variably among pernines:** **(2)** The foveae costales is positioned in line with the proximal margin of the facies articularis caudalis. **(3)** The foveae costales are prominent in *Pernis*, *Hamirostra*, and *Elanoides*, but small or flat in *Lophoictinia* and *Chondrohierax*. **(4)** A pneumatic foramina is present in all species except *Hamirostra*.

#### Gypaetinae.

**No characters differ for all gypaetines.**

**Two characters differ variably among gypaetines:** **(4)** The pneumatic foramina is small in *Neophron* and *Gypohierax*, but large in *Polyboroides*. **(6)** The processus ventralis is bifid in the 4th thoracic vertebrae in *Gypohierax* and *Polyboroides*, though narrower in width than the facies articularis cranialis and weakly projecting ventrally, while a bifid process is absent in *Neophron*.

#### Aegyptiinae.

**One character differs for all aegyptiines:** **(5)** The processus ventralis is under a third of the cranial articular facet width.

**Three characters differ variably among aegypiines: (3)** The foveae costales are positioned central in the corpus vertebra in *Gyps* and *Aegypius*, and adjacent to the facies articularis caudalis in *Necrosyrtes*. **(4)** Pneumatic foramina are present in *Necrosyrtes* and *Aegypius*, and absent in *Gyps*. **(6)** The processus ventralis lacks a bifid end in the 4<sup>th</sup> thoracic in *Gyps* and *Necrosyrtes*, while in *Aegypius* there is a small bifid tip narrower than the cranial articular facet with the tips weakly projecting ventrally.

#### Circaetinae.

**Three characters differ for all circaetines: (2)** The foveae costales are positioned in line with the proximal margin of the facies articularis caudalis. **(3)** The foveae costales weakly project from the corpus vertebra in cranial view. **(6)** There is no bifid process on the 4<sup>th</sup> thoracic vertebra.

**No characters differ variably among circaetines.**

#### Aquilinae.

**One character differs for all aquilines: (3)** The foveae costales weakly project from the corpus vertebra in cranial view.

**One character differs variably among aquilines: (6)** There is no bifid process on the 4<sup>th</sup> thoracic vertebra.

#### Haliaeetinae.

**One character differs for all haliaeetines: (2)** The foveae costales are positioned in line with the proximal margin of the facies articularis caudalis.

**Two characters differ variably among haliaeetines: (3)** The foveae costales are weakly projecting in *Haliaeetus* and moderately projecting in *Haliastur* and *Milvus*. **(6)** There is no bifid process on the 4<sup>th</sup> thoracic vertebra.

#### Buteoninae.

**Two characters differ for all buteonines: (2)** The foveae costales are positioned in line with the proximal margin of the caudal articular facet. **(5)** The processus ventralis shaft is less than a third of the cranial articular facet width.

**Three characters differ variably among buteonines: (3)** The foveae costales are weakly protruding in *Buteo* and prominent in *Ictinia*. **(4)** The foramen is present in *Ictinia* and absent in *Buteo*. **(6)** There is no bifid process on the 4<sup>th</sup> thoracic vertebra.

#### Summary

The fossil's size is a close match to the first synsacral vertebra of the pelvis from Victoria Fossil Cave, but it does not articulate well with it, most likely because the two bones are from different individuals. The shape of the facies articularis caudalis is flatter and less saddle-shaped

than the cranialis, which supports the interpretation that the vertebra is the 4<sup>th</sup> thoracic, or last vertebra before the pelvis. The subfamilies Aegyptiinae, Aquilinae and Haliaeetinae all differ by a single invariant character from the fossil (a different character for each subfamily), but only Aegyptiinae shares the character trait of having a bifid process on the 4<sup>th</sup> thoracic vertebra with the fossil. Therefore, it is most likely that the fossil is from an aegyptiine.

### ***Pelvis (Figure 4.7A–D).***

The pelvis is represented by a half-complete specimen SAMA P.41516 from the type locality, Victoria Fossil Cave. SAMA P.41516 has most of the right lateral side, excluding the caudal-most region, preserved and is short and robust compared to other Australian accipitrids of similar size.

**(1)** The crista iliaca dorsalis (Figure 4.7A: DIC) are not separated above the 5<sup>th</sup> and 6<sup>th</sup> synsacral vert (this is 15-20 mm in front of the acetabular region), but damage precludes assessing separation more anteriorly. **(2)** It lacks foramina intertransversaria. **(3)** The crista spinosa synsacri (Figure 4.7C: CSS) is flat, barely protruding from the dorsal surface. **(4)** The antitrochanter (Figure 4.7A, B, C: Ant) projects further laterally than the crista dorsolateralis ilii (Figure 4.7C: CD). **(5)** The fossa iliocaudalis is very shallow. **(6)** There is no processus ventralis on the extremitas cranialis synsacra (Figure 4.7D: ECS). **(7)** The anterior fossa renalis (Figure 4.7B: AFR) is extremely large and deep. **(8)** The sutura iliosynsacralis forms an angled line, with the dorsal half parallel to the dorsoventral axis and the lower half angled roughly 45° relative to the axis. **(9)** The processus costales (Figure 4.7B: PC) immediately cranial to the anterior fossa renalis are robust and fused laterally to brace the ilium.

Extant Accipitridae differ as follows (variable characters excluded):

#### Perninae.

**Two characters differ for all pernines:** **(4)** The crista dorsolateralis extends further laterally than the antitrochanter. **(8)** The sutura iliosynsacralis form vertical, parallel lines.

**Two characters differ variably among pernines:** **(1)** The dorsal iliac crests are well separated in all species except *Hamirostra melanosternon*, where they are adjacent. **(7)** The anterior fossa renalis is shallow in all species except *Pernis apivorus*, where it is slightly deepened.

#### Gypaetinae.

**One character differs for all gypaetines:** **(8)** The sutura iliosynsacralis form a vertical line.

**Five characters differ variably among gypaetines:** **(2)** Foramina closed in all species except *Neophron percnopterus*, where they are open. **(3)** Flat in all species except *N.*

*percnopterus*, where it is slightly inflated. (5) The fossa iliocaudalis is deep in *N. percnopterus* and *Gypohierax angolensis*, and shallow in *Polyboroides typus* and *Gypaetus barbatus*. (7) The anterior fossa renalis is shallow in all species except *G. angolensis*, where it is deep. (9) The processus costales immediately cranial to the anterior fossa renalis are the same as the fossil in all species except *G. angolensis*, which has thin struts.

#### Aegyptiinae.

**One character differs for all aegyptiines: (8)** The sutura iliosynsacralis form a straight line parallel to the dorsoventral axis.

**Three characters differ variably among aegyptiines: (5)** The fossa iliocaudalis is deep in *Necrosyrtes monachus*, and shallow in all other species. (6) A processus ventralis is present on the extremitas cranialis synsacra in species of *Gyps* and *Aegyptius monachus* and is absent in all other species. (7) The anterior fossa renalis is extremely large and deep in all species except *Necrosyrtes monachus*.

#### Circaetinae.

**Two characters differ for all circaetines: (3)** The crista spinosa synsacri is inflated. (8) The sutura iliosynsacralis form a straight line parallel to the dorsoventral axis.

**No characters differ variably among circaetines.**

#### Aquilinae.

The preacetabular region of the pelvis is longer and dorsoventrally narrower than in the fossil.

**One character differs for all aquilines: (8)** The sutura iliosynsacralis form a vertical line.

**Three characters differ variably among aquilines: (1)** The dorsal iliac crests are separated in *Aquila* and *Hieraetus*, but merge in *Spizaetus*. (3) Flat in all species except *Spizaetus tyrannus*, where it is inflated. (4) The antitrochanter projects further laterally than the crista dorsolateralis in species of *Aquila*, while the crista projects further laterally in all other species.

#### Haliaeetinae.

The preacetabular region of the pelvis is longer and dorsoventrally narrower than in the fossil. **One character differs for all haliaeetines: (8)** The sutura iliosynsacralis form a straight line parallel to the dorsoventral axis.

**Four characters differ variably among haliaeetines: (1)** Dorsal iliac crests are separated in all species except *Haliaeetus albicilla* (possible intraspecific variation). (2) Completely fused over in all species except *Haliastur sphenurus*. (4) The crista dorsolateralis projects further laterally than

the antitrochanter in all species except *Haliaeetus leucogaster*, where the antitrochanter projects further (possibly interspecific variation). **(7)** The anterior fossa renalis is shallow in all species except *Haliaeetus leucocephalus* and *H. albicilla*.

#### Buteoninae.

**Three characters differ for all buteonines:** **(4)** The crista dorsolateralis extends further laterally than the antitrochanter. **(7)** The anterior fossa renalis is shallow. **(8)** The sutura iliosynsacralis form a roughly vertical line.

**One character differs variably among buteonines:** **(9)** The processus costales are the same as the fossil in *Buteo*, and thin struts that do not connect to the sides of the pelvis in *Ictinia mississippiensis*.

#### Summary.

The fossil pelvis differs by one invariant character from the species in Gypaetinae, Aegypiinae, Aquilinae, and Haliaeetinae, which are also the subfamilies it matches in size. However, the fossil is distinct from species in the Aquilinae (excluding *Spizaetus*) and Haliaeetinae by character state **1** (separation of the dorsal iliac crests) and from all aquilines and haliaeetines by the preacetabular region being longer and narrower in these subfamilies. Therefore, the fossil overall has the most similarity to the vulturine subfamilies.

#### **Femur (Figure 4.7E–H).**

Two femora from Victoria Fossil Cave are nearly perfectly preserved, with all features intact. The most notable difference between them is their size, with the larger femur being 10% longer and 8% wider than its smaller counterpart (see Table 4.3). They exhibit the following features:

The femora are extremely large and robust compared to all living Australian accipitrids (see Table 4.3), and in Australasia only specimens of Haast's eagle *Hieraaetus moorei* outsize them. **(1)** The fovea lig. capitis (Figure 4.7H: FLC) is deep **(2)** and large relative to the caput. **(3)** The fossa trochanteris (Figure 4.7E: FT) is very shallow. **(4)** The crista trochanteris has one pneumatic foramen penetrating it medially (Figure 4.7E, F: CTF). **(5)** The depression distad to the facies articularis antitrochanterica on the caudal face is very shallow. **(6)** The linea intermuscularis cranialis (Figure 4.7E: LIC) is positioned laterally. **(7)** The proximal point of the epicondylus lateralis (Figure 4.7F: EL) is strongly projecting laterally. **(8)** The crista supracondylaris medialis is prominent in SAMA P.41514 and extremely prominent in SAMA P.41513, as formed by the tuberculum muscularis gastrocnemialis medialis (Figure 4.7H: TMGM). **(9)** The impressio gastrocnemialis lateralis (Figure 4.7F: IGL) is shallow and large. **(10)** The condylus lateralis and

medialis are separated by a deep notch caudally. **(11)** The impressio gastrocnemialis intermedia (Figure 4.7G, H: IGM) is circular in shape, **(12)** and is positioned centrally in the shaft. **(13)** The fossa poplitea (Figure 4.7G: FP) is deep. **(14)** The impressio lig. cruciati caudalis et cranialis (Figure 4.7G: ILCC) form two distinct shallow sulci. **(15)** The pars cranialis is relatively twice as wide as the pars caudalis. **(16)** The pars caudalis is slightly deeper than the pars cranialis. **(17)** The impressio lig. collaterale laterale (Figure 4.7F: ILCL) spans roughly two-thirds the caudo-cranial depth of the condylus lateralis.

Extant Accipitridae differ as follows (interspecifically variable characters excluded):

#### Perninae.

**Four characters differ for all pernines:** **(1)** The fovea lig. capitis is shallow. **(6)** The linea intermuscularis cranialis is positioned medially. **(8)** The crista supracondylaris medialis is flattened. **(16)** The impressio lig. cruciati caudalis et cranialis are of roughly equal depth.

**Two characters differ variably among pernines:** **(7)** The proximal point of the epicondylus lateralis is flat in all species except *Hamirostra melanosternon*, where it is weakly projecting. **(12)** The impressio gastrocnemialis intermedia is positioned centrally on the shaft in all species except *Hamirostra melanosternon*, where it is offset slightly medially.

#### Gypaetinae.

**Three characters differ for all gypaetines:** **(7)** The proximal point of the epicondylus lateralis is weakly projecting laterally. **(10)** The condylus lateralis et medialis are separated by a shallow notch. **(17)** The impressio lig. collat lateralis spans roughly half the caudo-cranial depth of the condylus lateralis.

**Seven characters differ variably among gypaetines:** **(1)** The fovea lig. capitis is deep in *Polyboroides typus* and shallow in all other species. **(3)** The fossa trochanteris is very shallow in all species except *Neophron percnopterus*. **(5)** The depression distad to the facies articularis antitrochanterica on the caudal face is very shallow in all species except *P. typus*, where it is deep. **(6)** The linea intermuscularis cranialis is positioned laterally in all species except *P. typus*, where it is positioned medially. **(8)** The crista supracondylaris medialis flattened in all species except *N. percnopterus*, where it is absent. **(12)** The impressio gastrocnemialis intermedia is offset medially in *Gypohierax angolensis* and positioned centrally in other species. **(16)** The impressio lig. cruciati caudalis et cranialis are equally shallow in all species except *P. typus*, where the pars cranialis is deeper.

### Aegyptiinae.

**Three characters differ for all aegyptiines: (3)** The fossa trochanteris is deepened. **(8)** The crista supracondylaris medialis is flattened. **(16)** The impressio lig. cruciati caudalis et cranialis are roughly the same depth.

**One character differs variably among aegyptiines: (12)** The impressio gastrocnemialis intermedia is positioned centrally in species of *Gyps* and *Aegyptius monachus* and is laterally offset in *Necrosyrtes monachus*.

### Circaetinae.

**Three characters differ for all circaetines: (8)** The crista supracondylaris medialis flattened. **(10)** The condylus lateralis et medialis are separated by a shallow notch. **(17)** The impressio lig. collaterale laterale spans roughly half the caudo-cranial depth of the condylus lateralis.

**No characters differ variably among circaetines.**

### Aquilinae.

**Four characters differ for all aquilines: (6)** The linea intermuscularis cranialis is positioned medially. **(8)** The crista supracondylaris medialis is barely prominent. **(9)** The impressio gastrocnemialis lateralis is deep and small. **(11)** The impressio gastrocnemialis intermedia is a horizontal line, slightly angled proximo-medially.

**Three characters differ variably among aquilines: (4)** The number of pneumatic foramina on the crista trochanteris ranges between one and two in species of *Aquila* and is limited to one in all other species. **(12)** The impressio gastrocnemialis intermedia is positioned centrally in species of *Aquila* and *Spizaetus* and offset laterally in species of *Hieraaetus*. **(17)** The impressio lig. collaterale laterale spans roughly half the caudo-cranial depth of the condylus lateralis in species of *Aquila* and over two thirds in all other species.

### Haliaeetinae.

**Five characters differ for all haliaeetines: (6)** The linea intermuscularis cranialis is positioned medially. **(8)** The crista supracondylaris medialis is weakly prominent. **(12)** The impressio gastrocnemialis intermedia is laterally offset. **(16)** The pars caudalis is slightly deeper than the pars cranialis. **(17)** The impressio lig. collaterale laterale spans roughly half the caudo-cranial depth of the condylus lateralis.

**No characters differ variably among haliaeetines.**

### Buteoninae.

**Six characters differ for all buteonines:** (6) The linea intermuscularis cranialis is positioned medially. (7) The proximal point of the epicondylus lateralis is moderately projecting. (8) The crista supracondylaris medialis is flattened. (12) The impressio gastrocnemialis intermedia is offset laterally. (13) The fossa poplitea is slightly deepened. (16) The impressio lig. cruciati caudalis et cranialis are of equal depth.

**One character differs variably among buteonines:** (5) The depression distad to the facies articularis antitrochanterica on the caudal face is shallow in *Buteo* and deepened in *Ictinia mississippiensis*.

### Summary.

The fossil most closely resembles the Aegyptiinae, Gypaetinae and Circaetinae in its morphology based on fewest number of differing characters (three invariant). Both Gypaetinae and Circaetinae differ from the fossil in characters **10** (condylus lateralis et medialis separated by notch) and **17** (impressio lig. collateralis lateralis spans half the caudo-cranial depth of the condylus lateralis), while both Aegyptiinae and Circaetinae differ from it by character **8** (flattening of crista supracondylaris medialis).

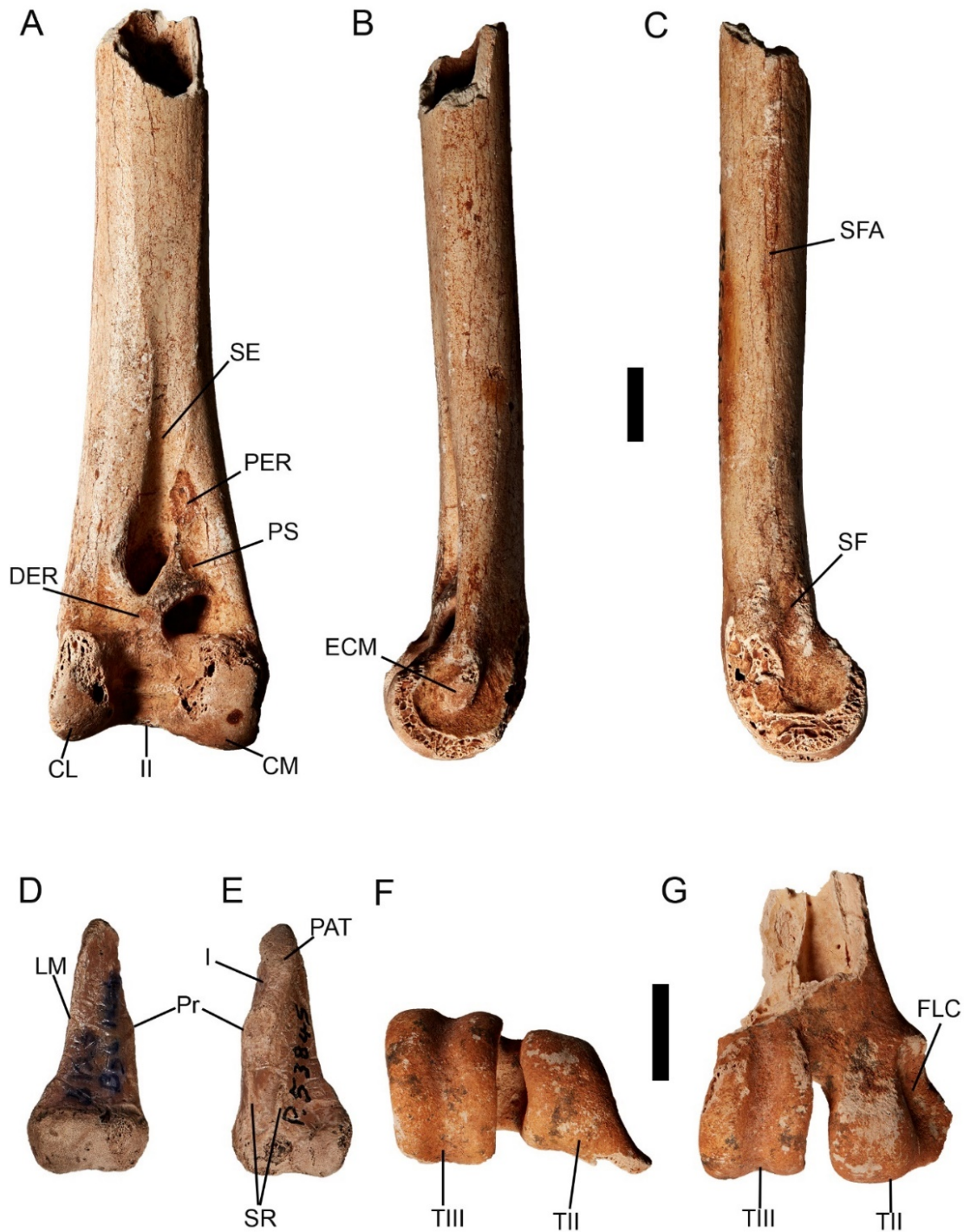


**Figure 4.8:** Accipitrid GWC/VFC distal tibiotarsus AMF 106562 in cranial (A), medial (B) and lateral (C), distal tarsometatarsus SAMA P.28008 in distal (F) and dorsal (G), and os metatarsale I SAMA P.53485 in plantar (D) and dorsal (E) view. Abbreviations: CL, condylus lateralis; CM, condylus medialis; DER, distal scar extensor retinaculum; ECM, epicondylus medialis; FLC, fovea lig. collateralis; I, indentation; II, incisura intercondylaris; LM, lateral margin; PAT, processus articularis tarsometatarsalis; PER, proximal scar extensor retinaculum; Pr, projection; PS, pons supratendineus; SE, sulcus extensorius; SF, sulcus m. fibularis; SFA, spina fibula attachment scar; SR, sulcus ridges; TII, trochlearis metatarsi II; TIII, trochlearis metatarsi III. Scale bars 10 mm.

### ***Tibiotarsus* (Figure 4.8A–C).**

Two tibiotarsi are referred to the new species, one from the Wellington Caves (AM F.106562) and the other from Waralamanko Waterhole, Cooper Creek (SAMA P25218) (see Gaff 2002 figures 5.1, 5.2); the whereabouts of the latter specimen is currently uncertain. We regard these fossils as belonging to the same species based on their morphological similarity, as per Gaff (2002). We base our description below on AM F.106562 and justify referring this fossil to accipitrid GWC/VFC based on the observation that it is much larger than would be predicted for “*Taphaetus*” *lacertosus* based on the size of the tarsometatarsus referred to the latter taxon, and that it is also much larger than those of the living *Aquila audax* and *Haliaeetus leucogaster*. Moreover, it is of an appropriate size to be associated with the femora and tarsometatarsus from Victoria Fossil Cave. The distal end is well-preserved except for the condylar margins, which are pitted and worn. The condylar margins on the caudal face are completely eroded away. The tibiotarsus has the following features:

(1) The width (27.5 mm) of the distal end is greater than its depth (18.1 mm). (2) The distal margin of the pons supratendineus (Figure 4.8A: PS) is angled between 30–40° relative to alignment of shaft. (3) The proximal margin of the condylus lateralis (Figure 4.8A: CL) is level with the distal-most margin of the pons supratendineus. (4) The proximal end of the pons is distinctly separated from the medial margin of the shaft. (5) The proximo-lateral scar for the extensor retinaculum (Figure 4.8A: PER) is positioned just proximal to the pons. (6) The distal scar for the extensor retinaculum (Figure 4.8A: DER) is positioned directly on the disto-medial end of the pons. (7) The sulcus m. fibularis (Figure 4.8C: SF) is deepened. (8) The condylus medialis (Figure 4.8A: CM) does not expand medially past the shaft margin. (9) The incisura intercondylaris (Figure 4.8A: II) is shallow (10) and U-shaped. (11) The distal end of the attachment scar for the spina fibulae (Figure 4.8C: SFA) is well proximal to the condylus lateralis. (12) The epicondylus medialis (Figure 4.8B: ECM) is weakly protruding, just projecting medially past the condylus medialis. (13) The sulcus extensorius (Figure 4.8A: SE) is deep.

Extant Accipitridae differ as follows (intraspecifically variable characters excluded):

#### Perninae.

**Three characters differ for all pernines:** (2) The distal margin of the pons supratendineus is angled relative to the shaft axis at 30° or less. (7) The sulcus m. fibularis is shallow. (8) The condylus medialis expands medially past the shaft margin.

**Two characters differ variably among pernines:** (4) The proximal end of the pons is separated from the medial margin of the shaft in all species except *Elanoides forficatus*, where it connects directly. (11) The distal end of the attachment scar for the spina fibulae is directly

proximal to the condylus medialis in all species except *Hamirostra melanosternon*, where it is set well proximal.

#### Gypaetinae.

**Two characters differ for all gypaetines: (4)** The proximal end of the pons is directly adjacent to the shaft margin. **(13)** The sulcus extensorius is shallow.

**Six characters differ variably among gypaetines: (2)** The distal margin of the pons supratendineus is angled  $>30^\circ$  in all species except *Polyboroides typus*, where it is almost horizontal/right angles to shaft axis. **(5)** The proximal scar for the extensor retinaculum is positioned one scar-length proximal to the pons in all species except *P. typus*, where it is two scar lengths. **(8)** The condylus medialis expands medially past the shaft margin in all species except *P. typus*, where it is not expanded. **(9)** The incisura intercondylaris is shallow in all species except *P. typus*. **(10)** The incisura intercondylaris is u-shaped in all species except *P. typus*, which is v-shaped. **(11)** The distal end of the attachment scar for the spina fibulae is just proximal to the condylus lateralis in all species except *Neophron percnopterus*, which terminates well proximal.

#### Aegyptiinae.

**Three characters differ for all aegyptiines: (1)** The width of the distal end is roughly equal to its depth. **(3)** The proximal margin of the condylus lateralis extends proximal to the distal margin of the pons supratendineus. **(7)** The sulcus m. fibularis is shallow.

**One character differs variably among aegyptiines: (11)** The distal end of the attachment scar for the spina fibulae is just proximal to the condylus lateralis in species of *Gyps* and *Necrosyrtes monachus* and is well proximal to the condyle in *Aegyptius monachus*.

#### Circaetinae.

**Four characters differ for all circaetines: (7)** The sulcus fibularis is shallow. **(8)** The condylus medialis expands medially past the shaft margin. **(11)** The distal end of the attachment scar for the spina fibulae is just proximal to the condylus lateralis. **(13)** The sulcus extensorius is moderately deep.

**No characters differ variably among circaetines.**

#### Aquilinae.

**Four characters differ for all aquilines: (2)** The distal margin of the pons supratendineus is angled  $45^\circ$  or more. **(8)** The condylus medialis expands medially past the shaft margin. **(9)** The incisura intercondylaris is deep. **(10)** The incisura intercondylaris is v-shaped.

**Two characters differ variably among aquilines: (5)** The proximal scar for the extensor retinaculum is positioned just proximal to the pons in all species except *Spizaetus ornatus*, where it

is well proximal. **(12)** The epicondylus medialis is well protruding in all species except those in *Spizaetus*, where they are weakly projecting.

#### Haliaeetinae.

**One character differs for all haliaeetines: (8)** The condylus medialis expands medially past the shaft margin.

**Four characters differ variably among haliaeetines: (2)** The distal margin of the pons supratendineus is angled between 30–40° in all species except those in *Haliaeetus*, which are angled 45° or more. **(5)** The proximal scar for the extensor retinaculum is positioned just proximal to the pons in species of *Haliaeetus*, and well proximal in all other species. **(11)** The distal end of the attachment scar for the spina fibulae is well proximal to the condylus lateralis in all species except *Haliastur indus*, where it ends directly proximal to the condyle. **(12)** The epicondylus medialis is well protruding in species of *Haliaeetus* and is weakly projecting in all others.

#### Buteoninae.

**Three characters differ for all buteonines: (2)** The distal margin of the pons supratendineus is angled at least 45°. **(5)** The medial scar for the extensor retinaculum is positioned at least one scar-length proximal to the pons. **(7)** The sulcus m. fibularis is shallow. **(8)** The condylus medialis expands medially past the shaft margin.

**No characters differ variably among buteonines.**

#### Summary.

The fossil shares the most features in common numerically with Aegypiinae, Circaetinae, and Buteoninae. However, Circaetinae and Buteoninae both differ from the fossil in that the condylus medialis expands past the medial shaft margin like most other accipitrids. Aegypiinae is the only subfamily to share the same state for this character as the fossil (condylus medialis not expanded past medial margin), which suggests that this is a feature unique to aegypiines and therefore aligns the fossil more strongly with them than buteonines and circaetines.

#### ***Tarsometatarsus (4.8F, G).***

Only trochleae metatarsorum II and III are preserved, limiting comparisons of this element. The following features are observed:

**(1)** The flange on trochlea metatarsi II (Figure 4.8F, G: TII) is oriented medioplantarly, and is long. **(2)** The fovea lig. collateralis (Figure 4.8G: FLC) is deep. **(3)** The distal margin of trochleae metatarsorum II and III (Figure 4.8F, G: TIII) are roughly equal in extent.

Extant Accipitridae differ as follows (variable characters excluded):

### Perninae.

**No characters differ for all pernines.**

**Two characters differ variably among pernines: (2)** The fovea lig. collateralis is shallow in all species except *Hamirostra melanosternon*, where it is deep. **(3)** The distal margin of trochlea metatarsi II extends further distally than III in all species except *H. melanosternon* and *Lophoictinia isura*, where trochleae metatarsorum II and III have roughly equal extent.

### Gypaetinae.

**One character differs for all gypaetines: (1)** The flange on trochlea metatarsi II is short.

**One character differs variably among gypaetines: (2)** The fovea lig. collateralis is deep in all species except *Neophron percnopterus*, which is shallow.

### Aegyptiinae.

**One character differs for all aegyptiines:(1)** The flange on trochlea metatarsi II is short.

**Two characters differ variably among aegyptiines: (2)** The fovea lig. collateralis is deep in all species except *Gyps coprotheres*. **(3)** The trochleae metatarsorum II and III are of equal extent in all species except those in *Gyps*, where trochlea metatarsi III has the greatest extent.

### Circaetinae, Aquilinae.

No significant differences.

### Haliaeetinae.

**One character differs for all haliaeetines: (3)** Trochlea metatarsi II has the greatest distal extent in all species.

**No characters differ variably among haliaeetines.**

### Buteoninae.

No significant differences.

### Summary.

The fossil bears the most similarity to the subfamilies Circaetinae, Aquilinae and Buteoninae. However, the available comparisons mainly relate to the grasping or functional ability of the toes and so are most similar to the accipitrids with large ungual phalanges and strong grasping capacity.

### ***Os metatarsale I (Figure 4.8D, E).***

The os metatarsale I is unbroken and has excellent preservation of detail.

(1) The os metatarsale I has a largely straight lateral margin (Figure 4.8D: LM), with slight curvature towards the distal end. (2) The lateral margin of the distal end is prominently inflated, forming a near 160° angle two-thirds of the way down the shaft. (3) The facet on the processus articularis tarsometatarsalis (Figure 4.8E: PAT) is long, taking up more than half the 'shaft' length, but not quite extending to the proximal point of the distal inflation. (4) A shallow indentation is present on the lateral margin of the processus articularis tarsometatarsalis (Figure 4.8E: I). (5) The medial margin has a very weak protrusion (Figure 4.8D, E: Pr) at the processus articularis tarsometatarsalis base. (6) The sulcus is bordered by low-projecting ridges (Figure 4.8E: SR) at its distal termination.

Extant Accipitridae differ as follows (variable characters excluded):

#### Perninae.

**One character differs for all pernines: (5)** The base of the processus articularis tarsometatarsalis is flat.

**Three characters differ variably among pernines: (1)** The os metatarsale I has a largely straight lateral margin, with slight curvature towards the distal end except *Chondrohierax uncinatus*, where the margin strongly curves out towards the distal end. **(2)** The angle between the lateral margin and distal end is between 160–180° in all species except *C. uncinatus*, where it is 100–120°. **(3)** The processus articularis tarsometatarsalis takes up over two-thirds of the length in *Hamirostra melanosternon* and *Lophoictinia isura*, and less than half in all other species.

#### Gypaetinae.

**No characters differ for all gypaetines.**

**Two characters differ variably among gypaetines: (1)** The lateral margin of the os metatarsale I is slightly sloped towards the distal end in all species except *Polyboroides typus*, which is largely straight. **(5)** The lateral margin has a very weak protrusion at the base of the attachment rugosity in all species except *Polyboroides typus*, where it is a prominent projection.

#### Aegyptiinae.

No significant differences.

#### Circaetinae.

**One character differs for all circaetines: (1)** The lateral margin of the os metatarsale I gradually slopes towards the distal end.

**One character differs variably among circaetines: (6)** The sulcus is bordered by a low-projecting ridge at the distal termination in *Terathopius ecaudatus*, which is absent in *Spilornis cheela*.

### Aquilinae.

**One character differs for all aquilines: (1)** The lateral margin of the os metatarsale I gradually slopes towards the distal end.

**No characters differ variably among aquilines.**

### Haliaeetinae.

**Three characters differs for all haliaeetines: (1)** The lateral margin of the os metatarsale I gradually slopes towards the distal end. **(5)** The lateral margin has a very prominent protrusion at the base of the attachment rugosity. **(6)** The sulcus is bordered by a strongly projecting ridge at its distal termination.

**No characters differ variably among all haliaeetines.**

### Buteoninae.

**One character differs for all buteonines: (1)** The os metatarsale I has a largely straight lateral margin, which sharply angles out towards the distal end.

**No characters differ variably among buteonines.**

### Summary.

The os metatarsale I has the strongest resemblance to aegyptine species, with no significant differences noted. However, it could also plausibly be a gypaetine as the distinguishing characters are present in all vulturine gypaetines, and only the non-vulturine genus *Polyboroides* differs.

### ***Comparisons with Australasian Pleistocene fossil taxa***

The accipitrid GWC/VFC taxon can be distinguished from "*Taphaetus*" *lacertosus* (whose state is in brackets) by the following features: greater physical size (smaller, especially in pelvic limb); **humerus** - the processus flexorius and condylus ventralis have roughly equal distal extent (processus flexorius shorter), interior margin of the tuberculum supracondylare ventrale is angled across the shaft (parallel to shaft), the dorsal sulcus of the m. humerotricipitalis is broad and takes up at least half the shaft width (narrow), deep fovea ligamenti collateralis (shallow), long flange of the trochleae metatarsi II (shortened).

Accipitrid GWC/VFC can be distinguished from *Hieraaetus moorei* (whose state is in brackets) by the following features: the sizes of the limb bones are significantly smaller than those of *H. moorei*; **quadrate** - there is no foramen basiorbitale (present), the processus orbitalis has a deep sulcus on the medial side (no sulcus), the processus orbitalis has a strongly proximo-medial angle (angled more medially), the condylus pterygoideus strongly projects medially, with almost

equal medial extent to the medial condyle (moderate projection with roughly half the extent of medial condyle); **coracoid** - the cotyla scapularis is small, about a quarter of the shaft width (large, nearly half shaft width), the foramen nervi supracoracoidei is on the shaft, roughly in line with the medial edge of the cotyla scapularis (set close to the medial margin of the processus procoracoideus); **scapula** - the corpus is strongly curved ventrally towards the distal end (weakly curved, mostly straight), the corpus does not increase in dorsoventral width towards the distal end (gradually increases in width); **humerus** - the proximal margin of the insertion for the m. pectoralis is equivalent to the distal margin of the crista bicipitalis (ends well distal of the crista bicipitalis), the distal end of the crista deltopectoralis is continuous with the shaft (at an angle with the shaft), the dorsal insertion of the sulcus lig. transversus is separated from the rest by a prominent ridge (continuous), the dorsal fossa m. humerotricipitalis is deep (shallow), the facies between the tuberculum supracondylare dorsale and the epicondylus dorsalis is weakly convex (prominently convex), the distance between the ventral margin of the fossa brachialis is narrow, between a quarter to a fifth of the shaft width (extremely narrow less than a fifth of shaft width), the interior margin of the tuberculum supracondylare ventrale is oriented at a high angle across the shaft (parallel to shaft); **ulna** - the depressio radialis is distinctly deepened (shallow, indistinct); **carpometacarpus** - the os metacarpale minus is arched (flattened), the processus extensorius is oriented at a 140° angle (90° angle); **pelvis** - the section of facies directly proximal to the antitrochanter has a deepened fossa present (no fossa in *H. moorei*), the antitrochanter has greater lateral projection than the crista dorsolateralis (less lateral extent in *H. moorei*), the vertebra acetabularis of the processus costalis merge to form a narrow bridge that connects to the lateral margins (broad bridge in *H. moorei*); **femur** - the tuberculum muscularis gastrocnemialis medialis is prominent (flattened in *H. moorei*), the proximal margin of the fossa poplitea is distinct from the rest of the cranial facies (continuous, less distinct in *H. moorei*), the muscular attachment proximal to the fossa poplitea is circular in shape and positioned central in the shaft (elongate oval, slightly offset laterally in *H. moorei*); **tibiotarsus** - the canalis extensorius is relatively deep (shallow), the proximal end of the pons supratendineus connects to a deepened depression adjacent to the medial shaft margin (connects to section of facies roughly equal in height to shaft margin), the proximal margin of the condylus medialis ends directly distal to the distal-most end of the pons supratendineus (ends at halfway point of pons); **os metatarsale I** - is elongate with a largely straight lateral margin (short/robust, proximodistally curving lateral margin), a small medial projection is present at the half-way point on the medial margin (prominent medial projection).

In conclusion, while accipitrid GWC/VFC shares great stoutness of the leg bones with *H. moorei*, many differences throughout the skeleton show these taxa are not closely related.

## Subfamily Gypaetinae (Vieillot, 1816)

### Mairs Cave Accipitrid Gen. et Sp. Nov. (Figs. 8–9)

**Holotype:** Cranial part of sternum SAMA P.19158.

**Diagnosis:** a large accipitrid distinguished by the following combination of characters: sternum with (1) distinct and prominently project processus labrum internum; (2) the spina externa is narrower than the apex carinae; (3) a crista medialis carinae that does not extend to the base of the spina externa. A humerus with (4) equal distance between the interior margin of the tuberculum supracondylare and proximal tip of the condylus dorsalis, and the tip of the condylus dorsalis and the dorsal margin.

**Etymology:** to be determined with naming of species.

**Age of Holotype:** Pleistocene (precise age unknown).

**Referred material:** partial distal humerus SAMA P.14528, unguis phalanx SAMA P.17139, unguis phalanx SAMA P.19157.

**Measurements (mm):** Sternum: preserved cranial width (between bases of processus craniolaterales) 69.0, height apex carinae (from apex to cranial margin of spina externa) 70.8, pila carinae width 7.8, depth sternum 51.0; Humerus: least shaft width 24.8, preserved distal width 38.9 (from ventral margin of tuberculum supracondylare ventrale to equivalently positioned lateral margin ); Unguis phalanx P.17139: length 37.1, articular facet height 15.4, width articular facet 12.9, height tuberculum flexorium 10.3, width tuberculum flexorium 8.8, length tuberculum flexorium 7.9; Unguis phalanx P.19157: length 35.5, height articular facet 16.1, width articular facet 12.5, height tuberculum flexorium 9.4, width tuberculum flexorium 9.5, tuberculum flexorium length 8.7.

**Locality and age:** 32° 10'30" S, 138° 52'23" E. Mairs Cave, Buckalowie Gorge, Flinders Ranges, SA, Australia, Pleistocene (precise age unknown).

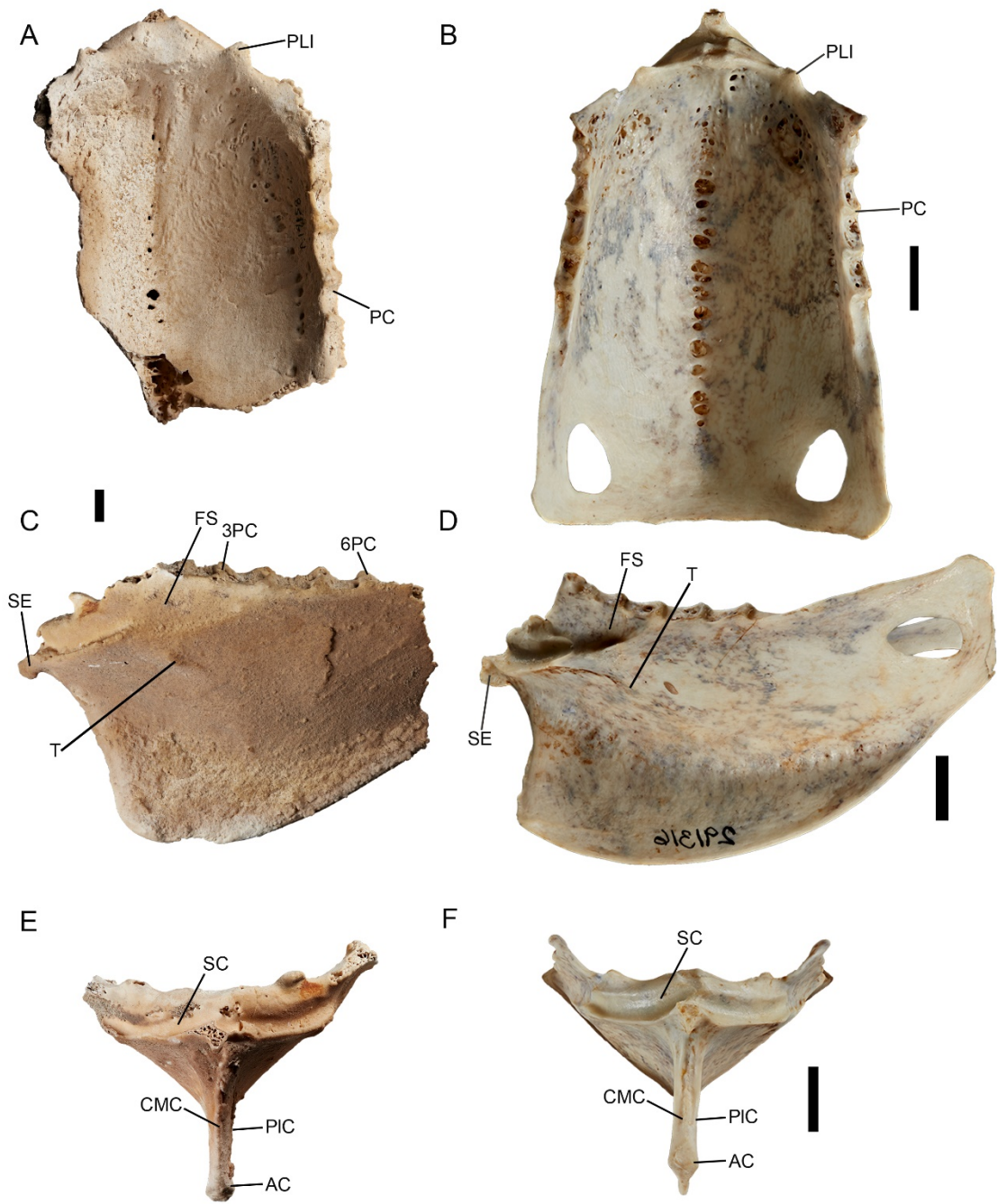


**Figure 4.9:** Sterna of the Mairs Cave accipitrid (SAMA P.19158) in dorsal (A), lateral (C) and cranial (E) view, and *Gypohierax angolensis* (USNM 291316) in dorsal (B), lateral (D) and cranial (F) view. Abbreviations: 3PC, third processus costalis; 6PC, sixth processus costalis; AC, apex carinae; CMC crista medialis carinae; FS, fossa sternocoracoidei; PC, processus costalis; PIC, pila carinae; PLI, processus labrum internum; SC, sulcus coracoidei; SE, spina externa; T, tuberculum. Scale bars 10 mm.



**Figure 4.10:** Accipitrid distal left humeri in cranial aspect (A-E) and ungual phalanges of Mairs Cave Accipitrid in lateral (H, G) and proximal H, I) aspect. (A) Mairs Cave Accipitrid SAMA P.14528, (B) *Gyps fulvus* B30269, (C) *Gypohierax angolensis* USNM 291316, (D) *Gypaetus barbatus* NHMUK S.1930.3.24.259, (E) “*Taphaetus*” *lacertosus* QM F.5507. Mairs Cave Accipitrid: (F, H) ungual phalanx SAMA P.17139, and (G, I) pedal phalanx SAMA P.19157. B–E are scaled to the same size as A. Abbreviations: AF, articular facet; CDt, condylus dorsalis tip; DECR, dorsal m. extensor carpi radialis scar; FB, fossa brachialis; LF, lateral fossa; PECR, palmar m. extensor carpi radialis scar; TF, tuberculum flexorium; TSV, tuberculum supracondylare ventrale. Scale bars 10 mm.

## Descriptions of Mairs Cave accipitrid.

### Sternum (Figure 4.9A, C, E).

The cranial half of the sternum (SAMA P.19158) is well preserved including the pila carinae, labrum internum, both processus labrum internum, sulcus coracoidei, processus costales, and pars cardiaca, while the spina externa is present but damaged.

(1) The spina externa (Figure 4.9C, D: SE) is short, (2) and appears to have been narrower than the apex carinae. (3) The left sulcus articularis coracoideus (Figure 4.9E, F: SC) overlaps the right sulcus articularis coracoideus immediately dorsal to the spina externa. (4) A pair of processus labra internum (Figure 4.9A, B: PLI) are present, (5) and are robust and cranially-prominent. (6) The crista medialis carinae (Figure 4.9E, F: CMC) does not extend to the base of the spina externa. (7) In lateral view, the apex carinae is positioned caudal to the spina externa base. (8) The apex carinae (Figure 4.9E, F: AC) is of roughly the same width as the pila carinae (Figure 4.9E, F: PIC). (9) Five processus costales (Figure 4.9A, B: PC) are preserved and a sixth likely was present

more proximally. **(10)** The pars cardiaca has very little pneumatization, with no distinct foramen pneumaticum. **(11)** There is no foramen present in the fossa sternocoracoidei (Figure 4.9C, D: FS). **(12)** The margin of the fossa sternocoracoidei extends to the (assumed) fourth processus costalis. **(13)** A tuberculum (Figure 4.8C, D: T) marks the origin point for the ligamenti sternocoracoideum laterale. **(14)** The carina depth is less than that of the sternum (measured from dorsal tip of processus costales to ventral base of pars cardiaca).

Living accipitrids differ as follows (variable characters excluded):

#### Across subfamilies.

The Elaninae and Accipitrinae are much smaller than the fossil taxon, excluding referral of the fossil species to either subfamily. **(2)** The apex carinae and the spina externa are of equal thickness in Elaninae, Perninae, most Gypaetinae, Circaetinae, Aquilinae, Haliaeetinae, Accipitrinae and Buteoninae, or the spina externa is thicker in *Gypaetus barbatus* (Gypaetinae), and all Aegypiinae excluding *Necrosyrtes monachus*.

#### Perninae.

**One character differs for all pernines: (6)** The crista medialis carinae terminates adjacent to the base of the spina externa.

**Two characters differ variably among pernines: (10)** The pars cardiaca has very little pneumatization, with no distinct foramen pneumaticum in all species except *Elanoides forficatus*, which has a deep foramen pneumaticum. **(12)** The margin of the fossa sternocoracoidei extends to the fifth or sixth processus costales in all species except *H. melanosternon*, where it extends to the fourth.

#### Gypaetinae.

**One character differs for all gypaetines: (6)** The crista medialis carinae extends to the base of the spina externa.

**Two characters differ variably among gypaetines: (3)** The left sulcus articularis coracoideus overlaps the right sulcus articularis coracoideus immediately dorsal to the spina externa in all species except *G. barbatus*, where they do not overlap. **(4)** Processus labrum internum are absent in *Neophron percnopterus*, and present in all other species.

#### Aegypiinae.

**One character differs for all aegypiines: (4)** Processus labrum internum are absent.

**Five characters differ variably among aegypiines: (3)** The left sulcus articularis coracoideus overlaps the right sulcus articularis coracoideus in species of *Gyps* and *Aegypius monachus*, and don't overlap in all other species. **(8)** The apex carinae is of roughly the same

width as the pila carinae in *N. monachus* and *Sarcogyps calvus*, while in all other species it is thinner. (9) There are six processus costales in all species except those in *Gyps* and *Aegyptius monachus*, which have five. (11) A foramen is present in all species except *Torgos tracheliotos* and *Trigonoceps occipitalis*, where it is absent. (12) The margin of fossa sternocoracoidei extends to the third processus costalis in all species except *A. monachus*, *T. tracheliotos* and *T. occipitalis*, where it extends to the fourth processus.

#### Circaetinae.

**Three characters differ for all circaetines:** (5) The processus labrum internum are weakly projecting. (6) The crista medialis carinae extends to the base of the spina externa. (7) The apex carina ends adjacent to the spina externa base.

**Several characters differ variably among circaetines:** (9) There are six processus costales in *Terathopius ecaudatus* and seven in *Spilornis cheela*. (12) The margin fossa sternocoracoidei extends to the fourth processus costalis in *S. cheela*, and the third in *T. ecaudatus*. (14) The carina is shallower than the sternum in *T. ecaudatus* and is of equal depth in *S. cheela*.

#### Aquilinae.

**Seven characters differ for all aquilines:** (4) Processus labrum internum are small or absent. (6) The crista medialis carinae extends to the base of the spina externa. (7) The apex carina ends adjacent to the spina externa base. (9) There are seven processus costales. (10) The pars cardiaca is pneumatized, though in some individuals it can be fused over. (12) The margin fossa sternocoracoidei extends to the fifth processus costalis. (14) The carina depth is equal to that of the sternum.

**No characters differ variably among aquilines.**

#### Haliaeetinae.

**Five characters differ for all haliaeetines:** (5) The processus labrum internum are small and weakly projecting. (6) The crista medialis carinae extends to the base of the spina externa. (7) The apex carina ends adjacent to the base spina externa. (9) There are seven processus costales. (14) The carina depth is equal to that of the sternum.

**No characters differ variably among haliaeetines.**

#### Buteoninae.

**Six characters differ for all buteonines:** (4) Processus labrum internum are absent. (6) The crista medialis carinae terminates adjacent to the base of the spina externa. (7) The apex carina ends adjacent to the base of the spina externa. (9) There are seven processus costales.

(12) The margin of the fossa sternocoracoidei extends to the fifth or sixth processus costalis. (14) The carina depth is equal to the sternum.

**One character differs variably among buteonines: (10)** A distinct foramen pneumaticum is present in *Ictinia mississippiensis*, and pneumatisation is present in the pars cardiaca of all species.

#### Summary.

Based on the listed differences above, the Mairs Cave Accipitrid bears the most similarity to species in Perninae and Gypaetinae. A pair of large, robust processus labrum internum (4, 5) are only seen in pernines and most gypaetines, which excludes the fossil from all other subfamilies. However, the fossil is much larger than any known pernine accipitrid. Additionally, while *Gypaetus barbatus* differs from the fossil in relation to having the left sulcus articularis coracoideus overlapping the right (3), sulci in most gypaetine species do not overlap. Pernines are much smaller taxa and among gypaetines only *Neophron percnopterus* lacks a processus labrum internum, thus overall, the fossil is more similar to species in the Gypaetinae than the Perninae.

#### **Humerus (Figure 4.10A).**

Only the distal shaft and proximal-most section of the distal end has been preserved, including the fossa brachialis, insertion scars for the m. extensor carpi radialis, tuberculum supracondylare dorsale, and tuberculum supracondylare ventrale. The condyles are completely broken off. The following features could be observed:

(1) The fossa brachialis (Figure 4.10A: FB) has a deepened, circular ventral scar, with a shallow section extending proximo-dorsally from it. (2) The fossa brachialis is not pneumatic. (3) The dorsal margin of the fossa brachialis is separated from the shaft margin by a distance less than a quarter of the fossa width. (4) The ventral margin of the fossa is curved parallel to the shaft margin (5) the intervening area between which is broad (1/3rd of fossa width). (6) The palmar insertion scar for the m. extensor carpi radialis (Figure 4.10A: PECR) is a broad, oval shape. (7) The dorsal insertion scar for the m. extensor carpi radialis (Figure 4.10A: DECR) is small, shallow and circular/round. (8) The interior margin of the tuberculum supracondylare ventrale (Figure 4.10A: TSV) is oriented at a 45–50° proximodorsally across the shaft. (9) The distance between the interior margin of the tuberculum supracondylare and proximal tip of the condylus dorsalis is roughly equal to the distance between the tip of the condylus dorsalis and the dorsal margin.

Extant accipitrids differ as follows (variable characters excluded):

#### Across Subfamilies.

(9) The distance between the interior margin of the tuberculum supracondylare and proximal tip of the condylus dorsalis is greater than that between the tip of the condylus dorsalis and the dorsal margin in all species except the Elaninae, *Elanoides forficatus*, *Lophoictinia isura*, *Hamirostra melanosternon* (Perninae), and Gypaetinae (excluding *Polyboroides typus*).

#### Perninae.

**One character differs for all pernines: (3)** The dorsal margin of the fossa brachialis is separated from the shaft margin by a quarter or less of the fossa width.

**Three characters differ variably among pernines (4, 5)** The ventral margin of the fossa forms a roughly straight line which is separated from the shaft margin by a third of the fossa width in all species except *Chondrohierax uncinatus*, where margin is curved and the distance is roughly a quarter of the fossa width. (8) The interior margin of the tuberculum supracondylare is aligned across the shaft in all species except *Elanoides forficatus*, where it is nearly parallel to the axis.

#### Gypaetinae.

**No characters differ for all gypaetines.**

**One character differs variably among gypaetines: (3)** The dorsal margin of the fossa brachialis is separated from the shaft margin by a quarter of the fossa width in *Polyboroides typus* and *Neophron percnopterus*, and less than a quarter of the width in *G. angolensis* and *Gypaetus barbatus*.

#### Aegyptiinae.

**Two characters differ for all aegyptiines: (7)** The dorsal insertion scar for the m. extensor carpi radialis is large. (8) The interior margin of the tuberculum supracondylare is aligned parallel to the shaft.

**No characters differ variably among aegyptiines.**

#### Circaetinae.

**Two characters differ for all circaetines: (1)** The fossa brachialis is consistently deep. (3) The dorsal margin of the fossa brachialis is separated from the shaft margin by a quarter of the fossa width.

**No characters differ variably among circaetines.**

#### Aquilinae.

**Five characters differ for all aquilines: (1)** The fossa brachialis is consistently shallow. (3) The dorsal margin of the fossa brachialis is separated from the shaft margin by a quarter of the

fossa width. (4) The ventral fossa margin forms a roughly straight line (5) roughly a quarter of the fossa width. (7) The dorsal insertion scar is large.

**No characters differ variably among aquilines.**

#### Haliaeetinae.

**Four characters differ for all haliaeetines: (1)** Same as fossil, though the ventral deepening is not as great. (4) The ventral fossa margin forms a roughly straight line (5) roughly a quarter of the fossa width. (7) The dorsal insertion scar is large.

**One character differs variably among haliaeetines: (3)** The dorsal margin of the fossa brachialis is separated from the shaft margin by a third of the fossa width in all species except *Milvus migrans*, which is roughly a quarter.

#### Buteoninae.

**Three characters differ for all buteonines: (1)** The fossa brachialis is consistently shallow. (4) The ventral fossa margin forms a roughly straight line (5) The ventral fossa margin is separated from the ventral shaft by a quarter or less of the fossa width.

**One character differs variably among buteonines: (3)** The dorsal margin of the fossa brachialis is separated from the shaft margin by a quarter of the fossa width in all species except *Buteo nitidus*, which is by a third.

#### Summary.

The humerus from the Mairs Cave Accipitrid most closely resembles species of Gypaetinae, as only one character consistently differs across all assessed gypaetines. It is notably larger than the compared species, although the unexamined *Gypaetus barbatus* might approach a similar size.

#### ***Ungual phalanx (Figure 4.10F–I).***

The two unguis phalanges are nearly perfectly preserved, missing only the very tip of the distal end. Due to a lack of associated pedal phalanges, it is uncertain to which digit these unguis belong. Both specimens are notably larger than unguis phalanges one and two in the observed specimens of *Aquila audax*. The following features are observed:

(1) In both, the height of the articular facet (Figure 4.10H, I: AF) is greater than its width. (2) The width of the tuberculum flexorium (Figure 4.10H, I: TF) in P.17139 is less than its height. (3) The width of the tuberculum flexorium in P.19157 is roughly equal to its height. (4) The foramina on the sides (Figure 4.10G: LF) of the tuberculum flexorium are distinct and deep in P.17139.

### **Comparisons to Australasian Pleistocene taxa**

The Mairs Cave Accipitrid can be separated from both "*Taphaetus*" *lacertosus* and accipitrid GWC/VFC taxon by the following features: the fossil represents birds that are significantly larger than both; the distance between the proximal tip of the condylus dorsalis and the margin of the tuberculum supracondylare ventrale on the humerus is equal to the distance between the condylus dorsalis and the lateral margin of the face between the tuberculum supracondylare dorsale and the epicondylus dorsalis (greater in "*Taphaetus*" *lacertosus* and accipitrid GWC/VFC).

The Mairs Cave Accipitrid can be distinguished from *Hieraaetus moorei* (state in brackets) by the following features: the sternum has prominent processus labrum internum present (absent in *H. moorei*), and in the humerus the palmar insertion for the m. extensor metacarpi radialis forms a distinct line (circle-shaped in *H. moorei*), the ventral margin of the fossa forms a curved line parallel to the shaft margin (straight in *H. moorei*), the distance between the ventral fossa brachialis margin and the ventral shaft margin is between 1/3 to 1/4 shaft width (less than 1/4 shaft width in *H. moorei*), the distance between the tip of the condylus ventralis and the margin of the tuberculum supracondylare ventrale equal to the distance between the condylus ventralis and the lateral margin of the face between the tuberculum supracondylare dorsale and the epicondylus dorsalis (greater width in *H. moorei*), the interior margin of the tuberculum supracondylare ventrale is oriented at least 45–50° across the shaft (oriented parallel to shaft).

### **Summary**

The Mairs Cave Accipitrid most closely resembles vulturine species of Gypaetinae in regards to the humerus (fossa m. brachialis depth, apneumatic state, ventral margin shape and width; shape of insertions for the m. extensor carpi radialis; orientation of the interior margin of the tuberculum supracondylare ventrale; distance between the interior margin of the tuberculum supracondylare and proximal tip of the condylus dorsalis) and sternum (with the only major difference being the extent of the crista medialis carinae to the spina externa). It differs from any living species of gypaetine by the spina externa being narrower than the apex carinae in cranial view and the crista medialis carinae terminating proximal to the spina externa. The fossil is significantly larger than *Neophron percnopterus* and *Gypohierax angolensis*, and is notably larger than *Gypaetus barbatus*, a species which is slightly larger than *Aquila audax*.

Based on the preserved section of the distal humerus, the Mairs Cave accipitrid differs markedly from accipitrid GWC/VFC in morphology as well as larger size. This reveals the coexistence of at least two large inland fossil accipitrids during the Pleistocene alongside "*Taphaetus*" *lacertosus* and *Aquila audax*.

In relation to extinct gypaetines from the Pleistocene, the Mairs Cave accipitrid would have been significantly larger than most known species. The Pleistocene *Neogyps errans* and *Neophrontops* species were close in size to the extant species of *Gypohierax* and *Neophron* respectively (see Galetti et al. 2017). It is also larger than the Miocene gypaetines *Mioneophron longirostris*, which was similar in size to the extant *Neophron* (Li et al. 2016), and *Anchigyps voorhiesi*, which was roughly the same size as *Gypohierax* (Zhang et al. 2012a). The holotype for the Miocene *Arikarornis macdonaldi* was specifically noted by the author to be equivalent in size to *Buteo borealis* (Howard 1966), a much smaller bird than the Mairs Cave accipitrid. *Palaeoborus rosatus* was within the size range of *Aquila audax* based on measurements of the holotype (Miller and Compton 1939), with *P. umbrosus* and *P. howardae* also falling into a similar range based on their holotypes (Cope 1874; Wetmore 1936).

#### **4.3.2 Body mass estimation**

Using the mass algorithms of Field et al. (2013), Campbell and Marcus (1992), and Campbell and Tonni (1983), body mass was predicted for accipitrid GWC/VFC (Table 4.4). Accipitrid GWC/VFC had a considerable range of predicted body masses, though some of the more extreme values are most likely the result of over- or under-estimates. The length of the humerus and coracoid gave the very low values of 2.9 kg and 3 kg respectively (Table 4.4), within the size range of a male *Aquila audax* (Marchant and Higgins 1993). This seems unlikely based on the other mass estimates and the overall robustness of the bones, and Worthy and Holdaway (2002) commented on how humerus length consistently produced low mass predictions compared to that of living raptors. In contrast the largest femur, SAMA P.41514, generated a predicted mass of 19.4–19.5 kg based on least shaft circumference (lsc) (Table 4.4), but it has been noted that predictions derived from the femur of birds tend to overestimate actual mass (Handley et al. 2016). The coracoid and tibiotarsus both generated similar predicted masses of 12.3 kg (coracoid HAF, Table 4.4) and 12.1–12.3 kg (tibiotarsus lsc, Table 4.4), more than twice the mass of the heaviest female *Aquila audax* (Marchant and Higgins 1993). The coracoid used for this prediction was part of the Green Waterhole Cave individual, which is assumed to be an individual of the smaller sex like the Victoria Fossil Cave humerus. Therefore, this mass predicted by the coracoid would be within the range of the smaller sex. Based on the size difference between the two femora from Victoria Fossil Cave (see Table 4.3, 4.4), individuals of the larger sex of accipitrid GWC/VFC could have been at least several kilograms heavier, perhaps even up to the 16 kg estimated for the largest specimens of *Hieraaetus moorei* (Worthy and Holdaway 2002).

Species	Humerus length	Humerus proximal width	Humerus least shaft width	Humerus distal width	Femur length	Femur proximal width	Femur least shaft width	Femur distal width	Tibiotarsus distal width	Tibiotarsus least shaft width
Accipitrid GWC/VFC	178.3	37.1	15.7	33.3	131.1–145.5	32.5–38.3	16.2–18.6	32.3–35.2	27.6	14.6
<i>Aquila Audax</i>	179.7, (10), 167.6–191.8, 9.0	34.4, (10), 32.7–36.5, 1.7	11.8, (10), 10.6–13.4, 0.9	29.5, (10), 28.1–31.4, 1.2	112.4, (10), 103.3–117.7, 4.4	24.9, (10), 23.1–27.7, 1.6	11.3, (10), 10.1–12.3, 0.8	23.3, (10), 21.5–25.6, 1.5	19.2, (10), 17.8–20.8, 1.2	10.1, (10), 9.4–11.1, 0.6
<i>Hieraaetus moorei</i>	232.4, (20), 208–259.9, 16.2	52.7, (18), 42.3–58.3, 4.5	17.9, (21), 15.6–21.0, 1.7	41.3, (21/20), 37.1–47.3, 3.0	162.8, (17), 140.3–176.0, 10.5	42.2, (17), 36.0–47.5, 3.8	18.3, (18), 15.3–19.9, 1.5	45.4, (18), 36.2–52.5, 5.1	34.1, (15), 27.3–39.8, 4.0	14.2, (17), 11.8–16.6, 1.6
<i>Haliaeetus leucogaster</i>	189.4, (10), 180.4–197.3, 6.4	35.5, (10), 32.9–37.8, 1.6	13.1, (10), 11.9–14, 0.6	30.6, (10), 28.6–32.7, 1.4	102.2, (10), 96.9–106.3, 3.4	24.3, (10), 22.4–25.8, 1.2	11.9, (10), 10.8–12.8, 0.6	21.6, (10), 20.1–23.1, 1.2	18.1, (10), 16.3–19.4, 1.2	9.9, (10), 8.8–11.4, 0.7
<i>Aegyptius monachus</i>	212.7	37.4	14.3	36.2	112.6	28.3	11.6	23.8	18.7	9.6
<i>Gyps coprotheres</i>	260.1	45.5	18.0	35.8	134.2	32.1	15.2	30.4	23.1	12.3
<i>Necrosyrtes monachus</i>	154.5	28.4	10.7	26.5	79.1	18.4	8.6	16.6	13.9	7.5

**Table 4.3:** Comparative measurements of the humerus, femora and tibiotarsus in accipitrid GWC/VFC to *Aquila audax*, *Hieraaetus moorei*, *Haliaeetus leucogaster*, *Aegyptius monachus*, *Gyps coprotheres* and *Necrosyrtes monachus*. In *Aquila audax*, *Haliaeetus leucogaster* and *Hieraaetus moorei* the data represents the average, number of specimens, range, and standard deviation of measurements. Specimens used: *Aquila audax* FUR 085, FUR 125, SAMA B46162, SAMA B46992, SAMA B31109, SAMA B46161, SAMA B47814, SAMA B32850, SAMA B32849, SAMA B49025; *Haliaeetus leucogaster* SAMA B49459, SAMA B58700, SAMA B46632, SAMA B56381, SAMA B59108, SAMA B56082, SAMA B48927, SAMA B49688, SAMA B48773, SAMA B37344; *Hieraaetus moorei* data taken from Worthy and Holdaway (2002); *Aegyptius monachus* R553; *Gyps coprotheres* ANWC 22724; *Necrosyrtes monachus* USNM 620646.

Accipitrid GWC/VFC						
Specimen	Element	Measurement (mm)	Regression output	BM regression output	Predicted BM (g)	Formula
AM F.106562	Distal tibiotarsus	45 (LSC)	1.6	4.1	12116.8	Campbell and Marcus 1992 tib LSC
		45 (LSC)	1.6	4.1	12280.0	Campbell and Tonni 1983 tib LSC
SAMA P.41513	Femur	55 (LSC)	4.0	9.5	13461.6	Field et al. 2013 fem LSC
		55 (LSC)	1.7	4.1	13521.2	Campbell and Marcus 1992 fem lsc
SAMA P.41514	Femur	64 (LSC)	4.2	9.9	19366.9	Field et al. 2013 fem LSC
		64 (LSC)	1.8	4.3	19485.0	Campbell and Marcus 1992 fem lsc
SAMA P.41517	Humerus	52 (LSC)	3.9	9.1	9023.8	Field et al. 2013 hum LSC
		178.3 (length)	5.2	7.9	2863.4	Field et al. 2013 hum L
SAMA P.42487	Coracoid	20.9 (HAF length)	3	9.4	12295.5	Field et al. 2013 cor HAF length
		16.1 (SW)	2.8	9.3	11247.7	Field et al. 2013 cor SW
		73	4.3	8	3037.5	Field et al. 2013 cor L (from lateral process)

**Table 4.4:** Mass estimates of the tibiotarsus, femur, humerus, and coracoid from accipitrid GWC/VFC. Predicted weight is measured in grams (g). Abbreviations: BM, body mass; cor, coracoid; fem, femur; HAF, humeral articular facet; hum, humerus; L, length; LSC, least shaft circumference; SW, shaft width; tib, tibiotarsus.

### 4.3.3 Phylogenetic Analyses

#### ***Analysis 1: Parsimony, morphology only, ordered characters***

The first analysis was restricted to morphological data, with 69 of the multistate characters ordered (see SI.1). The resulting 14 most parsimonious trees (hereafter MPTs) had a tree length of 1735 steps and the strict consensus tree is shown in (Figure 4.11). The topology of the consensus tree differed greatly from those proposed by recent molecular phylogenies, as anticipated due to the lack of molecular data or backbone constraints. The Accipitridae was strongly supported as

monophyletic (73% bootstrap support), as was its pairing with *Pandion* (97% bootstrap support). The non-Australian pernines were resolved as sister to all remaining accipitrids, the latter of which were weakly supported as a clade (49%). Within the remaining accipitrids the Elaninae was robustly supported as a monophyletic clade (99%), while all other subfamilies formed a very weakly supported polytomous clade (14%).

The Gypaetinae and Aegypiinae formed a weakly supported clade with *Polyboroides typus* as the most basal species (32%). The gypaetine species were not monophyletic and formed a grade of taxa wherein each branched off individually with weak support (40% or less). The Aegypiinae formed a monophyletic clade with moderate support (61%) sister to *Gypaetus barbatus*.

A monophyletic Aegypiinae clade was supported by 13 unambiguous (optimisation-independent) characters, but only one was compelling: Character 51 state 0 (CI 0.5) (the condylus caudalis of the quadrate is well differentiated from the other condyles). The Gypaetinae and Aegypiinae were separated from all other taxa by 11 unambiguous characters, three of which were compelling: Character 8 state 1 (CI 0.5) (the ossa supraorbitalia of the skull are present but reduced), character 56 state 0 (CI 0.5) (the caudal margin of the fossa aditus canalis neurovascularis of the mandible forms a crest), and character 247 state 1 (CI 0.5) (the sulcus hypotarsi is set plantar relative to sulcus flexorius on the tarsometatarsus).

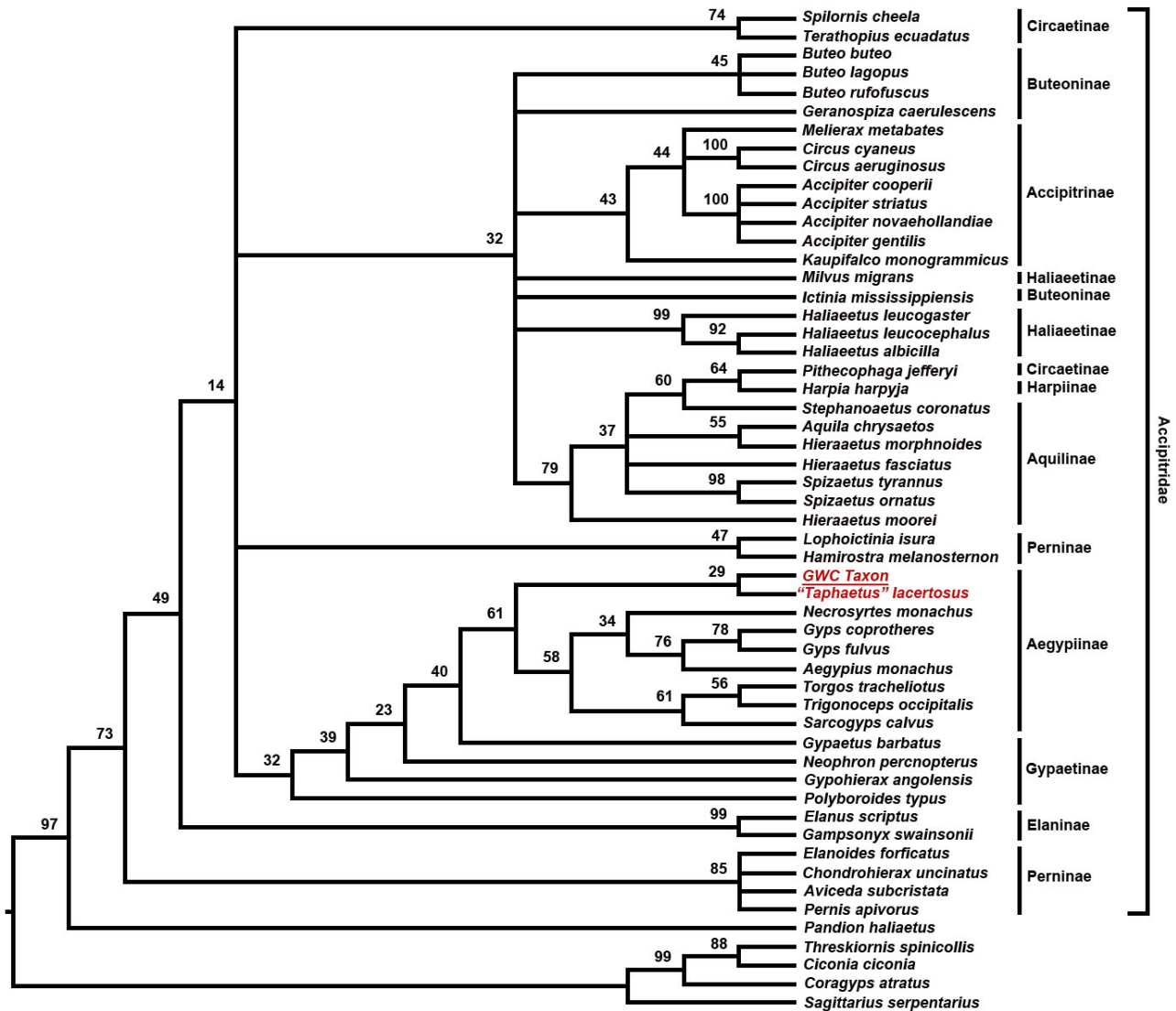


**Figure 4.11:** Results of phylogenetic analysis 1; Parsimony analysis of morphological (ordered) data. Strict consensus of 14 most-parsimonious trees. Tree length = 1735, MPT = 14, CI = 0.2294, HI = 0.7706, RI = 0.6080. Bootstrap values are given at each node. Fossil taxa are coloured red. Accipitrid GWC/VFC is listed as GWC Taxon and underlined.

### Analysis 2: Parsimony, morphology and molecular, ordered characters

In this second analysis, molecular data was added to the data matrix to constrain the extant species to accepted phylogenetic relationships based on abundant molecular data (Ronquist et al. 2012), and the analysis was rerun (Figure 4.12). Three MPTs were found, each with a tree length of 1869 steps. Monophyly of the Accipitridae was strongly supported (Bootstrap support 94%), and only four divergence nodes had support less than 50%.

The Aegyptiinae-Circaetinae clade had weak support (49%) but was strongly supported as sister to the Aquilinae-Harpiinae-Accipitrinae-Buteoninae-Haliaeetinae clade (84%). Accipitrid GWC/VFC formed a clade with "Taphaetus" and living aegyptiines with modest support (57%). "Taphaetus"-Aegyptiinae had strong support as a clade (82%), with "Taphaetus" lacertosus

resolved as basal to the living species. The genus *Aegypius* formed a clade with *Torgos* with very strong support (95%). The *Sarcogyps-Torgos-Trigonoceps-Aegypius* subclade had strong support (79%), while *Necrosyrtes-Gyps* had weak support (35%).

There are eight unambiguous (optimisation-independent) characters that distinguish Aegypiinae from Circaetinae and support the fossil's inclusion into the clade, though only three have low homoplasy: Character 51 state 0 (CI 0.5) (the condylus caudalis of the quadrate is well differentiated from the other condyles), 101 state 1 (CI 0.5) (the omal margin of the processus procoracoideus of the coracoid is oriented in a distal slope relative to the sternal margin), and 102 state 0 (CI 1.0) (the cotyla scapularis of the coracoid is less than a quarter of the shaft width in size).

The living Aegypiinae plus "*Taphaetus*" form a monophyletic clade sister to accipitrid GWC/VFC supported by three unambiguous characters: character 143 state 0 (CI 0.29) (humerus, processus flexorius does not project distal to the condylus ventralis), 151 state 2 (CI 0.18) (humerus, fossa m. brachialis separated from shaft margin by an intervening area <1/4 of the shaft width), and 154 state 0 (0.14) (humerus, interior margin of tuberculum supracondylare ventrale oriented parallel relative to shaft margin). However, all three characters have high homoplasy.

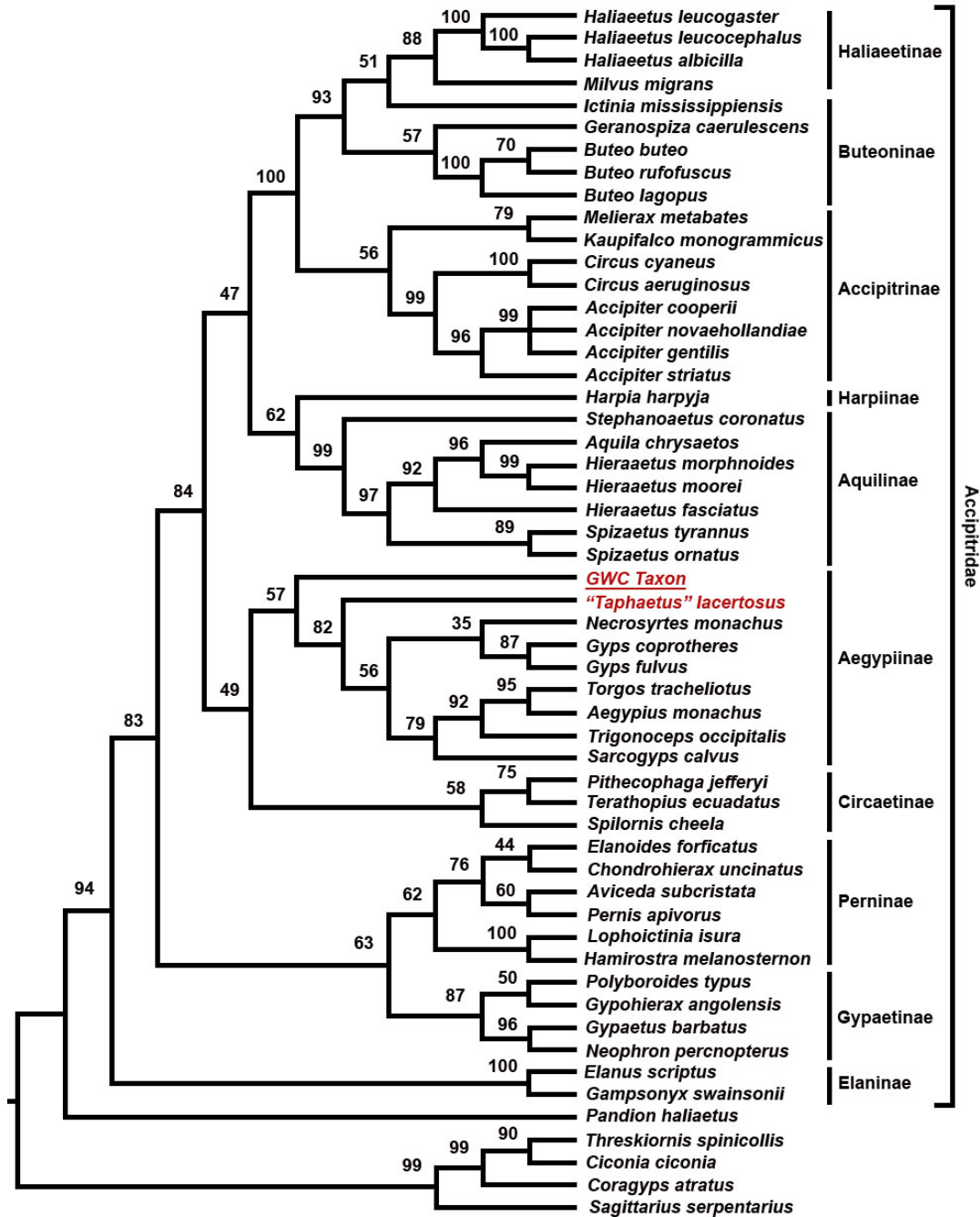


**Figure 4.12:** Results of phylogenetic analysis 2; Parsimony analysis of molecular and morphological data, characters ordered. Strict consensus of three most-parsimonious trees. Tree length = 1869, MPT = 3, CI = 0.2164, HI = 0.7836, RI = 0.5775. Bootstrap values are given at each node. Fossil taxa are coloured red. Accipitrid GWC/VFC is listed as GWC Taxon and underlined.

### Analysis 3: Bayesian inference, morphology + DNA, ordered

The Bayesian analysis produced a tree with very similar topology to that in the parsimony analysis using the same data, with support values for nodes very strong in all but a few cases (Figure 4.13).

The Circaetinae-Aegyptiinae had strong support as a monophyletic clade (95%). The Circaetinae clade had strong support (100%) as did the Aegyptiinae clade (95%). All the clades within Aegyptiinae had more than 80% support, except for the *Necrosyrtes-Gyps-Taphaetus* clade (65%) and the “*Taphaetus*”-*Gyps* clade (65%), likely due to “*Taphaetus*” lacking molecular data. The accipitrid GWC/VFC-Aegyptiinae clade had very strong support (95%), with the fossil being basal to all other species.

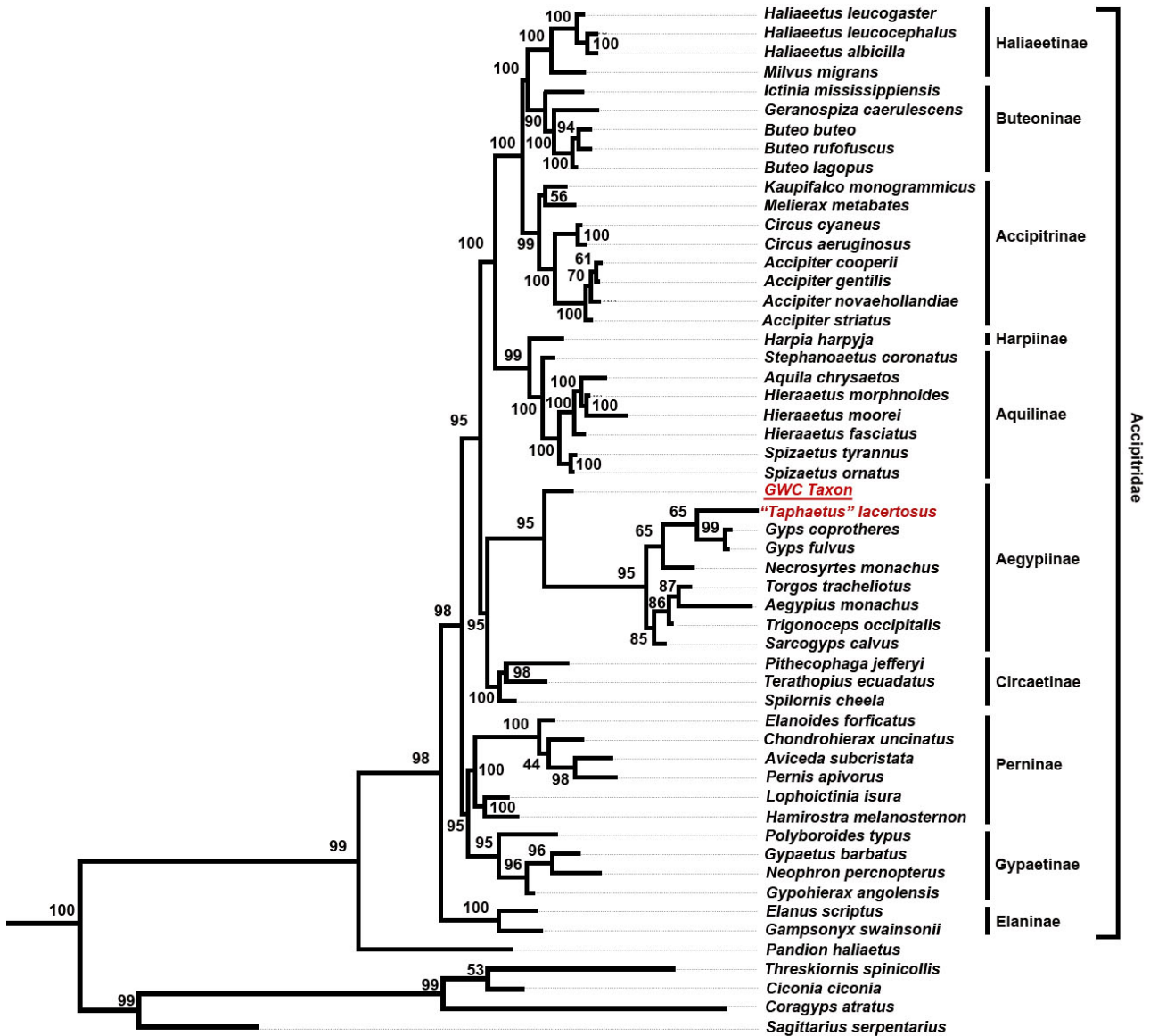


**Figure 4.13:** Results of phylogenetic analysis 3; combined molecular and morphological data (ordered, unlinked branches) analysed with Bayesian methods. Support values shown at nodes. Majority-rule consensus tree. Fossil taxa are coloured red. Accipitrid GWC/VFC is listed as GWC Taxon and underlined.

## Summary

All phylogenetic analyses resolved accipitrid GWC/VFC as sister to living Aegypiinae, with the only difference being the relationship of the fossil to "*Taphaetus*" *lacertosus* and the level of support for its position. Parsimony morphology-only analyses provided the weakest results (in terms of both topological comparisons to accepted relationships, and support values), while the Bayesian inference analysis combining morphology and molecular data provided the strongest. The parsimony molecular-morphology results indicate that the similarities between accipitrid GWC/VFC and other aegypiines were driven by unambiguous characters in the quadrate and coracoid, which are currently unknown in "*Taphaetus*" *lacertosus*. It was found that missing data do not have an impact on the position of the taxa, as an analysis using only the morphological characters the fossil had data for (plus molecular data) produced the same results. The accipitrid GWC/VFC taxon could be interpreted as either a basal species of Aegypiinae or as its immediate sister group.

## 4.4 DISCUSSION

The surveyed fossils could be separated into two taxa based on differences in size and morphology. The first, described as accipitrid GWC/VFC, has the most abundant fossil material, being present in deposits from Leana's Breath Cave (Nullarbor, Western Australia), Victoria Fossil Cave (Naracoorte, South Australia) Green Waterhole/Fossil Cave (Tantanoola, South Australia), and the Wellington Caves (Wellington, New South Wales). This species had a similar wingspan to *Aquila audax* but would have been more than twice as heavy (Table 4.3, 4.4), and phylogenetically resolved as a member of the Aegypiinae subfamily. The second taxon, described as Mairs Cave accipitrid, only had material present in Mairs Cave (Flinders Ranges, South Australia). Based on the size of the fossil material, this taxon was up to twice the size of *Aquila audax*.

### 4.4.1 Phylogenetic relationships

The diversity and phylogenetic relationships of Australian fossil accipitrids have been little studied, likely because of their incompleteness. Here we have described relatively fragmentary fossils and derived phylogenetic hypotheses that were constrained by molecular data for the extant compared species. Accipitrid GWC/VFC was consistently resolved as closely related to both the extinct aegypiine "*Taphaetus*" *lacertosus* and to the living Aegypiinae in all phylogenetic analyses, even though it is morphologically distinct from them in multiple ways.

If accipitrid GWC/VFC was a member of Aegypiinae, its basal position as the sister taxon to extant members of that clade would imply that it was part of a lineage that diverged a long time ago. Current estimates place the divergence of Aegypiinae into its extant genera at approximately 10–8 Ma during the late Miocene (Nagy and Tökölyi 2014; Mindell et al. 2018), which most likely

would also correlate with when the subfamily began to specialise in scavenging. The phylogenetic position of accipitrid GWC/VFC suggests it could have diverged prior to 10–8 Ma and so potentially originated before the shift towards obligate scavenging in this clade. However, it is also possible that the species is instead a derived (nested) Aegyptiinae that has reverted back to a plesiomorphic condition for certain characters, and its (apparent) basal position in the phylogeny is instead being driven by the more eagle-like features of the fossils. Missing data are known to drive taxa relatively basal in topologies (Sansom 2015) but in this case an analysis based only on morphological characters known for the fossils retrieved the same topology, suggesting missing data are not driving this relationship.

We consider that the Mairs Cave Accipitrid is too fragmentary to use in a phylogenetic analysis, but morphological comparisons suggest an affinity with the Gypaetinae subfamily, notably the presence of large processus labrum internum on the sternum, along with the equal distance between the proximal tip of the condylus dorsalis to both the interior margin of the tuberculum supracondylare and the dorsal margin.

#### **4.4.2 Diversity of Pleistocene Australian Accipitridae**

The accipitrid GWC/VFC and the Mairs Cave accipitrid increase the diversity of known Pleistocene Accipitridae in Australia. Added to "*Taphaetus*" *lacertosus* and *Aquila audax*, this brings the number of large inland Pleistocene accipitrid species up to at least four, three of which are now known to have had vulturine affinities. The fossil taxon *Necrastur alacer* is rather smaller and so not relevant here, and nor does it have a specific age assigned to the locality it came from (Worthy and Nguyen 2020) and could have occurred either during the Pliocene or the Pleistocene. Assuming the living species were also present during the Pleistocene, this brings the total diversity of Australian Accipitridae of that time up to at least 20 species and seven subfamilies.

More significantly, the presence of two additional large accipitrids during the Pleistocene in inland Australia fills a notably empty niche. In contemporary Australia, the only large inland accipitrid is *Aquila audax*, which both hunts and scavenges for food. The largest females of this species can potentially weigh just over 5 kg, though the average is 4.2, while males can reach up to 4 kg but on average weigh 3.1 (Marchant and Higgins 1993). Having only one large predatory accipitrid present in a continent the size of Australia is highly unusual, more especially so considering that until the late Pleistocene there was a diverse range of mammals that would have provided suitable food resources. In Africa, for example, there are now at least 10 predatory eagles of a similar size to or larger than *Aquila audax*, and 12 species of accipitrid vultures from both subfamilies (Dickinson and Renssen 2013). Africa is substantially larger than Australia, however, so a better comparison might be the accipitrid diversity present in the similarly-sized region of North America south of the arctic and sub-arctic zones. In present day North America, there are two species of large eagles commonly found: the bald eagle *Haliaeetus leucocephalus* and the golden

eagle *Aquila chrysaetos*, with the typically Eurasian white-tailed eagle *Haliaeetus albicilla* and Steller's sea eagle *Haliaeetus pelagicus* occasionally sighted in northern regions such as Alaska (Clark and Wheeler 1983). However, North America is also inhabited by three species of scavenging New World vultures Cathartidae: the turkey vulture *Cathartes aura*, the black vulture *Coragyps atratus*, and the California condor *Gymnogyps californianus*. The fossil record also reveals that the North American accipitrid fauna was much more diverse up until the Late Pleistocene, with an additional four large eagles, one New World vulture, two Old World vultures, and two teratorms known to have coexisted with the extant species at sites such as Rancho la Brea (Jefferson 1991). This is an extremely diverse assemblage of large predatory and scavenging birds compared to what is known from Pleistocene Australia. Therefore, the presence of two additional large Australian accipitrids, especially ones that appear to have been capable of hunting large prey or had an obligate scavenging ecology, brings the family's diversity closer to what might be expected from a continent of Australia's size.

#### **4.4.3 Palaeoecology**

##### ***Accipitrid GWC/VFC***

The morphology of accipitrid GWC/VFC is notably robust, with short robust wing bones and relatively larger robust pelvis and leg bones. The pelvis is especially deep and robust in the anterior ilial region, capable of housing large muscles, and the femora and tibiotarsi are very large, up to 20 percent longer and almost 40 percent wider in the shaft than *A. audax* in the case of the former (see Table 4.3). Having such a relatively robust pelvis and leg bones combined with a tarsometatarsal morphology suggesting the presence of robust talons is convergent on the morphology of *H. moorei* and indicates that this bird was capable of predating on large prey. The wing bones are short but robust, suggesting a predominantly flapping flight behaviour again similar to that envisaged for *H. moorei* (Holdaway 1991; Worthy and Holdaway 2002). If we are correct in thinking that the holotype humerus is from the smaller sex represented by the smaller femur, then a large female accipitrid GWC/VFC would likely have an even more robust humerus than the holotype. Given the few specimens referred to this taxon, it may be that the largest individuals of accipitrid GWC/VFC were equivalent in size to the largest of *H. moorei* (see Worthy and Holdaway 2002). The largest available femur of accipitrid GWC/VFC is 10% longer and 13% more robust than its smaller counterpart (Table 4.3), (Marchant and Higgins 1993), while the largest femur in *H. moorei* is up to 20% longer and 23% more robust than its smallest counterpart (see Table 4.3; Worthy and Holdaway 2002).

That the legs were so large and robust compared to the wings strongly indicates that accipitrid GWC/VFC was an active predator rather than a scavenger, much like *Hieraaetus moorei* (see Worthy and Holdaway 2002). Working on the assumption that both the holotype humerus and the GWC individual represent the smaller sex, the smaller femur SAMA P.41513 is 27% shorter in

length than the humerus (see Table 4.3). In the predatory *Aquila audax* it is an average of 38% shorter, and in *H. moorei* the average difference is 30% (Table 4.3). In contrast, the femur of *Necrosyrtes monachus* USNM 620646 is 49% shorter than the humerus, while in *Aegyptius monachus* R553 it is 47% shorter. The prominent lateral flanges on the trochleae of the tarsometatarsus in accipitrid GWC/VFC are also absent in scavenging aegyptiines but present in active hunters like *Aquila audax*. Based on the size of the trochleae, as well as the overall robustness of the pelvis and the pelvic limb bones, we predict that the ungual phalanges of accipitrid GWC/VFC would be much larger than those of *A. audax*, but smaller than *H. moorei*. We would also predict that ungual phalanges I and II would exhibit very distinct hypertrophy compared to III and IV, as predatory accipitrids – especially those that grapple with large prey – often exhibit this configuration.

To make estimates about the size range of the potential prey of accipitrid GWC/VFC, observations of other large accipitrids known to attack large animals can be compared. *Hieraaetus moorei* (Haast, 1872) is an example of an accipitrid specialised in hunting large prey. It is estimated to have had a wingspan of 2–3 m and a mass of 10–15 kg, making it the largest accipitrid known to have ever existed (Holdaway 1991; Brathwaite 1992; Worthy and Holdaway 2002). Despite its great size, its wings were comparatively short, which is thought to be an adaptation to flying through the forested landscape of Holocene New Zealand (Brathwaite 1992). Fossil evidence indicates that it regularly preyed upon species of the moa genera *Dinornis*, *Emeus*, *Euryapteryx* and *Pachyornis*, with fossil skeletons of individuals estimated to be up to 200 kg in weight bearing the marks of attacks (Worthy and Holdaway 2002; Bunce et al. 2005). Among living raptors, predation upon animals much larger than the hunter is not unheard of. *Stephanoaetus coronatus* is a living eagle native to Africa, documented as weighing up to 4.7 kg in females (Ferguson-Lees and Christie 2001). It has a notably powerful build compared to other eagles of a similar size, and has been documented hunting small antelopes, including suni (*Nesotragus moschatus*), and has been recorded killing a Harvey's Duiker (*Cephalophus harveyi*) that was roughly two-thirds the size of an adult (see Brown and Amadon 1968). The average adult Harvey's Duiker weighs 15 kg, so this juvenile was likely at least twice the weight of the attacking eagle. The diet of *Aquila audax* is typically dominated by rabbits, but it has also been documented attacking juvenile and small or weakened adult eastern grey kangaroos (*Macropus giganteus*), either in pairs or groups (Marchant and Higgins 1993; Fuentes and Olsen 2015). In these attacks, the eagles targeted the kangaroo's head in repeated strikes until it either escaped or collapsed from injury and exhaustion (Fuentes and Olsen 2015). The average adult *A. audax* weighs approximately 3.5 kg, excluding size differences between males and females (Marchant and Higgins 1993), while the average adult *M. giganteus* weighs 31 kg in females and 56 kg in males (Pearse 1981).

Based on these cases and its large, powerful build, it is entirely plausible for accipitrid GWC/VFC to have hunted the juveniles and weakened adults of extinct species of megafauna such as in the giant flightless bird *Genyornis newtoni* Stirling and Zietz, 1896, or species of giant kangaroos such as those in *Protemnodon*, *Sthenurus* and *Procoptodon*. These animals would have been slower and less agile compared to the kangaroos and ratites that survived the Pleistocene extinction and would have been easier for the heavily built accipitrid GWC/VFC to pursue and attack. Besides hunting, the accipitrid GWC/VFC would have probably supplemented its diet through scavenging from carcasses like most living eagles do today, though it would have been competing with the specialist scavenger species like "*Taphaetus*" *lacertosus*.

### **Mairs Cave Accipitrid**

It is more difficult to predict the ecology of the Mairs Cave accipitrid. While it had extremely large ungual phalanges, it was also an exceptionally large bird, and we lack the rest of the toe bones to determine their proportionate size. A lack of other pectoral limb material and complete wing bones means that it cannot be determined whether the limb proportions were more like those of hunting eagles or of scavenging vultures. The sternum, however, does give some hints, as it provides most of the surface area for muscle attachments of the wings. In the Mairs Cave accipitrid, the carina of the sternum is modestly projecting, and the apex carina is set well caudal of the spina externa in ventral view (see Figure 4.9). In species that are actively hunting, the carina is quite prominent, and extends equal to or cranially past the spina externa, providing most of the attachment for the pectoralis muscles controlling the downstroke of flapping flight. The morphology of the Mairs Cave accipitrid, therefore, indicates that it had less muscle mass for the downstroke motion, which would suggest it was not a flapping flier and would be a poor pursuit hunter. While its morphology is not as extreme as that seen in most aegyptine vultures like *Aegypius monachus* or species of *Gyps*, where the carina is a low ridge that is positioned extremely caudal of the spina externa, it does conform to the gypaetine species that primarily scavenge. The size of the distal humerus would also suggest that the wingspan was quite large and more suited for gliding than powered flight, as it is comparable to large vulture species such as *Gyps fulvus* and *Gyps coprotheres*. However, the morphology of the other wing bones, particularly the ulna for which length is a key factor in estimating the wingspan of a bird, are currently unknown. Based on this, we can assume the Mairs Cave accipitrid was for the most part a scavenger with some hunting capability like *Gypaetus barbatus* and *Gypohierax angolensis*.

### **Implications and Interpretations**

One aspect often noted about Pleistocene Australia is the paucity of large, terrestrial, mammalian predators; as of writing, the only species thought to have been capable of killing large prey animals is *Thylacoleo carnifex* Owen, 1859a, with evidence suggesting they were social animals that may have hunted in groups (see Arman and Prideaux 2016). While species of

*Thylacinus* and *Sarcophilus* were also present on mainland Australia at this time, it is thought that they would only have been capable of killing smaller prey (Wroe et al. 2007; Rovinsky et al. 2020). The giant varanid *Varanus priscus* (Owen 1859b) has been suggested to have hunted large mammals in a similar manner to the Komodo dragon (Fry et al. 2009), though others theorise that it mostly subsisted from scavenging (Wroe 2002). The low diversity of mammalian carnivores has led to suggestions that the Pleistocene carnivore guild of Australia was dominated by the large reptiles; the snake *Wonambi naracoortensis* Smith, 1976, the crocodylians *Quinkana fortirostrum* Molnar, 1981, *Gunggamarandu maunala* Ristevski et al., 2021, and *Paludirex gracilis* (Willis and Molnar, 1997), and the giant varanid lizard *Varanus priscus* (Owen, 1859b) lived during the same time as the extant *Crocodylus porosus* and *C. johnsoni*. However, most of these species are strongly associated with water, which would limit their range to riverine, coastal and wetland environments. In addition to this, the theory of reptilian predators playing a significant role in Australian ecosystems during the Pleistocene was disputed by Wroe (2002). The role of avian predators during this time period has been rarely discussed.

The presence of vulturine accipitrids present during the Pleistocene has very significant implications for our understanding of the dynamics of the Australian fauna at the time. Vultures play significant roles in scavenging guilds where they are present, being vital in the consumption of carcasses, potentially reducing the spread of harmful pathogens (Ogada et al. 2012a; 2012b), aiding in the location of food by other predators (Kane and Kendall 2017), and facilitating energy flow through food webs (Wilson and Wolkovich 2011). More interesting, however, is the presence of an aberrant aegyptiine vulture that morphologically appears more suited to being a hunter than a scavenger, indicating that the evolution of the subfamily in Australia took quite a different course compared to elsewhere in the world.

### ***Interactions between fossil vulture species***

The two fossil species described above seem to have had overlapping ranges with "*Taphaetus*" *lacertosus*. Accipitrid GWC/VFC and "*T.*" *lacertosus* are both known from the Wellington Caves of NSW, and as far west as the Nullarbor, WA, with accipitrid GWC/VFC also recorded in south-eastern SA, and "*T.*" *lacertosus* present as far north as the Warburton River, SA. The Mairs Cave accipitrid is currently only known from Mairs Cave in SA but would have existed within the same geographical range as the other species; *Aquila audax* juveniles are known to disperse up to 800 km from their parents' home range (Debus 1998), and it is quite likely that these extinct accipitrids would have also been wide-ranging dispersers. The presence of three large accipitrids coexisting in the same environments indicates that there was likely some form of niche partitioning, either in the form of preferred diet or preferred habitat. Modern vulture guilds are comprised of multiple species occupying the same environment, with coexistence allowed by a combination of behavioural and dietary adaptations to feeding on different parts of a carcass

(Hertel 1994; Kendall et al. 2012; Moreno-Opo et al. 2016). Hierarchy of species within a vulture guild is largely based on body size and agonistic behaviour, with the largest, most aggressive vultures typically being the most dominant and having the greatest access to carcasses (Moreno-Opo et al. 2020). Based on modern vulture guilds, we would predict species like the Mairs Cave accipitrid to be at the top of the hierarchy, using their size to maintain dominance, with smaller species like "*T. lacertosus*" either waiting for their turn at the carcass or using another strategy such as congregating in numbers to enforce their position. Accipitrid GWC/VFC might have been an active hunter rather than an obligate scavenger, but it likely also played a role in the scavenging guild. Most accipitrids will scavenge carrion, and it has been documented that some species of vultures often use eagles as a means of finding carcasses (Kane et al. 2014). Along with *Aquila audax*, accipitrid GWC/VFC may have been used as a visual indicator for the presence of a carcass based on observations of its flight behaviour by scavenging species. Compared to other vulture guilds around the world, the inclusion of an active hunter species in the vulture guild is quite unique.

#### 4.4.4 Role in the Australian Pleistocene

During the late Pleistocene, the Australian vultures would have been the primary avian scavengers on the continent until their extinction. The scavenging guild of the time would also have included facultative mammalian scavengers such as species of *Thylacinus* and *Sarcophilus*, which subsequently went extinct on the mainland roughly three thousand years ago (White et al. 2018), and larger mammalian predators like *Thylacoleo carnifex*, and large reptiles like the crocodylian *Quinkana fortirostrum* and monitor lizard *Varanus priscus* possibly also playing a role before their extinction in the late Pleistocene. In the present day, most scavenging across Australia is carried out primarily by avian species such as *Aquila audax* and the raven *Corvus coronoides*, and by the more recently introduced mammals such as wild dogs, feral cats, and foxes (Read and Wilson 2004; Forsyth et al. 2014).

While the environmental impacts of the extinction of Australian vultures is difficult to determine over 50–40 Ka later, it is possible to make inferences based on observations of current vulture declines across the globe. In India, the drastic decline in vulture populations means that carcasses are more frequently scavenged by feral dogs, resulting in their population booming and an increase in the transmission of diseases such as rabies (Markandya et al. 2008). This phenomenon is also observable in other places where vultures have declined or been extirpated, with facultative scavenging mammals arriving in greater numbers to feed on carrion and potentially increasing transmission of pathogens (Ogada et al. 2012b). The ecological release of less specialised avian scavengers can also occur following vulture decline, as the removal of apex scavengers has been documented to result in the less efficient 'mesosavengers' increasing in their abundance (O'Bryan et al. 2019). In the case of Australia, this is likely what has allowed

*Aquila audax* to become such a widespread generalist across the continent. In some cases, it seems that facultative scavengers are unable to replace vultures, leaving the carrion consumption role primarily to decomposers instead (Hill et al. 2018). The loss of these vultures from the Australian ecosystem in the late Pleistocene, regardless of whether they were hunters or scavengers, would have therefore had significant effects on the structure of the terrestrial Australian ecosystems.

## **Acknowledgements**

We would like to thank the following people: Phillipa Horton, Maya Penck and Mary-Anne Binnie (SAMA), Jacqueline Nguyen and Matthew McCurry (AM), Judith White (NHMUK), Chris Milensky (USNM), Mark Robbins (KU), Tim Ziegler and Karen Roberts (NMV), and Leo Joseph and Alex Drew (ANWC) for allowing access to their respective collections and specimens. We would also like to thank Rod Wells for providing copies of the original maps and documents regarding Green Waterhole/ Fossil Cave; Peter Horne, Dave Albano, Neville Skinner, Mark Neilsen, Ian Lewis, Dave Fielder, Andrea Gordon, and Katrin and Gerret Springer for their work in the diving expeditions that recovered the additional accipitrid material from Green Waterhole Cave; Jacqueline Nguyen for personally transporting the Wellington Caves material during the difficult times of 2020; John Hellstrom for his work on U-series dating the calcite rafts from Green Waterhole Cave.

We thank the SA Department for Environment and Heritage for their approval of permits allowing the collection of material from Green Waterhole Cave in 2006 (permit number C25141-1), 2007 (C25141-2) and 2008 (C25151-2).

## **Authors Contributions**

EKM and THW designed the study. EKM collected all morphological data, compiled the morphological matrix and did all analyses. DAF collected material from Cathedral Cave at Wellington Caves and provided dates for that site. MSYL collated the molecular data used in the analyses. THW and MSYL contributed to data interpretation. EKM wrote the manuscript, and all authors edited the manuscript.

## 4.5 Additional Information

### Thesis Appendices

Please see:

**Appendix 1: List of morphological characters.** Full descriptions of all 300 morphological characters used in the analyses, including character states and whether the character was ordered, with references.

### Supplementary Information

All files available at <https://figshare.com/s/7b9b1a551576ab5ce767>

**SI.1: Morphological character data matrix.** Mesquite file containing character states for all fossil and extant species used in this thesis.

**SI.6: Accipitrid GWC/VFC parsimony analysis file.** Command file for the parsimony analyses involving accipitrid GWC/VFC.

**SI.7: Accipitrid GWC/VFC Bayesian infile.** Command file for the Bayesian analysis involving accipitrid GWC/VFC.

## 4.6 References

- Arman, S. D. & Prideaux, G. J. (2016) Behaviour of the Pleistocene marsupial lion deduced from claw marks in a southwestern Australian cave. *Scientific Reports*, 6(1), 21372.
- Ayliffe, L. K., Marianelli, P. C., Moriarty, K. C., Wells, R. T., McCulloch, M. Y., Mortimer, G. E. & Hellstrom, J. C. (1998) 500 Ka precipitation record from southeastern Australia: Evidence for interglacial relative aridity. *Geology*, 26(2), 147–150.
- Baird, R. F. (1985) Avian fossils from Quaternary deposits in 'Green Waterhole Cave', south-eastern South Australia. *Records of the Australian Museum*, 37, 353–370.
- Baird, R. F. (1991) Avian fossils from the Quaternary of Australia. Chapter 21 in: *Vertebrate Palaeontology of Australasia*, P. Vickers-Rich, J. M. Monaghan, R. F. Baird & T. H. Rich (Eds). Pioneer Design Studio Ltd, Lilydale, & Monash University Publications Committee, Melbourne; p. 809–870.
- Baird, R. F., Rich, P. V. & van Tets, G. F. (1991) Localities yielding avian assemblages of Quaternary age in Australia. Appendix II, in Baird (1991), in: *Vertebrate Palaeontology of Australasia*, P. Vickers-Rich, J. M. Monaghan, R. F. Baird & T. H. Rich (Eds). Pioneer Design Studio Ltd, Lilydale, & Monash University Publications Committee, Melbourne: pp 850–870.
- Baumel, J. J., & Witmer, L. M. (1993) Osteologia. 45–132. In: J.J. Baumel, A.S. King, J.E. Breazile, H.E. Evans and J.C. Vanden Berge (Eds). *Handbook of avian anatomy: nomina anatomica avium, 2<sup>nd</sup> edition*. Publications of the Nuttall Ornithological Club 23. Nuttall Ornithological Club Cambridge, MA.
- Bickart, K. J. (1990) The birds of the Late Miocene–Early Pliocene Big Sandy Formation, Mohave County, Arizona. *Ornithological Monographs*, 44, 1–72.
- Boev, Z. (2010) *Gyps bochenskii* sp. n. (Aves: Falconiformes) from the Late Pliocene of Varshets (NW Bulgaria). *Acta Zoologica Bulgarica*, 62(2), 211–242.
- Boutakoff, N. (1963) The geology and geomorphology of the Portland area. *Geological Survey of Victoria Memoir*, 22, 1–117.
- Brathwaite, D. H. (1992) Notes on the weight, flying ability, habitat, and prey of Haast's eagle (*Harpagornis moorei*). *Notornis*, 39(4), 239–247.
- Brodkorb, P. (1964) Catalogue of Fossil Birds, Part 2 (Anseriformes through Galliformes). *Bulletin of the Florida State Museum*, 8(3), 195–335.
- Brown, Leslie and Amadon, Dean (Eds). (1968). *Eagles, hawks and falcons of the world*. Michelin House, London: Spring Books.

- Bunce, M., Szulkin, M., Lerner, H. R. L., Barnes, I., Shapiro, B., Cooper, A. & Holdaway, R. N. (2005) Ancient DNA provides new insights into the evolutionary history of New Zealand's extinct giant eagle. *PloS Biology*, 3(1), e9.
- Burchak-Abramovich, N. I. (1971) Materialy k izucheniyu pleystotsenovykh ptits Gruzii (peshchera Tsona). *Paleontologicheskiiy Sbornik*, 7(2): 45-51.
- Burleigh, J. G., Kimball, R. T. & Braun, E. D. (2015) Building the avian tree of life using a large-scale, sparse supermatrix. *Molecular Phylogenetics and Evolution*, 84, 53–63.
- Campbell, K. E. & Tonni, E. P. (1983) Size and locomotion in teratorns (Aves: Teratornithidae). *The Auk*, 100(2), 390–403.
- Campbell, K. E. Jr., & L. Marcus. (1992) The relationship of hindlimb bone dimensions to body weight in birds. In: *Papers in Avian Paleontology Honoring Pierce Brodkorb*. K. E. Campbell Jr. (ed.). Natural History Museum of Los Angeles County, Sciences Series 36; p. 395–412.
- Campbell, V. & Lapointe, F. J. (2009) The use and validity of composite taxa in phylogenetic analysis. *Systematic Biology*, 58(6), 560–572.
- Clark, W. S. & Wheeler, B. (1983) The field identification of North American eagles. *American Birds*, 37(5), 822–826.
- Coleman, M. (2002) Alluvial, aeolian and lacustrine evidence for climatic and flow regime changes over the past 250 ka, Cooper Creek near Innamincka, South Australia. Unpublished PhD thesis, University of Wollongong, New South Wales, Australia.
- Compton, L. V. (1935) Two avian fossil from the lower Pliocene of South Dakota. *American Journal of Science*, 178, 343–348.
- Condon, H. T. (1975) *Checklist of the birds of Australia. Part 1 Non-Passerines*. Royal Australasian Union.
- Cope, E. D. (1874) Notes on the Santa Fe marls, and some of the contained vertebrate fossils. *Proceedings of the Academy of Natural Sciences of Philadelphia*, 26, 147–152.
- Couzens, A. M. C. & Prideaux, G. J. (2018) Rapid Pliocene adaptive radiation of modern kangaroos. *Science*, 362(6410), 72–75.
- Dawson, L. (1985) Marsupial fossils from Wellington Caves, New South Wales; the historic and scientific significance of the collections in the Australian Museum, Sydney. *Records of the Australian Museum*, 37(2), 55–69.
- Dawson, L. & Augee, M. L. (1997) The late Quaternary sediments and fossil vertebrate fauna from Cathedral Cave, Wellington Caves, New South Wales. *Proceedings of the Linnean Society of New South Wales*, 117, 51–78.

- Dawson, L., Muirhead, J. & Wroe, S. (1999) The Big Sink Local Fauna: a lower Pliocene mammalian fauna from the Wellington Caves complex, Wellington, New South Wales. *Records of the Western Australian Museum*, supplement 57, 265–290.
- de Vis, C. W. (1889) Addition to the list of fossil birds. *Proceedings of the Royal Society of Queensland*, 6, 55–58.
- de Vis, C. W. (1892) Residue of the extinct birds of Queensland as yet detected. *Proceedings of the Linnean Society of New South Wales*, 6, 437–456.
- de Vis, C. W. (1905) A contribution to the knowledge of the extinct avifauna of Australia. *Annals of the Queensland Museum*, 6, 3–25.
- de Vis, C. W. (1911) *Palaeolestes gorei* n. sp. An extinct bird. *Annals of the Queensland Museum*, 10, 15–17.
- Debus, S. J. S. (1998) *The birds of prey of Australia: a field guide*. Oxford University Press.
- Dickinson, E. C. & Remsen J. V. Jr (Eds). 2013. *The Howard & Moore Complete Checklist of Birds of the World*. 4<sup>th</sup> edition, vol 1. Aves Press: Eastbourne, UK.
- Donders, T. H., Wagner, F. & Visscher, H. (2006) Late Pleistocene and Holocene subtropical vegetation dynamics recorded in perched lake deposits on Fraser Island, Queensland, Australia. *Palaeogeography, Palaeoclimatology, Palaeoecology*, 241(3–4), 417–439.
- Elzanowski, A. & Stidham, T. A. (2010) Morphology of the quadrate in the Eocene anseriform *Presbyornis* and extant galloanserine birds. *Journal of Morphology*, 271, 305–323.
- Elzanowski, A. & Zelenkov, N. V. (2015) A primitive heron (Aves: Ardeidae) from the Miocene of Central Asia. *Journal of Ornithology*, 156, 837–846.
- Emslie, S. D. (1998) Avian community, climate, and sea-level changes in the Plio-Pleistocene of the Florida Peninsula. *American Ornithological Society: Ornithological Monographs*, 50, 1–113.
- Feduccia, A. (1974) Another Old World vulture from the New World. *The Wilson Bulletin*, 86 (3), 251–255.
- Ferguson-Lees, J. & Christie, D. A. (Eds). (2001) *Raptors of the World*. Christopher Helm Publishers, London. 992 pp.
- Field, D. J., C. Lynner, C. Brown, & Darroch, S. A. (2013) Skeletal correlates for body mass estimation in modern and fossil flying birds. *PLoS ONE* 8: e82000. doi: 10.1371/journal.pone.0082000.

- Forsyth, D. M., Woodford, L., Moloney, P. D., Hampton, J. O., Woolnough, A. P. & Tucker, M. (2014) How does a carnivore guild utilise a substantial but unpredictable anthropogenic food source? Scavenging on hunter-shot ungulate carcasses by wild dogs/dingoes, red foxes and feral cats in south-eastern Australia revealed by camera traps. *PLOS One*, <https://doi.org/10.1371/journal.pone.0097937>.
- Fraser, R. A. & Wells, R. T. (2006) Palaeontological excavation and taphonomic investigation of the late Pleistocene fossil deposit in Grant Hall, Victoria Fossil Cave, Naracoorte, South Australia. *Alcheringa: An Australasian Journal of Palaeontology*, 30(1), 147–161.
- Fry, B. G., Wroe, S., Teeuwise, W., van Osch, J. P., Moreno, K., Ingle, J., McHenry, C., Ferrara, T., Clausen, P., Scheib, H., Winter, K. L., Greismana, L., Roelants, K., van der Weerd, L., Clemente, C. J., Giannakis, E., Hodgson, W. C., Luz, S., Martelli, P., Krishnasamy, K., Kochva, E., Kwok, H. F., Scanlon, D., Karas, J., Citron, D. M., Goldstein, E. J. C., Mcnaughtan, J. E., & Norman, J. A. (2009) A central role for venom in predation by *Varanus komodoensis* (Komodo Dragon) and the extinct giant *Varanus (Megalania) priscus*. *Proceedings of the National Academy of Sciences of the United States of America*, 106(22), 8969–8974.
- Fuentes, E. & Olsen, J. (2015) Observations of the killing of large macropods by Wedge-tailed Eagles *Aquila audax*. *Australian Field Ornithology*, 32, 160–166.
- Fusco, D. (2021) The impacts of environmental change on late Quaternary fossil fauna at Cathedral Cave, eastern Australia. Unpublished PhD thesis, Flinders University, College of Science and Engineering, South Australia, Australia.
- Gaff, P. (2002) The fossil history of the family Accipitridae in Australia. Master of Science thesis, Monash University, Victoria, Australia.
- Gaff, P. & Boles, W. E. (2010) A new eagle (Aves: Accipitridae) from the Mid Miocene Bullock Creek Fauna of northern Australia. *Records of the Australian Museum*, 62, 71–76.
- Galetti, M., Moleón, M., Fordano, P., Pires, M. M., Guimarães, P. R. Jr., Pape, T., Nichols, E., Hansen, D., Olesen, J. M., Munk, M., de Mattos, J. S., Schweiger, A. H., Owen-Smith, N., Johnson, C. N., Marquis, R. J. & Svenning, J. (2017) Ecological and evolutionary legacy of megafaunal extinctions. *Biological Reviews*, 93, 845–862.
- Gill, F., Donsker, D. & Rasmussen, P. (Eds). (2020) IOC World Bird List (v10.2). doi: 10.14344/IOC.ML.10.2.
- Gillespie, R., Brook, B. W. & Baynes, A. (2006) Short overlap of humans and megafauna in Pleistocene Australia. *Alcheringa: An Australasian Journal of Palaeontology*, 30(S1), 163–186.

- Griffiths, C. S., Barrowclough, G. F., Groth, J. G. & Mertz, L. A. (2007) Phylogeny, diversity, and classification of the Accipitridae based on DNA sequences of the RAG-1 exon. *Journal of Avian Biology*, 38, 587–602.
- Grün, R., Moriarty, K. & Wells, R. (2001) Electron spin resonance dating of the fossil deposits in the Naracoorte Caves, South Australia. *Journal of Quaternary Science*, 16(1), 49–59.
- Haast, J. 1872. Notes on *Harpagornis moorei*, an extinct gigantic bird of prey, containing description of femur, ungual phalanges, and rib. *Transactions and Proceedings of the New Zealand Institute*, 4, 192–196.
- Hackett, S. J., Kimball, R. T., Reddy, S., Bowie, R. C., Braun, E. L., Braun, M. J., Chojnowski, J. L., Cox, W. A., Han, K. L., Harshman, J., Huddleston, C. J., Marks, B. D., Miglia, K. J., Moore, W. S., Sheldon, F. H., Steadman, D. W., Witt, C. C. & Yuri, T. (2008) A phylogenomic study of birds reveals their evolutionary history. *Science*, 320, 1763–1768.
- Handley, W. D., Chinsamy, A., Yates, A. M. & Worthy, T. H. (2016) Sexual dimorphism in the late Miocene mihirung *Dromornis stirtoni* (Aves: Dromornithidae) from the Alcoota Local Fauna of central Australia. *Journal of Vertebrate Paleontology*, 36(5), e1180298.
- Hernandez, F. (2001) A new species of vulture (Aves, Aegypiinae) from the Upper Pleistocene of Spain. *Ardeola*, 48(1), 47–53.
- Hertel, F. (1994) Diversity in body size and feeding morphology within past and present vulture assemblages. *Ecology*, 75(4), 1074–1084.
- Hill, J. E., DeVault, T. L., Beasley, J. C., Rhodes, O. E. Jr & Belant, J. L. (2018) Effects of vulture exclusion on carrion consumption by facultative scavengers. *Ecology and Evolution*, 8(5), 2518–2526.
- Holdaway, R. N. (1991) *Systematics and palaeobiology of Haast's eagle (Harpagornis moorei Haast, 1872) (Aves: Accipitridae)*. Unpublished PhD thesis, Department of Zoology University of Canterbury, Christchurch, New Zealand.
- Holdaway, R. N. (1994). An exploratory phylogenetic analysis of the genera of Accipitridae, with notes on the biogeography of the family. *Raptor Conservation Today*, 601–647.
- Horne, P. (1988) "FOSSIL CAVE" (5L81) underwater palaeontological and surveying Report 1987-1988. *South Australian Underwater Speleological Society Inc.* Project Report Number 1. [Digitised Sept 2006; copy in SA Museum].
- Horton, D.R. (1984) Red kangaroos: last of the Australian megafauna. In: *Quaternary Extinctions: A Prehistoric Revolution*, P.S. Martin and R.G. Klein (Eds). Tucson, AZ: University of Arizona Press; p. 639–680.

- Hou, L. (1984) The Aragonian vertebrate fauna of Xiacaswan, Jiangsu 2. Aegypinae (Falcaniformes, Aves). *Vertebrata Palasiatica*, 22(1), 14–20.
- Hou, L., Zhou, Z., Zhang, F. & Li, J. (2000) A new vulture from the Miocene of Shandong, Eastern China. *Vertebrata Palasiatica*, 38(2), 104–110.
- Howard, H. (1952) The prehistoric avifauna of Smith Creek Cave, with a description of a new gigantic raptor. *Bulletin of the Society of California Academy of Sciences*, 51(2), 50–54.
- Howard, H. (1963) Fossil birds from the Anza-Borrego desert. *Los Angeles County Museum Contributions in Science*, 73, 1–33.
- Howard, H. (1966) Two fossil birds from the lower Miocene of South Dakota. *Los Angeles County Museum Contributions in Science*, 107(2), 1–8.
- Jarvis, E. D., Mirarab, S., Aberer, A. J., Li, B., Houde, P., Li, C., Simon, Y. W. H., Faircloth, B. C., Nabholz, B., Howard, J. T. & 95 others. (2014) Whole-genome analyses resolve early branches in the tree of life of modern birds. *Science*, 346, 1320–1331.
- Jefferson, G. T. (1991) A catalogue of late Quaternary vertebrates from California: part one, non-marine lower vertebrate and avian taxa. *Natural History Museum of Los Angeles County, Technical Reports*, 5, 60 pp.
- Johnson, C. N., Dortch, J. & Worthy, T. H. (2021) Interactions with megafauna. *The Oxford Handbook of the Archaeology of Indigenous Australia and New Guinea*. Edited by Ian J. McNiven and Bruno David. DOI: 10.1093/oxfordhb/9780190095611.013.10.
- Kane, A. & Kendall, C. J. (2017) Understanding how mammalian scavengers use information from avian scavengers: cue from above. *Journal of Animal Ecology*, 86, 837–846.
- Kane, A., Jackson, A. L., Ogada, D. L., Monadjem, A. & McNally, L. (2014) Vultures acquire information on carcass location from scavenging eagles. *Proceedings of the Royal Society B*, 281(1793), 20141072.
- Kendall, C., Virani, M. Z., Kirui, P., Thomsett, S. & Githiru, M. (2012) Mechanisms of coexistence in vultures: understanding the patterns of vulture abundance at carcasses in Masai Mara National Reserve, Kenya. *The Condor*, 114(3), 523–531.
- Kraehenbuehl, P., Lawrence, R. E., and Flavel, S. (1997) Caves of the Flinders Ranges. *Cave Exploration Group of South Australia Occasional Paper*, 9, 57 pp.
- Lawrence, R. E. (2009) The geological context of caves in the Flinders Ranges. *South Australian Geographical Journal*, 108, 59–78.

- Lerner, H. R. L. & Mindell, D. P. (2005) Phylogeny of eagles, Old World vultures, and other Accipitridae based on nuclear and mitochondrial DNA. *Molecular and Phylogenetic Evolution*, 37, 327–346.
- Li, Z., Clarke, J. A., Zhou, Z. & Deng, T. (2016) A new Old World vulture from the late Miocene of China sheds light on Neogene shifts in the past diversity and distribution of the Gypaetinae. *The Auk: Ornithological Advances*, 133, 615–625.
- Liddle, N. R., McDowell, M. C. & Prideaux, G. J. (2018) Insights into the pre-European mammal fauna of the southern Flinders Ranges, South Australia. *Australian Mammalogy*, 40, 262–268.
- Linnaeus, C. (1758) *Systema Naturae per Regna Tria Naturae*, 10th Edition, revised, Vol 1: Regnum Animale. Salvii, L. Holmiae, Stockholm, Sweden, iv + 824 pp.
- Livezey, B. C. & Zusi, R. L. (2007) Higher-order phylogeny of modern birds (Theropoda, Aves: Neornithes) based on comparative anatomy. II. Analysis and discussion. *Zoological Journal of the Linnean Society*, 149, 1–95.
- Lydekker, R. (1890) On the remains of some large extinct birds from the cavern-deposits of Malta. *Proceedings of the Zoological Society of London*, 28, 403–411.
- Macken, A. C. & Reed, E. H. (2013) Late Quaternary small mammal faunas of the Naracoorte Caves World Heritage Area. *Transactions of the Royal Society of South Australia*, 137(1), 53–67.
- Macken, A. C., Jankowski, N. R., Price, G. J., Bestland, E. A., Reed, E. H., Prideaux, G. J. & Roberts, R. G. (2011) Application of sedimentary and chronological analyses to refine the depositional context of a Late Pleistocene vertebrate deposit, Naracoorte, South Australia. *Quaternary Science Reviews*, 30(19–20), 2690–2702.
- Macken, A. C., McDowell, M. C., Bartholomeusz, D. N. & Reed, E. H. (2013) Chronology and stratigraphy of the Wet Cave fossil deposit, Naracoorte, and relationship to paleoclimatic conditions of the Last Glacial Cycle in south-eastern Australia. *Australian Journal of Earth Sciences*, 60(2), 271–281.
- Manegold, A. & Hutterer, R. (2021) First substantial evidence for Old World vultures (Aegypiinae, Accipitridae) from the early Palaeolithic and Iberomaurusian of Morocco. *PalZ*, <https://doi.org/10.1007/s12542-021-00548-9>.
- Manegold, A., Pavia, M. & Haarhoff, P. (2014) A new species of *Aegyptius* vulture (Aegypiinae, Accipitridae) from the early Pliocene of South Africa. *Journal of Vertebrate Paleontology* 34(6), 1394–1407.

- Manegold, A. & Zelenkov, N. (2015) A new species of *Aegyptius* vulture from the early Pliocene of Moldova is the earliest unequivocal evidence of Aegyptiinae in Europe. *Paläontologische Zeitschrift*, 89, 529–534.
- Marchant, S. & Higgins, P.J. (Eds) (1993). *Handbook of Australian, New Zealand & Antarctic Birds, Volume 2: Raptors to Lapwings*. Oxford University Press, Melbourne.
- Markandya, A., Taylor, T., Longo, A., Murty, M. N., Murty, S. & Dhavala, K. (2008) Counting the cost of vulture decline – an appraisal of the human health and other benefits of vultures in India. *Ecological Economics*, 67(2), 194–204.
- Mayr, G. (2009) *Paleogene fossil birds*. Springer-Verlag, Berlin, Heidelberg.
- Mayr G. (2014) Comparative morphology of the radial carpal bone of neornithine birds and the phylogenetic significance of character variation. *Zoomorphology*, 133: 425–434.
- Megirian, D., Prideaux, G. J., Murray, P. F. & Smit, N. (2010) An Australian land mammal age biochronological scheme. *Paleobiology*, 36(4), 658–671.
- Meijer, H. J. M. (2014) The avian fossil record in insular Southeast Asia and its implications for avian biogeography and palaeoecology. *PeerJ*, 2, e295.
- Meijer, H. J. M., Sutikna, T., Saptomo, E. W., Awe, R. D., Jatmiko, Wasisto, S., James, H. F., Morwood, M. J. & Tocheri, M. W. (2013) Late Pleistocene-Holocene non-passerine avifauna of Liang Bua (Flores, Indonesia). *Journal of Vertebrate Paleontology*, 33(4), 877–894.
- Migotto, R. (2013) Phylogeny of Accipitridae (Aves: Accipitriformes) based on osteological characters. PhD Dissertation, Universidade de São Paulo, Instituto de Biociências, Departamento de Zoologia.
- Miller, L. (1916). Two vulturid raptors from the Pleistocene of Rancho La Brea. *University of California Publications in Geological Sciences*, 9, 105–109.
- Miller, L. (1927a). The falcons of the McKittrick Pleistocene. *The Condor*, 29(3), 150–152.
- Miller, L. (1927b). Bird remains. *Science*, 66, 156.
- Miller, L. (1943). The Pleistocene birds of San Josecito Cavern, Mexico. *University of California Publications in Zoology*, 47, 54.
- Miller, A. H. & Compton, L. V. (1939) Two fossil birds from the lower Miocene of South Dakota. *The Condor*, 41(4), 153–156.

- Milne-Edwards A. 1863. Mémoire sur la distribution géologique des oiseaux fossils et description de quelques espèces nouvelles. *Annales des Sciences Naturelles Zoologie*, 4(20): 133–176.
- Milne-Edwards A. 1871. Des caracteres ostéologiques des oiseaux de proie diurnes. In: *Recherches anatomiques et paléontologiques pour servir a l'histoire des oiseaux fossils de la France*. Libraire de G. Masson, Paris, France. p. 406–473.
- Mindell, D. P., Fuchs, J. & Johnson, J. A. (2018) Phylogeny, taxonomy and geographic diversity of diurnal raptors: Falconiformes, Accipitriformes and Cathartiformes. In: *Birds of Prey*, J. H. Sarasola, J. Grande, J. Negro (Eds). Springer, Cham. pp 3–32.
- Mlíkovský, J. (2002) *Cenozoic birds of the world part 1: Europe*. Ninox Press, Praha, Czech Republic.
- Molnar, R. E. (1981) Pleistocene ziphodont crocodylians of Queensland. *Records of the Australian Museum*, 33(19), 803–834.
- Moreno-Opo, R., Trujillano, A. & Margalida, A. (2016) Behavioural coexistence and feeding efficiency drive niche partitioning in European avian scavengers. *Behavioural Ecology*, 27(4), 1041–1052.
- Moreno-Opo, R., Trujillano, A. & Margalida, A. (2020) Larger size and older age confer competitive advantage: dominance hierarchy within European vulture guild. *Scientific Reports*, 10(1), 2430.
- Nagy, J. & Tökölyi, J. (2014) Phylogeny, historical biogeography and the evolution of migration in accipitrid birds of prey (Aves: Accipitriformes). *Ornis Hungarica*, 22, 15–35.
- Newton, C. A. (1988) A taphonomic and palaeoecological analysis of the Green Waterhole (SL81): A submerged Late Pleistocene bone deposit in the lower southeast of South Australia. Unpublished honours thesis, Flinders University, South Australia.
- O'Bryan, C. J., Holden, M. H. & Watson, J. E. M. (2019) The mesoscavenger release hypothesis and implications for ecosystem and human well-being. *Ecology Letters*, 22, 1340–1348.
- Ogada, D. L., Keesing, F. & Virani, M. Z. (2012a) Dropping dead: causes and consequences of vulture population declines worldwide. *Annals of the New York Academy of Science*, 1249 (1), 57–71.
- Ogada, D. L., Torchin, M. E., Kinnaird, M. F. & Ezenwa, V. O. (2012b) Effects of vulture declines on facultative scavengers and potential implications for mammalian disease transmission. *Conservation Biology*, 26(3), 453–460.

- Olson, S. L. (1985) The fossil record of birds. In: *Avian Biology Vol. VIII*, D. S. Farner, J. R. King and K. C. Parkes (Eds). Elsevier Inc; p. 79–252.
- Osborne, R. A. L. (1991) Red earth and bones: the history of cave sediment studies in New South Wales, Australia. *Earth Sciences History*, 10(1), 13–28.
- Osborne, R. A. L. (1997) Rehabilitation of the Wellington Caves phosphate mine: implications for Cainozoic stratigraphy. *Proceedings of the Linnean Society of New South Wales*, 117, 175–180.
- Owen, R. (1859a) On the fossil mammals of Australia —Part I. Description of a mutilated skull of a large marsupial carnivore (*Thylacoleo carnifex*, Owen), from a calcareous conglomerate stratum, eighty miles SW of Melbourne, Victoria. *Philosophical Transactions of the Royal Society of London*, 149, 309–22.
- Owen, R. (1859b) Description of some remains of a gigantic land-lizard (*Megalania prisca*, Owen) from Australia. *Philosophical Transactions of the Royal Society of London*, 149, 43–48.
- Pearse, R. J. (1981) Notes on breeding, growth and longevity of the forester or eastern grey kangaroo, *Macropus giganteus* Shaw, in Tasmania. *Australian Wildlife Research*, 8, 229–35.
- Pledge, N. S. (1980) Macropodid skeletons, including *Simosthenurus* Tedford, from an unusual “drowned cave” deposit in the south east of South Australia. *Records of the South Australian Museum*, 18(6), 131–141.
- Prideaux, G. J., Long, J. A., Ayliffe, L. K., Hellstrom, J. C., Pillans, B., Boles, W. E., Hutchinson, M. N., Roberts, R. G., Cupper, M. L., Arnold, L. J., Devine, P. D. & Warburton, N. M. (2007b) An arid adapted middle Pleistocene vertebrate fauna from south-central Australia. *Nature*, 445, 422–425.
- Prideaux, G. J., R. G. Roberts, D. Megirian, K. E. Westaway, J. C. Hellstrom, and J. M. Olley. (2007a) Mammalian responses to Pleistocene climate change in south-eastern Australia. *Geology* 35, 33–36.
- Prum, R. O., Berv, J. S., Dornburg, A., Field, D. J., Townsend, J. P., Lemmon, E. M. & Lemmon, A. R. (2015) A comprehensive phylogeny of birds (Aves) using targeted next-generation DNA sequencing. *Nature*, 526, 569–573.
- Read, J. L. & Wilson, D. (2004) Scavengers and detritivores of kangaroo harvest offcuts in arid Australia. *Wildlife Research*, 31, 51–56.
- Reed, E. H. (2003). *Taphonomy of large mammal bone deposits, Naracoorte Caves*. Unpublished PhD thesis, Flinders University of South Australia, Australia.

- Reed, E. H. (2006) *In situ* taphonomic investigation of Pleistocene large mammal bone deposits from The Ossuaries, Victoria Fossil Cave, Naracoorte, South Australia. *Helictite*, 39(1), 5–15.
- Reed, E. H. & Bourne, S. J. (2000) Pleistocene fossil vertebrate sites of the south-east region of South Australia. *Transactions of the Royal Society of South Australia*, 124(2), 61–90.
- Reed, E. H. & Bourne, S. J. (2009) Pleistocene fossil vertebrate sites of the south-east region of South Australia II. *Transactions of the Royal Society of Australia*, 133(1), 30–40.
- Rich, P. V. (1980) 'New World vultures' with Old World affinities? *Contributions to Vertebrate Evolution*, 5, 1–115.
- Rich, P. & van Tets, G. F. (1982) Fossil birds of Australia and New Guinea: their biogeographic, phylogenetic and biostratigraphic input. In: *The Fossil Vertebrate Record of Australasia*, P. V. Rich & E. M. Thompson (Eds). Monash University Offset Printing Unit, Clayton: pp 235–384.
- Rich, P. V., Hou, L. H., Ono, K. & Baird, R. F. (1986) A review of the fossil birds of China, Japan and Southeast Asia. *Geobios*, 19(6), 755–772.
- Ristevski, J., Price, G. J., Weisbecker, V. & Salisbury, S. W. (2021) First record of a tomistomine crocodylian in Australia. *Scientific Reports*, 11, 12158.
- Roberts, R. G., Flannery, T. F., Ayliffe, L. k., Yoshida, H., Olley, J. M., Prideaux, G. J., Laslett, G. M., Baynes, A., Smith, M. A., Jones, R. & Smith, B. L. (2001) New ages for the last Australian megafauna: continent-wide extinction about 46,000 years ago. *Science*, 292(5523), 1888–1892.
- Ronquist F, Klopstein S, Vilhelmsen L, Schulmeister S, Murray DL, Rasnitsyn AP. 2012. A total-evidence approach to dating with fossils, applied to the early radiation of the Hymenoptera. *Systematic Biology*, 61(6): 973–999.
- Rovinsky, D. S., Evans, A. R., Martin, D. G. & Adams, J. W. (2020) Did the thylacine violate the costs of carnivory? Body mass and sexual dimorphism of an iconic Australian marsupial. *Proceedings of the Royal Society B: Biological Sciences*, 287, 20201537.
- Saltré, F. E., Rodríguez-Rey, M., Brook, B. W., Johnson, C. N., Turney, C. S. M., Alroy, J., Cooper, A., Beeton, N., Bird, M. I., Fordham, D. A., Gillespie, R., Herrando-Pérez, S., Jacobs, Z., Miller, G. H., Nogués-Bravo, D., Prideaux, G. J., Roberts, R. G. & Bradshaw, C. J. A. (2016) Climate change not to blame for late Quaternary megafauna extinctions in Australia. *Nature Communications*, 7, 10511, DOI: <https://doi.org/10.1038/ncomms10511>.

- Sánchez-Marco, A. (2007) New occurrences of the extinct vulture *Gyps melitensis* (Falconiformes, Aves) and a reappraisal of the paleospecies. *Journal of Vertebrate Paleontology*, 27(4), 1057–1061.
- Sansom, R. S. (2015) Bias and sensitivity in the placement of fossil taxa resulting from interpretations of missing data. *Systematic Biology*, 64, 256–266, doi:10.1093/sysbio/syu093.
- Shute, E. (2018) Early and Middle Pleistocene non-passerine birds from the Thylacoleo Caves, Nullarbor Plain. Unpublished PhD thesis, Flinders University, South Australia, Australia.
- Smith, J. (1976) Small fossil vertebrates from Victoria Cave, Naracoorte, South Australia. IV. Reptiles. *Transactions of the Royal Society of South Australia*, 100, 39–51.
- Sniderman, J. M. K. & Haberle, S. G. (2012) Fire and vegetation change during the Early Pleistocene in southeastern Australia. *Journal of Quaternary Science*, 27(3), 307–317.
- Sniderman, J. M., Jordan, G. & Porch, N. (2012) Plio-Pleistocene climate, vegetation and biogeography in southern Australia. *Japanese Journal of Palynology*, 58 (special issue), 220.
- Sniderman, J. M. K., Pillans, B., O’Sullivan, P. B. & Kershaw, A. P. (2007) Climate and vegetation in southeastern Australia respond to Southern Hemisphere insolation forcing in the late Pliocene–early Pleistocene. *Geology*, 35(1), 41–44.
- Sprigg, R. C. (1952) The geology of the Southeast Province, South Australia, with special reference to Quaternary coast-line migrations and modern beach developments. *Bulletin of the Geological Society of South Australia*, 29, 1–120.
- Stirling, E.C. & Zietz, A. H. C. (1896) Preliminary notes on *Genyornis newtoni*: a new genus and species of fossil struthious bird found at Lake Callabonna, South Australia. *Transactions of the Royal Society of South Australia*, 20, 171–190.
- Tedford, R. H. & Wells, R.T. (1990) Pleistocene deposits and fossil vertebrates from the “dead heart of Australia”. *Memoirs of the Queensland Museum*, 28(1), 263–284.
- Treble, P., Baker, A., Ayliffe, L. K., Cohen, T. J. & Hellstrom, J. C. (2017) Hydroclimate of the Last Glacial Maximum and deglaciation in southern Australia 's arid margin interpreted from speleothem records (23-15 ka). *Climate of the Past*, 13 (6), 667–687.
- Tugarinov, A. J. (1940) New data concerning the Tertiary ornithofauna of the USSR. *Comptes Rendus (Doklady) de l’Académie des Sciences de l’URSS*, 26, 197–200.
- Van Tets, G. F. (1984) A checklist of extinct fossil Australasian birds. In: *Vertebrate Zoogeography & Evolution in Australasia*, M. Archer & G. Clayton (Eds). Hesperian Press: p. 469–475.

- Van Tets, G. F. & Smith, M. J. (1974) Small fossil vertebrates from Victoria Cave, Naracoorte, South Australia. III Birds (Aves). *Transactions of the Royal Society of South Australia*, 98(4), 225–228.
- Van Tets, G. F. & Vickers-Rich, P. (1990) An evaluation of de Vis' fossil birds. *Memoirs of the Queensland Museum*, 28(1), 165–168.
- Vickers-Rich, P., van Tets, G. F. & McEvey, A. R. (1982) Pleistocene records of *Falco berigora* from Australia and the identity of *Asturaetus furcillatus* de Vis (Aves: Falconidae). *Memoirs of the Queensland Museum*, 20(3), 687–693.
- Vieillot, L. J. P. (1816) *Analyse d'une nouvelle ornithology elementaire*. D'eterville, Paris, France; 70 pp.
- Vigors, N. A. (1824) Sketches in ornithology; or, observations on the leading affinities of some of the more extensive groups of birds. On the groups of the Falconidae. *Zoological Journal* 1: 308–346.
- Wells, R. T. (1975) Reconstructing the past: excavating in caves. *Australian Natural History*, 18, 208–211.
- Wells, R. T., Moriarty, K. & Williams, D. L. G. (1984) The fossil vertebrate deposits of Victoria Fossil Cave Naracoorte: an introduction to the geology and fauna. *The Australian Zoologist*, 21(4), 305–333.
- Wetmore, A (1936) Two new species of hawks from the Miocene of Nebraska. *Proceedings of the United States National Museum*, 84, 73–78.
- Wetmore, A. (1940) Avian remains from the Pleistocene of central Java. *Journal of Paleontology*, 14(5), 447–450.
- Wetmore, A. (1943) Two more fossil hawks from the Miocene of Nebraska. *The Condor*, 45 (6), 229–231.
- White, L. C., Saltré, F., Bradshaw, C. J. A. & Austin, J. J. (2018) High-quality fossil dates support a synchronous, Late Holocene extinction of devils and thylacines in mainland Australia. *Biology Letters*, 14, 20170642.
- Willis, P. M. A. & Molnar, R. E. (1997) A review of the Plio-Pleistocene crocodylian genus *Pallimnarchus*. *Proceedings of the Linnean Society of New South Wales*, 117, 223–242.
- Wilson, E. E. & Wolkovich, E. M. (2011) Scavenging: how carnivores and carrion structure communities. *Trends in Ecology and Evolution*, 26(3), 129–35.

- Woodhead, J., Hellstrom, J., Maas, R., Drysdale, R., Zanchetta, G., Devine, P. & Taylor E. (2006) U-Pb geochronology of speleothems by MC-ICPMS. *Quaternary Geochronology*, 1, 208–221.
- Worthy, T. H., & Holdaway, R. N. (2002). *The lost world of the moa: prehistoric life of New Zealand*. Indiana University Press.
- Worthy, T. H., Mitri, M., Handley, W. D., Lee, M. S., Anderson, A. & Sand, C. (2016) Osteology supports a stem-galliform affinity for the giant extinct flightless bird *Sylviornis neocaledoniae* (Sylviornithidae, Galloanseres). *PLOS ONE*, 11(3), DOI: 10.1371/journal.pone.0150871.
- Worthy, T. H., & Nguyen, J. M. T. (2020) An annotated checklist of the fossil birds of Australia. *Transactions of the Royal Society of Australia*, 144(1), 66–108.
- Wroe, S. (2002) A review of terrestrial mammalian and reptilian carnivore ecology in Australian fossil faunas, and factors influencing their diversity: the myth of reptilian domination and its broader ramifications. *Australian Journal of Zoology*, 50, 1–24.
- Wroe, S., Clausen, P., McHenry, C., Moreno, K. & Cunningham, E. (2007) Computer simulation of feeding behaviour in the thylacine and dingo as a novel test for convergence and niche overlap. *Proceedings of the Royal Society B: Biological Sciences*, 274(1627), 2819–2828.
- Wroe, S., Field, J. H., Archer, M., Grayson, D. K., Price, G. J., Louys, J., Faith, J. T., webb, G. E., Davidson, I. & Mooney, S. D. (2013) Climate change frames debate over the extinction of megafauna in Sahul (Pleistocene Australia-New Guinea). *Proceedings of the National Academy of Sciences of the United States of America*, 110(22), 8777–8781.
- Zhang, Z., Feduccia, A. & James, H. F. (2012a) A Late Miocene accipitrid (Aves: Accipitriformes) from Nebraska and its implications for the divergence of Old World vultures. *PLOS ONE*, 7(11), e48842.
- Zhang, Z., Huang, Y., James, H. F. & Hou, L. (2012b) Two Old World vultures from the middle Pleistocene of northeastern China and their implications for interspecific competition and biogeography of Aegypiinae. *Journal of Vertebrate Paleontology*, 32(1), 117–124.
- Zhang, Z., Zheng, X., Zheng, G. & Hou, L. (2010) A new Old World vulture (Falconiformes: Accipitridae) from the Miocene of Gansu Province, northwest China. *Journal of Ornithology*, 151, 401–408.

## **Chapter 5. Discussion**

### **5.1 Thesis summary and aims**

The aim of this thesis was to increase our knowledge of the Australian fossil accipitrids by describing Oligocene and Pleistocene species and determining their phylogenetic position in Accipitridae where possible. The precise objectives were as follows:

1. Taxonomically describe the fossil accipitrids using a wide selection of extant species and close relatives for comparison.
2. Using a comprehensive morphological and molecular data matrix, resolve the phylogenetic position of selected fossil Australian accipitrids in relation to the living species.
3. Based on their morphology, determine the likely ecology of the fossil species.
4. Based on the findings of the above objectives, discuss their implications for the history of accipitrid diversity, ecologies and evolution in Australia.

## 5.2 Project Findings

Each data chapter was written with the intent of becoming an independent publication, and so the results for each part were discussed within them. The findings for each chapter are summarised below.

### 5.2.1 An exceptionally complete new basal raptor (Aves: Accipitridae) from the late Oligocene Namba Formation, South Australia

In this chapter, we described the fossil accipitrid material from Lake Pinpa and Lake Namba, located in the Callabonna Sub-basin of the Lake Eyre Basin, SA. This material included a partial skeleton comprised of 63 bones and a distal humerus from sites 12 and 11 respectively at Lake Pinpa, and a distal femur from Ericmas Quarry, Lake Namba. All these fossils derive from the Namba Formation, which is dated to roughly 28–24 Ma (see Martin 1990; Woodburne et al. 1994). The partial skeleton is described as *Archaeohierax sylvestris* gen. et sp. nov. (Mather et al. 2021; Chapter 2 herein) and is the oldest and most complete fossil accipitrid known from Australia.

The Lake Pinpa accipitrid, *Archaeohierax sylvestris* gen. et sp. nov., is the second species to be documented from the late Oligocene of Australia following *Pengana robertbolesi* from Riversleigh deposits in Queensland (Boles 1993). Despite a lack of material from the latter, *Archaeohierax* is easily distinguished from *Pengana* by the morphology of the distal tibiotarsus.

Like *Pengana robertbolesi*, *Archaeohierax sylvestris* inhabited a forested environment, albeit in central-south Australia as opposed to the north. It was well suited for flying through the forest and canopy, with shortened wings relative to its body size (Figure 2.13) allowing for greater manoeuvrability. Based on the morphology of its legs, it was unlikely to have been able to probe the hollows of trees like *P. robertbolesi* is theorised to have done (Boles 1993). Instead, we argue above that it was most likely an ambush hunter that perched in wait until potential prey wandered into range, pursuing them in short but rapid chases and grabbing them with the claws on the ends of its long, powerful legs.

*Archaeohierax sylvestris* has multiple unique features across many parts of the skeleton that set it apart from other species and subfamilies of accipitrids, including the proximally-low projecting caput of the humeri (Figure 2.5), two pneumatic fossae separated by the pila medialis within the pars cardiaca of the sternum (Figure 2.4), a deep and circular scar for the laterodistal insertion of the transverse ligament on the tibiotarsus (Figure 2.8), widely separated trochleae of the tarsometatarsi, and a large, distinct incisura for the m. flexor hallucis brevis tendon that extends distal to the fossa metatarsi I (Figure 2.9). In Bayesian analyses, it is resolved within the Accipitridae clade with reasonably good support, placing above the Elaninae and below the Perninae (Figure 2.14). It is strongly excluded from any living subfamily clade. Based on these factors and the age of the fossil we argue that *Archaeohierax sylvestris* was a member of a now extinct subfamily, erected above as Archaeohieraxinae, which was endemic to the Australasian

region. As *Archaeohierax sylvestris* and *Pengana robertbolesi* differed greatly and were roughly of contemporary age, this indicates the presence of at least two major clades of Accipitridae present by the late Oligocene of Australia.

The distal humerus from site 11 at Lake Pinpa and the femur from the slightly younger Ericmas Fauna at Ericmas Quarry, Lake Namba, represent a smaller accipitrid species that also inhabited the Lake Pinpa region at the same time as *Archaeohierax sylvestris*. There is not enough material to reliably describe these intriguing fossils as a species at this time, but they point to further accipitrid diversity waiting to be uncovered in both the Pinpa and Ericmas Local Faunas of the Namba Formation in South Australia.

Reviewers noted that the plantar orientation of digit II present in *Archaeohierax* was also characteristic of other basal accipitrids such as elanines, further supporting the results.

### **5.2.2 *Taphaetus lacertosus*, a widespread aegyptine vulture from the Pleistocene of Australia.**

In this chapter, the lectotype distal humerus for "*Taphaetus*" *lacertosus* de Vis, 1905 was reassessed for its taxonomic distinction and affinities within accipitrids. The fossil was unable to be obtained on loan from the Queensland Museum where it is held; instead, we used high quality photographic images and 3D scanning images for comparisons of the lectotype to fossil and extant specimens. In addition, undescribed fossils excavated from the Wellington Caves (NSW) and Leaena's Breath Cave (WA) were assessed to determine if they were referable to "*T.*" *lacertosus*.

The reassessment of the lectotype of "*T.*" *lacertosus* upheld the original assessment by de Vis (1905) that the fossil represented a species of accipitrid distinct from *Aquila audax* and *Haliaeetus leucogaster*, but of similar size. However, the quadrate that de Vis (1905) had attributed to this taxon was found to not represent an accipitrid at all and was in fact a large species of heron Ardeidae, most likely belonging to the genus *Ardea* or *Egretta*. The nomen *lacertosus* cannot retain the generic name "*Taphaetus*" as the type species of this genus as originally proposed (de Vis 1891) is *Uroaetus brachialis* de Vis, 1889. Later de Vis (1905) recognised that the holotype of *Uroaetus brachialis* de Vis, 1889, which taxon he had erected the genus *Taphaetus* for in 1891, was correctly identified originally and so transferred it back to *Uroaetus* as *Uroaetus brachialis*, which is now a synonym of *Aquila audax*, and thus *Taphaetus* de Vis, 1891 is a synonym of *Aquila* (see Worthy and Nguyen 2020). However, de Vis (1905) immediately after restoring *brachialis* back to *Uroaetus*, erected a new species *lacertosus* in the genus *Taphaetus* which therefore became a new nomen *Taphaetus* de Vis, 1905 with the type species by monotypy of *T. lacertosus* de Vis, 1905. As *Taphaetus* de Vis, 1905 is a junior homonym of *Taphaetus* de Vis, 1891, the nomen *lacertosus* therefore must be placed in a new genus. Pending submission of this chapter for publication, we did not propose a new name herein due to names being unavailable for

nomenclature when erected in theses; instead the parataxonomic term “Nov. gen. *lacertosus*” is provisionally used.

In surveying other large fossil accipitrid bones in museum collections we identified further fossil material that can be assigned to Nov. gen. *lacertosus*. These are two fragmented distal humeri and a single complete tarsometatarsus from the Wellington Caves, Wellington, NSW, along with a proximal tarsometatarsus from Leaena’s Breath Cave WA, on the Nullarbor. The humeri from the Wellington Caves were assigned to Nov. gen. *lacertosus* on the basis of similar morphology and size (see Table 3.1, Figure 3.2) with the lectotype, while the tarsometatarsus from the Wellington Caves was assigned on the basis of its association with the humeri, with both also being of an appropriate size to belong to the same species (see Table 3.1, 3.2) and sharing aegyptine characteristics. The tarsometatarsus from Leaena’s Breath Cave was referred on the basis of similarity in morphology and size (see Table 3.2, Figure 3.3) to the specimen from the Wellington Caves.

Both the lectotype humerus and newly assigned material were found to most closely resemble species of Old World vultures in their morphology, which confirms previous unsupported suggestions by van Tets (1984) that Nov. gen. *lacertosus* was an Old World vulture, and the claims that fossil material from this group of Accipitridae is present in Australia (Rich and van Tets 1982). While this may initially seem unusual, as the extant species of Old World vultures now/currently only inhabit Africa, Europe and Asia, the Pleistocene fossil record for South-east Asia includes vultures from Java (Wetmore 1940) and Flores, Indonesia (Meijer et al. 2013). In this context of a much greater palaeogeographic range, the presence of vultures in Australia would be expected.

A parsimony phylogenetic analysis of Nov. gen. *lacertosus* found that the taxon was nested within the Aegyptiinae clade (Figure 3.5), a subfamily of Old-World vultures. Nov. gen. *lacertosus* specifically resolved as sister to species in the extant genus *Gyps*, although the fossil differs enough morphologically to be placed in its own genus. The species is therefore to be given a new genus name to reflect this when this chapter is submitted for publication.

### **5.2.3 New large Pleistocene Old World vultures (Accipitridae) from Australia: morphology, systematics and palaeoecological implications.**

In the third and final data chapter, we conducted a survey of fossil material of large, unidentified accipitrids from Australian Pleistocene deposits in the collections of the South Australian Museum, Western Australian Museum and Australian Museum. This material was sourced from Leaena’s Breath Cave (WA), Mairs Cave (SA), Victoria Fossil Cave (SA), Green Waterhole/Fossil Cave (SA), Wellington Caves (NSW) and Cooper Creek (SA). Specimens were located by searching collections, communications with collection managers, and previous literature (Gaff 2002). We determined the number of species represented by these fossils and compared

them to living species of Accipitridae and performed phylogenetic analyses on them where possible.

The fossil material was distinguishable into two taxa: a taxon known solely from material in Mairs Cave, and one distributed across all other sites. Both taxa were larger than *Aquila audax*, the only large accipitrid present across inland Australia today, and Nov. gen. *Iacertosus*.

We used the parataxonomic nomen 'accipitrid GWC/VFC' pending formal submission for publication wherein a name will be given/introduced. It was slightly larger than *A. audax* but with more robust limb bones and drastically different limb proportions (see Table 4.3). While the morphology of most of the tibiotarsus and tarsometatarsus are currently unknown due to lack of preservation, the femora, distal tibiotarsus and frags of tarsometatarsus reveals that the leg bones were very large and robust compared to a relatively short wingspan (see Table 4.3). This morphology indicates an accipitrid specialised for grappling and killing large prey, possibly even species of megafauna present at the time. The leg bones of accipitrid GWC/VFC are only slightly smaller than those of *Hieraaetus moorei* which preyed upon species of Dinornithiformes (moa) many times larger than itself (Worthy and Holdaway 1996; Holdaway and Worthy 1997; Worthy and Holdaway 2002), it is entirely plausible that accipitrid GWC/VFC may have hunted megafauna such as the large, flightless bird *Genyornis newtoni* or the large macropodid species in *Procoptodon*, *Sthenurus* and *Protemnodon*. Even the extant *Aquila audax* has been documented killing young or unhealthy eastern grey kangaroos *Macropus giganteus*, albeit in pairs or groups (Marchant and Higgins 1993; Fuentes and Olsen 2015). However, when the fossil taxon was subjected to phylogenetic analysis, it was resolved as a member of the (scavenging) Aegypiinae clade in both parsimony and Bayesian analyses. This suggests that accipitrid GWC/VFC was either a member of a basal lineage of aegypiines that originated before the subfamily began to specialise in scavenging, or that it represents a derived lineage in an otherwise scavenging group that reverted to the ancestral active hunting niche (as found in Elaninae, Perninae, Pandionidae and Sagittariidae).

The Mairs Cave accipitrid is represented by a sternum, partial distal humerus and two ungual phalanges, seemingly from a single individual that was much larger than *A. audax*. The size of the humerus is equivalent to species of large vultures in the genus *Gyps*, indicating a wingspan up to or greater than 2.5 m (Brown and Amadon 1968) compared to 2.3 m for a female *Aquila audax* (see Debus 1998). The ungual phalanges, on the other hand, are larger than those of *A. audax* and much larger than those of *Gyps* vultures, which indicates an active hunter. Without more elements of the pectoral and pelvic limbs to determine their size relative to each other, it is difficult to confidently say whether the Mairs Cave accipitrid was more inclined towards hunting or scavenging. The morphology of the sternum provides robust evidence that the species belonged to the Gypaetinae subfamily of Old-World vultures, which are more diverse in their ecologies and

behaviours than the vultures of the Aegypiinae (Brown and Amadon 1968). Based on this interpretation of the taxonomy of the accipitrid from Mairs Cave, it is entirely possible for it to have been primarily a scavenger but with some hunting capability.

Both the accipitrid GWC/VFC and Mairs Cave accipitrid had the same geographic range as each other, along with Nov. gen. *lacertosus* and *Aquila audax*. This indicates that some form of niche partitioning was in place to allow their coexistence. Their presence also demonstrates the existence of a vulture guild in the Australian Pleistocene, which is unique in that it seems to have included active predators alongside scavengers.

The presence of three vulture species increases the large, inland raptor diversity to be much closer to what we would expect for a continent the size of Australia. In contrast to modern inland Australia having a single large raptor (*Aquila audax*), the similarly sized region of North America south of the sub-arctic zone has four extant large, inland birds of prey; the golden eagle *Aquila chrysaetos* (Accipitridae), turkey vulture *Cathartes aura*, black vulture *Coragyps atratus*, and California condor *Gymnogyps californianus* (Cathartidae) (Brown and Amadon 1968; de Graaf et al. 1985). Notably, North America also had many of its large raptors go extinct towards the end of the Pleistocene (see Jefferson 1991), yet the modern depauperate diversity is still greater than present day Australia's.

Accipitrid GWC/VFC is the only example of a predatory species of Aegypiinae recorded from anywhere in the world. Its existence has revealed a previously unknown diversity of ecology in aegypiines and has major implications for the evolution of the subfamily. With the paucity of large, mammalian predators in Australia during the Pleistocene (see Wroe 2002), accipitrid GWC/VFC would have been one of the top terrestrial predators of its time.

Based on the stratigraphic age of the sites the fossils come from, it is likely that these species died out during the Pleistocene megafaunal mass extinction event of Australia, alongside many other large species of mammals, reptiles and birds (see Figure 5.1). This reveals that this extinction event had major impacts on the Australian avian predatory guild, and drastically changed the scavenging guild.

## Extinct and Extant Megafauna of Australia (Pleistocene to present)

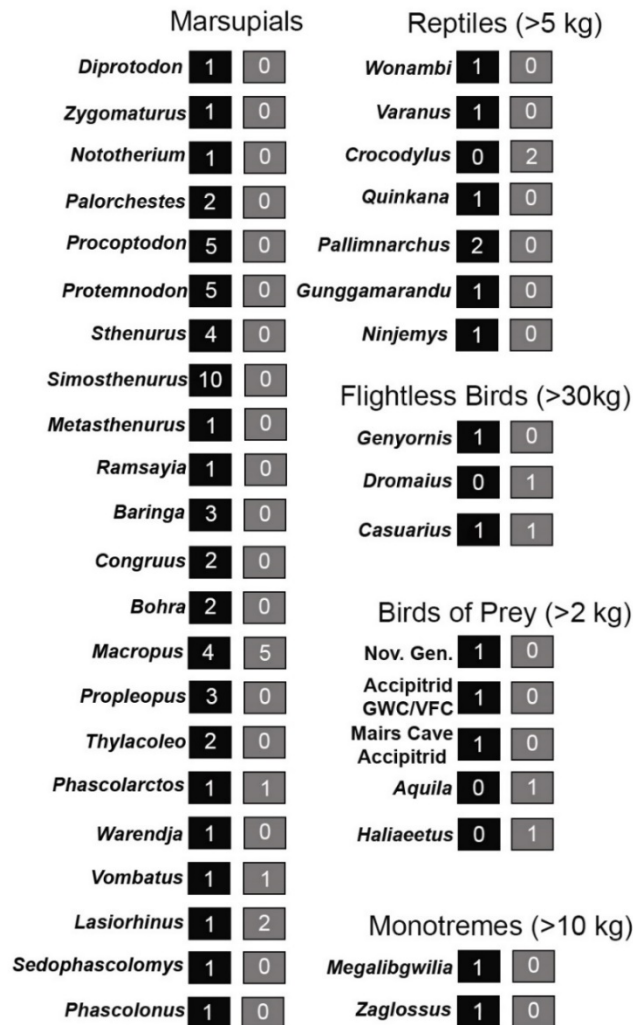


**Figure 5.1:** A simplified depiction of the number of extinct Pleistocene species (black boxes) versus the number of extant Australian megafaunal species (grey boxes). Genera and number of species sourced from Johnson and Prideaux (2004), Wroe et al. (2013).

## 5.3 Suggestions for future research

### 5.3.1 Oligocene Accipitridae of Australia

Future studies will be largely dependent on the acquisition of more fossil material from late Oligocene sites such as the Etadunna and Namba Formations and Riversleigh. Finding more material from the undescribed second taxon of the Namba Formation would go a long way to resolving the relationship of the fossil to *Archaeohierax sylvestris*.

However, there are other avenues of interest that could be pursued with the material that is already collected. A phylogenetic analysis of *Archaeohierax sylvestris* including other Oligocene

accipitrids globally would better resolve relationships of Accipitridae at this time. Alternatively, as most of the skeleton is known in *A. sylvestris*, digital scans could be used to reconstruct the articulated skeleton and predict the musculature of the living animal based on extant examples (see Lautenschlager 2016a; 2016b). This could be used to test the validity of our hypotheses regarding the palaeoecology of the species.

### 5.3.2 Pleistocene Accipitridae of Australia

Examination of fossils from Pleistocene sites across the southern half of Australia have confirmed the existence of at least three extinct species of Accipitridae in minimally eight sites. When these and other sites are further explored in the future, it is recommended that researchers closely examine fossil material for the bones of large birds, as these could represent more material from one or more of these taxa. More fossil material, especially of bone elements that are not represented among the current collected specimens, would increase our understanding of the morphology and ecology of these species, and would provide more information for phylogenetic analyses.

With scavenging vultures and giant predatory accipitrids confirmed to have been present in Australia, it is possible that they may have left taphonomic traces on the bones of carcasses they foraged on that subsequently underwent fossilisation. In the case of vultures, these marks tend to be subtle, such as irregular, shallow score marks which can form straight lines or be L- or V-shaped, small pits, and occasionally punctures (Reeves 2009; Domínguez-Solera and Domínguez-Rodrigo 2011; Fetner and Sołtysiak 2013). The majority of these marks tend to be concentrated on the ribs and meat-bearing bones, while the epiphyses are typically left untouched (Domínguez-Solera and Domínguez-Rodrigo 2011). In future, it might be worthwhile for studies involving megafaunal skeletons, particularly from sites where mass deaths occurred such as Lake Callabonna, to carefully examine fossils bones for such marks. This might require observation via magnifying lenses, as many of these marks are small and easily mistaken for other taphonomic processes.

It is also possible that accipitrid GWC/VFC left traces on fossils, like that inferred to have been made by *Hieraaetus moorei* in New Zealand. Fossilised moa pelvises from sites such as Pyramid Valley and Glencrieff Swamp, where these giant birds became trapped in the mire, have been found with lesions and rends consistent with the damage produced by large eagle claws (Holdaway 1991; Worthy and Holdaway 1996; Holdaway and Worthy 1997; Worthy and Holdaway 2002). To have caused this damage, the talons would have to have pierced through the feathers and skin, up to 5 cm of muscle mass, and then 5 mm of bone while creating these gashes – Some of which are 10 cm long (TH Worthy, pers. comms). Given the violent nature of these marks, *H. moorei* must have attacked these bogged moas while they were still alive. It is quite likely that accipitrid GWC/VFC, being a predatory bird not much smaller than *H. moorei*, would have also

attacked and killed bogged megafaunal animals or somewhat weakened ones out in the open in Australia. Therefore, similar damage to bones from sites such as Lake Callabonna, where Australian megafauna became trapped in the mud, should be assessed for similarities to those from Pyramid Valley in NZ.

### 5.3.3 Bridging the Oligocene and Pleistocene: Miocene Accipitridae

While this study focused on the fossil species of the Oligocene and Pleistocene, we did not study material of accipitrids representing the intermediate time period of the Miocene from Bullock Creek and Alcoota. As of the time of writing, only one species has been described from this time period, *Aquila bullockensis* from the middle Miocene Camfield Beds near Bullock Creek, Northern Territory (Gaff and Boles 2010). This species is currently the oldest referred to the extant genus *Aquila*; however, it was described based off a distal humerus, which is not the most diagnostic of accipitrid bones. There are also several distinct differences between the fossil and extant *Aquila audax*: the processus flexorius has less distal projection, the tuberculum supracondylare dorsale is less projecting cranially and lacks any narrowing proximally, there is little or no convexity between the tuberculum supracondylare dorsale and the epicondylus dorsalis, and the dorsal insertion for the m. extensor radii is positioned offset from the tuberculum supracondylare dorsale. Furthermore, molecular phylogenies predict that *Aquila* only evolved during the Pliocene (Nagy and Tökölyi 2014; Mindell et al. 2018), several million years after *A. bullockensis* is known to have existed.

Accipitrid material representing at least two taxa is also known from Alcoota, Northern Territory (Vickers-Rich 1991; Worthy and Yates 2017). A distal tarsometatarsus from Lake Palankarinna was previously thought to be an accipitrid (Vickers-Rich 1991; Boles 2006) but was later discovered to be a falconid (Gaff 2002) but given the coeval nature of the deposits there with those of the Namba Formation, accipitrids can be expected to occur.

We highly recommend that the type specimen for *A. bullockensis*, along with undescribed material known to include proximal and distal ulnae at least, and the four large pedal and ungual phalanges and distal right tarsometatarsus from the Alcoota Local Fauna (Worthy and Yates 2017), be reassessed using a broad sample of extant accipitrid genera. We would also suggest that this material be compared to those found across Miocene sites that preserve bird fossils to determine how many species are represented in the fossil record of this time. By phylogenetically comparing material from Alcoota and *A. bullockensis* with *Archaeohierax sylvestris* and a broad sample of extant species, the following questions could be addressed; was *A. bullockensis* correctly assigned to the genus *Aquila*? Did *Aquila* originate earlier than molecular predictions estimated? Is there is any relationship between *Archaeohierax sylvestris* and the Australian accipitrids of the Miocene?

Somewhat farther afield, but geographically still in the Australasian realm, at least two fossil accipitrids are also known but undescribed from the Miocene-age St Bathans Fauna of New

Zealand (see Worthy et al. 2014; Worthy et al. 2017). While obviously distinct from that of Australia, the New Zealand avifauna is partially influenced by the Australian one, as many species in the former have their origins from the latter (see Falla 1953; Trewick and Gibb 2010). This is observable even in the present day; the New Zealand marsh harrier *Circus approximans* is identical to those found in Australia, and only appeared in the New Zealand fossil record a few hundred years ago (Worthy and Holdaway 2002; Gill et al. 2010). Therefore, a greater understanding of the New Zealand Miocene accipitrids could provide some information on the Australian Miocene accipitrid diversity by proxy.

### **5.3.4 Phylogeny and systematics of Australia's fossil Accipitridae**

As demonstrated by this study and previous works, it is possible to get well resolved phylogenetic trees that include fossil taxa using molecular data in the character matrix along with morphological data (see Ksepka et al. 2006; Ronquist et al. 2012). Future descriptions of limited material of fossil accipitrids, even if only single elements such as the tarsometatarsus are available, should consider also performing at least parsimony-based phylogenetic analyses to qualitatively assess if perceived similarities are plesiomorphies or useful synapomorphies relevant to relationships.

The extraction of ancient DNA from Pleistocene fossil material has been revolutionary in understanding the phylogeny of extinct megafauna and changes in population genetics of extant species (Willerslev and Cooper 2005; Orlando and Cooper 2014; Phillips and Zakaria 2021). The potential for Pleistocene accipitrid species to have ancient DNA extracted from their fossils is low: it is possible but highly unlikely for specimens preserved in the predominantly warm-hot arid environment of Australia. Late Pleistocene species from Europe and North America have had great success using partial DNA sequences extracted from fossils to resolve phylogenies (see Heintzman et al. 2015; Knapp 2019), but these fossils were preserved in environments favourable for DNA preservation. These conditions are rare in Australia, and while it has been achieved in the case of two extinct macropodids from caves in the Tasmanian highlands (Llamas et al. 2015; Cascini et al. 2019), environmental DNA representing 33 species of animals from cave deposits on Kangaroo Island (Seersholm et al. 2021), and for mainland devils and thylacines across southern Australia prior to their extinction roughly 3 Ka (Brüniche-Olsen et al. 2018; White et al. 2018), the likelihood of a fossil in the Naracoorte Caves that is 50 Ka or older containing DNA is very low (Grealy et al. 2016). Therefore, fossils in open environments farther north than Naracoorte are even less likely to preserve DNA, especially if they are over a few thousand years in age.

## **5.4 Conclusions**

This study has revealed that Australia has a long history of unique endemic Accipitridae spanning millions of years back to the late Oligocene. Most notably, the diversity of Australian

accipitrids during the Pleistocene, a crucial era in understanding the evolution of the modern fauna, was much greater than it is in the present day. The confirmed presence of vultures from the Aegypiinae and Gypaetinae subfamilies drastically changes our understanding of the scavenging and predation dynamics of the Australian Pleistocene, especially with the presence of a vulture that occupied an active predator niche. This demonstrates that the native accipitrid fauna was highly impacted by the megafaunal extinction event, and that we still have much to learn about this crucial period in Australia's faunal history.

## **Appendices**

### **Appendix 1: Morphological character list**

A total of 154 characters were derived from Migotto (2013, unpublished thesis), two from Elzanowski and Stidham (2010), two from Elzanowski and Zelenkov (2015), six from Gaff and Boles (2010), one from Worthy et al. (2016), three from Mayr (2014) and three from Mayr (2018). The remaining characters were novel traits derived from observations and comparisons between the extant and fossil specimens.

Ordered characters shown by \* at end of character states.

## Skull

1. Transverse ridge on frontal behind hinge (Migotto 2013, char. 1): 0 = absent; 1 = present.
2. Depression in the os frontale (Migotto 2013, char. 2): 0 = absent; 1 = present.
3. Width of depression in the frontal (Migotto 2013, 3): 0 = narrow; 1 = broad.
4. Type of articulation of the lacrimal and frontal (Migotto 2013, 4; modified from Migotto 2008, 01): 0 = sutured; 1 = fused.
5. Processus supraorbitale lacrimale (Migotto 2013, 5; modified from Brito 2008, 05): 0 = undifferentiated from frontal; 1 = differentiated from frontal.
6. Medial face of processus supraorbitale lacrimale (Migotto 2013, 6; modified from Brito 2008, 09): 0 = connected to frontal; 1 = free from frontal.
7. Size of processus supraorbitale lacrimale (Migotto 2013, 7; modified from Brito 2008, 07): 0 = reduced; 1 = short; 2 = long. \*
8. Ossa supraorbitalia (Migotto 2013, 8; modified from Jollie 1977): 0 = absent; 1 = reduced; 2 = present. \*
9. Shape of processus orbitalis lacrimale (Migotto 2013, 9; modified from Holdaway 1994, 11): 0 = thin; 1 = inflated.
10. Lateral projection of processus orbitalis lacrimale (Migotto 2013, 10; Brito 2008, 13): 0 = absent; 1 = present.
11. Lateral concavity of processus orbitalis lacrimale (Migotto 2013, 11; Brito 2008, 09): 0 = absent; 1 = slightly accentuated; 2 = accentuated. \*
12. Rostromedial fenestra in processus supraorbitalis lacrimale (Migotto 2013, 12; modified from Migotto 2008, 12): 0 = absent; 1 = present (foramen); 2 = present (notch/fenestra).
13. Contact between processus orbitalis lacrimale and os ectethmoidale (Migotto 2013, 13; modified from Migotto 2008, 10): 0 = present (articulated); 1 = present (fused).
14. Size of lateral portion of ectethmoidale (Migotto 2013, 14): 0 = long; 1 = average; 2 = short. \*
15. Foramen orbitonasalis medialis (Migotto 2013, 15; Migotto 2008, 13): 0 = confluent with sulcus n. olfactorii; 1 = not confluent.
16. Fonticuli interorbitales (Migotto 2013, 16; modified from Jollie 1977b): 0 = absent; 1 = present.

17. Shape of processus postorbitalis (Migotto 2013, 17; modified from Holdaway 1994, 25): 0 = gracile; 1 = thickened; 2 = robust. \*
18. Length of processus postorbitalis relative to zygomatic process (Migotto 2013, 18; modified from Migotto 2008, 19): 0 = short (dorsal to); 1 = long (ventral to).
19. Lamina parasphenoidalis processus medialis (Migotto 2013, 19; Brito 2008, 29): 0 = barely evident; 1 = short; 2 = long. \*
20. Lateral fusion of lamina parasphenoidalis to base of rostrum parasphenoidale (Migotto 2013, 20; modified from Migotto 2008, 22): 0 = present; 1 = absent; 2 = incomplete. \*
21. Tuberculum basilaris (Migotto 2013, 21; modified from Migotto 2008, 24): 0 = absent; 1 = present.
22. Medial process of crista parabasalis dorsally bounding tympanic fossa (Migotto 2013, 22): 0 = reduced; 1 = long.
23. Processus basipterygoideus (Migotto 2013, 23; Jollie 1977b): 0 = present (functional); 1 = present (vestigial); 2 = absent. \*
24. Processus zygomaticus (Migotto 2013, 24; modified from Migotto 2008, 26): 0 = vestigial; 1 = developed; 2 = highly developed (*Ciconia*). \*
25. Crista otica dorsalis (Migotto 2013, 25; modified from Migotto 2008, 28): 0 = vestigial; 1 = short; 2 = laterally expanded. \*
26. Position of crista otica dorsalis in relation to jugal bar (Migotto 2013, 26; modified from Migotto 2008, 29): 0 = oblique; 1 = perpendicular.
27. Squamosal overlapping quadrate-squamosal joint (Migotto 2013, 27): 0 = hidden; 1 = exposed.
28. Conformation of pterygoid-palatine joint (Migotto 2013, 28; Migotto 2008, 33): 0 = pterygoid articulates/abuts to parasphenoidal and palatine; 1 = pterygoid articulates/abuts only to palatine.
29. Alignment of lateral edges of processus paroccipitalis in caudal view (Migotto 2013, 29): 0 = parallel or near parallel; 1 = convergent ventrally.
30. Direction of plane of foramen magnum (Migotto 2013, 30; modified from Migotto 2008, 36): 0 = caudal; 1 = caudoventral; 2 = ventral. \*
31. Prominentia cerebellaris (modified from Migotto 2013, 31; modified from Migotto 2008, 37): 0 = little or no inflation; 1 = inflated.

32. Shape of crista nuchalis transversa in caudal aspect (Migotto 2013, 32; Brito 2008, 53): 0 = inverted 'u'-shape; 1 = 'm'-shape.
33. Angle between processus maxillaris nasale and jugal bar (Migotto 2013, 33; modified from Migotto 2008, 40): 0 = acute (around 30°); 1 = around 50°; 2 = broad (around 80°). \*
34. Crista tomialis (Migotto 2013, 34): 0 = absent; 1 = present.
35. Shape of angulus tomialis maxillaris (Migotto 2013, 35; modified from Migotto 2008, 41): 0 = continuous with jugal bar; 1 = discrete projection ventral to jugal.
36. Position of angulus tomialis maxillaris relative to the maxillary bar/process of nasal (Migotto 2013, 36): 0 = rostral portion of maxilla; 1 = equal to maxillary bar; 2 = extends past maxillary bar. \*
37. Openness of nares (Migotto 2013, 37; modified from Migotto 2008, 43): 0 = completely open; 1 = partially covered by nasal bone (caudal part covered); 2 = partially covered by nasal bone (dorsal part covered).
38. Palatines ventrally concave when paired in caudoventral view (Migotto 2013, 38; modified from Migotto 2008, 45): 0 = absent; 1 = present.
39. Medial angle of palatine (Migotto 2013, 39; Brito 2008, 69): 0 = present; 1 = absent.
40. Dorsoventral height of rostrum relative to tomial margin (Migotto 2013, 40; modified from Brito 2008, 78): 0 = long; 1 = short.
41. Contact between medial borders of caudal palatines (Migotto 2013, 41): 0 = partial, separated by parasphenoid caudally; 1 = complete.
42. Processus maxillopalatinus (Migotto 2013, 42): 0 = reduced; 1 = developed.
43. Contact between processus maxillopalatinus (Migotto 2013, 43; modified from Migotto 2008, 47): 0 = fused; 1 = adjacent to each other; 2 = widely separated. \*
44. Fenestra ventromedialis (Migotto 2013, 44; modified from Holdaway 1994, 06; also refer to Livezey and Zusi 2007, 0289): 0 = absent; 1 = present (narrow); 2 = present (wide). \*
45. Fenestra ventrolateralis (Migotto 2013, 45; Migotto 2008, 49; Livezey and Zusi 2007, 0290): 0 = absent or small; 1 = present.
46. Vomer (Migotto 2013, 46; modified from Jollie 1977b): 0 = absent; 1 = present.
47. Shape of rostral extremity of vomer (Migotto 2013, 47): 0 = pointed; 1 = inflated.
48. Foramen in palatine lamina dorsale (Migotto 2013, 48): 0 = absent; 1 = present.
49. Pterygoid foramina (Migotto 2013, 49; Brito 2008, 76): 0 = absent; 1 = present.

50. Position of quadrato-quadratojugal joint relative to processus postorbitalis on dorsoventral axis (Migotto 2013, 50; modified from Migotto 2008, 53): 0 = rostral or close to it; 1 = caudal.
51. Quadrate, condylus mandibularis caudalis differentiation from condylus lateralis and condylus medialis (Elzanowski and Zelenkov 2015; Migotto 2013, 51; modified from Migotto 2008, 54): 0 = well differentiated; 1 = slightly differentiated; 2 = absent. \*
52. Processus retroarticularis (Migotto 2013, 52; Holdaway 1994, 34): 0 = absent; 1 = present (vestigial); 2 = present (developed). \*
53. Position of mandibular symphysis relative to rostrocaudal axis of mandible (Migotto 2013, 53; modified from Holdaway 1994, 27): 0 = coincides with axis; 1 = does not coincide, noticeably depressed below axis.
54. Processus lateralis of mandible (Migotto 2013, 54; modified from Migotto 2008, 59): 0 = slightly differentiated from mandible; 1 = short; 2 = long. \*
55. Processus coronoideus (Migotto 2013, 55): 0 = absent; 1 = present
56. Mandible, caudal margin of fossa aditus canalis neurovascularis (Migotto 2013, 56): 0 = forms a crest; 1 = forms a distinct tuberculum pseudotemporale; 2 = flat.
57. Position of processus coronoideus relative to external muscle adductor of mandible (Migotto 2013, 57): 0 = close; 1 = separate.
58. Cranium, cranial base, number of foramina nervi hypoglossi (Mayr, 2018): 0 = 4 or more; 1 = 3; 2 = 2. \*
59. Cranium, cranial base, configuration of foramina nervi hypoglossi (Mayr, 2018): 0 = clustered into tight group; 1 = one or more foramina separated clearly from rest of group; 2 = foramina arranged into vertical line.
60. Cranium, cranial base, position of foramen nervi glossopharyngealis relative to ostium canalis ophthalmicus externus and ostium canalis carotici (Mayr, 2018): 0 = forms relatively straight line falling between ostium canalis ophthalmicus externus and ostium canalis carotici; 1 = forms peak of 'triangle' or angle outwards between the two ostia; 2 = set well outside the two ostia. \*
61. Quadrate, proximal end, processus oticus, size of capitulum oticum relative to capitulum squamosum: 0 = equal size; 1 = unequal size (capit. otic. larger).
62. Quadrate, proximal end, processus oticus, caudal foramen under capitulum: 0 = present; 1 = absent.

63. Quadrate, proximal end, foramen pneumaticum caudomediale (Elzanowski and Zelenkov 2015): 0 = present; 1 = absent.
64. Quadrate, distal end, foramen pneumaticum basiorbitale (Elzanowski and Stidham 2010): 0 = present; 1 = absent.
65. Quadrate, distal end, foramen pneumaticum rostromediale (Elzanowski and Stidham 2010): 0 = present; 1 = absent.
66. Quadrate, size of condylus lateralis relative to condylus medialis: 0 = greatly enlarged, more than twice the size of condylus medialis; 1 = twice to 1.5 times the size; 2 = roughly equal. \*
67. Quadrate, processus orbitalis orientation relative to corpus of processus oticus: 0 = medial orientation (continuing out in straight line); 1 = medioventral; 2 = mediodorsal.
68. Quadrate, condylus lateralis, size of arcus jugal facet: 0 = moderate, roughly half of lateral facies; 1 = large, over two thirds of lateral facies.

## Sternum

69. Number and position of incisura/fenestra sterni (Migotto 2013, 58): 0 = none; 1 = shallow incisura medialis; 2 = outer incisura/fenestra (fenestra lateralis extends close to trabecula lateralis) present; 3 = both fenestra/incisura medialis and lateralis present.
70. Conformation of fenestra/incisura lateralis (Migotto 2013, 59): 0 = open; 1 = enclosed.
71. Abutment of crista medialis carinae to spina externa (modified from Migotto 2013, 60): 0 = absent; 1 = present; 2 = separated by deep fossa (*Ciconia*).
72. Contiguity of caudal end of carina to caudal margin of sternum (Migotto 2013, 61): 0 = absent, carina terminates before caudal margin; 1 = present, carina terminates at caudal margin.
73. Size of region between caudal end of carina and caudal margin of sternum (Migotto 2013, 62): 0 = absent or small; 1 = large.
74. Projection of spina externa in rostrum sterni (Migotto 2013, 63; Holdaway 1994, 55): 0 = short; 1 = long (compressed in *Ciconia*, *Sagittarius*).
75. Position of apex of carina relative to the sulcus sellaris medialis on a dorsoventral axis (Migotto 2013, 64): 0 = separated caudally; 1 = adjacent; 2 = overlapping cranially. \*
76. Position of sulci articularis coracoidei (Migotto 2013, 65; modified from Jollie 1977b): 0 = separate; 1 = overlapping.

77. Processus of labrum internum sternae (Migotto 2013, 66): 0 = absent or vestigial; 1 = small; 2 = robust. \*
78. Caudolateral extremity of fossa sternocoracoidei (Migotto 2013, 67): 0 = distinct with thick border; 1 = little differentiation, forms line.
79. Number of processus costales: 0 = 4; 1 = 5; 2 = 6; 3 = 7; 4 = 8.
80. Caudolateral extension of fossa sternocoracoidei (modified from Migotto 2013, 68; modified from Holdaway 1994, 51): 0 = reaches 2nd processus costalis; 1 = reaches 3rd processus costalis; 2 = reaches 4th processus costalis; 3 = reaches 5th or 6th processus costalis; 4 = reaches past 6<sup>th</sup> processus costalis or not visible (*Ciconia*).
81. Foramen in fossa sternocoracoidei (Migotto 2013, 69; Holdaway 1994, 48): 0 = absent; 1 = present.
82. Anteromedial projection on processus craniolateralis (Migotto 2013, 70): 0 = absent; 1 = present (short); 2 = present (developed). \*
83. Pneumatic foramen on dorsal face of processus craniolateralis (Migotto 2013, 71): 0 = absent; 1 = present.
84. Thickened carina apex relative to spina externa of rostrum sterni (Migotto 2013, 72): 0 = proportionate; 1 = spina externa thicker than carina apex; 2 = carina apex thicker than spina externa. \*
85. Carinae apex thickness (Migotto 2013, 73): 0 = absent, apex carinae tapers from pila carinae; 1 = present, apex thick as or thicker than pila.
86. Type of origin point for lig. sternocoracoideum laterale (Migotto 2013, 74): 0 = crest; 1 = tuberculum.
87. Sternum, ventral surface, position of dorsolateral intermuscular line relative to point of origin for lig. sternocoracoideum laterale (Migotto 2013, 75): 0 = adjacent; 1 = separated medially.
88. Caudal extension of dorsolateral intermuscular line down body of sternum (Migotto 2013, 76): 0 = extends to cranial third of body; 1 = extends to middle third of body; 2 = extends to caudal third of body. \*
89. Depth of carina: 0 = greater than depth of sternum; 1 = roughly equal to depth of sternum; 2 = less than depth of sternum. \*
90. Extension of spina interna: 0 = present; 1 = absent.
91. Distinct foramen pneumaticum in dorsal face of sternum depth: 0 = absent; 1 = present.

## Scapula

92. Pneumatic foramen in cranial region of acromion (Migotto 2013, 82): 0 = absent; 1 = present.
93. Cranial projection of acromion in ventral or medial view: 0 = low projection; 1 = distinct projection.
94. Presence of a foramen on medial facies (derived from Migotto 2013, 83): 0 = absent; 1 = present on medial facies.
95. Presence of a foramen on ventral facies caudal to humeral facet (derived from Migotto 2013, 83): 0 = absent; 1 = present.

## Coracoid

96. Incisura/foramen nervi supracoracoidei (Migotto 2013, 84; modified from Olson 1987): 0 = absent; 1 = present.
97. Position of incisura/foramen nervi supracoracoidei (modified from Migotto 2013, 85): 0 = directly adjacent to medial margin of shaft; 1 = set adjacent to medial margin of cotyla scapularis; 2 = set almost central between the medial and lateral margins of shaft.
98. Coracoid, shaft, medial edge, incisura n. supracoracoidei enclosed by bridge of bone: 0 = open; 1 = enclosed.
99. Coracoid, shaft, medial edge, incisura n. supracoracoidei size: 0 = large, takes up at least half of shaft length omal to impressio m. sternocoracoidei (see *Falco berigora*); 1 = small, takes up  $\frac{1}{4}$  or less of shaft length.
100. Foramen opening into corpus from foramina nervi supracoracoidei (Migotto 2013, 86): 0 = absent; 1 = present.
101. Coracoid, omal end, orientation of omal margin of processus procoracoideus relative to sternal margin: 0 = parallel; 1 = orientated in a distal slope.
102. Coracoid, omal end, size of cotyla scapularis relative to the shaft width: 0 = small, less than  $\frac{1}{4}$  width; 1 = large,  $\frac{1}{4}$  or more width.
103. Sternal margin of facies articularis clavicularis forms crest overhanging sulcus supracoracoideus (Migotto 2013, 87; modified from Holdaway 1994, 59): 0 = present; 1 = absent.
104. Coracoid, omal end, position of pneumatic foramina relative to sides of sulcus supracoracoideus (Migotto 2013, 88): 0 = ventral; 1 = dorsal.

105. Coracoid, omal end, presence of pneumatic foramina in sulcus supracoracoideus: 0 = present; 1 = absent.
106. Coracoid, omal end, depth of pneumatic foramina in sulcus supracoracoideus: 0 = deep, pneumatic holes extend well into shaft; 1 = shallow, mildly pneumatized, barely goes past facies of sulcus.
107. Shape of coracobrachial ligament attachment (Migotto 2013, 89): 0 = triangular; 1 = rectangular, 2 = absent (*Falco*).
108. Coracoid, omal end, position of tuberculum for insertion of coracobrachial ligament on dorsal facies of coracoid body (Migotto 2013, 90; modified from Holdaway 1994, 68): 0 = medial; 1 = central; 2 = lateral. \*
109. Contiguity of coracobrachial ligament attachment to the cranial border of sulcus m. sternocoracoidei (Migotto 2013, 91): 0 = absent; 1 = present.
110. Depth of impression m. sternocoracoidei (Migotto 2013, 92): 0 = shallow; 1 = deep.
111. Coracoid, omal end, dorsal view, facies articularis humeralis, lateral projection: 0 = long and little projection; 1 = short and projecting (see *Accipiter fasciatus*); 2 = long and projecting.
112. Coracoid, length vs sternal articular width: 0 = short, robust; 1 = moderate; 2 = elongate, narrow. \*
113. Coracoid, sternal end, lateral edge, processus lateralis projection: 0 = non-projecting, barely extends past lateral-most point of facies articularis sternalis; 1 = well projecting, extends distinctly lateral of facies articularis sternalis.
114. Coracoid, distal end, lateral edge, processus lateralis robustness: 0 = the process is broad, with the distal edge approximately the same height as the proximal-most end; 1 = the process is tapered and narrow, distal edge narrower in height than proximal-most end, sternal edge quite compressed in relation to coracoid sternal end.
115. Coracoid, distal end, omal-sternal width of the facet on the facies articularis sternalis: 0 = narrow, consistent along facies; 1 = widened into a flange at angulus medialis end.
116. Coracoid, distal end, projection of dorsal flange relative to distal margin of facies articularis: 0 = set well proximal of margin; 1 = set near adjacent to margin.

## Humerus

117. Humerus, proximal end, cranial surface, pneumatic fossa set in base of caput humeri: 0 = absent; 1 = present (see *Coragyps atratus* B36873).
118. Humerus, proximal end, dorsal side, tuberculum dorsale presence (modified from Migotto 2013, char. 93): 0 = projecting caudally; 1 = projecting dorsoproximally.
119. Humerus, proximal end, dorsal side, level of tuberculum dorsale relative to sulcus lig. transversus (Migotto 2013, char, 94): 0 = distal to; 1 = aligned with.
120. Humerus, proximal end, cranial surface, depth of sulcus lig. transversus: 0 = shallow; 1 = deep, makes very distinct impression into bone.
121. Humerus, proximal end, cranial surface, inflation of the intumescencia humeri: 0 = surface inflated in rounded mound; 1 = surface flattened or slightly concave.
122. Humerus, proximal end, caudal surface, shape of fossa pneumotricipitalis ventralis: 0 = narrowed, half-oval; 1 = broadened, semicircular.
123. Humerus, proximal end, caudal surface, depth of fossa pneumotricipitalis dorsalis (Migotto 2013, char. 96): 0 = absent or barely differentiated; 1 = distinct/deep.
124. Humerus, proximal end, caudal surface, crus ventrale fossa, scar for attachment for M. scapulohumeralis caudalis/ dorsalis scapulae (see Matsuoka and Hasegawa 2007): 0 = elevated on crus ventrale fossa; 1 = not prominent on surface.
125. Humerus, proximal end, caudal surface, towards ventral side, depth of incisura capitis: 0 = shallow, no excavation present; 1 = secondarily deepened.
126. Humerus, proximal end, located ventral of incisura capitis, capital ridge on shaft (Migotto 2013, char. 95): 0 = absent; 1 = present.
127. Humerus, proximal end, caudal surface, distal of incisura capitis, adjacent to crus dorsale fossa, size of insertion at dorsal side of incisura capitis (see Matsuoka and Hasegawa 2007): 0 = quite large and round; 1 = oval shaped and narrow (see *Circus assimilis*).
128. Humerus, proximal end, caudal surface, distal of incisura capitis, visibility of insertion at dorsal side of incisura capitis: 0 = well defined, distinct shape; 1 = faint, poorly defined .
129. Humerus, proximal end, dorsal side, position of angulus deltopectoralis relative to distal end of crista bicipitalis (analogous to Migotto 2013 char. 99 and Holdaway 1994 char. 98): 0 = level or positioned just distal of crista bicipitalis; 1 = positioned well distal of crista bicipitalis.

130. Humerus, proximal end, proximal end, profile of proximal part of crista (Migotto 2013 char. 100, Holdaway 1994 char. 71): 0 = concave; 1 = flat
131. Humerus, proximal end, dorsal side, angulus deltopectoralis (Migotto 2013, char. 98): 0 = rounded; 1 = angled.
132. Humerus, proximal end, alignment of distal end of crista deltopectoralis relative to shaft (Migotto 2013, char. 97): 0 = perpendicular; 1 = parallel (Perpendicular is taken to mean deltoid crest directed cranially e.g. *Lophoictinia*, parallel directed dorsally e.g. *Aegyptius*).
133. Humerus, proximal end, ventral view, angle between distal crista deltopectoralis and shaft (Migotto 2013 char.101, Holdaway 1994 char. 72): 0 = shallow; 1 = markedly angled.
134. Humerus, proximal end, caudal aspect, presence of sulcus on caudal surface of crista deltopectoralis: 0 = in proximal half of crista, quite deep; 1 = in proximal half of crista, shallow; 2 = no sulcus. \*
135. Humerus, proximal end, ventrally on the crista deltopectoralis, breadth of insertion scar of m. pectoralis: 0 = narrow; 1 = robust.
136. Humerus, proximal end, crista deltopectoralis, in cranial view, length and distal end of scar for m. pectoralis (analogous to Migotto 2013 char. 104): 0 = long, extends level with base of crista bicipitalis; 1 = short, ends well before base of crista bicipitalis.
137. Humerus, proximal end, ventral side, distal margin of crista bicipitalis in caudal view (analogous to Migotto 2013 char. 102, Holdaway 1994 char. 84): 0 = little flaring, terminates close to shaft; 1 = forms distoventrally convex flange.
138. Humerus, proximal end, cranial facies, distal of crista bicipitalis, sulcus nervus coracobrachialis (modified from Migotto 2013, char. 103): 0 = absent; 1 = present (faint); 2 = present (distinct). \*
139. Humerus, shaft, curvature: 0 = straight, little or none; 1 = slightly sigmoid; 2 = markedly sigmoid (see *Accipiter fasciatus*). \*
140. Humerus, shaft, scar for m. latissimus dorsi on caudal facies: 0 = faint, poorly defined line down shaft; 1 = distinct line down shaft.
141. Humerus, shaft width, measured just proximal to epicondylus dorsalis, as a proportion of distal width from condylus ventralis to condylus dorsalis (Gaff and Boles 2010, character 7): 0 = less than 25%; 1 = more than 25% (broad).

142. Humerus, distal end, ventral side, projection of processus flexorius in medial view (Gaff and Boles 2010, character 5): 0 = protrudes caudally out from shaft (*Aquila*); 1 = caudal protrusion reduced/flattened (*Haliaeetus*).
143. Humerus, distal end, ventral side, projection of processus flexorius in cranial view (Migotto 2013, character 106; Gaff and Boles 2010, character 5): 0 = small, does not project past condylus ventralis; 1 = medium, equal with condylus ventralis; 2 = large, projects past condylus ventralis. \*
144. Humerus, distal end, ventral side, shape of processus flexorius in medial view (Gaff and Boles 2010, character 5): 0 = base well rounded (*Aquila*); 1 = base less round/flattened (*Haliaeetus*).
145. Humerus, distal end, ventral side, width of fossa on tuberculum supracondylare ventrale relative to gap between condyles: 0 = large (equal to or greater than size of gap); 1 = small (less than size of gap).
146. Humerus, distal end, ventral side, depth of fossa for pronator superficialis on tuberculum supracondylare ventrale: 0 = deep; 1 = shallow.
147. Humerus, distal end, projection of tuberculum supracondylare dorsale in cranial view (modified from Migotto 2013 char. 105): 0 = barely projecting dorsad of condyle; 1 = projecting noticeably dorsal from condyle; 2 = projecting strongly from condyle. \*
148. Humerus, distal end, caudal view, depth fossa olecrani (Gaff and Boles 2010, char. 2): 0 = shallow (see *Aquila*); 1 = deep and defined (see *Haliaeetus*); 2 = secondary deepening within fossa (see *Falco berigora*). \*
149. Humerus, distal end, cranial view, ventral side, shape of scar for m. pronator superficialis (Gaff and Boles 2010, char. 3): 0 = quite circular (see *Aquila*); 1 = ovoid, not as well defined (see *Haliaeetus*).
150. Humerus, distal end, cranial face, fossa m. brachialis depth: 0 = shallow; 1 = deep.
151. Humerus, distal end, cranial face, proximity of fossa m. brachialis to dorsal facies of shaft: 0 = distant, intervening shaft very broad (1/2 width of fossa (see *Falco berigora*); 1 = moderate separation, intervening area 1/4 width of fossa; 2 = narrow separation <1/4 width of fossa (see *Aegyptius monachus*). \*
152. Humerus, distal end, cranial face, orientation of dorsal margin of fossa brachialis proximally: 0 = curving dorsally towards shaft edge; 1 = curving ventrally.
153. Humerus, distal end, cranial face, extent of pneumatisation in fossa brachialis: 0 = little or none; 1 = highly pneumatic, fossae large.

154. Humerus, distal end, cranial face, orientation of interior margin of tuberculum supracondylare ventrale relative to the shaft axis: 0 = parallel to shaft; 1 = angled across shaft.
155. Humerus, distal end, cranial face, distance between interior margin of tuberculum supracondylare ventrale and tip of condylus dorsalis relative to distance between condylus dorsalis and dorsal margin: 0 = wider; 1 = equal.

## **Ulna**

156. Ulna, proximal end, delimitation dorsally and ventrally of incisura radialis (Migotto 2013, 107): 0 = crests; 1 = tuberosities or single tubercule.
157. Ulna, proximal end, pneumatic foramina in incisura radialis (Migotto 2013, 108): 0 = absent or small; 1 = present (conspicuous).
158. Ulna, proximal end, pneumatic foramen in impressio m. brachialis (Migotto 2013, 109): 0 = absent; 1 = present.
159. Ulna, proximal end, ventral side, impressio m. brachialis depth: 0 = shallow, little deepening in towards proximal end; 1 = well deepened.
160. Ulna, proximal end, size of projection of olecranon above cotyla (Migotto 2013, 110): 0 = small; 1 = large.
161. Ulna, proximal end, pneumatic foramen located between olecranon and cotyla dorsalis in cranial view (Migotto 2013, 111): 0 = absent; 1 = present.
162. Ulna, proximal end, shape of distal and lateral margins of processus cotylaris dorsalis (Migotto 2013, 112): 0 = rounded; 1 = pointed.
163. Ulna, proximal end, dorsal aspect, projection of shaft past cotyla ventralis: 0 = flattened to weak projection, does not project past cotyla; 1 = moderate projection, projects equal to or slightly past edge of cotyla ventralis; 2 = strongly projecting, projects well past edge of cotyla ventralis. \*
164. Ulna, proximal end, depth of impressio m. scapulothoracalis: 0 = small; 1 = large
165. Ulna, distal end, shape of dorsal side of tuberculum carpale (Migotto 2013, 113): 0 = undifferentiated from rest of tuberculum; 1 = differentiated (flat facies); 2 = differentiated (shallow fossa). \*
166. Ulna, distal end, tuberculum carpale, presence of foramen on ventral side (Migotto 2013, 114): 0 = absent; 1 = present.
167. Ulna, distal end, sulcus intercondylaris (Migotto 2013, 115): 0 = shallow; 1 = deep.

168. Ulna, distal end, tuberculum carpalae status: 0 = flattened, weakly to moderately protruding; 1 = pointed, well protruding.
169. Curvature of shaft in ventral or dorsal aspect: 0 = straight, little or none; 1 = distinct, especially proximally (see *Accipiter fasciatus*).

### **Radius**

170. Radius, proximal end, presence of pneumatic foramen associated with the tuberculum bicipitalis radialis (Migotto 2013, 116): 0 = absent; 1 = present.
171. Radius, distal end, presence of a pneumatic foramen in the depressio ligamenti (modified from Migotto 2013, 117): 0 = absent; 1 = present.
172. Radius, distal end, position of pneumatic foramen in the depressio ligamenti (modified from Migotto 2013, 117): 0 = medial side; 1 = lateral side.

### **Carpometacarpus**

173. Carpometacarpus, proximal end, pneumatic foramina in fovea carpalis cranialis (Migotto 2013, 119): 0 = absent; 1 = present.
174. Carpometacarpus, proximal end, angle formed between processus extensorius and external rim of trochlea carpalis (Migotto 2013, 120): 0 = obtuse (greater than 100°); 1 = right angle (roughly 90°).
175. Carpometacarpus, proximal end, contiguity between facies articularis digiti alulae and proximal region of os metacarpale majus (Migotto 2013, 121; Holdaway 1994, 141): 0 = present, connected to os metacarpale majus; 1 = absent, not connected.
176. Carpometacarpus, proximal end, pneumatic surface on proximal region of os metacarpale minus (derived from Migotto 2013, 122; Holdaway 1994, 132): 0 = present; 1 = absent.
177. Carpometacarpus, proximal end, shape of surface of proximal region of os metacarpale minus (derived from Migotto 2013, 122; Holdaway 1994, 132): 0 = concave; 1 = flat.
178. Carpometacarpus, proximal end, position of distal end of ventral rim of trochlea carpalis relative to processus alularis: 0 = located well proximal to; 1 = equivalent to or slightly proximal of.
179. Carpometacarpus, proximal end, pneumatisation of fossa infratrochlearis: 0 = present; 1 = absent.

180. Carpometacarpus, proximal end, ventral facies, deep sulcus separating the processus pisiformis and the processus extensorius: 0 = absent; 1 = present
181. Carpometacarpus, proximal end, dorsally, pneumatization of fossa supratrochlearis: 0 = present; 1 = absent.
182. Carpometacarpus, proximal end, distance between processus pisiformis and proximal-most point of spatium intermetacarpale: 0 = long, greater than proximal width of carpometacarpus; 1 = short, equal or less than proximal width.
183. Carpometacarpus, curvature of os metacarpale minus: 0 = flattened; 1 = arched caudally.
184. Carpometacarpus, distal end, projection of facies articularis digitalis minor past facies articularis digitalis major: 0 = greatly projecting; 1 = slightly projecting; 2 = roughly level. \*
185. Carpometacarpus, distal end, projection of ridge bordering sulcus tendineus distally in dorsal view: 0 = low; 1 = distinct thickening on either side of groove.
186. Carpometacarpus, distal end of os metacarpale majus, ventral projection: 0 = projects weakly cranially in low angle; 1 = protrudes out strongly cranially in steep angle.
187. Carpometacarpus, distal end, length of distal synostosis to facet for digit 2 relative to spatium intermetacarpale (modified from Worthy et al 2016): 0 = short, less than width of spatium intermetacarpale; 1 = moderate, equal width of spatium intermetacarpale; 2 = elongate, up to twice as long. \*

### **Ossa Carpi**

188. Os carpi radiale, projection of facies articularis metacarpalis (see Mayr 2014): 0 = not projecting in cranial view; 1 = partially projecting in cranial view (rounded or low prominence); 2 = strongly projecting in cranial view (both ends visible, pointed edges). \*
189. Os carpi radiale, notch for m. ulnometacarpalis ventralis (see Mayr 2014): 0 = low profile of inner edge; 1 = distinct inner edge projecting ventrally.
190. Os carpi radiale, facies articularis ulnaris, indentation depth (see Mayr 2014): 0 = shallow or slight; 1 = deep, distinct.

### **Pelvis**

191. Pelvis, dorsal view, shape of pelvis: 0 = short and broad; 1 = elongate.
192. Pelvis, dorsal view, ala preacetabularis ilii, canalis iliosynsacri: 0 = absent; 1 = present.

193. Pelvis, dorsal view, proximity of dorsal iliac crests in preacetabular zone (Migotto 2013, 124): 0 = close set or touching; 1 = separated.
194. Pelvis, dorsal view, foramina intertransversaria (Migotto 2013, 125): 0 = open; 1 = partially or completely closed.
195. Pelvis, crista iliosynsacralis in interacetabular region (Migotto 2013, 126): 0 = flat or slightly grooved; 1 = inflated.
196. Pelvis, Lateral extremity of crista dorsolateralis ilii (Migotto 2013, 127): 0 = laterally expanded; 1 = retracted/withdrawn.
197. Pelvis, fossa iliocaudalis depth: 0 = shallow or absent; 1 = deep.
198. Pelvis, processus ventralis on extremitas cranialis synsacra: 0 = absent; 1 = present.
199. Pelvis, anterior fossa renalis: 0 = shallow; 1 = deep.
200. Pelvis, caudal fossa renalis (Migotto 2013, 128): 0 = shallow; 1 = deep.
201. Pelvis, caudal margin of foramen obturatum (Migotto 2013, 129): 0 = open, confluent to ischiopubica fenestra; 1 = closed.
202. Pelvis, incisura of terminal region of ischium (Migotto 2013, 130): 0 = absent; 1 = present (slight, see *Pandion haliaetus*); 2 = present (pronounced, see *Coragyps atratus*). \*
203. Pelvis, sutura iliosynsacralis conformation of postacetabular zone in dorsal aspect from caudal margin up: 0 = abruptly strikes out in 45° angle line before turning inwards (forms a right angle 'L' shape, *Falco berigora*); 1 = forms a gradually angled line that follows outward towards edges of ala postacetabularis (*Pandion haliaetus*); 2 = roughly forms a straight line following proximally up pelvis (*Aquila audax*).
204. Pelvis, ventral view, caudal of foramen acetabuli, conformation of widest distal processus costales of vertebrae acetabulum: 0 = thin struts limited to synsacrum; 1 = thin struts, forms a thin bridge attaching directly to ventral side of antitrochanter; 2 = thick struts, forms robust bridge attaching directly to ventral side of antitrochanter. \*

## Femur

205. Femur, proximal end, proximal projection of crista trochanteris from facies articularis antitrochanterica (Migotto 2013, 131): 0 = high; 1 = low.
206. Femur, proximal end, fossa trochanteris (Migotto 2013, 132): 0 = distinct depression; 1 = shallow or absent.

207. Femur, proximal end, cranial aspect, number of pneumatic foramina on crista trochanteris (Migotto 2013, 133): 0 = none; 1 = one; 2 = two. \*
208. Femur, proximal end, caudal surface, depth of depression immediately distad of facies articularis antitrochanterica: 0 = shallow or no depression; 1 = deep, distinct impression.
209. Femur, proximal end, cranial aspect, position of linea intermuscularis cranialis on the upper corpus femoris (Migotto 2013, 134): 0 = lateral connects to end of crista trochanterica; 1 = medial, passing to medial side of pneumatic zone.
210. Femur, proximal end, projection of facies articularis antitrochanterica over cranial facies: 0 = overhanging; 1 = not overhanging.
211. Femur, proximal end, position of fovea lig. capitis: 0 = set high in caput femoris, small and circular (see *Falco berigora*); 1 = set high in caput femoris, large and circular; 2 = set low in caput femoris, large and ovalar.
212. Femur, distal end, shape of proximal part of condylus fibularis in caudal aspect (Migotto 2013, 135): 0 = short; 1 = extended out to the side.
213. Femur, distal end, crista supracondylaris medialis (Migotto 2013, 136): 0 = absent or minute; 1 = present.
214. Femur, distal end, depth of fovea tendineus m. tibialis cranialis: 0 = deep and distinct; 1 = shallow.
215. Femur, distal end, depth of impressio m. gastrocnemialis lateralis: 0 = deep; 1 = shallow.
216. Femur, distal end, size of impressio m. gastrocnemialis lateralis: 0 = large; 1 = small.
217. Femur, distal end, caudal view, connectivity of lateral and medial condyles: 0 = connected by proximodistally compressed ridge; 1 = no connection, separated by distinct sulcus.
218. Femur, distal end, shape of ligament attachment point proximal to fossa poplitea: 0 = line/ridge; 1 = circular; 2 = oval; 3 = absent.
219. Femur, distal end, depth of fossa poplitea: 0 = shallow; 1 = moderately deep; 2 = very deep, (see *Pandion*). \*

## **Tibiotarsus**

220. Tibiotarsus, proximal end, linearity of proximal profile of crista patellaris assessed in cranial aspect (Migotto 2013, 137): 0 = straight; 1 = convex proximally.
221. Tibiotarsus, proximal end, level of distal extremity of crista cnemialis cranialis in relation to proximal end of crista fibularis (Migotto 2013, 138): 0 = proximal; 1 = coinciding; 2 = caudal. \*
222. Tibiotarsus, proximal end, crista cnemialis cranialis length distally on shaft and cranial projection: 0 = markedly projects from shaft; 1 = does not project.
223. Proximal end, caudal facies, depth of fossa flexoria: 0 = shallow; 1 = deep, distinct fossa in shaft adjacent to facies articularis.
224. Tibiotarsus, proximal end, depression in the facies gastrocnemialis lateral of crista cnemialis cranialis (Migotto 2013, 139): 0 = deep; 1 = shallow or none.
225. Tibiotarsus, proximal end, depth of fossa retropatellaris: 0 = shallow, faint impression into proximal articular surface; 1 = deep, distinct impression.
226. Tibiotarsus, distal end, alignment of pons supratendineus in relation to long axis of shaft (Migotto 2013, 140; Holdaway 1994, 215): 0 = perpendicular (e.g. *Polyboroides*); 1 = oblique; 2 = nearly parallel (e.g. *Accipiter*). Note the canalis extensorius runs at right angle to the alignment of the pons. \*
227. Tibiotarsus, distal end, depth of sulcus extensorius under bridge of pons (Migotto 2013, 141): 0 = shallow; 1 = deep; 2 = very deep. \*
228. Tibiotarsus, distal end, condylus lateralis, sulcus m. fibularis (peronei) depth (Migotto 2013, 142): 0 = shallow; 1 = deep.
229. Tibiotarsus, distal end, expansion of condyles beyond shaft margins (anterior view): 0 = condyles expanded; 1 = condyles not expanded.
230. Tibiotarsus, distal end, condylus medialis, epicondylus medialis (Migotto 2013, 143): 0 = weakly present; 1 = developed, prominent of condyles; 2 = developed, occluded by condyles.
231. Tibiotarsus, distal end, cranial view, distal notch of incisura intercondylaris (modified from Migotto 2013, 144; modified from Holdaway 1994, char. 244): 0 = shallow; 1 = deep (u-shape); 2 = deep (v-shape).
232. Tibiotarsus, distal end, caudal surface of trochlea cartilaginosis tibialis (modified Migotto 2013, 145): 0 = flat or bound by low caudal projections of condyli; 1 = deep groove bound by high caudal projections of condyli.

233. Tibiotarsus, distal end, number of openings to canalis extensorius: 0 = 2; 1 = 3 (as per falconids eg *Falco berigora*).
234. Tibiotarsus, distal end, distal view, level of cranial margin of condyles: 0 = equal; 1 = lateral condyle more cranial; 2 = medial condyle more cranial.
235. Tibiotarsus, distal end, distal view, medial condyle depth relative to width: 0 = deeper than wide; 1 = depth equals width; 2 = depth less than width (>0.5 mm). \*
236. Tibiotarsus, distal end, cranial view, ratio of height to width of medial condyle: 0 = roughly equal ratio (<15% difference); 1 = wider than high; 2 = higher than wide.
237. Tibiotarsus, distal end, cranial view, ratio of height to width of lateral condyle: 0 = roughly equal ratio (<15% difference); 1 = wider than high; 2 = higher than wide.
238. Tibiotarsus, distal end, projection of epicondylus lateralis from condylus lateralis: 0 = projects markedly from condyle (*Falco berigora*); 1 = no projection.
239. Tibiotarsus, distal end, position of proximal/medial attachment for tuberositas retinaculum extensoriiis medialis (ligamentum transversum): 0 = set close to proximal side of pons supratendineus; 1 = set well proximal to pons supratendineus.
240. Tibiotarsus, distal end, position of distal/lateral attachment for ligamentum transversum: 0 = at end of distal side of pons supratendineus bridge, well offset from margin (*Elanus*); 1 = level with distal pons supratendineus; but extending to lateral margin.
241. Tibiotarsus, distal end, projection of crista on medial margin of trochlea cartilaginis tibialis: 0 = strongly projecting, forms rough 90° angle between main shaft and condyle; 1 = strongly projecting, flat line; 2 = weakly projecting.

### **Tarsometatarsus**

242. Tarsometatarsus, proximal end, hypotarsus structure (terminology after Mayr 2016) plantar connection of crista lateralis flexoris hallucis longus and crista medialis flexoris digitorum longus to enclose a canal (based on Migotto 2013 char. 147): 0 = fully overlapping, monosulcate; 1 = partial overlap, cristae approach one another plantarly and join at some points but do not form a complete bridge over the length of the cristae (see *Aviceda subcristata* and *Pernis apivorus*); 2 = no overlap, sulcus hypotarsi completely open. \*
243. Tarsometatarsus, proximal end, dorsoplantar depth of cristae relative to each other (analogous to Migotto 2013 char. 148): 0 = crista medialis flexor digitorum longus and crista lateralis flexor hallucis longus of roughly equal depth; 1 = crista medialis flexor digitorum longus distinctly deeper than crista lateralis flexor hallucis longus.

244. Tarsometatarsus, proximal end, proximodistal length of crista medialis hypotarsi relative to crista lateralis hypotarsi: 0 = crista medialis hypotarsi much longer than crista lateralis hypotarsi; 1 = crista medialis and lateralis hypotarsi of roughly equal length.
245. Tarsometatarsus, proximal end, length of crista medialis lateralis relative to width: 0 = wider than long (1.5- 2x); 1 = roughly equal; 2 = longer than wide (1.5-2x). \*
246. Tarsometatarsus, proximal end, proximal aspect, cristae hypotarsi, depth of sulcus hypotarsi relative to the cotylae: 0 = sulcus hypotarsi set well plantar of cotylae (see *Coragyps atratus*); 1 = sulcus hypotarsi in line or close to cotylae.
247. Tarsometatarsus, proximal end, proximal aspect, sulcus hypotarsi, position of sulcus hypotarsi relative to sulcus flexorius: 0 = roughly equal; 1 = sulcus hypotarsi set plantar to sulcus flexorius.
248. Tarsometatarsus, proximal end, proximal view, incisura at base of crista lateralis flexoris hallucis longus hypotarsi, canal for m. fibularis longus (Migotto 2013, 149; modified from Jollie 1977b): 0 = absent; 1 = present (shallow); 2 = present (deep). \*
249. Tarsometatarsus, proximal end, lateral side, plantar aspect, length of sulcus for musculus fibularis longus on shaft (see Mayr 2016): 0 = absent or reduced; 1 = medium length, forms short, shallow sulcus (that extends to proximal third of length; 2 = very long sulcus, extends to at least halfway down shaft (*Pandion haliaetus*). \*
250. Tarsometatarsus, proximal end, depth of fossa infracotylaris dorsalis (Migotto 2013, 155): 0 = shallow; 1 = deep.
251. Tarsometatarsus, proximal end, lateral side, distinctness of impressio ligamentum collateralis lateralis: 0 = prominent tuberosity; 1 = indistinct scar, no prominence.
252. Tarsometatarsus, proximal end, length of crista medialis hypotarsi relative to depth: 0 = depth greater than length; 1 = depth equal to length; 2 = depth lesser than length. \*
253. Tarsometatarsus, proximal end, distal projection/hook on plantar end of crista medialis hypotarsi (modified from Migotto 2013, 151): 0 = none present; 1 = short, barely projects from crista; 2 = long, projects distinctly from crista. \*
254. Tarsometatarsus, proximal end, position of crista medialis hypotarsi: 0 = in line with outer edge of cotyla medialis; 1 = in line with centre of cotyla medialis; 2 = centred proximally between cotylae (see *Falco berigora*). \*
255. Tarsometatarsus, proximal end, proximal prominence of eminentia intercotylaris in dorsal view: 0 = little to moderate proximal projection; 1 = hyperprotruding, extends well proximal to cotyla (see *Coragyps atratus*).

256. Position of distal end of crista medianoplantaris relative to foramina vascularia proximalia medialis (Migotto 2013, 152): 0 = proximal; 1 = coinciding; 2 = distal. \*
257. Tarsometatarsus, proximal end, plantar aspect, position of foramen vasculare proximale medialis in lateromedial axis (Migotto 2013, 153): 0 = medial to crista medianoplantaris; 1 = lateral to crista medianoplantaris.
258. Tarsometatarsus, proximal end, plantar aspect, size of foramina vascularia proximalia: 0 = small, pinhole like; 1 = large, distinct holes.
259. Tarsometatarsus, proximal end, plantar and dorsal aspect, foramina vascularia proximalia, openness: 0 = both foramina open plantarly; 1 = foramina lateralis closed plantarly; 2 = foramina medialis closed plantarly.
260. Tarsometatarsus, proximal end, medial side, plantar aspect, width of proximal end of fossa parahypotarsalis medialis: 0 = very narrow; 1 = broad and poorly defined; 2 = broad and distinct.
261. Attachment ridges for impressiones retinaculi extensorii (Migotto 2013, 154 [modified]): 0 = absent; 1 = present (open, forms attachment for bridge); 2 = present (enclosed). \*
262. Tarsometatarsus, proximal end, prominence of tuberositas m. tibialis cranialis in lateral view: 0 = barely visible or none; 1 = very distinct protuberance from shaft.
263. Tarsometatarsus, proximal end, dorso-plantar depth of medial shaft adjacent to midlength fossa parahypotarsalis medialis: 0 = very thick; 1 = dorso-plantarly compressed but slightly thickened; 2 = highly dorso-plantarly compressed, thin. \*
264. Tarsometatarsus, proximal end, shape of tuberositas m. tibialis cranialis: 0 = elongate ridge; 1 = roughly circular or semi-ovular.
265. Tarsometatarsus, proximal end, proximity of tuberositas m. tibialis cranialis to foramina vascularia proximalia (analogous to Migotto 2013, 156, but slightly different states): 0 = abutting or just distal to foramina; 1 = set well distal from foramina.
266. Tarsometatarsus, proximal end, mediolateral position of tuberositas m. tibialis cranialis relative to foramina vascularia proximalia: 0 = offset medially, located distal to medial foramen (see *Falco berigora*); 1 = set roughly central between foramina (but see *Elanus scriptus* for unusual foramina positions); 2 = offset laterally, located distal to lateral foramen. \*
267. Tarsometatarsus, proximal end, central shaft, number of scars for tuberosities m. tibialis cranialis: 0 = 1; 1 = 2.

268. Tarsometatarsus, proximal end, shaft on medial side of tuberositas m. tib. cranialis, depth of sulcus extensorius (analogous to Migotto 2013, 157): 0 = distinct, noticeable groove between outer shaft edge and tuberositas; 1 = indistinct, flattened.
269. Tarsometatarsus, shaft, dorsal facies subcutanea lateralis at midlength of shaft: 0 = flat, ends level; 1 = strongly concave.
270. Tarsometatarsus, shaft, dorsal facies, position and depth of sulcus extensorius: 0 = deep, positioned strictly on dorsal facies; 1 = deep, pressing medially towards distal end; 2 = shallow, pressing medially towards distal end.
271. Tarsometatarsus, proximal end + shaft, plantar aspect, merging of fossa parahypotarsalis medialis and sulcus flexorius: 0 = not merged (see *Pandion haliaetus*); 1 = merge close to proximal end; 2 = merge roughly halfway along the shaft or more distal; 3 = non-conventional sulcus flexorius, not applicable (*Falco*).
272. Tarsometatarsus, shaft, development of lateral crista on plantar surface of shaft (modified from Migotto 2013, 158): 0 = lateral crista absent to weakly developed; 1 = lateral crista well developed.
273. Tarsometatarsus, distal end, extension of incisura for m. flexor hallucis brevis relative to fossa metatarsi I: 0 = ends more proximally; 1 = ends equidistant with; 2 = ends distally to; 3 = absent or positioned differently. \*
274. Tarsometatarsus, distal end, plantar facies, width of sulcus for abductor muscle IV: 0 = narrow; 1 = broad; 2 = indistinct.
275. Tarsometatarsus, distal end, position of fossa metatarsi I: 0 = located on the medial facies of the shaft; 1 = offset medially on plantar facies; 2 = on plantar facies well-separated from medial edge. \*
276. Tarsometatarsus, distal end, relative distal extent of trochleae, in dorsal aspect: 0 = all roughly equal; 1 = trochlea metatarsi IV ends proximal to trochleae metatarsorum III and II which have equal distal extent; 2 = trochlea metatarsi IV has least distal extent and trochlea metatarsi III the most distal extent; 3 = trochlea metatarsi IV has least distal extent and trochlea metatarsi II the most distal extent.
277. Tarsometatarsus, distal end, plantar development of external rim of trochlea metatarsi II: 0 = projecting plantarly; 1 = projecting medio-plantarly; 2 = no projection.
278. Tarsometatarsus, distal end, plantar development of external rim of trochlea metatarsi IV: 0 = short to moderately projecting; 1 = very long, flange strongly projecting out from trochlea plantarly (see *Pandion*).

279. Tarsometatarsus, Angle of distal face of trochlea metatarsi IV relative to lateromedial axis (modified from Migotto 2013, 160): 0 = absent, distal facies parallel; 1 = present, distal facies oblique on medial facing edge; 2 = present, distal facies oblique on lateral facing edge.
280. Tarsometatarsus, distal end, plantar aspect, diameter of foramen vasculare distale compared to width of incisura intertrochlearis lateralis: 0 =  $\frac{1}{2}$  width or less (see *Falco berigora*); 1 = between  $\frac{1}{2}$  to equal width; 2 = greater width (see *Aviceda subcristata*).

## Digits

### Pedal digit I, phalanx 1

281. Os metatarsale I, presence of projecting ridge on lateral section of sulcus on anterior facies (that facing plantar facies of tarsometatarsus) of trochlea metatarsi I: 0 = absent; 1 = present, slightly protruding; 2 = present, highly protruding (see *Haliaeetus*, *Haliastur*, *Milvus*). \*
282. Os metatarsale I, tuberculum located at mid-length on medial edge of metatarsal; 0 = absent; 1 = present, slight projection; 2 = present, large projection. \*
283. Os metatarsale I, shape of lateral edge of shaft leading distally to lateral side trochlea metatarsi I: 0 = straight (see *Pernis*, *Aviceda*); 1 = concave.
284. Os metatarsale I, sulcus distomedial to articular facet: 0 = small, 1 = large.
285. Robustness of digit 1 phalanx 1 compared to phalanges on all other digits: 0 = least robust (*Coragyps atratus*); 1 = equal or slightly more robust than most phalanges on other digits (*Falco berigora*); 2 = significantly more robust than any other phalanx (*Aquila audax*). \*
286. Digit 1, unguis phalanx, length of facies articularis relative to length of tuberculum flexorius: 0 = roughly equal; 1 = tuberculum longer; 2 = facies articularis longer.

### Pedal digit II

287. Fusion between 1st and 2nd phalanges of digit II (Migotto 2008, ch. 161): 0 = absent; 1 = present.
288. Size difference between phalanges one and two (if unfused): 0 = one as long as, or slightly longer than, two (*Coragyps atratus*); 1 = one shortened, roughly half the length of two (*Falco berigora*); 2 = one greatly shortened, compressed cube less than half the length of two (*Aquila audax*). \*

289. Digit 2, unguis phalanx, length of facies articularis relative to length of tuberculum flexorium: 0 = roughly equal; 1 = tuberculum longer; 2 = facies articularis longer.

### **Pedal digit III**

290. Size difference between phalanges two and three: 0 = equal in size (*Coragyps atratus*); 1 = 3 larger than 2; 2 = 2 larger than 3.
291. Phalanx 4, prominent ridge on medial side of corpus phalangis (from juncture cotyla articularis): 0 = absent; 1 = present.
292. Phalanx 4, ridge at juncture of lateral and plantar sides of corpus phalangis: 0 = rounded; 1 = sharp/pointed.
293. Phalanx 4, height to width ratio of cotyla articularis: 0 = higher than wide; 1 = equal height to width; 2 = wider than high.
294. Phalanx 4, symmetry of tuberculum flexorium in plantar aspect: 0 = medial side larger than lateral; 1 = complete or almost complete symmetry; 2 = lateral side larger than medial. \*
295. Phalanx 4, width to length ratio of tuberculum flexorium in plantar aspect: 0 = wider than long; 1 = longer than wide; 2 = equal width and length.
296. Phalanx 4, ridge on midline of tuberculum flexorium: 0 = absent, 1 = present.
297. Digit 3, unguis phalanx, length of facies articularis relative to length of tuberculum flexorium: 0 = roughly equal; 1 = tuberculum longer; 2 = facies articularis longer.

### **Pedal digit IV**

298. Length of phalanx 1 relative to phalanx 4: 0 = as long as, or longer than, 4 (*Coragyps atratus*); 1 = slightly shorter than 4 (2/3 to 1/2 length, see *Aquila audax*); 2 = considerably shorter than 4 (1/3 or less, see *Falco berigora*). \*
299. Shortening of phalanges 2 and 3 relative to 4: 0 = slightly shorter than 4 (*Coragyps atratus*); 1 = greatly shorter than 4, almost cube-shaped (Accipitridae, Falconidae).
300. Digit 4, unguis phalanx, length of facies articularis relative to length of tuberculum flexorium: 0 = roughly equal; 1 = tuberculum longer; 2 = facies articularis longer.

### **References**

- Brito GRR. 2008. *Análise filogenética de Cathartidae (Aves) com base em caracteres osteológicos*. PhD dissertation, Universidade de São Paulo, Instituto de Biociências, Departamento de Zoologia.
- Elzanowski A, Stidham TA. 2010. Morphology of the quadrate in the Eocene anseriform *Presbyornis* and extant galloanserine birds. *J Morphol*, 271: 305–323.
- Elzanowski A, Zelenkov NV. 2015. A primitive heron (Aves: Ardeidae) from the Miocene of Central Asia. *J Ornithol*, 156: 837–846.
- Gaff P, Boles WE. 2010. A new eagle (Aves: Accipitridae) from the Mid Miocene Bullock Creek Fauna of northern Australia. *Rec Aust Mus*, 62: 71–76.
- Holdaway, RN. 1994. An exploratory phylogenetic analysis of the genera of the Accipitridae, with notes on the biogeography of the family. In: Meyburg, B. U.; Chancellor, R. D. (eds.). Berlin, *Proceedings of the IV World Conference on birds of prey and owls*, p. 601–649.
- Jollie M. 1977. A contribution to the morphology and phylogeny of the Falconiformes, part III. *Evolutionary Theory*, 2(5): 209–300.
- Livezey BC, Zusi RL. 2007. Higher-order phylogeny of modern birds (Theropoda, Aves: Neornithes) based on comparative anatomy: II. Analysis and discussion. *Zool J Linnean Soc*, 149(1): 1–95.
- Matsuoka H, Hasegawa Y. 2007. Myology and osteology of the Whooper Swan *Cygnus cygnus* (Aves: Anatidae) Part 1. Muscles attached to the sternum, coracoid, clavicle, scapula and humerus. *Bull Gunma Nat Hist Mus*, 11: 7–14
- Mayr G. 2014. Comparative morphology of the radial carpal bone of neornithine birds and the phylogenetic significance of character variation. *Zoomorphology*, 133: 425–434.
- Mayr G. 2018. Size and number of the hypoglossal nerve foramina in the avian skull and their potential neuroanatomical significance. *J Morphol*, 279(2): 274–285.
- Migotto R. 2008. *Inferência filogenética em gaviões buteoninos (Aves: Accipitridae), com base em caracteres osteológicos cranianos*. Masters dissertation, Universidade de São Paulo, Instituto de Biociências, Departamento de Zoologia.
- Migotto R. 2013. Phylogeny of Accipitridae (Aves: Accipitriformes) based on osteological characters. PhD dissertation, Universidade de São Paulo, Instituto de Biociências, Departamento de Zoologia.
- Worthy TH, Mitri M, Handley WD, Lee MS, Anderson A, Sand C. 2016. Osteology supports a stem-galliform affinity for the giant extinct flightless bird *Sylviornis neocaledoniae* (Sylviornithidae, Galloanseres). *PLOS ONE*, 11(3), DOI: 10.1371/journal.pone.0150871.

## Appendix 2: Additional Measurements

### Measurements from *Archaeohierax sylvestris* holotype

Sternum: carina apex height (from cranial margin of spina interna to apex of carina) 35.1; L Coracoid: facies articularis humeralis width 7.7; proximal height (from base of cotyla scapularis to cranial margin of processus acrocoracoideus) 12.8; L Scapula: PW (acromion to ventral side of facies articularis humeralis) 14.0; L Ulna: length (from distal end to cranial margin of cotyla dorsalis) 158.8; least-shaft width 6.5; maximum DW, from tuberculum carpale to caudal margin condylus dorsalis ulnare 12.9; L Radius: length 156.3; L Carpometacarpus: length 78.2; PW 19.6; L Tibiotarsus: length, from distal side condylus lateralis to proximal end crista fibularis, 135.7; least SW 9.7; DW 16.5; depth condylus lateralis 12.9; height condylus lateralis 9.4; depth condylus medialis 13.1 mm; height condylus medialis 9.2; R Tibiotarsus: length N/A; least SW 9.7; DW 17.6; craniocaudal depth condylus lateralis N/A; proximodistal height condylus lateralis 9.3; craniocaudal depth condylus medialis 13.4; proximodistal height condylus medialis 9.2; L Tarsometatarsus: length 110.1 (considered to approximate total length despite the twisted nature of the partially

reconstructed element resulting in proximal end being rotated 90 degrees to most of the bone); PW 16.0 from cotyla medialis medial margin to crista lateralis lateral margin; plantar depth 17.8 from eminentia intercotylaris to plantar margin of crista medialis hypotarsus, 8.8 from eminentia intercotylaris to sulcus hypotarsi middle, and 13.6 from medial condyle dorsal margin to crista lateralis hypotarsi plantar margin; SW immediately proximal to the fossa metatarsi I 9.3; DW (excluding flange on trochlea metatarsi II) 17.7; width of trochlea metatarsi II 4.3; width of trochlea metatarsi III 5.2; width of trochlea metatarsi IV N/A; depth of trochlea metatarsi II 9.3; depth of trochlea metatarsi III 7.7; depth of trochlea metatarsi IV N/A; shaft width 9.4; Pedal phalanges: see Table 1.

element	side	TL	PW	Prox H	DW	Tub flex W	Tub Flex L
Os metatarsal I	R	18.1	-	-	10.6	-	-
Phalanx I.1	R	30.0	11.8	-	7.6	-	-
Phalanx I.2	R	23.2	7.7	8.7	-	4.2	4.6
Phalanx II.1	R	-	9.3	-	-	-	-
Phalanx II.2	R	26.1	7.5	-	6.4	-	-
Phalanx II.3	R	20.0	6.7	8.4	-	4.1	4.9
Phalanx III.1	R	24.1	8.4	-	6.1	-	-
Phalanx III.2	R	13.0	6.3	-	5.5	-	-
Phalanx III.4	R	-	6.1	6.4	-	3.7	3.3
Os metatarsal I	L	18.7	-	-	10.5	-	-

Phalanx I.1	L	30.1	12.0	-	7.4	-	-
Phalanx II.1	L	11.9	9.9	-	6.1	-	-
Phalanx II.2	L	26.7	7.5	-	6.4	-	-
Phalanx II.3	L	-	-	8.3	-	-	4.4
Phalanx III.1	L	24.0	8.1	-	6.1	-	-
Phalanx III.2	L	13.5	6.3	-	5.2	-	-
Phalanx III.4	L	-	6.1	6.4	-	3.6	4.1
Phalanx IV.1	L	12.2	6.8	-	4.7	-	-
Phalanx IV.2	L	6.0				-	-
Phalanx IV.3	L	5.6				-	-
Phalanx IV.4	L	19.1	4.5	-	4.6	-	-
Phalanx IV.5	L	-	4.7	5.8	-	2.8	2.7

**Table A2.1:** Measurements for phalanges of all pedal digits of *Archaeohierax sylvestris* gen. et. sp. nov. Abbreviations: R = right, L = left, TL = total length, PW = proximal width, Prox H = proximal height, DW = distal width, Tub flex W = tuberculum flexorium width, Tub Flex L = tuberculum flexorium length.

Species	Hum PW	Hum DW	Hum PW/DW	Tib DW	Fem DW	Tib DW/Fem DW
<i>Archaeohierax sylvestris</i>	29.3	?	?	17.6	?	?
NMV P222435 (distal femur)	?	?	?	?	12.8	?
SAMA P.58917 (distal humerus)	?	15.4	?	?	?	?
<i>Gampsonyx swainsonii</i>	8.4	6.7	0.8	6.3	5.7	1.1
<i>Buteo lagopus</i>	22.7	19.6	0.86	13.3	16.8	0.79
<i>Accipiter striatus</i> (ssp. <i>velox</i> )	11.6	10.5	0.90	6.3	8.2	0.76
<i>Accipiter cooperii</i>	17.4	14.3	0.82	10	11.8	0.85
<i>Accipiter cooperii</i>	14.2	12.5	0.88	8	9.8	0.82
<i>Accipiter nisus</i>	10.6	?	?	5.9	6.5	0.91
<i>Aquila chrysaetos</i>	41.1	35.9	0.87	23.3	29.2	0.80
<i>Aviceda subcristata</i>	15	13.8	0.91	8.3	9.7	0.85
<i>Circus approximans</i>	19.2	17.3	0.9	10.8	13.9	0.78
<i>Circus approximans</i>	20	17.9	0.9	11.7	13.7	0.86

<i>Aquila audax</i>	36.4	31.3	0.86	20	24.3	0.82
<i>Hieraaetus morphnoides</i>	21.9	19.1	0.87	13.4	15.4	0.87
<i>Elanus scriptus</i>	14.3	12.4	0.87	9.2	9.3	0.99
<i>Hamirostra melanosternon</i>	26.8	22.5	0.84	13.2	15.6	0.85
<i>Haliaeetus leucogaster</i>	36.7	31.8	0.87	19.3	22.6	0.85

**Table A2.2:** Chapter 2 Measurements of humerus proximal and distal width, femur distal width, and tibiotarsus distal width of fossil specimens and extant species and the derived ratios Hum PW/DW, ratio between the proximal and distal width of the humerus, and Tib DW/Fem DW, the ratio between the distal widths of the tibiotarsus and femur.

## Appendix 3: Chapter 2 comparative descriptions with extant species

### *Archaehierax sylvestris*

#### *Rostrum maxillare*

Other accipitrids differ as follows (variable characters excluded):

#### Elaninae.

(4) In ventral view, the ossified rostral section of the palate is relatively small (only a few millimetres long at most), in part due to (5) the presence of a large fenestra ventromedialis.

#### Perninae.

(3) All species possess a large, fully open nasal cavity, with the exception of those in *Aviceda subcristata*, where the nasal cavity is narrow but still completely open, and in *Hamirostra melanosternon*, which had a small nasal shield in all observed specimens.

#### Gypaetinae.

(2) *Neophron percnopterus* lacks a crista tomialis, which is a state only shared with the species *Gypaetus Barbatus* (not included in this analysis [pers. obs.]). (3) All species have quite distinctive rostra, with elongate nasal cavities (with the exception of *Polyboroides typus*, in which it is non-elongate, like most Accipitridae). (4) The ossified rostral section of the palatal face of the rostrum is of moderate to large length relative to the total length of the rostrum. (5) The presence of an incisura ventromedialis varies between species; it is completely fused over its length in *N. percnopterus* but is narrow in *P. typus*.

#### Aegyptiinae.

(3) All species have large nasal cavities which are partially covered by a bony shield originating from the posterior half of the nasal. (4) The ossified rostral section of the palatal face of the rostrum is of moderate to large length relative to the total length of the rostrum. (5) The incisura ventromedialis varies from present and narrow in species of *Gyps* and *Aegyptius monachus*, to absent due to complete fusion of pars maxillaris palatini in *Sarcogyps calvus*.

#### Circaetinae.

(4) The ossified rostral section of the palatal face of the rostrum is of moderate to large length relative to the total length of the rostrum.

#### Aquilinae.

(5) A narrow and small incisura ventromedialis is present in all species except for *Stephanoaetus coronatus*.

Haliaeetinae, Accipitrinae, Buteoninae.

**(5)** The incisura ventromedialis is lacking due to completely ossified pars maxillaris palatini.

**Vertebrae**

Other accipitrids differ as follows (variable characters excluded):

Elaninae.

**(Trait 1)** The arcus atlantis is almost completely flat in cranial and caudal view and does not overhang the fossa condyloidea. **(5)** The cranioventral margin of the fossa condyloidea does not notably project cranially in lateral aspect. **(6)** The zygopophyses caudales are peaked and rounded in shape.

Perninae.

No atlas or axis was available for *Aviceda subcristata*. In other pernines, only **(5)** the ventral margin of the fossa condyloidea having slightly cranial projection differed consistently from the fossil.

Gypaetinae.

The atlas and axis vertebrae were missing in the observed specimen of *Polyboroides typus*. **(1)** The arcus atlantis is arched in *Neophron percnopterus* and does not exhibit craniodistal curvature. **(4)** The proximal margin of the lateral margin corners of the fossa condyloidea do not project proximally into points, **(5)** and the cranioventral margin is non-projecting. **(6)** The zygopophyses caudales form a low, rounded peak, and are weakly projecting caudally. **(11)** The incisurae caudales arcus are distinct and fully enclosed by a bridge of bone.

Aegyptiinae.

**(2)** The incisura fossae forms a broad and deep semicircle. **(5)** The ventral margin of the fossa condyloidea projects slightly cranially. **(7)** The incisurae caudales arcus are deep, with distal projections from the corpus partially enclosing them. **(11)** The axis incisurae caudales arcus are open but partially enclosed by a thin bridge of bone.

Circaetinae.

**(1)** The arcus atlantis has very little curvature in a craniodistal projection. **(5)** The fossa condyloidea ventral margin weakly projects cranially. **(7)** The incisurae caudales arcus are deep, with small distal projections from the corpus partially enclosing them. **(11)** The axis incisurae caudales arcus are enclosed by a bridge of bone.

Aquilinae.

**(2)** The incisura fossae is a half-circle shape and is broad in all taxa except for species of *Aquila*, where it forms an almost complete circle and is narrow. **(4)** The proximal margin of the lateral

corners of the fossa condyloidea have low proximal projections in all taxa except for *Aquila audax*, where they are quite prominent. **(5)** The ventral margin of the fossa condyloidea projects prominently cranially in all species of *Aquila*, and weakly projects cranially in species of *Spizaetus*, *Hieraaetus morphnoides* and *Hieraaetus fasciatus*. **(6)** The zygopophyses caudales are broad and flat, and barely project caudal of the arcus atlantis. **(7)** The incisurae caudales arcus are deep and distinct with prominent enclosing projections in all taxa except for *Hieraaetus morphnoides*, where it is shallow and the projections are short. **(11)** The atlas incisurae caudales arcus are enclosed.

#### Haliaeetinae.

**(4)** The proximal margin of the fossa condyloidea strongly projects proximally into points in *Haliaeetus leucogaster*, and weakly projects proximally in all other taxa. **(5)** The ventral margin of the fossa projects weakly cranially in species of *Haliaeetus* and *Haliastur* and is pointed and strongly projecting cranially in species of *Milvus*. **(6)** The zygopophyses caudales are flat and barely project caudal of the arcus atlantis. **(11)** The atlas incisurae caudales arcus are enclosed in species of *Milvus*, and open in species *Haliaeetus* and *Haliastur*. The axis neural spine is long and distinctly curves caudally at the proximal end into a rounded point in species of *Haliaeetus*, and caudoproximally straight in species of *Milvus* and *Haliastur*.

#### Accipitrinae.

**(1)** The arcus atlantis forms a flattened arch. **(5)** The fossa condyloidea ventral margin has slight cranial projection. **(6)** The zygopophyses caudales form rounded peaks, and barely extends caudal of the arcus atlantis. **(11)** The atlas incisurae caudales arcus are enclosed by a bridge in *Circus aeruginosus*, and open in all other taxa.

#### Buteoninae.

**(1)** The arcus atlantis is arched in caudal and cranial view with craniodistal curvature in *Buteo buteo*, *Buteo rufofuscus* and *Buteo nitidus*, while *Ictinia* has a flattened arch with craniodistal curvature, and *Buteo lagopus* has a completely flat arcus atlantis with craniodistal curvature. **(5)** The ventral margin of the fossa condyloidea projects cranially in *Buteo buteo*, *Buteo rufofuscus*, and *Buteo lagopus*, and does not project in *Buteo nitidus* and *Ictinia*. **(6)** The zygopophyses caudales form rounded peaks that slightly projects caudally from the arcus atlantis. **(11)** The atlas incisurae caudales arcus are open, though thin partial bridges are present.

#### **Quadrate**

Other accipitrids differ as follows (variable characters excluded):

#### Across Subfamilies.

**(Trait 8)** The sulcus running along the ventral crista is broad and indistinct in all other taxa except in species of *Milvus* and *Haliaeetus* (Haliaeetinae) where it is narrow and indistinct. **(9)** The fossa caudomedialis is practically absent in the subfamilies Circaetinae and Aegyptiinae, as well as the species in *Hamirostra*, *Lophoictinia* (Perninae), *Neophron* (Gypaetinae), and *Haliaeetus* (Haliaeetinae); shallow in Aquilinae and species of *Elanoides*, *Chondrohierax* (Perninae), *Polyboroides* and *Gypohierax* (Gypaetinae); and deep in Elaninae, Accipitrinae and Buteoninae, as well as species in *Pernis* (Perninae). The depressio was indistinctly shaped (i.e. a gradually deepened area rather than a defined pit) in all species, and apneumatic in all species except in *Pernis* and *Haliaeetus*.

Key characters distinguishing subfamilies are listed below.

#### Elaninae.

**(2)** The capitulum squamosum lacks a prominent hook on the cranial margin. **(5)** A foramen pneumaticum basiorbitale is lacking with only a fossa present. **(7)** The crista medialis is prominent. **(10)** The condylus pterygoideus is contiguous with the dorsal margin of the condylus medialis and barely projecting in a distinct condyle.

#### Perninae.

**(2)** The capitulum squamosum is not hooked cranially, though some species (*Pernis apivorus*, *Hamirostra melanosternon*, *Lophoictinia isura*) have it slightly projected. **(5)** Most pernines have a fossa pneumaticum basiorbitale rather than a foramen, except for *L. isura* and *H. melanosternon*, which lack either. **(11)** The condylus pterygoideus is variably prominent. **(12)** The condylus caudalis is very small and triangle-shaped in *P. apivorus*, but in species in all other genera it has a prominent semicircular shape (slightly triangular in *C. uncinatus*) akin to what the fossil likely looked like.

#### Gypaetinae.

All gypaetines have the same morphology of the processus oticus as *Archaeohierax sylvestris* gen. et. sp. nov., but only *Polyboroides typus* was observed to have **(2)** a cranial hook on the capitulum squamosum. **(5)** Lack a foramen pneumaticum basiorbitale.

#### Aegyptiinae.

**(5)** There is no fossa or foramen pneumaticum basiorbitale. **(11)** The general morphology of the condylus medialis is similar to that in the fossil, though in aegyptiines the ventral facet is much more bulbous. **(12)** The condylus caudalis prominently projects caudally into a laterally off-set triangular shape, rather than a semicircular shape.

#### Circaetinae.

**(2)** The Circaetinae possess a less prominent cranial hook on the capitulum squamosum. **(5)** Lack a foramen pneumaticum basiorbitale. **(9)** Foramen pneumaticum caudomediale present, variably small (*S. cheela*), or large (*T. ecaudatus*). **(11)** The medial extent of both condyles is roughly equal. **(12)** The condylus caudalis is shaped like a rounded off triangle in ventral view.

#### Aquilinae.

**(2)** Most species have a cranial hook on the capitulum squamosum, quite slight in species of *Spizaetus* and *Hieraaetus morphnoides*, prominent in those of *Aquila* including *A. fasciata*. **(5)** All lack a foramen pneumaticum basiorbitale and instead have a fossa basiorbitale. **(10)** The condylus pterygoideus and condylus medialis are well separated in all observed aquilines. **(12)** The condylus caudalis forms a rounded triangle shape in all aquilines except *A. chrysaetos*, which has a condylus caudalis shaped more like a semicircle.

#### Haliaeetinae.

**(5)** A small foramen pneumaticum basiorbitale is present in species of *Haliastur* and *M. migrans*, but no foramen or fossa basiorbitale is present in those of *Haliaeetus* (a large foramen is present in *Haliaeetus leucocephalus*, but is likely to be ventrally offset pneumatisation of the depressio rostromediale). **(9)** The foramen pneumaticum caudomediale is small in *Haliastur sphenurus* and species of *Haliaeetus*, and large in *Haliastur indus* and *M. migrans*. **(10)** All species have the condylus pterygoideus separated from the condylus medialis, though they are relatively more close-set than in the fossil. **(12)** The condylus caudalis is triangular-shaped in species of *Haliaeetus*, and semicircular in species of *Haliastur* and *M. migrans*.

#### Accipitrinae.

**(2)** Projection on the cranial capitulum squamosum small or slightly hooked ventrally. **(11)** Medial extent of the condylus pterygoideus ranges from equal to the medial condyle (*Circus cyaneus*, *C. aeruginosus*, *Accipiter gentilis*, *A. cirrocephalus* and *A. novaehollandiae*) to extending further than the medial condyle (*Circus assimilis*, *Accipiter nisus*, *A. fasciatus* and *A. striatus*). **(12)** The condylus caudalis forms a rounded triangle shape in ventral view in species of *Circus* and is semicircular in species of *Accipiter*.

#### Buteoninae.

**(2)** All species have a slight ventral hook on the cranial side of the capitulum squamosum. **(7)** The crista medialis is elevated into a ridge in the ventral half. **(9)** The foramen pneumaticum caudomediale is large in species of *Buteo*, and tiny in *Ictinia mississippiensis*. **(11)** The condylus pterygoideus has equal extent medially with the condylus medialis. **(12)** The condylus caudalis has a triangular shape in *I. mississippiensis* and is triangular with rounded corners in species of *Buteo*.

## **Sternum**

Extant accipitrids differ as follows:

### Across Subfamilies.

**(3)** The crista medialis extends to the base of the spina externa in members of all subfamilies except Aegyptiinae. **(8)** The apex carinae lies directly ventral to the base of the spina externa, or projects more cranial, in species in all subfamilies except for Gypaetinae and Aegyptiinae. **(11)** The sulci articularis coracoidei overlap in all species except for *Gampsonyx swainsonii* (Elaninae) and *Sarcogyps calvus* (Aegyptiinae). **(13)** No species in any subfamily has a distinct pila medialis separating pneumatic fossae in the pars cardiaca, which is thus an autapomorphy suggesting subfamilial distinction for the new species.

Key characters distinguishing members of extant subfamilies are listed below.

### Aegyptiinae.

**(5)** The carina apex is tapered into a thin point. **(7)** The carina has less depth than the basal sternum, making up less than 50% of total depth.

### Accipitrinae.

**(2)** The cranial projection of the spina externa is long in *Melierax metabates* and *Accipiter*, and short in *Kaupifalco monogrammicus* and species of *Circus*. **(5)** The carina apex is tapered into a thin point in species of *Accipiter* and *M. metabates*.

## **Coracoid**

Extant accipitrids differ as follows:

### Across Subfamilies.

**(Trait 5)** The sternal margin of the facies articularis clavicularis does not form a crest overhanging the sulcus supracoracoideus in Elaninae, Perninae (except *Chondrohierax uncinatus*), Gypaetinae (except *Polyboroides typus*), Aegyptiinae, Haliaeetinae, Accipitrinae, and Buteoninae. **(8)** The impressio lig. acrocoracohumeralis is shallow in Elaninae, Perninae, Gypaetinae, Accipitrinae, and Buteoninae. **(9)** In all subfamilies, the processus procoracoideus does not, or barely, angle ventrally towards the medial face.

Other key characters distinguishing subfamilies are listed below.

### Elaninae.

**(2)** The foramen nervi supracoracoidei opens to the corpus in species of *Elanus* but not *Gampsonyx swainsonii*. **(10)** The angulus medialis is well projecting medially but forms a  $>90^\circ$  angle.

### Perninae.

(1) The foramen nervi supracoracoidei is similar to the fossil in all taxa except *Aviceda subcristata*, where it is an incisura. (2) The foramen opens to the corpus in all taxa except for *A. subcristata*, *Pernis apivorus*, and *Lophoictinia isura*.

### Gypaetinae and Aegyptiinae.

(2) The foramen nervi supracoracoidei opens to the corpus.

### Circaetinae.

(2) The foramen nervi supracoracoidei opens to the corpus. (10) The angulus medialis barely projects medially from the facies articularis sternalis.

### Aquilinae.

(1) An incisura nervi supracoracoidei is present in most species of *Aquila* and *Spizaetus*, but a foramen nervi supracoracoidei is present in *Hieraaetus morphnoides* and *Aquila fasciata*. In all species, the foramen or incisura is set against medial margin. (8) The impressio lig. acrocoracohumeralis is deep in all taxa except for species of *Spizaetus*, where it is shallow. (10) The angulus medialis is very short, and barely projects medially from the facies articularis sternalis in all taxa, except in species of *Spizaetus*, where it is well projecting.

### Haliaeetinae.

(1) A foramen nervi supracoracoidei is present and adjacent to the shaft in all taxa except *Haliaeetus leucocephalus* (on the medial margin). (8) The impressio lig. acrocoracohumeralis is deep in all taxa except for *Milvus migrans* and species of *Haliastur*, where it is shallow.

### Accipitrinae.

(1) All species of *Accipiter* lack either a foramen or incisura nervi supracoracoidei; species of *Circus* have either a foramen (*C. cyaneus*, *C. aeruginosus*) or incisura (*C. assimilis*, *C. approximans*) close to the medial margin.

### Buteoninae.

(1) The foramen nervi supracoracoidei is located against the medial margin in species of *Buteo* and closer to the shaft in *Ictinia mississippiensis*.

## **Scapula**

Extant accipitrids differ as follows (key characters only):

### Elaninae.

**(9)** The corpus scapula deepens slightly distally.

#### Perninae.

**(3)** All taxa are similar to the fossil in lacking a foramen in the acromion (except for *Aviceda subcristata* and *Lophoictinia isura*). **(4)** Pneumatic foramina are variably present in *Hamirostra melanosternon* (medially), *L. isura* (medially, one specimen had it and the other not), *Chondrohierax uncinatus* (laterally), but are lacking in *Elanoides forficatus*, *Pernis apivorus* and *A. subcristata*. **(9)** The corpus scapulae is slightly deeper caudal to the margo dorsalis attachment point.

#### Gypaetinae.

**(3)** A pneumatic foramen in the acromion is variably present, lacking in *Polyboroides typus*, but present in *Neophron percnopterus*. **(4)** A foramen is present in the medial face in *P. typus*, and one in the lateral face in *N. percnopterus*. **(9)** The corpus scapulae is slightly deeper caudal to the margo dorsalis attachment point.

#### Aegyptiinae.

**(3)** A foramen is present in the acromion. **(4)** Species of *Gyps* lack a foramen on either the medial or lateral face, but one is present laterally in *Aegyptius monachus* and *Sarcogyps calvus*. **(9)** The corpus scapulae does not get deeper distal to the ligamental attachment point on the margo dorsalis.

#### Circaetinae.

**(1)** The tuberculum coracoideum slightly projects cranially. **(3)** A foramen is present in the acromion in *Spilornis cheela*, but not in *Terathopius ecaudatus*. **(4)** *S. cheela* lacks any foramina on the medial or lateral face of the cranial end, but *T. ecaudatus* has a foramen present on the medial face.

#### Aquilinae.

**(1)** The tuberculum coracoideum slightly projects cranially. **(3)** A foramen is present in the acromion. **(4)** Foramina are absent in the medial or lateral face in *Stephanoaetus*, *Aquila audax*, *Hieraaetus moorei* and species of *Spizaetus*, but a medial foramen is present in *Aquila chrysaetos*, *Hieraaetus morphnoides*, and *Aquila fasciata*. **(9)** The corpus scapulae deepens towards the extremitas caudalis.

#### Haliaeetinae.

**(3)** A foramen is present in the acromion in *Haliaeetus leucocephalus*, *Haliaeetus albicilla*, and *Milvus migrans*, but is absent in *Haliaeetus leucogaster* and species of *Haliaastur*. **(4)** Foramina are

absent in the medial and/or lateral face in *H. leucocephalus*, *H. albicilla*, *Haliastur sphenurus* and *M. migrans*, while a medial foramen is present in *H. leucogaster* and *Haliastur indus*.

#### Accipitrinae.

**(1)** The tuberculum coracoideum slightly projects cranially. **(3)** A foramen is present in the acromion in *Melierax metabates*, is absent in species of *Accipiter* and *Circus*, and could not be assessed in *Kaupifalco monogrammicus*. **(4)** A foramen is present medially in all taxa except for *M. metabates*. This feature was not assessable in our specimen of *K. monogrammicus*.

#### Buteoninae.

**(1)** The tuberculum coracoideum slightly projects cranially. **(3)** A foramen is present in the acromion in all taxa except *I. mississippiensis*.

#### **Humerus**

Extant accipitrids differ as follows:

#### Elaninae.

**(2)** An indistinct ligament attachment about the same width of the incisura capitis is present at the dorsal side of the incisura. **(5)** The crus dorsale fossae is narrow and caudally flat. **(8)** The angulus cristae of the crista deltopectoralis is rounded in profile.

#### Perninae.

**(2)** A faint, circular ligamental attachment point is present dorsally in the incisura capitis. **(4)** The fossa pneumotricipitalis is wide and deep in all species but *Pernis apivorus*, where it is narrow and deep. **(7)** The proximal section of the crista deltopectoralis is flat in ventro-cranial view in all taxa except *C. uncinatus*, where the proximal crista deltopectoralis is slightly concave. **(8)** The angulus cristae of the crista deltopectoralis is rounded in most species but is weakly pointed in *P. apivorus* and strongly pointed in *C. uncinatus*.

#### Gypaetinae.

**(2)** A faint, round ligament attachment point is present dorsally in the incisura capitis. **(4)** The fossa pneumotricipitalis is deep and narrow in *P. typus* and deep and wide in *N. percnopterus*. **(5)** The crus dorsale fossae is flat and broad in *Polyboroides typus*, and narrow and flat with proximal pneumatization in *Neophron percnopterus*. **(8)** The angulus cristae of the deltopectoralis is rounded. **(9)** The distal termination of the crista deltopectoralis is perpendicular to the shaft in *P. typus* but parallel to it in *N. percnopterus*.

#### Aegyptiinae.

(2) Species have a faint, ovular ligament attachment dorsally in the incisura. (5) The crus dorsale fossae is flat. (6) The sulcus lig. transversus is separated into ventral and dorsal sections. (8) The angulus cristae of the deltopectoralis is rounded. (9) The distal end of the crista deltopectoralis is steeply angled to the shaft in *Aegyptius monachus* and species of *Gyps*, but parallel in *Sarcogyps calvus*.

#### Circaetinae.

(1, 2) *Spilornis cheela* has a shallow incisura capitis with a faint, very small ligament attachment dorsally, while *Terathopius ecaudatus* has a deep incisura capitis with a distinct, prominent and small ligament attachment dorsally. (5) The crus dorsale fossae is narrow in *S. cheela*, and broad in *T. ecaudatus*. (6) The sulcus lig. transversus has separate ventral, dorsal parts. (8) The angulus cristae of the deltopectoralis is rounded. (9) The distal end of the crista deltopectoralis arises steeply from the shaft in *S. cheela* but parallel in *T. ecaudatus*.

#### Aquilinae.

(2) A large, faint and round ligament attachment is present dorsally in the incisura capitis. (5) The crus dorsale fossae is flat. (6) Ventrally, the sulcus lig. transversus is deep and round in species of *Aquila* including *Aquila fasciata*, but shallow in species of *Spizaetus* and *Hieraaetus morphnoides*. In all taxa, the ventral sulcus is separate from the dorsal section which is a shallow notch. (7) The proximal section of the crista deltopectoralis is flat in ventro-cranial view in all species except *Spizaetus tyrannus*, where it is concave.

#### Haliaeetinae.

(2) A large, faint and round ligament attachment is present dorsally in the incisura capitis. (5) The crus dorsale fossae is flat. (9) The distal end of the crista deltopectoralis is parallel to the shaft.

#### Accipitrinae.

(2) A faint, round ligament attachment point is present dorsally in the incisura capitis. (5) The crus dorsale fossae is flat. (7) The proximal section of the crista deltopectoralis is flat in ventro-cranial view in *Accipiter gentilis* and *Circus aeruginosus*, but concave in all other species observed in this study. (9) The distal end of the crista deltopectoralis is parallel to the shaft in all species.

#### Buteoninae.

(2) A large, faint, circular attachment point is present dorsally in the incisura capitis. (5) The crus dorsale fossae is flat. (6) The sulcus lig. transversus is separated into larger deeper ventral section and a shallow, narrow dorsal notch. (9) The distal end of the crista deltopectoralis is aligned parallel to the shaft.

## ***Ulna***

Extant accipitrids differ as follows:

### Elaninae.

**(5)** *Elanus* species possess an incisura radialis that is moderately deepened, while in *Gampsonyx swainsonii* the incisura is shallow and flat. **(6)** Two round tubercula are present in species of *Elanus*, which are large and positioned adjacent to each other on the cranial face; in *G. swainsonii* they are small, and well-separated, with one central on the cranial face and the other on the edge of the ventral face. **(9)** The tuberculum carpale is rounded, and has little projection in all species, except for *Elanus axillaris* (well-projecting). **(10)** The proximal face of the tuberculum carpale is undifferentiated from the rest of the tuberculum.

### Perninae.

**(5)** Species exhibit an incisura radialis depth ranging from moderate (*L. isura*, *H. melanosternon*) to shallow (*P. apivorus*, *A. subcristata*). **(6)** Two oval tubercula or scars are present on the cranial face (except for *E. forficatus*, with one prominent tuberculum central on the cranial face). **(9)** Cranial projection of the tuberculum carpale is slight in *A. subcristata*, moderate in *L. isura* and *C. uncinatus*, and strong in *P. apivorus*, *E. forficatus* and *H. melanosternon*. **(10)** The proximal face of the tuberculum carpale is undifferentiated from the rest of the tuberculum in all species except for *H. melanosternon* and *L. isura*, which have a strongly flattened ventral margin. **(15)** The sulcus intercondylaris is deep in *E. forficatus*, *C. uncinatus* and *A. subcristata*, and shallow in *P. apivorus*, *L. isura* and *H. melanosternon*.

### Gypaetinae.

**(1)** The proximal shaft is notably curved cranially in *Polyboroides typus*, but *Neophron percnopterus* has a largely straight profile. **(4)** The impressio scapulo-tricipitis is moderately deep in all taxa. **(5)** The incisura radialis is deep. **(9)** The tuberculum carpale projects moderately in *N. percnopterus*, and strongly in *P. typus*. **(10)** The proximal face of the tuberculum carpale is undifferentiated from the rest of the tuberculum. **(15)** The sulcus intercondylaris is deep in *P. typus*, and shallow in *N. percnopterus*.

### Aegyptiinae.

**(4)** The impressio scapulo-tricipitis is moderately deep. **(5)** The incisura radialis is deep. **(6)** Two oval tubercula are present on the cranial face. They are flattened, and slightly separated by the deepened extension of the incisura radialis. *Aegyptius monachus* differs from species of *Gyps* in that the ventral-most tuberculum extends onto the ventral face and is much longer than the dorsal tuberculum. **(9)** The tuberculum carpale is strongly projecting cranially. **(10)** In species of *Gyps* and *A. monachus*, the ventral margin of the proximal face of the tuberculum carpale is strongly

flattened, which is absent in *Sarcogyps calvus*. **(14)** In *S. calvus*, there is a pneumatic fossa on the proximodorsal face of the tuberculum carpale, which is absent in species of *Gyps* and *A. monachus*. **(15)** The sulcus intercondylaris is deep in species of *Gyps* and *A. monachus*, and shallow in *S. calvus*.

#### Circaetinae.

**(4)** The impressio scapuloaltricipitis is deep. **(5)** The incisura radialis is deep. **(9)** The tuberculum carpale is moderately projecting cranially. **(10)** The proximal face of the tuberculum carpale is undifferentiated from the rest of the tuberculum. **(15)** The sulcus intercondylaris is shallow in *S. cheela*, and deep in *T. ecaudatus*.

#### Aquilinae.

**(1)** Most taxa have little to no shaft curvature, with the exception of *Stephanoaetus coronatus* and species of *Spizaetus*. **(4)** The impressio scapuloaltricipitis is large and shallow in species of *Aquila*, while in those of *Hieraaetus* and *Spizaetus* it is small and shallow. **(6)** Species of *Aquila* and *Spizaetus* have three attachment points forming the tubercula, two on the cranial face and one on the ventral face. On the cranial face, the more dorsally positioned tubercula is circular and proximal to the others, while the more ventral one is oval and located beside the one on the ventral face and is roughly twice its size. In species of *Hieraaetus*, there are two tubercula on the cranial face, a larger dorsal one and a smaller ventral one beside it. **(9)** The tuberculum carpale is moderately projecting cranially. **(10)** The proximal face of the tuberculum carpale is undifferentiated from the rest of the tuberculum. **(15)** The sulcus intercondylaris is deep in all taxa except *Hieraaetus moorei*.

#### Haliaeetinae.

**(4)** The impressio scapuloaltricipitis is deep being larger in *Haliaeetus* species than in *Haliastur* species and *M. migrans*. **(5)** The incisura radialis is deep in all genera except for *Milvus migrans*, where it is shallow. **(6)** Species of *Haliaeetus* have four tubercula, three of which are located on the cranial face. Only one oval tuberculum positioned on the ventral-most edge of the cranial face is present in *M. migrans* and species of *Haliastur*. **(9)** The tuberculum carpale is moderately projecting cranially in species of *Haliaeetus*, and strongly projecting in species of *Haliastur* and *M. migrans*. **(10)** The proximal face of the tuberculum carpale is undifferentiated from the rest of the tuberculum. **(14)** There is no foramen on the ventral face of the tuberculum carpale base. **(15)** The sulcus intercondylaris is deep.

#### Accipitrinae.

**(5)** Species of *Accipiter* have a shallow incisura radialis, while for species in *Circus* it is moderately deepened. **(6)** Species of *Accipiter* have three round tubercula, two on the cranial face (the dorsal one most proximal) and one central on the ventral face. In species of *Circus*, there are two

tubercula/attachment points on the cranial face, with the ventral tuberculum being elongate, and the more proximal dorsal one roughly circular. **(9)** The tuberculum carpale is moderately to strongly projecting cranially in all taxa. **(10)** The proximal face of the tuberculum carpale is undifferentiated from the rest of the tuberculum. **(15)** The sulcus intercondylaris is deep.

#### Buteoninae.

**(4)** The impressio scapulo-tricipitis is shallow in species of *Buteo*, but deep in *Ictinia mississippiensis*. **(5)** The incisura radialis is moderately deepened. **(6)** Two round tubercula are present in species of *Buteo*, with the dorsal-most one positioned roughly central in the cranial face, and the ventral tuberculum positioned on the ventral-cranial margin and positioned proximally to the dorsal tuberculum. *I. mississippiensis* has a single oval tuberculum on the ventral-most edge of the cranial face. **(9)** The tuberculum carpale is moderately projecting cranially. **(10)** The proximal face of the tuberculum carpale is undifferentiated from the rest of the tuberculum. **(15)** The sulcus intercondylaris is deep.

#### **Radius**

Extant accipitrids differ as follows:

#### Elaninae.

**(7)** The depressio ligamentosa is very shallow. **(8)** There is no notch in the proximal margin of the facies articularis ulnaris.

#### Perninae.

**(1, 7)** Most species lack pneumatic foramina associated with the tuberculum bicipitale radiale or the depressio ligamentosa. The exception is *Chondrohierax uncinatus*, which has pneumatic foramina in both regions. **(8)** The proximal margin of the facies articularis ulnaris is notched in *H. melanosternon*, *L. isura* and *P. apivorus*, but flat in *E. forficatus* and *C. uncinatus*.

#### Gypaetinae.

No notable differences.

#### Aegyptiinae.

**(7)** Species have pneumatic foramina in the lateral half of the depressio ligamentosa. **(8)** The proximal margin of the facies articularis ulnaris has a sulcus that bisects the articular surface of the facies, which is shallow in species of *Gyps* and deep in *Aegyptius monachus*.

#### Circaetinae.

**(8)** The proximal margin of the facies articularis ulnaris is notched in *Spilornis cheela* but is not in *Terathopius ecaudatus*.

### Aquilinae.

(8) The proximal margin of the facies articularis ulnaris is notched in all taxa, distinct in *Hieraaetus morphnoides*, *Aquila fasciata*, and *Aquila chrysaetos*, but shallow in species of *Spizaetus* and *Aquila audax*.

### Haliaeetinae.

No notable differences.

### Accipitrinae.

(8) The proximal margin of the facies articularis ulnaris is notched in *A. gentilis*, *A. cirrocephalus*, *A. novaehollandiae*, and *C. cyaneus*, but is flat in *C. assimilis*, *C. aeruginosus*, and *A. striatus*.

### Buteoninae.

(2) The tuberculum bicipitalis is distinctly projecting ventrally.

### ***Os carpale radiale***

Extant accipitrids differ as follows (key characters only):

### Elaninae.

(Trait 3) The facies articularis metacarpalis barely projects distally from the cranial facies in cranial view. (6) The dorsal cranial fossa is shallow. (8) A shallow fossa is present in the facies articularis ulnaris on the caudal face, set approximately halfway between the ventral and dorsal margins.

### Perninae.

(3) The facies articularis metacarpalis barely projects distally from the cranial face in cranial view. (6) The dorsal cranial fossa is present in all taxa, but varies in depth, shallow in *H. melanosternon*, *E. forficatus*, and *C. uncinatus* (the latter is also pneumatic), and deep in *L. isura* and *P. apivorus*.

### Gypaetinae.

(5) There is a shallow fossa ventrally on the cranial face. (6) The dorsal cranial fossa is deep in *P. typus* and shallow in *N. percnopterus*. (8) A small, shallow fossa is present on the facies articularis ulnaris, fossa is extremely small in *P. typus*.

### Aegyptiinae.

(5) The cranial face ventrally has a shallow and pneumatic fossa covering most of the surface. (6) The dorsal cranial fossa is shallow and pneumatic (8) A large and shallow fossa is present on the facies articularis ulnaris.

### Circaetinae.

(5) A shallow fossa covers most of the cranial face ventrally. (6) The dorsal cranial fossa is shallow. (8) A small, shallow fossa is present on the facies articularis ulnaris.

#### Aquilinae.

(1) The distoventral projection is of approximately equal ventral extent as the ventral margin. (4) The sulcus for the musculus extensor carpi radialis is broad, shallow, and quite flattened. (5) A shallow fossa covers most of the cranial face ventrally. (6) The dorsal cranial fossa is shallow in species of *Spizaetus* and deep in species of *Hieraaetus* and *Aquila*. (8) The caudal fossa in the facies articularis ulnaris is small and deep in species of *Spizaetus*, and large and deep in species of *Aquila* and *Hieraaetus*.

#### Haliaeetinae.

(1) The distoventral projection does not project ventral of the ventral margin. (4) The sulcus for the musculus extensor carpi radialis is shallow and flat. (5) The cranial face ventrally is mostly covered by a shallow fossa, which is deeper towards the ventral margin. (6) The dorsal cranial fossa is shallow (8) The facies articularis ulnaris is occupied by a fossa that is shallow in *M. migrans* and species of *Haliastur*, and deep in species of *Haliaeetus*.

#### Accipitrinae.

(1) The distoventral projection is very short, and barely projects ventrally of the ventral margin. (4) The sulcus for the musculus extensor carpi radialis flat. (6) The dorsal cranial fossa is deep in all taxa except in *Accipiter nisus*, *A. striatus*, and *A. cirrocephalus*, where it is shallow.

#### Buteoninae.

(1) The distoventral projection is very short and does not project ventrally of the ventral margin of the cranial face. (3) The facies articularis metacarpalis is weakly projecting distally, from the cranial face in cranial view. (4) The sulcus for the musculus extensor carpi radialis is flat.

#### ***Os carpale ulnare***

Extant accipitrids differ as follows:

#### Elaninae.

(1) The cranial projection is relatively small but connected to the proximodorsal margin by a prominent ridge. (4) The ligamental attachment scar on the proximal margin just ventral to the crus longus is small and weakly projecting proximally. (7) There is no caudal projection on the proximal margin of the caudal face.

#### Perninae.

(4) The ligamental attachment on the proximal margin is barely projecting in *C. uncinatus* and *P. apivorus*, and absent or extremely reduced in *H. melanosternon* and *L. isura*. (7) A caudal projection on the proximal margin is variably present, lacking in *C. uncinatus*, present in *H. melanosternon*, *P. apivorus*, and *L. isura*.

#### Gypaetinae.

(4) The ligamental attachment scar on the proximal margin of the crus longus is very faint and does not project proximally. (7) The caudal face has a distinct caudal projection on the proximal margin.

#### Aegyptiinae.

There is pneumatisation of the crus longus in species of *Gyps*, and of both the crus longus and crus brevis in *Aegyptius monachus*. (1) The cranial projection is connected to the proximal margin by a prominent ridge. (4) The ligamental attachment scar on the proximal margin of the crus longus, is faint and does not project proximally. (7) The caudal projection is prominent on the proximal margin of the caudal face offset towards the crus brevis. (10) The incisura metacarpalis forms a deep, broad 'u'-shape.

#### Circaetinae.

(4) The ligamental attachment scar adjacent to the proximal margin of the crus longus, is faint and does not project proximally. (7) The caudal projection on the proximal margin of the caudal face adjacent to the crus brevis is prominent in *T. ecaudatus* and weak in *S. cheela*. (10) The incisura metacarpalis is deep and forms a broad 'u'-shape.

#### Aquilinae.

(4) The ligamental attachment scar adjacent to the proximal end of the crus longus, is faint and does not project proximally. (7) The caudal projection on the proximal margin of the caudal face adjacent to the crus brevis projects prominently in species of *Aquila* and weakly in species of *Hieraaetus* and *Spizaetus*.

#### Haliaeetinae.

(4) The ligamental attachment scar on the proximal end of the crus longus, barely projects proximal of the proximal margin. (7) The projection on the proximal margin of the caudal face adjacent to the crus brevis is prominent in species of *Haliaeetus* but not so in species of *Haliastur* and *Milvus*. (10) The incisura metacarpalis is deep and broad, forming a 'U' shape.

#### Accipitrinae.

(4) The ligamental attachment scar on the proximal margin is moderately projecting proximally. (7) A small caudal projection is present on the proximal margin of the caudal face adjacent to the crus brevis. (10) The incisura metacarpalis is deep and 'U'-shaped.

### Buteoninae.

(4) The ligamental attachment scar on the proximal margin adjacent to the proximal end of the crus longus, is very small and does not project proximally. (7) The caudal projection on the proximal margin of the caudal face adjacent to the crus brevis is small. (10) The incisura metacarpalis is deep and forms a broad 'U'-shape.

### ***Carpometacarpus***

Extant accipitrids differ as follows:

### Elaninae.

(7) The fovea carpalis caudalis is deep. (9) The proximal margin of processus extensorius forms a 90° angle with the trochlea carpalis. (14) The area between the distal base of the processus pisiformis and the proximal end of the spatium intermetacarpale has no distinct sulcus. (18) The sulcus tendineus is narrow. (20) The os metacarpale minus is largely flat caudally, with little curvature. (22) The length of the distal synostosis is greater than its width.

### Perninae.

(3) The sulcus is shallower in all taxa. (5) A similar shallow sulcus is present in *P. apivorus* but is absent in all other taxa. (6) The fovea carpalis cranialis is shallow, and in *C. uncinatus* is also pneumatic. (7) The fovea carpalis caudalis is shallow in *H. melanosternon*, *L. isura* and *P. apivorus*, but is deep in *E. forficatus* and *C. uncinatus*. (12) The processus alularis is not separated from the shaft by a notch in all taxa, except for *C. uncinatus*, where is a distinct notch. (18) The sulcus tendineus is narrow. (19) The groove on the proximal caudal face of the os metacarpale minus in *C. uncinatus* is pneumatic.

### Gypaetinae.

(12) The processus alularis is weakly projecting cranially and is not separated from the shaft by a notch. (17, 18) The sulcus tendineus is restricted to the dorsal face and is narrow. (20) The os metacarpale minus is mainly flat caudally, with slight curvature towards the distal end. (21) The facies articularis digitalis minor extends well distal of the facies articularis digitalis major in *P. typus* but is co-level with it in *N. percnopterus*.

### Aegyptiinae.

(1) The fossa infratrochlearis is pneumatic. (3) The sulcus is shallow. (4) The fossa supratrochlearis is deep and apneumatic. (5) A sulcus is present ventrally on the proximal margin of the processus extensorius, which is shallow in *A. monachus* and deep in species of *Gyps*. (6) The fovea carpalis cranialis is deep and pneumatic. (7) The fovea carpalis caudalis is deep. (8) The caudal margin of the trochlea carpalis is shorter and ends roughly in line with the processus

pisiformis. **(18)** The sulcus tendineus is narrow. **(19)** The proximal section of the caudal face of the os metacarpale minus is pneumatic. **(20)** The os metacarpale minus is flat caudally.

#### Circaetinae.

**(7)** The fovea carpalis caudalis is shallow in *S. cheela* and deep in *T. ecaudatus*. **(8)** The caudal margin of the trochlea carpalis is shorter ends roughly in line with the base of the processus pisiformis. **(18)** The sulcus tendineus is narrow. **(22)** The distance between the distal point of the facies articularis digitalis minor and the distal end the spatium intermetacarpale is short, roughly equal to the width of the distal synostosis in *S. cheela*, and long, greater than the width of the synostosis in *T. ecaudatus*.

#### Aquilinae.

**(3)** The sulcus is shallow. **(7)** The fovea carpalis caudalis is shallow in all taxa except *Aquila chrysaetos*, where it is deep. **(9)** The proximal margin of the processus extensorius forms a roughly 90° angle with the proximal trochlea carpalis. **(18)** The sulcus tendineus is narrow. **(20)** The os metacarpale minus is flat caudally in all taxa except for species of *Spizaetus*, which have slight caudal arching. **(22)** The length of the distal synostosis is shorter than its width.

#### Haliaeetinae.

**(18)** The sulcus tendineus is narrow **(20)** The os metacarpale minus is largely flat caudally.

#### Accipitrinae.

**(7)** The fovea carpalis caudalis has moderate depth. **(9)** The proximal margin of the processus extensorius forms a 90° angle with the trochlea carpalis. **(18)** The sulcus tendineus is narrow. **(20)** The os metacarpale minus is mainly flat caudally.

#### Buteoninae.

**(3)** The sulcus is shallow. **(9)** The proximal margin of the processus extensorius forms a 90° angle with the trochlea carpalis. **(20)** The os metacarpale minus is mainly flat caudally.

### ***Manus***

Extant accipitrids differ as follows (key characters only):

#### Elaninae.

**(Trait 3)** MI.1 lacks a tuberculum on the caudal margin of the ventral face. **(4)** MI.1 there are no visible ligament scars on the dorsal face adjacent to the proximal end. **(7)** A distinct depression is present on the ventral face of MIII.1, directly cranial to the caudal tuberosity.

#### Perninae.

**(9)** MII.2, the caudal margin is rounded.

### Gypaetinae.

**(3)** A small but prominent tuberculum is present on the caudal margin of the ventral face of MI.1 in *Polyboroides typus*, just distal to the proximal end, but is completely absent in *Neophron percnopterus*. **(4)** MI.1, two ligamental scars are present on the dorsal face just distal of the proximal margin, which are distinct in *N. percnopterus* and shallow in *P. typus*. **(6)** MIII.1, a projection is present on the caudal margin, which is caudally oriented in *P. typus* and proximocaudally oriented in *N. percnopterus*. **(9)** MII.2, the caudal margin is rounded in *N. percnopterus*.

### Aegyptiinae.

Proximally on the MII.1, the caudal face has notable pneumatization. **(3)** The MI.1 has a flat ligamental attachment scar, rather than a tuberculum on the caudal margin of the ventral face. **(9)** MII.2, the caudal margin is rounded and broad. **(11)** MII.2, a low ridge is present proximally on the dorsal face; no fossae are present. **(12)** MII.2, a prominently projecting tuberculum is present at the caudal side of the proximal end of the ridge. **(13)** MII.2, a pneumatic fossa is present on the ventral face, which is large in *Aegyptius monachus* and small in species of *Gyps*.

### Circaetinae.

**(2)** In the MI.1 of *Terathopius ecaudatus*, the proximal end of the cranial margin crista connects to a distinct projection that extends cranial to the crista itself, which is absent in *Spilornis cheela*. **(3)** MI.1, the ligamental attachment on the caudal margin of the ventral face just distal to the proximal end is a flat scar not a tuberculum. **(4)** MI.1, a single, very faint ligamental scar is present on the proximal margin of the dorsal face. **(9)** MII.2, the caudal margin is rounded and broad. **(11)** MII.2, a shallow fossa is present caudal to the ridge adjacent to the proximal end. **(13)** MII.2, the fossa proximally on the ventral face is deep in *T. ecaudatus*, but shallow in *S. cheela*.

### Aquilinae.

**(3)** MI.1, a small tuberculum is present on the caudal face at approximately mid-length, and a small, flat ligamental attachment scar is present on the caudal margin of the ventral face just distal of the proximal end. **(6)** The MIII.1 has a prominent projection on the caudal margin, positioned offset centre towards the proximal and oriented caudally. **(9)** MII.2, the caudal margin is rounded and broad. **(11)** MII.2, a low ridge is present in the dorsal face, most prominent proximally, with a shallow fossa caudal to it. In *Aquila audax*, a second shallow fossa is present caudal to the ridge slightly distal of the proximal margin.

### Haliaeetinae.

**(3)** MI.1, the ligamental scar on the caudal margin of the ventral face is flat. **(6)** The MIII.1 has a prominent projection on the caudal margin which is caudally oriented in species of *Haliaeetus*,

proximocaudally oriented in species of *Haliastur*, but small and proximocaudally oriented in *Milvus migrans*. **(7)** MIII.1, a shallow depression is present on the ventral face, just cranial of the caudal projection. **(9)** MII.2, the caudal margin is rounded and broad.

#### Accipitrinae.

**(3)** MI.1, the ligamental attachment point on the caudal margin of the ventral face is flat. **(6)** The MIII.1 has a prominent caudally oriented projection on the caudal margin. **(11)** MII.2, a shallow fossa is present in the proximal margin, caudal to the ridge. **(12)** MII.2, the proximal end of the ventral face has a shallow depression.

#### Buteoninae.

**(3)** MI.1 lacks a tuberculum on the caudal margin of the ventral face. **(11)** In MII.2 a shallow fossa is present in the proximal margin, caudal to the ridge.

#### ***Tibiotarsus***

Extant accipitrids differ as follows:

#### Elaninae.

**(1)** The impressio lig. collateralis medialis is barely evident. **(3)** The crista fibularis is barely prominent, only projecting from the shaft at its distal end. **(7)** The linea present on the medial margin of the shaft is faint. **(15)** The cranial tuberculum of the retinaculum m. fibularis is barely evident. **(22)** The incisura intercondylaris is very shallow. **(24)** The epicondylus medialis is lacking. **(25)** The depressio medialis is shallow. **(27)** The caudal surface of the tibialis cartilaginis is slightly concave.

#### Perninae.

**(1)** The impressio lig. collateralis medialis is not prominent. **(3)** The crista fibularis has less projection in all taxa. **(10)** The crista is absent in *H. melanosternon* and *P. apivorus*, but present in *C. uncinatus*, *E. forficatus*, and *L. isura*. **(13)** The pons is flat in *H. melanosternon*, *L. isura*, *P. apivorus* and *C. uncinatus*, but arched cranially in *E. forficatus*. **(16)** There is no caudal tuberculum retinaculi m. fibularis in the examined taxa. **(22)** The incisura intercondylaris is very shallow. **(24)** The epicondylus medialis barely projects medially past the medial condyle in cranial view. **(25)** The depressio medialis is shallower in all taxa. **(27)** The caudal surface of the tibialis cartilaginis is flat in *P. apivorus* and *C. uncinatus*, inflated in *E. forficatus*, and concave in *H. melanosternon* and *L. isura*.

#### Gypaetinae.

**(7)** A faint linea is present on the medial margin. **(9)** The sulcus extensorius is narrower, approximately a third of shaft width. **(11)** The canalis extensorius is of moderate depth and has a

small diameter. **(12)** The pons supratendineus forms a 90° angle relative to the long axis in *Polyboroides typus*, and a 30–45° angle in *Neophron percnopterus*. **(13)** The pons supratendineus is cranially flattened. **(19)** Distal width is roughly equal to distal depth (*P. typus*), and slightly wider than deep in *N. percnopterus*. **(20)** Distal width is less expanded relative to shaft width in *P. typus*, and gradually widens in *N. percnopterus*. **(21)** The condylus medialis is slightly deeper craniocaudally than the condylus lateralis. **(22)** The incisura intercondylaris is moderately deep (about 25% of the distal depth) in *P. typus*, and very shallow in *N. percnopterus*. **(24)** The epicondylus medialis is flat or small and not projecting past the medial condyle in cranial view. **(25)** The depressio medialis is shallower. **(26)** The depressio lateralis is deep. **(27)** The caudal surface of the tibialis cartilaginosa is slightly concave in *P. typus* and flattened in *N. percnopterus*.

#### Aegyptiinae.

**(1)** The impressio lig. collateralis medialis is a flat scar. **(3)** The crista fibularis is barely distinct from the shaft, **(4)** with no differentiation in width along the crista in species of *Gyps* and the distal end of the crista being the widest point in *Aegyptius monachus*. **(15, 16)** The tubercula for the retinaculi m. fibularis are small and flat and do not project laterally. **(17)** The medial/proximal attachment scar for the extensor retinaculum is positioned immediately proximal to the pons supratendineus. **(19)** Distal width approximates craniocaudal depth of the distal end. **(24)** The epicondylus medialis is small and does not project medially past the margin of the medial condyle in cranial view.

#### Circaetinae.

**(1)** The impressio lig. collateralis medialis is not prominent. **(3)** The crista fibularis is narrow, less than a quarter of the width of the shaft. **(5)** The cranial face directly adjacent to the crista fibularis is flattened. **(9)** The sulcus extensorius is narrower at roughly a third of shaft width. **(15, 16)** The tuberculum for the retinaculi m. fibularis are flat and non-projecting in *Terathopius ecaudatus*, and small ridges (cranial larger than caudal) that are weakly projecting laterally in *Spilornis cheela*. **(17)** The medial/proximal attachment scar for the extensor retinaculum is immediately proximal to the pons supratendineus in *T. ecaudatus* and is one pons-length proximal to it in *S. cheela*. **(22)** The incisura intercondylaris is shallow, less than 25% of distal depth. **(24)** The epicondylus medialis is short, barely projecting medial of the medial condyle.

#### Aquilinae.

**(9)** The sulcus extensorius occupies about a third of the shaft width. **(17)** The medial/proximal attachment scar for the extensor retinaculum is just proximal to the medial margin of the pons in species of *Aquila* including *A. fasciata* and *Spizaetus*, and moderately proximal (one pons-length) to the pons in *H. morphnoides*. **(24)** The epicondylus medialis is moderately projecting, just visible past the margin of the medial condyle in cranial view.

#### Haliaeetinae.

(15) The cranial tuberculum retinaculi m. fibularis is weakly projecting laterally. (17) The medial/proximal attachment scar is just proximal to the pons supratendineus in *Haliaeetus*, and one pons-length proximal to the pons in species of *Haliastur* and *M. migrans*. (22) The incisura intercondylaris is shallow, <25% of distal depth. (24) The epicondylus medialis is moderately projecting, barely visible past the margin of the medial condyle in cranial view.

#### Accipitrinae.

(1) The impressio lig. collateralis medialis is prominent. (7) The linea is faint on the medial margin of the shaft. (9) The sulcus extensorius is narrower at a third of shaft width. (14) The medial side of the pons supratendineus abuts the medial shaft margin in all taxa except for *Accipiter striatus* and *Accipiter gentilis*, where it is separated from the shaft margin. (16) The caudal tuberculum retinaculi m. fibularis is slightly less projecting laterally than the cranial tuberculum in *A. gentilis*, *A. nisus*, *A. cirrocephalus*, *A. striatus*, and *C. aeruginosus*, and flat in *C. assimilis*. (17) The medial/proximal attachment scar for the extensor retinaculum is set well proximal to the medial margin of the pons (at least two pons-lengths).

#### Buteoninae.

(5) The cranial face directly adjacent to the crista fibularis is flattened. (9) The sulcus extensorius is roughly a third of the shaft width in species of *Buteo* and half the shaft in *Ictinia*. (17) The medial/proximal attachment scar for the extensor retinaculum is proximal to the pons supratendineus by at least one pons-length. (21) The medial condyle is slightly deeper craniocaudally than the lateral condyle. (26) The depressio lateralis is deep.

#### ***Tarsometatarsus***

Extant accipitrids differ as follows:

#### Elaninae.

(2) Tarsometatarsi are short relative to distal width. (8) A prominent distal hook is present on the plantar margin of the medial hypotarsal crista. (18) The crista plantaris lateralis is weakly projecting. (20) The fossa metatarsi I is set on the medial face and is medially oriented. (29) The trochlea metatarsi III is aligned with shaft axis. (31) The flange on trochlea metatarsi II is oriented medioplantarly.

#### Perninae.

(8) A prominent distal hook is present on the medial hypotarsal crista in *Hamirostra melanosternon* and *Elanoides forficatus*, and a small, barely distinct hook in *P. apivorus*, *Lophoictinia* and *C. uncinatus*. (16) The shaft medially is slightly compressed dorsoplantarly, greatest at the mid-length. (18) The crista plantaris lateralis is weakly projecting. (33) The trochlea metatarsi II is the most

distal extending of the three trochleae, followed by trochlea metatarsi III then IV, in all species except *L. isura*, where II and III have equal extent and extend distal to IV, and in *H. melanosternon*, where III has the most extent and IV the least.

#### Gypaetinae.

**(4)** The eminentia intercotylaris is very prominent in *P. typus*, extending well proximal to the cotylae as a sharp peak, but is low and flat in *N. percnopterus*. **(10)** The tuberositas is positioned centrally in the shaft. **(16)** The shaft medially has little to no compression dorsoplantary. **(29)** The trochlea metatarsi III is aligned with shaft axis in *P. typus*, and slightly oriented laterally in *N. percnopterus*.

#### Aegyptiinae.

**(6)** The lateral and medial hypotarsal cristae are of roughly equal proximodistal length. **(16)** The shaft medially lacks marked dorsoplantar compression. **(17)** The crista plantaris lateralis is weakly developed, ending proximal of fossa metatarsi I. **(18)** The crista plantaris is weakly projecting. **(29)** The trochlea metatarsi III is aligned with shaft axis. **(33)** The trochlea metatarsi III has the greatest distal extent and trochlea metatarsi IV the least in species of *Gyps*, while in all other aegyptiines II and III have roughly equal extent and IV the least.

#### Circaetinae.

**(12)** The tuberositas is distally adjacent to the foramina vascularia proximalia. **(17)** The crista plantaris lateralis strongly projects in *Spilornis cheela* and weakly projects in *Terathopius ecaudatus*. **(29)** The trochlea metatarsi III is laterally oriented in *T. ecaudatus* and aligned with shaft axis in *S. cheela*. **(31)** The flange on the plantar margin is medioplantary oriented and long. **(32)** The flange on trochlea metatarsi IV is plantary oriented and is long.

#### Aquilinae.

**(4)** The eminentia intercotylaris is low and not/barely projected proximally in species of *Aquila* and *Hieraaetus* but is projecting proximally of the cotylae in species of *Spizaetus*. **(12)** The tuberositas is positioned roughly two lengths of the tuberositas distal to the foramen. **(14)** The fossa infracotylaris dorsalis is deep. **(31)** The flange on the plantar margin of the trochlea metatarsi II is medioplantary oriented and is long. **(32)** The flange on trochlea metatarsi IV is plantary oriented and is long. **(33)** The trochleae metatarsorum II and III have equal distal extent and surpass trochlea metatarsi IV in *Spizaetus tyrannus* and species of *Aquila* including *Aquila fasciata*, while in *Hieraaetus morphnoides*, trochlea metatarsi has the most extent and IV the least, and in *H. moorei*, III has the most extent and IV the least.

#### Haliaeetinae.

**(4)** The eminentia intercotylaris is flat, barely extending proximal of the cotylae. **(31)** The flange on the plantar margin of the trochlea metatarsi II is oriented medioplantary and is long. **(32)** The

flange on trochlea metatarsi IV is plantar oriented and is long. **(33)** The trochlea metatarsi II has the greatest distal extent, and trochlea metatarsi IV least.

#### Accipitrinae.

**(6)** The lateral and medial hypotarsal cristae are of equal proximodistal length in all taxa except for *Accipiter gentilis*, where the crista lateralis is half the proximodistal length of the crista medialis. **(8)** The distal hook on the plantar margin of the medial hypotarsal crista is small. **(33)** The trochlea metatarsi IV terminates proximal to the other trochleae in all taxa except those in *Circus*, *Accipiter cooperii* and *A. fasciatus* and *Accipiter striatus*, where they have equal extent.

#### Buteoninae.

**(6)** The proximodistal length of the lateral hypotarsal crista is half that of the medial hypotarsal crista in all taxa except *Buteo nitidus*, where the proximodistal lengths of the cristae are identical. **(7)** The lateral hypotarsal crista shallower, two-thirds the plantar depth of the medial hypotarsal crista in species of *Buteo*, and just over half the depth of the medial hypotarsal crista in *Ictinia mississippiensis*. **(18)** The crista plantares lateralis projects strongly in species of *Buteo* and weakly in *I. mississippiensis*. **(33)** The trochleae have roughly equal distal extent in species of *Buteo*, while in *I. mississippiensis*, trochlea metatarsi II has the greatest distal extent, followed by trochlea metatarsi III and then trochlea metatarsi IV in all species except *Buteo lagopus*, where II and III have equal extent past IV.

### **Gen. et sp. Indet.**

#### ***Humerus***

Extant accipitrids differ as follows:

#### Elaninae.

**(2)** The dorsal face between the tuberculum supracondylare dorsale and the epicondylus dorsalis is not inflated and does not project dorsal of either point. **(3)** The palmar attachment point for the m. extensor carpi radialis is a very shallow, narrow, relatively smaller insertion scar positioned directly ventral to the tuberculum. **(8)** The sulcus humerotricipitalis is narrower, covering approximately one-third of the total shaft width. **(18)** The distal margin of the condylus dorsalis in cranial view is well proximal to the distal margin of the condylus ventralis, but the notch between the two is shallow. **(21)** The ventral-distal margin of the condylus ventralis is not continuous with the entepicondyle, and the two can be seen separately in cranial view

#### Perninae.

(7) The fossa olecrani is continuous with the rest of the face in all taxa except *L. isura*, where a distinct deepening in the face is present adjacent to the processus flexorius in distal view. (9) The fossa m. brachialis is moderately deep. (10) The fossa is narrowly separated from the dorsal margin of the shaft. (11) The epicondylus ventralis is flat, barely projecting ventrally. (18) The distal margin of the condylus dorsalis is proximal of the distal margin of the condylus ventralis, and the notch of the distal margin between the two is shallow. (20) The processus flexorius has equal distal extent with the condylus ventralis in caudal view and extends prominently ventrally.

#### Gypaetinae.

(3) The palmar insertion scar of the m. extensor carpi radialis is large and round. (9) The fossa m. brachialis is deep. (11) The epicondylus ventralis weakly projects ventrally. (12) The distal section of the epicondylus ventralis has one large, deep distinct insertion scar on the ventral margin of the cranial face, and a second, smaller and shallow scar on the ventral face directly adjacent to the first. (18) The distal margin of the condylus dorsalis is positioned proximal to that of the condylus ventralis in cranial view, forming a shallow, broad notch between the two. (20) The distal margin of the processus flexorius has equal distal extent to that of the condylus ventralis in caudal view, and prominently extends ventrally.

#### Aegyptiinae.

(2) The dorsal face between the tuberculum supracondylare dorsale and the epicondylus dorsalis is greatly prominent dorsally. (3) The palmar insertion of the m. extensor metacarpi radialis is large, very shallow and oval. (9) The fossa m. brachialis is deep and takes up three-quarters of the shaft at its maximum width. (10) The fossa is narrowly separated from the dorsal margin of the shaft. (12) Three insertion scars are present on the distal epicondylus ventralis on the ventral margin, with the proximal-most insertion being the largest and deepest, with two smaller, shallower insertion scars immediately distal to it. (14) The insertion scar for the pronator superficialis is large, deep and positioned ventrally and slightly distal to the tuberculum supracondylaris ventrale, with a second large, very shallow insertion scar directly distal to the first. (19) The incisura intercondylaris is moderately wide. (20) The processus flexorius extends just distal to the condylus ventralis.

#### Circaetinae.

(3) The palmar insertion scar for the m. extensor carpi radialis is dorsoventrally long and narrow. (9) The fossa m. brachialis is deep. (12) Two insertion scars are associated with the distal section of the epicondylus ventralis cranial face. Both are large and located on the ventral face, with the cranial-most insertion scar being deep and the caudal-most scar being shallow. (14) The insertion scar for the pronator superficialis is large, positioned ventral to the tuberculum on the cranial face and is deep. A second scar is present distal to the first on the ventral margin, which is small and

shallow. **(19)** The incisura intercondylaris is wide. **(20)** The processus flexorius has equal distal extent with the condylus ventralis in caudal view.

#### Aquilinae.

**(2)** The dorsal face between the tuberculum supracondylare dorsale and the epicondylus dorsalis is projecting dorsally into a prominence that projects dorsal of both points. **(3)** The palmar insertion scar of the m. extensor carpi radialis is large and oval. **(12)** There are two large insertion scars present on the ventrodiscal face of the epicondylus ventralis. The cranial-most scar is deep, and the caudal-most scar is shallow. A third large, very faint, very shallow scar is present on the distal face distal to the other two insertions. **(19)** The incisura intercondylaris is broad. **(20)** The distal margin of the processus flexorius extends distal to the condylus ventralis in caudal view, and projects well ventrally. **(21)** The condylus ventralis is not continuous with the entepicondylar distal margin, with the two visibly distinct in cranial view.

#### Haliaeetinae.

**(3)** The palmar insertion scar of the m. extensor carpi radialis is large and linear. **(9)** The fossa m. brachialis is deep. **(12)** Two large, deep insertion scars are present on the ventral margin of the epicondylus ventralis, with the caudal-most of the pair shallower than the cranial-most. Two faint, large, very shallow scars are present on the distal margin distally adjacent to the former pair. **(14)** The insertion scar for the pronator superficialis is positioned ventral to the tuberculum supracondylare ventrale, and is small, round and deep. A second scar, which is small, round and very shallow, is located distal to the former insertion. **(19)** The incisura intercondylaris is broad. **(20)** The distal margin of the processus flexorius is of roughly equal extent to that of the condylus ventralis in caudal view and is well projecting ventrally.

#### Accipitrinae.

**(2)** The dorsal face between the tuberculum supracondylaris and the epicondylus dorsalis is flat. **(3)** The palmar insertion scar of the m. extensor carpi radialis is large and linear. **(9)** The fossa m. brachialis spans between a third (*Accipiter*) to two-thirds (*Circus*) of the shaft width. **(12)** Two large, deep insertion scars are present on the distal section ventral margin of the epicondylus ventralis, with the caudal-most of the pair shallower than the cranial-most. **(14)** The insertion scar for the pronator superficialis is positioned ventral to the tuberculum supracondylare ventrale and is round and shallow, with a second small, very shallow insertion distal to the first on the ventral margin. **(20)** The processus flexorius extends well distal of the condylus ventralis in caudal view. **(21)** The ventrodiscal margin of the condylus ventralis is not continuous with the entepicondyle, with the two visibly distinct in cranial view.

#### Buteoninae.

(2) The dorsal face between the tuberculum supracondylare dorsale and the epicondylus dorsalis is flat. (3) The palmar insertion scar of the m. extensor carpi radialis is large and linear. (12) Two large, deep insertion scars are present on the distoventral margin of the epicondylus ventralis, with the caudal-most of the pair shallower than the cranial-most. (14) The insertion scar for the pronator superficialis is positioned ventral to the tuberculum supracondylare ventrale and is round and shallow, with a second small, very shallow scar distal to the first on the ventral margin. (18) The distal margin of the condylus dorsalis is proximal to the condylus ventralis, forming a shallow notch between the two condyles. (20) The processus flexorius extends well distal to that of the condylus ventralis. (21) The ventrodistal margin of the condylus ventralis is not continuous with the entepicondyle, with the two visually distinct in cranial view.

### ***Femur***

Recent accipitrids differ in key features as follows (variable characters excluded):

#### Elaninae.

(2) A crista supracondylaris medialis is present in all species except for *Gampsonyx swainsonii*. (6) The attachment scar on the planum popliteum is centred on the shaft. (8) The epicondylar projection on the lateral condyle is extremely short, barely projecting from the condylar surface.

#### Perninae.

(2) A crista supracondylaris medialis is present. (5) The fossa poplitea is deep in the majority of taxa, with the exception of *Chondrohierax uncinatus* (shallow). (8) The epicondylaris does not project from the lateral condyle in most species of pernines, except for *H. melanosternon* and *L. isura*, where it is short and robust.

#### Gypaetinae.

(2) A crista supracondylaris medialis is present in *Polyboroides typus* and absent in *Neophron percnopterus*. (6) The attachment scar on the planum popliteum is centred on the shaft. (8) The lateral epicondylar projection is short and robust in *P. typus* and is very short in *N. percnopterus*.

#### Aegyptiinae.

(6) The attachment scar on the planum popliteum is centred on the shaft. (8) The lateral epicondylaris is robust and projects strongly from the lateral condyle in all taxa.

#### Circaetinae.

(6) The attachment scar on the planum popliteum is centred on the shaft. (8) The lateral epicondylar projection is robust and distinctly projecting laterally from the lateral condyle in all taxa.

#### Aquilinae.

**(4)** The fovea tendineus is deep in all taxa. **(6)** The attachment scar on the planum popliteum is centred on the shaft in all taxa, except for species of *Hieraaetus*, where it is offset laterally. **(7)** The impressio gastrocnemialis lateralis is large and deep in all taxa. **(8)** The lateral epicondylar projection is short and robust in all taxa except for species of *Hieraaetus*, where the projection is long.

Haliaeetinae.

**(2)** A crista supracondylaris medialis is present. **(4)** The fovea tendineus is deep in all taxa except for species of *Haliastur*, where it is shallow. **(6)** The attachment scar on the planum popliteum is laterally offset. **(7)** The impressio m. gastrocnemialis lateralis is large and deep in all taxa.

Accipitrinae.

**(2)** A crista supracondylaris medialis is present in all species except for *Melierax metabates*. **(6)** The attachment scar on the planum popliteum is laterally offset. **(7)** The impressio m. gastrocnemialis lateralis is large and deep in all taxa. **(8)** The lateral epicondylar projection is short and robust in all taxa except for species of *Accipiter*, where it is long.

Buteoninae.

**(2)** A crista supracondylaris is present. **(6)** The attachment scar on the planum popliteum is laterally offset.

## Appendix 4: Chapter 2 PCA analyses data, scree plots and biplots

	Ulna L	Ulna SW	Ulna DW	CMC L	CMC PW	Tib L	Tib SW	Tib DW	Tib CLD	Tib CLH	Tib CMD	Tib CMH	Tmt L	Tmt SW	Tmt DW	Tmt T2W	Tmt T2D	Tmt T3W	Tmt T3D	Tmt T4W	Tmt T4D	D1.1 L	D1.2 L	D2.2 L
<i>Archaeohierax sylvestris</i>	158.8	6.5	12.9	78.2	19.7	135.7	9.7	16.5	12.9	9.4	13.4	9.2	110.1	9.4	17.7	4.3	9.3	5.2	7.7	3.4	9.6	29.9	24	25.9
<i>Elanus scriptus</i>	92.7	4.3	7.5	49.2	11.1	57.4	4.8	9.2	6.4	5	6.4	5.1	37	4.8	9.3	2.1	3.3	3.1	4.3	2.2	6.3	14	11.7	13.5
<i>Hamirostra melanosternon</i>	152.6	6.9	13.5	77.8	19.1	86.1	7.3	13.5	9.6	7.2	10.5	7.1	68.7	7.6	15.3	4.1	5.9	4.8	6.4	3	8.1	21.2	18.3	21.3
<i>Pernis apivorus</i>	112.5	6.2	10.7	57.1	15.2	71.7	6.4	11.2	7.6	6	8.1	7	51.8	6.3	10.8	2.6	4	3.6	4.4	2.4	5.5	19.4	16.8	18.1
<i>Lophoictinia isura</i>	116.7	6.1	10.9	61.1	15.7	65.5	6	10.9	7.6	6.3	7.6	5.3	48.3	5.8	10.5	2.9	3.9	3.6	4.2	2.3	5.6	18.7	16.4	17.2
<i>Aquila audax</i>	219.2	9.6	17.5	91.4	25.1	137.2	12.2	20.1	14.1	10.3	14.8	10.6	107.2	11.1	21.4	5.7	8.1	6.9	11.2	4.6	12.8	37	29.7	32.2
<i>Hieraaetus morphnoides</i>	132.9	6.3	10.8	65.8	15.6	87	7.2	13.5	8.9	7.1	8.9	7.5	63.2	8.3	14.1	3.6	5.3	4.5	6.7	3.4	9.2	25.6	19	22.3
<i>Spizaetus tyrannus</i>	135.3	6.1	10.7	63.5	15.8	108.6	9.1	15.1	10.1	7.7	9.5	7.5	84	8.7	16.3	4.1	5.5	4.8	7.4	3.2	9.1	28.9	23.1	25.5
<i>Haliaeetus leucogaster</i>	228.6	9.9	17.8	110.1	25.7	134.3	11.7	19.3	14	10.9	13.4	9.7	104.1	11	21.1	6.9	8.3	6.7	10.5	4.3	11.4	35.6	31.5	31
<i>Circus assimilis</i>	128.8	5.6	10.4	66.2	15.3	110.6	6.1	11	9.4	7.4	8.9	6	98.6	4.8	11.3	2.6	4.6	4	5.2	2.4	7.3	21.7	17.7	19.9
<i>Spilornis cheela</i>	115.5	5.7	10.4	55.5	14.6	93.5	7.4	12.8	8.1	6.1	8	6.4	78.8	6.9	11.9	3.3	4.4	3.8	5.6	2.5	6.8	16.2	15.9	16.6
<i>Aegyptius monachus</i>	277.1	9.6	19.5	112.7	25.7	132.9	9.8	18.6	16.2	13.4	17.5	10.8	96.3	11.1	20.8	5	8.7	7.8	11.9	4.9	12.5	30.4	23.4	29.1
<i>Gyps coprotheres</i>	318.2	12.3	24.4	135.6	32.7	152.7	12.7	22.4	20.1	16.8	21.8	14.2	105.2	14.3	26.4	7.1	11.2	9.9	14.3	6.4	14.6	30.9	?	31.6
<i>Neophron percnopterus</i>	164.1	6.7	13.4	77.4	19.4	99.8	8.05	14.7	10.9	8.8	10.9	7.4	81	7.9	16	4.4	5.1	5.7	7.9	3.5	8.2	21.8	17.8	23.1

**Table A4.1:** Absolute data (mm) from *Archaeohierax sylvestris* and selected extant species for PCA (A). Abbreviations: CMC, carpometacarpus; D1.1, pedal digit 1 phalanx 1; D1.2, pedal digit 1 phalanx 2; D2.2, pedal digit 2 phalanx 2; DW, distal width; L, length; PW, proximal width; SW, shaft width; Tib, tibiotarsus; Tmt, tarsometatarsus.

PC	Eigenvalue	% variance	Eig 2.5%	Eig 97.5%
1	6436.72	92.15	83.633	96.875
2	488.783	6.9976	2.6934	15.185
3	28.0255	0.40122	0.10483	1.1336
4	17.3289	0.24809	0.030877	0.53801
5	7.16593	0.10259	1.50E-31	0.15927
6	3.26073	0.046682	2.01E-41	0.090476
7	1.62274	0.023232	0	0.061295
8	1.09431	0.015667	0	0.030364
9	0.405474	0.0058049	0	0.012179
10	0.2811	0.0040243	0	0.003747
11	0.161578	0.0023132	0	0.006421
12	0.0927182	0.0013274	0	0.001941
13	0.0766038	0.0010967	0	0.001769

**Table A4.2:** Statistics for absolute data PCA (A) using a variance-covariance matrix, iterative imputation and 1000 bootstraps.

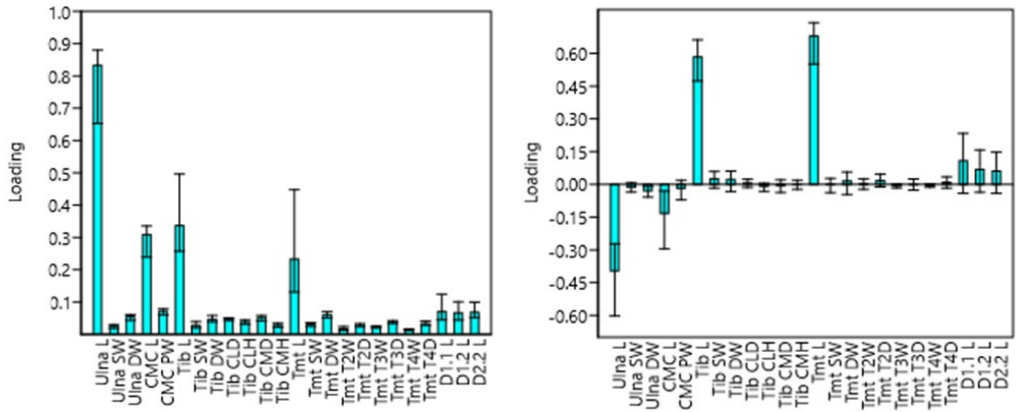


**Figure A4.1:** PC1 Biplot (left) and PC2 Biplot (right) of absolute data PCA (A).

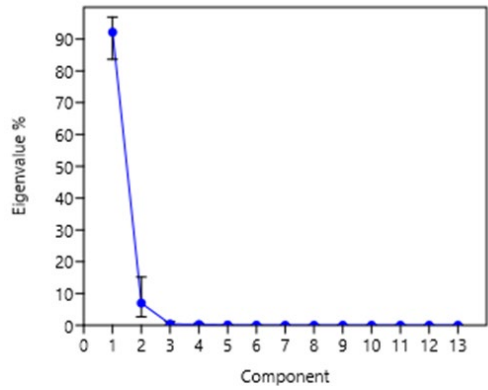


**Figure A4.2:** Scree plot for eigenvalue % of each PC component for absolute data PCA (A).

	Ulna L	Ulna SW	Ulna DW	CMC L	CMC PW	Tib L	Tib SW	Tib DW	Tib CLD	Tib CLH	Tib CMD	Tib CMH	Tmt L	Tmt SW	Tmt DW	Tmt T2W	Tmt T2D	Tmt T3W	Tmt T3D	Tmt T4W	Tmt T4D	D1.1 L	D1.2 L	D2.2 L
<i>Archaeohierax sylvestris</i>	2.2	0.8	1.1	1.9	1.3	2.1	1.0	1.2	1.1	1.0	1.1	1.0	2.04	1.0	1.2	0.6	1.0	0.7	0.9	0.5	1.0	1.5	1.4	1.4
<i>Elanus scriptus</i>	2.0	0.6	0.9	1.7	1.04	1.8	0.7	1.0	0.8	0.7	0.8	0.7	1.6	0.7	1.0	0.3	0.5	0.5	0.6	0.3	0.8	1.1	1.07	1.1
<i>Hamirostra melanosternon</i>	2.2	0.8	1.1	1.9	1.3	1.9	0.9	1.1	1.0	0.9	1.0	0.8	1.8	0.9	1.2	0.6	0.8	0.7	0.8	0.5	0.9	1.3	1.3	1.3
<i>Pernis apivorus</i>	2.05	0.8	1.03	1.7	1.2	1.8	0.8	1.05	0.9	0.8	0.9	0.8	1.7	0.8	1.03	0.4	0.6	0.6	0.6	0.4	0.7	1.3	1.2	1.3
<i>Lophoictinia isura</i>	2.1	0.8	1.04	1.8	1.2	1.8	0.8	1.04	0.9	0.8	0.9	0.7	1.7	0.8	1.02	0.5	0.6	0.6	0.6	0.4	0.7	1.3	1.2	1.2
<i>Aquila audax</i>	2.3	1.0	1.2	2.0	1.4	2.1	1.1	1.3	1.1	1.01	1.2	1.02	2.03	1.04	1.3	0.7	0.9	0.8	1.05	0.7	1.1	1.6	1.5	1.5
<i>Hieraaetus morphnoides</i>	2.1	0.8	1.03	1.8	1.2	1.9	0.9	1.1	0.9	0.8	0.9	0.9	1.8	0.9	1.1	0.5	0.7	0.6	0.8	0.5	1.0	1.4	1.3	1.3
<i>Spizaetus tyrannus</i>	2.1	0.8	1.03	1.8	1.2	2.03	0.9	1.2	1.0	0.9	1.0	0.9	1.9	0.9	1.2	0.6	0.7	0.7	0.9	0.5	1.0	1.5	1.4	1.4
<i>Haliaeetus leucogaster</i>	2.4	1.0	1.2	2.04	1.4	2.1	1.1	1.3	1.1	1.04	1.1	1.0	2.02	1.04	1.3	0.8	0.9	0.8	1.02	0.6	1.1	1.5	1.5	1.5
<i>Circus assimilis</i>	2.1	0.7	1.02	1.8	1.2	2.04	0.8	1.04	1.0	0.9	0.9	0.8	2.0	0.7	1.05	0.4	0.7	0.6	0.7	0.4	0.9	1.3	1.2	1.3
<i>Spilornis cheela</i>	2.1	0.7	1.02	1.7	1.2	2.0	0.9	1.1	0.9	0.8	0.9	0.8	1.9	0.8	1.07	0.5	0.6	0.6	0.7	0.4	0.8	1.2	1.2	1.2
<i>Aegypius monachus</i>	2.4	1.0	1.3	2.05	1.4	2.1	1.0	1.3	1.2	1.1	1.2	1.03	2.0	1.04	1.3	0.7	0.9	0.9	1.1	0.7	1.1	1.5	1.4	1.5
<i>Gyps coprotheres</i>	2.5	1.1	1.4	2.1	1.5	2.2	1.1	1.3	1.3	1.2	1.3	1.1	2.02	1.1	1.4	0.8	1.05	1.0	1.1	0.8	1.2	1.5	?	1.5
<i>Neophron percnopterus</i>	2.2	0.8	1.1	1.9	1.3	2.0	0.9	1.2	1.04	0.9	1.04	0.9	1.9	0.9	1.2	0.6	0.7	0.8	0.9	0.5	0.9	1.3	1.2	1.4

**Table A4.3:** Log transformed data (mm, rounded up to two digits) from *Archaeohierax sylvestris* and selected extant species for PCA (B). Abbreviations: CMC, carpometacarpus; D1.1, pedal digit 1 phalanx 1; D1.2, pedal digit 1 phalanx 2; D2.2, pedal digit 2 phalanx 2; DW, distal width; L, length; PW, proximal width; SW, shaft width; Tib, tibiotarsus; Tmt, tarsometatarsus.

PC	Eigenvalue	% variance	Eig 2.5%	Eig 97.5%
1	0.426831	91.486	0.88325	95.612
2	0.0152836	3.2758	1.8154	26.401
3	0.00862215	1.848	1.02E-28	5.7641
4	0.00541231	1.1601	1.75E-01	5.1699
5	0.00348796	0.7476	0	3.1823
6	0.00305587	0.65499	0	1.7328
7	0.00159113	0.34104	0	2.8329
8	0.000839514	0.17994	0	0.36368
9	0.000568529	0.12186	0	0.23489
10	0.000329	0.070517	0	0.14318
11	0.000276503	0.059265	0	0.084151
12	0.00017126	0.036707	0	0.051759
13	8.60E-05	0.018428	0	0.017749

**Table A4.4:** Statistics for log transformed data PCA (B) using a variance-covariance matrix, iterative imputation and 1000 bootstraps.

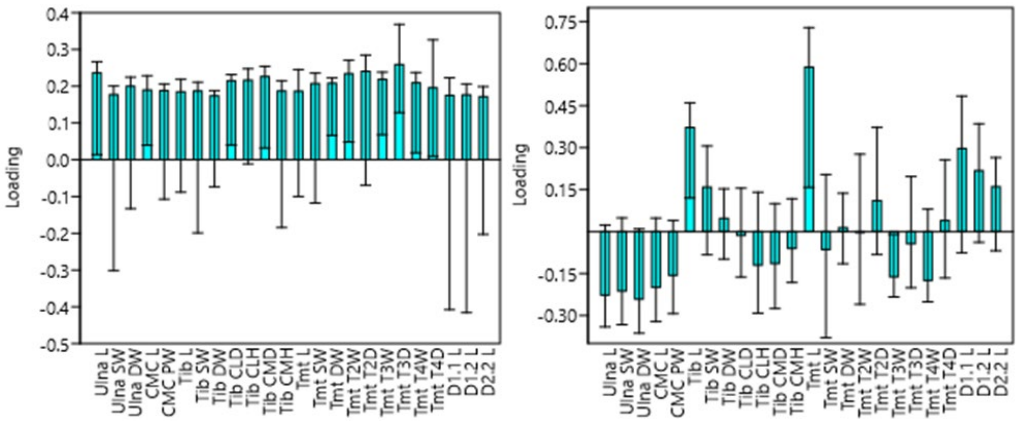


**Figure A4.3:** PC1 Biplot (left) and PC2 Biplot (right) of log transformed data PCA (B).

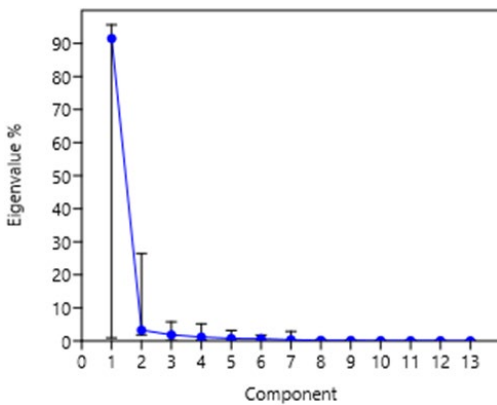


**Figure A4.4:** Scree plot for eigenvalue % of each PC component for log transformed data PCA (B).

	Ulna L	Ulna SW	Ulna DW	CMC L	CMC PW	Tib L	Tib SW	Tib DW	Tib CLD	Tib CLH	Tib CMD	Tib CMH	Tmt L	Tmt SW	Tmt DW	Tmt T2W	Tmt T2D	Tmt T3W	Tmt T3D	Tmt T4W	Tmt T4D	D1.1 L	D1.2 L	D2.2 L
<i>Archaeohierax sylvestris</i>	7.8	0.32	0.63	3.8	0.97	6.7	0.48	0.81	0.63	0.46	0.66	0.45	5.4	0.46	0.87	0.21	0.46	0.26	0.38	0.17	0.47	1.5	1.2	1.3
<i>Elanus scriptus</i>	7.7	0.36	0.62	4.1	0.92	4.8	0.4	0.77	0.53	0.42	0.53	0.42	3.1	0.4	0.77	0.17	0.27	0.26	0.36	0.18	0.52	1.2	0.97	1.1
<i>Hamirostra melanosternon</i>	8.1	0.37	0.72	4.1	1	4.6	0.39	0.72	0.51	0.38	0.56	0.38	3.6	0.4	0.81	0.22	0.31	0.25	0.34	0.16	0.43	1.1	0.97	1.1
<i>Pernis apivorus</i>	8.3	0.45	0.79	4.2	1.1	5.3	0.47	0.82	0.56	0.44	0.59	0.51	3.8	0.46	0.79	0.19	0.29	0.26	0.32	0.18	0.4	1.4	1.2	1.3
<i>Lophoictinia isura</i>	7.9	0.41	0.74	4.1	1.1	4.4	0.41	0.74	0.52	0.43	0.52	0.36	3.3	0.39	0.71	0.2	0.26	0.24	0.28	0.16	0.38	1.3	1.1	1.2
<i>Aquila audax</i>	9.3	0.41	0.74	3.9	1.1	5.8	0.52	0.85	0.6	0.44	0.63	0.45	4.6	0.47	0.91	0.24	0.34	0.29	0.48	0.19	0.54	1.6	1.3	1.4
<i>Hieraaetus morphnoides</i>	8.1	0.39	0.66	4	0.96	5.3	0.44	0.83	0.55	0.43	0.55	0.46	3.9	0.51	0.86	0.22	0.32	0.28	0.41	0.21	0.56	1.6	1.2	1.4
<i>Spizaetus tyrannus</i>	7.8	0.35	0.62	3.7	0.91	6.3	0.53	0.87	0.58	0.44	0.55	0.43	4.8	0.5	0.94	0.24	0.32	0.28	0.43	0.18	0.53	1.7	1.3	1.5
<i>Haliaeetus leucogaster</i>	10.5	0.45	0.82	5	1.2	6.2	0.54	0.88	0.64	0.5	0.61	0.44	4.8	0.5	0.97	0.32	0.38	0.31	0.48	0.2	0.52	1.6	1.4	1.4
<i>Circus assimilis</i>	8.1	0.35	0.66	4.2	0.97	7	0.39	0.7	0.59	0.47	0.56	0.38	6.2	0.3	0.71	0.16	0.29	0.25	0.33	0.15	0.46	1.4	1.1	1.2
<i>Spilornis cheela</i>	7.4	0.36	0.67	3.5	0.93	6	0.47	0.82	0.52	0.39	0.51	0.41	5	0.44	0.76	0.21	0.28	0.24	0.36	0.16	0.43	1	1	1.1
<i>Aegypius monachus</i>	12.5	0.43	0.88	5.1	1.1	6	0.44	0.84	0.73	0.6	0.79	0.49	4.3	0.5	0.94	0.22	0.39	0.35	0.54	0.22	0.56	1.4	1	1.3
<i>Gyps coprotheres</i>	12	0.46	0.92	5.1	1.2	5.8	0.48	0.84	0.76	0.63	0.82	0.53	4	0.54	1	0.27	0.42	0.37	0.54	0.24	0.55	1.2	?	1.2
<i>Neophron percnopterus</i>	8.8	0.36	0.72	4.2	1	5.4	0.43	0.79	0.59	0.47	0.59	0.4	4.3	0.42	0.86	0.24	0.27	0.31	0.42	0.19	0.44	1.2	0.96	1.2

**Table A4.5:** Size standardised (divided by height of quadrate) data (mm) from *Archaeohierax sylvestris* and selected extant species for PCA (C). Abbreviations: CMC, carpometacarpus; D1.1, pedal digit 1 phalanx 1; D1.2, pedal digit 1 phalanx 2; D2.2, pedal digit 2 phalanx 2; DW, distal width; L, length; PW, proximal width; SW, shaft width; Tib, tibiotarsus; Tmt, tarsometatarsus.

PC	Eigenvalue	% variance	Eig 2.5%	Eig 97.5%
1	2.94748	67.234	18.565	86.592
2	1.26769	28.917	10.327	73.794
3	0.079347	1.81	0.42632	4.5664
4	0.0435879	0.99427	1.01E-28	2.1266
5	0.0244473	0.55766	7.49E-31	1.1866
6	0.00962939	0.21965	4.91E-34	0.37911
7	0.00465463	0.10618	0	0.1758
8	0.00308716	0.07042	0	0.13991
9	0.0017012	0.038805	0	0.070876
10	0.000850945	0.019411	0	0.043144
11	0.000793983	0.018111	0	0.017466
12	0.000381583	0.0087042	0	0.015299
13	0.000260246	0.0059364	0	2.05E-29

**Table A4.6:** Statistics for size standardised data PCA (C) using a variance-covariance matrix, iterative imputation and 1000 bootstraps.

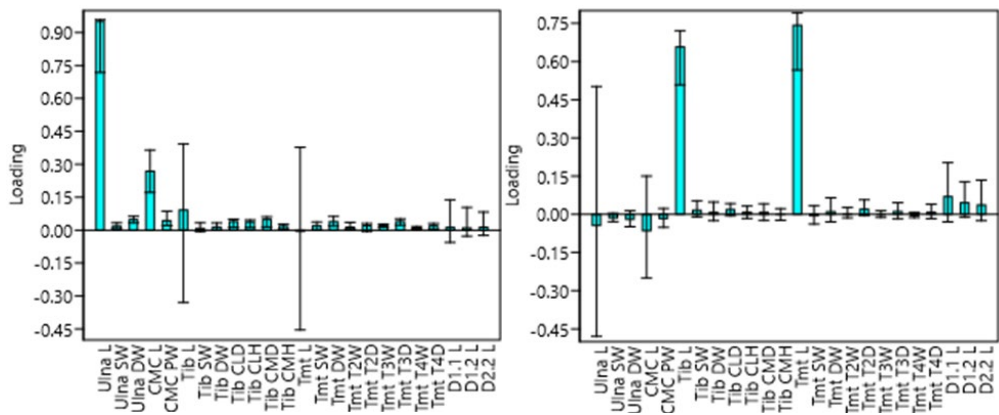


**Figure A4.5:** PC1 Biplot (left) and PC2 Biplot (right) of size standardised data PCA (C).

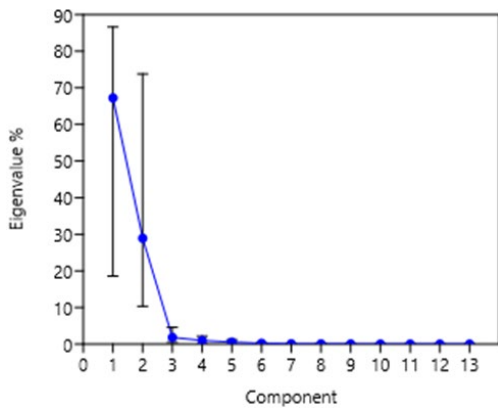


**Figure A4.6:** Scree plot for eigenvalue % of each PC component for size standardised data PCA (C).

## Appendix 5: Chapter 2 additional phylogenetic trees

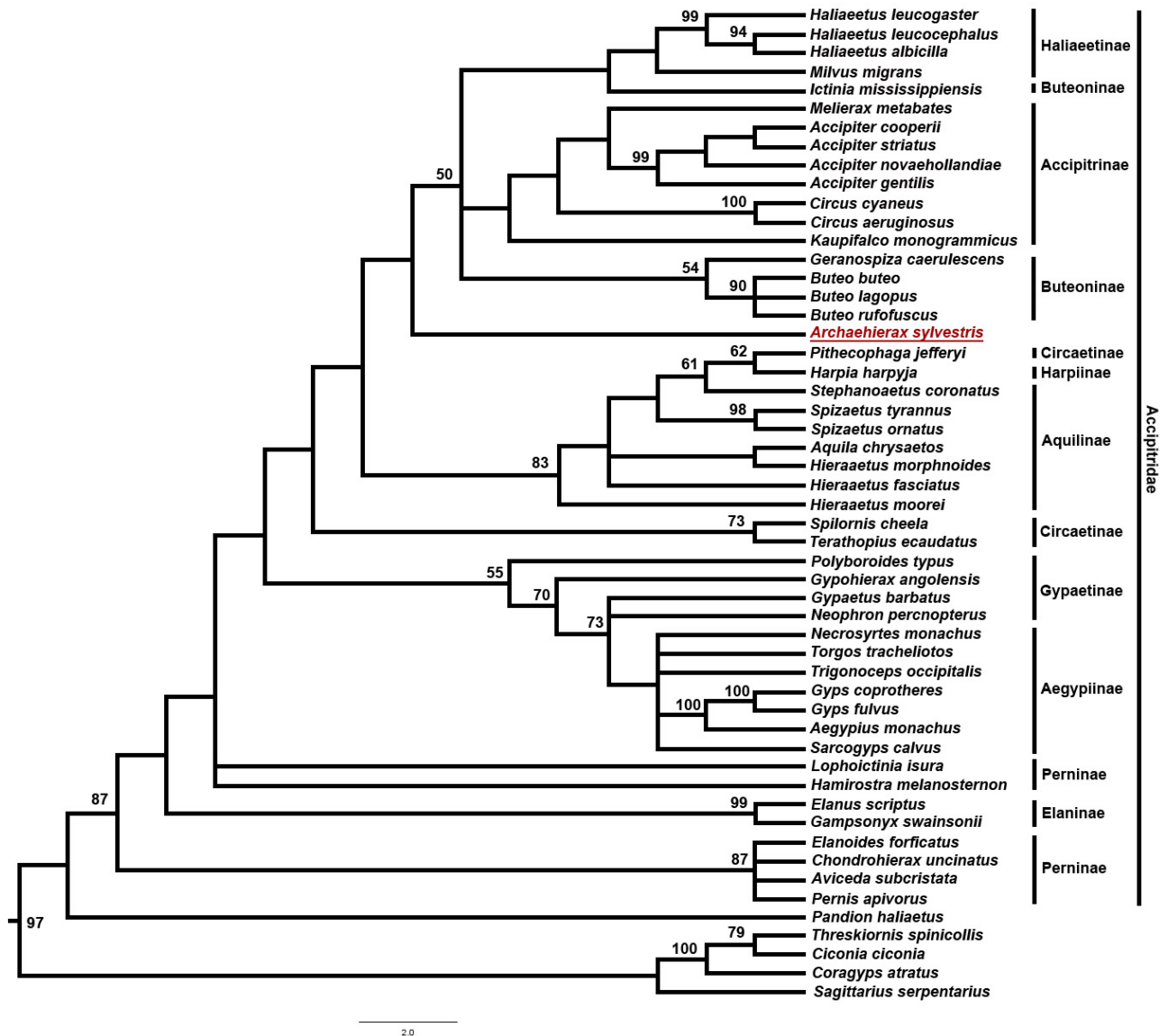
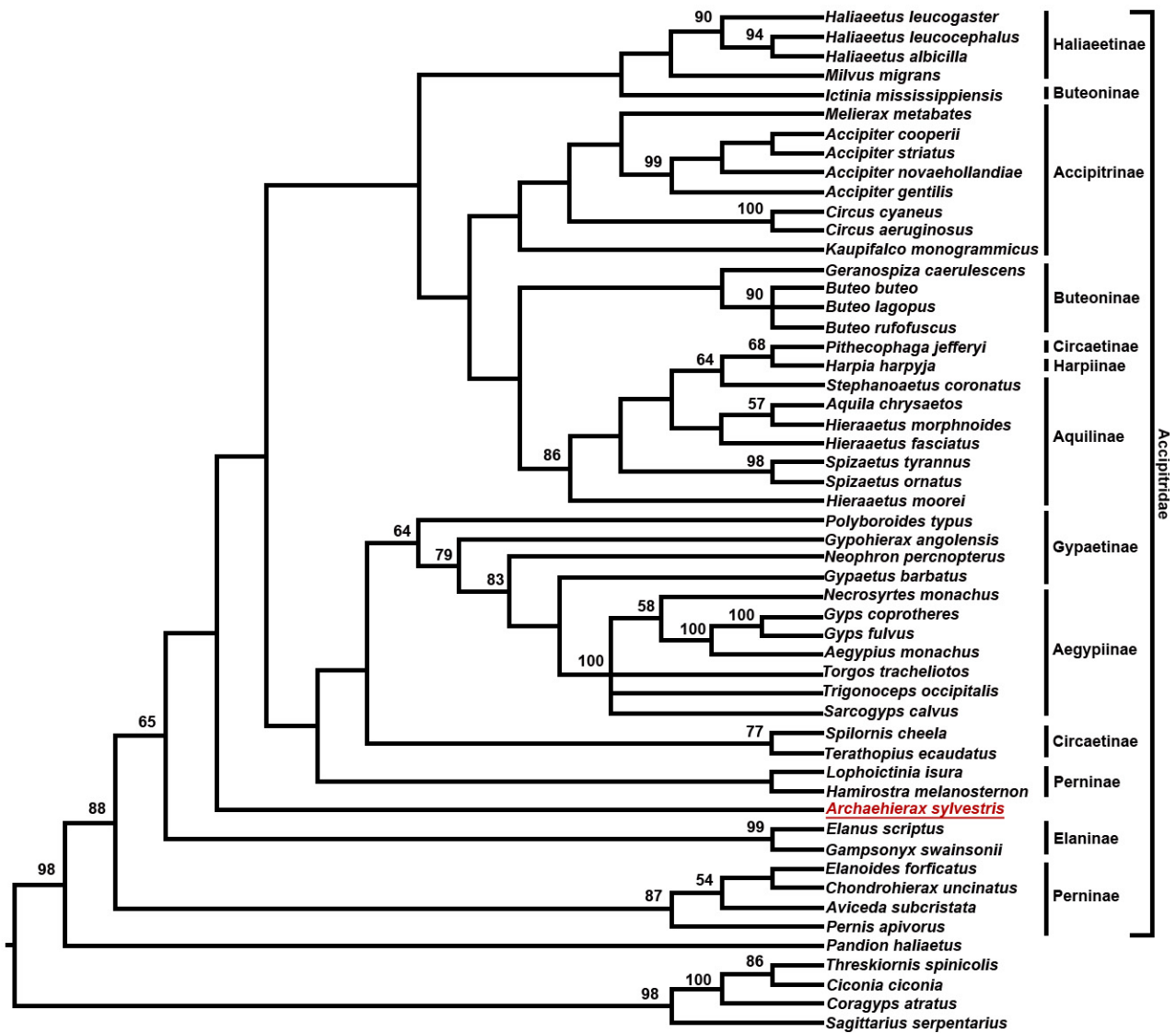


**Figure A5.1:** Analysis 1: Parsimony analysis of morphological (unordered) data. Strict consensus of 30 most-parsimonious trees. Tree Length = 1686, MPT = 30, CI = 0.2361, HI = 0.7639, RI = 0.6072. Bootstrap values are given at each node where they are greater than 50.



2.0

**Figure A5.2:** Analysis 2: Parsimony analysis of morphological (ordered) data. Strict consensus of four most-parsimonious trees. Tree Length = 1720, MPT = 4, CI = 0.2314, HI = 0.7686, RI = 0.6096. Bootstrap values are given at each node where they are greater than 50.

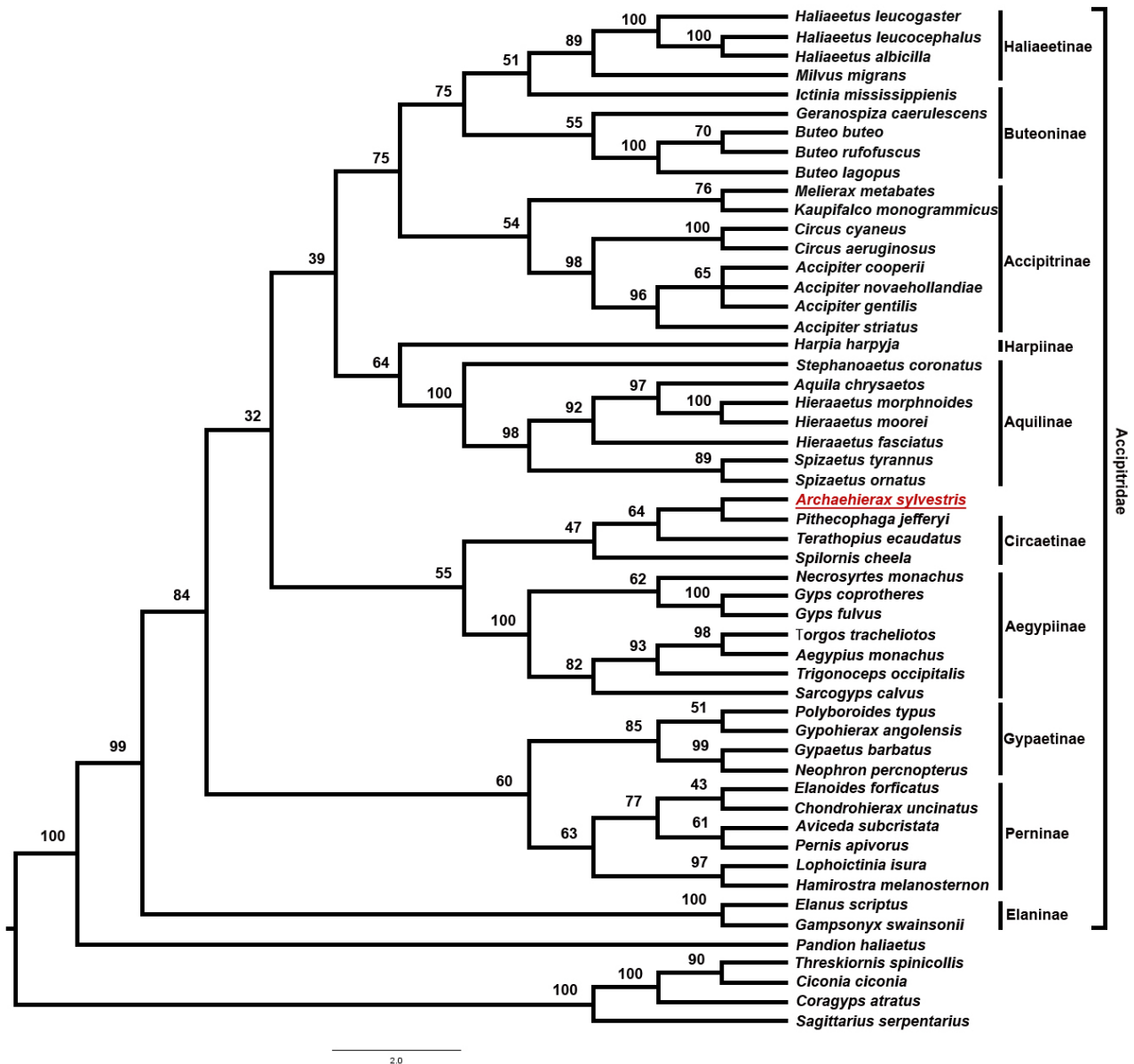


**Figure A5.3:** Analysis 3: Parsimony analysis of combined morphological (ordered) and molecular data. Strict consensus of 3 most-parsimonious trees. Tree Length = 1831, MPT = 3, CI = 0.2174, HI = 0.7826, RI = 0.5768. Bootstrap values are given at each node.



## BIBLIOGRAPHY

- Agnolin, F. (2006) Notas sobre el registro de Accipitridae (Aves, Accipitriformes) fósiles Argentinos. *Studia Geologica Salmanticensia*, 42, 67–80.
- Agnolin, F., Brissón Egli, F., Soibelzon, E., Rodríguez, S. G., Soibelzon, L. H., Iacona, F. & Piazza, D. (2017) A new large Cathartidae from the Quaternary of Argentina, with a review of the fossil record of condors in South America. *Contribuciones Científicas del Museo Argentino de Ciencias Naturales*, 7, 1–16.
- Alley, N. F. (1998) Cainozoic stratigraphy, palaeoenvironments and geological evolution of the Lake Eyre Basin. *Palaeogeography, Palaeoclimatology, Palaeoecology*, 144 (3–4), 239–263.
- Alvarenga, H. M. F. (1985) Notas sobre os Cathartidae (Aves) e descrição de um novo gênero do Cenozóico Brasileiro. *Anais da Academia Brasileira de Ciências*, 57, 349–357.
- Alvarenga, H., Brito, G. R. R., Migotto, R., Hubbe, A. & Höfling, E. (2008) *Pleistovultur nevesi* gen. et sp. nov. (Aves: Vulturidae) and the diversity of condors and vultures in the South American Pleistocene. *Ameghiniana*, 45 (3), 613–618.
- Amadon, D. (1977) Notes on the taxonomy of vultures. *The Condor*, 79, 413–416.
- Amadon, D. (1982) The genera of Booted Eagles: *Aquila* and relatives. *Journal of the Yamashina Institute for Ornithology*, 14, 108–121.
- Amaral, F. S. R., Miller, M. J., Silveira, L. F., Bermingham, E. & Wajntal, A. (2006) Polyphyly of the hawk genera *Leucopternis* and *Buteogallus* (Aves, Accipitridae): multiple habitat shifts during the Neotropical buteonine diversification. *BMC Evolutionary Biology*, 6, article number 10, doi: 10.1186/1471-2148-6-10
- Amaral, F. S. R., Sheldon, F. H., Gamauf, A., Haring, E., Riesing, M., Silveira, L. F. & Wajntal, A. (2009) Patterns and processes of diversification in a widespread and ecologically diverse avian group, the buteonine hawks (Aves, Accipitridae). *Molecular Phylogenetics and Evolution*, 53, 703–715.
- Ameghino, F. (1895) Sur les oiseaux fossiles de la Patagonia. *Boletín del Instituto Geográfico Argentino*, 15, 501–602.
- Ameghino, F. (1899) Sinópsis geológico-paleontológica. Suplemento (adiciones y correcciones). La Plata.

- Archer, M. & Hand, S. J. (2006) The Australian marsupial radiation. In: *Evolution and Biogeography of Australasian Vertebrates*, Merrick, J. R., Archer, M., Hickey, G. M., Lee, M. S. Y. (Eds.). Auscipub Pty Ltd, Oatlands, NSW; p. 575–646.
- Arredondo, O. (1970) Nueva especie de ave pleistocénica del orden Accipitriformes (Accipitridae) y nuevo género para las Antillas. *Ciencias Biológicas*, 4(8), 1–19.
- Arredondo, O. & Arredondo, C. (2002) [for 1999 volume] Nuevos género y especie de ave fósil (Falconiformes: Accipitridae) del Cuaternario de Cuba. *Poeyana*, 470–475: 9–14.
- Arshad, M., Gonzalea, J., El-Sayed, A. A., Osborne, T. & Wink, M. (2009) Phylogeny and phylogeography of critically endangered *Gyps* species based on nuclear and mitochondrial markers. *Journal of Ornithology*, 150, 419–430.
- Awise, J. C., Nelson, W. S. & Sibley, C. G. (1994) DNA sequence support for a close phylogenetic relationship between some storks and New World vultures. *Proceedings of the National Academy of Sciences USA*, 91, 5173–5177.
- Baird, R. F. (1985) Avian fossils from Quaternary deposits in 'Green Waterhole Cave', south-eastern South Australia. *Records of the Australian Museum*, 37, 353–370.
- Baird, R. F. (1991) Quaternary avifauna of Australia. In: *Vertebrate palaeontology of Australasia*, P. Vickers-Rich, J. M. Monaghan, R. F. Baird, T. H. Rich, E. M. Thomson, C. Williams (Eds). Pioneer Design Studio Pty Ltd, Lilydale, and Monash University Publications Committee, Melbourne; p. 809–849.
- Ballmann, P. (1973) Fossile Vögel aus dem Neogen der Halbinsel Gargano (Italien). *Scripta Geologica*, 17, 1–75.
- Barrowclough, G. F., Groth, J. G., Lai, J. E. & Tsang, S. M. (2014) The phylogenetic relationships of the endemic genera of Australo-Papuan hawks. *Journal of Raptor Research*, 48, 36–43.
- Becker, J. J. (1985) *Pandion lovensis*, a new species of osprey from the Late Miocene of Florida. *Proceedings of the Biological Society of Washington*, 98, 314–320.
- Bickart, K. J. (1990) The birds of the late Miocene–early Pliocene Big Sandy Formation, Mohave County, Arizona. *Ornithological Monographs*, 44 1–72.
- Bildstein, K. L. (2004) Raptor migration in the neotropics: patterns, processes, and consequences. *Ornitologia Neotropical*, 15, 83–99.
- Boev, Z. (2012) *Circaetus rhodopensis* sp. n. (Aves: Accipitriformes) from the Late Miocene of Hadzhidimovo (SW Bulgaria). *Acta Zoologica Bulgarica*, 64 (1), 5–12.
- Boev, Z. (2014) *Gyps bochenskii* sp. n. (Aves: Falconiformes) from the Late Pliocene of Varshets (NW Bulgaria). *Acta Zoologica Bulgarica*, 62 (2), 211–242.

- Boev, Z. (2015) An Early Pleistocene Snake Eagle, *Circaetus haemusensis* sp. n. (Aves, Accipitriformes) from Varshets, northwestern Bulgaria. *Acta Zoologica Bulgarica*, 67 (1), 127–138.
- Boev, Z. N. (2013) *Aquila kurochkini* sp. n., a new Late Pliocene eagle (Aves, Accipitriformes) from Varshets (NW Bulgaria). *Palaeontological Journal*, 47 (11), 1344–1354.
- Boev, Z. N & Korachev, D. (1998) *Buteo spassovi* sp. n. – a Late Miocene buzzard (Accipitridae, Aves) from SW Bulgaria. *Geologica Balcanica*, 29, 125–129.
- Boles, W. E. (1993) *Pengana robertbolesi*, a peculiar bird of prey from the Tertiary of Riversleigh, northwestern Queensland, Australia. *Alcheringa*, 17(1), 19–25.
- Boles, W. E. (2006) The avian fossil record of Australia: an overview. In: *Evolution and Biogeography of Australasian Vertebrates*, Merrick, J. R., Archer, M., Hickey, G. M., Lee, M. S. Y. (Eds.). Auscipub Pty Ltd, Oatlands, NSW; p. 387–411.
- Brandt, J. F. (1853) Die Gruppen und Gattungen der Raubvögel Russlands in exomorphischer und craniologischer Beziehung. *Journal für Ornithologie (Journal for Ornithology)*, 1 (3), 178–195.
- Breman, F. C. Jordaens, K., Sonet, G., Nagy, Z. T., Van Houdt, J. & Mouette, M. (2013) DNA barcoding and evolutionary relationships in *Accipiter* Brisson, 1760 (Aves, Falconiformes: Accipitridae) with a focus on African and European representatives. *Journal of Ornithology*, 154, 265–287.
- Brodkorb, P. (1956) Two new birds from the Miocene of Florida. *The Condor*, 58 (5), 367–370.
- Brodkorb, P. (1964) Catalogue of fossil birds, Part 2 (Anseriformes through Galliformes). *Bulletin of the Florida State Museum Biological Sciences*, 8 (3), 195–335.
- Brown, L. H. (1970) *Eagles*. Arco Publishing, New York.
- Brown L. & Amadon D. (Eds.) (1968) *Eagles, hawks and falcons of the world*. Michelin House, London, England.
- Brunet, J. (1970), Oiseaux de l'Éocène supérieur du Bassin de Paris. *Annales de Paléontologie (Vertébrés)*, 56, 3–57.
- Brüniche-Olsen, A., Jones, M. E., Burrige, C. P., Murchison, E. P., Holland, B. R. & Austin, J. J. (2018) Ancient DNA tracks the mainland extinction and island survival of the Tasmanian devil. *Journal of Biogeography*, 45(5), 963–976.
- Bunce, M., Szulkin, M., Lerner, H. R. L., Barnes, I., Shapiro, B., Cooper, A. & Holdaway, R. N. (2005) Ancient DNA provides new insights into the evolutionary history of New Zealand's extinct giant eagle. *PloS Biology*, 3, e9.

- Burchak-Abramovich, N. I. (1971) Materialy k izucheniyu pleystotsenovykh ptits Gruzii (peshchera Tsona). *Paleontologicheskii Sbornik*, 7(2): 45-51.
- Cade, T. J. (1955) Variation of the common rough-legged hawk in North America. *The Condor*, 57 (6), 313–346.
- Campbell, K. E. & Tonni, E. P. (1980) A new genus of teratorn from the Huayquerian of Argentina (Aves: Teratornithidae). *Natural History Museum of Los Angeles County, Contributions in Science*, 330, 59–68.
- Campbell, K. E. & Tonni, E. P. (1983) Size and locomotion in teratorns (Aves: Teratornithidae). *The Auk*, 100, 390–403.
- Campbell, K. E. (1979) The non-passerine Pleistocene avifauna of the Talara Tar Seeps, north-western Peru. *Royal Ontario Museum Life Sciences Contributions*, 118, 1–203.
- Cascini, M., Mitchell, K. J., Cooper, A. & Phillips, M. J. (2019) Reconstructing the evolution of giant extinct kangaroos: comparing the utility of DNA, morphology and total evidence. *Systematic Biology*, 68(3), 520–537.
- Chapman, F. M. (1926) The distribution of bird life in Ecuador: a contribution to a study of the origin of Andean bird life. *Bulletin of the American Museum of Natural History*, 55, 1–783.
- Claramunt, S. & Cracraft, J. (2015) A new time tree reveals Earth history's imprint on the evolution of modern birds. *Science Advances*, 1, e1501005.
- Clark, W. S. (2012) The eagle genus *Hieraaetus* is distinct from *Aquila*, with comments on the name Ayres' Eagle. *Bulletin of the British Ornithologists Club*, 132, 295–298.
- Compton, L. V. (1935) Two avian fossil from the lower Pliocene of South Dakota. *American Journal of Science*, 178, 343–348.
- Condon, H. T. (1975) *Checklist of the Birds of Australia: Non-passerines (Vol. 1)*. Royal Australasian Ornithologists Union.
- Cope, E. D. (1874) Notes on the Santa Fe marls, and some of the contained vertebrate fossils. *Proceedings of the Academy of Natural Sciences of Philadelphia*, 26, 147–152.
- Cracraft, J. & Vickers-Rich, P. (1972) The systematics and evolution of the Cathartidae in the Old World Tertiary. *The Condor*, 74, 272–283.
- Dawson, E. W. (1961) An extinct sea eagle in the Chatham Islands. *Notornis*, 5, 171–172.
- Dawson, T. J. & Dawson, L. (2006) Evolution of arid Australia and consequences for vertebrates. In: *Evolution and Biogeography of Australasian Vertebrates*, Merrick, J. R., Archer, M., Hickey, G. M., Lee, M. S. Y. (Eds.). Auscipub Pty Ltd, Oatlands, NSW; p. 51–70.

- de Graaf, R. M., Tilghman, N. G. & Anderson, S. H. (1985) Foraging guilds of North American birds. *Environmental Management*, 9(6), 493–536.
- de Oliveira, E. H. C., Tagliarini, M. M., dos Santos, M. S., O'Brien, P. C. M. & Ferguson-Smith, M. A. (2013) Chromosome painting in three species of Buteoninae: a cytogenetic signature reinforces the monophyly of South American species. *PLoS ONE*, 8 (7), e70071, doi:10.1371/journal.pone.0070071.
- de Vis, C. W. (1889) Addition to the list of fossil birds. *Proceedings of the Royal Society of Queensland*, 6, 55–58.
- de Vis, C. W. (1890) On a bone of an extinct eagle. *Proceedings of the Royal Society of Queensland*, 6, 161–162.
- de Vis, C. W. (1891) Note on an extinct eagle. *Proceedings of the Linnean Society of New South Wales*, 16, 123–125.
- de Vis, C. W. (1892) Residue of the extinct birds of Queensland as yet detected. *Proceedings of the Linnean Society of New South Wales*, 16, 437–456.
- de Vis, C. W. (1905) A contribution to the knowledge of the extinct avifauna of Australia. *Annals of the Queensland Museum*, 6, 3–25.
- de Vis, C. W. (1911) *Palaeolestes gorei*, n. sp., an extinct bird. *Annals of the Queensland Museum*, 10, 15–17.
- Debus, S. J. S. (1998) *The birds of prey of Australia: a field guide*. Oxford University Press.
- Delacour, J. (1947) *Birds of Malaysia*. Macmillan, New York.
- Dickinson, E. C. & Remsen J. V. Jr (Eds). 2013. *The Howard & Moore Complete Checklist of Birds of the World*. 4<sup>th</sup> edition, vol 1. Aves Press: Eastbourne, UK.
- Domínguez-Solera, S. & Domínguez-Rodrigo, M. (2011) A taphonomic study of a carcass consumed by griffon vultures (*Gyps fulvus*) and its relevance for the interpretation of bone surface modifications. *Archaeological and Anthropological Sciences*, 3(4), 385–392.
- Ducey, J. E. (1992) Fossil birds of the Nebraska region. *Transactions of the Nebraska Academy of Sciences*, 19, 83–96.
- Emslie, S. D. (1988a) An early condor-like vulture from North America. *The Auk*, 105(3) 529–535.
- Emslie, S. D. (1988b) The fossil history and phylogenetic relationships of Condors (Ciconiiformes: Vulturidae) in the New World. *Journal of Vertebrate Paleontology*, 8(2), 212–228.
- Emslie, S. D. (1998) Avian community, climate, and sea-level changes in the Plio-Pleistocene of the Florida peninsula. *Ornithological Monographs*, 50, 1–113.

- Emslie, S. D. & Czaplewski, N. J. (1999) Two new fossil eagles from the Late Pliocene (Late Blancan) of Florida and Arizona and their biogeographic implications. *Smithsonian Contributions to Palaeobiology*, 89, 185–198.
- Engelmann, F. (1928) Die Raubvögel Europas: Naturgeschichte, Kulturgeschichte und Falknerei. Neudamm, J. Neumann.
- Etherington, G. J. & Mobley, J. A. (2016) Molecular phylogeny, morphology and life-history comparisons within *Circus cyaneus* reveal the presence of two distinct evolutionary lineages. *Avian Research*, 7 (17), DOI 10.1186/s40657-016-0052-3.
- Falla, R. A. (1953) The Australian element in the avifauna of New Zealand. *Emu*, 53, 36–46.
- Feduccia, A. (1974) Another Old World vulture from the New World. *The Wilson Bulletin*, 86 (3), 251–255.
- Feduccia, A. & Voorhies, M. R. (1989) Miocene hawk converges on secretarybird. *Ibis*, 131, 349–354.
- Fetner, R. A. & Sołtysiak, A. (2013) Shape and distribution of griffon vulture (*Gyps fulvus*) scavenging marks on a bovine skull. *Journal of Taphonomy*, 11(1), 41–47.
- Fitzinger, L. J. (1856) Über das System und die Charakteristik der Natürlichen Familien der Vögel. *Sitzungber. Kais. Akad. D. Wiss. Math. Nat.* (Vienna), 21, 277–318.
- Fleischer, R. C., Olson, S. L., James, H. F. & Cooper, A. C. (2000) Identification of the extinct Hawaiian Eagle (*Haliaeetus*) by mtDNA sequence analysis. *The Auk*, 117 (4), 1051–1056.
- Forbes, H. O. (1892) Preliminary notice of additions to the extinct avifauna of New Zealand. *Transactions and Proceedings of the New Zealand Institute*, 24, 185–189.
- Friedmann, H. (1950) The birds of North and Middle America. Part XI. Cathartidae to Falconidae. *United States National Museum Bulletin*, 50. Washington D.C., Smithsonian Institution.
- Fuentes, E. & Olsen, J. (2015) Observations of the killing of large macropods by Wedge-tailed Eagles *Aquila audax*. *Australian Field Ornithology*, 32, 160–166.
- Fusco, D. (2021) The impacts of environmental change on late Quaternary fossil fauna at Cathedral Cave, eastern Australia. Unpublished PhD thesis, Flinders University, College of Science and Engineering, South Australia, Australia.
- Fürbringer, M. (1888) Untersuchungen zur Morphologie und Systematik der Vögel zugleich ein Beitrag zur Anatomie der Stutz und Bewegungsorgane. K. Zool. Genoots. Bidr. Tot de Dierkunde (Amsterdam, I. J. Van Holkema), 15.

- Gadow, H. (1893) Vogel. In: *Klassen und Ordnungen des Thier-Reichs, wissenschaftlich dargestellt in Wort und Bild*, H. G. Bronn (ed). Sechster Band. C.F. Winter'sche, Leipzig und Heidelberg.
- Gaff, P. (2002) The Fossil History of the Family Accipitridae in Australia. Master of Science dissertation, Monash University, Victoria, Australia.
- Gaff, P. & Boles, W. E. (2010) A new eagle (Aves: Accipitridae) from the Mid Miocene Bullock Creek Fauna of northern Australia. *Records of the Australian Museum*, 62, 71–76.
- Gaillard, C. (1908) Les oiseaux des Phosphorites du Quercy. In: *Annales de L'Universite de Lyon*, A. Rey (ed). J. B. Balliere et Fils, Paris. No. 23, 178 pp.
- Gaillard, C. (1939) Contribution à l'étude des oiseaux fossiles. *Nouvelles Archives du Muséum d'histoire naturelle de Lyon*, 15 (2), 1–100.
- Gamauf, A. & Haring, E. (2004) Molecular phylogeny and biogeography of Honey-Buzzards (genera *Pernis* and *Henicopernis*). *Journal of Zoological Systematics and Evolutionary Research*, 42, 145–153.
- Gamauf, A. & Haring, E. (2005) Phylogenetic analysis of Old World Perninae based on mitochondrial DNA sequences. *Zoologische Mededelingen*, 79 (3), 175–177.
- Gamauf, A., Gjershaug, J. O., Kvaløy, K. & Haring, E. (2005) Molecular phylogeny of the hawk-eagles (genus *Spizaetus*). *Zoologische Mededelingen*, 79 (3), 179–180.
- Giebel, C. G. (1847) *Fauna der Vorwelt mit steter Berücksichtigung der lebenden Thiere*. Vol I (2): Vögel und Amphibien. Leipzig: Brockhaus.
- Gill, B. J., Bell, B. D., Chambers, G. K., Medway, D. G., Palma, R. L., Scofield, R. P., Tennyson, A. J. D. & Worthy, T. H. (2010) *Checklist of the birds of New Zealand, Norfolk and Macquarie Islands, and the Ross Dependency, Antarctica*. 4th edition. Ornithological Society of New Zealand & Te Papa Press, Wellington.
- Goodman, S. M. (1994a) Description of a new species of subfossil eagle from Madagascar-*Stephanoaetus* (Aves, Falconiformes) from the deposits of Ampasambazimba. *Proceedings of the Biological Society of Washington*, 107 (3), 421–428.
- Goodman, S. M. (1994b) The enigma of antipredator behaviour in lemurs: evidence of a large extinct eagle on Madagascar. *International Journal of Primatology*, 15 (1), 129–134.
- Goodman, S. M. and Rakotozafy, L. M. A. (1995) Evidence for the existence of two species of *Aquila* on Madagascar during the Quaternary. *Geobios*, 28 (2), 241–246.
- Grassé, P-P. (1950) *Traité de Zoologie: Anatomie, Systématique, Biologie*. Tome XV, *Oiseaux*, Libraires de l'Académie de Médecine. Masson et Cie, Paris.

- Grealy, A., Macken, A., Allentoft, M. E., Rawlence, N. J., Reed, E. & Bunce, M. (2016) An assessment of ancient DNA preservation in Holocene-Pleistocene fossil bone excavated from the world heritage Naracoorte Caves, South Australia. *Journal of Quaternary Science*, 31(1), 33–45.
- Gregory, S. M. S. & Dickinson, E. C. (2012) *Clanga* has priority over *Aquiloides* (or how to drop a clanger). *Bulletin of the British Ornithologists' Club*, 132, 135–136.
- Griffiths, C. S., Barrowclough, G. F., Groth, J. G. & Mertz, L. A. (2007) Phylogeny, diversity, and classification of the Accipitridae based on DNA sequences of the RAG-1 exon. *Journal of Avian Biology*, 38, 587–602.
- Griscom, L. (1932) The distribution of bird life in Guatemala; a contribution to a study of the origin of Central American bird life. *Bulletin of the American Museum of Natural History*, 64, 1–425.
- Groth, J. G. & Barrowclough, G. F. (1999) Basal divergences in birds and the phylogenetic utility of the nuclear RAG-1 gene. *Molecular Phylogenetics and Evolution*, 12, 115–123.
- Haast, J. V. (1872) Notes on *Harpagornis moorei*, an extinct gigantic bird of prey, containing description of femur, ungual phalanges, and rib. *Transactions and proceedings of the New Zealand Institute*, 4, 192–196.
- Haast, J. V. (1874) On *Harpagornis*, an extinct genus of gigantic raptorial birds of New Zealand. *Transactions and proceedings of the New Zealand Institute*, 6, 62–75.
- Hackett, S. J., Kimball, R. T., Reddy, S., Bowie, R. C. K., Braun, E. L., Braun, M. J., Chojnowski, J. L., Cox, W. A., Han, K., Harshman, J., Huddleston, C. J., Marks, B. D., Miglia, K. J. Moore, W. S., Sheldon, F. H., Steadman, D. W., Witt, C. C. & Yuri, T. (2008) A phylogenomic study of birds reveals their evolutionary history. *Science*, 320, 1763–1768.
- Haring, E., Kvaløy, K., Gjershaug, J. O., Rørv, N. & Gamauf, A. (2007) Convergent evolution and paraphyly of the hawk-eagles of the genus *Spizaetus* (Aves, Accipitridae) – phylogenetic analyses based on mitochondrial markers. *Journal of Zoological Systematics and Evolutionary Research*, 45(4), 353–365.
- Harrison, C. J. O. & Walker, C. A. (1973) An undescribed extinct fish-eagle from the Chatham Islands. *Ibis*, 115, 274–277.
- Harrison, C. J. O., & Walker, C. A. (1976) Birds of the British Upper Eocene. *Zoological Journal of the Linnean Society*, 59, 323–351.
- Harrison, C. J. O., & Walker, C. A. (1979) Birds of the British Middle Eocene. *Tertiary Research Special Paper*, 5, 19–27.

- Heintzman, P. D., Zazula, G. D., Cahill, J. A., Reyes, A. V., MacPhee, R. D. E. & Shapiro, B. (2015) Genomic data from extinct North American *Camelops* revise camel evolutionary history. *Molecular Biology and Evolution*, 32(9), 2433–2440.
- Helbig, A. J., Kocum, A., Seibold, I. & Braun, M. J. (2005) A multi-gene phylogeny of aquiline eagles (Aves: Accipitriformes) reveals extensive paraphyly at the genus level. *Molecular Phylogenetics and Evolution*, 35, 147–164.
- Hernández Carrasquilla, F. (2001) A new species of vulture (Aves, Aegypiinae) from the Upper Pleistocene of Spain. *Ardeola*, 48 (1), 47–53.
- Holdaway, R. N. (1991) Systematics and palaeobiology of Haast's Eagle (*Harpagornis moorei* Haast, 1872) (Aves: Accipitridae). Unpublished PhD thesis. Department of Zoology, University of Canterbury, Christchurch, New Zealand. 472 pp.
- Holdaway, R. N. (1994) An exploratory phylogenetic analysis of the genera of the Accipitridae, with notes on the biogeography of the family. In: Meyburg, B.-U. and Chancellor, R. D. (Eds). *Raptor Conservation Today*. World Working Group on Birds of Prey and Owls; p. 601–647.
- Holdaway, R.N. & Worthy, T. H. (1997) A reappraisal of the late Quaternary fossil vertebrates of Pyramid Valley Swamp, North Canterbury, New Zealand. *New Zealand Journal of Zoology*, 24, 69–121.
- Holdaway, R. N., Worthy, T. H. & Tennyson, A. J. D. (2001) A working list of breeding bird species of the New Zealand region at first human contact. *New Zealand Journal of Zoology*, 28, 119–187.
- Hou, L. (1984) The Aragonian vertebrate fauna of Xiaocaowan, Jiangsu-2. Aegypinae (Falconiformes, Aves). *Vertebrata PalAsiatica*, 22, 14–20. [In Chinese].
- Hou, L. (1998) Aves. In: *Luobidang Cave Site*, Hao S., Wanbo H. (Eds). South Press; p. 40–47.
- Hou, L., Zhou, Z., Zhang, F. and Li, J. (2000) A new vulture from the Miocene of Shandong, Eastern China. *Vertebrata PalAsiatica*, 38 (2), 104–110.
- Howard, H. (1932) Eagles and eagle-like vultures of the Pleistocene of Rancho La Brea. *Carnegie Institute Washington Publications*, 429, 1–82.
- Howard, H. (1935) A new species of eagle from a Quaternary cave deposit in eastern Nevada. *The Condor*, 37, 206–209.
- Howard, H. (1944) A Miocene hawk from California. *The Condor*, 46, 236–237.
- Howard, H. (1962) Bird remains from a prehistoric cave deposit in Grant County, New Mexico. *The Condor*, 64 (3), 241–242.

- Howard, H. (1963) Fossil birds from the Anza-Borrego desert. *Los Angeles County Museum Contributions in Science*, 73, 1–33.
- Howard, H. (1966) Two fossil birds from the lower Miocene of South Dakota. *Los Angeles County Museum Contributions in Science*, 107, 1–8.
- Hudson, G. E. (1948) Studies on the muscles of the pelvic appendage in birds II; the heterogeneous order Falconiformes. *American Midland Naturalist*, 39, 102–127.
- Jánossy, D. (1977) Plio-Pleistocene bird remains from the Carpathian Basin III, Strigiformes, Falconiformes, Caprimulgiformes, Apodiformes. *Aquila*, 84, 9–36.
- Jánossy, D. (1983) Die mittelpleistozäne Vogelfauna von Přezletice bei Prag (ČSSR). In: *Wirbeltier-Evolution und Faunenwandel in Känozoikum*, W.-D. Heinrich (Ed.). Akademie-Verlag, Berlin; p. 247–269.
- Jarvis, E. D. et al. (2014) Whole genome analyses resolve early branches in the tree of life of modern birds. *Science*, 346, 1320–1331.
- Jefferson, G. T. (1991) A catalogue of late Quaternary vertebrates from California: part one, non-marine lower vertebrate and avian taxa. *Natural History Museum of Los Angeles County, Technical Reports*, 5, 60 pp.
- Jetz, W., Thomas, G. H., Joy, J. B., Hartmann, K. & Mooers, A. O. (2012) The global diversity of birds in space and time. *Nature*, 491, 444–448.
- Jiang, L., Chen, J., Wang, P., Ren, Q., Yuan, J., Qian, C., Hua, X., Guo, Z., Zhang, L., Yang, J., Wang, Y., Zhang, Q., Ding, H., Bi, D., Zhang, Z., Wang, Q., Chen, D. & Kan, X. (2015) The mitochondrial genomes of *Aquila fasciata* and *Buteo lagopus* (Aves, Accipitriformes): sequence, structure and phylogenetic analyses. *PLoS ONE*, 10 (8), e0136297, doi:10.1371/journal.pone.0136297.
- Johnson, C. N. & Prideaux, G. J. (2004) Extinctions of herbivorous mammals in the late Pleistocene of Australia in relation to their feeding ecology: No evidence for environmental change as cause of extinction. *Austral Ecology*, 29, 553–557.
- Jollie, M. (1976) A contribution to the morphology and phylogeny of the Falconiformes – Part 1. *Evolutionary Theory*, 1, 285–298.
- Jollie, M. (1977a) A contribution to the morphology and phylogeny of the Falconiformes – Part 2. *Evolutionary Theory*, 2, 115–208.
- Jollie, M. (1977b) A contribution to the morphology and phylogeny of the Falconiformes – Part 3. *Evolutionary Theory*, 2, 209–300.

- Jollie, M. (1977c) A contribution to the morphology and phylogeny of the Falconiformes – Part 4. *Evolutionary Theory*, 3, 1–142.
- Kerley, L. L. & Slaght, J. C. (2013) First documented predation of Sika Deer (*Cervus nippon*) by Golden Eagle (*Aquila chrysaetos*) in Russian Far East. *Journal of Raptor Research*, 47 (3), 328–330.
- Kessler, J. (E.) (2018) Evolution and presence of diurnal predatory birds in the Carpathian Basin. *Ornis Hungarica*, 26(1), 102–123.
- Knapp, M. (2019) From a molecules' perspective – contributions of ancient DNA research to understanding cave bear biology. *Historical Biology*, 31(4), 442–447.
- Kocum, A. (2008) Phylogenie der Accipitriformes (Greifvögel) anhand verscheidener nuklearer und mitochondrialer DNA-Sequenzen. *Vogelwarte*, 46, 141–143.
- Kretzoi, M. (1977) The fauna of small vertebrates of the Middle Pleistocene at Petralona. *Anthropos*, 4, 131–143.
- Kruckenhauser, L., Haring, E., Pinsker, W., Riesing, M. J., Winkler, H., Wink, M. & Gamauf, A. (2004) Genetic vs. morphological differentiation of Old World buzzards (genus *Buteo*, Accipitridae). *Zoologica Scripta*, 33 (3), 197–211.
- Ksepka, D. T., Bertelli, S. & Giannini, M. P. (2006) The phylogeny of the living and fossil Sphenisciformes. *Cladistics*, 22, 412–441.
- Kurochkin, E. N. (1968) Fossil remains of birds from Mongolia. *Ornitologija*, 9, 323–330. [In Russian].
- Kurochkin, E. N. (1976) A survey of the Paleogene birds of Asia. *Smithsonian Contributions to Paleobiology*, 27, 75–86.
- Kurochkin, E. N. (1985) Birds of the Central Asia in Pliocene. *Transactions of the Joint Soviet-Mongolian Paleontological Expedition*, 26, 1–120.
- Lambrecht, K. (1933) *Handbuch der Palaeornithologie*. Borntraeger, Berlin.
- Laube, (1909) Ein neuer Vogelrest aus den Tonen von Preschen bei Bilin. *Lotos*, 57, 159–161.
- Lautenschlager, S. (2016a) Digital reconstruction of soft-tissue structures in fossils. *The Paleontological Society Papers*, 22, 101–117. doi:10.1017/scs.2017.10
- Lautenschlager, S. (2016b) Reconstructing the past: methods and techniques for the digital restoration of fossils. *Royal Society Open Science*, 3, 160342.

- Lerner, H. R. L. & Mindell, D. P. (2005) Phylogeny of eagles, Old World vultures, and other Accipitridae based on nuclear and mitochondrial DNA. *Molecular Phylogenetics and Evolution*, 37, 327–346.
- Lerner, H. R. L., Christidis, L., Gamauf, A., Griffiths, C., Haring, E., Huddleston, C. J., Kabra, S., Kocum, A., Krosby, M., Kvaløy, K., Mindell, D., Rasmussen, P. R., Røv, N., Wadleigh, R., Wink, M. & Gjershaug, J. O. (2017). Phylogeny and taxonomy of the Booted Eagles (Accipitriformes: Aquilinae). *Zootaxa*, 4216(4), 301–320.
- Lerner, H. R. L., Klaver, M. C. & Mindell, D. P. (2008) Molecular phylogenetics of the buteonine birds of prey (Accipitridae). *The Auk*, 304(2), 304–315.
- Li, Z., Clarke, J. A., Zhou, Z. & Deng, T. (2016) A new Old World vulture from the late Miocene of China sheds light on Neogene shifts in the past diversity and distribution of the Gypaetinae. *The Auk*, 133, 615–625.
- Ligon, J. D. (1967) Relationships of the cathartid vultures. *Occasional Papers of the Museum of Zoology, University of Michigan*, 651, 1–26.
- Linnaeus, C. (1758) *Systema Naturae per Regna Tria Naturae*, 10th Edition, revised, Vol 1: Regnum Animale. Salvii, L. Holmiae, Stockholm, Sweden, iv + 824 pp.
- Llamas, B., Brotherton, P., Mitchell, K. J., Templeton, J. E. L., Thomson, V. A., Metcalf, J. L., Armstrong, K. N., Kasper, M., Richards, S. M., Camens, A. B., Lee, M. S. Y. & Cooper, A. (2015) Late Pleistocene Australian marsupial DNA clarifies the affinities of extinct megafaunal kangaroos and wallabies. *Molecular Biology and Evolution*, 32(3), 574–584.
- Louchart, A., Bedetti, C. & Pavia, M. (2005) A new species of eagle (Aves: Accipitridae) close to the Steppe Eagle, from the Pleistocene of Corsica and Sardinia, France and Italy. *Palaeontographica*, 272, 128–148.
- Louchart, A., Haile-Selassie, Y., Vignaud, P., Likius, A. & Brunet, M. (2008) Fossil birds from the Late Miocene of Chad and Ethiopia and zoogeographical implications. *Oryctos*, 7, 147–167.
- Louys, J. and Price, G. J. (2015) The Chinchilla Local Fauna: An exceptionally rich and well-preserved Pliocene vertebrate assemblage from fluvial deposits of south-eastern Queensland, Australia. *Acta Palaeontologica Polonica*, 60(3), 551–572.
- Lydekker, R. (1890) On the remains of some large extinct birds from the cavern-deposits of Malta. *Proceedings of the Zoological Society of London*, 403–411.
- Manegold, A. & Hutterer, R. (2021) First substantial evidence for Old World vultures (Aegypiinae, Accipitridae) from the early Palaeolithic and Iberomaurusian of Morocco. *Paläontologische Zeitschrift*, <https://doi.org/10.1007/s12542-021-00548-9>.

- Manegold, A. & Zelenkov, N. (2014) [2015] A new species of *Aegyptius* vulture from the early Pliocene of Moldova is the earliest unequivocal evidence of Aegyptiinae in Europe. *Paläontologische Zeitschrift*, 89, 529–534.
- Manegold, A., Pavia, M. & Haarhoff, P. (2014) A new species of *Aegyptius* vulture (Aegyptiinae, Accipitridae) from the early Pliocene of South Africa. *Journal of Vertebrate Paleontology*, 34, 1394–1407.
- Marchant, S., & P.J. Higgins (1993) *Handbook of Australian, New Zealand and Antarctic Birds. Volume 2: Raptors to Lapwings*. Oxford University Press, Melbourne.
- Marsh, O. C. (1871) Notice of some new fossil mammals and birds from the Tertiary formation of the West. *American Journal of Science*, 2 (8), 120–127.
- Martin, H. A. (1990) The palynology of the Namba Formation in the Wooltana-1 bore, Callabonna Basin (Lake Frome), South Australia, and its relevance to Miocene grasslands in central Australia. *Alcheringa: an Australasian Journal of Palaeontology*, 14 (3): 247–255.
- Martin, H. A. (2006) Cenozoic climate change and the development of the arid vegetation in Australia. *Journal of Arid Environments*, 66(3), 533–563.
- Martin, L. D. (1971) An early Pleistocene eagle from Nebraska. *The Condor*, 73 (2), 248–250.
- Martin, L. D. (1975) A new species of *Spizaetus* from the Pliocene of Nebraska. *The Wilson Bulletin*, 87 (3), 413–416.
- Mather, E. K., Lee, M. S. Y., Camens, A. B. & Worthy, T. H. (2021) An exceptional partial skeleton of a new basal raptor (Aves: Accipitridae) from the late Oligocene Namba Formation, South Australia. *Historical Biology*, DOI: 10.1080/08912963.21.1966777.
- Mayr, G. (2005) The postcranial osteology and phylogenetic position of the Middle Eocene *Messelastur gratulator* Peters, 1994 – a morphological link between owls (Strigiformes) and falconiform birds? *Journal of Vertebrate Paleontology*, 25(3), 635–645.
- Mayr, G. (2006a) An osprey (Aves: Accipitridae: Pandionidae) from the early Oligocene of Germany. *Senckenbergiana lethaea*, 86(1), 93–96.
- Mayr, G. (2006b) A new raptorial bird from the Middle Eocene of Messel, Germany. *Historical Biology*, 18(2), 99–106.
- Mayr, G. (2009) *Paleogene fossil birds*. Springer-Verlag, Berlin, Heidelberg.
- Mayr, G. (2011) Well-preserved new skeleton of the Middle Eocene *Messelastur* substantiates sister group relationship between Messelasturidae and Halcyornithidae (Aves, ?Pan-Psittaciformes). *Journal of Systematic Palaeontology*, 9, 159–171.

- Mayr, G. (2017) *Avian Evolution*. John Wiley & Sons, Chichester, West Sussex.
- Mayr, G. & Clarke, J. (2003) The deep divergences of neornithine birds: a phylogenetic analysis of morphological characters. *Cladistics*, 19(6), 527–553.
- Mayr, G. & Hurum, J. H. (2020) A tiny, long-legged raptor from the early Oligocene of Poland may be the earliest bird-eating diurnal bird of prey. *The Science of Nature*, 107, article number 48, 6 pp. doi.org/10.1007/s00114-020-01703-z.
- Mayr, G. & Perner, T. (2020) A new species of diurnal birds of prey from the late Eocene of Wyoming (USA)—one of the earliest New World records of the Accipitridae (hawks, eagles, and allies). *Neues Jahrbuch für Geologie und Paläontologie-Abhandlungen*, 297, 205–215.
- McGowran, B. & Hill, R. S. (2015) Cenozoic climatic shifts in southern Australia, *Transactions of the Royal Society of South Australia*, 139(1), 19–37.
- Meijer, H. J. M., Sutikna, T., Saptomo, E. W., Awe, R. D., Jatmiko, Wasisto, S., James, H. F., Morwood, M. J. & Tocheri, M. W. (2013) Late Pleistocene-Holocene non-passerine avifauna of Liang Bua (Flores, Indonesia). *Journal of Vertebrate Paleontology*, 33(4), 877–894.
- Migotto, R. (2013) Filogenia de Accipitridae (Aves: Accipitriformes) com base em caracteres osteológicos. PhD dissertation, Universidade de São Paulo.
- Miller, A. H. & Compton, L. V. (1939) Two fossil birds from the lower Miocene of South Dakota. *The Condor*, 41, 153–156.
- Miller, A. H. & Sibley, C. G. (1942) An Oligocene hawk from Colorado. *The Condor*, 44, 39–40.
- Miller, L. H. (1911) A series of eagle tarsi from the Pleistocene of Rancho La Brea. *University of California Publications, Bulletin of the Department of Geological Sciences*, 6, 305–316.
- Miller, L. H. (1915) A walking eagle from Rancho La Brea. *The Condor*, 17 (5), 179–181.
- Miller, L. H. (1916) Two vulturid raptors from the Pleistocene of Rancho La Brea. *University of California Publications, Bulletin of the Department of Geological Sciences*, 9, 105–109.
- Miller, L. H. (1928) Generic reassignment of *Morphnus daggetti*. *The Condor*, 30, 255–256.
- Miller, L. H. (1937) Skeletal studies of the tropical hawk *Harpagus*. *The Condor*, 39(5), 219–221.
- Millsap, B. A., Seipke, S. H. & Clark, W. S. (2011) The Gray Hawk (*Buteo nitidus*) is two species. *The Condor*, 113 (2), 326–339.
- Milne-Edwards, A. (1863) Mémoire sur la distribution géologique des oiseaux fossiles et description de quelques espèces nouvelles. *Comptes Rendus des Séances hebdomadaires de l'Académie des Sciences (Paris)*, 56, 1219–1222.

- Milne-Edwards, A. (1867–1871) *Rechères anatomiques et paléontologiques pour servir à l'histoire des oiseaux fossils de la France*. 2 vol. Victor Masson et Fils, Paris.
- Milne-Edwards, A. (1892) *Sur les oiseaux fossiles des dépôts éocènes de phosphate de chaux du Sud de la France*. C R Second Congress Ornithology International, 60–80.
- Mindell, D. P., Fuchs, J. & Johnson, J. A. (2018) Phylogeny, taxonomy and geographic diversity of diurnal raptors: Falconiformes, Accipitriformes and Cathartiformes. In: *Birds of Prey*, J. H. Sarasola, J. Grande, J. Negro (Eds). Springer, Cham; p. 3–32.
- Mlíkovský, J. (1997) Taxonomic identity of *Haliaeetus angustipes* Jánossy, 1983 (Aves: Accipitridae) from the early Pleistocene of the Czech Republic. *Buteo*, 9, 51–56.
- Mlíkovský, J. & Švec, P. (1989) Review of the Tertiary waterfowl (Aves: Anseridae) of Czechoslovakia. *Časopis pro Mineralogii a Geologii*, 34, 199–203.
- Moreno, F. P. & Mercerat, A. (1891) Catálogo de los pájaros fósiles de la Republica Argentina conservados in el Museo de La Plata. *Anales del Museo de La Plata: Paleontologia Argentina*, 1, 7–71.
- Mourer-Chauviré, C. (1975) Un exemple d'évolution chez les oiseaux au quaternaire: *Buteo rufinus jansonii* nov. subsp. (Aves, Falconida, Accipitridae) du Pleistocene moyen de Saint-Estève-Janson (Bouches-du Rhône, France). *Colloque internat. C.N.R.S., 218 (Paris, 4–9 juin 1972). Problemes actuelles de paleontologie-evolution des vertebres*; 533–543.
- Mourer-Chauviré, C. (1991) Les Horusornithidae nov. fam., Accipitriformes (Aves) a articulation intertarsienne hyperflexible de l'Éocène du Quercy. *Geobios*, 13, 183–192.
- Mourer-Chauviré, C. (2002) Revision of the Cathartidae (Aves, Ciconiiformes) from the Middle Eocene to the Upper Oligocene Phosphorites du Quercy, France. In: *Proceedings of the 5<sup>th</sup> Symposium of the Society of Avian Palaeontology and Evolution, Beijing, 1–4 June 2000*, Zhou Z, Zhang F (Eds). Science Press, Beijing; p. 97–111.
- Mourer-Chauviré, C. (2003) Birds (Aves) from the Middle Miocene of Arrisdrift (Namibia). Preliminary study with description of two new genera: *Amanuensis* (Accipitriformes, Sagittariidae) and *Namibiavis* (Gruiformes, Idiornithidae). *Memoir of the Geological Survey of Namibia*, 19, 103–113.
- Mourer-Chauviré, C. (2006) The avifauna of the Eocene and Oligocene Phosphorites du Quercy (France): An updated list. *Strata*, 13, 135–149.
- Mourer-Chauviré, C. & Cheneval, J. (1983) Les Sagittariidae fossiles (Aves, Accipitriformes) de l'Oligocène des phosphorites du Quercy et du Miocène inférieur de Saint-Gérard-le-Puy. *Geobios*, 16(4), 443–459.

- Nagy, J. & Tökölyi, J. (2014) Phylogeny, historical biogeography and the evolution of migration in accipitrid birds of prey (Aves: Accipitriformes). *Ornis Hungarica*, 22, 15–35.
- Nitzsch, C. L. & Burmeister, C. H. (1840) *System der Pterylographie*. Halle, Eduard Anton.
- Noriega, J. I., Areta, J. I., Vizcaíno, S. F. & Bargo, M. S. (2011) Phylogeny and taxonomy of the Patagonian Miocene falcon *Thegornis musculosus* Ameghino, 1895 (Aves: Falconidae). *Journal of Palaeontology*, 85 (6), 1089–1104.
- Oatley, G., Simmons, R. E. & Fuchs, J. (2015) A molecular phylogeny of the harriers (*Circus*, Accipitridae) indicate the role of long distance dispersal and migration in diversification. *Molecular Phylogenetics and Evolution*, 85, 150–160.
- Olson, S. L. (1982) The distribution of fused phalanges of the inner toe in the Accipitridae. *Bulletin of the British Ornithologists' Club*, 102, 8–12.
- Olson, S. L. (1984) The relationships of the extinct Chatham Island Eagle. *Notornis*, 31 (4), 273–277.
- Olson, S. L. (1985) The fossil record of birds. In: *Avian Biology*, vol. 8, D. S. Farner, J. R. King, K. C. Parkes (eds). Academic Press, New York, pp 79–238.
- Olson, S. L. (2000) Fossil Red-shouldered Hawk in the Bahamas: *Calohierax quadratus* Wetmore synonymised with *Buteo lineatus* (Gmelin). *Proceedings of the Biological Society of Washington*, 113, 298–301.
- Olson, S. L. (2007) The “Walking Eagle” *Wetmoregyps daggetti* Miller: a scaled-up version of the Savanna Hawk (*Buteogallus meridionis*). *Ornithological Monographs*, 63, 110–114.
- Olson, S. L. (2008) A new genus and species of buteonine hawk from Quaternary deposits in Bermuda. *Proceedings of the Biological Society of Washington*, 121 (1), 130–141.
- Olson, S. L. & Alvarenga, H. M. F. (2002) A new genus of small teratorn from the Middle Tertiary of the Taubaté Basin, Brazil (Aves, Teratornithidae). *Proceedings of the Biological Society of Washington*, 115, 701–705.
- Olson, S. L. & James, H. F. (1991) Descriptions of thirty-two new species of birds from the Hawaiian Islands: Part I. Non-passeriformes. *Ornithological Monographs*, 45.
- Olson, S. L. & Rasmussen, P. C. (2001) Miocene and Pliocene birds from the Lee Creek Mine, North Carolina. In: *Geology and Palaeontology of Lee Creek Mine, North Carolina, III*, C. E. Ray, D. J. Bohaska (Eds.); and: *Smithsonian Contributions to Palaeobiology*, 90, 233–365.
- Orlando, L. & Cooper, A. (2014) Using ancient DNA to understand evolutionary and ecological processes. *Annual Review of Ecology, Evolution and Systematics*, 45, 573–598.

- Owen, R. (1879) *Memoirs on the extinct and wingless birds of New Zealand*. 2 vol. John van Voorst, London.
- Panteleyev, A. V., Sablin, M. V. & Zabelin, V. I. (2006) A find of remains of birds and mammals in the Neogene of Tuva. In: *Materialy Mezhdunarodnogo simpoziuma: Pozdněkainozoiskaya istoriya severa aridnoi zony*. Rostov-on-Don: Yuzhn. Nauchn, Tsentr Ross. Akad. Nauk. Pp 246–247.
- Peters, D. S. (1994) *Messelastur gratulator* n. gen. n. spec., ein Greifvogel aus der Grube Messel (Aves: Accipitridae). *Courier Forschungsinstitut Senckenberg*, 170, 3–9.
- Peters, J. L. (1931) *Checklist of the birds of the world. Volume 1*. Harvard University Press, Cambridge.
- Phillips, M. J. & Zakaria, S. S. (2021) Enhancing mitogenomic phylogeny and resolving the relationships of extinct megafaunal placental mammals. *Molecular Phylogenetics and Evolution*, 158, 107082, <https://doi.org/10.1016/j.ympev.2021.107082>.
- Picasso, M. B. J., Tambussi, C. & Dozo, M. T. (2009) Neurocranial and brain anatomy of a late Miocene eagle (Aves, Accipitridae) from Patagonia. *Journal of Vertebrate Paleontology*, 29 (3), 831–836.
- Prum, R. O., Berv, J. S., Dornburg, A., Field, D. J., Townsend, J. P., Lemmon, E. M. & Lemmon, A. R. (2015) A comprehensive phylogeny of birds (Aves) using targeted next-generation DNA sequencing. *Nature*, 526(7574), 569–573.
- Rasmussen, D. T., Olson, S. L. & Simons, E. L. (1987) Fossil birds from the Oligocene Jebel Qatrani Formation, Fayum Province, Egypt. *Smithsonian Contributions to Paleobiology*, 62, 1–20.
- Reed, E. H. & Bourne, S. J. (2000) Pleistocene fossil vertebrate sites of the south-east region of South Australia. *Transactions of the Royal Society of South Australia*, 124 (2), 61–90.
- Reeves, N. M. (2009) Taphonomic effects of vulture scavenging. *Journal of Forensic Science*, 54(3), 523–528.
- Rich, P. V. (1980) 'New World vultures' with Old World affinities? *Contributions to Vertebrate Evolution*, 5, 1–115.
- Rich, P. V. & van Tets, G. F. (1982) Fossil birds of Australia and New Guinea; their biogeographic, phylogenetic and biostratigraphic input. Pp. 235–384 in P. V. Rich, and E. M. Thompson, (Eds). *The fossil vertebrate record of Australasia*. Monash University Offset Printing Unit, Clayton, Victoria.

- Rich, P. V., Hou, L. H., Ono, K. & Baird, R. F. (1986) A review of the fossil birds of China, Japan and Southeast Asia. *Geobios*, 19(6), 755–772.
- Rich, P., Van Tets, G. F. & McEvey, A. R. (1982) Pleistocene records of *Falco berigora* from Australia and the identity of *Asturaetus furcillatus* De Vis (Aves: Falconidae). *Memoirs of the Queensland Museum*, 20, 687–693.
- Rich, T. H., Archer, M., Hand, S. J., Godthelp, H., Muirhead, J., Pledge, N. S., Flannery, T. F., Woodburne, M. O., Case, J. A., Tedford, R. H., Turnbull, W. D., Lundelius, E. L. Jr, Rich, L. S. V., Whitelaw, M. J., Kemp, A., Vickers-Rich, P. (1991) Australian Mesozoic and Tertiary terrestrial mammal localities. In: *Vertebrate palaeontology of Australasia*, P Vickers-Rich, JM Monaghan, RF Baird, TH Rich (Eds.). Pioneer Design Studio Ltd, Lilydale, & Monash University Publications Committee, Melbourne; p. 1005–1057.
- Riesing, M. J., Kruckenhauser, L., Gamauf, A. & Haring, E. (2003) Molecular phylogeny of the genus *Buteo* (Aves: Accipitridae) based on mitochondrial marker sequences. *Molecular Phylogenetics and Evolution*, 27, 328–342.
- Ronquist, F., Klopstein, S., Vilhelmsen, L., Schulmeister, S., Murray, D. L. & Rasnitsyn, A. P. (2012) A total-evidence approach to dating with fossils, applied to the early radiation of the Hymenoptera. *Systematic Biology*, 61 (6), 973–999.
- Sánchez Marco, A. (2007) New occurrences of the extinct vulture *Gyps melitensis* (Falconiformes, Aves) and a reappraisal of the palaeospecies. *Journal of Vertebrate Paleontology*, 27, 1057–1061.
- Scarlett, R. J. (1953) A sub-fossil hawk from New Zealand. *Records of the Canterbury Museum*, 6 (3), 245–252.
- Scheider, J., Wink, M., Stubbe, M., Hille, S. & Wiltschko, W. (2004) Phylogeographic relationships of the Black Kite *Milvus migrans*. In: *Raptors Worldwide*, Chancellor, RD and Meyburg B.-U. (Eds). Berlin & Budapest, WWGBP & MME/Birdlife Hungary; p. 467–472.
- Schreiber, A., Stubbe, M. & Stubbe, A. (2000) Red kite (*Milvus milvus*) and black kite (*M. migrans*): minute genetic interspecies distance of two raptors breeding in a mixed community (Falconiformes: Accipitridae). *Biological Journal of the Linnean Society*, 69, 351–365.
- Seersholm, F. V., Grealy, A., McDowell, m. C., Cole, T. L., Arnold, L. J., Prideaux, G. J. & Bunce, M. (2021) Ancient DNA from bulk bone reveals past genetic diversity of vertebrate fauna on Kangaroo Island, Australia. *Quaternary Science Reviews*, 262, 106962.
- Seibold, I. & Helbig, A. J. (1995) Evolutionary history of New and Old World vultures inferred from nucleotide sequences of the mitochondrial cytochrome *b* gene. *Philosophical Transactions of the Royal Society of London B: Biological Sciences*, 350, 163–178.

- Sharpe, R. B. (1891) *A review of recent attempts to classify birds: An address delivered before the Second International Ornithological Congress on the 18<sup>th</sup> of May, 1891*. Published at the office of the Congress, pp 90.
- Sharpe, R. B. (1899) *A hand-list of the genera and species of birds*. British Museum of Natural History, London.
- Shufeldt, R. W. (1891) Tertiary fossils of North American birds. *The Auk*, 8, 365–368.
- Shufeldt, R. W. (1892) Fossil birds from the Equus beds of Oregon. *American Naturalist*, 25, 818–821.
- Shufeldt, R. W. (1913) Further studies of fossil birds with descriptions of new and extinct species. *Bulletin of the American Museum of Natural History*, 32, 285–306.
- Sibley, C. & Ahlquist, J. (1990) *Phylogeny and classification of birds of the world*. Yale University Press, New Haven, Connecticut.
- Siewwright, H. & Macleod, N. (2012) Eigensurface analysis, ecology, and modelling of morphological adaptation in the falconiform humerus (Falconiformes: Aves). *Zoological Journal of the Linnean Society*, 165, 390–419.
- Sobolev, D. & Marisova, I. (2011) New species of Miocene buzzards (Falconiformes, Accipitridae). In: *Modern ecological problems of the Ukrainian polissya and adjacent areas*, G. G. Senchenko, I. V. Smal, P. P. Nezhin, M. M. Liskenko (Eds). Nizhyn Gogol State University; p. 158–163.
- Song, X., Huang, J., Yan, C., Xu, G., Zhang, X. & Yue, B. (2014) The complete mitochondrial genome of *Accipiter virgatus* and evolutionary history of the pseudo-control regions in Falconiformes. *Biochemical Systematics and Ecology*, 58, 75–84.
- Steadman, D. W. & MacFadden, B. J. (2016) A large eagle (Aves, Accipitridae) from the early Miocene of Panama. *Journal of Paleontology*, 90 (5), 1012–1015.
- Stejneger, L. (1885) Birds. In: *The Standard Natural History*, vol. 4, J. S. Kingley (Ed.). Boston, S. E. Cassino.
- Stucchi, M. & Emslie, S. D. (2005) A new condor (Ciconiiformes, Vulturidae) from the late Miocene/early Pliocene Pisco Formation, Peru. *The Condor*, 107, 107–113.
- Stucchi, M., Emslie, S.D., Varas-Malca, R.M. & Urbina-Schmitt, M. (2015) A new late Miocene condor (Aves, Cathartidae) from Peru and the origin of South American condors. *Journal of Vertebrate Paleontology*, 35, e972507.
- Suárez, W. (2004) The identity of the fossil raptor of the genus *Amplibuteo* (Aves: Accipitridae) from the Quaternary of Cuba. *Caribbean Journal of Science*, 40, 120–125.

- Suárez, W. & Olson, S. L. (2007) The Cuban fossil eagle *Aquila borraasi* Arredondo: a scaled up version of the Great Black-hawk *Buteogallus urubitinga* (Gmelin). *Journal of Raptor Research*, 41 (4), 288–298.
- Suárez, W. & Olson, S. L. (2009) The generic position of *Miraquila terrestris* Campbell: Another addition to the buteogalline radiation from the Pleistocene of Peru. *Journal of Raptor Research*, 43(3), 249–253.
- Sushkin, P. P. (1905) Zur Morphologie des Vogelskelets; Vergleichende Osteologie der Normalen Tagraubvogel (accipitres) und die Fragen der Classification. Teil I; Grundeinteilung der Accipitres. Teil II; Falken undihrenachsten Verwandten. *Nouveaux mémoires de la Société impériale des naturalistes de Moscou*, 16, 4–247.
- Tambussi, C. & Noriega, J. I. (1996) Summary of the avian fossil record from southern South America. *Muenchner Geowissenschaftliche Abhandlungen*, 30, 245–264.
- Tambussi, C. & Noriega, J. I. (1999) The fossil record of condors (Ciconiiformes: Vulturidae) in Argentina. *Smithsonian Contributions to Palaeobiology*, 89, 177–184.
- Tonni, E. P. (1970) *Foetopterus ambiguous* Moreno et Mercerat, 1891 (Aves, Falconiformes): su asignación a *Chloephaga picta* (Aves, Anseriformes). *Ameghiniana*, 7, 279–280.
- Tonni, E. P. (1980) The present state of knowledge of the Cenozoic birds of Argentina. *Natural History Museum of Los Angeles County, Contributions in Science*, 330, 104–114.
- Tonni, E. P. & Noriega, J. I. (1998) Los condors (Ciconiiformes: Vulturidae) de la Región Pampeana de la Argentina durante el Cenezoico Tardío: distribución interacciones y extinciones. *Ameghiniana*, 35 (2), 141–150.
- Travouillon, K. J., Legendre, S., Archer, M. & Hand, S. J. (2009) Palaeoecological analyses of Riversleigh's Oligo-Miocene sites: implications for Oligo-Miocene climate change in Australia. *Palaeogeography, Palaeoclimatology, Palaeoecology*, 276, 24–37.
- Trewick, S. A. & Gibb, G. C. (2010) Vicars, tramps and assembly of the New Zealand avifauna: a review of molecular phylogenetic evidence. *Ibis*, 152, 226–253.
- Twenty-fifth supplement to the American Ornithologists' Union check-list of North American birds (1950). *The Auk*, 67, 368–370.
- Van Tets, G. F. (1984) A checklist of extinct fossil Australasian birds. In: *Vertebrate Zoogeography & Evolution in Australasia*, M. Archer & G. Clayton (Eds). Hesperian Press; p. 469–475.
- Van Tets, G. F. & Rich, P. V. (1990) An evaluation of De Vis' fossil birds. *Memoirs of the Queensland Museum*, 28, 165–168.

- Vickers-Rich, P. (1991) The Mesozoic and Tertiary history of birds on the Australian plate. In: *Vertebrate palaeontology of Australasia*, P. Vickers-Rich, J. M. Monaghan, R. F. Baird, T. H. Rich, E. M. Thomson, C. Williams (Eds). Pioneer Design Studio Pty Ltd, Lilydale, and Monash University Publications Committee, Melbourne; p. 721–808.
- Vigors, N. A. (1825) Sketches in ornithology; or Observations on the leading affinities of some of the more extensive groups of birds. *The Zoological Journal*, 2, 37–70.
- Walker, C. A. & Dyke, G. J. (2006) New records of fossil birds of prey from the Miocene of Kenya. *Historical Biology*, 18 (2), 95–98.
- Warter, S. L. (1976) A new osprey from the Miocene of California (Falconiformes, Pandionidae). In: *Collected Papers in Avian Paleontology Honoring the 90th Birthday of Alexander Wetmore*, S. L. Olson (ed.). – *Smithsonian Contributions to Paleobiology* 27: 133–139.
- Wells, D. R. & Inskipp, T. P. (2012) A proposed new genus of booted eagles (Tribe Aquilini). *Bulletin of the British Ornithologists' Club*, 132, 70–72.
- Wetmore, A. (1923) Avian fossils from the Miocene and Pliocene of Nebraska. *Bulletin of the American Museum of Natural History*, 48, 483–507.
- Wetmore, A. (1926) Description of a fossil hawk from the Miocene of Nebraska. *Annals of the Carnegie Museum*, 16, 403–408.
- Wetmore, A. (1927) Fossil birds from the Oligocene of Colorado. *Proceedings of the Colorado Museum of Natural History*, 7, 1–13.
- Wetmore, A. (1933) An Oligocene eagle from Wyoming. *Smithsonian Miscellaneous Collections*, 87 (19), 1–9.
- Wetmore, A. (1934) A systematic classification for the birds of the world, revised and amended. *Smithsonian Miscellaneous Collections*, 89(13), 1–13.
- Wetmore, A. (1936) Two new species of hawks from the Miocene of Nebraska. *Proceedings of the United States National Museum*, 84, 73–78.
- Wetmore, A. (1937). Bird remains from cave deposits on Great Exuma Island in the Bahamas. *Bulletin of the Museum of Comparative Zoology*, 130, 427–441 + plate.
- Wetmore, A. (1940) Avian remains from the Pleistocene of central Java. *Journal of Paleontology*, 14(5) 447–450.
- Wetmore, A. (1943) Two more fossil hawks from the Miocene of Nebraska. *The Condor*, 45 (6), 229–231.

- Wetmore, A. (1956) A check-list of the fossil and prehistoric birds of North America and the West Indies. *Smithsonian Miscellaneous Collections*, 131 (5), 1–105.
- Wetmore, A. (1958) Miscellaneous notes on fossil birds. *Smithsonian Miscellaneous Collections*, 135 (8), 1–11.
- Wetmore, A. & Case, E. C. (1934) A new fossil hawk from the Oligocene beds of South Dakota. *Contributions from the Museum of Palaeontology, University of Michigan*, 4, 129–132.
- White, C. M. N. (1950) Systematic notes on African birds. *Ostrich*, 21, 31–32.
- White, C. M. N. (1951) Systematic notes on African birds. *Ostrich*, 22, 25–26.
- White, L. C., Mitchell, K. J. & Austin, J. J. (2018) Ancient mitochondrial genomes reveal the demographic history and phylogeography of the extinct, enigmatic thylacine (*Thylacinus cynocephalus*). *Journal of Biogeography*, 45(1), 1–13.
- Willerslev, E. & Cooper, A. (2005) Ancient DNA. *Proceedings of the Royal Society B: Biological Sciences*, 272, 3–16.
- Wink, M. I. (2000) Advances in DNA studies of diurnal and nocturnal raptors. In: *Raptors at Risk*, R. D. Chancellor and B. U. Meyburg (eds). WWGBP/Hancock House. pp. 831–844.
- Wink, M. I. & Sauer-Gürth, H. (2004) Phylogenetic relationships in diurnal raptors based on nucleotide sequences of mitochondrial and nuclear marker genes. *Raptors worldwide*. WWGBP, Berlin, 483–498.
- Wink, M. I. & Seibold, I. (1996) Molecular phylogeny of Mediterranean raptors (Families Accipitridae and Falconidae). In: *Biología y Conservación de las Rapaces Mediterráneas, 1994*, J. Muntaner and J. Mayol (eds). Monografías, 4 SEO, Madrid.
- Wink, M. I., Seibold, F. L. & Bednarek, W. (1998) Molecular systematics of Holarctic raptors (order Falconiformes) In: *Holarctic birds of prey*, R. D. Chancellor, B. U. Meyburg and J. J. Ferrero (Eds). IGRAMEX, Calamonte, Spain; p. 29–47.
- Woodburne, M. O., MacFadden, B. J., Case, J. A., Springer, M. S., Pledge, N. S., Power, J. D., Woodburne, J. M. & Springer, K. B. (1994) Land mammal biostratigraphy and magnetostratigraphy of the Etadunna Formation (Late Oligocene) of South Australia. *Journal of Vertebrate Paleontology*, 13(4): 483–515.
- Worthy, T. H. & Holdaway, R. N. (1996) Quaternary fossil faunas, overlapping taphonomies, and palaeofaunal reconstruction in North Canterbury, South Island, New Zealand. *Journal of the Royal Society of New Zealand*, 26, 275–361.
- Worthy, T. H. & Holdaway, R. N. (2002) *The lost world of the moa: prehistoric life of New Zealand*. Indiana University Press: Bloomington, Indiana.

- Worthy, T. H. & Yates, A. (2017) A review of the smaller birds from the late Miocene Alcoota local faunas of Australia with a description of a new anatinid species. In: *Proceedings of the 9<sup>th</sup> International Meeting of the Society of Avian Palaeontology and Evolution, Diamante (Argentina), 1–6 August 2016 –Palaeontología y Evolución de las Aves*, 7: 221–252.
- Worthy, T. H., De Pietri, V. L. & Scofield, R. P. (2017) Recent advances in avian palaeobiology in New Zealand with implications for understanding New Zealand's geological, climatic and evolutionary histories. *New Zealand Journal of Zoology*, 44(3), 177–211.
- Worthy, T. H., Tennyson, A. J. D., Jones, C., McNamara, J. A. & Douglas, B. J. (2007) Miocene waterfowl and other birds from central Otago, New Zealand. *Journal of Systematic Palaeontology*, 5(1), 1–39.
- Worthy, T. H., Tennyson, A. J. D., Marshall, B. A., Salisbury, S. W., Hand, S. J. & Scofield, R. P. (2014) Updating the record from the Early Miocene St Bathans Fauna, Central Otago and its significance for documenting the assembly of New Zealand's terrestrial biota. *Geogenes* 2014, 31–33.
- Wroe, S. (2002) A review of terrestrial and mammalian carnivore ecology in Australian fossil faunas, and factors influencing their diversity: the myth of reptilian domination and its broader implications. *Australian Journal of Zoology*, 50(1), 1–24.
- Wroe, S., Field, J. H., Archer, M., Grayson, G. J., Louys, J., Faith, J. T., Webb, G. E., Davidson, I. & Mooney, S. D. (2013) Climate change frames debate over the extinction of megafauna in Sahul (Pleistocene Australia-New Guinea). *Proceedings of the National Academy of Sciences of the United States of America*, 110(22), 8777–8781.
- Zelenkov, N. V. (2013) New finds and revised taxa of Early Pliocene birds from Western Mongolia. In: *Proceedings Volume of the 8<sup>th</sup> International Meeting of the Society of Avian Paleontology and Evolution*, Ursula B. Göhlich and Andreas Kroh (Eds); p. 153–170.
- Zelenkov, N. V. (2016) Evolution of bird communities in the Neogene of Central Asia, with a review of the Neogene fossil record of Asian birds. *Paleontological Journal*, 50 (12), 1421–1433.
- Zelenkov, N. V. & Kurochkin, E. N. (2015) Class Aves. In: *Fossil vertebrates of Russia and adjacent countries, Fossil Reptiles and Birds. Part 3*. E. N. Kurochkin, A. V. Lopatin, N. V. Zelenkov (eds.). Moscow: GEOS.
- Zhang, Z., Feduccia, A. & James, H. F. (2012b) A Late Miocene accipitrid (Aves: Accipitriformes) from Nebraska and its implications for the divergence of Old World vultures. *PLoS ONE*, 7 (11), e48842, doi:10.1371/journal.pone.0048842.

Zhang, Z., Huang, Y., James, H. F. & Hou, L. (2012a) Two Old World vultures from the middle Pleistocene of northeastern China and their implications for interspecific competition and biogeography of Aegypiinae. *Journal of Vertebrate Paleontology*, 32, 117–124.

Zhang, Z., Zheng, X., Zheng, G. & Hou, L. (2010) A new Old World vulture (Falconiformes: Accipitridae) from the Miocene of Gansu Province, northwest China. *Journal of Ornithology*, 151, 401–408.